Molecular mechanisms of drug resistance, invasion and metastasis in pancreatic carcinoma

A thesis submitted for the degree of Ph.D.

by

Naomi Walsh B.Sc. Hons

This research work described in thesis was performed under

the supervision of

Prof. Martin Clynes and Dr. Norma O'Donovan

National Institute for Cellular Biotechnology

Dublin City University

2007

I hereby certify that this material, which I now submit for assessment on the programme of study leading to the award of Ph D. is entirely my own work, that I have exercised reasonable care to ensure that the work is original, and does not to the best of my knowledge breach any law of copyright, and has not been taken from the work of others save and to the extent that such work has been cited and acknowledged within the text of my work.

Signed:_____   ID No.: 99421976

Date:_____

Abbreviations

%	-	Percentage
Ab	-	Antibody
ABC	-	ATP Binding Cassette
ALDH1A1	-	Aldehyde dehydrogenase 1A1
ATCC	-	American Tissue Culture Collection
ATP	-	Adenosine Triphosphate
BSA	-	Bovine Serum Albumin
cDNA	-	Complementary DNA
CFE	-	Colony forming efficiency
CI	-	Combination Index
CM	-	Conditioned media
DMEM	-	Dublecco's Minimum Essential Medium
DMSO	-	Dimethyl Sulfoxide
DNA	-	Deoxyribonucleic Acid
DTT	-	Dithiothreitol
ECACC	-	European Collection of Animal Cell Culture
ECM	-	Extracellular matrix
ED	-	Effective dose
EDTA	-	Ethylene Diamine Tetraacetic Acid
EGF	-	Epidermal Growth Factor
EGFR	-	Epidermal Growth Factor Receptor
EMT	-	Epithelial to Mesenchymal Transition
erbB2	-	HER2
FCS	-	Foetal Calf Serum
FGF	-	Fibroblast Growth Factor
GAL-1	-	Galectin-1
GAPDH	-	Glyceraldehyde-6-Phosphate Dehydrogenase
GSN	-	Gelsolin
IC_{50}	-	Inhibitory Concentration 50%
IHC	-	Immunohistochemistry

HGFR	-	Hepatocyte Growth Factor Receptor
IGFR	-	Insulin-like Growth Factor Receptor
kDa	-	Kilo Daltons
LRP	-	Lung resistance-related protein
MAPK	-	Mitogen Activated Protein Kinase
MDR	-	Multiple drug resistance
Min	-	Minutes
miRNA	-	microRNA
MMPs	-	Matrix Metalloproteases
mRNA	-	Messenger RNA
MRP	-	Multi-drug resistance-associated protein
NDPK	-	Nucleotide diphosphate kinase
NSCLC	-	Non-Small Cell Lung Cancer
OD	-	Optical density
PBS	-	Phosphate Buffered Saline
P-gp	-	P-glycoprotein
RISC	-	RNA-Induced Silencing Complex
RNA	-	Ribonucleic Acid
RNase	-	Ribonuclease
RPM	-	Revolutions Per Minute
RT	-	Room termperature
RT-PCR	-	Reverse Transcription Polymerase Chain Reaction
SD	-	Standard Deviation
SF	-	Serum-free
siRNA	-	Small interfering RNA
STIP1	-	Stress-induced phosphoprotein 1
TBS	-	Tris Buffered Saline
TGFβ1	-	Transforming Growth Factor β1
UHP	-	Ultra High Pure Water
v/v	-	Volume/Volume
VIM	-	Vimentin

Abstract

The research outlined in this thesis aims to further our knowledge of the biological characteristics underlying the aggressive behaviour by which pancreatic cancer invades and metastasises at an early stage and is refractory to most chemotherapeutic drugs. Investigation into drug resistance in pancreatic cancer involved pulse-selection of three cell lines with epirubicin, taxotere and gemcitabine. The drug-selected cell lines, in general, displayed low changes in sensitivity to their respective selecting drugs and no obvious cross-resistance profile. However, drug treatment modulated the invasive potential of the pulse-selected cell lines.

Expression of multi-drug resistant proteins (P-gp and MRP-1) was also determined by IHC in 45 pancreatic tumour specimens, results suggested a contributory role for P-gp expression in pancreatic cancer.

An *in vitro* pancreatic invasion model was established by single cell cloning of MiaPaCa-2, yielding sub-clones displaying diverse invasive properties. The malignant phenotypes of MiaPaCa-2, Clone #3 (highly invasive) and Clone #8 (poorly invasive) were characterised, comparative proteomic profiling by 2-D DIGE, MALDI-TOF MS and RNAi revealed three targets, ALDH1A1, VIM and STIP1 with functional involvement in the invasion process. ALDH1A1 appeared to play a role in the aggressive invasive phenotype; expression was associated with increased invasion, drug resistance and decreased adhesion. VIM and STIP expression was also linked to increased invasion and decreased adhesion, with STIP1 displaying a role in proliferation, which has not previously been described. Factors secreted into conditioned media of Clone #3 and Clone #8 was also examined by proteomics. Targets, GSN and ALDH1A1 were chosen for functional analysis and their potential involvement in cancer cell invasion assessed.

EGFR/HER2 expression was analysed in 5 pancreatic cancer cell lines, and two cell lines which co-expressed EGFR and HER2 were tested with lapatinib. Lapatinib, a dual EGFR/HER2 inhibitor in combination with chemotherapeutic drugs showed additive interactions, suggesting the possibility of a therapeutic role for lapatinib in combination with chemotherapy in pancreatic cancer patients co-expressing EGFR/HER2.

Table of contents

Chapter 1.0   Introduction

Chapter 3.0   Results

1.0   Introduction

1.1   Pancreatic cancer

Pancreatic cancer is a devastating disease and is the tenth most common cause of cancer in Europe (Ferlay *et al.*, 2007). Approximately 170,000 new cases of pancreatic cancer (2.1% of total cancers) occur worldwide every year (Parkin *et al.*, 1999). In Ireland, pancreatic cancer is the 11th most common invasive cancer in men and women, is responsible for 5% of cancer related deaths and has the lowest 5-year relative survival for patients diagnosed between 1995 and 2000 (National Cancer Registry Ireland, 2000).

It is the most fatal malignancy; all-stage 5-year survival rate is less than 5% (Jemal *et al.*, 2002). The lethality of this cancer is related to its rapid growth and tendency to invade adjacent organs and metastasise at an early stage. Patients generally present at an unresectable stage, due to the asymptomatic nature of the disease. Surgery offers the best possibilities for survival; however, fewer than 15% of patients are eligible for resection at time of diagnosis. Cancer of the pancreas is more common in males than females and in the older individual; the highest incidence has been reported in black American males. Several causes and associations have been linked to the occurrence of pancreatic cancer. The risk of pancreatic cancer is increased 3-fold by diabetes. Other factors such as pancreatitis, pernicious anemia, cystic fibrosis and familial adenomatous polyposis increase the risk of contracting the disease (Ghadirian *et al.*, 2003). Smoking is the strongest environmental cause of pancreatic cancer with an increased risk of approximately 2-fold (Lowenfels and Maisonneuve, 2004).

Apart from surgical resection at early diagnosis, no therapy has been found to elicit a good response. At present radiation and chemotherapy only show a limited effect in fighting pancreatic cancer.

Pancreatic carcinoma appears to be inherently resistant to a wide variety of chemotherapeutic agents, which can differ greatly and are unrelated with respect to molecular structure and target specificity.

1.1.1   Genetics of pancreatic cancer

Pancreatic cancer can occur through the accumulation of inherent and acquired genetic alterations. Tumour suppressors and oncogenes contribute to the development of pancreatic cancer. Tumour suppressor genes code for proteins which control cell proliferation, and loss of these genes through mutations, deletion or chromosomal reorganisation leads to deregulated growth. Oncogenes are mutated forms of proto-oncogenes that cause normal cells to grow out of control and cause cancer. Proto-oncogenes are the genes that control normal cell division and differentiation. When a proto-oncogene mutates into an oncogene, the gene is permanently turned-on or activated which leads to increased cell division.

1.1.2 Tumour suppressors in pancreatic cancer

Pancreatic cancer is associated with several inactivated tumour suppressor genes such as p53, p16, p21, SMAD4/DPC4 and p27. Both copies of a tumour suppressor gene must be inactivated, i.e. mutations in both alleles must occur for there to be a loss in the gene product (Hruban *et al*., 1998).

The p53 tumour suppressor gene is inactivated in approximately 50% of pancreatic cancers (Pellegata *et al*., 1994; Slebos *et al*., 2000). P53 controls cell cycle at the G1/S interface and plays a vital role in inducing programmed death in response to DNA damage. Taghavi *et al*. (2007) determined that restoration of wild-type p53 function could be used to eliminate the tumourigenic phenotype in two pancreatic tumour cell lines; CRL1420, which contains elevated levels of mutant p53, and CRL1682, with no detectable p53 protein. Expression of wild-type p53 decreased the growth rate of CRL1420 and completely suppressed its potential for tumour formation in nude mice. The size of the tumours formed in nude mice by CRL1682 was reduced drastically. Neither of the cell lines irrespective of the status of p53 was arrested at G1 in response to x-irradiation. Thus, these results provide functional evidence that the deletion or mutational inactivation of the p53 gene represents an important step in the tumourigenicity of pancreatic cancer. Cascalló *et al*. (2005) showed that in a human xenograft model, sequential administration of gemcitabine and restoration of p53 resulted in potent tumour

2

growth inhibition. Statistical differences were observed with respect to the growth of tumours receiving only gemcitabine or p53. This data indicates that reintroduction of p53 function in human pancreatic tumours *in vivo* allows the restoration of molecular pathways improving the response to gemcitabine. Eisold *et al*. (2004) examined whether the combination of adenovirus-mediated (Ad) wild-type (wt) p53 gene transfer and 5-fluorouracil (5FU) chemotherapy effects pancreatic cancer cells with different p53 gene status. Human and rat pancreatic cancer cell lines, with p53 mutation, wild-type and null were used for *in vitro* studies. Ad-p53 gene transfer combined with 5-FU significantly inhibited tumour cell proliferation and substantially enhanced apoptosis in all cell lines with an alteration in the p53 gene compared to cell lines containing (Ad) wt-p53. *In vivo* experiments showed the most effective tumour regression in animals treated with Ad-p53 plus 5-FU. Both *in vitro* and *in vivo* analyses revealed that a sublethal dose of Ad-p53 increased the apoptotic response induced by 5-FU. These results suggest that Ad-p53 may synergistically enhance 5-FU-chemosensitivity most strikingly in pancreatic cancer cells lacking p53 function. These findings illustrate that the anticancer efficacy of this combination treatment is dependent on the p53 gene status of the target tumour cells.

P16 is an inhibitor of cyclin-dependent kinases (CDKs), which complexes with cyclin-D. Loss of p16 function results in release of activated transcription factors and progression of the cell cycle through the G1/S checkpoint (Cowgill *et al*., 2003). P16 acts on retinoblastoma (RB1) to form a negative feed-back loop that regulates the ability of RB1 to prevent cell proliferation. Deletions or mutations in p16 expression can affect the relative balance of functional p16 and cyclin-D, resulting in abnormal cell growth (Sirivatanauksorn *et al*., 1998). Liu *et al*. (1995) observed deletions of both exons 1 and 2 of MTS-1 (MTS-1 encodes p16, an inhibitor of cyclin-dependent kinase 4 (cdk4) which complexes with cyclin D1) in 50% of pancreatic cancer cell lines and an additional 30% of pancreatic cancer cell lines show point mutations or microdeletions based on DNA sequencing. Loss of p16 expression has been reported in 25-100% of pancreatic cancers (Xu *et al*., 2006; Caldas *et al*., 1994; Naumann *et al*., 1996) and is associated with higher incidence of lymph node metastasis (Jeong *et al*., 2005). Loss of p16 expression is associated with decreased survival, increased tumour size and risk of metastasis (Garcea *et*

al., 2005). The presence p16 alterations, correlates with a worse prognosis in resected pancreatic cancer patients (Gerdes *et al*., 2002).

SMAD4/DPC4 tumour suppressor gene is deleted/lost in approximately 50% of invasive pancreatic cancers (Hahn *et al*., 1996; Tang *et al*., 2002). SMAD4 regulates signal transduction of the transforming growth factor β (TGFβ) superfamily (Levy *et al*., 2005). SMAD4 mediates down-regulation of E-cadherin induced by TGF-β in the pancreatic cancer cell line, Panc-1, at least in part, through Snail and Slug induction (Takano *et al*., 2007). Peng *et al*. (2002) determined the role of SMAD4 in the suppression of tumor cell growth and in the regulation of TGF-β-mediated expression of cell-cycle regulatory genes p15 (ink4b) and p21(waf1). Over-expression of SMAD4 by adenoviral infection in pancreatic cancer cell line, Capan-1 (no SMAD4 expression) reduced anchorage-independent growth by more than 50%, and inhibited xenograft tumour growth. However, over-expression of SMAD4 in CFPac-1 cells (SMAD4 homozygously deleted) did not inhibit CFPac-1 growth. Interestingly, SMAD4 induced expression of p15(ink4b), p21(waf1), and TGF-β-responsive reporter gene in Capan-1 but not in CFPac-1 cells.

1.1.3 Tumour oncogenes in pancreatic cancer
Pancreatic cancer is associated with many mutated oncogenes. These oncogenes can be classified into groups; growth factors and their receptors, signal transducers, transcription factors and programmed cell death receptors. Examples of oncogenes associated with pancreatic cancer include c-met, platelet-derived growth factor (PDGF), EGFR and HER2, abl and K-ras, myc and bcl-2.

Mutations in K-ras are found in 80-100% of pancreatic cancer patients (Lemoine *et al*., 1992; Rozenblum *et al*., 1997). The ras family of oncogenes encode for proteins with GTPase activity and can switch on signal transduction pathways. Ji *et al*. (2007) reported that K-ras activates hedgehog signalling in pancreatic cancer, utilising a down-stream effector pathway mediated by RAF/MEK/MAPK but not PI3K/AKT. Brummelkamp *et al*. (2002) used a retroviral RNA interference (RNAi) system to inhibit the expression of mutated K-ras^{v12} while leaving other ras isoforms unaffected. These studies showed that

small interfering RNA (siRNA) for K-ras decreases anchorage-independent growth in the pancreatic cancer cell line, Capan-1. Fleming *et al*. (2005) found that silencing mutant K-ras through RNAi results in alteration of pancreatic cancer tumour cell behaviour *in vitro*. Furthermore, after K-ras RNAi, there was a reduction in angiogenic potential of both pancreatic cancer cell lines. Panc-1 cells increased the level of expression of thrombospondin-1, an endogenous inhibitor of angiogenesis, whereas MiaPaCa-2 cells decreased the production of vascular endothelial growth factor, a primary stimulant of angiogenesis in pancreatic tumours. This study suggested that targeting mutant K-ras specifically might be effective against pancreatic cancer *in vivo*.

Rejiba *et al*. (2007) examined whether combining K-ras siRNA with gemcitabine has therapeutic potential for pancreatic cancer. *In vitro*, the treatment of tumour cell cultures with the corresponding K-ras siRNA resulted in a significant inhibition of endogenous k-ras expression and cell proliferation. *In vivo*, tumour xenografts were significantly reduced with K-ras siRNA (GAT) delivered by electroporation. The combined treatment with K-ras siRNA(GAT) plus gemcitabine resulted in strong growth inhibition of orthotopic pancreatic tumours. Survival rate was significantly prolonged and the mean tumour volume was dramatically reduced in mice receiving the combined treatment compared with single agents.

These recent reports show that targeting mutant K-ras through specific siRNA might be effective for K-ras oncogene silencing and tumour growth inhibition.

The oncogene c-Met is a 190 kDa tyrosine kinase receptor, consisting of a heterodimer of two disulphide linked chains of 50 kDa (alpha) and 145 kDa (beta) which is synthesised as a 170 kDa precursor that is glycosylated and cleaved to give the active protein (Giordano *et al*., 1989). The c-met proto-oncogene encodes a transmembrane tyrosine kinase receptor (Met) that has the capacity to modulate cell proliferation and differentiation; it is activated by the hepatocyte growth factor (HGF) or scatter factor (SF).

 Over-expression of c-Met has been reported in biliary tract carcinomas (Nakazawa *et al*., 2005) and colorectal cancers (Zeng *et al*., 2004). Ebert *et al*. (1994) reported co-over-expression of c-Met and HGF in pancreatic cancer, indicating that both regulatory proteins may participate via an autocrine or paracrine mechanism to promote pancreatic cancer cell

invasion. Hansel *et al.* (2004) examined global gene expression profiles from well-differentiated non-metastatic (n=5) and metastatic (n=7) pancreatic endocrine neoplasms to determine molecular markers that predict disease progression. This study confirmed the over-expression of Met in metastatic versus non-metastatic pancreatic endocrine neoplasms (5 of 15, 33% versus 4 of 24, 17%), as well as in lymph node metastases (4 of 7, 57%) and liver metastases (5 of 9, 56%) by immunohistochemistry.

1.1.4 Genetic alterations predisposition for pancreatic cancer

Familial pancreatic cancer is hereditary predisposition that is responsible for approximately 3% of pancreatic cancer cases. Analysis of the family history can help individuals to identify risks of developing pancreatic cancer. These include distinct hereditary cancer syndromes such as; Peutz-Jeghers syndrome, hereditary pancreatitis, familial atypical multiple mole melanoma syndrome, hereditary breast and ovarian cancer syndrome and hereditary non-polyposis colorectal cancer.

BRCA1 and BRCA2 encode proteins that are involved in cell cycle regulation and DNA repair (Boulton, 2006). Inherited or germ-line mutations in these genes has been identified as predictors of breast and ovarian cancer (Wooster *et al.*, 2003). Recently, Couch *et al.* (2007) suggested that BRCA2 mutations accounts for 6% of moderate and high-risk pancreatic cancer families. Other genetic mutations such as STK11/LKB1, CDKN2A/p16, PRSS1 are association with pancreatic cancer (Zalatnai, 2006). The identification of germline mutations in genes predisposing to pancreatic cancer could be used for a more precise risk assessment for the development of pancreatic cancer. This may allow the application of screening methods for the detection of early pancreatic cancer in high-risk individuals, and allow potentially curative pancreatectomy treatment.

1.2   Chemotherapy for pancreatic cancer

Chemotherapeutic drugs used in combination assays and proliferation assays throughout this thesis will also be outlined and their modes of action will be discussed in the following section.

1.2.1   Anthracyclines

Epirubicin (Figure 1.2.1), doxorubicin (adriamycin) and daunorubicin are members of the anthracycline class of antineoplastic drugs. Doxorubicin is an anthracycline antibiotic isolated from *Streptomyces peucetius*. Epirubicin is the semi-synthetic drug derived from doxorubicin; it forms a complex with DNA by intercalation of its planar rings between nucleotide base pairs. Intercalation results in complex formation which inhibits DNA, RNA and protein synthesis. It also triggers DNA cleavage by topoisomerase II α, resulting in initiation of cell death (Minotti *et al*., 2004). Binding to cell membranes and proteasomes may also be involved in the compound's cytotoxic effects. The drug binds to the proteasome in the cytoplasm forming an anthracycline-proteasome complex that translocates into the nucleas via nuclear pores. The drug then dissociates from the proteasome and binds to DNA (Kiyomiya *et al*., 2001).

Epirubicin also generates free radicals that cause cell and DNA damage. It inhibits DNA helicase activity, preventing the enzymatic separation of double-stranded DNA and interfering with replication and transcription. The anti-proliferative and cytotoxic activity of epirubicin is thought to result from these or other possible mechanisms.

Epirubicin is favoured over doxorubicin, the most popular anthracycline, in some chemotherapy regimens as it appears to cause less side-effects. Epirubicin has a different spatial orientation of the hydroxyl group at the 4' carbon of the sugar, which may account for its faster elimination and reduced toxicity. Epirubicin is primarily used against breast and ovarian cancer, gastric cancer, lung cancer, and lymphomas. Epirubicin and gemcitabine have been tested in combination to treat advanced pancreatic cancer (Neri *et al*., 2002). In a phase II trial, Ianniello *et al.* (2001) showed how the regime offered a feasible approach for the improvement of treatment for advanced pancreatic cancer.
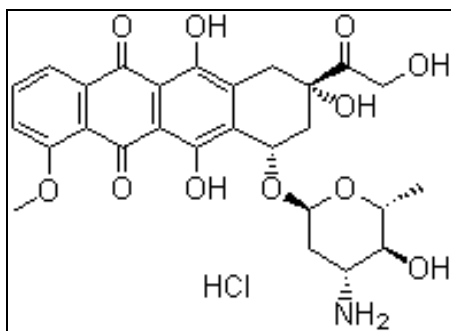
Figure 1.2.1 Chemical structure of epirubicin (www.chemblink.com).

Common methods of resistance to epirubicin include increased drug efflux, due to the over-expression of MDR-1 gene product P-glycoprotein (Pesic *et al*., 2006) and multidrug resistance associated protein, MRP-1 (Breuninger *et al*., 1995).

1.2.2   Taxanes

Docetaxel (taxotere) and paclitaxel (taxol) are members of a group of anti-neoplastic chemotherapeutic drugs known as the taxanes. Taxotere (Figure 1.2.2) is a semi-synthetic taxane derived from a taxane intermediate extracted from the needles of *Taxus baccata*, while taxol was originally isolated from the yew tree *Taxus brecifolia*. The anti-tumour activity of taxanes is attributed to their ability to disrupt the normal process of microtubule assembly and disassembly. Microtubules within a cell support cell shape and can act as a transport network. They are essential for the reproduction, growth and spread of tumour cells. Microtubules are normally reorganised during the mitosis process to form a spindle. Guanosine triphosphate (GTP) is required during the assembly of microtubules from tubulin. When mitosis is complete, the spindle disappears and the microtubule network reforms. Taxanes have a high binding affinity to tubulin, and taxotere has a higher binding affinity than taxol (Georgoulias, 2002). Tubulin-binding promotes polymerisation and prevents de-polymerisation of the microtubules in the absence of GTP, forming stable microtubules that exhibit resistance to microtubule physiologic disassembly. Taxotere accumulates within the tumour cells, inhibiting cell proliferation and promoting cell death (Eisenhauer and Vermorken, 1998).

Taxotere displayed variable activity (0-28% response rate) in the treatment of pancreatic cancer and has shown a median survival of > 6 months (Okada *et al*., 1999; Rougier *et al*.,

2000). Taxotere has been combined with gemcitabine for treatment of unresectable metastatic pancreatic cancer; results show response rates of 7.4-33% and the best median survival of 7 months (Androulakis *et al*., 1999).

Resistance to taxotere is associated with two major mechanisms: over-expression of P-gp (Bradley and Ling, 1994; Gottesman and Pastan, 1993) and altered expression α- and β-tubulin binding activity (Cabral and Barlow, 1989; Haber *et al*., 1995).

The unique chemical structure of Taxotere®
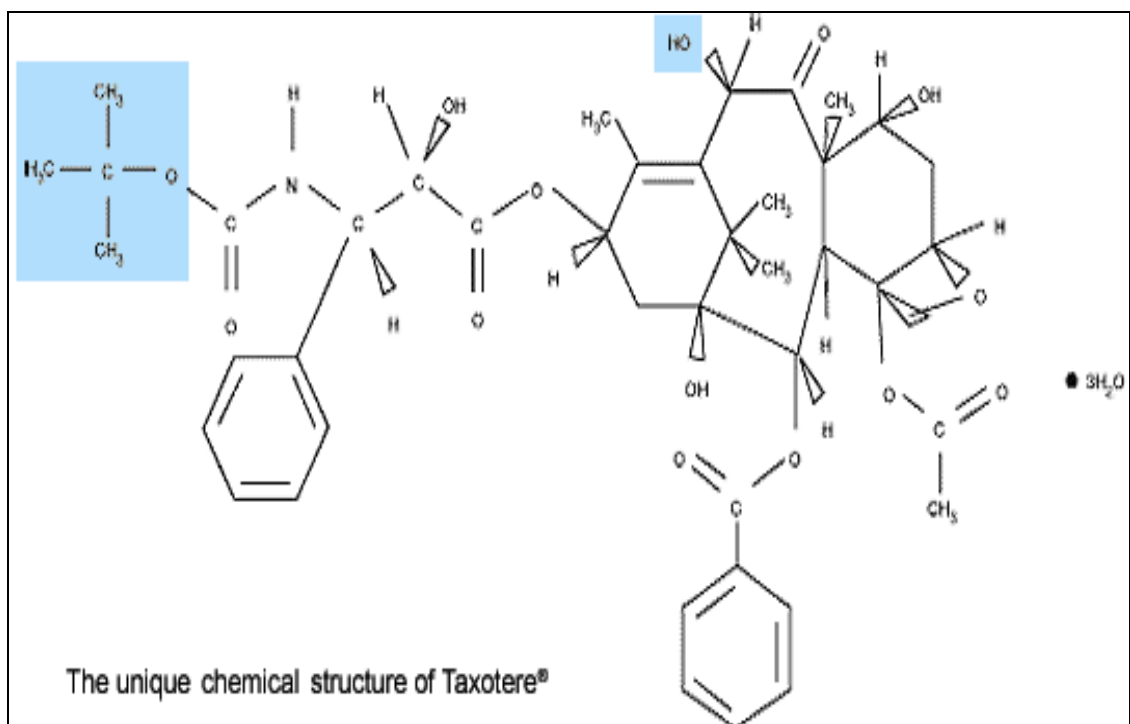
Figure 1.2.2 Chemical structure of taxotere (www.taxotere.com).

1.2.3   Gemcitabine

Gemcitabine (2', 2'-difluorodeoxycytidine: dFdC), an anti-metabolite, is an S-phase nucleoside deoxycytidine analogue. It is a pro-drug that needs to be metabolised before it can exert its toxic effects. It has three modes of action: it competes for incorporation into DNA, hence inhibiting DNA synthesis (Huang *et al*., 1991); prevents DNA repair by masked termination; and undergoes self potentiation and inhibits ribonucleotide reductase (Shore *et al*., 2003) (Figure 1.2.3).

Gemcitabine has been widely used for the treatment of head and neck, non-small lung cancer and has now emerged as the keystone of chemotherapy for pancreatic cancer.
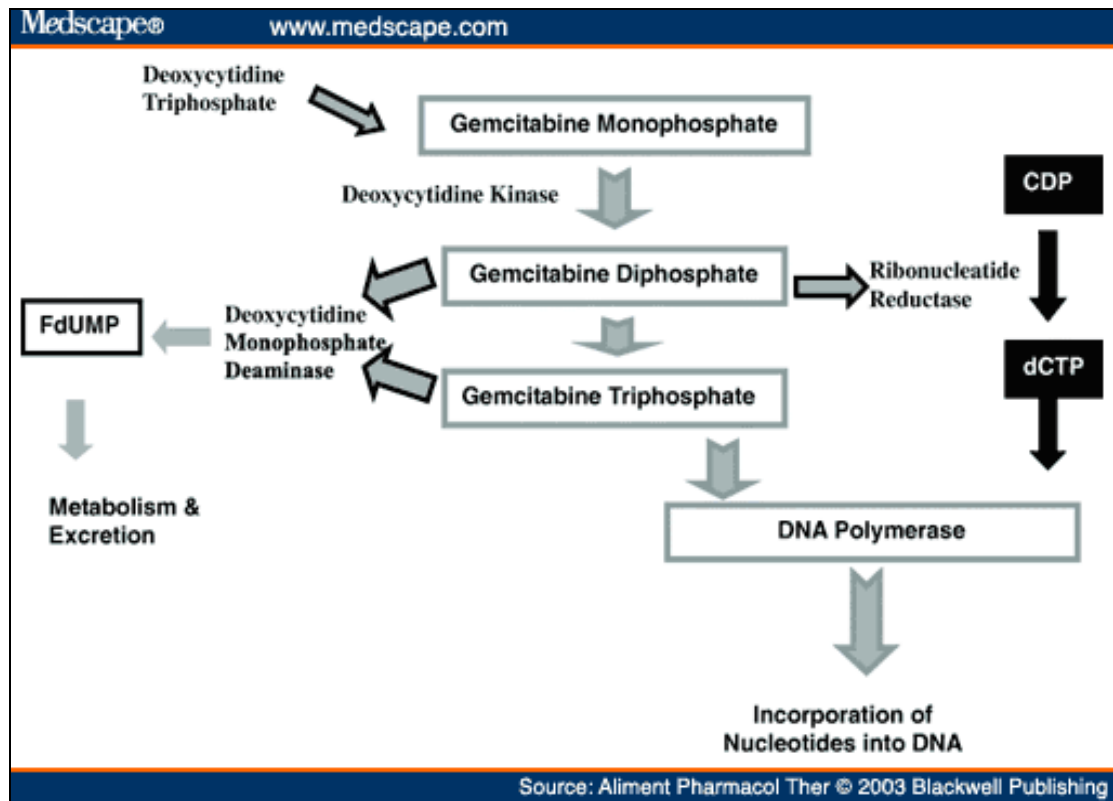
Figure 1.2.3 Mode of Action of Gemcitabine (Shore *et al.,* 2003).

Gemcitabine resistance may be caused by increased ribonucleotide reductase activity (Jordheim *et al*., 2005) and decreased dCK activity (Achiwa *et al*., 2004), which decreases the phosphorylation of gemcitabine (Figure 1.2.4). Feng *et al*. (2006) reported that treatment of two human head and neck cancer cell lines with gemcitabine stimulates phosphorylation of EGFR. EGFR down-regulation did not occur at the level of transcription (RT-PCR), but instead occurred via phosphorylation and ubiquitination of the receptor along a proteosome/lysosome-mediated pathway. These results suggest that EGFR degradation may be a novel mechanism for gemcitabine-mediated cell death.
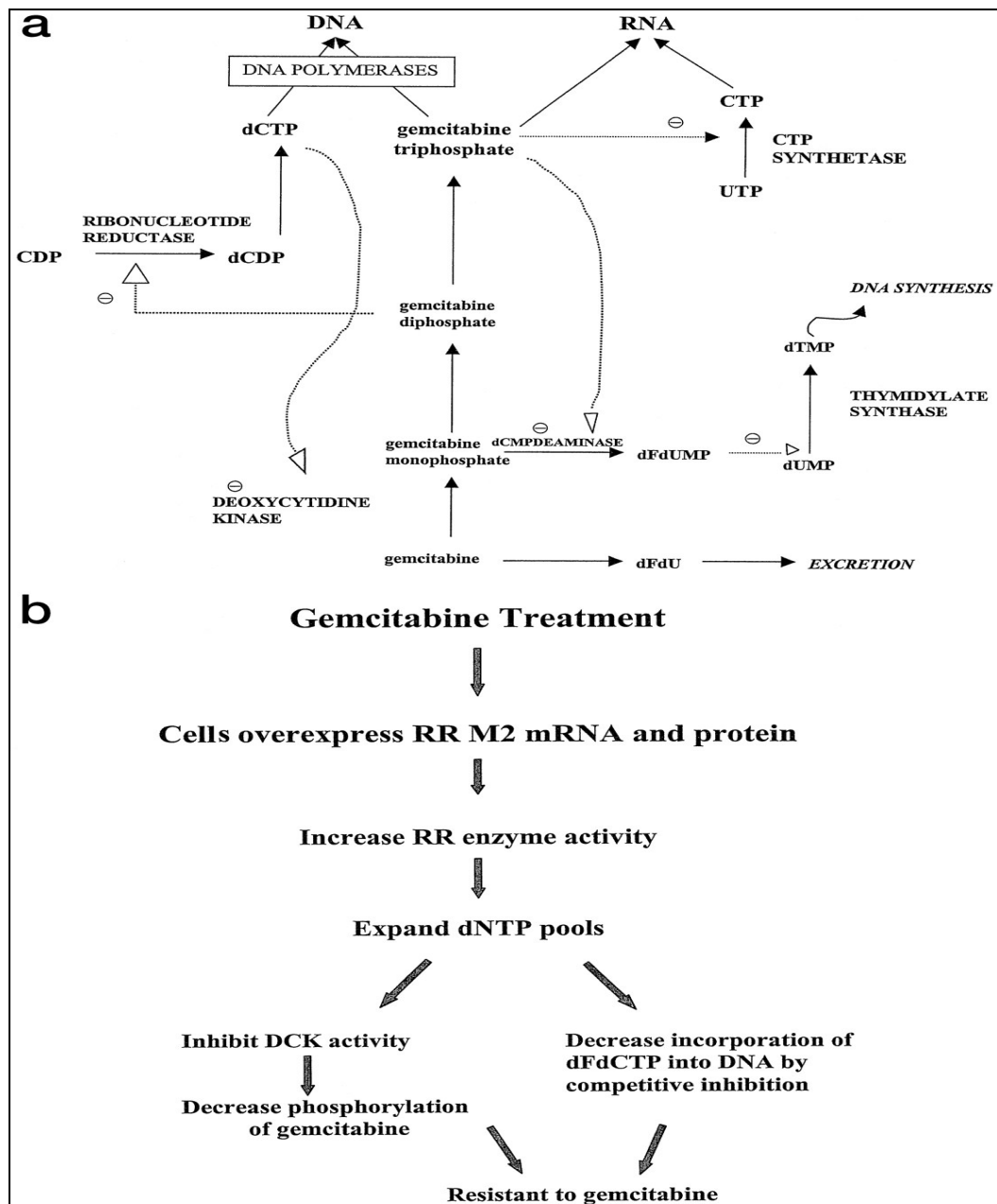
Figure 1.2.4 A. Schematic diagram of the metabolism of gemcitabine. B. The hypothesis of the role of ribonucleotide reductase in gemcitabine resistance. (Goan *et al.*, 1999).

11

1.2.4 Platinum compounds

Cisplatin (cis-diamminedichloro-platinum (II)) (Figure 1.2.5 (A)) and carboplatin (cis-diammine-1,1-cyclobutandicarboxylateplatinum (II)) (Figure 1.2.5 (B)) are platinum compounds commonly used in cancer chemotherapy. These platinum agents form strong chemical bonds with thiol sulphurs and amino nitrogens in proteins and nucleic acids. The cytotoxicity of platinum agents is due to the formation of intrastrand cross-links in the DNA (Brabec and Kasparkova, 2002). The cross-link adducts in the DNA lead to G2 arrest and apoptosis, due to the inability of the cells to transcribe the Pt-damaged DNA and produce mRNA essential for mitosis (Sorenson and Eastman, 1988).

Cisplatin is mainly used to treat solid tumours such as testicular, germ cell, bladder, head and neck cancer. Palmer *et al*. (2007) performed a randomised phase 2 trial of neoadjuvant chemotherapy in resectable pancreatic cancer: gemcitabine alone versus gemcitabine combined with cisplatin. This study concluded that combination therapy with gemcitabine and cisplatin is associated with a high resection rate and an encouraging survival rate, suggesting that further study is warranted.
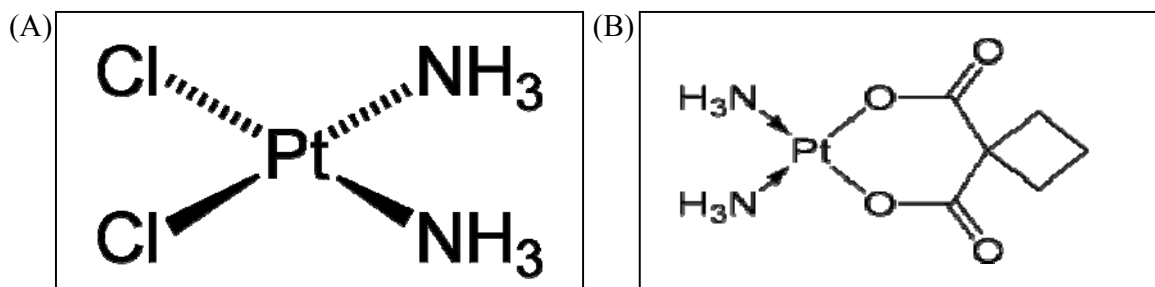
Figure 1.2.5 Chemical structure of (A) cisplatin and (B) carboplatin (www.dsch.univ.trieste.it)

Mechanisms of platinum resistance include decreased uptake of the drug into the cells, inactivation of the drug by cellular thiol compounds, enhanced repair of the platinum-related DNA damage and the absence of mismatch repair (Papouli *et al*., 2004), and increased GSH-based detoxification (Godwin *et al*., 1992).

1.2.5 Capecitabine (5'dFUrd)

XELODA (capecitabine) is a fluoropyrimidine carbamate with anti-neoplastic activity. It is an orally administered systemic prodrug of 5'-deoxy-5-fluorouridine (5'-DFUR or 5'dFUrd)) which is converted to 5-fluorouracil.

Capecitabine has substantial activity in patients with locally advanced or metastatic breast cancer, after failure of taxane or anthracycline chemotherapy (Blum *et al*., 1999). Capecitabine is metabolised in the liver by carboxylesterase to 5'-deoxy-5-fluorocytidine (5'dFCR), and then converted to 5'dFUR. Finally, 5'dFUR is converted to the cytotoxic 5-FU by thymidine phosphorylase (Figure 1.2.6) in tumour and normal tissue (Ishikawa *et al*., 1998). These metabolites exert their toxic effects by thymidylate synthase (TS) inhibition and incorporation into RNA and DNA (Schellens, 2006). TS is bound by capecitabine metabolite, FdUMP. This binding complex prevents the formation of thymidylate from 2'-deoxyuridylate. TS is essential for the synthesis of 2'-deoxythymidine-5'-monophosphate, a precursor for DNA synthesis (Rustum, 2004). Therefore, deficiency of this compound inhibits cell division. Nuclear transcription enzymes can incorporate FUTP in place of UTP during RNA synthesis; this metabolic error interferes with RNA processing and protein synthesis (FDA, 2000).

Capecitabine in combination with gemcitabine, in the treatment of advanced/metastatic pancreatic cancer improved the median overall survival, but not significantly compared to gemcitabine alone (Herrmann *et al*., 2007). Capecitabine in combination with trastuzumab (Herceptin) caused complete remission of a patient with recurrent breast cancer and liver metastasis (Morohashi *et al*., 2007). The combination of capecitabine and trastuzumab has been further validated in a phase II study of HER2 over-expressing advanced/metastatic breast cancer. Schaller *et al*. (2007) showed that the combination of capecitabine and trastuzumab is highly active in patients with HER2 over-expressing anthracycline- and/or taxane-pretreated breast cancer, with only slight restrictions regarding quality of life. These recent studies suggest that the combination of capecitabine and EGFR/HER2 targeting therapies could possibly be used to treat other cancer at advanced/metastatic stage. Geyer *et al*. (2006) demonstrated in a randomised trial that lapatinib, an EGFR/HER2 inhibitor, increases the efficacy of capecitabine, compared to capecitabine

alone in patients with advanced or metastatic breast cancer who have developed resistance to trastuzumab-based therapy. The median time to progression was 8.4 months in the combination-therapy group as compared with 4.4 months in the monotherapy group. Lapatinib plus capecitabine is superior to capecitabine alone in women with HER2-positive advanced breast cancer that has progressed after treatment with regimens that included an anthracycline, a taxane, and trastuzumab.
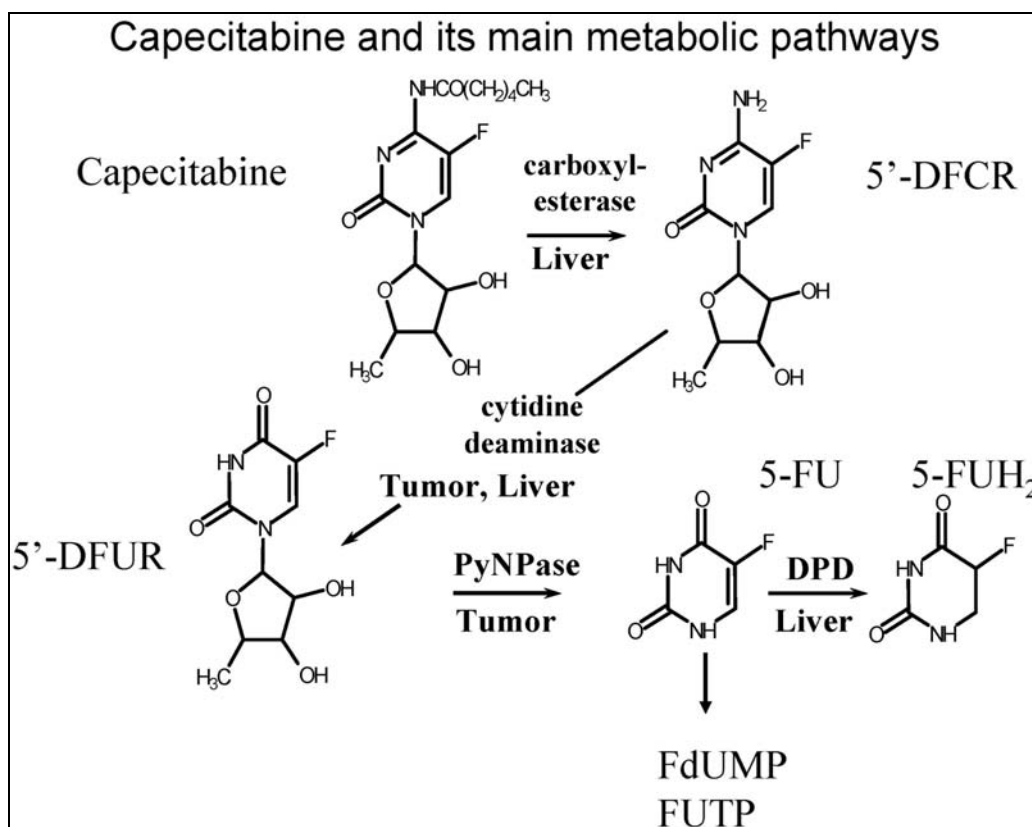
Figure 1.2.6 Chemical structure of capecitabine and its main metabolites. Abbreviations: 5'-DFCR, 5'-deoxy-5-fluorocytidine; 5'-DFUR, 5'-deoxy-5-fluorouridine; 5-FU, 5-fluorouracil; 5-FUH2, 5-fluorodihydrouracil; FdUMP, 5-fluoro-2'-deoxyuridine-monophosphate; FUTP, 5-fluorouridine-5'-triphosphate (Schellens, 2006).

1.3   Multi-drug resistance

Multi-drug resistance (MDR) is defined as the ability of cancer cells to develop cross-resistance to chemotherapeutic drugs. The resistance profile seems to be unrelated to molecular structure or target specificity. The multi-drug resistance increases during chemotherapy treatment and is multi-factorial, as several pathways and cellular mechanisms are involved. The most widely studied MDR mechanisms are the over-expression of the MDR-1 gene/P-glycoprotein (P-170/P-gp) and the multi-drug resistance associated protein (MRP-1). Other factors associated with increased drug resistance include, the lung resistance protein (LRP), topoisomerase IIα, glutathione S transferase (GST), increased repair of drug-induced DNA damage, blocked apoptosis and alterations in cell cycle control and signalling pathways (Filipits *et al*., 2000).

The MDR phenotype represents a major obstacle for effective chemotherapy. Such resistance may develop during drug treatment, referred to as acquired resistance, or maybe an inherent feature of the tumour known as intrinsic resistance.

1.3.1   Drug resistance in pancreatic cancer

Resistance of pancreatic cancer to multiple drugs is frequently encountered. Such resistance may be acquired during drug treatment, or may be an inherent feature of pancreatic cancer. This severe resistance is linked with treatment failure and poor prognosis.

Over-expression of the multidrug resistance protein, P-glycoprotein (P-gp) and the multidrug resistance protein (MRP-1) in cancer cells have been linked with the development of simultaneous resistance to a great variety of cytotoxic drugs. P-glycoprotein is a 170-kDa integral plasma membrane protein, which contains 12 putative transmembrane regions and two ATP binding sites. It confers multidrug resistance by functioning as an energy-dependent drug efflux pump (Germann *et al.,* 1993). MRP-1 is involved in cancer drug resistance and in the transport of glutathione and glucuronate conjugates, as well as anionic drugs out of the cell (Figure 1.3.1).

This ability of P-gp and MRP-1 to act as drug efflux pumps, transporting chemotherapeutic drugs out of the cells, renders the chemotherapy ineffective.

Chemotherapy for advanced pancreatic cancer is often considered palliative and due to the intrinsic and/or acquired resistance to chemotherapeutic drugs the rate of survival of pancreatic cancer is very low.

Lage and Dietel (2002) established a P-glycoprotein-mediated multidrug resistant pancreatic cell line induced by daunorubicin (DRB)-selection, and an alternative drug resistant phenotype due to treatment with mitoxantrone (MTX) to investigate further the complex multimodal mechanisms of resistance in pancreatic cancer. The DRB-variant was 1,800 times more resistant and the MTX-selected cell line was 8 times more resistant than the parental cell line. The DRB-selected variant showed considerable over expression of ABC-transporter protein P-gp by Western blot and RT-PCR, while the MTX cell line exhibited no enhanced expression of P-gp at either the mRNA or protein level. There was however, a constitutive expression of MRP-1 protein in both drug selected cell lines and the parent. Accumulation assays were performed to investigate the level of drug uptake in these cell lines. The results showed decreased accumulation of drugs, mitoxantrone and daunorubicin in the DRB selected variant, which may be explained by the activity and presence of P-gp in this cell line. However, in the MTX-variant reduced accumulation of the drugs was also observed indicating that an alternative mechanism unrelated to P-gp/MRP-1 transport proteins is involved in the decreased up-take of drugs in this cell line.

Recently, it has been shown that MRP-1 has been found in some MDR phenotypes in the absence of P-gp. The structurally distinct MRP-1 drug resistant protein is similar to P-gp as it also causes resistance to a wide variety of hydrophobic drugs. It is located in the plasma membrane and causes decreased drug accumulation and increased drug efflux in cells (Zamann *et al.,* 1994).
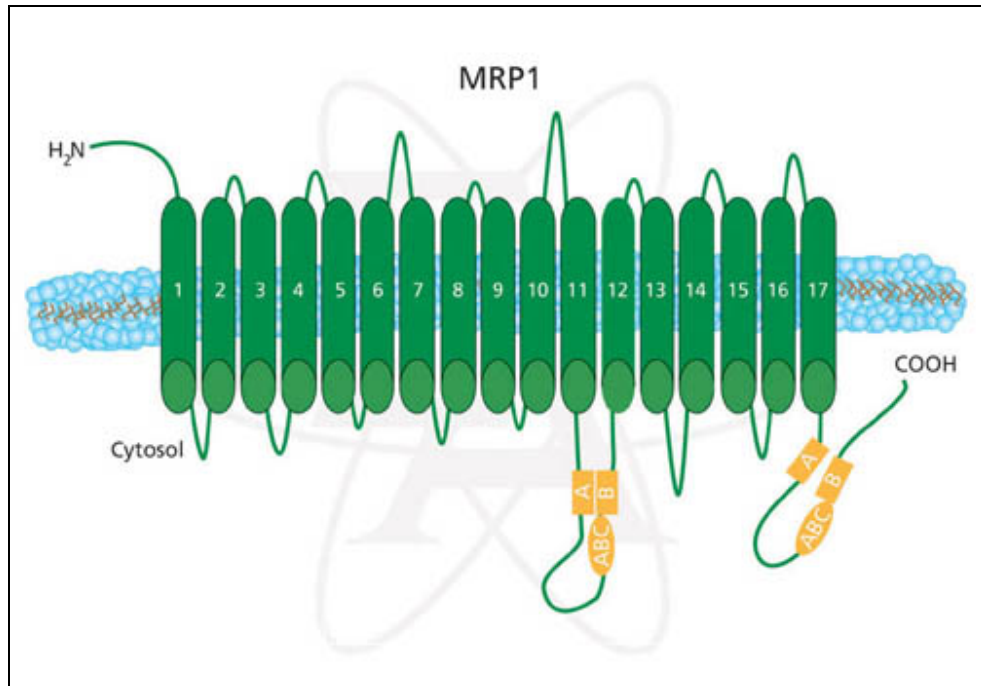
Figure 1.3.1: Schematic Diagram of MRP-1 (www.sigmaaldrich.com).

Miller *et al.* (1996) examined the expression of both P-gp and MRP-1, and their function as drug efflux systems in pancreatic ductal adenocarcinoma (PDA). Functional expression of P-gp was examined using Rhodamine 123 (R123), an indicator of P-gp activity; results suggested there was no functional P-gp present in the cell lines PANC-1, BxPc-3 and AsPc-1 whereas the incidence of MRP-1 expression in the cell lines (3 out of 4 cell lines) suggests that MRP-1 is an important contributor to the resistance of pancreatic cancer to chemotherapeutic drugs.

Verovski *et al.* (1996) developed a pancreatic tumour cell line resistant to doxorubicin, which displayed multidrug resistance not conferred by P-gp. Over-expression of the vesicular marker lung resistance-related protein (LRP) and MRP-1 were associated with the MDR phenotype.

However, P-gp may have an important contribution in the development of acquired resistance after exposure to drug treatment.

Liu *et al.* (2001) verified the acquired resistance caused by P-gp in a study examining the effect of taxotere on the pancreatic carcinoma cell line SUIT-2 and its taxotere selected variant S2/TXT, established by drug selection with increasing taxotere concentrations (0.1 nM to 2 nM). The TXT-variant was 9.5-fold more resistant than the parental cell line. RT-PCR was used to establish the level of MDR-1 expression in both cell lines. The parental line SUIT-2 showed no MDR-1 expression while the S2/TXT line expressed MDR-1. However, MDR-1 was also expressed when the parental line was exposed to 0.4 nM taxotere for 24 hrs. This shows that the MDR-1 gene is expressed when treated with a chemotherapeutic agent and highlights the fact that P-gp may mediate acquired resistance to taxotere in pancreatic cancer.

König *et al.* (2005) studied the expression and localisation of the human MRP family, (MRP1-MRP9) and the breast cancer resistance protein, (BCRP) in normal human pancreas (n=6) and pancreatic carcinoma (n=31). Quantification of mRNA levels showed BCRP, MRP-1, MRP-3, MRP-4 and MRP-5 were most abundantly expressed in 37 tissue samples. The expression of BCRP, MRP-1 and MRP-4 mRNA did not show a relationship with tumour stage or grading. However, the mRNA level of MRP-3 was up-regulated in pancreatic carcinoma samples and correlated with tumour grading. The MRP-5 mRNA showed significantly increased expression in pancreatic carcinoma samples compared to normal pancreas samples.

Among the MRP family members, MRP-3 shares the highest amino acid sequence identity (58%) with MRP-1 and both localise to the basolateral membranes of polarised cells (König *et al.*, 1999). In humans, MRP-3 expression is highest in the adrenal glands and the intra-hepatic bile ducts, followed by moderate to low expression in the small intestine, kidney and pancreas (Kool *et al.*, 1997). Zelcer *et al.* (2001) characterised the drug specificity of MRP-3, and showed that MRP-3 conferred resistance to etoposide and methotrexate.

MRP-5 is an organic anion transporter, as it pumps efflux anionic fluorochromes. In addition, intracellular glutathione levels have been shown to be depressed in MRP5-transfected cells (Wijnholds *et al.*, 2000).

This data suggests that both MRP-3 and MRP-5 may play a considerable role in drug resistance in pancreatic carcinoma and that quantitative investigation into their expression may prove to be a predictive advantage for patients with pancreatic cancer.

1.4 Multi-drug resistance, invasion and metastasis

The relationship between drug resistance, invasion and metastasis has not been fully elucidated. However, there is evidence suggesting a link, as cell lines selected for drug resistance are more invasive/metastatic compared to non-resistant parental cells (Liang *et al.*, 2002).

1.4.1 Invasion and metastasis

Metastasis is defined by the ability of tumour cells at the primary site to invade local tissue and to cross basement membrane and tissue barriers and to re-establish at distant secondary locations.

Tumour invasion and metastasis are major causes of treatment failure and death in cancer patients. Intrinsic aggressiveness of the tumour and histological grade may be responsible for the divergence of metastasis in cancers of comparable size. The heterogeneous nature of some tumours leads to sub-populations of highly metastatic tumour cells existing at very early stages of primary tumour development (Fearon and Vogelstein, 1990).

Secondary metastases *in vivo* are commonly more resistant to chemotherapeutic treatment compared to the primary tumours (Goswami *et al.*, 2004).

1.4.2 The metastatic cascade

The process of metastasis is not random. A cascade of complex interactions between the cancer cell and its surroundings results in the metastatic cascade (Table 1.4.1). To initiate the metastatic cascade, tumour cells must first break signalling contact with neighbouring cells, degrade and penetrate the basement membrane and then invade the interstitial stroma in order to reach blood/lymph vessels (Ray *et al.*, 1994). Intravasation requires penetration of the blood/lymph systems. The tumour cells must then exit the lymph system

or blood stream at a new site (extravasation) and proliferate in the secondary organ (Deryugine *et al.,* 2006) (Figure 1.4.1).

It is important to note that although metastasis is an intentional, effective event it is an inefficient development, as the majority of invading/metastatic cells do not survive the process. Millions of tumour cells are shed into the circulation daily. However only 0.01% of circulating tumour cells initiate a successful metastatic focus, the rest having been destroyed by a combination of mechanical stresses, proteolytic degradation and surveillance by the immune system (Cameron *et al.*, 2000).

1.4.3 Invasion and metastasis in pancreatic cancer

The process of invasion and metastasis in pancreatic cancer is responsible for 90% of pancreatic cancer deaths in patients. At diagnosis, nodal involvement is found in 80% of cases and visual metastases are detected in 50% of cases. Among the remaining non-metastatic patients, approximately 1 in 5 has undetected peritoneal cancer (André *et al.*, 1998). The most common sites of metastasis of pancreatic adenocarcinoma are the liver, the peritoneum (the thin membrane lining of the abdominal cavity) and the lungs (Nakahashi *et al.*, 2003; Neoptolemos *et al.*, 2003).

Numerous *in vitro* studies and *in vivo* analyses of animal models have indicated that cells isolated from metastases differ greatly (both genetically and phenotypically) from cells isolated from their parental primary tumours. Therefore, sub-populations of primary tumour cells seem to obtain metastatic properties during later stages of tumour progression (Fidler and Kriple, 1977). In contrast, studies also indicate that it is not small sub-populations of the primary tumour that have metastatic capacity, but rather most of the cells in the tumour. Bernards and Weinberg (2001) suggest that the potential for metastasis is determined early in tumourigenesis, which explains why most cells in a primary tumour express the molecular signature that is associated with metastatic tumours.

A review by Pantel and Brakenhoff (2004) suggests metastatic spread might follow two models; both of which are complementary but take different specific routes. The first model is refers to lymph node metastasis. Cancer cells during the early stages of tumour growth disseminate from the original primary tumour to the lymphatic or vascular system.

In this model, cancer cells form solid metastases in the lymph nodes. Further metastases then occur from the lymph nodes to distant sites, and it is possible that this ability was gained during the selection of these cells in the lymph-node environment. The second model involves the development of solid metastases at distant sites as a result of dissemination through the blood. In this model cells do not passage through the lymphatic system. Kayahara *et al*. (2007) investigated the precise pattern of neural invasion and the relationship between neural invasion and nodal involvement in pancreatic cancer. Histological evaluation of pancreatic cancer specimens revealed a connection between cancer cells inside lymph nodes and cancer cells within the perineural space, suggesting tumour cells in the perineural space grow in a continuous fashion and may be responsible for some cases of lymphatic spread.

There is increasing evidence that in epithelial malignancies, loss or down-regulation of expression of the structures responsible for the maintenance of tissue integrity correlates with an increasing tendency for metastatic spread. Such de-adhesion acts as a prelude to the cells invading the extracellular matrix (Ahmad and Hart., 1997).

Steps	Mechanisms involved
Transformation and growth	**Oncogene activation/ suppressor inactivation**
Detachment from original tumour and attachment to extracellular matrix (ECM) components	**Loss of E-cadherin, integrins**
Disruption and invasion through surrounding tissue or ECM/basement membrane	**MMP, uPA, cathepsin activity**
Attachment to basement membrane of the vascular endothelium of the lymphatic or blood vascular channel	**Altered integrin expression**
Intravasculation into the blood/lymph vascular channel	**Protease activity**
Adhesion to the blood/lymph wall	**E-selectin, mucins, V-CAM, I-CAM, Integrins**
Survival and transportation through the blood/lymph vessels and avoid immune mediated destruction	**IGF survival factors, Downregulation of intrinsic immunogenicity**
Lodgement in the capillary of tissue and attachment to the endothelium or basement membrane of the tissue	**Integrins, laminin, collagens, fibronectin**
Extravasation- exit the vessel wall and enter perivascular, interstitial connective tissue	**Protease activity**
Proliferation and induce angiogenesis within new environment	**Organ specific growth factors, VEGF, HGF,EGFR**

Table 1.4.1 The metastatic cascade and molecules and mechanisms involved
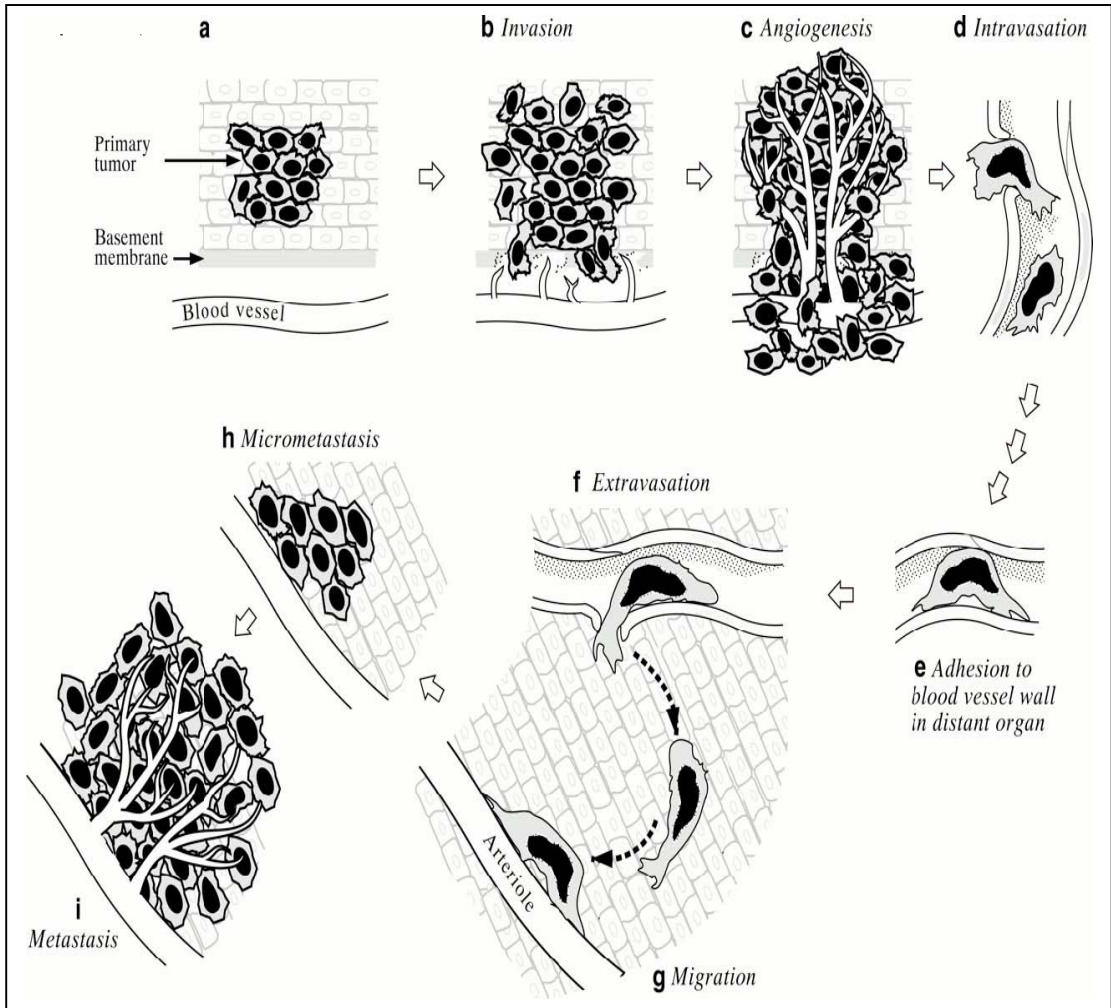
Figure 1.4.1 The metastatic process (www.home_uchicago.edu)

1.4.4 The extracellular matrix- basement membrane

The extracellular matrix (ECM) is a complex structural entity surrounding and supporting cells and organs within the body. The main function of the basement membrane is cell and tissue support. Epithelial, endothelial and many mesenchymal cells are supported by this thin sheet-like ECM structure. It consists of 4 main components; structural proteins, collagens and elastin; specialised proteins, fibronectin and laminin; proteoglycans and glycosaminoglycans.

Three main proteins will be discussed, collagens, fibronectin and laminin.

1.4.4.1 Collagen

The collagens are the most abundant family of fibrous proteins found in all animals. It is the major protein comprising the ECM. Collagens are secreted in the form of propeptides and are converted to collagen molecules by specific proteolytic enzymes, which reside outside the cells. The collagens then assemble in the extracellular space to form collagen fibres. There are at least 12 types of collagen. Type I, II and III are the most abundant and form fibrils of similar structure. These collagens are characterised by their long, helical structure. Three alpha chains coil together to form a triple superhelix. Collagens are also rich in proline and hydroxyproline. The bulky pyrollidone rings of proline reside on the outside of the triple helix (Brown *et al.*, 2006).

Type IV collagen forms a two-dimensional reticulum and is a major component of the ECM organised as a thin sheet beneath the epithelia known as the basal lamina (40-120 nm thick). Collagens are predominantly synthesised by fibroblasts but epithelial cells also synthesise these proteins. These basic structures organise the extracellular matrix and give it resilience. Molecules of this type of collagen have a more flexible structure then collagen type I, II or III. They form a flexible, sheet-like multilayered network.

1.4.4.2 Fibronectin

Fibronectin was the first well-characterised adhesive protein. It is built up of multiple domains, each with specific binding sites for other matrix macromolecules and for receptors on the surfaces of cells. Fibronectin is a large glycoprotein that is found in all vertebrates. It exists as a dimer composed of two very large subunits, 60-70 nm long and 2-3 nm thick, joined by a pair of disulfide bonds near their carboxyl termini. Each subunit is folded into a series of functionally distinct domains separated by regions of flexible polypeptide chain. Fibronectin contains at least six folded domains, each with a high affinity for collagen, heparin, fibrin and specific integrins on the surfaces of various types of cells. Expression of fibronectin has been shown to have a direct influence on the establishment and maintenance of the transformed phenotype (Ruoslahti *et al.*, 1999). Adhesion to fibronectin mediated by integrin $\alpha 5\beta 1$ is responsible for improved survival of different cell lines, including breast carcinoma (Varner *et al.*, 1995) and pancreatic cancer (Vogelmann *et al.*, 1999).

1.4.4.3 Laminin

Laminin anchors cell surfaces to the basal lamina. Laminins are flexible four-armed, 850 kDa glycoproteins. Laminin monomers polymerise into 3D structures in a time- and concentration- dependent manner. As an initial step in metastasis, many epithelial tumours exhibit altered localisation or expression of laminin-binding integrins (e.g. $\alpha 6\beta 4/\alpha 6\beta 1$). This promotes invasion through the basement membrane and increases motility in the stroma, where tumour cells can remodel the matrix by depositing laminin (Hood and Cheresh, 2002). Increased expression of laminin binding proteins correlates with aggressive growth and with the ability to metastasise in pancreatic tumour tissues (Vogelmann *et al.*, 1999).

1.4.5 The proteases involved in metastasis

Proteolytic enzymes play a fundamental role in cancer progression. The process of invasion is not a passive one due to pressure from excessive cellular proliferation alone but is an active, dynamic process that requires protein synthesis and degradation. A critical proteolytic event early in the metastatic cascade appears to be the degradation of basement membrane (Gobin and West, 2002).

Tumour cells secrete enzymes to degrade the extracellular matrix barriers in order to intravasate successfully. Almost all cells of the tumour and host environment over-express one or more of these enzymes. Degradation of the basement membrane is not dependent solely on the amount of proteolytic enzymes present but on the balance of activated proteases and their naturally occurring inhibitors (Kohn *et al*., 1995).

Many proteases are capable of degrading ECM components and can be classified into 4 major classes:

1. Matrix metallproteinases (MMPs)
2. Serine proteinases
3. Cathepsins
4. Cysteine proteinases.

1.4.5.1 Matrix metalloproteinases

Matrix metalloproteinases are a family of secreted or transmembrane proteins that are capable of digesting basement membrane components. These proteolytic enzymes have been involved in the remodelling of connective tissue in many conditions such as embryonic growth and development, ovulation, menstruation and wound healing. However over-production of these proteases is known to contribute to cancer progression (Coussens and Werb 1996).

Currently there are over 20 known members, which share functional and structural characteristics and can be categorised into the collagenases, gelatinases, stromelysin and membrane-type MMP sub families (Table 1.4.2).

Table 1.4.2 Family of matrix metalloproteinases (MMPs)

Stromelysins	Collagenases	Gelatinases	Membrane-type MMPs	Other MMPs
MMP-3	MMP-1	MMP-2	(MT-MMP1) MMP-14	MMP-18
MMP-7	MMP-8	MMP-9	(MT-MMP2) MMP-15	MMP-19
MMP-10	MMP-13		(MT-MMP3) MMP-16	MMP-20
MMP-11			(MT-MMP4) MMP-17	MMP-21
MMP-12			MMP-24	MMP-23

MMPs have a zinc-binding domain at their catalytic site; they are secreted as zymogens and are regulated through gene transcription, proteolytic cleavage and by their natural inhibitors, the tissue-specific inhibitors of matrix metalloproteinases (TIMPs). Biologically active agents such as growth factors, hormones, oncogenes and tumour promoters transcriptionally regulate MMP activation. TIMPs inhibit MMPs by forming tight 1:1 stoichiometric, non-covalent complexes with either the pro-enzyme or the activated MMP, or by controlling their autocatalytic activation. Their expression is also influenced by local cytokines and growth factors.

MMP-2 activation involves the membrane bound MMP type I (MT-MMP1). TIMP2 binds to the inactive MT-MMP1, which allows proMMP-2 to bind and form a complex on the cell surface and then acts as a substrate for a second MT-MMP1 molecule. This results in the conversion of MMP-2 into its active form, suggesting that MT-MMP1 expression level is closely related to invasion and malignancy of tumours (Sato *et al*., 2005).

Four TIMPs have been identified (Brew *et al.*, 2000). TIMP-1, TIMP-2, TIMP-4 are secreted proteins while TIMP-3 is anchored in the ECM.

Studies have demonstrated a positive correlation between MMP expression, invasive behaviour and metastatic potential in tumours such as breast (Kim *et al*., 2006), prostate

(Aalinkeel *et al*., 2004), colon (Murray *et al*., 2004), lung (Fang *et al*., 2005), ovarian (Herrera *et al*., 2002) and pancreatic cancers (Bloomston *et al*., 2002).

Degradation of extracellular membrane proteins in the basement membrane such as collagen type IV is a critical event in early tumour invasion, suggesting that MMP-2 and MMP-9, which degrade collagen IV are particularly important. MMP-2 and MMP-9 expression in pancreatic cell lines correlates with the *in vitro* invasive potential of cell lines (Yang *et al*., 2001).

Jones *et al*. (2004) showed that MMPs 7, 8, 9, 11 and TIMPs 1 and 3 were highly expressed in 75 pancreatic adenocarcinomas compared to 10 normal pancreas samples by immunohistochemistry and real time RT-PCR. MMP-15 was under expressed in the tumours by RT-PCR; however this was not confirmed by immunohistochemistry. MMP-11 expression is associated with lymph node involvement, while MMP-7 predicted survival. MMP-7 up regulation has been identified as an early event in tumour development (Yamamoto *et al*., 2001). MMP-7 expression is limited to epithelial cells, rather than the stroma and is produced mainly by the tumour cells and can increase the invasive potential of the tumour cells (Powell *et al*., 1993).

1.4.5.2 Serine proteases

Serine proteases are characterised by a serine residue at their active site and are produced in an inactive form. Members of this family include elastin, cathepsin G and B, thrombin, plasmin, plasminogen, tissue-type plasminogen activator (tPA) and urokinase type plasminogen-activator (uPA). uPA converts inactive plasminogen to active plasmin. Plasmin is capable of degrading a wide variety of ECM components as well as activating other proteinases, such as MMPs. uPA is mainly detected in the cell membrane fraction and high levels have been found in gastric tumours with metastatic spread occurring between normal colonic epithelium and carcinoma (Plebani *et al*., 1995).

1.4.5.3 Cathepsins

Cathepsins are lysosomal enzymes involved in cancer due to their proteolytic activity. Cathepsin D is an aspartic proteinase, cathepsin B and L are cysteine proteinases and cathepsin G is a serine proteinase.

Cathepsin D has been extensively studied in tumour invasion and metastasis. Over-expression of cathepsin D has been shown in several neoplasms including gastric, colon and breast, where relapse and metastasis is related to high levels of cathepsin D (Ahamad and Hart, 1997). However, in pancreatic cancer expression of cathepsin D did not correlate to nodal invasion or metastasis to liver or lung (Ruppert *et al.*, 1997).

Cathepsin B and L are cysteine-rich proteases, characterised by a cysteine-rich residue at their active site and are lysosomol proteases capable of ECM degradation (Ahmad and Hart, 1997). Cathepsin B levels in B16 murine melanoma correlated with metastatic potential of the tumour (Qian *et al.*, 1989). Cathepsin B expression has been demonstrated to have prognostic implications, whereby expression levels correlate with tumour grade, lymph node metastasis in some tumours. Ohta *et al.* (1994) demonstrated that over-expression of cathepsin B relates to invasive behaviour but not to metastatic spread in pancreatic carcinoma.

1.5 Integrins

Integrins are a large family of heterodimeric transmembrane glycoproteins that attach cells to extracellular matrix proteins of the basement membrane or to ligands on other cells i.e. they mediate direct cell-cell recognition and cell-matrix interactions (Hynes, 1992). Integrins contain large α (120-170KDa) and small β (90-100KDa) subunits non-covalently bound (Figure 1.5.1 A). To date, 24 distinct heterodimers have been described. These heterodimers are integral cell membrane receptors that form focal adhesion contacts with various ECM-ligands, such as collagens, fibronectin, laminin, vitronectin. Ligand binding specificity depends on the specific α and β chains present in the heterocomplex. Members of integrin subfamilies bind to many ECM ligands therefore the presence of multiple integrins on cells that identify the same ligands allows for overlapping recognition (Mizejewski, 1999) (Figure 1.5.1 B).
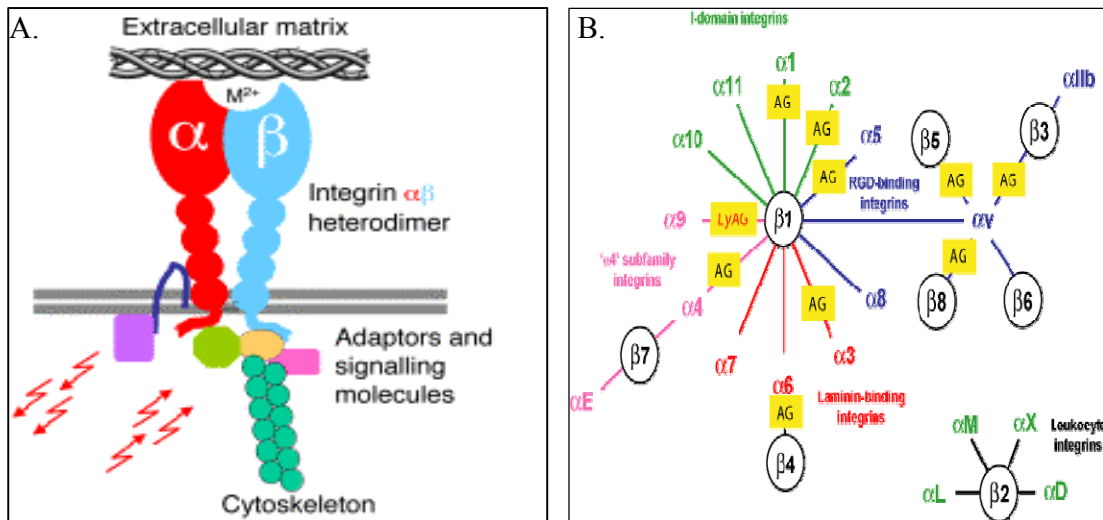
Figure 1.5.1 A. Structure of integrin heterodimer (dan1.medkem.gu.se) and B. The integrin family of adhesion receptors and their main ligands (www.chuv.ch).

1.5.1 Integrins in invasion and metastasis

Malignant transformation is characterised by disruption of the basement membrane, cytoskeletal remodelling, decreased adhesion and altered cell motility. Many studies suggest that various integrin subunits can contribute either positively or negatively to the transformed cell phenotype. Changes in the expression of fibronectin-binding integrins have been observed in malignant cells. Integrin α5β1, the main fibronectin receptor, is down-regulated in poorly differentiated breast carcinoma. However over-expression of the fibronectin receptor in transfected sarcoma S180 cells enhances their motility on fibronectin. Increased integrin αvβ3, the vitronectin receptor appears to be positively correlated with increased malignancy in melanoma, whereby the integrin complex expression is a molecular marker for the change from radial growth phase (RGP) to the metastatically competent vertical growth phase (VGP). Hsu *et al*. (1998) introduced β3 into RGP melanoma cell lines subsequently converting them to VGP-like melanoma cells. Altered expression of α6-containing integrins is found in various tumours. In hepatoma cell lines, attachment to laminin is mediated by integrin α6β1 (Torimura *et al*., 1999). This complex was also over-expressed and functionally active in metastatic human pancreatic carcinoma cells and participates in metastasis formation through binding to laminin (Vogelmann *et al*., 1999). The expression of the fibronectin-binding subunit α5

appears to be decreased in pancreatic tumour tissue. In general, the loss or gain of expression of particular integrins appears to be indirectly implicated in malignant transformation and may be directly involved in tumour progression and metastasis.

1.5.2   Integrins and proteolytic enzymes

Integrins are needed in cell movement, but they may also have other roles in cancer invasion and metastasis. Importantly, they induce the expression of different ECM degrading proteases, especially members of the MMP family. The interplay between integrins and the matrix metalloproteinases may be one of the key phenomena in the invasion process. Integrin complex $\alpha3\beta1$ recognises fibronectin, collagen type IV and laminin, and is up-regulated in certain tumours. Sugiura *et al.* (1999) demonstrated that ligation of $\alpha3\beta1$, in the breast cell line MDA-MB-231, with monoclonal antibodies specifically stimulates production of MMP-2 and induces invasive protusions within matrigel. Integrin adhesion to laminin and antibody-induced clustering of integrin $\alpha3\beta1$, also enhanced the secretion of MMP-2 in rhabdomyosarcoma and glioblastoma cells (Kubota *et al.*, 1997; Chintala *et al.*, 1996). Other integrins have been associated with tumour progression and metastasis; $\alpha v\beta3$ has been identified as a tumour progression marker in melanoma. It co-localises with MMP-2 on the surface of melanoma cells thereby facilitating tumour cell invasion by degradation of the ECM (Hofmann *et al.*, 2000). The signalling pathways that link integrin receptors and MMP activation are poorly understood. Up-regulation of collagen by MMP-1 was prevented by tyrosine kinase inhibitors in osteosarcoma cells (Riikonen *et al.*, 1995). Klemke *et al.* (1994) observed that the epidermal growth factor (EGF) promotes $\alpha v\beta5$-dependent pancreatic carcinoma cell migration on vitronectin and is dependent on the activation of the EGF receptor and protein kinase C (PKC).

1.5.3   Integrins and anoikis

Anchorage-dependent cells that are deprived of the ability to bind immobilised ECM undergo apoptosis, a process referred to as anoikis (Frisch and Screaton, 2001). Anoikis is the apoptosis of cells that have lost contact with extracellular matrix, or that interact with matrix through an inappropriate integrin-matrix combination. It is important for

embryonic development (gastrulation) and mammary gland involution. Anoikis occurs through established apoptotic signalling pathways, which depend upon cell type. These include caspases of the initiator (caspase-8) and effector (caspase-3, 7) types as well as protein kinases such as MEKK- 1. Cells undergoing anoikis display typical apoptopic characteristics: nucleosomal DNA ladder formation, cell shrinkage, caspase activation/cleavage of caspase substrates and cytochrome c release from mitochondria (Marco *et al.*, 2003). Protection against anoikis is afforded by the activation of certain other kinases such as FAK and PI3K/Akt. Upon integrin ligation, FAK is phosphorylated and begins a signalling complex (Figure 1.5.2). The FAK signalling complex mediates and activates pathways such as PI3K and its downstream targets protein kinase B (PKB/AKT), the ERK and JNK/MAPK pathway (Grossmann, 2002). Sensitivity to anoikis is frequently lost in tumour cells, which probably contributes to their ability to grow independently of anchorage and metastasise. This sensitivity can be lost by activation of oncogenes such as ras, alterations in intracellular apoptosis components, over-expression of growth factors such as EGF, HGF or IGF-related molecules, or breakdown of cadherin-catenin complexes.
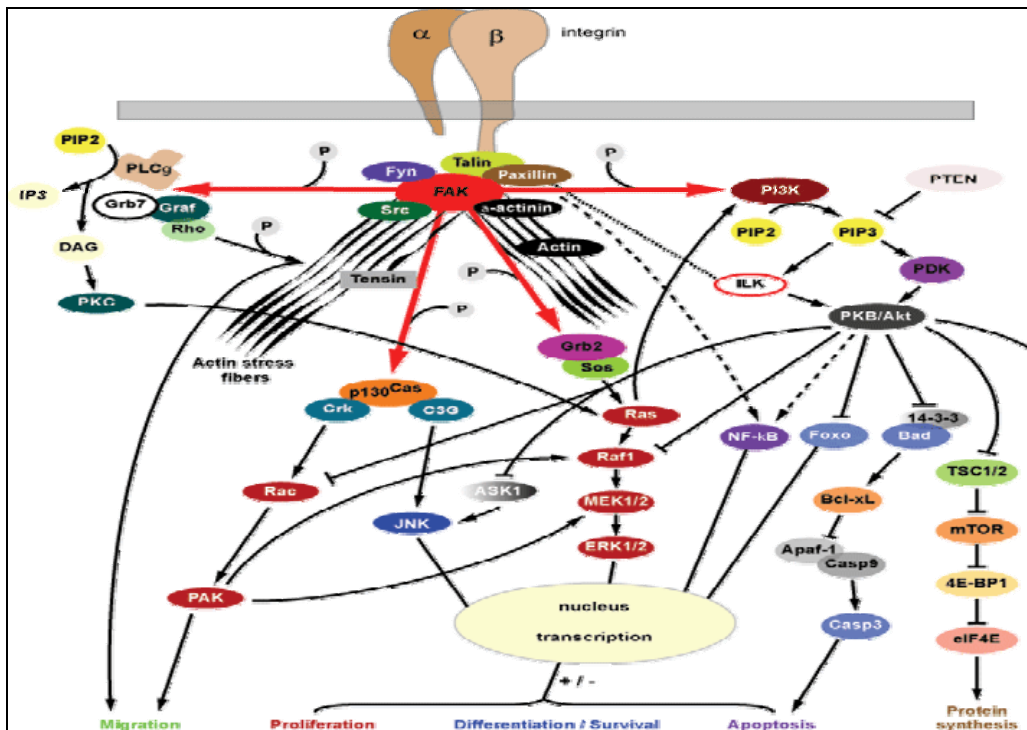
Figure 1.5.2 Integrin signalling pathways (www.chuv.ch).

1.6 The epithelial to mesenchymal transition (EMT)

Epithelial to mesenchymal transition (EMT) is the process by which epithelial cells lose their strong intracellular adhesion and their basolateral polarity to gain front-end to back-end polarity, and the ability to migrate through the ECM (Savagner, 2001). As cells lose cell-cell contact, new cell-ECM interactions are generated. Thus, many cell surface-associated adhesion molecules change function and are the source of signals that activate growth, ECM degradation and metastasis (DeClerck, 2004).

A variety of indicators exist for the EMT phenotype (Figure 1.6.1). Intermediate filament proteins provide a convenient and abundant marker, with keratins indicating an epithelial phenotype and vimentin indicating a mesenchymal phenotype (Hay, 1995). The epithelial state is characterised by the presence of the epithelial cell adhesion molecule E-cadherin and/or the associated catenins, forming the adherens junctions. These cell-cell adhesion-related criteria are almost entirely absent in mesenchymal cells (Birchmeier *et al.*, 1996). Several other groups of molecules have been implicated in physiological and pathological EMT pathways, including cell-cell adhesion molecules, cell-ECM adhesion molecules, proteases, transcription factors, growth factors and cytoskeletal proteins.

The molecular changes that occur during EMT also include reorganisation of other cell-cell contact complexes (tight junctions, desmosomes), modification of cell-substrate adhesion complexes, synthesis of ECM proteins normally expressed by mesenchymal cells, and the expression of several proteases including matrix metalloproteases (MMPs). The ability to scatter, migrate and degrade ECM components is associated with a mesenchymal phenotype, more aggressive cancer and poor prognosis (Gilles *et al.*, 1996).

MET

Epithelial

Cell-cell contact
Adherens junctions (E-cadherin complexes)
Desmosomes
Tight junctions

Cytoskeleton
Cytokeratins

ECM synthesis
Laminin, collagen type IV

Protease expression
Low or absent

Mesenchymal

Cell-cell contact
Weak, nonexistent or inactive

Cytoskeleton
Vimentin

ECM synthesis
Fibronectin, collagen type I/III

Protease expression
High (MMPs)

EMT

Figure 1.6.1 Molecular traits of the EMT. Epithelial and mesenchymal cells are shown schematically, and the differences commonly seen between them are grouped into four major categories: Cell-cell contacts, cytoskeleton, ECM synthesis, and protease expression (Holland and Frei, 2003).

EMT plays an important role in tumour invasion and metastases, and its detection may have a significant prognostic implication in pancreatic cancer. Yosuico *et al.* (2006) examined the expression of EMT related proteins in resected pancreatic cancers and correlated the results with clinical outcome. Pancreatic cancer patients (n=34) who underwent pancreatectomy were included. Immunohistochemical staining for vimentin, E-cadherin, MIB-1 (Ki-67 nuclear fraction) and cytokeratin were performed on formalin fixed paraffin-embedded tissues. The results were correlated with clinicopathological parameters and survival. There was a significant negative association between vimentin and E-cadherin expression. Vimentin expression correlated with histological grade.

Therefore, decreased E-cadherin expression (<50% expression) was associated with poorer survival, as E-cadherin expression had an inverse correlation with vimentin.

The role of cadherins (calcium-dependent adhesion molecules) has been investigated as inducers of EMT. E-cadherin (epithelial cadherin) has been implicated in EMT, as the loss of its expression has been found to correlate with an invasive and undifferentiated phenotype in pancreatic carcinoma (Karayiannakis *et al.*, 2001; Joo *et al.*, 2002) as well as gastric (Jawhari *et al.*, 1997), prostate (Richmond *et al.*, 1997) and colorectal cancer (Karatzas *et al.*, 1999; Hugh *et al.*, 1999). N-cadherin (neural cadherin) over-expression is associated with high invasive potential. Nakajima *et al.* (2004) immunohistochemically investigated N-cadherin expression and the role of EMT in pancreatic carcinoma. N-cadherin expression was observed in 13/30 primary tumours and 8/15 metastatic tumour samples. Its expression correlated with neural invasion, histological type, fibroblast growth factor expression in primary tumours and with TGF and vimentin expression in metastatic tumours. Vimentin, a mesenchymal marker, was observed in a few cancer cells of primary tumour but was substantially expressed in liver metastasis. TGF stimulated N-cadherin and vimentin protein expression and decreased E-cadherin expression of Panc-1 cells with morphological change. This study provides morphological evidence of EMT in pancreatic carcinoma and revealed that over expression of N-cadherin is involved in EMT and is affected by growth factors.

Yin *et al.* (2006) studied the implication of EMT induced by TGF-β1 in pancreatic cancer invasion. TGF-β1 expression was determined in 29 cases of human pancreatic carcinoma (PC) by immunohistochemistry and the results were compared with those of pathological examination. The effects of TGF-β1 on the phenotype and invasion of pancreatic cancer cell line Panc-1 were also investigated. TGF-β1 was detected in 12 cases (41.4 %) of PC. Significant correlation was found between the expression of TGF-β1 and lymph node involvement and the depth of invasion. TGF-β1 promoted EMT of Panc-1 cell lines and their invasion ability was substantially enhanced. TGF-β1 may promote the malignancy of pancreatic cancer by triggering EMT. TGF-β1 induces EMT in A549 alveolar epithelial cells via Smad2 activation (Kasai *et al.*, 2005).

The transcription factors Snail and Slug (zinc-finger proteins) have been linked as repressors of E-cadherin expression (Bolos *et al.*, 2003). Barrallo-Gimeno *et al.* (2005) proposed that Snail genes act primarily as survival factors and inducers of cell movement, rather than as inducers of EMT. Twist, another transcription factor, is also known to trigger EMT. Twist is essential in the expression of N-cadherin in *Drosophilia* embryogenesis (Oda *et al.*, 1998). Studies have shown that up-regulation of Twist is associated with the malignant transformation of melanoma and T-cell lymphoma (Yang *et al.*, 2006). An increased N-cadherin level in gastric carcinomas is due to Twist over-expression (Rosivatz *et al.*, 2002). Hotz *et al.* (2007) reported that Snail and Slug are expressed in pancreatic cancer but not normal tissue.

Recent reports have shown that MMPs can stimulate Snail expression, and consequently activate the EMT (Radisky, 2005). Przybylo and Radisky (2007) showed that by exposing mouse mammary cells SCp2, to MMP-3 the EMT phenotype is stimulated. Increased cell motility, down-regulation of epithelial cytokeratins, expression of Snail and up-regulation of mesenchymal marker vimentin were observed. Expression of Snail was dependent on MMP-3, as withdrawal of MMP-3 caused a rapid decrease in Snail levels. Yokoyama *et al.* (2003) showed that three E-cadherin negative squamous cell carcinoma (SCC) cell lines had a fibroblastic morphology, strong expression of vimentin, and expressed Snail. Compared to other E-cadherin positive SCC cells, these cells showed higher invasive ability and expression of MMP-2. Over-expression of Snail in A431 cells resulted in the loss of E-cadherin expression, the change of their morphology to fibroblastic, and the up-regulation of vimentin, indicating that an EMT was induced by Snail. Furthermore, these cells became more invasive and showed higher levels of MMP-2 activity and its gene expression. Luciferase analysis demonstrated that the MMP-2 promoter activity was induced by Snail transfection and the promoter region from -262 to -411 relative to the transcriptional start site was necessary for this induction. These results indicate that Snail is a new inducer of MMP-2 expression and suggest that the EMT contributes to the increased invasion not only through the inhibition of cell-cell adhesion but also the up-regulation of MMP-2 expression in SCC cells. Several signaling pathways have been found to be important in EMT, these include tyrosine kinase signaling, the Ras pathway, integrin-linked kinase (ILK) and integrin signaling, Wnt/β-catenin, Notch, Rac1b and

reactive oxygen species (ROS), and the phosphatidylinositol 3' kinase (PI3K)/AKT pathway (Figure 1.6.2) (Larue and Bellacosa, 2005).
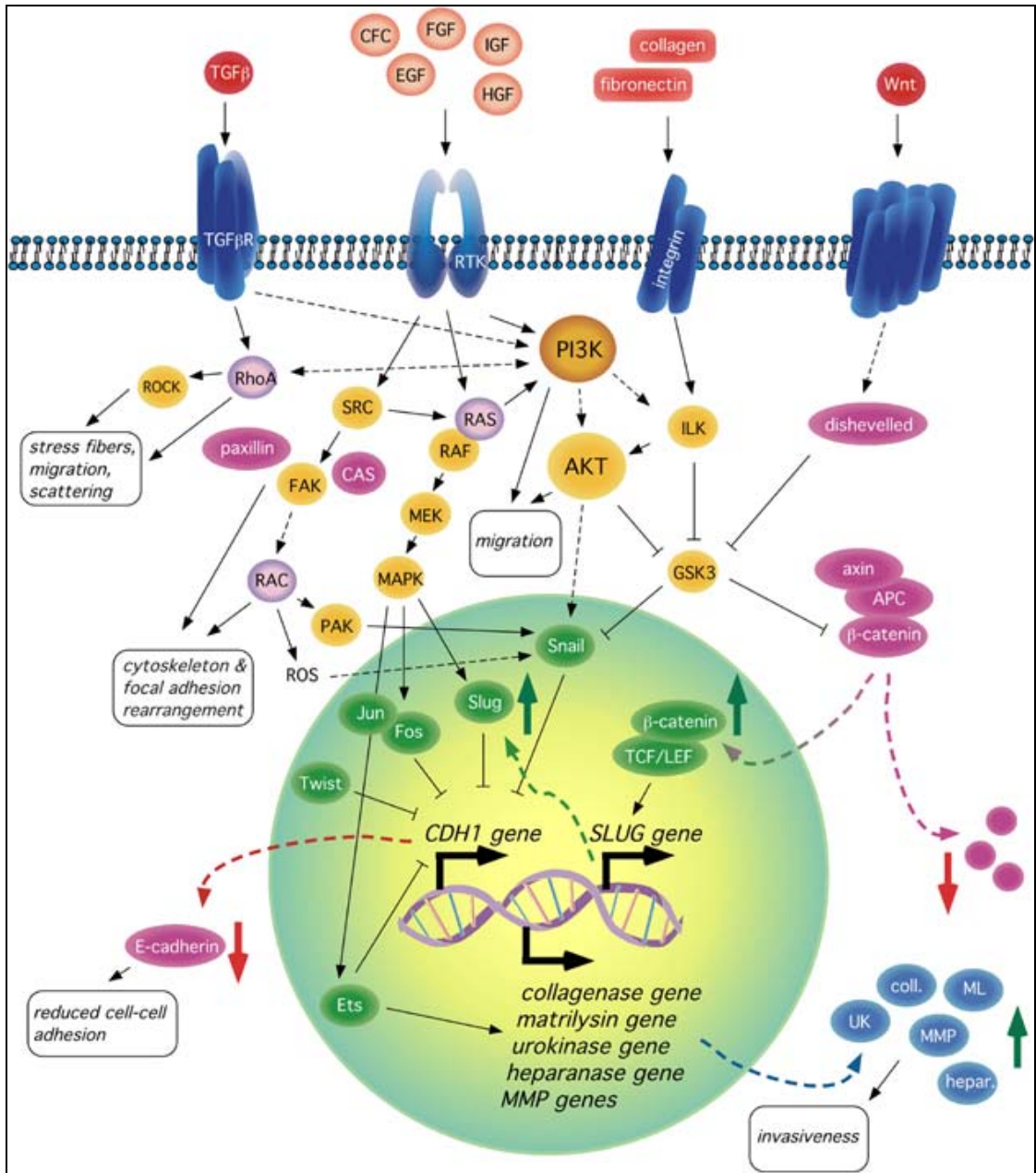
Figure 1.6.2 Diagram of the signal transduction pathways involved in the epithelial–mesenchymal transition (Larue and Bellacosa, 2005).

Activation of the PI3K/AKT signaling cascade is a central feature of EMT. The oncogenic serine/threonine kinase AKT is a downstream effector of PI3K (Batlle *et al.*, 2000).

AKT is frequently up-regulated and activated in ovarian (Altomare *et al.*, 2004), breast (Bakin *et al.*, 2000) and pancreatic tumours (Javle *et al.*, 2007). AKT is involved in many basic cellular processes, including cell cycle progression, cell proliferation, cell survival, metabolism and EMT (Grille *et al.*, 2003). AKT activation can contribute to the neoplastic phenotype. AKT can enhance invasiveness of pancreatic carcinoma cells via up-regulation of IGF-I (Tanno *et al.*, 2001). Furthermore, EMT induced by activated AKT involves loss of cell–cell adhesion (including down-regulation of E-cadherin) and morphological changes, caused by the up-regulation of the mesenchymal marker vimentin (Grille *et al.*, 2003). Induction of cell motility, enhanced tumour cell invasion, decrease in cell–matrix adhesion and suppression of apoptosis link AKT activation to metastatic tumour progression (Jallal et al., 2007; Kim *et al.*, 2002).

During tumour progression loss of cell-cell adhesion leads to the invasive phenotype. Integrins, which mediate adhesion to extracellular matrix components, play a critical role in directing the migration of cells and these receptors also may have an important role in EMT. Bates *et al.* (2005) found that EMT activated the integrin β6 subunit and consequently caused induction of the complex αvβ6 in colon carcinoma. Enhancement of tumourigenetic properties were observed, including activation of autocrine TGF-ß and migration on interstitial fibronectin. Kaplan-Meier analysis of β6 expressions in 488 colorectal carcinomas revealed a reduction in median survival time of patients with high β6 expression. Cox regression analysis confirmed that this integrin is an independent variable for these tumours. These findings define the αvβ6 integrin as an important risk factor for early-stage disease and a novel therapeutic candidate for colorectal cancer.

Promotion of EMT in cancer cells has been shown to be activated by signalling of integrins through integrin-linked kinase (ILK), activating rac and downstream pathways (Persad and Dedhar, 2003). Over-expression of constitutively active ILK results in loss of cell-cell adhesion, anchorage-independent growth and tumourigenicity in nude mice. Down-regulation of E-cadherin and loss of β-catenin from cell–cell adherence junctions are also induced by activated ILK signalling (Novak *et al.*, 1998). ILK over-expression can activate AP-1 transcription factor that regulates genes required for EMT. Sawai *et al.* (2006) demonstrated that ILK and β1-integrin play important roles in the enhancement of

adhesive and invasive capabilities of pancreatic cancer cells through p38 MAPK signaling pathway and AP-1 activation. Over-expression of ILK enhanced the IL-1α-induced p38 MAPK phosphorylation more strongly through GSK-3 activation, and subsequently induced AP-1 DNA-binding activity, promoting expression of genes involved in pancreatic cancer cell adhesion and invasion.

1.7 Proteomic analysis

Since the successful sequencing and mapping of the human genome, proteomic analysis has focused on identification, localisation and functional analysis of protein complements expressed by the genome (Neet and Lee, 2000).

Genomic technologies such as microarrays are used for the detection of specific gene changes within, for example, diseased tissue compared to normal tissue. Microarrays are artificially constructed grids of DNA in which each element of the grid contains a specific oligodeoxynucleotide probe. Microarray experiments rely on the ability of RNA to bind specifically to a corresponding sequence-complementary probe. This enables researchers to simultaneously measure the expression of thousands of genes in a given sample. High throughput sequencing of DNA and the subsequent storage and annotation of the data is an advantage of gene profiling. However, interpreting data and adapting the results to a particular application remains a challenge. Also, the process is complex and focuses on the information of one target molecule, DNA, in the nucleus of cells. Studies have shown that differential mRNA expression does not always correlate with protein expression (Gygi *et al*., 1999; Anderson and Seilhamer, 1997)

Distinct changes may occur during the transformation of a healthy cell to a neoplastic cell that may not be apparent in gene changes. The location, structure and function of proteins can change dramatically within an organism due to malignant transformation, cell cycle and external/internal signalling. Thus, the quantity and complexity of the data derived from the sequencing and mapping of the human proteome are estimated to be at least three times greater than that involved in the human genome project (Sellers *et al*., 2003).

The field of proteomics is particularly important because most diseases are manifested at the level of protein activity. Therefore, proteomics is an invaluable tool in the direct correlation of the involvement of specific proteins, protein complexes and their modification status to a disease state.

1.7.1 2D-DIGE MALDI-TOF MS

Two-dimensional difference gel electrophoresis (2D-DIGE) is a high performance proteomic technology, allowing quantitative protein expression profiles across many clinical specimens in a reproducible, sensitive and high-throughout manner. Initially described by O'Farrell (1975), proteins in a 2D gel are separated by two separate unrelated elements. The first dimension step is isoelectric focusing (IEF), which separates proteins according to their isoelectric points (pI). The second dimension step, SDS-polyacrylamide gel electrophoresis (SDS-PAGE), separates proteins according to their molecular weights.

Fluorescent spectrally resolvable dyes used to prelabel proteins have added to the multiplexing capability of 2D DIGE methodology. The CyDye DIGE Fluor dyes (Cy2, Cy3 and Cy5) are matched for mass and charge, but possess distinct excitation and emission spectra. The Cy dyes minimally label the lysine residues of proteins; the dyes undergo nucleophilic substitution reaction with the epsilon-amino group of lysine residues on the protein resulting in the formation of an amide bond. The dye: protein ratio is optimised so that only 3-5% of the protein sample is labelled. This method ensures that proteins with a single dye molecule are visualised, resulting in co-migration of proteins originating from separate samples. Consequently, the same protein labelled with any of the dyes will migrate to the same position on the 2D gel. By using different dyes to separately label proteins isolated from normal and diseased tissues, multiple samples (up to three) can be co-separated and quantitated by three different set of wavelengths (Figure 1.7.1). The inclusion of a pooled internal standard (Cy2), containing every protein from all samples is used to match protein patterns across gels. This feature, counteracts inter-gel variation, allows normalisation of individual experiments and accurate quantification of differences between samples with significance (Alban *et al.*, 2003; Unlu *et al.*, 1997; Gharbi *et al.*, 2002).
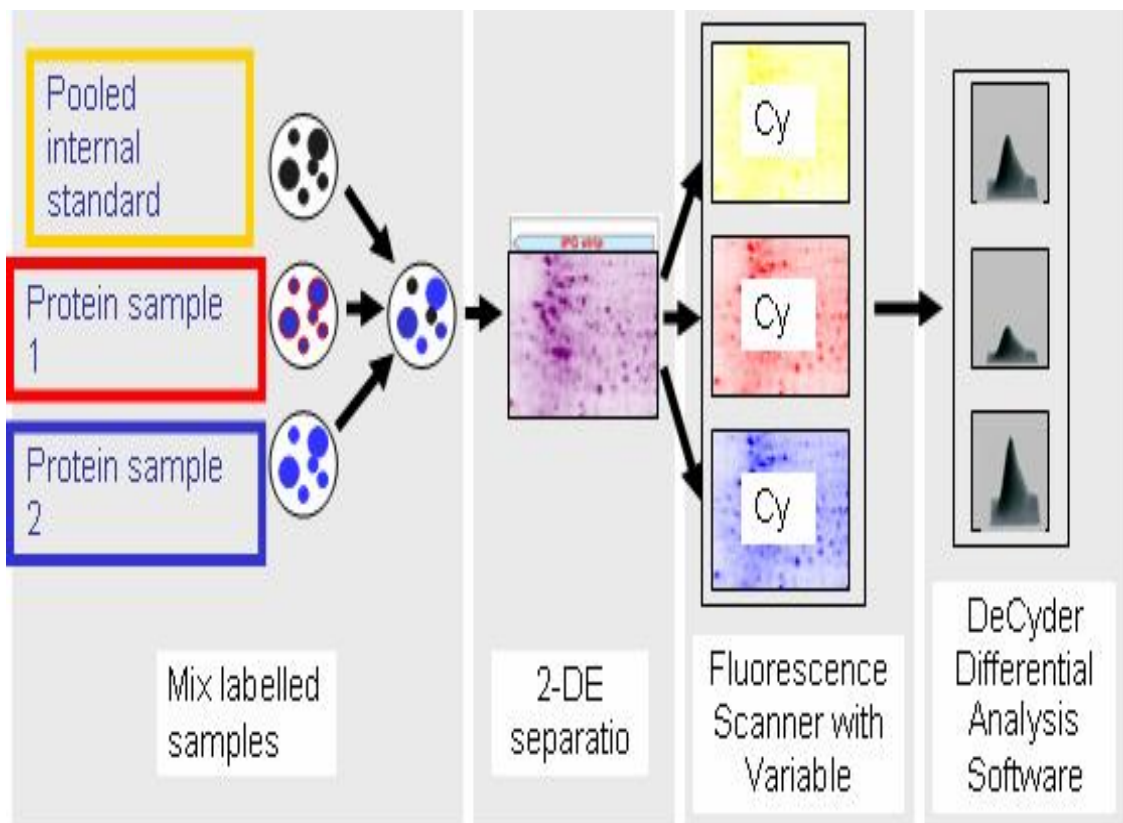
Figure 1.7.1 Outline of 2D DIGE system where three CyDye DIGE Fluor minimal dyes are separated in one gel

The fully optimised system (including CyDye fluorescent dyes, imager, and DeCyder Differential Analysis Software) offers increased throughput, ease of use, reproducibility, and accurate quantitation of protein expression differences. Reduced system variability enables accurate study of protein expression differences against a baseline of biological variation. DeCyder biological variation analysis (BVA) processes multiple gel images, performs gel-gel spot matching and quantatively compares protein abundance across gels.

Mass spectrometry identifies the proteins corresponding to any spots observed by 2D-DIGE and utilises the gene and literature database to interpret the proteomic data. Matrix-assisted Laser Desorption/Ionisation (MALDI) developed by Karas and Hillenkamp, (1988, 1990) involves the precipitation of sample molecules with an excess of matrix material (α-cyano-4-hydroxycinnamic acid or dihydroxybenzoic acid), the precipitant is then bombarded with a laser pulses and imparts energy. The matrix materials have absorbances at the wavelength of the laser, and are subject to desorption and ionisation,

41

accompanied by fragmentation. The MS measures the mass-to-charge ratio (m/z) of the protein, peptide or peptide fragments (Figure 1.7.2). The time-of-flight (TOF) analyser separates ions according to their m/z ratios by measuring the time it takes for ions to travel through a field free region known as the flight or drift tube. The smaller ions possess higher velocity relative to larger/heavier ions. Separated ion fractions arriving at the end of the drift tube are detected by an appropriate recorder that produces a signal upon impact of each ion group. The TOF mass spectrum is a recording of the detector signal as a function of time. This peptide mass fingerprint can then be used to search databases to identify the protein (Blackstock & Weir, 1999; Yates, 2000).
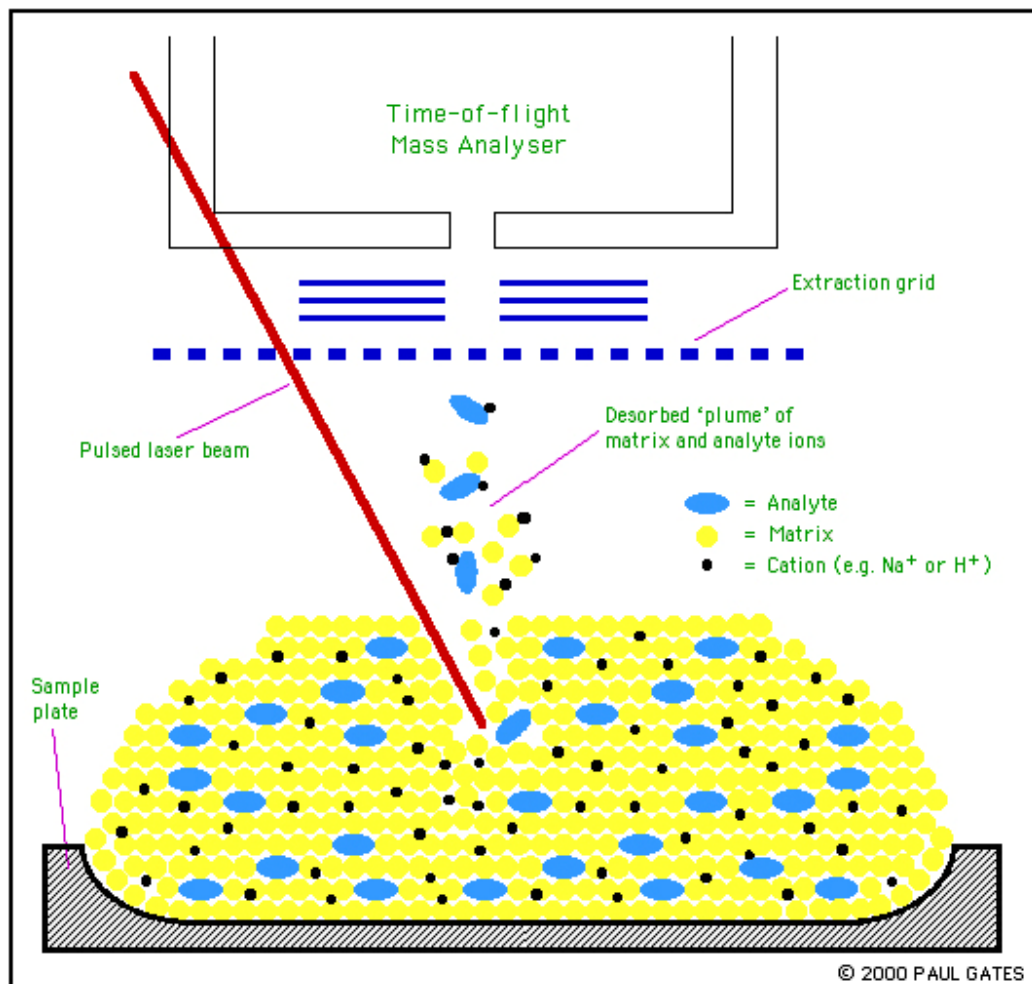
Figure 1.7.2 A schematic diagram of the mechanism of MALDI-TOF-MS (Yates, 2000)

1.7.2 Bioinformatics

Bioinformatic approaches can determine the proteomic signatures responsible for the important clinical-pathological features and identify a small number of key proteins, which may be candidates for disease markers and therapeutic targets. Bioinformatics is the collection, organisation and analysis of large amounts of biological data, using networks of computers and databases. General information about proteins can be obtained using SWISS-PROT and NCBI. Other proteomic databases, such as Bioinfomatic harvester, Open proteomics and Pubmed, search all that is known about a protein's interactions and its related gene. Software packages are available to analyse proteomic data e.g. PathwayStudio and Gene Ontology (GO STAT). PathwayStudio is a product aimed at the visualisation and analysis of biological pathways, gene regulation networks and protein interaction maps. It comes with a comprehensive database that gives a snapshot of all information available in PubMed, with the focus on pathways and cell signalling networks. This product allows visualisation of results in the context of automatically created pathways, gene regulation networks and protein interaction maps. The GO STAT consortium provides structural description of protein function that is used as a common language for gene annotation in many organisms. Large-scale techniques have generated many valuable protein-protein interaction datasets that are useful for the study of protein function (Deng *et al*., 2004).

Combination between 2D-DIGE, mass spectrometry and bioinformatics approach is a powerful tool for disease proteomics. The efforts to understand the overall features of the proteome by using a bioinformatics approach to analyse 2D-DIGE data, together with the integrated information of the individual proteins identified by 2D-DIGE, will give us novel molecular backgrounds for diseases.

1.7.3 Proteomics and cancer

Genetic mutations within cancer cells can modify protein signalling through expression of differential isoforms, post-translational modifications and altered pathways. Therefore, cancer proteomics can be characterised into expression proteomics and functional genomics. Expression proteomics seeks to identify proteins that are differently displayed in tissues that can be used as markers for cancer detection, diagnosis, and in the development of novel treatments. Functional proteomics, on the other hand, is related to how proteins interact with each other, with DNA and RNA, or as components of larger complexes. This approach recognises that proteins are part of a dynamic system, and that just identifying individual proteins is not adequate to explain their function. The capability of proteomics to identify and determine proteins associated with cancer is enhancing and improving molecular classifications of tumours and furthermore, developing more sensitive bio-markers for disease prognosis and treatment sensitivity.

Page *et al*. (1999) carried out an extensive study of the protein expression map (PEM) of the normal human breast (luminal and myoepithelial), which can be compared to future breast cancer studies. Using 2D gel proteome analysis, 43,302 proteins were detected across 20 samples; each cell type comprising a total of 1,738 unique proteins. Differential analysis detected 170 proteins that were elevated two-fold or more between the cell types indicating the scope of protein abundance between cell types.

A strategy for combining proteomic analysis and microdissection of human normal tissue versus tumour tissue was described by Emmert-Buck *et al*. (2000). Normal squamous epithelium and corresponding tumour cells from two patients with esophageal cancer were obtained by laser-capture microdissection and studied by two-dimensional polyacrylamide gel electrophoresis (2D-PAGE). 50,000 cells resolved approximately 675 distinct proteins (or isoforms). Comparison of the microdissection protein profiles identified 17 proteins with tumour-specific alterations, including 10 that were unique to tumour cells and 7 that were observed only in normal epithelium. Two of the altered proteins were characterised by mass spectrometry and immunoblot analysis, and were identified as cytokeratin 1 and annexin I. In the future, comparison of 2D-PAGE protein profiles, visualisation of

deregulated proteins, and subsequent determination of the identity of selected proteins through high-sensitivity MS-MS microdissection protein profiles can be used to analyse suspected malignant tumours and diagnose patients with cancer.

The correlation of large-scale protein expression profiles with clinical data could be used to gain insights into the molecular aspects of cancer. Voss *et al.* (2001) systematically compared the protein expression patterns by two-dimensional gel electrophoresis with clinical features in human B-cell chronic lymphocytic leukaemia (B-CLL), a disease characterised by broad clinical variability. Analysis of the pattern from 24 patient samples by statistical methods allowed the identification of proteins that clearly discriminated between the patient groups with defined chromosomal characteristics or whose expression levels did correlate with clinical parameters such as patient survival. The data described showed that B-CLL patient populations with shorter survival times exhibited changed levels of redox enzymes, heat shock protein 27 and protein disulfide isomerase, suggesting a potential role for these molecules in drug resistance.

1.7.4   Proteomics and pancreatic cancer

Identification of the pancreatic cancer proteome may help to unravel the molecular events that underlie the early invasive/metastatic, inherent chemo-resistant phenotype of this disease. Chen *et al.* (2005) studied the quantitative protein expression of normal pancreas versus pancreatic cancer tissue, using isotope-coded affinity tag technology (ICAT) and MS. A total of 656 proteins were identified and quantified in two pancreatic cancer samples, of which 151 were differentially expressed in cancer by at least 2-fold. Many proteins identified provided candidates for future early diagnosis biomarkers and targets for therapy. Several differentially expressed proteins were further validated by tissue microarray immunohistochemistry. Several of the differentially expressed proteins identified were determined to be involved in protein-driven interactions between the ductal epithelium and the extracellular matrix that orchestrate tumour growth, migration, angiogenesis, invasion, metastasis, and immunologic escape.

Mikuriya *et al.* (2007) identified proteins that might be available for early diagnosis and effective therapies by proteomic profiling of pancreatic cancer tissues. Pancreatic

cancerous and paired non-cancerous tissues were analysed by two-dimensional gel electrophoresis. The differential display showed 11 spots whose expression was increased in cancerous tissues compared with the paired non-cancerous tissues. The liquid chromatography-mass spectrometry/mass spectrometry (LC-MS/MS) system identified the spots as alpha-enolase, glyceraldehyde-3-phosphate dehydrogenase (GAPDH), triosephosphate isomerase, transgelin, calmodulin, superoxide dismutase(Mn) mitochondrial precursor, glutathione S-transferase P, cyclophilin A, protein disulfide isomerase A3 precursor, and apolipoprotein A-I precursor. Two of the 11 spots were detected as GAPDH. Four of 11 spots were enzymes involved in glycolytic pathway. Increased glycolysis in cancer cells has been regarded as the effect of intratumoural hypoxia and is possibly associated with tumour invasion, metastasis or resistance to therapies.

1.7.4.1 Proteomics and biomarkers in pancreatic cancer

As pancreatic cancer invades and metastasises at an early stage without symptoms, it is vital to develop early detection systems for the diagnosis of pancreatic cancers. Some studies have reported proteomic analyses of pancreatic tissue, pancreatic juice as well as blood plasma and sera (Kuramitsu and Nakamura, 2006). Molecular markers and biomarkers constitute major targets for the early detection of cancer and identification of cancer risk (Negm *et al*., 2002). Proteomics provides an excellent means for analysis of body fluids for classifying proteins and identifying biomarkers for early detection of cancers. Biomarkers currently available for pancreatic cancer detection, such as CA19-9, lack adequate sensitivity and specificity, which may contribute to late diagnosis of this deadly disease. Approximately 10% of the population with the Lewis negative genotype are not able to produce CA 19-9 due to the lack of the enzyme involved in its synthesis, even if they have advanced pancreatic cancer (Goggins, 2005). Honda *et al*. (2005) demonstrated a set of four mass peaks using surface-enhanced laser desorption/ionization coupled with hybrid quadrupole time-of-flight mass spectrometry in pancreatic cancer plasma, accurately distinguishing their expression from healthy controls in a training cohort with a sensitivity of 97.2% and a specificity of 94.4% and in the validation cohort with a sensitivity of 90.9% and a specificity of 91.1%. The introduction of this technology

has increased the possibility of identifying novel markers with the potential to overtake and replace CA 19-9.

Sun *et al*. (2007) analysed, by two-dimensional gel electrophoresis (2-DE) and mass spectroscopic identification, 10 protein spots significantly changed in pancreatic carcinoma and successfully identified 5 proteins including cyclin I, Rab GDP dissociation inhibitor beta (GDI2), alpha-1 antitrypsin precursor, Haptoglobin precursor, and Serotransferrin precursor. The increased levels of cyclin I and GDI2 found to be associated with pancreatic carcinoma were further confirmed by Western blot analyses in an independent series of serum samples and/or pancreatic juice samples. Applying immunohistochemistry further validated the expression of cyclin I and GDI2 in additional pancreatic carcinomas. These results indicate that cyclin I and GDI2 may be potential molecular targets for pancreatic cancer diagnostics and therapeutics.

In a study to characterise the "pancreatic juice proteome" in patients with pancreatic adenocarcinoma, Gronborg *et al*. (2004) identified a total of 170 unique proteins including known pancreatic cancer tumour markers (e.g., CEA, MUC1) and proteins over-expressed in pancreatic cancers (e.g. hepatocarcinoma-intestine-pancreas/pancreatitis-associated protein (HIP/PAP) and lipocalin 2). In addition, novel proteins that had not been previously described in pancreatic juice (e.g., tumour rejection antigen (pg96) and azurocidin) were detected. The proteins identified in this study could be directly assessed for their potential as biomarkers for pancreatic cancer. Hong *et al*. (2004) identified, by proteomic analysis, autoantibodies to calreticulin isoforms in the sera of pancreatic cancer patients. The identification of circulating tumour antigens or their related autoantibodies provides a means for early cancer diagnosis as well as leads for therapy, as they can arise in sera at a relatively early stage of pancreatic cancer.

1.8   RNA interference (RNAi)

RNA interference (RNAi) is the mechanism for RNA-guided regulation of gene expression, in which the introduction of double-stranded RNA (dsRNA) into a diverse range of organisms and cell types causes degradation of the complementary mRNA. Small interfering RNAs (siRNA) are double-stranded RNA molecules, 20-25 nucleotides in length (Elbashir *et al.*, 2001). The natural role of RNAi is a mechanism for protecting against viral infection. The genetic material of most viruses is RNA rather than DNA. Eukaryotic cells recognise dsRNA and degrade it into small fragments of 20 nucleotide pairs in length by an enzyme known as dicer. These small interfering RNA fragments are then used as a template by an enzyme complex called RISC (RNA induced silencing complex) to destroy single stranded RNA with the same sequence (Baulcombe, 2006). RNAi controls gene expression at the post-transcriptional level, resulting in selective silencing of specific proteins (Figure 1.8.1).

Initial evidence of RNAi emerged from work on the genetic modification of petunia flowers; over-expression of the gene involved in the purple pigment resulted in loss of their original colour and occurrence of white flowers. This was termed 'cosuppression' as the introduction of extra copies of the transgene caused decreased expression as well as in the endogeneous gene (Van der Krol *et al.*, 1990; Napoli *et al.*, 1990). RNAi was first termed by Fire *et al.* (1998) in the nematode *Caenorhabditis elegans*.
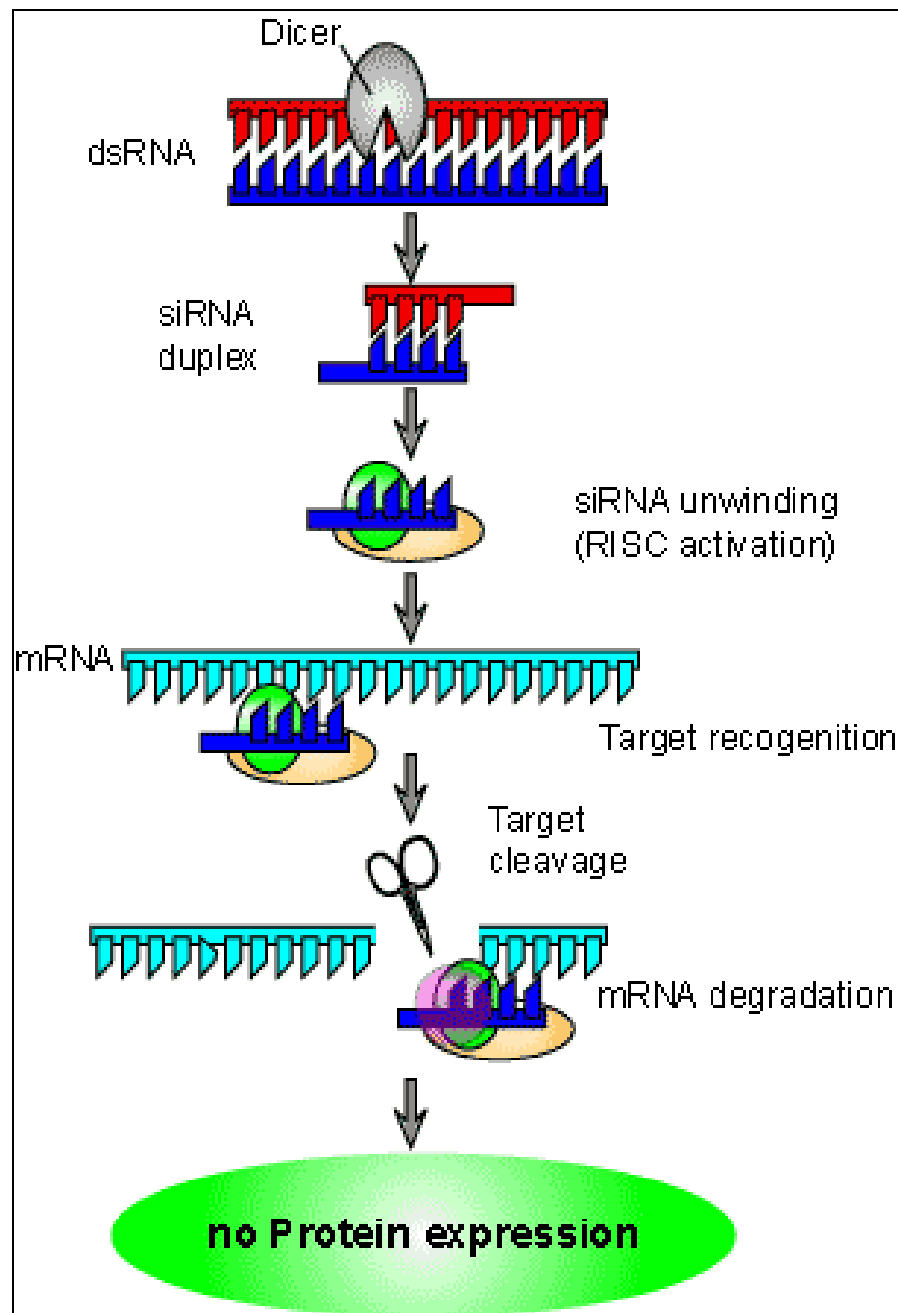
Figure 1.8.1 Mechanism of RNAi (www.scq.ubc.ca)

1.8.1 Applications of RNAi

RNAi is commonly used in biological and biomedical research to study the effect of blocking expression of a given gene. Synthetic siRNAs are the most widespread application of RNAi; this involves transient transfection of *in vitro* cultured mammalian cells, effectively mediating post-transcriptional gene silencing in cells without inducing interferon responses (Elbashir *et al*., 2001), followed by a downstream assay to monitor the RNAi effect. However, the effective delivery of RNAi agents and serum stability *in vivo* is critical for the therapeutic use of siRNA in cancer. SiRNA-mediated RNAi has a short duration *in vivo*; therefore, enhancing the durability of siRNA is essential.

1.8.2 Delivery of siRNAs *in vivo*

Many different methods for siRNA delivery have been developed,

- Direct injection delivering siRNA to target organ
- Viral vector delivery
- Liposomes
- Atelocollagen

Direct delivery of unmodified/naked siRNA in mice is often administrated intravenously by hydrodynamic transfection (high pressure tail vein injection). Lewis *et al*. (2002) co-injected mice with plasmids expressing luciferase (reporter gene) along with synthetically prepared siRNA targeted to luciferase mRNA. Successful suppression of luciferase was observed in the liver, spleen, lung, kidney and pancreas. The inherent simplicity and easy manipulation of naked RNA makes it an attractive delivery target (Wolff and Budker, 2005). While this method is widely used and in some cases led to efficient target gene inhibition, it may suffer from certain technical and practical limitations at least in a therapeutical setting, since it relies on the rapid IV injection of a comparably large volume (Aigner, 2006). Alternative strategies for the application of naked siRNAs include various delivery routes which, however, often provide a local administration or rely on an administration at least close to the target tissue or target organ, thus restricting the number of target organs, which may not be relevant for certain diseases. Intranasal administration of naked siRNA targeting heme oxygenase-1 (HO-1), a cytoprotective enzyme, led to

effective gene suppression and consequently enhanced apoptosis, via increased Fas expression and caspase 3 activity, in mouse lung during ischemia-reperfusion (I-R) injury (Zhang *et al.*, 2004).

siRNA delivery by viral vectors utilises 3 main classes of viruses, including the retrovirus, adenovirus and lentivirus. Retroviruses were one of the first vectors used to transduct cells with plasmids expressing hairpin-shRNA constructs. Despite the relative ease of use *in vitro*, use of the retrovirus *in vivo* has safety concerns and significant limitations. Retroviruses integrate their DNA into the hosts genomic DNA, bringing with it, the risk of mutagenesis and carcinogenesis (Xi and Grandis, 2003). Another problem is that retroviral transduction is limited to actively dividing cells, which means that the majority of mammalian cells will not receive the siRNA.

Adenoviruses do not commonly integrate DNA into the host's genome and the effects are short-lived, usually lost after several cell divisions. Therefore are used when a short duration of action is required, such as tumour-targeting therapy. Zhang *et al.* (2004) intratumourally injected an adenovirus encoding the hypoxia-inducible factor-1 (HIF-1)-targeted siRNA. Down-regulation of HIF-1 protein *in vivo* had a small but significant effect on tumour growth when combined with ionising radiation. These results suggest that an adenovirus-based siRNA gene transfer approach may be a potentially effective adjuvant strategy for cancer treatment. However, despite the lowered risk of insertional mutagenesis, the adenovirus is associated with significant dose-dependent liver toxicity that can severely limit therapy. Another major disadvantage of adenoviral vectors is the dependence on specific surface receptors on the target cell which are often absent, rendering transduction impossible in many cases.

Lentiviral vectors are a promising subclass of viruses that lack the risk of insertional mutagenesis and are able to transfect primary and non-dividing cells. Lentiviral vectors have been shown to successfully transduce and stably express siRNAs in muscle cells (Rubinson *et al.*, 2003). Chen *et al.* (2007) employed lentivirus-mediated siRNA targeted to the gene, enhancer of zeste homolog 2 (EZH2). Suppression of EZH2 in hepatocellular carcinoma (HCC) cells, reduced their growth rate *in vitro* and markedly diminished their

tumourigenicity *in vivo*. Moreover, in a mouse model of established large-sized HCC, intratumoural injection of lentiviral (Lenti)-shRNA (short hairpin RNA) or siRNA (small interfering RNA) targeting EZH2 produced significant tumour regression.

Non-viral vectors such as liposomes have the advantage of low toxicity, ease of synthesis and low immune response over viral vectors. Cationic liposomes and polymer particles have been shown to be suitable for the delivery of siRNA. Yano *et al*. (2004) determined that intravenous administration of a liposome complexed with bcl-2 siRNA induced strong anti-tumour effects in a mouse model of liver metastasis. Ochiya *et al*. (2001) developed a safe non-vector-based siRNA delivery system, termed atelocollagen. Atelocollagen is a biomaterial obtained from type I collagen of calf dermis by pepsin treatment. The atelocollagen-based transfer method has great potential for site-specific transportation of target siRNAs because the complex of siRNA/atelocollagen becomes solid when transplanted and remains so for a defined period *in vivo*. In addition, an atelocollagen complex can be delivered as micro-particles for intravenous injection, making systemic delivery of siRNA possible (Sano *et al*., 2003).

Minakuchi *et al*. (2004) determined that atelocollagen complexed with human fibroblast growth factor (FGF)-4 siRNA was resistant to nucleases and was efficiently transduced into cells, thereby allowing long-term gene silencing. Site-specific *in vivo* administration of an anti-luciferase siRNA/atelocollagen complex reduced luciferase expression in a xenografted tumour. Atelocollagen-mediated transfer of siRNA *in vivo* showed efficient inhibition of tumour growth in an orthotopic xenograft model of a human non-seminomatous germ cell tumour. Clinical applications of siRNA indicate that an atelocollagen-based non-viral delivery method could be a reliable approach to achieve maximal function of siRNA *in vivo*.

RNAi is an invaluable tool, allowing rapid characterisation of the function of known genes, as well as aiding the identification of novel genes in disease processes such as the cancer invasion/metastatic cascade.

1.8.3 RNAi-mediated therapy in pancreatic cancer

Many molecular alerations play a role in pancreatic tumour progression, early invasion and metastasis as well as inherent resistance to chemotherapy and radiation. Therefore, challenges exist to identify molecular pathways and genes that are involved in the aggressiveness of this cancer.

Inhibition of target genes through siRNA is an effective therapy to determine the potential involvement of specific genes in the pancreatic cancer malignancy. Recent developments in RNAi-mediated targeting research in pancreatic cancer are summarised in table 1.8.1.

The k-ras gene is frequently mutated in pancreatic cancer (Lemoine *et al*., 1992; Rozenblum *et al*., 1997). Brummelkamp *et al*. (2002) developed a siRNA retroviral vector targeting the mutant oncogenic k-ras gene, rather than the wild-type in the pancreatic cancer cell line, Capan-1. Down-regulation of k-ras (mut) abolished colony formation *in vitro* and formation of tumours *in vivo*. In agreement with this study, reduced cell proliferation, migration, colony growth and VEGF expression was observed in pancreatic cancer cell lines, MiaPaCa-2 and Panc-1 after k-ras knockdown (Flemming *et al*., 2005).

Targeting the molecules associated with pancreatic cancer progression, including, invasion, metastasis and angiogenesis by RNAi represent a powerful tool in anti-cancer therapy. Today, numerous genes and proteins have been used to reverse the neoplastic phenotype *in vitro* and *in vivo* through gene translation silencing. Suppression of genes such as, carcinoembryonic antigen-related cell adhesion molecule 6 (CEACAM6) (Duxbury *et al*., 2006), EphA2 (Duxbury *et al*., 2004), glucose transporter-1 (GLUT-1) (Ito *et al*., 2004) and MUC-1 (Tsutsumida *et al*., 2006) at the post-transcriptional level inhibited tumour cell growth, invasion and metastasis of pancreatic cancer cell lines.

Nitori *et al*. (2005) examined the clinicopathologic significance of tissue factor (TF) expression in pancreatic ductal adenocarcinoma by immunohistochemistry using a newly raised anti-TF monoclonal antibody in 113 patients who had undergone surgical resection of pancreatic ductal adenocarcinoma. Increased TF expression correlated with the extent of the primary tumour, lymph node metastasis, lymphatic distant metastasis, advanced

tumour-node-metastasis stage, and high tumour grade. Multivariate analysis using the Cox proportional hazards model showed that high TF expression was an independent negative predictor for survival, and patients with TF-negative tumours had a significantly better prognosis even if lymph node metastasis was present. Furthermore, this study corroborated the clinical data with *in vitro* TF knockdown by RNA interference. *In vitro*, siRNA targeting TF suppressed the invasiveness of a pancreatic adenocarcinoma cell line, suggesting that TF expression may contribute to the aggressiveness of pancreatic ductal adenocarcinoma by stimulating tumour invasiveness and that evaluation of the primary tumour for TF expression may identify patients with a poor prognosis.

The inherent drug and radiation resistance of pancreatic cancer is another area for RNAi targeted therapy. P-gp, encoded by the MDR-1 gene, has been shown to play a role in pancreatic cancer mediated drug resistance (Liu *et al*., 2001). Nieth *et al*. (2003) inhibited MDR1 expression by RNAi. SiRNA duplexes specifically inhibited MDR1 expression up to 91% at the mRNA and protein level in the human pancreatic carcinoma cell line, EPP85-181RDB, and resistance against daunorubicin was decreased to 89%. The data proved that siRNA-targeting of P-gp expression could be an effective method for reversal of drug resistance. The role of survivin, ILK and RRM2 in pancreatic tumour cell resistance to chemotherapy and radiation was evaluated by RNAi. Kami *et al*. (2005) silenced survivin at mRNA and protein level in AsPc-1 cells by siRNA, and radiation treatment of the cells caused increased capase-3 activity and DNA fragmentation. This study is in accordance with others determining that survivin may play a role as a radioresistance factor in pancreatic cancer (Asanuma *et al*., 2000; Rodel *et al*., 2005; Guan *et al*., 2006). Further studies have implicated survivin in proliferation and apoptosis (Tsuji *et al*., 2005; Guan *et al*., 2006).

Enhancing the chemotherapeutic effects of drugs in pancreatic cancer has further been evaluated by down-regulated tumourigenetic-related genes which are over-expressed in pancreatic cancer. ILK has been previously shown to be linked to the progression of the aggressive nature of pancreatic cancer (Sawai *et al*., 2006). Yau *et al*. (2005) reported that the ILK inhibitor QLT0254 blocked tumour growth and enhanced gemcitabine-induced apoptosis in a pancreatic cancer xenograft. This study was further validated, whereby ILK

siRNA-mediated knockdown in pancreatic cancer cells induced chemosensitisation to gemcitabine via increased caspase 3-mediated apoptosis, suggesting a role for ILK as a determinant of pancreatic cancer resistance to gemcitabine (Duxbury *et al.*, 2005).

Activation of RRM2 which catalyses the conversion of ribonucleotide 5'-diphosphate to 2'-deoxynucleotide, is associated with chemoresistance to gemcitabine and with the invasive potential of pancreatic cancer cells (Jung *et al.*, 2001; Zhou *et al.*, 1998). Duxbury *et al.* (2004) determined that suppression of RRM2 by RNAi resulted in enhanced gemcitabine-induced cytotoxicity *in vitro*, as well as reduced tumour growth, increased tumour apoptosis and inhibition of metastasis in pancreatic cancer xenografts *in vivo*. This study demonstrates that systemic delivery of siRNA-based therapy can enhance the efficacy of gemcitabine.

Investigation of potential therapeutic targets in pancreatic cancer has demonstrated that RNAi technology can be directed against specific characteristics of this malignant disease. Selective and efficient knockdown of genes enables researchers to monitor the specificity of siRNA targeting. Therefore, siRNA-mediated therapy is a valid therapeutic strategy in anticancer intervention.

Table 1.8.1 Summary of potential targets by RNAi for developing therapeutic in pancreatic cancer

Therapeutic strategy	Target gene	Therapeutic effects	Reference
Oncogene	K-ras	Reduction of cell proliferation, migration and VEGF expression	Brummelkamp *et al*. (2002) Fleming *et al*. (2005)
Tumour progression, angiogenesis and apoptosis	CEACAM6	Inhibition tumour growth, angiogenesis and enhancement of apoptosis	Duxbury *et al*. (2006)
	TF	Suppression of invasion	Nitori *et al*. (2005)
	EphA2	Inhibition of tumour growth and metastasis	Duxbury *et al*. (2004)
	GLUT-1	Inhibition of metastasis	Ito *et al*. (2004)
	MUC-1	Decreased proliferation and reduction of metastasis	Tsutsumida *et al*. (2006)
	Notch-1	Decreased cell invasion through reduced MMP-2, NF-kappa and VEGF expression *in vitro*	Wang *et al*. (2006)
Chemo-resistance	P-gp	Enhancement of chemotherapy	Nieth *et al*. (2003)
	Survivin	Increased caspase-3 and apoptosis	Kami *et al*. (2005); Asanuma *et al*, (2000) Rodel *et al*. (2005); Guan *et al*. (2006)
	ILK	Increased capase-3-mediated apoptosis	Duxbury *et al*. (2005)
	RRM2	Enhanced gemcitabine induced toxicity Reduced tumour growth and increased apoptosis	Duxbury *et al*. (2004)

Adapted from Chang (2007)

1.9   Epidermal growth factor receptor tyrosine kinase family

Receptors of the epidermal growth factor (erbB) family play principal roles in mediating the proliferation and differentiation of normal cells and are expressed in a wide variety of tissues. The role of growth factors in the pathogenesis of cancers has been increasingly studied as they have been shown to function in cell proliferation, survival, adhesion, migration and differentiation (Yarden, 2001).

The ErbB family consists of four closely related transmembrane receptors, erbB-1 (EGFR/HER1), erbB-2 (HER2), erbB-3 (HER3) and erbB-4 (HER4). All four receptors share the same basic structure composed of three regions; an extracellular region consisting of glycosylated domains- two of which are cysteine-rich, a transmembrane domain containing a single hydrophobic anchor sequence, and an intracellular region containing the catalytic tyrosine kinase domain which is responsible for the regulation of intracellular signalling (Schlessinger, 2000). The receptors share 40-50% sequence identity in their extracellular domains, 60-80% similarity in their kinase domains and 10-30% in their tails (Yarden *et al.*, 1991). EGFR binds the ligands, epidermal growth factor (EGF), transforming growth factor α (TGF-α) and amphiregulin (AR). Betacellulin (BTC), heparin binding EGF-like growth factor (HB-EGF) and epiregulin bind to both EGFR and HER4. However the latter two ligands also bind to HER3. Neuregulins -1, -2 and heregulins are ligands for HER3 and HER4. HER4 also binds neuregulin -3 and 4 (Figure 1.9.1). These ligands activate the receptor by binding to the extracellular domain and inducing the formation of receptor homodimers or heterodimers allowing the receptors to signal. Although HER2 does not act as a receptor, the ligands induce tyrosine phosphoylation by triggering heterodimerisation and cross-phosphorylation. The major partner of EGFR is HER2. These complexes containing HER2 are more stable than other dimers containing members of the EGF receptor family. HER3 lacks tyrosine kinase activity and is activated by the tyrosine kinases on other receptors. HER4 isoforms differ in the composition and structure of their membrane regions and C-terminal tails.
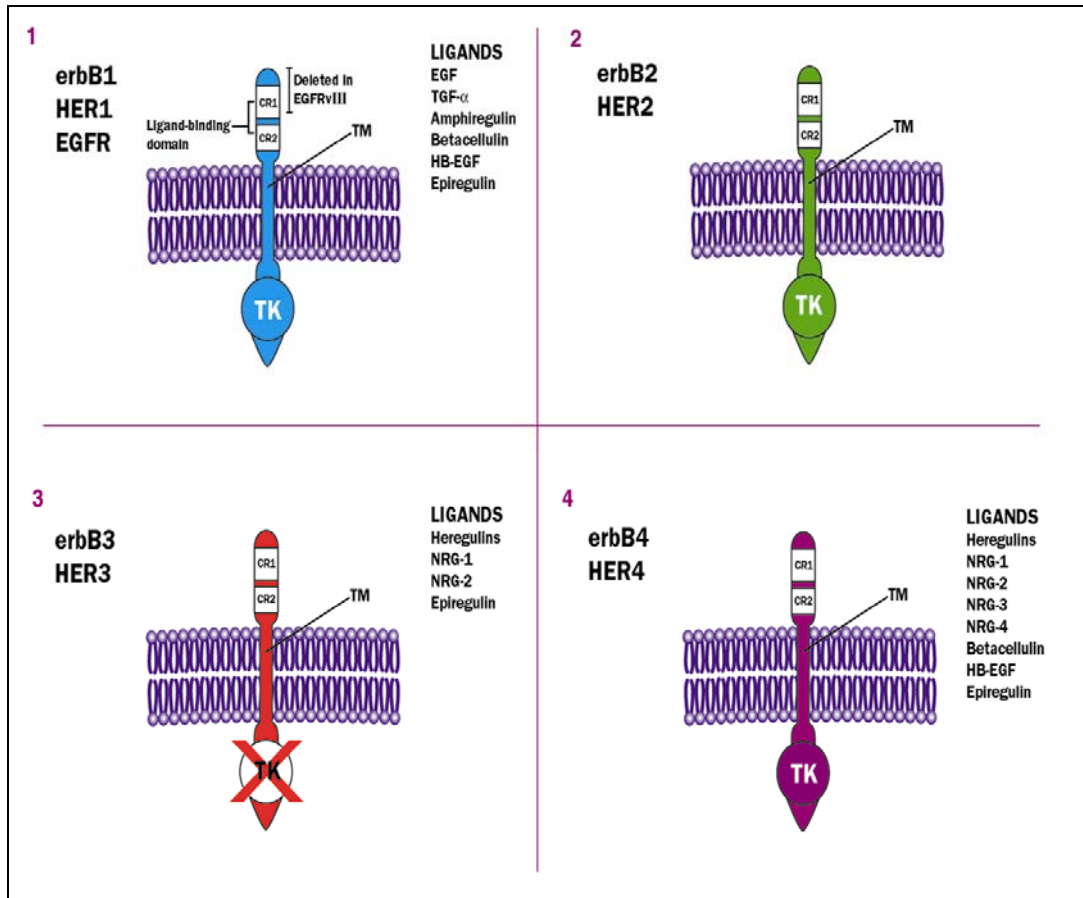
Figure 1.9.1 Structure of erbB family and their cognate ligands (Horizons in cancer therapeutics, 2001).

1.9.1 Epidermal growth factor receptor (EGFR)

EGFR is a 170 kDa cell surface molecule that mediates signal transduction from the cell surface to the cytoplasm (Xiong *et al*., 2002). When activated, EGFR phosphorylates and activates other intracellular proteins, including the Ras/Raf/MAPK pathway and the AKT pathway, which affects cell signalling pathways, cellular proliferation, control of apoptosis and angiogenesis (Figure 1.9.2). EGFR plays an important role in tumour development and maintenance. EGFR over-expression occurs in 30% to 65% of pancreatic ductal adenocarcinomas (Fjällskog *et al.,* 2003; Dancer *et al*., 2007) and EGFR over-expression is thought to confer a poor prognosis in several malignancies. It often correlates with poorly differentiated histology and a more advanced stage of cancer. Tobita *et al*. (2003) investigated the expression of EGFR in 77 cases of invasive ductal adenocarcinoma of the

pancreas. They detected EGFR on 42% of cancer cell membranes by IHC. EGFR expression correlated with the histological differentiation and metastatic status of the TNM tumour classification, but was not related to other clinicopathological features. EGFR status in pancreatic cancer may therefore be a potential marker for differentiation and liver metastasis in cancer cells rather than tumourgenesis. Recent studies have described a relationship between EGFR and metastasis and suggest that EGFR expression may be useful as a predictive marker for invasion and metastasis in cancer (Wang *et al*., 2007; Festuccia *et al*., 2005).

Therefore EGFR is an attractive target for treatment because of its presence and over-expression in many tumour types.
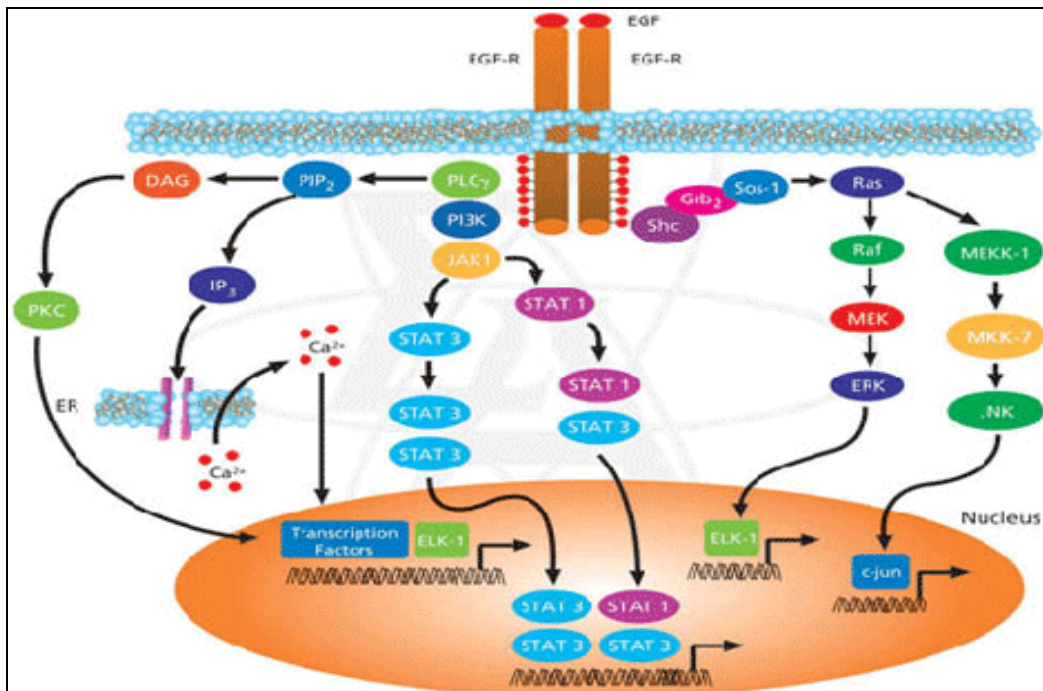
Figure 1.9.2 EGF Receptor Signal Transduction Pathway (www.sigmaaldrich.com).

1.9.2 HER2

HER2 is a proto-oncogene that encodes a transmembrane glycoprotein with tyrosine kinase activity, which is closely related to EGFR. Although HER2 is a more potent oncoprotein than other members of the erbB family, it has no high affinity ligands. EGFR

and HER2 can form heterodimeric complexes; HER2 has also been linked with the formation of heterodimeric complexes with HER3 and HER4. Up-regulation or amplification of the HER2 gene has been associated with a poor prognosis in breast cancer and in 30% of ovarian cancers (McKenzie *et al.*, 1993). Approximately 30% of prostate, 20% of gastric, 2% of colorectal cancer have been reported to over-express HER2 (Markogiannakis *et al.*, 1997). Safran *et al.* (2001) establish the frequency of over-expression of HER2 in patients with pancreatic adenocarcinoma in order to determine the potential role of trastuzumab (Herceptin) as a therapeutic agent in this disease. IHC staining revealed HER2 over-expression in 21% of samples (n=154), indicating that HER2 over-expression occurs in a subset of pancreatic cancer patients. Over-expression is more common in well and moderately differentiated tumours. Yamanaka *et al.* (1993) examined the expression of HER2 in normal pancreas and pancreatic cancer tissue. Immunostaining was observed in acinar and ductal cells of normal pancreas, where as HER2 expression was observed in 45% of pancreatic carcinomas. A slight correlation existed between well-differentiated tumours and HER2 expression. HER2 over-expresison in pancreatic cancer has also been determined to reduce survival times. Lei *et al.* (1995) reported that over-expression of HER2 was found in 10 of 21 (47.6%) pancreatic cancers of ductal origin and in 2 of 6 (33.3%) ampullary adenocarcinomas. Over-expression of HER2 was closely and inversely related to the survival of the patients with pancreatic cancer of ductal origin: 19.1 ± 11.7 months for those not over-expressing compared to 7.3 ± 3.8 months for the over-expressing patients. Among the pancreatic cancer group, 11 patients underwent cancer resection. The average survival for the 7 with non over-expressing cancer was 21.4 ± 14.3 months compared to 10.5 ± 3.6 months for those with over-expressing tumour. Among the 4 patients not undergoing resection, the average survival with non over-expressing cancer was 15.0 ± 3.8 months as contrasted to 5.2 ± 2.1 months for the over-expressers.

The oncogene HER2 is variably expressed in pancreatic cancer cases, between 17-82% (Bũchler *et al.*, 2001; Dancer *et al.*, 2007). Therefore, it may be a target for therapeutic strategies for a sub-population of patients with pancreatic cancer.

1.9.3 HER3 and HER4

HER3 and HER4 are structurally related family members of the erbB receptor family. HER3 lacks tyrosine kinase activity and is activated by the tyrosine kinases on other receptors. HER4 isoforms differ in the composition and structure of their membrane regions and C-terminal tails, which contain key phosphorylation sites responsible for binding with downstream targets.

The formation of erbB homodimers and heterodimers, following ligand binding and receptor aggregation causes the activation of intrinsic tyrosine kinase activity of the receptor via phosphorylation and generates a cascade of downstream events. HER3 and HER4 proteins have been increasingly referred to in literature as potential prognostic markers in pancreatic cancer. Expression of HER3, in particular was shown to be expressed in 47% (27/58) of pancreatic cancer. This expression of HER3 was associated with advanced tumour stage and shorter survival postoperatively. The study concluded that a significant quantity of human pancreatic cancers over express HER3, and that the presence of HER3 might contribute to disease progression (Friess *et al.,* 1995).

A study was conducted to investigate the presence of HER4 in pancreatic cancer. Graber *et al.* (1999) showed that mRNA expression of HER4 is decreased (6 fold) in non-metastatic pancreatic cancer when compared to tumours with lymph node or distant metastasis or to the normal pancreas. IHC showed that the HER4 antigen is predominantly located in the cell membrane and cytoplasm of ductal and acinar cells. 61 out of 75 pancreatic samples showed weak to moderate expression of HER4. However, the level of HER4 in pancreatic cancer had no influence on patient survival, yet may be an important receptor involved in the tumourigenesis of pancreatic cancer.

1.9.4 Clinical implications of the mechanism of EGFR family inhibitors in cancer

Novel therapeutic agents that target the epidermal growth factor receptor family and signalling pathways represent an important addition to the therapy for the treatment of a variety of cancers.

Inhibitors of the EGFR family can be divided into two categories:

1. Monoclonal antibodies
2. Small molecule inhibitors

1.9.4.1 Erlotinib/ Tarveca

Erlotinib (tarveca) is an oral anti-cancer drug under development by OSI Pharmaceuticals, Genentech and Roche (Figure 1.9.3). It is a member of the epidermal growth factor receptor (EGFR) inhibitor class of agents, approved in 2004 by the FDA for the treatment of patients with local or advanced metastatic NSCLC and in 2005 as a first line treatment of locally advanced, unresectable or metastatic pancreatic cancer, in combination with gemcitabine. Furthermore, Moore *et al*. (2007) recently published a phase III trial of erlotinib plus gemcitabine compared with gemcitabine alone in 569 patients with advanced pancreatic cancer. Overall survival based on an intent-to-treat analysis was significantly prolonged on the erlotinib/gemcitabine arm; median survival 6.24 months v 5.91 months. One-year survival was also greater with erlotinib plus gemcitabine (23% v 17%). Progression-free survival was significantly longer with erlotinib plus gemcitabine. Objective response rates were not significantly different between the arms, although more patients on erlotinib had disease stabilisation.
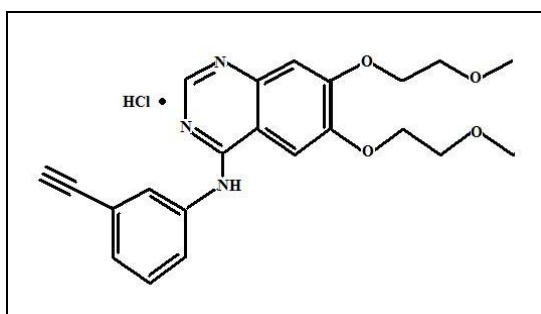
6,7-bis(2-methoxy-ethoxy)-quinazolin-4-yl-(3-ethylnylphenyl) amine

Chemical formula $C_{22}H_{23}N_3O_4HCl$.

Figure 1.9.3 Structure of erlotinib (Tsao *et al*., 2005)

Erlotinib is a member of the quinazoline family. It is a reversible, ATP-competitive inhibitor of the internal tyrosine kinase domain of EGFR. Erlotinib is capable of inducing cell cycle arrest with an accumulation of cells in G_0/G_1, loss of the hyperphosphorylated form of the retinoblastoma protein and accumulation of p27^{Kip1} (Moyer *et al.,* 1997). Durkin *et al.* (2003) investigated the effect of erlotinib on pancreatic cell lines *in vitro*. Five out of six cell lines showed growth inhibition at 72 hrs at both 50 μM and 100 μM concentrations of erlotinib. No significant difference in cell growth was noted between the two concentrations. This may suggest that saturation of the EGF receptor was achieved at the lower concentration and no additional benefits were observed at greater concentrations. This study promotes the use of EGFR blockade as a targeted therapeutic strategy for the treatment of pancreatic cancer using small molecule tyrosine inhibitors such as erlotinib.

EGFR-mediated signal transduction pathways are important in cellular response to ionizing radiation. High EGFR expression on cancer cells may contribute to radioresistance. Kim *et al*. (2005) evaluated the radiosensitising effect of erlotinib in three human cancer cell lines with different EGFR expression, A431 (very high expression), H157 (moderate expression) and H460 (low expression). A431 was the most radioresistant and the most sensitive to erlotinib, while H460 was the most radiosensitive and the most resistant to erlotinib. H157 had intermediate sensitivity to radiation and erlotinib. Treatment with erlotinib for 24 hr at 300 nM increased G1 arrest by 18.6, 2.0 and 4.8% in A431, H157 and H460, respectively. Erlotinib-induced apoptosis was augmented by radiation in A431 cells only. In conclusion, high EGFR expression may result in a high degree of radiosensitiation when treated with erlotinib combined with radiation. The extent of erlotinib-induced radiosensitisation was proportional to EGFR expression, as well as autophosphorylation of the human epidermal growth factor receptor.

1.9.4.2 Iressa/Gefitinib

Gefitinib is an oral anti-cancer drug developed by AstraZeneca (Figure 1.9.4). It is a member of the quinazoline family. The drug works by competitively inhibiting ATP binding to the ATP binding site of the internal tyrosine kinase domain of EGFR. The drug

causes numerous effects on tumour cells over expressing EGFR, such as blocking receptor autophosphorylation, inducing cell cycle arrest and reducing cell proliferation. This tumour growth inhibition is associated with up-regulation of the CDK2 inhibitor p27^{Kip1}, which accounts for the cell cycle arrest in the G_1 phase (Di Gennaro *et al.*, 2003).
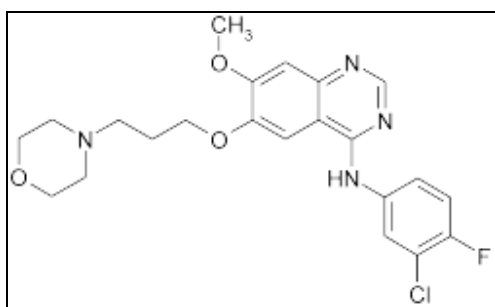
Figure 1.9.4 Structure of gefitinib (Barker *et al.*, 2001)

This EGFR tyrosine kinase inhibitor has shown clinical activity against EGFR-expressing tumours. Li *et al.* (2004) investigated the potential role of gefitinib in pancreatic cancer *in vitro*. Gefitinib inhibited EGF-induced cell growth and eradicated EGF-induced phosphorylation of EGFR and MAP kinase. Gefitinib inhibited basal and EGF-induced anchorage-dependant cell growth and invasion through EGFR-dependent pathways. Gefitinib has been indicated as offering a new treatment option for pancreatic cancer. Czito *et al.* (2006) initiated two phase I clinical trials assessing the combination of gefitinib, capecitabine and radiation on patients with localised pancreatic or rectal cancer. This combination resulted in increased patient toxicity and further investigation of this combination is needed. Gefitinib use in clinical trials is now limited due to its unfavourable outcome in many NSCLC trials.

1.9.4.3 Lapatinib/Tykerb

Lapatinib is a dual EGFR and HER2 tyrosine kinase inhibitor (Figure 1.9.5). Its dual mode of action distinguishes it from existing TKIs, which are selective EGFR inhibitors. Dual inhibition of EGFR and HER-2 tyrosine kinases has been found to exert greater biologic effects in the inhibition of signalling pathways promoting cancer cell proliferation and survival than inhibition of either receptor alone.
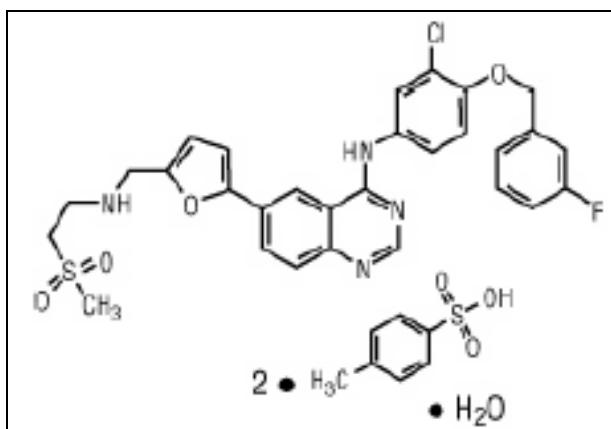
Figure 1.9.5 Structure of lapatinib (Arora *et al*., 2005)

Rusnak *et al.* (2001) developed potent quinazoline and pyrido-[3,4- *d*]-pyrimidine small molecules that are dual inhibitors of the EGFR and HER2. These dual inhibitors demonstrated *in vitro* inhibition of EGFR and HER2 kinase domains. Cell lines over-expressing EGFR and HER2 showed significant inhibition of growth at concentrations of <0.5 μM. Dose-responsive inhibition was observed in tumour growth in mouse subcutaneous xenograft models of BT-474 and NH5 breast cancer cell lines. This data highlighted the potential use of dual EGFR and HER2 inhibitors in cancers over expressing EGFR and HER2.

The novel dual EGFR/HER2 tyrosine kinase inhibitor lapatinib (GlaxoSmithKline; Research Triangle Park, NC) has been shown to inhibit tumour cell growth *in vitro* and in xenograft models for a variety of human tumours. Lapatinib reduced the tyrosine phosphorylation of EGFR and HER2, and cell survival and proliferation *in vitro*. Downstream effectors, Erk1/2 and AKT were also inhibited. *In vivo* mouse xenograft models of BT-474 and NH5 were used to show that activation of EGFR, HER2, Erk1/2 and AKT were inhibited by treatment with lapatinib (Xia *et al.,* 2002).

Phase I clinical trials using lapatinib to treat solid tumours were performed. Preliminary data showed good response and no grade 4 toxicities. Phase IB trial of lapatinib in

pretreated metastatic cancer patients using varied doses showed stable disease in most cancer types and partial/minor response in breast cancer previously treated with Herceptin-containing regimens (Burris H.A, 2004).

More clinical trials are ongoing for the treatment of breast cancer with lapatinib in various regimens, including Herceptin, plus paclitaxel and lapatinib together with letrozole. Recently, lapatinib in combination with capecitabine has gained FDA approval for the treatment of patients with HER2 positive, advanced, metastatic breast cancer. Geyer *et al*. (2006) treated women with HER2-positive, locally advanced or metastatic breast cancer that had progressed after treatment with regimens that included an anthracycline, a taxane, and trastuzumab (Herceptin) with capecitabine alone or in combination with lapatinib. Results show that the median time to progression was 8.4 months in the combination therapy group compared to 4.4 months in the monotherapy group. These improvements were achieved without an increase in serious toxic effects or symptomatic cardiac events. The trial was stopped and women receiving capecitabine alone were allowed transfer to the combination therapy arm and continue treatment. Overall survival data is not currently available.

The positive results from these trials have opened up more combinations of lapatinib to treat different types of cancers over expressing EGFR and HER2. Lapatinib has not yet been tested in pancreatic cancer.

1.9.4.4 Erbitux/ Cetuximab

Erbitux is a human-mouse chimerised IgG_1 monoclonal antibody with a high affinity to EGFR, derived from the murine anti-EGFR monoclonal antibody 225.

Erbitux inhibits EGF receptor activity by blocking the binding of EGFR ligands such as EGF and the transforming growth factor-α (TGF-α), resulting in the increased activity of pro-apoptotic molecules, inhibition of cyclin dependent kinase-2 (CDK-2) activity and enhancement of the cytotoxicity of chemotherapeutic drugs and radiation.

Erbitux inhibits tumour growth *in vivo* and cell proliferation *in vitro*. The mechanisms involved include inhibition of angiogenesis, invasion and metastasis, activation of immune responses, arrest in cell cycle progression, activation of pro-apoptotic agents and increased sensitivity to chemotherapeutic drugs (Mendelsohn, 2001).

Buchsbaum *et al.* (2002) investigated the treatment of pancreatic cell lines and mouse xenografts with combinations of erbitux, gemcitabine and radiation. Erbitux inhibited EGF-induced tyrosine kinase phosphorylation of EGFR in cell lines, MiaPaCa-2 and BxPc-3. The combination of erbitux, gemcitabine and radiation in the cell lines showed high apoptosis and inhibition of proliferation *in vitro*. While *in vivo* the combination showed 100% complete regression of MiaPaCa-2 tumours for 250 days and the greatest growth inhibition for BxPc-3 compared to single treatment of erbitux, gemcitabine or radiation alone.

Xiong *et al.* (2004) carried out a phase II trial to evaluate the combination of erbitux and gemcitabine in the treatment of advanced pancreatic cancer. This trial included 41 patients who had not received prior chemotherapy. Following treatment, 12% of patients achieved a partial response and 63% achieved stabilisation of their cancer. The average duration of survival for the entire group of patients was 7 months, with a one-year survival of over 30%. The most common side effect of treatment was rash, which occurred in 87% of patients.

The researchers concluded that the addition of erbitux to gemcitabine appears promising for the treatment of pancreatic cancer and may improve survival in patients with advanced pancreatic cancer, compared to gemcitabine alone.

1.10 Aims of Thesis:

The aims of this thesis were as follows;

- To investigate the sensitivity of a panel of pancreatic cancer cell lines to a panel of chemotherapeutic drugs.
- To develop drug-resistant variants of pancreatic cancer cell lines and investigate the occurrence of cross-resistance to other structurally and functionally unrelated drugs; and also to investigate any correlation between acquired drug resistance and invasion.
- To study the incidence of multi-drug resistance pumps (P-gp and MRP-1) in pancreatic cancer tissue sections by immunohistochemistry.

- To investigate clonal variation within a pancreatic cancer cell line with respect to invasion, adhesion and drug resistance.
- To identify key target proteins by proteomic analysis, followed by functional analysis such as gene expression knockdown using siRNA, in order to investigate the mechanisms of invasion, adhesion, anoikis, proliferation and drug resistance within human pancreatic cancer cell lines.

- To investigate and characterise the role of secreted factors in the conditioned media (CM) in *in vitro* invasion, adhesion and anoikis assay.

- To determine the role of the tyrosine kinase inhibitor, lapatinib, in EGFR/HER2 expressing cell lines.

2.0   Materials & Methods

2.1   Cell Culture

Cell culture procedures were strictly adhered to as outlined in NICB SOP.

2.1.1   Cell lines

Table 2.1 outlines details and sources of the human pancreatic tumour cell lines used in this thesis. All cells were maintained under standard culture conditions, 5% CO_2 at 37 ^{o}C. Table 2.2 outlines the media components and serum concentration for the cell lines. All cell lines are mycoplasma free; testing was carried out in-house by Michael Henry.

Table 2.1   Cell lines used in this thesis

Cell Line	Details-Histology	Source
AsPc-1	Pancreatic adenocarcinoma from metastatic ascites	ATCC
BxPc-3	Pancreatic adenocarcinoma	ATCC
Bx/Epi	Epirubicin-selected variant of BxPc-3	NICB
Bx/Gem	Gemcitabine-selected variant of BxPc-3	NICB
KCI-MOH1	Pancreatic adenocarcinoma	DSMZ
KCI/Epi	Epirubicin-selected variant of KCI-MOH1	NICB
KCI/Txt	Taxotere-selected variant of KCI-MOH1	NICB
KCI/Gem	Gemcitabine-selected variant of KCI-MOH1	NICB
MiaPaCa-2	Pancreatic carcinoma	ECACC
Mia/Epi	Epirubicin-selected variant of MiaPaCa-2	NICB
Mia/Txt	Taxotere-selected variant of MiaPaCa-2	NICB
Mia/Gem	Gemcitabine-selected variant of MiaPaCa-2	NICB
Clone #3	Clonal population of MiaPaCa-2	NICB
Clone #8	Clonal population of MiaPaCa-2	NICB
Panc-1	Pancreatic ductal carcinoma	ATCC

NICB, National Institute for Cellular Biotechnology, DCU, Dublin, Ireland

ATCC, American Type Culture Collection, Rockville, MD, USA.

DSMZ, Deutsche Sammlung von Mikroorganism und Zellkulturen GmbH (German Collection of Microorganisms and Cell Cultures), Braunschweig, Germany.

ECACC, European Collection of Animal Cell Cultures, Salisbury, Wiltshire, UK.

Table 2.2 Additional components in media.

Cell Line	Basal Media	FCS (%)	Additions
AsPc-1	RPMI 1640	5	Sodium pyruvate
BxPc-3	RPMI 1640	5	Sodium pyruvate
KCI-MOH1	RPMI 1640	5	Sodium pyruvate
MiaPaCa-2	DMEM	5	N/A
Panc-1	DMEM	5	N/A

2.2 Isolation of sub-populations by clonal dilution

Clonal populations were isolated by plating cells in 96-well plates at a concentration of 1 cell per 3 wells (15 cells/ml). After 1 day, the 96-well plates were monitored for single cells in wells. Single cell wells were marked and then allowed to grow until they reached levels that allowed them to be scaled up initially into 24-well plates.

2.2.1 Collection of conditioned media

Cells were cultured until 50-60% confluent. Cells were washed x3 in serum-free (SF) media. Cells were incubated in SF media (5 ml/T25 cm^2 flask) for 60 min. After this time, cells were washed again x3 in SF media. SF media was added to the cells and incubated for 72 hrs. After such time, conditioned media (CM) was collected, centrifuged for 5 min at 1000 rpm, filtered through 0.22 μm filter and stored at −80 ^{o}C.

Experiments varying the pH of CMs were carried out by the addition of differing volumes of HCL (acidic pH) and NaOH (alkaline pH) and pH determined using a pH meter. Aliquots of pH altered CMs were left at RT for 2 hrs then brought back to their original pH and added into the invasion chamber as outlined in section 2.5.2.

2.2.1.1 Proteomic analysis of conditioned media

CM was collected as outlined in section 2.2.1. CM was concentrated using 10,000 molecular weight cut-off concentrators (Millipore); samples were cleaned-up using ready-prep 2D clean-up kit (BioRad) and protein quantification was carried out on precipitates as outlined in section 2.9.2

2.3 *In vitro* proliferation assays

Cells in the exponential phase of growth were harvested by trypsinisation. Cell suspensions containing 1×10^4 cells/ml were prepared in cell culture medium. 100 μl/well of the cell suspension was added to 96-well plates (Costar, 3599). Plates were agitated gently in order to ensure even dispersion of cells over the surface of the wells. Cells were then incubated overnight. Cytotoxic drug dilutions were prepared at 2X their final concentration in cell culture medium. 100 μl of the drug dilutions were then added to each well. Plates were then mixed gently as above. Cells were incubated for a further 6-7 days until the control wells had reached approximately 80-90% confluency. Assessment of cell survival in the presence of drug was determined by the acid phosphatase assay (section 2.3.2). The concentration of drug which caused 50% cell kill (IC_{50} of the drug) was determined by using CalcuSyn software (Biosoft, version 2.0). Results were graphed as percentage survival (relative to the control cells) versus cytotoxic drug concentration.

2.3.1 Combination toxicity assays

Cells were set up as for *in vitro* proliferation assays (section 2.3). Following overnight incubation, a volume of 50 μl of 3x lapatinib dilutions was added to appropriate wells, 24 hrs prior to addition of 50 μl of the 5x chemotherapeutic drug. All wells contained a total final volume of 250 μl in each well (including controls). All agents were dissolved in DMSO, ethanol or media. Cells were incubated for a further 6 days. Cell number was assessed using the acid phosphatase assay (section 2.3.2). The concentration of drug, which caused the greatest efficiency in cell kill, was determined by using CalcuSyn software (Biosoft, version 2.0). Results were plotted as the percentage survival (relative to the control cells) versus cytotoxic drug concentration.

2.3.2 Assessment of cell number - Acid Phosphatase assay

A. Acid Phosphatase in 96-well plate format.
1.   Following an incubation period of 6-7 days, media was removed from the plates.

2. Each well on the plate was washed with 100 μl PBS. This was removed and 100 μl of freshly prepared phosphatase substrate (10 mM *p*-nitrophenol phosphate (Sigma 104-0) in 0.1 M sodium acetate (Sigma, S8625), 0.1% triton X-100 (BDH, 30632), pH 5.5) was added to each well. The plates were wrapped in tinfoil and incubated in the dark at 37°C for 1.5 hours.

3. The enzymatic reaction was stopped by the addition of 50 μl of 1 M NaOH to each well.

B. Acid Phosphatase in 6-well plate format.

1. Following an incubation period of 72 hours, media was removed from the plates.

2. Each well on the plate was washed with 1 ml PBS. This was removed and 2ml of freshly prepared phosphatase substrate (10 mM *p*-nitrophenol phosphate (Sigma 104-0) in 0.1 M sodium acetate (Sigma, S8625), 0.1% triton X-100 (BDH, 30632), pH 5.5) was added to each well. The plates were wrapped in tinfoil and incubated in the dark at 37°C for 2 hours.

3. The enzymatic reaction was stopped by the addition of 1 ml of 1 M NaOH to each well.

Plates were read in a dual beam plate reader at 405 nm with a reference wavelength of 620 nm.

2.3.3 CalcuSyn

CalcuSyn Version 2.0 software uses the median effect method to quantify the effects of drug combinations to determine whether they give greater effects together that expected from a simple summation of their individual effects (Chou and Talalay, 1984). CalcuSyn analysed dose effects for single and multiple drugs. Data was processed for non-mutually exclusive (drugs that are non-competitive inhibitors of each other), constant ratio combinations for two compounds. The programme graphs the data and produces reports of summary statistics for all drugs and detailed analysis of drug interactions including the Combination Index (CI) and effective dose (ED) values. CI<0.8 indicates synergism, CI > 0.8 but < 1.2 indicates an additive effect and CI > 1.2 indicates antagonism (van Waardenburg *et al*., 2004)**.**

2.4 Pulse selection of parent cell lines

A number of drug resistant variants were established from the cell lines BxPc-3, KCI-MOH1 and MiaPaCa-2 by pulse-selection with epirubicin, taxotere and gemcitabine.

2.4.1 Determination of drug concentration for pulse selection

Cells were seeded into twelve T25 cm^2 flasks at 1.5×10^5 cells per flask and allowed to attach overnight. The following day media was removed from the flask and a range of concentrations of appropriate drug was added to the flasks in duplicate. Complete media was added to two flasks as a 100% survival control. Flasks were returned to the incubator for a 4-hour incubation, after which the drug was removed. The flasks were rinsed and fed with fresh complete media. The flasks were then incubated for 5-7 days until the cells in the control flasks had reached approximately 80% confluency. At this point, medium was removed from the flasks and cells were trypsinised and counted in duplicate. The concentration of drug that caused appropriate cell kill was determined from a plot of the percentage survival relative to the control cells versus cytotoxic drug concentration. Concentrations chosen for pulse selection of BxPc-3, KCI-MOH1 and MiaPaCa-2 gave a 50-60% kill, i.e. IC50 – IC60 (Table 2.3).

Table 2.3　　　Concentrations for pulse-selection

Cell Line	Epirubicin (ng/ml)	Taxotere (ng/ml)	Gemcitabine (ng/ml)
BxPc-3	50	2	60
KCI-MOH1	100	2	50
MiaPaCa-2	64	1.2	20

2.4.2 Pulse selection

Cells at low confluency in T75 cm^2 flasks were exposed to the chosen concentration of epirubicin, taxotere or gemcitabine for 4 hours. After this period, the drug was removed and the flasks were rinsed and fed with fresh complete media. The cells were then grown in drug-free media for 6 days, refeeding every 2-3 days. This was repeated once a week for ten weeks. Some drug-selected variants could not be selected for 10 pulses as low viability was observed.

73

2.5 Extracellular matrix assays

2.5.1 Reconstitution of ECM proteins

Matrigel (Sigma, E-1270) was diluted to a working stock of 1 mg/ml in serum free DMEM. Collagen type IV (Sigma, C-5533), fibronectin (Sigma, F-2006) and laminin (Sigma, L-2020) were reconstituted in PBS to a stock concentration of 500 μg/ml. Each of the ECM proteins, collagen type IV, fibronectin and laminin were diluted to a working stock concentration of 25 μg/ml in PBS. Collagen type I (Sigma, C4361) at a stock concentration of 3.1 mg/ml was used at a working concentration of 10 μg/ml in PBS. Aliquoted stocks were stored at –20°C.

2.5.2 *In vitro* invasion assays

Invasion assays were performed using the method of Albini *et al.* (1987). 100 μl of matrigel, laminin, fibronectin and collagen type IV and I were placed into each insert (Falcon 3097) (8.0μm pore size, 24 well format) and kept at 4 °C for 24 hours. The insert and the plate were then incubated for one hour at 37 °C to allow the proteins to polymerise. Cells were harvested and resuspended in culture media containing 5% FCS at 1×10^6 cells/ml. Excess media/PBS was removed from the inserts, and they were rinsed with culture media. 100 μl of the cell suspension was added to each insert. A further 100 μl of culture media was added to each insert and 500 μl of culture media containing 5% FCS was added to the well underneath the insert. Cells were incubated for 24 hours. After this time period, the inside of the insert was wiped with a cotton swab dampened with PBS, while the outer side of the insert was stained with 0.25% crystal violet for 10 minutes and then rinsed in distilled water (dH$_2$O) and allowed to dry. The inserts were then viewed and photographed under the microscope. The invasion assays were quantified by counting cells in 10 random fields within a grid at 20x objective and graphed as the total number of cells invading at 200x magnification.

For conditioned media experiments, CM (diluted 1:1 in fresh media) was added above and below the insert and assayed as above.

2.5.3   Motility assay

Motility assays were carried out as described in section 2.5.2, without the addition of extracellular proteins.

2.5.4   Adhesion assay

Adhesion assays were performed using an adapted method of Torimura *et al.* (1999). 250 µl aliquots of ECM proteins were placed into wells of a 24-well plate. The plates were gently mixed to ensure the base of each well was completely covered with the solution. The plates were then incubated overnight at 4 ^{o}C. The excess solution was then removed from the wells and washed twice with sterile PBS. To reduce non-specific binding, 0.5 ml of sterile 0.1% BSA/PBS solution was dispensed into each well. The plates were incubated at 37 ^{o}C for 20 minutes and then rinsed twice again with sterile PBS.

Cells were harvested and resuspended in media at a concentration of 2.5×10^{4} cells/ml. 1 ml of cells were plated onto 24 wells plates in triplicate and incubated for 60 minutes. Wells that had been coated with ECM proteins but contained no cells were used as blanks. Wells containing cells but not coated with ECM proteins were used as positive controls. After 60 minutes, the medium was removed from the wells and rinsed gently with sterile PBS. Cell number attached was assessed using the acid phosphatase assay (section 2.3.2 B).

2.5.5   Preincubation of cells with matrigel coated flasks

Matrigel was coated onto flasks (1 ml/25 cm^{2}) at a concentration of 1 mg/ml. Flasks were shaken gently to ensure complete coverage of the bottom of the flask. The coated flasks were then placed at 4 ^{o}C overnight to allow the matrigel settle. Before seeding flasks with cells, the flasks were placed into an incubator at 37 ^{o}C for approximately 2 hours to allow the matrigel polymerise. The excess media in the flasks was then removed and fresh complete media containing the cell suspension was added. Cells attached to the matrigel on the bottom of the flask and after 24 hrs were removed with 0.5 ml/25 cm^{2} dispase (BD Biosciences, 354235). Dispase is a bacillus derived neutral metalo protease that recovers cells cultured on matrigel.

2.6   Soft agar assays

1.548 g of agar (Bacto Difco, 214040) was dissolved in 100 ml of ultra pure water and autoclaved. This agar was then melted in a microwave oven immediately prior to use and incubated at 44 ^{o}C. RPMI-1640 10x medium (Sigma, R1145) and DME 10x medium (Sigma, D5271) were diluted to 2x stock in dH$_2$O, filter sterilised and pH adjusted. Agar Medium (AgM) was prepared by adding equal parts agar and 2x medium. This solution was then dispensed onto 35 mm sterile petri dishes (Lux Scientific Corp., 5217). The agar was allowed to set at room temperature and the remaining AgM was returned to the water bath with the temperature reduced to 41 ^{o}C. The thermo-labile serum was added last to the Agar Medium.

Cells were harvested and resuspended in medium without serum, ensuring that a single cell suspension was obtained. The cells were diluted to give a concentration of 2×10^4 cells/ml in a total of 5 ml. 5 ml of Agar Medium was then added to each suspension, mixed well and 1.5 ml was dispensed onto each pre-set agar plate, in triplicate, giving a final concentration of 1.5×10^4 cells/plate. The plates were placed on trays containing a small volume of water to prevent the agar from drying out and incubated at 37 ^{o}C, 5% CO$_2$ for 10 days. Percentage colony forming efficiency (%CFE) was evaluated by counting the number of single cells in ten random fields on day 1 at 40x magnification. Colonies greater than 50 μm were counted on day 10, and the percentage of cells forming colonies determined.

2.7   Anoikis assay

Poly- (2-hydroxyethyl methacrylate) (poly-HEMA, Sigma, P3932) was dissolved at 12 mg/ml in 95% ethanol. To coat 24-well plates, 100 μl of poly-HEMA solution was added and allowed to dry in a laminar flow cabinet. After full evaporation, the coating step was repeated. Once evaporation was complete, wells were washed twice with sterile PBS. Cells (1×10^5 cells/ml/well) were then plated onto standard 24-well tissue plates (adherent controls) or poly-HEMA-coated plates (non-adherent) and incubated for 24 hrs at 37°C in 5% CO$_2$. After this time, 100 μl of alamar blue vital dye (Serotec, BUF012B) was added to the 24-well plates to quantitatively measure cell survival. The plate was read in a dual beam plate reader at 570 nm with a reference wavelength of

600 nm. The level of anoikis was assessed as the percentage cell death relative to adherent controls over 24 hours.

2.8   Tissue samples

Formalin-fixed paraffin-embedded tissue was kindly provided by the Histopathology Department of St. Vincent's Hospital, Dublin. 5 μm sections of tissue blocks were cut using a microtome, mounted onto poly-l-lysine coated slides. Slides were stored at room temperature until required.

2.8.1   Immunohistochemistry

All immunohistochemical studies on formalin-fixed paraffin-embedded tissue sections were performed following the method of Hsu *et al.* (1981) using an avidin-biotin horseradish peroxidase (HRP) conjugated kit (ABC) plus an appropriate secondary antibody.

Paraffin-embedded tissue samples were dewaxed in xylene (2 x 5 minutes), rehydrated in grading alcohols, 100%, 90% and 70% (2 x 3 minutes), and placed in Tris Buffered Saline (TBS/0.05% Tween-20). Endogenous peroxidase activity was quenched by placing tissue sections in 3% (vol/vol) H_2O_2/distilled water for 5-7 minutes at room temperature. All slides were blocked for non-specific staining with 20% normal rabbit serum (Dako, X-902)/TBS for 20 minutes at room temperature. Primary antibodies were applied to each sample optimally diluted in TBS/0.05% Tween-20 (antibody MDR-1, 6/1C: ascites diluted 1:40; MRP-1: neat supernatant) (Table 2.4). Primary antibodies were incubated overnight at 4^oC. Samples were then washed (3 x 5 minutes) with TBS/0.05% Tween-20; this was followed by a 30 minute incubation with biotinylated secondary antibody (rabbit anti-mouse IgG (1/300 dilution in TBS/0.05% Tween-20) (Dako, E345) or rabbit anti-rat (1/500 dilution in TBS/0.05% Tween-20). Finally, following another 3 x 5 minute wash step, Vectastain Elite ABC reagent (HRP conjugated) (Vector Laboratories, UK PK-7100) was applied for 25 minutes at room temperature. The peroxidase substrate, 3',3-daminobenzidine tetrahydrochloride (DAB) containing 0.02% H_2O_2 (Vector Laboratories, UK SK-4100) was added for 5-10 minutes at room temperature. All slides were then washed (3 x 5 minutes) TBS/0.05% Tween-20. Tissue sections were then lightly counter stained with haematoxylin (Vector Laboratories, H-3401). Slides were then dehydrated in grading alcohols, 70%,

90% and 100% (2 x 3 minutes). Samples were then cleared in xylene and mounted in DPX (BDH, UK). Negative control samples in which primary antibody were replaced by 1x TBS/0.05% Tween-20 were included in all experiments. Positive controls (normal kidney and lung tissue) using the same experimental conditions were included in all experiments.

Table 2.4 Antibodies used in Immunohistochemical analysis

Antibody	Dilution/concentration	Supplier	Reference
MDR-1, Clone 6/1C (M)	1/40	NICB	Moran *et al*. (1997).
MRP-1, (Rat)	1/40	Alexis	Filipitis *et al*. (2000).

2.8.2 Immunofluorescence

Aliquots of 100 µl of 1×10^6 cells/ml from actively growing cultures were plated directly onto coated slides. Cells were allowed to attach overnight under culture conditions. After such time, slides were washed 3x in PBS and allowed to air dry. Slides were then foil wrapped and stored at -80 ^{o}C until required. Cells were later thawed and fixed in ice-cold acetone for 5-10 minutes and allowed to air dry for 15 min prior to immunostaining. Slides were blocked for non-specific staining with 20% (v/v) normal rabbit serum for 20 min. The primary antibody was added and incubated for 1 hr at RT. Cells were washed 3x in PBS and secondary antibody, fluorescein isothicyanate-linked (FITC) anti-goat (Sigma) was added for 30 min at RT. Secondary antibody was removed and cells washed as outlined. Slides were mounted with Vectashield (Vector Laboratories, U.K) mounting medium and covered using a glass cover slip. Cells were viewed and photographed using a Nikon phase contrast microscope fitted with an FITC filter.

2.9 Western blotting techniques

2.9.1 Whole cell extract preparation

Cells were grown to 80-90% confluency in cell culture grade petri dishes. Media was removed and cells were washed twice with ice cold PBS. All procedures from this point forward were performed on ice. Cells were lysed with 200-300 μl of NP-40 lysis buffer and incubated on ice for 20 minutes. Table 2.5 below provides the details of the lysis buffer. Immediately before use, 10 μl of the 100X protease and phosphatase inhibitors listed in table 2.6 were added to 1 ml of lysis buffer.

Table 2.5   NP-40 lysis buffer

Addition required per 500ml stock	Final concentration
425 ml dH$_2$O water	-
25 ml 1 M Tris-HCl (pH 7.5)	50 mM Tris-HCl (pH 7.5)
15 ml 5 M NaCl	150 mM NaCl
2.5 ml NP-40	0.5% NP-40

Table 2.6   NP-40 lysis buffer 100X stocks

100X stock	Preparation instructions
100 mM DTT	154 mg in 10 ml dH$_2$O
100 mM PMSF	174 mg in 10 ml 100% ethanol
100X Protease inhibitors	2.5 mg/ml leupeptin, 2.5 mg/ml aprotinin, 15 mg/ml benzamidine and 1 mg/ml trypsin inhibitor in dH$_2$O

Cells were then removed with a cell scraper and further homogenised by passing through a 21 G syringe. Sample lysates were centrifuged at 14000 rpm for 10 minutes at 4 $^{\circ}$C. Supernatant containing extracted protein was transferred to a fresh chilled eppendorf tube. Protein concentration was quantified using the Biorad assay as detailed in Section 2.9.2. Samples were then stored in aliquots at -80°C.

2.9.2 Protein Quantification

Protein levels were determined using the Bio-Rad protein assay kit (Bio-Rad, 500-0006) as follows. A 2 mg/ml bovine serum albumin (BSA) solution (Sigma, A9543)

was prepared freshly in lysis buffer. A protein standard curve (0, 0.2, 0.4, 0.6, 0.8 and 1.0 mg/ml) was prepared from the BSA stock with dilutions made in lysis buffer. The Bio-Rad reagent was diluted 1:5 in dH_2O water. 8 µl of protein standard dilution or sample (diluted 1:10) was added to 392 µl of diluted dye reagent and the mixture vortexed. The protein standards and samples were added in triplicate onto a 96-well plate. After 5 minutes incubation, absorbance was assessed at 570 nm. The concentration of the protein samples was determined from the plot of the absorbance at 570 nm versus concentration of the protein standard.

2.9.3 Gel electrophoresis

Proteins for analysis by Western blotting were resolved using SDS-polyacrylamide gel electrophoresis (SDS-PAGE). The stacking and resolving gels were prepared as illustrated in table 2.7 or precast 7.5% gels were used (Lonza).

Table 2.7   Preparation protocol for SDS-PAGE gels (2 x 0.75mm gels)

Components	10% Resolving Gel	5% Stacking Gel
Acrylamide stock	4.6 ml	670 µl
dH_2O	5.6 ml	2.7 ml
1.875 M Tris-HCl pH 8.8	3.5 ml	-
1.25 M Tris-HCl pH 6.8	-	500 µl
10% SDS	140 µl	40 µl
10% NH_4- persulfate	140 µl	40 µl
TEMED	**5.6 µl**	4 µl

The acrylamide stock in table 2.7 consists of a 30% (29:1) ratio of acrylamide:bis-acrylamide (Sigma, A2792). In advance of samples being loaded in to the relevant sample wells, 20-40 µg of protein was diluted in 10x loading buffer. Molecular weight markers (Sigma, C4105) were loaded alongside samples. The gels were run at constant amplitude (45mA) until the bromophenol blue dye front reached the end of the gel, at which time sufficient resolution of the molecular weight markers was achieved.

2.9.4 Western blotting

Western Blotting was performed by the method of Towbin *et al*. (1979). Once electrophoresis was complete, the SDS-PAGE gel was equilibrated in transfer buffer (25 mM Tris (Sigma, T8404), 192 mM glycine (Sigma, G7126), pH 8.3-8.5) for approximately 15 minutes. Six sheets of Whatman 3 mm filter paper were soaked in freshly prepared transfer buffer. These were then placed on the cathode plate of a semi-dry blotting apparatus (Bio-rad). Air pockets were then removed from between the filter paper. Nitrocellulose membrane (GE Healthcare, RPN 303D), which had been equilibrated in the same transfer buffer, was placed over the filter paper on the cathode plate. Air pockets were once again removed. The gels were then aligned on to the membrane. Six additional sheets of transfer buffer soaked filter paper were placed on top of the gel and all air pockets removed. The anode was carefully laid on top of the stack and the proteins were transferred from the gel to the membrane at a current of 34 mA at 15 V for 30-40 minutes, until all colour markers had transferred. Following protein transfer, membranes were stained using PonceauS (Sigma, P7170) to ensure efficient protein transfer. The membranes were then blocked overnight using 5% skimmed milk powder in PBS at 4 °C. Membranes were incubated with primary antibody for 2-3 hours at RT (Table 2.8) and a negative control where the membrane was exposed to antibody diluent was also performed. Antibodies were prepared in 1% skimmed milk powder in PBS. Primary antibody was removed after this period and the membranes rinsed 3 times with PBS containing 0.5% Tween 20 (Sigma P1379) for a total of 15-30 minutes. Secondary antibody (1 in 1,000 dilution of anti-mouse IgG peroxidase conjugate (Sigma, A4914)) in PBS, was added for 1.5 hour at room temperature. The membranes were washed thoroughly in PBS containing 0.5% Tween for 15 minutes.

Table 2.8   List of primary, secondary antibodies and dilutions

Primary Antibody	Dilution	
MDR-1/P-gp	1/100	sc-59589, Santa Cruz Biotechnology
MRP-1	1/100	sc-59607, Santa Cruz Biotechnology
Integrin Beta 1	1/500	MAB1951Z-20, Chemicon
Integrin Alpha 4	1/500	MAB1945, Chemicon
Integrin Alpha 5	1/500	AB1949, Chemicon

Integrin Alpha 6	1/200	MAB1982, Chemicon
Aldehyde dehydrogenase 1A1	1/500	Ab9893, Abcam
Vimentin	1/500	V4630, Sigma
Cytokeratin 18	1/200	sc-6259, Santa Cruz Biotechnology
Triosephosphatase 1	1/500	Ab28760, Abcam
Stress-induced phosphoprotein 1	1/200	sc-15276, Santa Cruz Biotechnology
GAPDH	1μg/ml	AM4300, Ambion
Gelsolin	1/500	G4896, Sigma
Galectin 1	1/500	Ab25138, Abcam
Nucleotide diphosphate kinase	1/200	Ab37627, Abcam
Bip	1/200	610978, BD Bioscience
β-actin	1:10,000	A5441, Sigma
α-Tubulin	1/1000	T6199, Sigma
EGFR	1/100	Ab-15, Lab Vision
HER2	1/1000	OP15, Oncogene Research Products
Secondary Antibody	**Dilution**	
Anti-mouse	1/1000	A6782, Sigma
Anti-rat	1/1000	R5130, Sigma
Anti-rabbit	1/500	18772, Sigma
Anti-goat	1/500	Sc2098, Santa Cruz Biotechnology

2.9.5 Enhanced chemiluminescence (ECL) detection

Immunoblots were developed using Luminol (Santa Cruz), which facilitated the detection of bound peroxidase-conjugated secondary antibody. Following the final washing membranes were incubated with Western blot Luminol reagent (Santa Cruz, sc-2048). 3 ml of a 50:50 mixture of Luminol reagent was used to cover the membrane. The membrane was wrapped in clingfilm. The membrane was then exposed to autoradiographic film (Kodak, X-OMATS) for various times (from 10 seconds to 30 minutes depending on the signal). The exposed autoradiographic film was developed for 3 minutes in developer (Kodak, LX-24). The film was then washed in water for 15 seconds and transferred to a fixative (Kodak, FX-40) for 5 minutes. The film was then washed with water for 5-10 minutes and left to dry at room temperature.

2.10 Proteomic analysis

2.10.1 Sample preparation

Cells were grown to 60-70% confluency in 175cm^2 flasks, trypsinised and allowed to attach to matrigel for 24 hrs and managed according to section 2.5.5. Cell pellets were then washed twice in ice cold PBS and twice in sucrose buffer and the resulting pellet was stored at -80 ^{o}C.

2.10.2 Total protein extraction

All proteomic analysis detailed in this thesis was carried out by Dr. Paul Dowling. Cell pellets were reconstituted with 1ml of the following complete lysis buffer: (4% w/v CHAPS, 7 M urea, 2 M thiourea, 10 mM Tris-HCL, 5 mM magnesium acetate pH 8.5). Immediately before use, 10μl of 100x stocks of DNase and RNase were added to 1ml of lysis buffer. The lysate was then homogenised by passing though a 25-gauge needle 6 times. The cell lysate was placed on an orbital shaker and shaken for 1 hour at room temperature. The protein lysate was then transferred to an eppendorf and centrifuged at 14,000 rpm for 20 minutes at 10 ^{o}C to remove insoluble material. The resulting supernatant was transferred to a fresh microcentrifuge tube and its pH was checked to ensure it was between pH 8.0-9.0 by spotting 3 μl onto a pH indicator strip. The sample was then divided into smaller aliquots and stored at –80 ^{o}C. The protein concentration was quantified using the Biorad method. Biological replicates (n=3) of each cell line were prepared.

2.11 Protein sample labelling

2.11.1 Preparation of dye stock solution (1 nmol/μl)

The three CyDye DIGE Fluor Minimal dyes (Cy3, Cy5 and Cy2 (GE Healthcare, 25-8010-65) were thawed from –20 ^{o}C to room temperature for 5 minutes. To each microfuge tube dimethylformamide (DMF) (Aldrich, 22,705-6) was added to a concentration of 1 nmol/μl. Each microfuge tube was vortexed vigorously for 30 sec to dissolve the dye. The tubes were then centrifuged for 30 sec at 14,000 rpm in a microcentrifuge. The reconstituted dyes were stored at –20 ^{o}C for up to two months.

2.11.2 Preparation of 10 μl working dye solution (200 pmol/μl)

On thawing, the dye stock solutions were centrifuged in a microcentrifuge for 30 seconds. To make 10 μl of the three working dye solutions, 8 μl of DMF was added to 2 μl of 1 nmol/μl stock of Cy2, Cy3 and Cy5 i.e. 200 pmol/μl working stock. The dyes were stored at -20 ^{o}C in tinfoil in the dark for 3 months.

2.11.3 Protein labelling

The comparative protein samples equivalent to 50 μg was placed into eppendorf tubes and labelled with the Cy3 and Cy5 minimal dyes. Each tube was mixed by vortexing, centrifuged and then left on ice for 30 minutes in the dark. The reaction was quenched with a 50-fold molar excess of free lysine to dye for 10 minutes on ice in the dark. The labelled samples were stored at –80 ^{o}C. The Cy2 pool for each gel (50 μg) contained an equal concentration aliquot of each of the protein samples. To this 1 μl of each dye (200 pmol/μl) was added to 50 μg of protein sample. An equal volume of 2x sample buffer (2.5 ml rehydration buffer stock solution (7 M urea, 2 M thiourea, 4 % CHAPS), pharmalyte broad range pH 4-7 (2%) (GE Healthcare, 17-6000-86), DTT (2%) (Sigma, D9163)) was added to the labelled protein samples. The mixture was left on ice for at least 10 minutes then applied to Immobiline DryStrips for isoelectric focussing.

2.12 First dimension separation - isoelectric focussing

2.12.1 Strip rehydration

Immobiline 24 cm linear pH gradient (GE Healthcare, IPG) strips, pH 3-11 were rehydrated in rehydration buffer solution (7 M urea, 2 M thiourea, 4% CHAPS, 0.5% IPG buffer, 50 mM DTT). Each strip was overlaid with about 3 ml IPG Cover Fluid (GE Healthcare, 17-1335-01) and allowed to rehydrate overnight (or at least 12 hours) at RT.

2.12.2 Isoelectric focussing

IEF was performed using an IPGphor apparatus (GE Healthcare). The cover of the IPGphor unit was closed and the desired programme selected (40 kV/h at 20 ^{o}C with resistance set at 50 mA). On completion of the IEF run, the strips were drained of the

cover fluid and stored in glass tubes at –80 $^{\circ}$C or used directly in the second dimension.

2.13 Second Dimension – SDS polyacrylamide gel electrophoresis

2.13.1 Equilibration of focussed Immobiline DryStrips

Strips were equilibrated for 20 min in 50 mM Tris-HCL, pH 8.8, 6 M urea, 30% v/v glycerol, 1% w/v SDS containing 65 mM DTT and then for 20 min in the same buffer containing 240 mM iodoacetamide. The 12.5 % acrylamide gel solution was prepared in a glass beaker (acrylamide/bis 40 %, 1.5 M Tris pH 8.8, 10 % SDS). Prior to pouring, 10 % ammonium persulfate and 100 µl neat TEMED were added. The gels were overlaid with 1 ml saturated butanol. The gels were left to set for at least three hours at RT. Equilibrated IPG strips were transferred onto 24 cm 12.5% uniform polyacrylamide gels poured between low fluorescence glass plates. Strips were overlaid with 0.5% w/v low melting point agarose in running buffer containing bromophenol blue. Gels were run at 2.5 W/gel for 30 min and then 100 W total at 10 $^{\circ}$C until the dye front had run off the bottom of the gels. All the images were collected on a Typhoon 9400 Variable Mode Imager (GE Healthcare).

2.13.2 Scanning DIGE labelled samples

The appropriate emission filters and lasers were then selected in the Typhoon Variable Mode Imager (GE Healthcare) for the separate dyes (Cy2 520 BP40 Blue (488), Cy3 580 BP30 Green (532) and Cy5 670 BP 30 Red (633)). Gels were scanned at 100 pixel resolution, resulting in the generation of three images, one each for Cy2, Cy3 and Cy5. Once the scanning was completed, the gel images were imported into the ImageQuant software. All gels were cropped identically to facilitate spot matching in the Decyder BVA module.

2.14 Analysis of gel images

2.14.1 Differential in-gel analysis (DIA)

The DIA module processes a triplet of images from a single gel. The internal standard is loaded as the primary image followed by the secondary and tertiary image, derived from, for example, a control and treated sample. Spot detection and calculation of

spots properties were performed for each image from the same gel. The software determined the margins of the spots, quantified the spot intensities and calculated the relative spot intensity as the ratio between the total intensity of the gel and the intensity of each individual spot. The protein spots were then normalised using the in-gel linked internal standard. The data from the first gel was XML formatted and exported into the Biological Variation Analysis (BVA) software for further analysis. This procedure was repeated for each gel in the experiment.

2.14.2 Biological variation analysis (BVA)

Once all gels from the experiment were loaded into the BVA module, the experiment design was set up and the images were assigned into three groups (standard, control and treated). The spots on the gels were then matched across all gels in the experiment. This module detects the consistency of the differences between samples across all the gels. The software standardises the relative spot intensity of the Cy5 image to that of the Cy3 image in the same gel. The standardised spot intensity was then averaged across the triplicate gels. The BVA module detected the consistency of the differences between samples across all the gels and applied statistics to associate a level of confidence for each of the differences. The protein spots with statistically significant protein expression changes were designated "proteins of interest" and placed in a pick list.

Preparative gels for spot picking with 300 μg of protein/gel were focussed and run out on SDS-PAGE gels. The gels were then stained with colloidal coomassie and deep purple (section 2.14.3, 2.14.4). Spots that showed differential protein expression were picked with the ETTAN Spot Picker (section 2.14.3).

2.14.3 Staining- Brilliant blue G Colloidal coomassie and Deep purple staining of preparative gels for spot picking

After electrophoresis, the smaller lower plates with the gels attached were placed in the gel boxes containing fixing solution (7% glacial acetic acid in 40% (v/v) methanol (Aldrich, 200-659-6)) for at least 1 hour. During this step a 1X working solution of Brilliant Blue G colloidal coomassie (Sigma, B2025) was prepared by adding 800ml UHP to the stock bottle. When the fixing step had nearly elapsed a solution containing 4 parts of 1X working colloidal coomassie solution and 1 part methanol was made,

mixed by vortexing for 30 seconds and then placed on top of the gels. The gels were left to stain for 2 hours. To destain, a solution containing 10% acetic acid in 25% methanol was poured over the shaking gels for 60 seconds. The gels were then rinsed with 25% methanol for 30 seconds and then destained with 25% methanol for 24 hours. Alternatively, after fixing solution, gels were washed 3x in wash buffer (35 mM sodium hydrogen and 300 mM sodium carbonate in water) and further washed in water. Deep purple stain (GE Healthcare, RPN6305) was then added to the gels, diluted 1/200 in water, and incubated for 1 hr. Gels were destained in 7.5% (v/v) acetic acid in the dark for 15 min and repeated. The glass surface was dried and two reference markers (GE Healthcare) attached to the underside of the glass plate before scanning. The resulting image was imported into the ImageMaster software (GE Healthcare) and the spots were detected, normalised and the reference markers selected. All spots of interest were manually selected. The resulting image was saved and exported into the Ettan Spot Picker software.

2.14.4 Spot picking

The stained gel was placed in the tray of the Ettan Spot Picker (GE Healthcare, 18-1145-28) with reference markers (GE Healthcare, 18-1143-34), aligned appropriately and covered with UHP. The imported pick list was opened, the syringe primed and the system was set up for picking the spots from the pick list. The spots were robotically picked and placed in 96-well plates (Greiner), which were stored at 4°C until spot digestion.

2.14.5 Spot digestion

The 96-well plate was placed in the Ettan Digester (GE Healthcare, 18-1142-68) to digest the protein. The gel plugs were washed 3x for 20 minutes each with 50µl 50mM ammonium bicarbonate (Sigma, A6141) in 50% methanol, followed by 3x wash for 15 min with 50µl 70% acetonitrile (Sigma, 34967). The gel plugs were left to dry. After drying, the individual gel pieces were rehydrated in 10µl digestion buffer (12.5ng trypsin (Promega, V5111) per µl of 10% acetonitrile, 40mM ammonium bicarbonate). Exhaustive digestion was carried out overnight at 37°C. A volume of 40µl of 0.1% trifluoroacetic acid (Sigma, 302031) in 50% acetonitrile was added to the wells, mixed and left for 20 minutes. A volume of 60µl of this solution was transferred to a fresh 96-

well plate. A volume of 30 µl of 0.1% trifluoroacetic acid in 50% acetonitrile was added to the wells, mixed and left for 20 minutes. A volume of 50µl of this solution was transferred to the fresh 96-well plate. The liquid in the plate was vacuum-dried in a Maxi dry plus (Speed Vac, MSC, Dublin). After drying, the 96-well plate was placed in the Ettan Spotter (GE Healthcare, 18-1142-67) for spotting onto the target plates. A volume of 3 µl of 0.5% trifluoroacetic acid in 50% acetonitrile was added to the desiccated peptides and mixed 5 times. A volume of 0.3 µl of this mixture was spotted onto the target plate after which a volume of 0.3 µl matrix solution [7.5 mg/ml a-cyano-4-hydroxycinnamic acid (LaserBio labs, 28166-41-8) in 0.1% trifluoroacetic acid in 50% acetonitrile] was added.

2.14.6 Identification of proteins with MALDI-TOF

The target plate was placed in the MALDI-ToF (GE Healthcare, 11-0010-87) instrument. Mass spectra were recorded operating in the positive reflectron mode at the following parameters: accelerating voltage 20 kV; and pulsed extraction: on (focus mass 2500). Internal calibration was performed using trypsin autolysis peaks at 842.509 m/z, 2211.104 m/z and external calibration was performed using PepMix 4 respectively. Calibration using Pep4 was performed. The mass spectra generated for each of the proteins were analyzed using MALDI evaluation software (GE Healthcare). Protein identification was achieved with the PMF Pro-Found search engine for peptide mass fingerprints.

2.15 PathwayStudio of identified proteins

PathwayStudio 4.0 is a bioinfomatic product aimed at the visualisation and analysis of biological pathways, gene regulation networks and protein interaction maps. It comes with a comprehensive database that gives a snapshot of all information available in PubMed, with the focus on pathways and cell signalling networks. PathwayStudio permits the identification of biological interactions among genes and proteins of interest from the published literature, and provides links to the supporting sentences in the matching journal article citations (for articles available online in PubMed). The software can also connect two genes/proteins with the shortest possible path, import a list of genes/proteins, which can then be arranged into a pathway and finally find

common upstream and downstream regulators of a gene/protein. Graph drawing, layout optimisation, data filtering, pathway expansion and classification and prioritisation of proteins were all possible. PathwayStudio workes by identifying relationships among genes, small molecules, cell objects and processes and builds pathways based on these relationships.
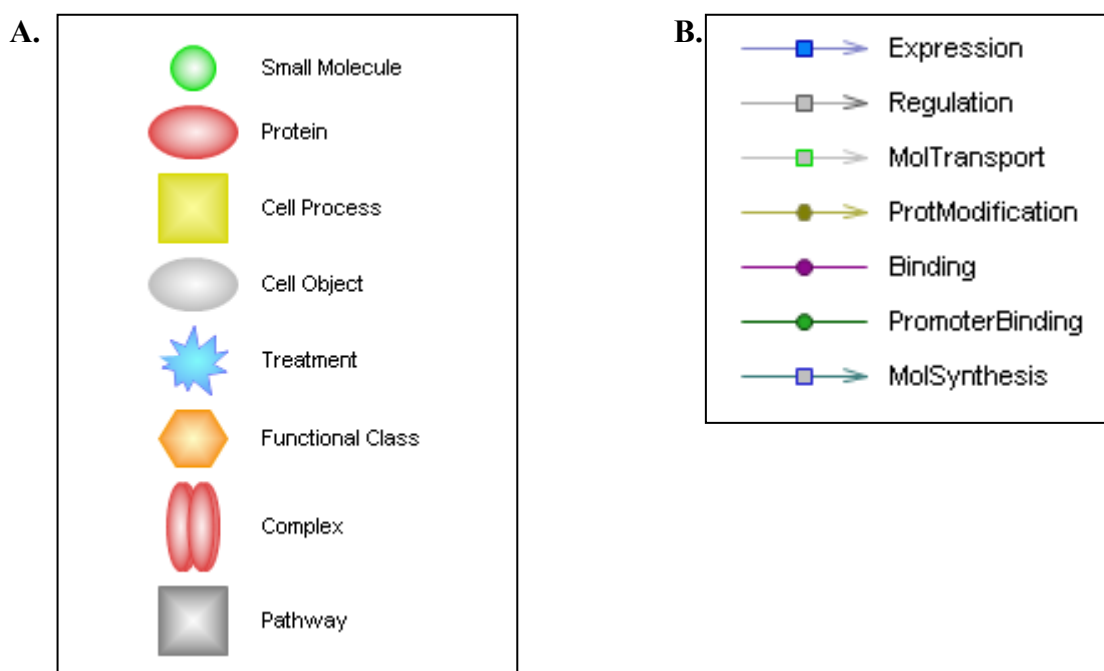
Figure 2.1: PathwayStudio® A. Eight different types of 'nodes' are represented in a unique graphical form. Each 'node' details the molecule name, alias, description, HUGO ID, Swiss Prot ID, MGI ID, OMIM ID, Locuslink ID, RGD ID, Unigene ID, Gene Ontology terms, and organism name. **B.** 'Controls' are represented as arrows with different colours in the network, each representing a type of control/interaction. The dots on each 'control' arrow is clickable to obtain the description of an interaction and the relevant MedLine articles.

2.16 RNA interference (RNAi)

RNAi using small interfering RNAs (siRNAs) was carried out to silence specific genes. The siRNAs used were chemically synthesised (Ambion Inc). These siRNAs were 21-23 bps in length and were introduced to the cells via reverse transfection with the transfection agent siPORT^{TM} *Neo*FX^{TM} (Ambion Inc., 4511).

2.16.1 Transfection optimisation

In order to determine the optimal conditions for siRNA transfection, optimisation with kinesin siRNA (Ambion Inc., 16704) was carried out for each cell line. There were a number of different parameters that had to be determined to establish an optimised protocol for the siRNA transfection of MiaPaCa-2 and its single cell population clones. Cell suspensions were prepared at 1×10^5, 3×10^5 and 5×10^5 cells per ml. Solutions of negative control and kinesin siRNAs at a final concentration of 30 nM were prepared in optiMEM (Gibco^{TM}, 31985). NeoFX solutions at a range of concentrations were prepared in optiMEM in duplicate and incubated at room temperature for 10 minutes. After incubation, either negative control or kinesin siRNA solution was added to each neoFX concentration. These solutions were mixed well and incubated for a further 10 minutes at room temperature. 100 µl of the siRNA/neoFX solutions were added to each well of a 6-well plate. 1 ml of the relevant cell concentrations were added to each well. The plates were mixed gently and incubated at 37°C for 24 hours. After 24 hours, the transfection mixture was removed from the cells and the plates were fed with fresh medium. The plates were assayed for changes in proliferation at 72 hours using the acid phosphatase assay (Section 2.3.2 B). Optimal conditions for transfection were determined as the combination of conditions which gave the greatest reduction in cell number after kinesin siRNA transfection and also the least cell kill in the presence of transfection reagent.

Optimisation of siRNA for GAPDH was also carried out using the above parameters to determine accurate transfection knock down at the protein level. Western blot analysis was used to establish the optimum conditions for a siRNA transfection. The optimised conditions for the cell lines are shown in Table 2.11.

Table 2.11   Optimised conditions for siRNA transfection

Cell line	Seeding density per 96-well	Seeding density per 6-well	Volume NeoFX per 96 well (µl)	Volume NeoFX per 6 well (µl)
MiaPaCa-2	2.5×10^3	3×10^5	0.2	2
Mia clone #3	2.5×10^3	3×10^5	0.2	2
Mia clone #8	2.5×10^3	3×10^5	0.2	2

2.16.2 siRNA functional analysis of targets MiaPaCa-2 and its sub-populations Clone #3 and Clone #8

Three pre-designed siRNAs were chosen for each of the protein/gene targets and transfected into cells. Two siRNAs were used if a validated siRNA was available. Validated siRNAs have been verified by real-time RT-PCR to reduce gene expression of >70% 48 hours post-transfection. For each set of siRNA transfections carried out, control, non-transfected (NT) cells and a scrambled (SCR) siRNA transfected control were used. Scrambled siRNA are sequences that do not have homology to any genomic sequence. The scrambled non-targeting siRNA used in this study is commercially produced, and guarantees siRNA with a sequence that does not target any gene product. It has also been functionally proven to have no significant effects on cell proliferation, morphology and viability. For each set of experiments investigating the effect of siRNA, the cells transfected with target-specific siRNAs were compared to cells transfected with scrambled siRNA. This took account of any effects due to the transfection procedure, reagents, and also any random effects of the scrambled siRNA. Kinesin was used as a control to assess the efficiency of the siRNA transfection. Kinesin plays an important role in cell division; facilitating cellular mitosis. Therefore, transfection of siRNA kinesin resulted in cell cycle arrest and confirmed efficient transfection. Western blots (section 2.9) were used to determine if siRNA had an efficient knock-down effect at a protein level. Table 2.12 outline the list of siRNAs and IDs used in this thesis.

Table 2.12   List of siRNAs used

Target name	Ambion IDs
Scrambled	17010
Kinesin	14851
GAPDH	4300
Integrin Beta 1 #1	109877 (validated)
Integrin Beta 1 #2	109878
Integrin Beta 1 #3	109879
Integrin Alpha 5 #1	111113
Integrin Alpha 5 #2	106729
Integrin Alpha 5 #3	106728

Integrin Alpha 6 #1	103827 (validated)
Integrin Alpha 6 #2	8146
ALDH1A1 #1	106197
ALDH1A1 #2	106196
ALDH1A1 #3	106195
VIM #1	13111
VIM #2	138994
VIM #3	138993
STIP1 #1	136103
STIP1 #1	136104
STIP1 #1	18523
GSN #1	8127
GSN #2	8031

2.16.3 Invasion assays on siRNA transfected cells

Using the optimised conditions in Table 2.11, each of the siRNAs was tested to see changes in invasion of the cells after transfection. Two-three separate siRNAs were used for each target gene (Table 2.12). All siRNAs were purchased from Ambion Inc.

To assay for changes in invasive capacity, siRNA experiments in 6-well plates were set up using 2 μl NeoFx to transfect 30 nM siRNA at a cell density of $3x10^5$ per well of a 6-well plate. Transfection medium was removed after 24 hours and replaced with fresh growth medium. The transfected cells were assayed for changes in invasion capacity at 48 hours using the *in vitro* invasion assay described in Section 2.5.2. All experiments were carried out independently at least three times.

2.16.4 Adhesion assays on siRNA transfected cells

To assay for changes in adhesion abilities, siRNA experiments in 6-well plates were set up using 2 μl NeoFx to transfect 30nM siRNA in a cell density of $3x10^5$ per well of a 6-well plate. Transfection medium was removed after 24 hours and replaced with fresh growth medium. The transfected cells were assayed for changes in adhesion abilities at 48 hours using the optimised *in vitro* adhesion assay described in section 2.5.3. All experiments were carried out independently at least three times.

2.16.5 Anoikis assays on siRNA transfected cells

Forty-eight hrs post transfection (as previously described, table 2.11) in 6-well plates, cells were tested in anoikis assays (section 2.6) to determine changes in the ability to survive in suspension conditions. All experiments were carried out independently at least three times.

2.16.6 Proliferation assays on siRNA transfected cells

As described in table 2.11, cells were seeded using 0.2 µl Neofx to transfect 30 nM siRNA in a cell density of 2.5×10^3 per well of a 96-well plate. After 24 hrs, transfection medium was replaced with fresh media and cells were allowed to grow until they reached 80-90% confluency, a total of 5 days. Cell number was assessed using the acid phosphatase assay (section 2.3.2). All experiments were carried out independently at least three times.

2.16.7 Chemosensitivity assay on siRNA transfected cells

Assays were set up as described above (section 2.12.6). 24 hrs after addition of fresh media, appropriate concentrations (2x) of chemotherapeutic drugs were added to the wells in duplicate and incubated for 3 days. Drug was aspirated and cells washed 3x with PBS. Cells were then trypsinised and resuspended to 150 µl in fresh media. From the suspension, 30 µl was transferred to a fresh 96-well plate in the presence of fresh media. The plates were assayed for changes in proliferation at 96 hrs using the acid phosphatase assay (Section 2.3.2).

2.16.8 Transfection of Clone #8 with ALDH1A1 cDNA

The target cell line was trypsinised in 6-well plates and set up at 50-70% confluency. Following incubation overnight at 37^oC, transfection mixtures were prepared and combined as outlined in table 2.13, and incubated for 15 minutes at RT. Control wells were untreated and empty vector controls contained transfection mixture without cDNA in the presence of empty plasmid, pCMV6-XL5 (Figure 2.3) (Origene). The transfection mixture was added directly onto cells in 6-well plate and incubated for a further 48 hrs. Western blotting (section 2.9) and invasion assays (section 2.5.2) were then carried out.

Table 2.13 Volumes for efficient cDNA transfection

Vessel type	Optimem	Transfection reagent	Optimem	ALDH1A1 cDNA expression plasmid
6-well plate	**125 μl**	**5 μl**	**125 μl**	**2 μg- ALDH1A1 cDNA (Origene)**
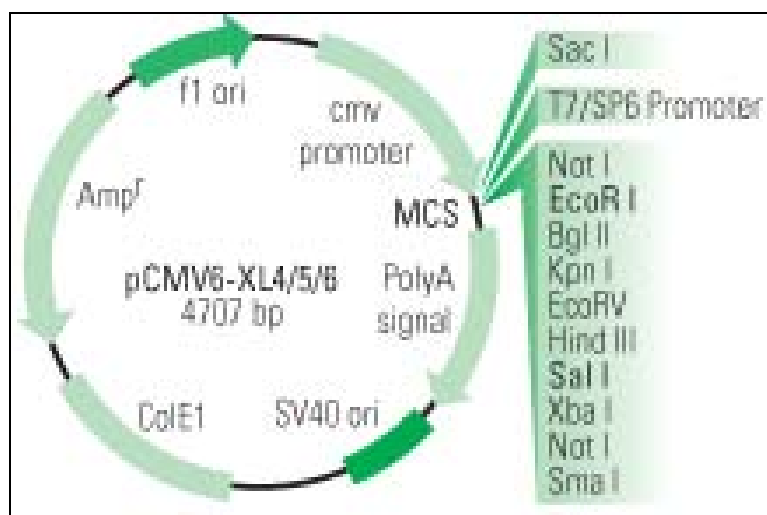
Figure 2.3 Schematic of plasmid vector

2.17 Statistical analysis

Analysis of the difference of comparisons, as well as untreated versus siRNA treated mean invasion and motility counts, adherence absorbance, anoikis and percentage survival calculated, were performed using a student t-test (two-tailed with unequal variance), on Microsoft Excel. In the siRNA experiments, siRNA scrambled transfected cells were used as control compared to siRNA treated samples. This was to ensure no 'off-target' effects of the transfection procedure. Non-treated controls were used to ensure scrambled siRNA was having no effects and to normalise data.

*, A p value of ≤ 0.05 was deemed significant

**, A p value ≤ 0.01 was deemed more significant

***, A p value ≤ 0.005 was deemed highly significant

3.0   Results

3.1   Chemosensitivity profile of BxPc-3, KCI-MOH1 and MiaPaCa-2 cell lines

In order to determine the relative resistance of the pancreatic cancer cell lines to a range of structurally distinct and molecularly different chemotherapeutic drugs, proliferation assays were performed (Chapter 2.3). The cell lines were analysed using an *in vitro* proliferation assay to determine the IC_{50} (concentration of drug that inhibits proliferation of 50% of the cell population) of the following drugs: epirubicin, taxotere, gemcitabine, taxol, 5-fluorouracil, vincristine, VP-16, adriamycin, carboplatin and cisplatin.

There was a considerable difference in sensitivity between the cell lines to the panel of chemotherapeutic drugs studied. BxPc-3 showed high resistance to epirubicin and VP-16 compared to both KCI-MOH1 and MiaPaCa-2. MiaPaCa-2 also displayed sensitivity to adriamycin and vincristine. The chemo-sensitivity profiles for several drugs are similar in the three pancreatic cell lines, such as taxotere, taxol, carboplatin and cisplatin. However, there are significant differences in sensitivity to certain drugs, for example, gemcitabine, which is the drug of choice for pancreatic cancer. The KCI-MOH1 cell line appears to be more sensitive to gemcitabine than either BxPc-3 or MiaPaCa-2. Interestingly BxPc-3 appears to be less sensitive to epirubicin, although not to adriamycin or to VP-16 as compared to the other two cell lines (Table 3.1.1).

In conclusion, the pancreatic cancer cell lines generally displayed a modest inherent resistance to the panel of ten chemotherapeutic drugs analysed. In some cases, the resistance profile seems to indicate the same mechanistic mode of resistance, whereby cells showing increased resistance to gemcitabine also display resistance to 5-fluorouracil.

Table 3.1.1 IC_{50} values of pancreatic cell lines to a panel of chemotherapeutic agents (results are expressed as $IC_{50} \pm$ SD, *n*=3).

Chemotherapeutic agent (ng/ml)	BxPc-3	KCI-MOH1	MiaPaCa-2
Epirubicin	37.2 ± 6.7	5.6 ± 0.7	14 ± 2.2
Gemcitabine	1.7 ± 0.2	0.5 ± 0.1	1.3 ± 0.1
5-Fluorouracil (µg/ml)	0.5 ± 0.04	0.17 ± 0.02	0.5 ± 0.1
Taxotere	0.4 ± 0.05	0.43 ± 0.1	0.4 ± 0.04
Taxol	1.4 ± 0.2	1.8 ± 0.7	1.7 ± 0.1
Adriamycin	42.3 ± 3.0	40.3 ± 4.4	16.7 ± 2.3
Carboplatin (µg/ml)	2.8 ± 0.3	4.3 ± 0.4	6.1 ± 0.4
Cisplatin (µg/ml)	0.2 ± 0.05	0.2 ± 0.01	0.4 ± 0.05
VP-16	477.4 ± 49.5	33.2 ± 3.7	171.5 ± 9.4
Vincristine	2.3 ± 0.2	2.6 ± 0.3	0.6 ± 0.1

3.1.1 Pulse selection of cell lines

Three pancreatic cancer cell lines, BxPc-3, KCI-MOH1 and MiaPaCa-2 were chosen for drug treatment. The cell lines were pulsed with epirubicin, taxotere and gemcitabine for four hours, once a week for 10 weeks (Chapter 2.4.2). These drugs are clinically relevant and were used at different concentrations based on cell line sensitivity to the chemotherapeutic drugs as outlined in table 3.1.2. All drug concentrations were within the range of physiological achievable concentration *in vivo*.

Table 3.1.2   Concentrations for pulse-selection

Cell line	Epirubicin (ng/ml)	Taxotere (ng/ml)	Gemcitabine (ng/ml)
BxPc-3	50	n/a	60
KCI-MOH1	100	2	50
MiaPaCa-2	64	1.2	20

(n/a refers to the unsuccessful establishment of taxotere-selected BxPc-3 variant)

3.1.1.1 Changes in resistance to chemotherapeutic drugs in selected variants

Pulse selection of the above cell lines with epirubicin, taxotere and gemcitabine resulted in the establishment of nine novel cell lines. Cell lines selected with epirubicin, taxotere and gemcitabine were denoted "/Epi", "/Txt" and "/Gem" respectively.

After the 10 pulses, the pulse selected cell lines exhibited a modest increase in resistance to the selecting drug (Tables 3.1.3-3.1.5).

3.1.2 Cross-resistance profile of pulse-selected variants

When cell lines are repeatedly exposed to a chemotherapeutic drug, they may develop resistance to the selecting drug and also develop to a variety of other chemotherapeutic drugs which are unrelated in molecular structure and target specificity; this is termed cross-resistance. To investigate this phenomenon, the cross-resistance profiles to a variety of drugs were tested in the BxPc-3, KCI-MOH1 and MiaPaCa-2 selected variants.

3.1.2.1 BxPc-3 pulse-selected variants

The IC_{50} concentrations, fold resistance information and p values of the BxPc-3 pulse-selected variants are shown in table 3.1.3.

Bx/Epi was generated after 10 pulses with 50 ng/ml epirubicin. The epirubicin variant exhibits a modest 1.4-fold increase in resistance to epirubicin and cross-resistance to adriamycin (1.7-fold) and vincristine (1.5-fold). The cell line showed similar sensitivity to gemcitabine, taxol and VP-16 as the parental cell line. Bx/Epi exhibited cross-sensitivity to 5-fluorouracil, taxotere, carboplatin and cisplatin.

The gemcitabine-selected variant was established after 10 pulses with 60 ng/ml gemcitabine. Bx/Gem exhibited no increase in resistance to gemcitabine or VP-16. However, cross-resistance was observed with epirubicin (1.7-fold) and vincristine (1.2-fold). Increased sensitivity was observed to 5-fluorouracil and taxotere. Carboplatin sensitivity was increased whereas resistance to cisplatin was increased 1.3-fold.

A taxotere variant of BxPc-3 could not be successfully established.

Table 3.1.3 IC_{50} concentrations and fold resistance of BxPc-3 drug selected variants (results are expressed as $IC_{50} \pm SD$, *n*=3).

Chemotherapeutic agent (ng/ml)	BxPc-3 IC_{50}	Bx/Epi IC_{50}	Fold resistance Bx/Epi	Bx/Gem IC_{50}	Fold resistance Bx/Gem
Epirubicin	38.7 ± 6.3	52.3 ± 26.0	1.4	54.7 ± 26.1	1.7
Gemcitabine	1.7 ± 0.2	1.5 ± 0.1	0.8	1.7 ± 0.1	1.0
5-Fluorouracil (µg/ml)	0.5 ± 0.04	0.2 ± 0.2	0.4	0.3 ± 0.1	0.6**
Taxotere	0.4 ± 0.3	0.3 ± 0.04	0.7*	0.2 ± 0.2	0.8
Taxol	1.4 ± 0.2	1.5 ± 0.1	1.2	1.5 ± 0.1	1.1***
Adriamycin	42.3 ± 3.0	72.2 ± 17.0	1.7*	65.3 ± 30.8	1.1
Carboplatin (µg/ml)	3.3± 0.7	2.1 ±0.05	0.6	2.6 ± 0.6	0.9**
Cisplatin (µg/ml)	0.2 ± 0.04	0.2 ± 0.01	0.8	0.28 ± 0.08	1.3*
VP-16 (µg/ml)	0.5 ± 0.05	0.4 ± 0.1	0.9	0.5 ± 0.09	1.0
Vincristine	2.3 ± 0.2	3.5 ± 0.3	1.5	2.6 ± 1.0	1.2***

* p value ≤ 0.05, ** p value ≤ 0.01, *** p value ≤ 0.005

3.1.2.2 KCI-MOH1 pulse-selected variants

The IC_{50} concentrations, fold resistance information and p values denoted by; $* \leq 0.05$, $** \leq 0.01$, $*** \leq 0.005$ of the KCI-MOH1 pulse-selected variants are shown in table 3.1.4.

KCI/Epi was established after 10 pulses with 100 ng/ml epirubicin. The selected variant displayed 8-fold resistance to epirubicin compared to the parental cell line. Cross-resistance profiling showed that an increase in resistance was also observed for gemcitabine (2.1-fold), taxol (1.5-fold), carboplatin (1.4-fold) and VP-16 (2.5-fold). A significant decrease in response to adriamycin and vincristine was demonstrated suggesting an alternative mode of multidrug resistance other than MDR-1 and MRP-1.

The gemcitabine-selected variant was generated after 10 pulses with 50 ng/ml gemcitabine. A significant increase in resistance of 2608-fold was observed to the selecting drug. KCI/Gem also displayed cross-resistance to epirubicin (7.3-fold), taxol (2.6-fold) and VP-16 (3.0-fold). A slight increase in resistance to taxotere and cisplatin was observed. Resistance to 5-fluorouracil, adriamycin, carboplatin and vincristine were decreased.

The taxotere-selected variant, KCI/Txt was established after 10 pulses with 2 ng/ml taxotere. No resistance was developed against the selecting drug; in fact the cells displayed a marked sensitivity to taxotere. Cells also showed a decrease in resistance to adriamycin, cisplatin, and vincristine. An increase in resistance was observed for epirubicin (9.0-fold), gemcitabine (2.5-fold), 5-fluorouracil (1.5-fold), taxol (2.4-fold), carboplatin (1.4-fold), and VP-16 (3.0-fold).

Table 3.1.4   IC$_{50}$ concentrations and fold resistance of KCI-MOH1 drug selected variants

Chemotherapeutic agent	KCIMOH1 IC$_{50}$	KCI/Epi IC$_{50}$	Fold resistance KCI/Epi	KCI/Gem IC$_{50}$	Fold resistance KCI/Gem	KCI/Txt IC$_{50}$	Fold resistance KCI/Txt
Epirubicin	5.6 ± 0.7	45.1 ± 4.7	8.0***	41.1 ± 5.2	7.3**	50.2 ± 8.8	9.0
Gemcitabine	0.5 ± 0.1	1.1 ± 0.2	2.1*	1394 ± 219	2608**	1.3 ± 0.2	2.5
5-Fluorouracil (µg/ml)	0.17 ± 0.02	0.2 ± 0.2	1.1	0.1 ± 0.01	0.5**	0.3 ± 0.03	1.5*
Taxotere	0.43 ± 0.1	0.2 ± 0.002	1.1	0.5 ± 0.03	1.1	0.3 ± 0.1	0.8*
Taxol	1.8 ± 0.7	2.6 ± 0.2	1.4	4.5 ± 0.8	2.5**	4.2 ± 0.4	2.3**
Adriamycin	40.3 ± 4.4	25.1 ± 3.6	0.6**	25.1 ± 1.7	0.6*	28.6 ± 1.3	0.7
Carboplatin (µg/ml)	4.3 ± 0.4	5.8 ± 0.1	1.4**	2.6 ± 0.1	0.6**	6.1 ± 1.0	1.4
Cisplatin (µg/ml)	0.2 ± 0.01	0.2 ± 0.05	1.1	0.3 ± 0.05	1.5*	0.2 ± 0.02	0.9
VP-16	33.2 ± 3.7	82.2 ± 8.3	2.5***	99.1 ± 9.0	3.0***	99.1 ± 7.4	3.0*
Vincristine	2.6 ± 0.3	1.7 ± 0.3	0.6**	1.8 ± 0.2	0.7*	1.8 ± 0.1	0.7

3.1.2.3 MiaPaCa-2 pulse-selected variants

The IC_{50} concentrations, fold resistance information and *p* values denoted by; * ≤ 0.05, ** ≤ 0.01, *** ≤ 0.005 of the MiaPaCa-2 pulse selected variants are shown in table 3.1.5.

Mia/Epi was established after 10 pulses with 64 ng/ml epirubicin. The selected variant displayed a significant 1.7-fold increase in resistance to epirubicin compared to the parental cell line. Cross-resistance profiling showed an increase in resistance to gemcitabine (1.6-fold), taxotere (1.4-fold), adriamycin (2.6-fold), carboplatin (1.4-fold), cisplatin (1.5-fold), VP-16 (2.3-fold) and vincristine (2.8-fold). No change in resistance was observed for taxol.

The taxotere-selected variant, Mia/Txt was established after 10 pulses with 1.2 ng/ml taxotere. Table 2.3.3 shows that resistance to taxotere was increased 1.2-fold, while taxol resistance was similarly increased (1.2-fold). Cross-resistance profiling showed modest increases in resistance to gemcitabine (2.5-fold), cisplatin (1.5-fold) and carboplatin (1.2-fold). A decrease in resistance was observed for epirubicin, 5-fluorouracil, adriamycin, VP-16 and vincristine.

Mia/Gem established through 10 pulses with 20 ng/ml gemcitabine displayed a significant increase in resistance to gemcitabine (1.3-fold). Cross-resistance was also observed to 5-fluorouracil (1.2-fold), epirubicin (1.2-fold), taxotere (1.3-fold), taxol (1.4-fold), adriamycin (2.6-fold), VP-16 (1.3-fold) and vincristine (2.8-fold). Cells displayed a modest increase in resistance to carboplatin while, a slight decrease in resistance to cisplatin was observed.

Table 3.1.5   IC$_{50}$ concentrations and fold resistance of MiaPaCa-2 drug selected variants

Chemotherapeutic agent	MiaPaCa-2 IC$_{50}$	Mia/Epi IC$_{50}$	Fold resistance Mia/Epi	Mia/Gem IC$_{50}$	Fold resistance Mia/Gem	Mia/Txt IC$_{50}$	Fold resistance Mia/Txt
Epirubicin	14 ± 2.2	24.3 ± 2.1	1.7***	17.9 ± 1.5	1.2*	3.9 ± 0.5	0.3***
Gemcitabine	1.3 ± 0.1	2 ± 0.1	1.6***	1.7 ± 0.1	1.3**	3.1 ± 0.3	2.5*
5-Fluorouracil (µg/ml)	0.5 ± 0.1	0.5 ± 0.1	1.1	0.6 ± 0.0.4	1.2	0.2 ± 0.0.3	0.5***
Taxotere	0.4 ± 0.04	0.5 ± 0.01	1.4**	0.5 ± 0.1	1.3	0.5 ± 0.2	1.2
Taxol	1.7 ± 0.1	1.6 ± 0.2	1.0	2.3 ± 0.3	1.4	2.0 ± 0.2	1.2
Adriamycin	16.7 ± 2.3	44.0 ± 2.9	2.6***	42.8 ± 7.0	2.6*	6.0 ± 1.0	0.4***
Carboplatin (µg/ml)	6.1 ± 0.4	8.6 ± 0.7	1.4	6.6 ± 1.3	1.1	7.4 ± 1.3	1.2
Cisplatin (µg/ml)	0.4 ± 0.05	0.7 ± 0.02	1.5*	0.4 ± 0.1	0.9	0.6 ± 0.09	1.5*
VP-16	171.5 ± 9.4	400.8 ± 57.7	2.3*	222.8 ± 14.2	1.3***	82.2 ± 12.8	0.5***
Vincristine	0.6 ± 0.1	1.7 ± 0.3	2.8*	1.7 ± 0.1	2.8***	0.5 ± 0.3	0.9

3.1.3 P-gp and MRP-1 expression in pulse-selected variants

Expression of two drug resistance pumps (P-gp and MRP-1) were investigated by Western blot in our panel of drug selected cell lines (Chapter 2.9). Figure 3.1.1 (A) shows no detection of P-gp in our panel of pulse-selected variants. (B) MRP-1 protein was detected at very low levels in the BxPc-3 cell line; however, there is no distinguishable difference in MRP-1 expression between parental BxPc-3 and epirubicin and gemcitabine-selected variants. MRP-1 was not detected in KCI-MOH1 and MiaPaCa-2 or their drug-selected variants.
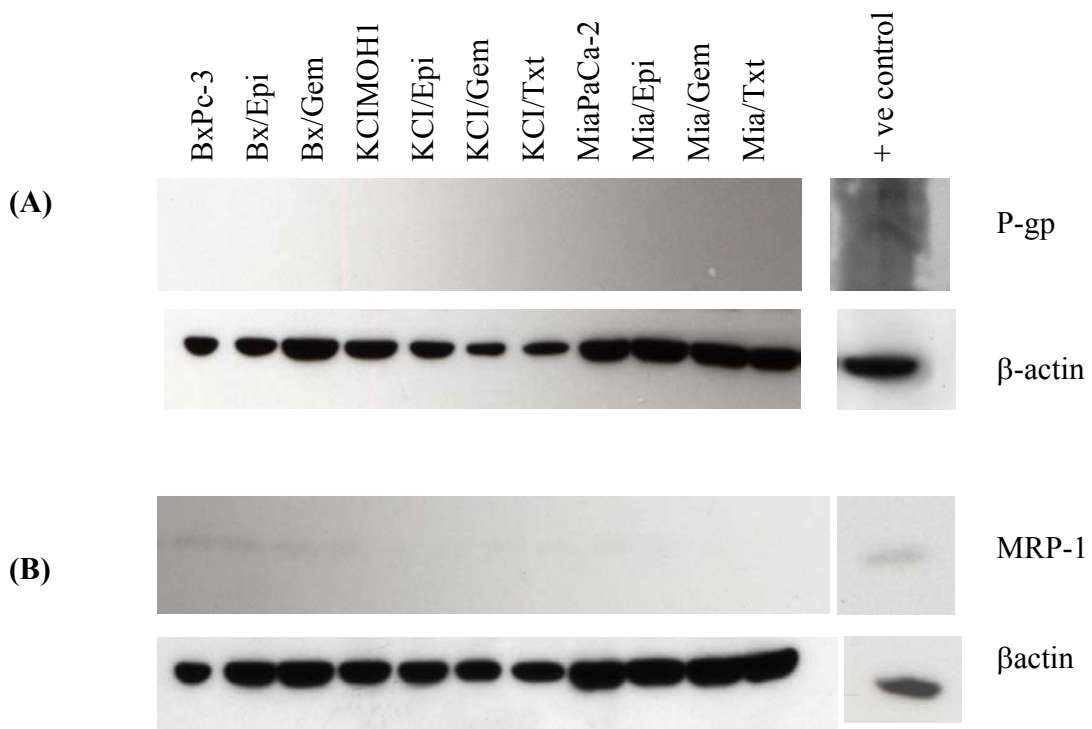
Figure 3.1.1 Western blot analysis of (A) P-gp and (B) MRP-1 in our panel of drug-selected pancreatic cancer cell lines. B-actin was used as loading control.

3.1.4 Invasion assays

Invasion assays were performed on the drug selected variants to investigate the possible association between drug resistance and invasion. Invasion assays were performed on epirubicin, taxotere and gemcitabine selected variants of BxPc-3, KCI-MOH1 and MiaPaCa-2 as outlined in Chapter 2.5.2.

3.1.4.1 Invasion assay of parental cell lines

The invasion assays performed on the parental cell lines show variable degrees of invasion. BxPc-3 displays the highest level of invasion through matrigel-coated invasion inserts. The scale of invasion as shown in figure 3.1.2 is as follows: BxPc-3>KCI-MOH1>MiaPaCa-2.
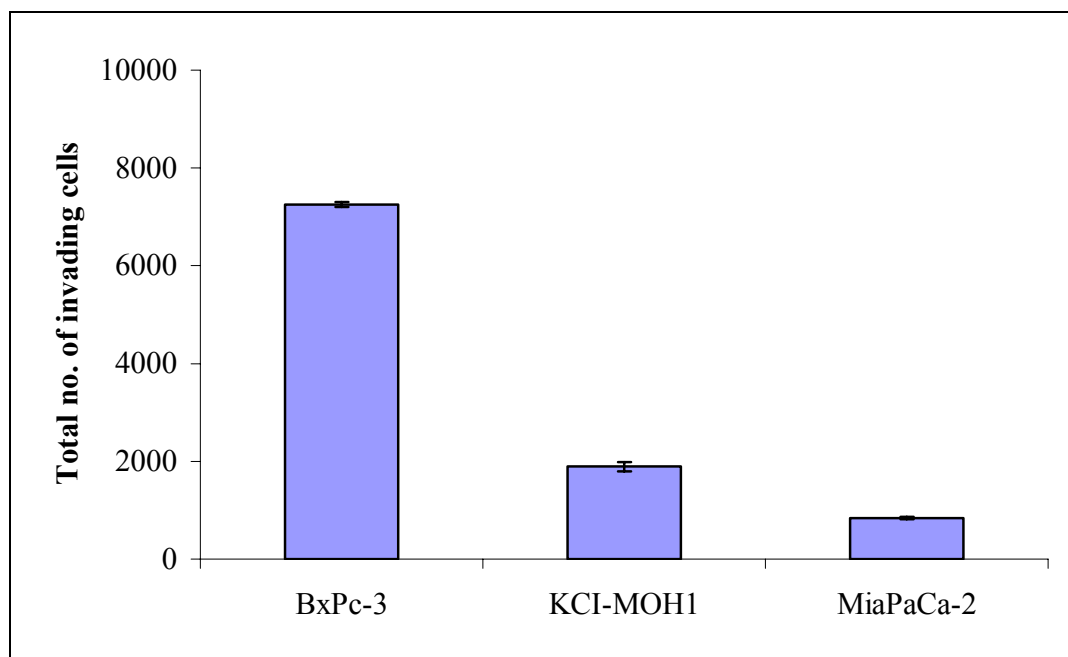
Figure 3.1.2 Invasion assays of BxPc-3, KCI-MOH1 and MiaPaCa-2

3.1.4.2 Invasion of drug-selected cell lines

The BxPc-3 parent cell line was the most invasive cell line used in this study. After pulse-selecting the cells with epirubicin and gemcitabine, the variants showed increased invasion activity compared to the parental line (Figure 3.1.3). Bx/Epi displayed a significant increase in invasion ($p=0.002$), while Bx/Gem also displayed a slight but significant increase in invasion ($p=0.05$).

The KCI-MOH1 cell line showed modest invasion through the matrigel-coated insert, however, the epirubicin and gemcitabine-selected variants showed a significant increase in invasion compared to the parental cell line ($p \leq 0.001$). The taxotere-selected cell line, KCI/Txt showed a slight decrease in invasion (Figure 3.1.4).

MiaPaCa-2 displayed the lowest level of invasion. After pulse-selecting the cells with epirubicin and gemcitabine, the selected variants became significantly more invasive than the parent cell line ($p \leq 0.001$). Mia/Txt showed no significant change in invasion capacity compared MiaPaCa-2 (Figure 3.1.5).

(A)
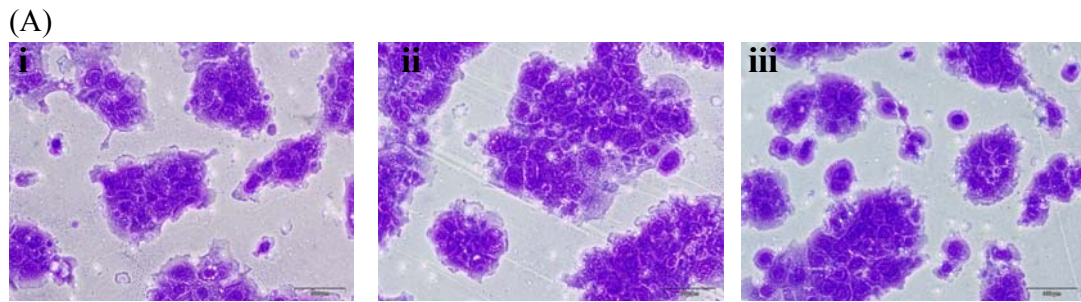
(B)
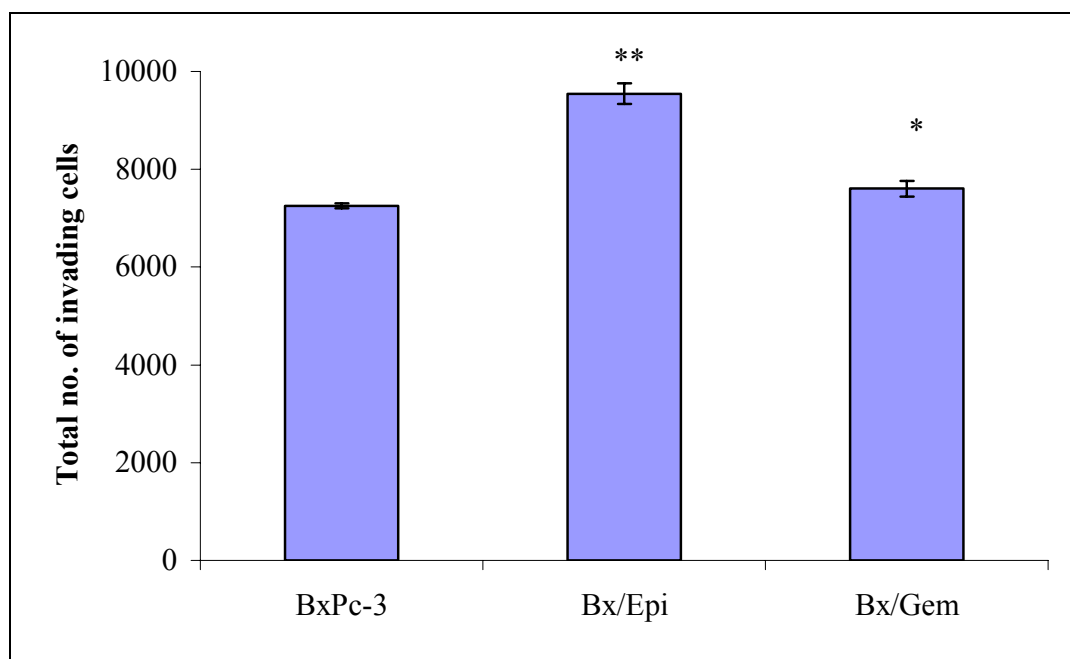
Figure 3.1.3 (A) Invasion assay of (i) BxPc-3, (ii) Bx/Epi, (iii) Bx/Gem through matrigel. Magnification, 200x. Scale bar, 200 μm. (B) Quantified invasion assay of BxPc-3, Bx/Epi and Bx/Gem.

Statistics; * p ≤ 0.05, ** p ≤ 0.01, *** p ≤ 0.005 Student's t-test

(A)
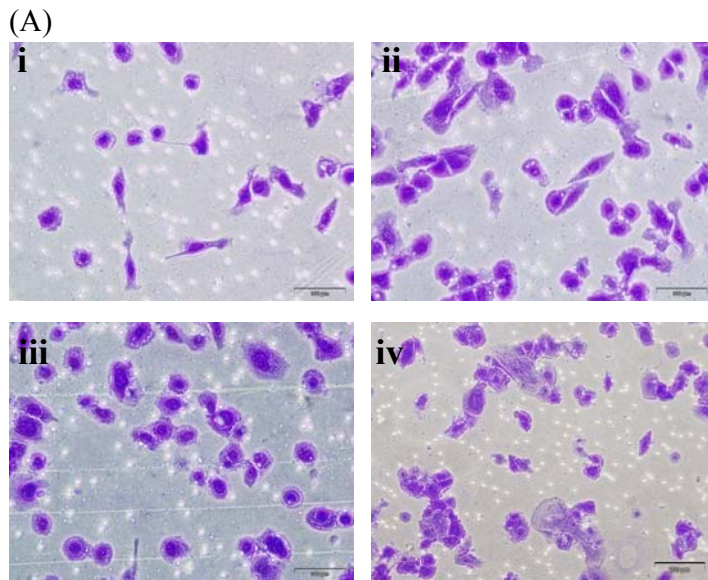
(B)
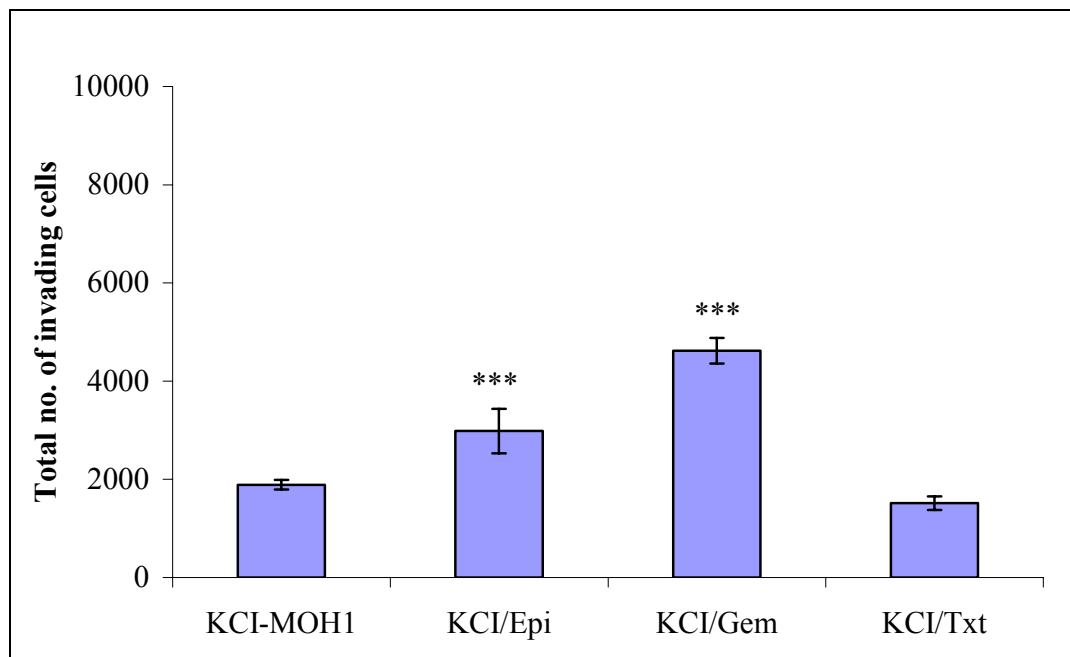
Figure 3.1.4 A. Invasion of (i) KCI-MOH1, (ii) KCI/Epi, (iii) KCI/Gem through matrigel. Magnification, 200x. Scale bar, 200 μm. B. Quantified invasion assay of KCI-MOH1, KCI/Epi, KCI/Gem and KCI/Txt.

Statistics; * p ≤ 0.05, ** p ≤ 0.01, *** p ≤ 0.005 Student's t-test.

(A)

(B)
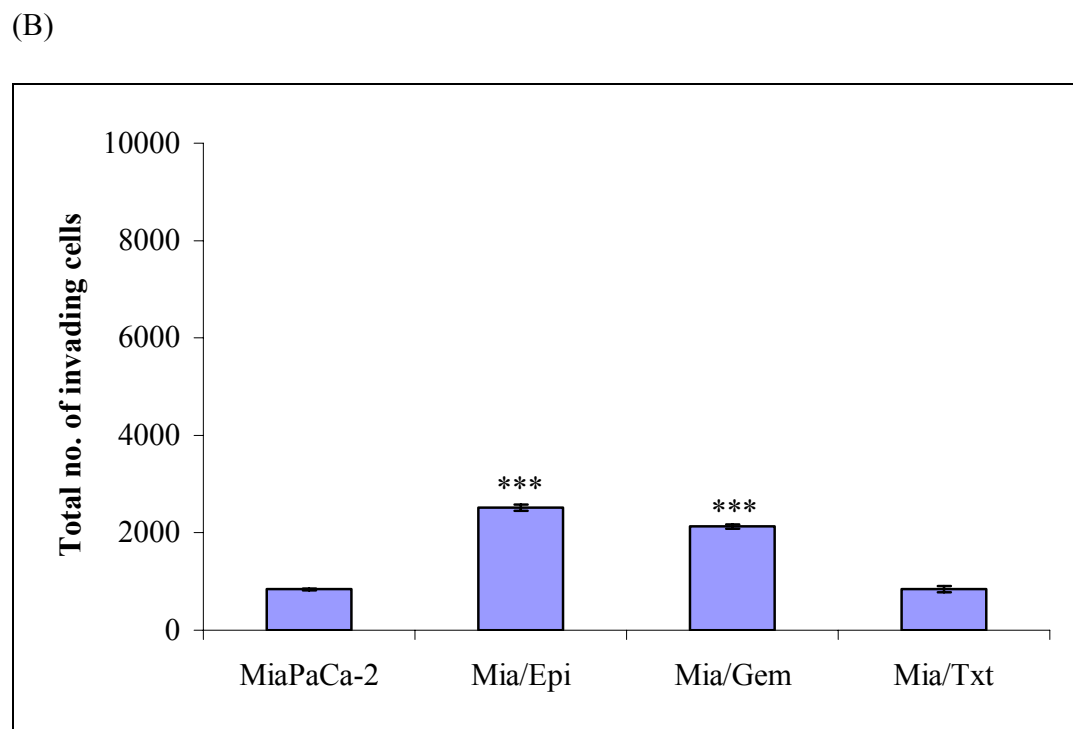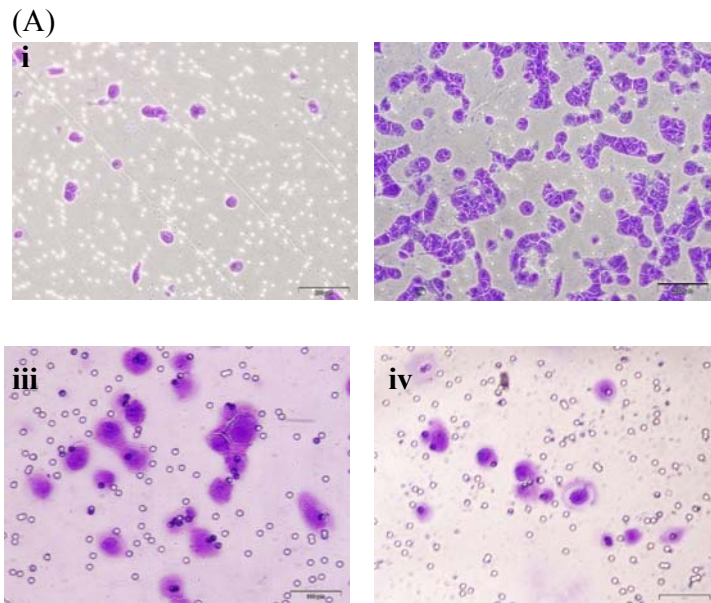
Figure 3.1.5 A. Invasion of (i) MiaPaCa-2, (ii) Mia/Epi, (iii) Mia/Gem and (iv) Mia/Txt through matrigel. Magnification, 200x. Scale bar, 200 μm. B. Quantified invasion assay of MiaPaCa-2, Mia/Epi, Mia/Gem and Mia/Txt

Statistics; * p ≤ 0.05, ** p ≤ 0.01, *** p ≤ 0.005 Student's t-test.

3.2 MDR-associated protein expression in pancreatic carcinoma patients

Drug resistance is one of the major obstacles in the treatment of pancreatic cancer. Increased export of cytotoxic drugs from tumour cells is one of the key mechanisms of drug resistance. Many of the proteins responsible in this drug efflux belong to the family of ABC transporters.

Primary pancreatic carcinoma specimens from 45 patients were included in this study. Formalin-fixed paraffin embedded tumour samples from the 45 patients were analysed by means of immunohistochemistry for expression of MDR-1/P-gp and MRP-1 using monoclonal antibodies (MAbs) (Chapter 2.8.1, table 2.3.1). Tumours stained with appropriate MAbs were scored and presented as the percentage of positive tumour cells and intensity (Table 3.2.1).

Relevant histopathological information was available for 42 cases (Table 3.2.2). Information on patient age at diagnosis was available for 37 cases; age ranged from 32 to 73 years and the median age was 62 years. Data on tumour type was available for 42 cases; 34 tumours were classified as adenocarcinoma, 4 were endocrine/neuro-endocrine, 3 were cholangiocarcinoma and one was a retro-pancreatic malignant GIST. Six tumours were poorly differentiated, twenty-five were moderately differentiated and seven were well differentiated (data was unavailable for 7 cases). Table 3.2.3 outlines the grade system used to classify the extent of differentiation in cancer cells.

Table 3.2.1 Percentage and intensity grade of staining

Percentage grade of staining	Intensity grade of staining
1= 10<25%	Level 1 = weak staining
2= 25-50%	Level 2 = strong staining
3= 50<75%	Level 3 = intense staining
4= 75<100%	

Table 3.2.2 Summary of histopathological information for 42 patients

Age (years)	Tumour type	Differentiation status
Range, 32-73	Adenocarcinoma, 34	Poorly differentiated, 6
Median, 62	Endocrine/neuro-endocrine, 4	Moderately differentiated, 25
	Cholangiocarcinoma, 3	Well differentiated, 7
	Retro-pancreatic malignant, GIST 1	

Table 3.2.3 Histological grading of tumours

Histopathological grade	Classification
Grade X	Cannot be assessed
Grade I	Well differentiated (greater than 95% of tumour composed of glands)
Grade II	Moderately differentiated (50-95% of tumour composed of glands
Grade III	Poorly differentiated (40% or less of tumour composed of glands)

3.2.1 MDR-1/P-glycoprotein protein expression

MDR-1/P-glycoprotein (P-gp) protein expression was studied in 45 pancreatic tumour specimens. Immunohistochemical analysis results are presented in table 3.2.4. Representative tumours stained with the P-gp specific MAb, 6/1C (Moran *et al*., 1997) are shown in figure 3.2.1.

Our findings show that P-gp was expressed in 93% (42/45) of pancreatic tumours (Table 3.2.4). Approximately 12% (5/42) scored 1+, 10% (4/42) scored 2+, 24% (10/42) scored 3+, while 55% (23/42) scored 4+. Weak staining was observed in 10% (4/42) of cases, intermediate staining in 52% (22/42) and strong staining in 38% (16/42) of cases. Three cases showed no P-gp expression.

Table 3.2.5 shows the distribution and percentage of P-gp positive tumours in relation to age at diagnosis, tumour size, histological grade and nodal status. The majority of patients in this study were over 50 and displayed a higher expression of P-gp positivity (93%) than patients under 50 (89%). A weak association between P-gp expression and larger tumour size was displayed; higher P-gp expression levels (93%) were observed in larger size tumours ($\geq$ 2cm), while 67% of smaller tumours ($\leq$ 2cm) displayed P-gp positivity. Histological grade II appeared to be more strongly associated with P-gp expression (100%). In node positive patients, 94% of specimens expressed P-gp, while 87% of samples from node negative patients expressed P-gp. It is important to note that no statistical significant association was determined for P-gp positivity and histopathological features.

Table 3.2.4   Summary of P-gp staining and intensity expression

Percentage grade of staining	Number of cases	Intensity grade of staining		
		Strong (+3)	Intermediate (+2)	Weak (+1)
0	3	-------------	-------------	-------------
1+ (1<25%)	5	--------------	3	2
2+ (25-50%)	4	--------------	4	--------------
3+ (50<75%)	10	3	6	1
4+ (>75%)	23	13	9	1

Table 3.2.5   P-gp expression in pancreatic carcinomas and association with age at diagnosis, tumour size, histological grade and nodal status (*n*=45)

	Number positive	Percentage positive
Age		
<50 years	8/9	89%
>50 years	26/28	93%
Unknown n=8		
Tumour size		
≤2 cm	2/3	67%
≥2 cm	26/28	93%
Unknown n=14		
Histological grade		
Grade I (well-differentiated)	5/7	71.5%
Grade II (moderately-differentiated)	25/25	100%
Grade III (poorly-differentiated)	5/6	83%
Unknown n=7		
Nodal status		
Node positive patients	16/17	94%
Node negative patients	13/15	87%
Unknown n=13		

A.
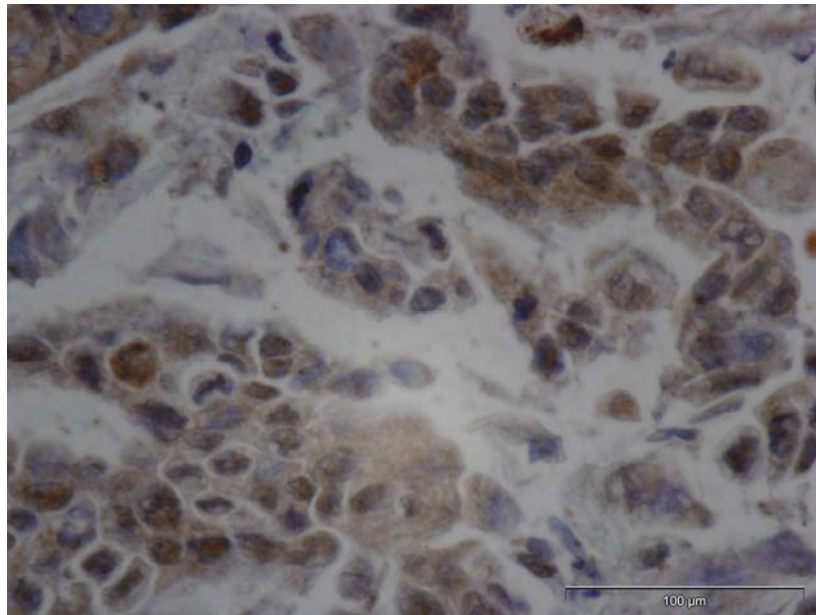
B.
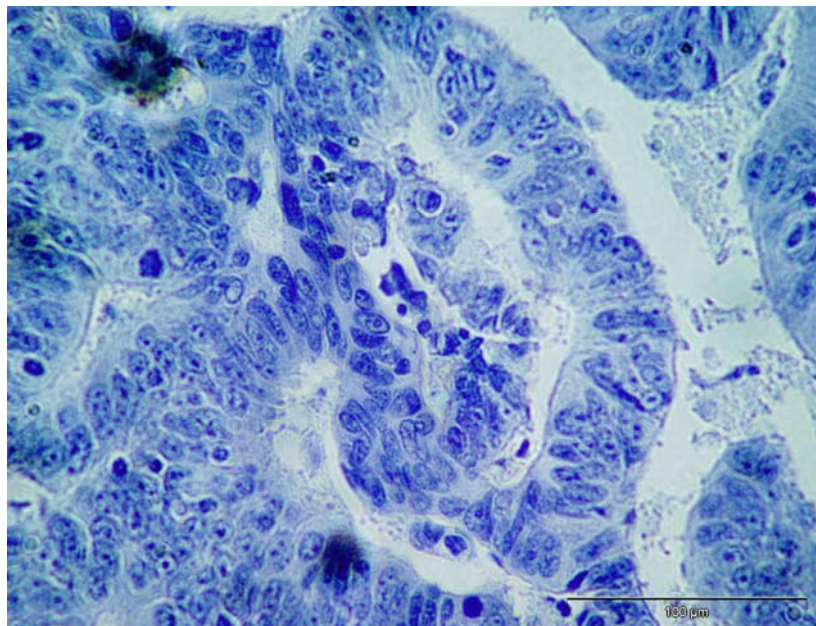
Figure 3.2.1 Immunohistochemical analysis of P-gp expression
A. Intense P-gp positivity is observed in the pancreatic tumour sample (4+3), stained with anti- MDR-1, 6/1C. B. Negative control specimen. Magnification, 400x, scale bar, 100 μm.

3.2.2 MRP-1 protein expression

MRP-1 protein expression was studied in 45 specimens from pancreatic tumour patients. Immunohistochemical analysis results are presented in table 3.2.6. Representative tumours stained with the MRP-1 specific MAb, (Alexis, ALX-801-007-C250) are represented in figure 3.2.2.

We found that MRP-1 protein was expressed in 31% of pancreatic tumours (Table 3.2.6). Approximately 14% (2/14) scored 1+, 14% (2/14) scored 2+, 57% (8/14) scored 3+ and 14% (2/14) scored 4+. Weak staining was observed in 36% (5/14) of cases, intermediate staining in 29% (4/14) and strong staining in 36% (5/14).

Sixty-nine percent (31/45) of tumours did not show MRP-1 protein expression.

Patients over 50 years displayed a higher percentage of MRP-1 expression (46.5%) than patients under 50 (11%). A weak association between MRP-1 expression and larger tumour size was observed; higher MRP-1 expression levels (39%) were observed in larger tumours ($\geq$ 2 cm) compared to smaller tumours ($\leq$ 2 cm) of which all specimens were MRP-1 negative. Histological grade II appeared to be more strongly associated with MRP-1 expression (40%). In specimens from node positive patients, 29% of samples expressed MRP-1, while 53% of samples from node negative patients expressed MRP-1 (Table 3.2.7). No statistical significant association was observed for MRP-1 expression and histopathological features.

Table 3.2.6   Summary of MRP-1 staining and intensity expression

Percentage grade of staining	Number of cases	Intensity grade of staining		
		Strong (+3)	Intermediate (+2)	Weak (+1)
0	31	--------------	--------------	--------------
1+ (1<25%)	2	1	---------------	1
2+ (25-50%)	2	1	---------------	1
3+ (50<75%)	8	2	3	3
4+ (>75%)	2	1	1	---------------

Table 3.2.7   MRP-1 expression in pancreatic cancer and association with age at diagnosis, tumour size, and histological grade and nodal status (*n*=45)

	Number positive	Percentage positive
Age		
<50 years	1/9	11%
>50 years	13/28	46.5%
Unknown n=8		
Tumour size		
≤2 cm	0/3	0%
≥2 cm	11/28	39%
Unknown n=14		
Histological grade		
Grade I (well-differentiated)	1/7	14%
Grade II (moderately-differentiated)	10/25	40%
Grade III (poorly-differentiated)	2/6	33%
Unknown n=7		
Nodal status		
Node positive patients	5/17	29%
Node negative patients	8/15	53%
Unknown n=13		
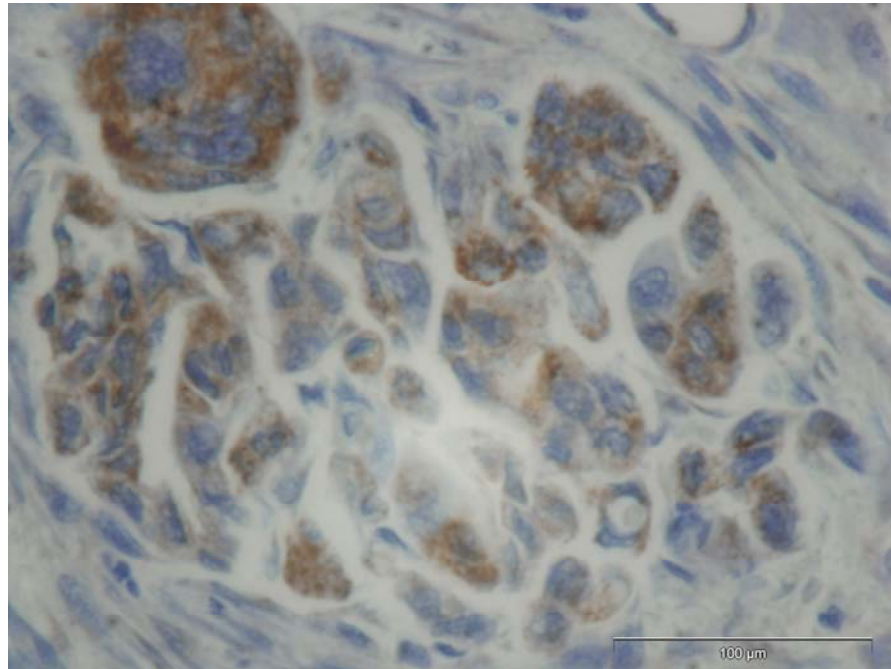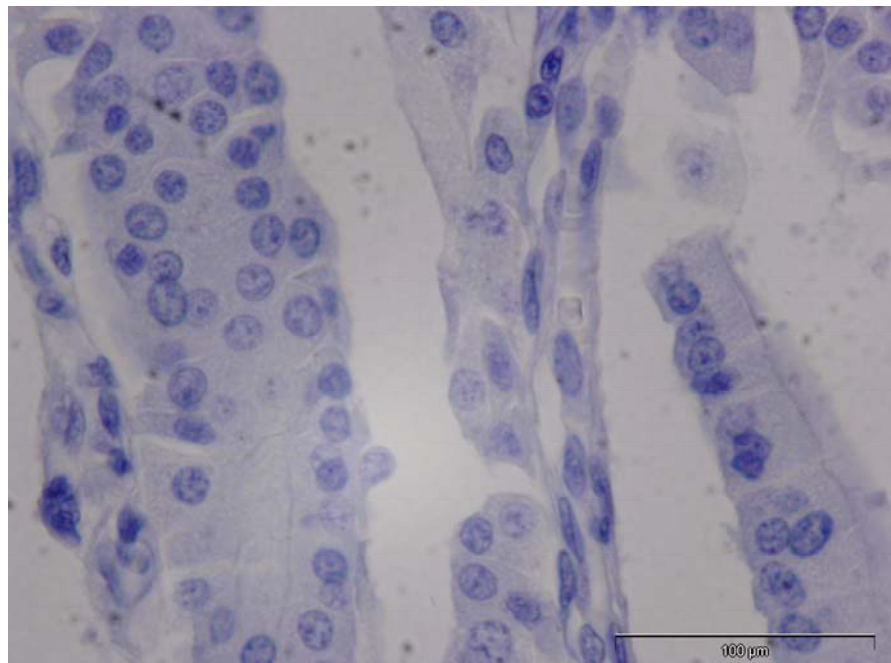
Figure 3.2.2 Immunohistochemical analysis of MRP-1 expression

A. Intense MRP-1 positivity is observed in the pancreatic tumour sample (3+3), stained with anti-MRP-1. B. Negative control specimen. Magnification, 400x. Scale bar, 100 μm.

3.2.3 MDR-1/P-gp and MRP-1 protein expression

Table 3.2.8 outlines the co-expression of P-gp and MRP-1 observed in the samples. In this study, 31% of samples stained positive for both P-gp and MRP-1. However from section 3.3.1-3.3.2, P-gp expression (93%) is found more frequently in pancreatic cancer than MRP-1 expression (31%). Interestingly, 62% of patients stained positive for P-gp and negative for MRP-1. Only, three cases (6.7%) expressed neither P-gp nor MRP-1. No cases of MRP-1 positive, P-gp negative were observed.

Table 3.2.8 **Summary slide number stained positive and negative for P-gp and MRP-1.**

MDR-1$^+$	MDR-1$^-$	MRP-1$^+$	MRP-1$^-$	MDR-1$^+$ MRP-1$^+$	MDR-1$^-$ MRP-1$^-$	MDR-1$^+$ MRP-1$^-$
42	3	14	31	14	3	28

3.3 Investigation into clonal variation in the invasive phenotype in sub-populations of MiaPaCa-2

An objective of this thesis was to establish pancreatic cancer cell line models differing in invasion status from single cell clonal populations of the cell line, MiaPaCa-2 (Chapter 2.2). Initially clonal populations were screened using *in vitro* invasion assays to determine intrinsic differences in the invasive phenotype (Chapter 2.5.2).

Invasion through specific extracellular matrix proteins was assessed using laminin, fibronectin, collagens type IV and I.

3.3.1 Isolation of sub-clonal populations of the pancreatic cancer cell line, MiaPaCa-2

Single cell cloning was performed as described in chapter 2.2. The cell line, MiaPaCa-2 was chosen as other cell lines did not culture well in single cell colonies. Four clones were isolated and successfully established as cell lines from MiaPaCa-2. The invasion status of the clones was tested on matrigel (Figure 3.3.1). Two sub-populations, Clone #3 and Clone #8 showing a large increase and decrease in invasion were chosen for further analysis.
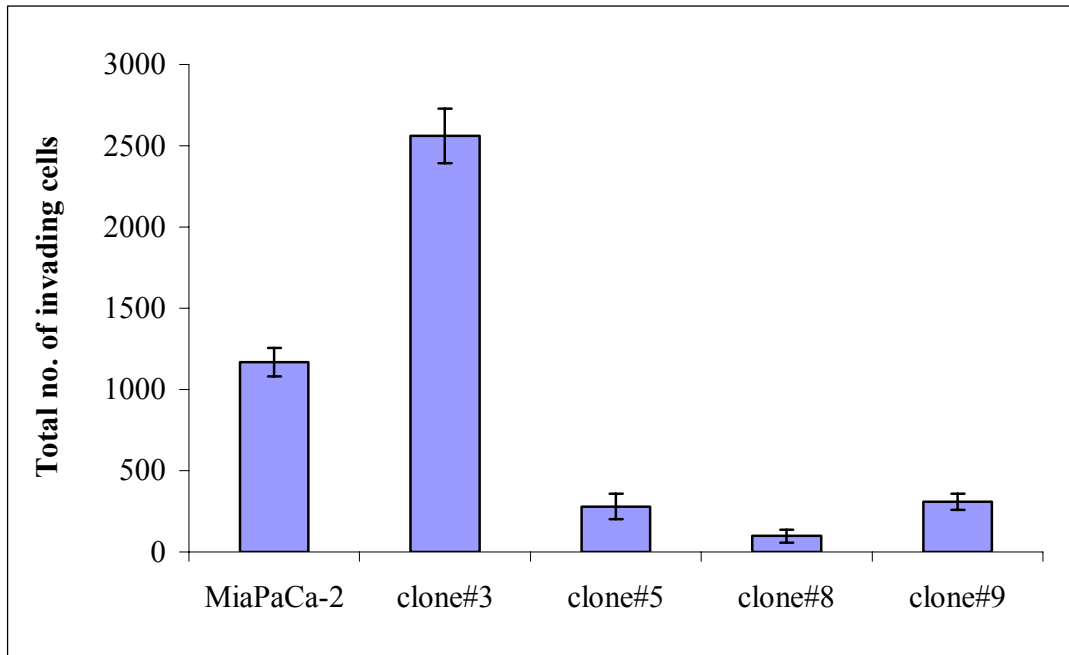
Figure 3.3.1 Invasion assay of sub-populations of the pancreatic cell line, MiaPaCa-2, through matrigel.

3.3.2 Invasion assays through matrigel, laminin, fibronectin, collagens type IV and I

The invasion assays were carried out using a range of extracellular matrix proteins: matrigel, laminin, fibronectin, collagens type IV and I (Figures 3.3.2-6). Motility assays were also performed without extracellular matrices (Figure 3.3.7). The assays were performed in triplicate and each figure illustrates a representative experiment. Invasion and motility assay results are summarised in figure 3.3.8.

Clone #3 is a highly invasive clonal population displaying significantly increased invasion through matrigel ($p=0.001$) compared to the parent MiaPaCa-2. Invasion is also increased through laminin and fibronectin, although not significantly. Clone #3 also displays significantly increased motility compared to the parental cell line ($p=0.00005$).

Clone #8 shows a significant decrease in invasion through matrigel ($p=0.00001$), laminin ($p=0.002$), fibronectin ($p=0.008$), and collagens type IV ($p=0.02$) and I ($p=0.03$). Motility of Clone #8 is similar to MiaPaCa-2.

Overall, the highest level of invasion was observed through fibronectin for each of the cell lines. In contrast, the lowest level of invasion displayed by the cell lines was through the collagens, type IV and I. This lack of invasion through the collagens could be explained by the reduced expression of collagen receptors, integrin $\alpha 1$, in the pancreatic cancer cell line, MiaPaCa-2 (Grzesiak and Bouvet, 2007).
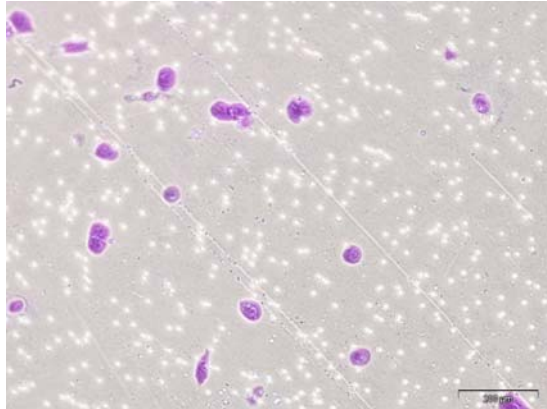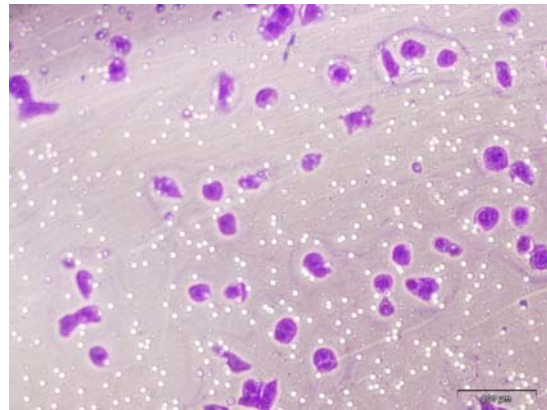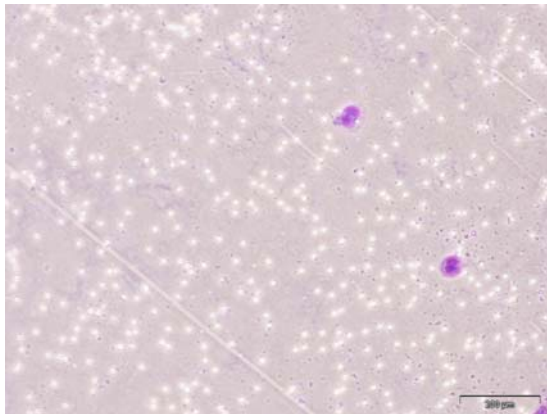
Figure 3.3.2 Invasion of (A) MiaPaCa-2 (B) Clone #3 and (C) Clone #8, through matrigel. Magnification, 100x. Scale bar, 200µm.

(A)
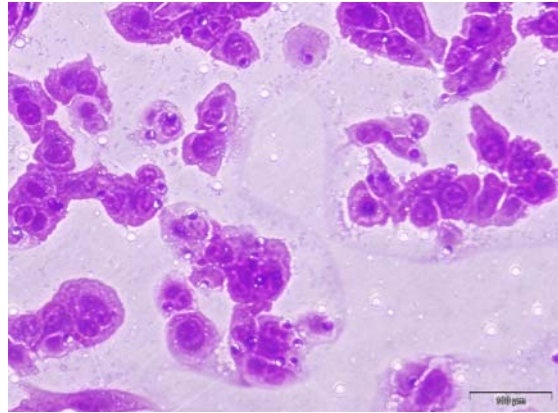
(B)
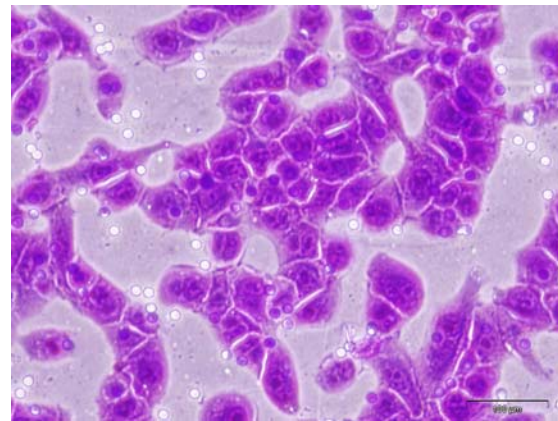
(C)
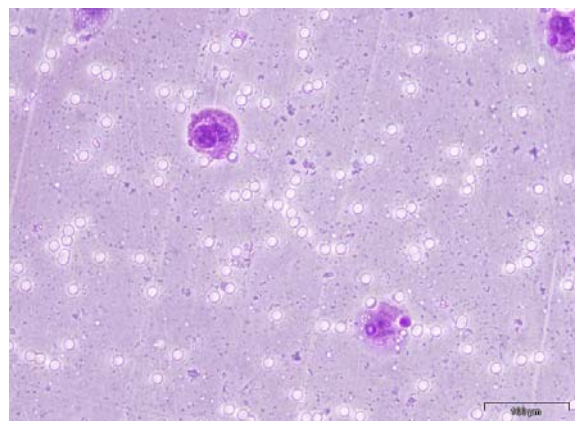
Figure 3.3.3 Invasion of (A) MiaPaCa-2 (B) Clone #3 and (C) Clone #8, through laminin. Magnification, 200x. Scale bar, 100μm.

(A)

(B)

(C)
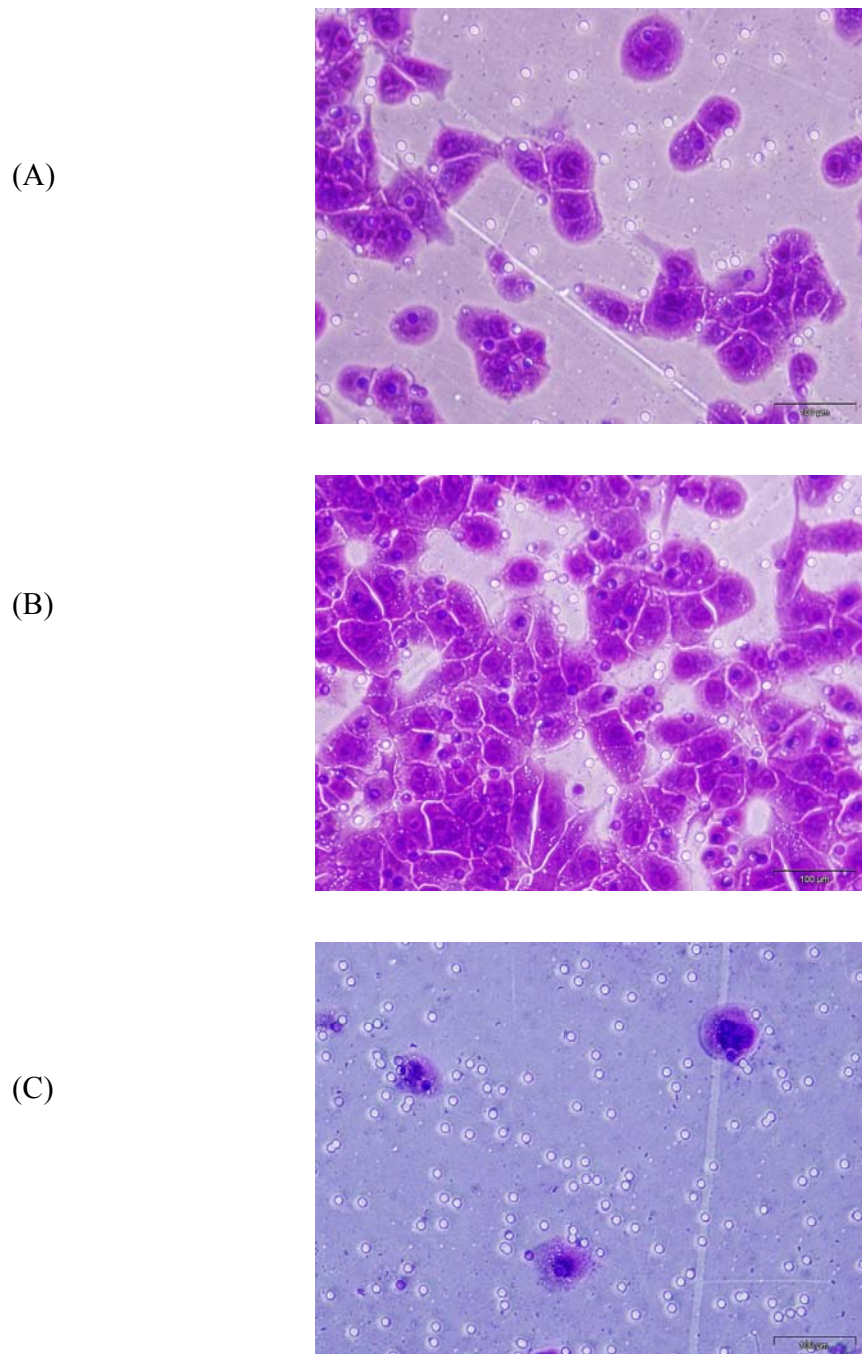
Figure 3.3.4 Invasion of (A) MiaPaCa-2 (B) Clone #3 and (C) Clone #8, through fibronectin. Magnification, 200x. Scale bar, 100μm.

(A)
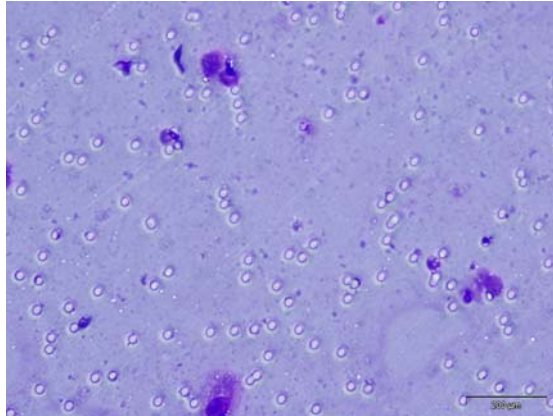
(B)
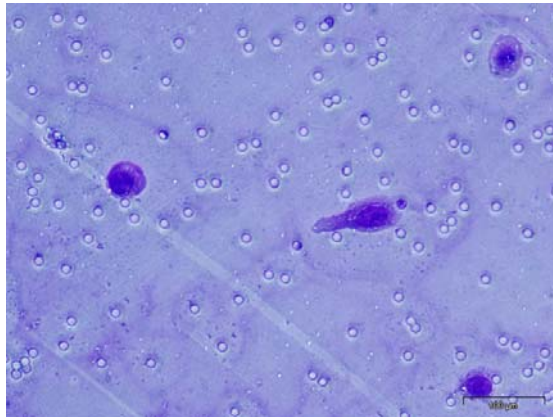
(C)
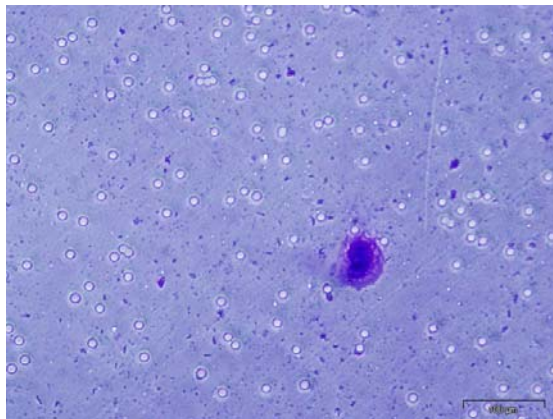
Figure 3.3.5 Invasion of (A) MiaPaCa-2 (B) Clone #3 and (C) Clone #8, through collagen type IV. Magnification, 200x. Scale bar, 100µm.

(A)

(B)

(C)
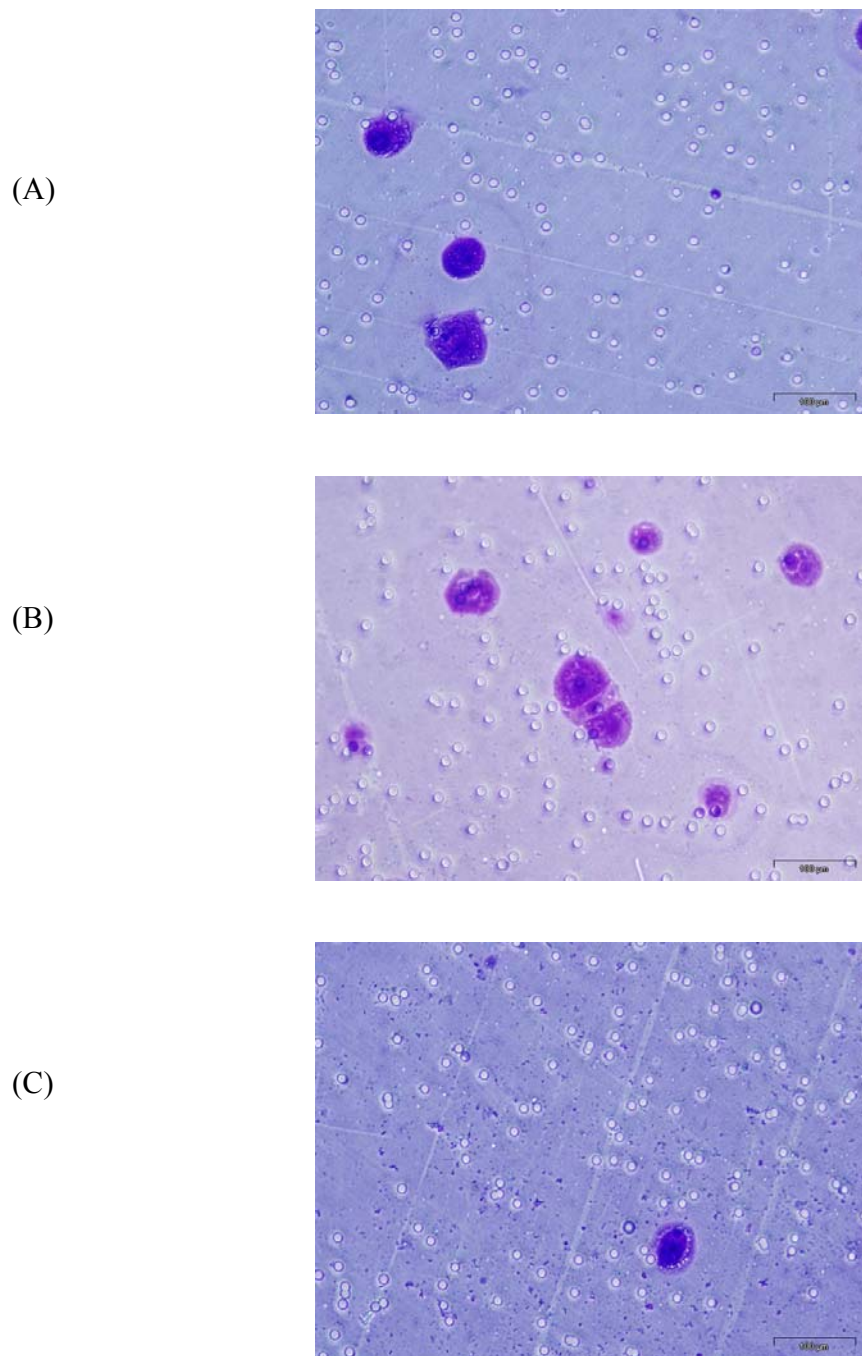
Figure 3.3.6 Invasion of (A) MiaPaCa-2 (B) Clone #3 and (C) Clone #8, through collagen type I. Magnification, 200x. Scale bar, 100μm.

(A)
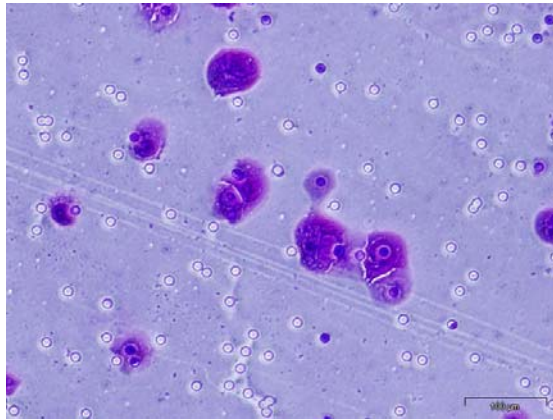
(B)
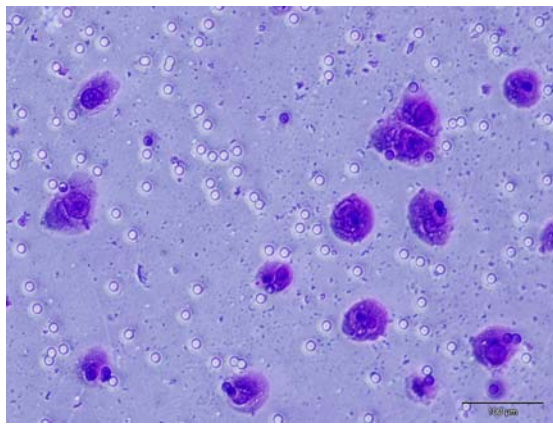
(C)
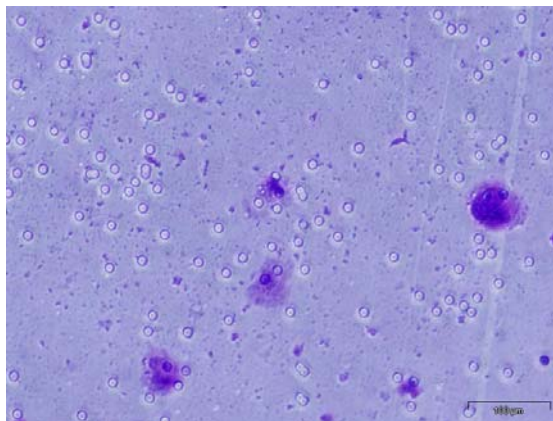
Figure 3.3.7 Motility of (A) MiaPaCa-2 (B) Clone #3 and (C) Clone #8. Magnification, 200x. Scale bar, 100μm.
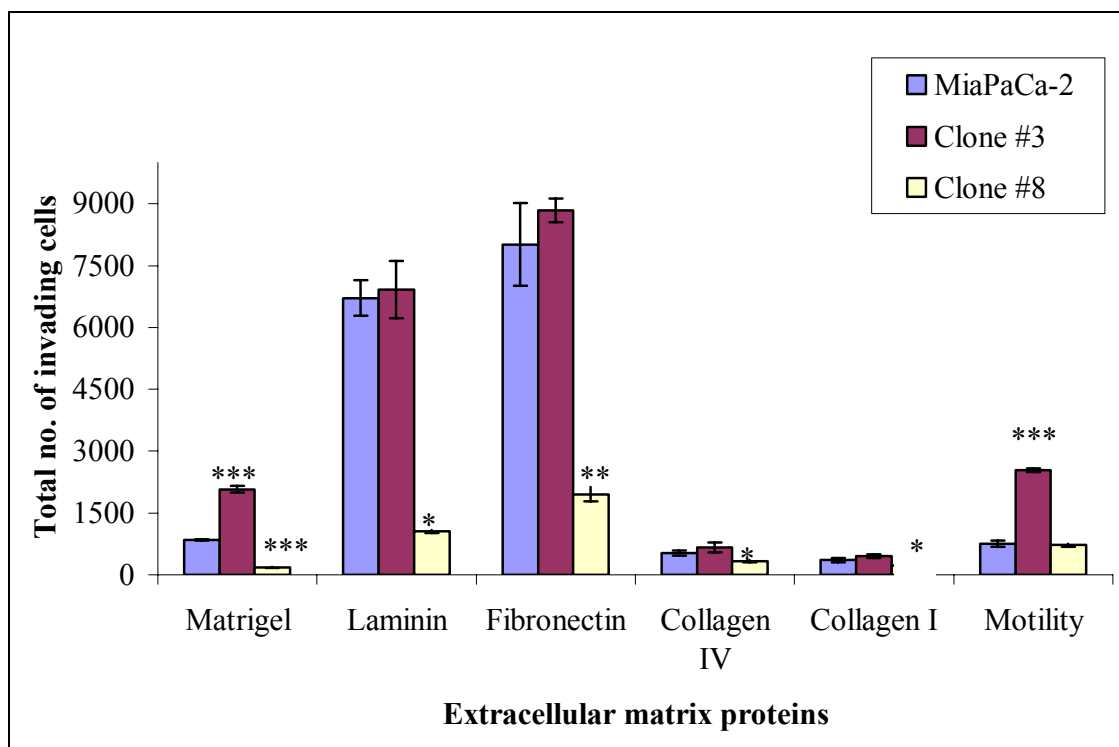
Figure 3.3.8 Invasion of MiaPaCa-2, Clone #3 and Clone #8 through ECM proteins and motility assay. Results are displayed as the total number of cells invading as counted at 200x magnification ± SD ($n = 3$). Ten random fields were counted, averaged and the total no. of cells invading calculated and statistical analysis was carried out using the student *t*-test.

Statistics: $p \leq 0.05^*$, 0.01^{**}, 0.005^{***} (unpaired *t*-test).

3.3.3 Adhesion properties of MiaPaCa-2 and sub-populations Clone #3 and Clone #8

The sub-populations, Clone #3 and Clone #8 were characterised further by assessing the adhesive abilities of the clones to ECM proteins, matrigel, laminin, fibronectin, collagen type IV and I compared to the parental cell line, MiaPaCa-2 (Chapter 2.5.4).

Figure 3.3.9 illustrates the level of adhesion of the pancreatic cell line, MiaPaCa-2 and its sub-clones, Clone #3 and Clone #8. The more invasive cell line, Clone #3 displays significantly decreased adhesion to matrigel ($p=0.01$), laminin ($p=0.02$), fibronectin ($p=0.01$) and collagen type IV ($p=0.01$) compared to the parental line. In contrast, a significant increase in adhesion was observed to collagen type I ($p=0.003$), although the level of adhesion to the collagens was lower than to laminin or fibronectin.

The less invasive cell line, Clone #8 shows significantly increased adhesion to matrigel ($p=0.04$) and laminin ($p=0.002$). The adhesion to fibronectin and collagen type I were also increased, but not significantly. In contrast, adhesion to collagen type IV was decreased significantly ($p=0.001$).

Interestingly, it is evident from figure 3.3.9, that there is no difference in adherence to collagens type IV and I between Clone #3 and Clone #8. Adhesion to collagen type IV is significantly decreased for both clonal populations compared to the parental cell line, while adhesion to collagen type I is increased for both Clone #3 and Clone #8.
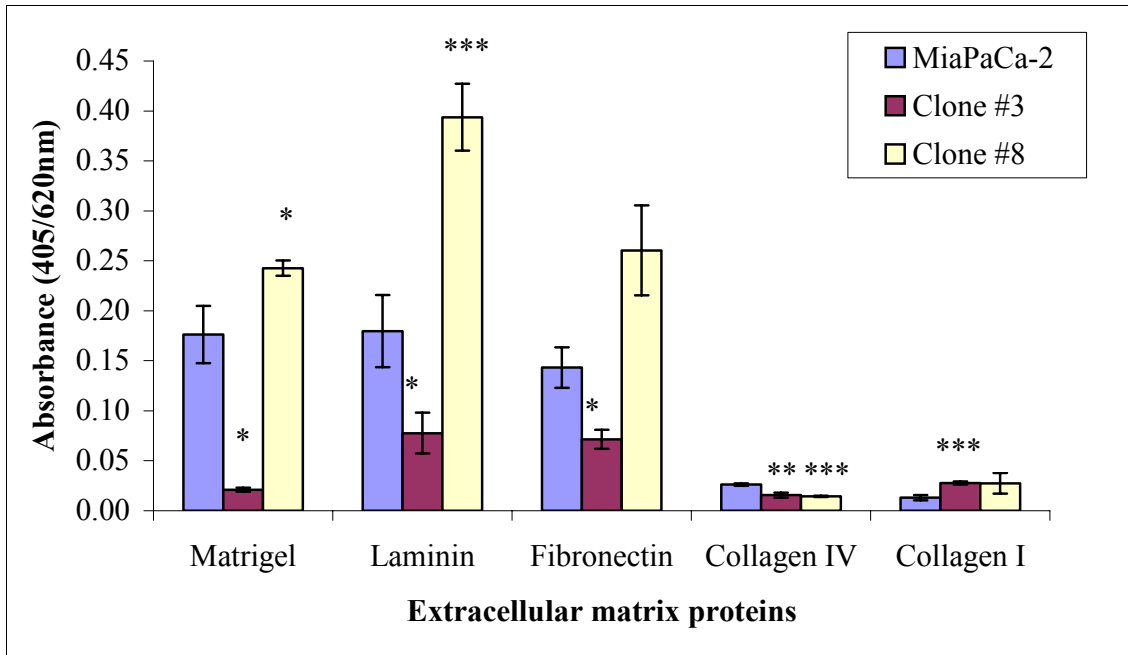
Figure 3.3.9 Adhesion of MiaPaCa-2, Clone #3 and Clone #8 to extracellular matrix proteins. Results are expressed as absorbance at 405nm with a reference wavelength of 620nm. Data shown is mean ± standard deviation (n = 3).
Statistics: $p \leq 0.05^*$, 0.01^{**}, 0.005^{***} (unpaired t-test).

3.3.4 Anchorage independent growth of MiaPaCa-2 and sub-populations Clone #3 and Clone #8

The ability of MiaPaCa-2, Clone #3 and Clone #8 to form colonies under anchorage independent conditions was evaluated in order to further characterise the inherent differences in the sub-populations, Clone #3 and Clone #8 (Chapter 2.6).

Figure 3.3.10 illustrates the different appearance of the colonies after 10 days of anchorage independent growth. MiaPaCa-2 shows modest colony formation with an average colony size of 75 μm, Clone #3 forms more and larger colonies with an average size of 120 μm. In contrast, Clone #8 in single cell suspension had the ability to form very few colonies; single cells appeared to undergo apoptosis, possibly due to the lack of cell-ECM or cell-cell attachment as pictured in figure 3.3.11. The average size of Clone #8 colonies was 60 μm. The parental cell line, MiaPaCa-2 has a percentage colony forming efficiency (%CFE) of 48%; however Clone #3, the cell line that has shown increased invasion and decreased adhesion displays a %CFE of 69% (Figure 3.3.11). In contrast, Clone #8, which displays decreased invasion and increased adhesion, shows a significantly reduced ability (32% CFE) to form colonies (p=0.006).
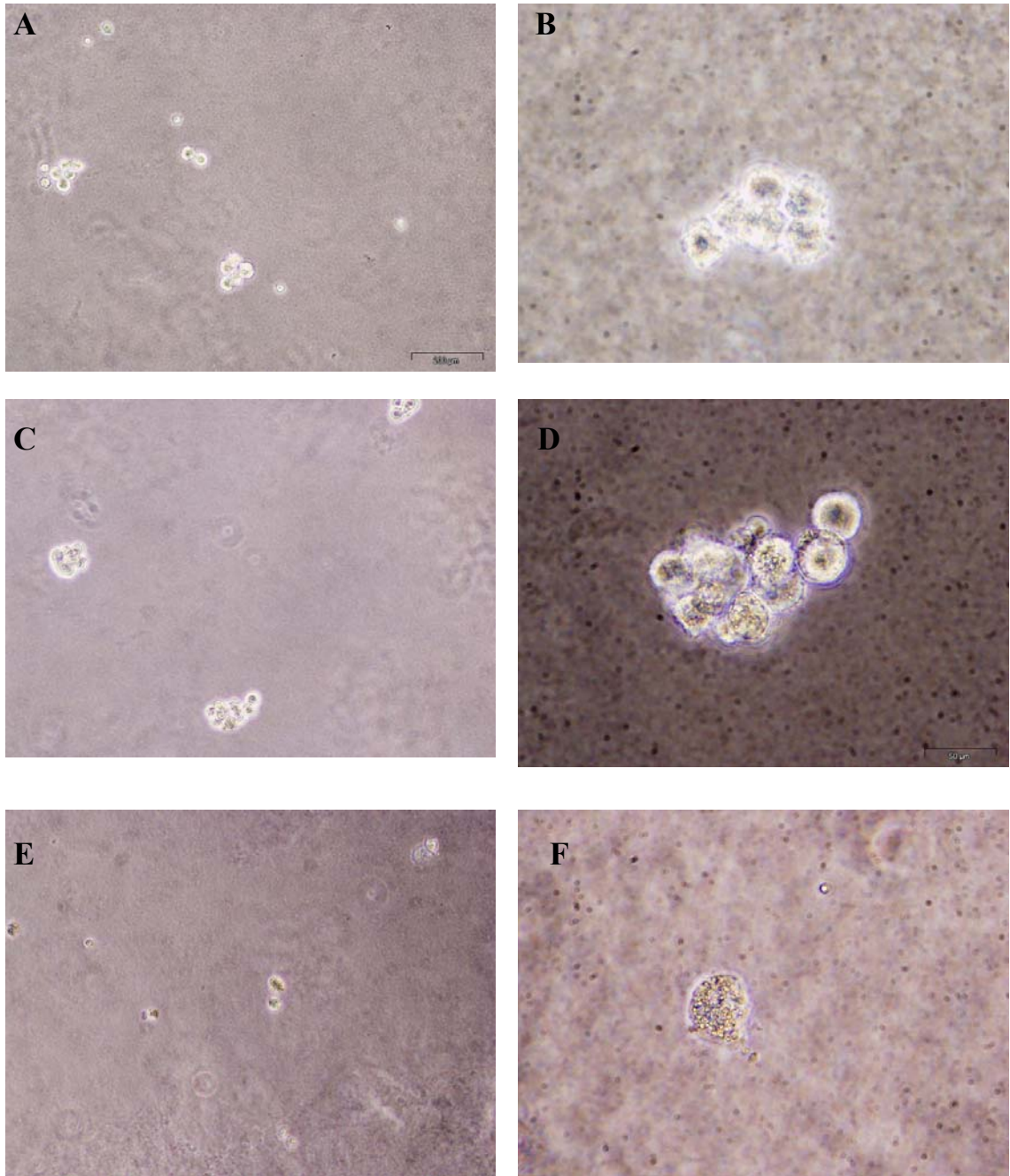
Figure 3.3.10 Colony formation after 10 days of MiaPaCa-2 (A) and (B), Clone #3 (C) and (D) and Clone #8 (E) and (F). Magnification, 100x (A,C,E) and 400x (B,D,F). Scale bar, 200μm.
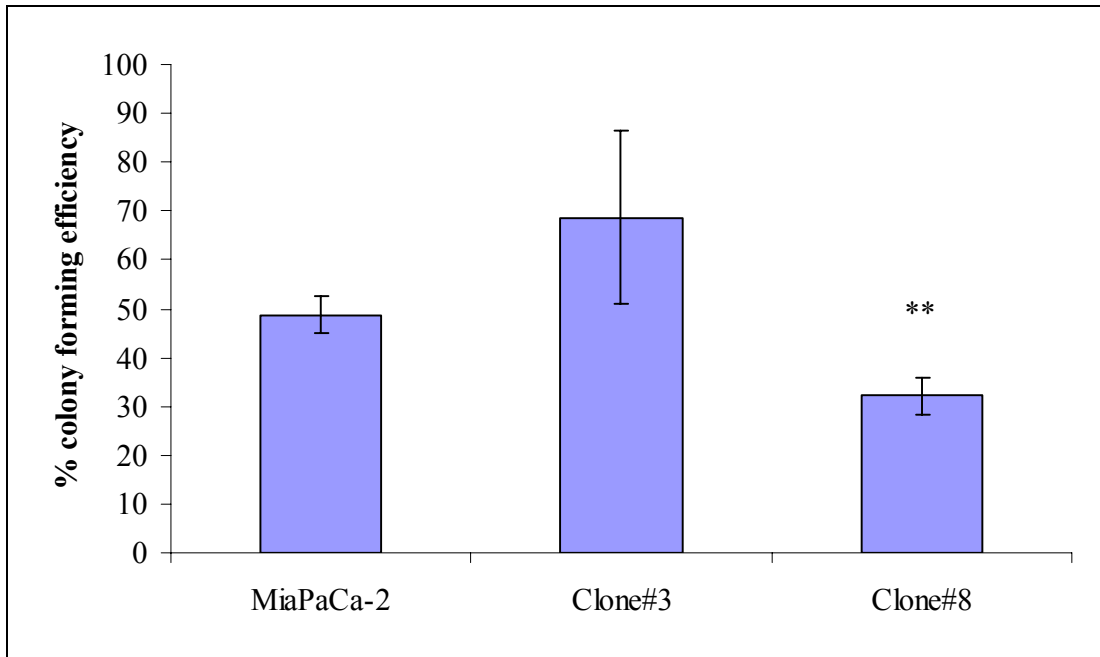
Figure 3.3.11 Percentage colony forming efficiency (%CFE) of MiaPaCa-2, Clone #3 and Clone #8 under anchorage independent conditions. Data shown is mean ± standard deviation (*n* = 3).

Statistics: *p* ≤ 0.05*, 0.01**, 0.005*** (unpaired *t*-test).

3.3.5 Anoikis induction in MiaPaCa-2 and sub-populations Clone #3 and Clone #8

Anoikis is a specific form of apoptosis induced by the loss or alteration of cell-cell or cell-matrix anchorage. An *in vitro* anoikis assay was used to assess sensitivity to anoikis of MiaPaCa-2 and its sub-populations Clone #3 and Clone #8 (Chapter 2.7).

Figure 3.3.12 shows the percentage survival of non-adherent cells (24 hrs poly-HEMA treated plastic) relative to adherent cells (non-treated plastic). The evaluation of survival in suspension shows that Clone #3 displays increased resistance in anoikis compared to the parental cell line, although this difference did not reach statistical significance ($p=0.07$). Clone #8 demonstrates a significant sensitivity to anoikis ($p=0.02$) compared to the parental cell line, MiaPaCa-2.
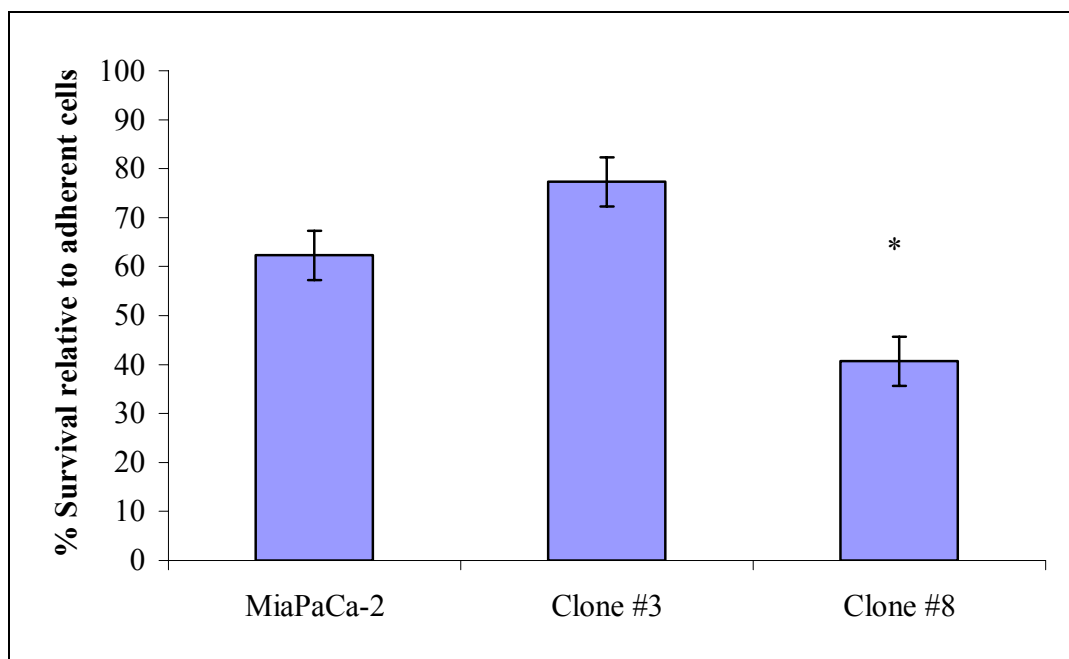
Figure 3.3.12 Percentage survival of MiaPaCa-2, Clone #3 and Clone #8 in suspension compared to adherent cells. Data shown is mean ± standard deviation (n = 3). Statistics: $p \leq 0.05^*$, 0.01^{**}, 0.005^{***} (unpaired t-test).

3.3.6 Analysis of the expression of integrins β1, α2, α5 and α6 in MiaPaCa-2 and sub-populations Clone #3 and Clone #8

Altered changes in invasion and adhesion to fibronectin and laminin were observed in Clone #3 and Clone #8. Therefore, expression of integrins β1, α2, α5 and α6 which are associated with the adhesion to fibronectin and laminin were examined by Western blot analysis in the cell lines (Chapter 2.9).

Figure 3.3.13 (A) illustrates the Western blot of integrin β1 (130kDa) in MiaPaCa-2, Clone #3 and Clone #8. Integrin β1 is highly expressed in the low-invasive, Clone #8 compared to the parent cell line, MiaPaCa-2. Clone #3 and MiaPaCa-2 showed low expression of integrin β1.

Integrin α2 (130 kDa) protein was expressed at low levels, the expression was unaltered between MiaPaCa-2, Clone #3 and Clone #8 (Figure 3.3.13 B).

Integrin α5 (135kDa) expression in Clone #8 was increased compared to MiaPaCa-2, while a significant decrease in expression of Clone #3 was observed (Fig 3.3.13 C.).

Integrin α6 shows higher protein expression in Clone #8 compared to the parental MiaPaCa-2 and Clone #3 (Figure 3.3.13 D).
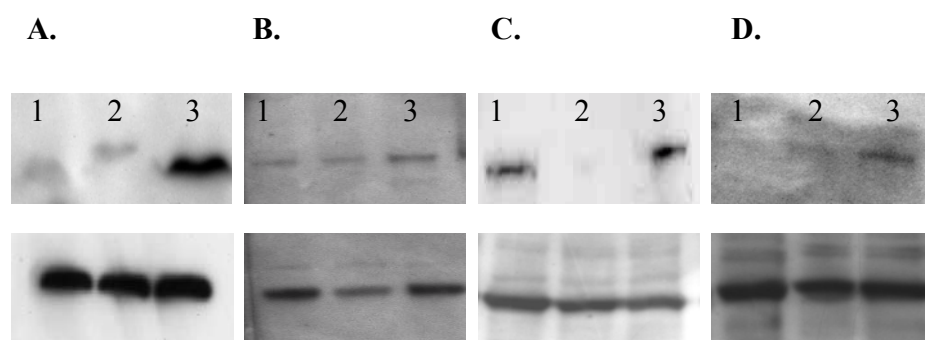
Figure 3.3.13 Western blot of (A) Integrin β1 (130kDa) (B) Integrin α2 (130 kDa) (C) Integrin α5 (135 kDa) (D) Integrin α6 (120 kDa) and β-actin (42 kDa) (below) used as loading control in (1) MiaPaCa-2, (2) Clone #3 and (3) Clone #8.

3.3.6.1 Effect of siRNA transfection of integrin β1 on Clone #8

Integrin β1 was shown to be abundantly expressed in the Clone #8 cell line compared to the parental cell line, MiaPaCa-2 and its high invasive sub-population Clone #3. Figure 3.3.14 shows a representative Western blot of the knockdown of integrin β1 in Clone #8 cells after integrin β1 siRNA transfection.
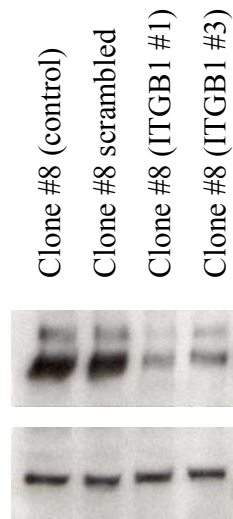
Figure 3.3.14 Knockdown of integrin β1 in Clone #8 cells confirmed by Western blot 48 hours post transfection. SiRNAs ITGB1 #1 and #3 were chosen as target siRNAs.

3.3.6.2 Effect of integrin β1 siRNA transfection on invasion and motility

The role of integrin β1 in the low invasive, highly adhesive cell line, Clone #8 was assessed using siRNA (Figure 3.3.15). Forty-eight hours following transfection of two independent siRNAs, cells were subjected to invasion and motility assays as described previously in chapter 2.16.3 and 2.16.4. Integrin β1 siRNA transfected into Clone #8 resulted in a significant increase in invasion through matrigel (p=0.005 and p=0.04), however invasion through laminin was not significantly altered. Invasion through fibronectin significantly increased (p=0.04 and p=0.02). Motility of Clone #8 after siRNA β1 transfection was also significantly increased (p=0.01 and p=0.03) compared to the scrambled control.
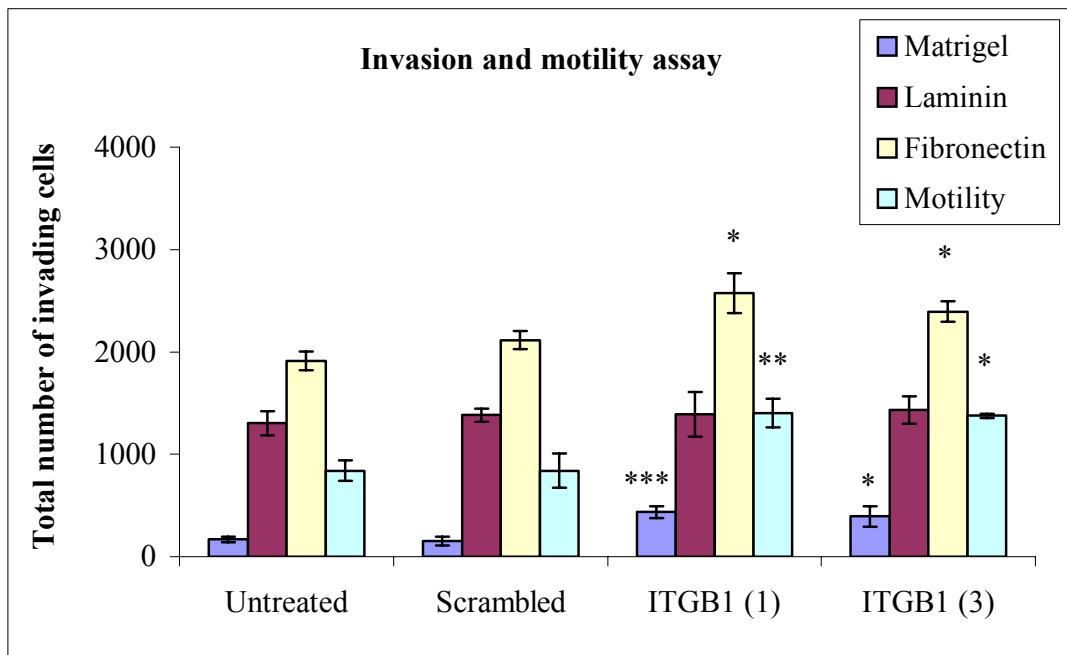
Figure 3.3.15 Invasion and motility of Clone #8 control, treated with scrambled siRNA and two independent integrin β1 siRNA targets through matrigel, laminin and fibronectin. Experiments were performed 48 hours post-transfection with two different exon targeted siRNA integrin β1. Untransfected- and scrambled siRNA transfected- cell lines were the controls for this experiment.
Statistics: $p \leq 0.05^*$, 0.01^{**}, 0.005^{***} (unpaired t-test).

3.3.6.3 Effect of integrin β1 siRNA transfection on adhesion

The role of adhesion in Clone #8 cells transfected with integrin β1 siRNA was also assessed (Figure 3.3.16). A significant decrease in adhesion to matrigel (45% and 47% decrease) was observed ($p=0.02$ and $p=0.002$) compared to the scrambled control. Adhesion to fibronectin ($p=0.02$ and $p=0.04$) was also decreased with the integrin β1 siRNA treatment (49% and 37%). Adhesion to laminin was not altered after transfection with integrin β1 siRNAs (3% and 2%).
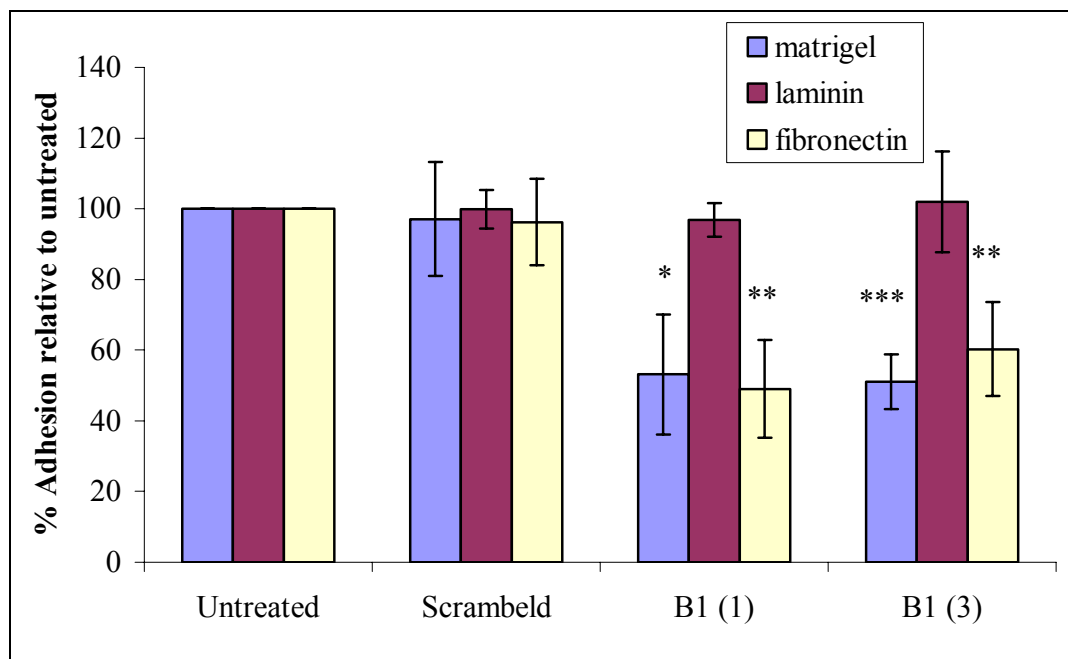
Figure 3.3.16 Adhesion of Clone #8 control, treated with scrambled siRNA and two independent integrin β1 siRNA targets to matrigel, laminin and fibronectin. Experiments were performed 48 hours post-transfection with two different exon targeted siRNA integrin Beta 1. Untransfected- and scrambled siRNA transfected-cell lines were the controls for this experiment.

Statistics: $p \leq 0.05*$, $0.01**$, $0.005***$ (unpaired t-test).

3.3.6.4 Effect of integrin β1 siRNA transfection on anoikis

Anoikis assays were also carried out to investigate whether the knockdown of integrin β1 had any effect on the survival of Clone #8 in suspension (Chapter 2.16.5). Figure 3.3.17 shows a significant increase in the percentage of cells surviving in suspension, when treated with integrin β1 siRNA compared to cells treated with scrambled control relative to adherent cells (p=0.01, p=0.003).
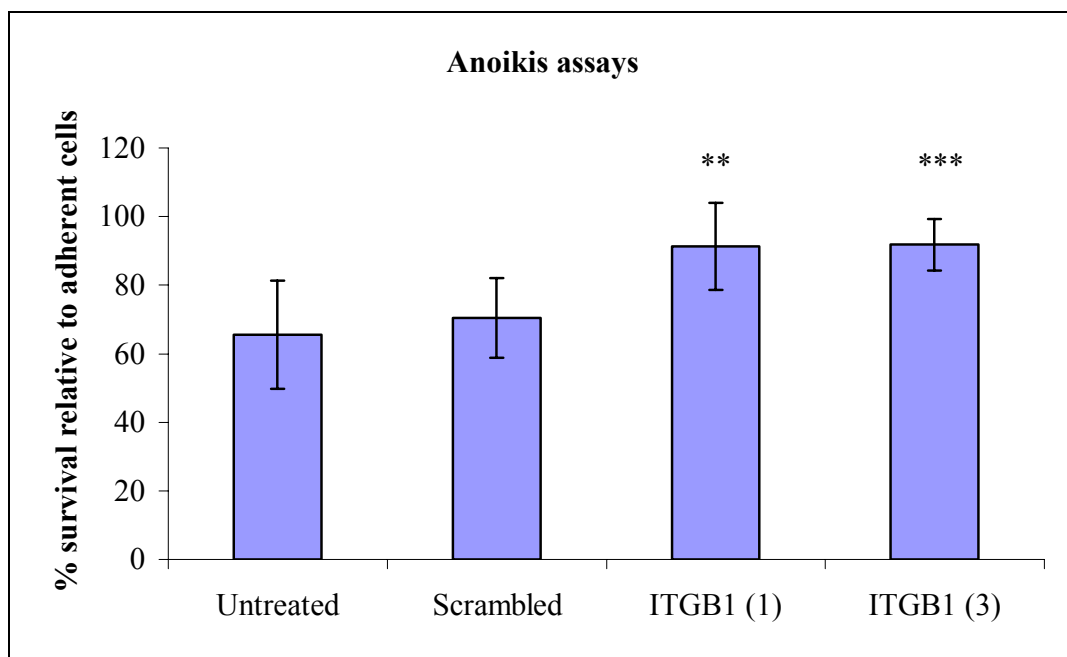
Figure 3.3.17 Anoikis assay of Clone #8 control, treated with scrambled siRNA and two independent integrin β1 siRNA targets. Experiments were performed 48 hours post-transfection with two different exon targeted siRNA integrin Beta 1 and in triplicate. Untransfected- and scrambled siRNA transfected- cell lines were the controls for this experiment.

Statistics: $p \leq 0.05^*$, 0.01^{**}, 0.005^{***} (unpaired t-test).

3.3.6.5 Effect of integrins α5 and α6 siRNA transfection in Clone #8

Integrins α5 and α6 were shown to be expressed in the Clone #8 cell line compared to the parental cell line, MiaPaCa-2 and its sub-population Clone #3. Figure 3.3.18 shows a representative Western blot of the knockdown of integrins α5 (ITGA5) and α6 (ITGA6) in Clone #8 cells after integrins α5 and α6 siRNA transfection.
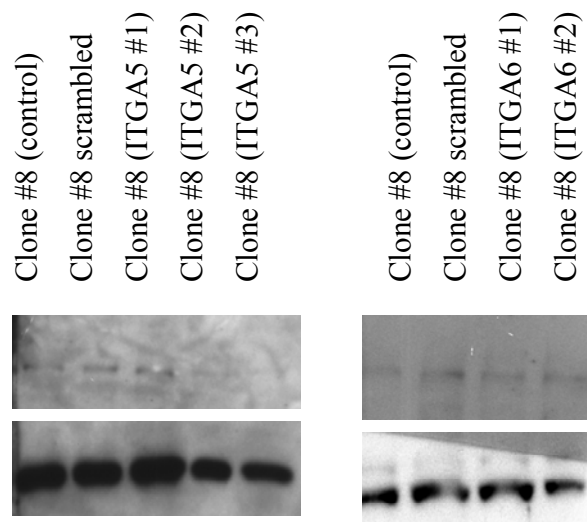
Figure 3.3.18 Knockdown of integrin α5 and integrin α6 in Clone #8 cells confirmed by Western blot 48 hours post transfection. SiRNAs ITGA5 #1, #2 and #3 were chosen as target integrin α5 siRNAs. SiRNAs ITGA6 #1 (validated) and #2 were chosen as integrin α6 target siRNAs.

3.3.6.6 Effect of integrins α5 and α6 siRNA transfection on invasion

Transfection of integrin α5 siRNA into Clone #8 resulted in significant increase in invasion through matrigel ($p=0.0003$, $p=0.005$ and $p=0.005$), laminin ($p=0.07$, $p=0.008$ and $p=0.0002$) and fibronectin ($p=0.0002$, $p=0.0001$ and $p=0.008$) compared to the scrambled control.

Transfection of siRNA α6 into Clone #8 also resulted in significant increase in invasion through matrigel ($p=0.00009$ and $p=0.02$), no significant increase in invasion through laminin, but significantly increased invasion through fibronectin ($p=0.004$ and $p=0.04$) was observed (Figure 3.3.19).
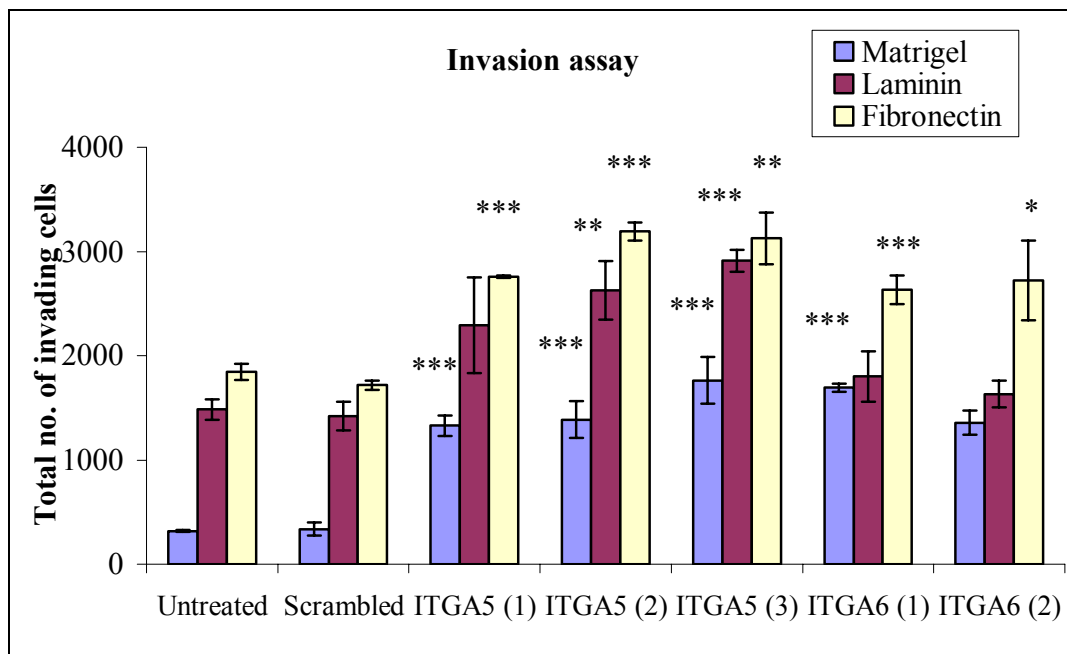
Figure 3.1.19 Invasion of Clone #8 control, treated with scrambled siRNA and three independent integrin α5 siRNA targets and two integrin α6 target siRNAs through matrigel, laminin and fibronectin. Experiments were performed 48 hours post-transfection and in triplicate. Untransfected- and scrambled siRNA transfected- cell lines were the controls for this experiment.

Statistics: $p \leq 0.05*$, $0.01**$, $0.005***$ (unpaired t-test).

3.3.6.7 Effect of integrins α5 and α6 siRNA transfection on motility

Transfection of integrin α5 siRNA into Clone #8 resulted in a significant increase in motility. Integrin α5 siRNA (1) resulted in a 1.7-fold increased in motility (p=0.03), integrin α5 siRNA (2) increased motility by 1.9-fold (p=0.0007) and integrin α5 siRNA (3) also increased motility 1.7-fold (p=0.06) compared to scrambled siRNA transfected control.

Transfection of integrin α6 siRNA (1) into Clone #8 also resulted in a 1.4-fold increase in motility (p=0.2) and integrin α6 siRNA (2) showed a significant 1.6-fold increase in motility (p=0.004) compared to scrambled siRNA transfected control (Figure 3.3.20).
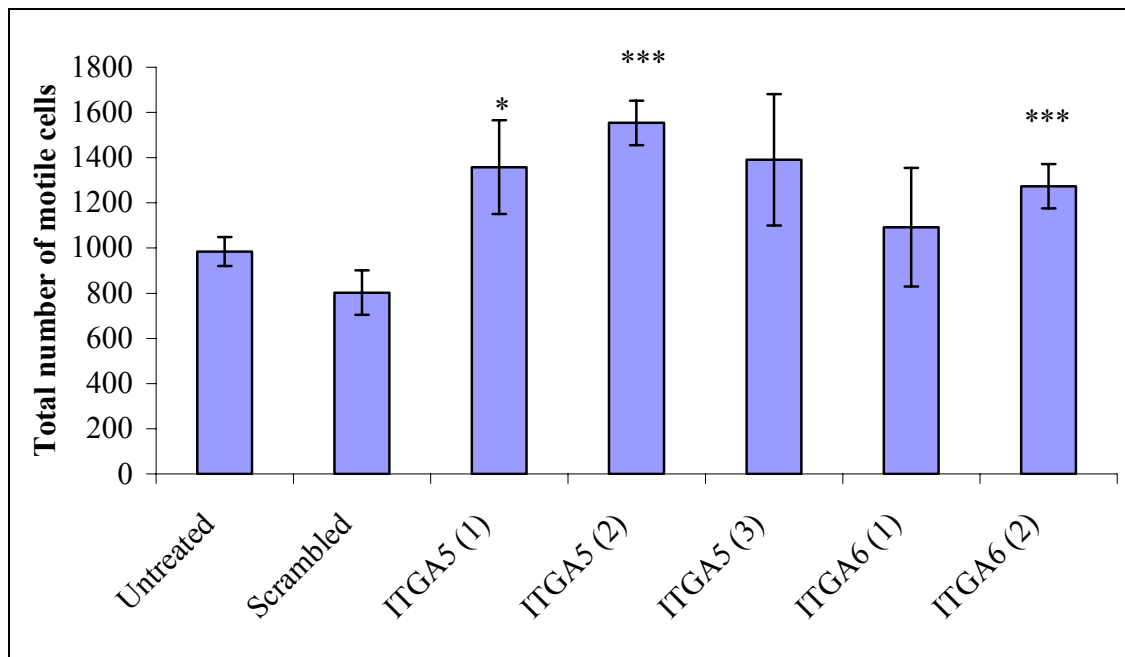
Figure 3.3.20 Motility of Clone #8 control, treated with scrambled siRNA and three independent integrin α5 siRNA targets and two integrin α6 target siRNAs. Experiments were performed 48 hours post-transfection and in triplicate. Untransfected- and scrambled siRNA transfected- cell lines were the controls for this experiment. Statistics: $p \leq$ 0.05*, 0.01**, 0.005*** (unpaired t-test).

3.3.6.8 Effect of integrins α5 and α6 siRNA transfection on adhesion

Figure 3.3.21 shows the percentage adhesion relative to untreated control cells. A decrease in adhesion to matrigel and laminin was observed although not significantly, while a more pronounced reduction of 40%, 29% and 38% in adhesion to fibronectin was seen after integrin α5 siRNA treatment ($p=0.02$, $p=0.03$ and $p=0.02$).

Adhesion to matrigel and fibronectin was not altered with integrin α6 siRNAs treatment; however adhesion to laminin was reduced by 37% and 42% ($p=0.08$ and $p=0.01$).
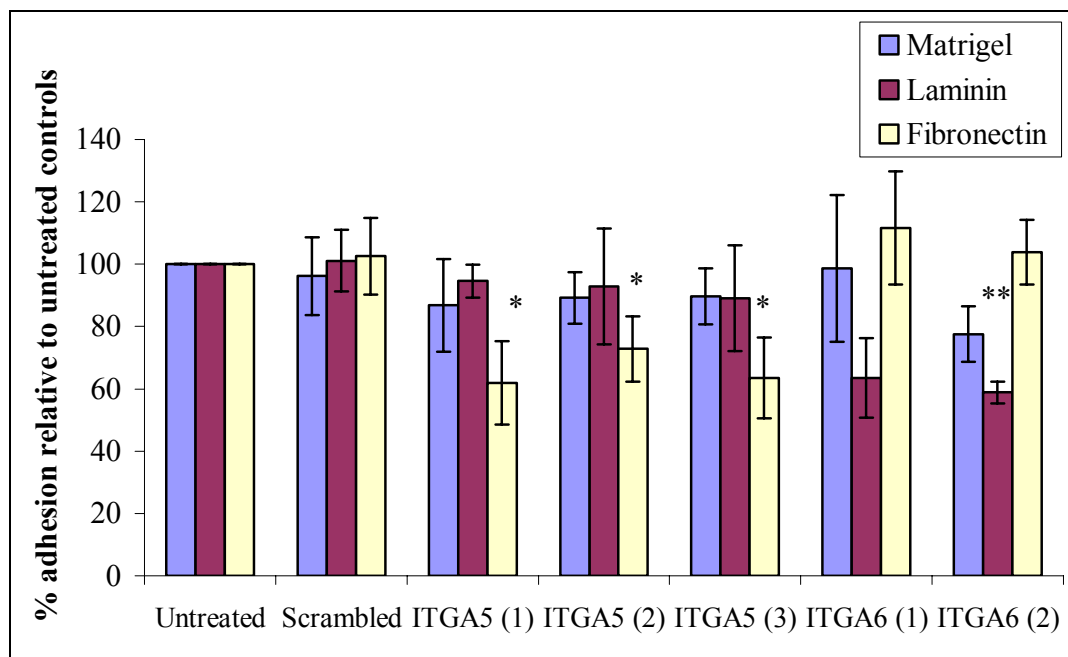
Figure 3.3.21 Adhesion of Clone #8 control, treated with scrambled siRNA, three independent integrin α5 siRNA targets and two integrin α6 siRNA targets to matrigel, laminin and fibronectin. Experiments were performed 48 hours post-transfection and in triplicate. Untransfected- and scrambled siRNA transfected- cell lines were the controls for this experiment.

Statistics: $p \leq 0.05^*$, 0.01^{**}, 0.005^{***} (unpaired t-test).

3.3.6.9 Effect of integrins α5 and α6 siRNA transfection on anoikis

Anoikis assays were also carried out to investigate the role of integrins α5 and α6 on the survival of Clone #8 in suspension. No significant increase in resistance to anoikis was observed after either integrins α5 and α6 siRNA transfection compared to cells treated with scrambled control relative to adherent cells (Figure 3.3.22).
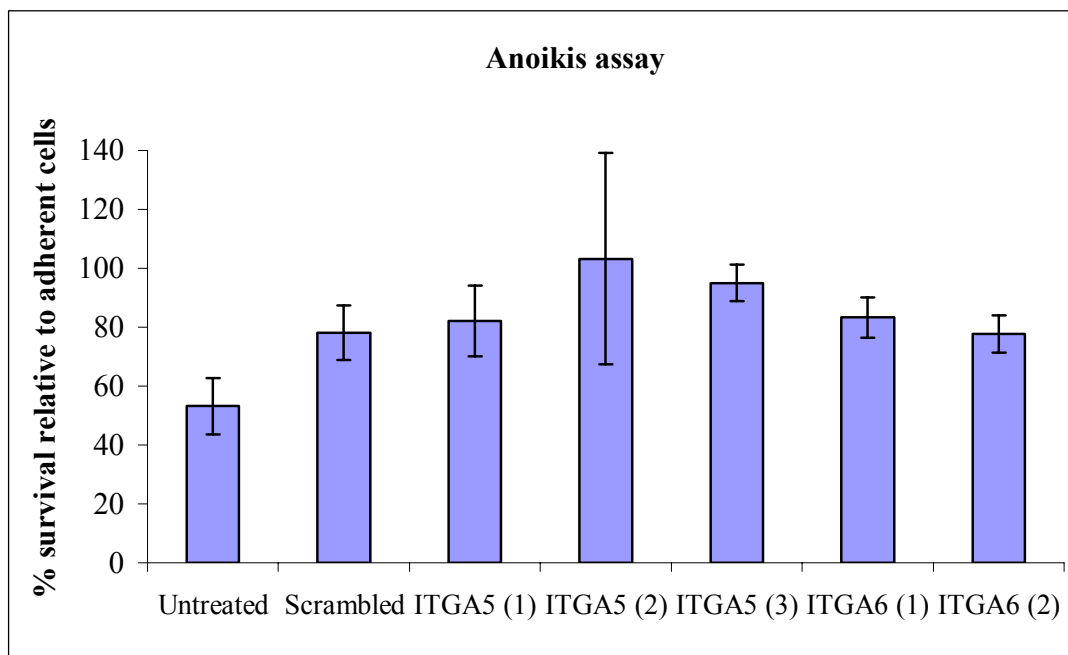
Figure 3.3.22 Anoikis of Clone #8 control, treated with scrambled siRNA, three independent integrin α5 siRNA targets and two integrin α6 siRNA targets. Experiments were performed 48 hours post-transfection and in triplicate. Untransfected- and scrambled siRNA transfected- cell lines were the controls for this experiment.

Statistics: $p \leq 0.05^*$, 0.01^{**}, 0.005^{***} (unpaired t-test).

3.3.7 Drug resistance of MiaPaCa-2 and sub-populations, Clone #3 and Clone #8

To determine if there is any link between altered invasion, adhesion, anchorage independent survival and drug resistance, proliferation assays were performed to compare drug sensitivity in MiaPaCa-2 and its sub-populations, Clone #3 and Clone #8 (Chapter 2.3).

The IC_{50} values of each of the chemotherapeutic agents were determined for the parental cell line and its sub-populations, Clone #3 and Clone #8 (Table 3.3.1). Clone #3 exhibited a significantly higher level of resistance to taxotere ($p=0.02$) and VP-16 ($p=0.05$), while resistance levels to epirubicin ($p=0.13$), adriamycin ($p=0.06$) and vincristine ($p=0.08$) were also increased compared to MiaPaCa-2, although not significantly. No increase in resistance was observed for 5-FU, taxol, cisplatin and carboplatin. Interestingly, a significant sensitivity to gemcitabine was observed ($p < 0.005$). Clone #8 displayed an increase in sensitivity to all ten chemotherapeutic drugs compared to the parental cell line (Figure 3.3.23).
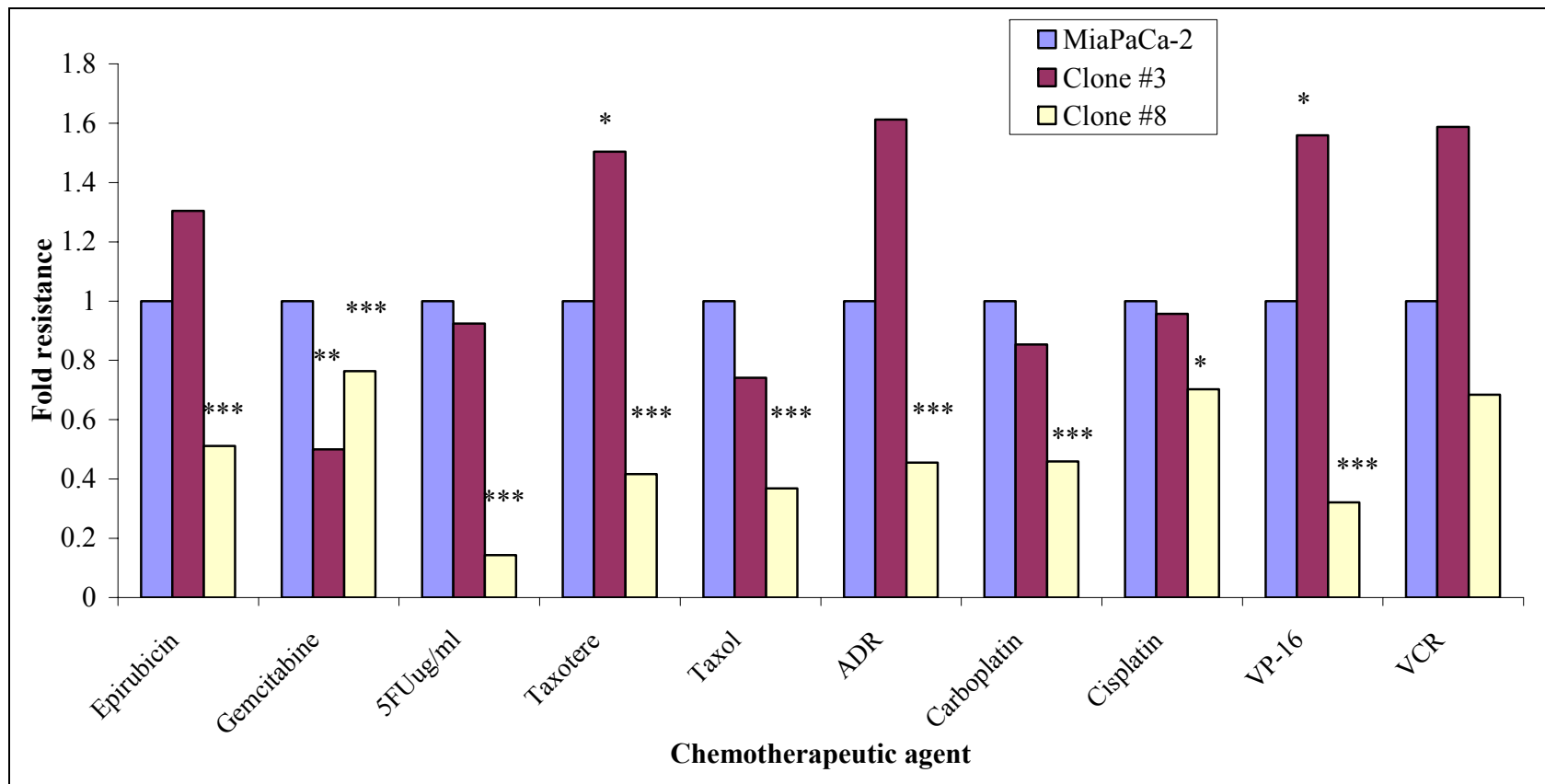
Figure 3.3.23 Fold resistance levels of MiaPaCa-2, Clone #3 and Clone #8 to a panel of 10 drugs. Cell viability was determined by acid phosphatase assay, read at 405nm with a reference wavelength of 620nm.

Statistics, * p ≤ 0.05, ** p ≤ 0.01 *** p ≤ 0.005 Student's t-test.

Table 3.3.1 Comparison of chemo-sensitivity and IC$_{50}$ results between MiaPaCa-2 and sub-clones, Clone #3 and Clone #8. Mean IC$_{50}$ values from triplicate experiments ± standard deviation are displayed.

Chemo agents (ng/ml)	MiaPaCa-2	Clone #3	Fold resistance	Clone #8	Fold resistance
Epirubicin	14 ± 2.3	18.3 ± 3.1	1.3	7.2 ± 0.3	0.5***
Gemcitabine	1.3 ± 0.1	0.6 ± 0.0	0.5***	1.0 ± 0.1	0.8*
5-FU (ug/ml)	0.5 ± 0.1	0.4 ± 0.0	0.9	0.1 ± 0.0	0.1***
Taxotere	0.4 ± 0.0	0.6 ± 0.1	1.5*	0.2 ± 0.0	0.4***
Taxol	1.7 ± 0.1	1.2 ± 0.4	0.7	0.6 ± 0.1	0.4***
Adriamycin	16.7 ± 2.3	26.9 ± 5.2	1.6	7.6 ± 1.5	0.5***
Carboplatin	6140 ± 392	5243 ± 762	0.9	2820 ± 556	0.5***
Cisplatin	431.6 ± 53.7	413.1 ± 26.1	1.0	303.5 ± 52.9	0.7*
VP-16	171.5 ± 9.4	267.5 ± 42.2	1.6*	55.1 ± 10.3	0.3***
Vincristine	0.6 ± 0.1	1.0 ± 0.2	1.6	0.4 ± 0.1	0.7

* p ≤ 0.05, ** p ≤ 0.01 *** p ≤ 0.005 Student's t-test.

Table 3.3.2 Summary of different characteristics between Clone #3 and Clone #8 compared to the parental cell line, MiaPaCa-2.

	Clone #3	Clone #8
Motility	Increased	Unchanged
Invasion through matrigel	Increased	Decreased
Invasion through laminin	Slightly increased	Decreased
Invasion through fibronectin	Slightly increased	Decreased
Invasion through collagen IV	Slightly increased	Decreased
Invasion through collagen I	Slightly increased	Decreased
Adhesion to matrigel	Decreased	Increased
Adhesion to laminin	Decreased	Increased
Adhesion to fibronectin	Decreased	Slightly increased
Adhesion to collagen IV	Decreased	Decreased
Adhesion to collagen I	Increased	Slightly increased
Colony growth	Slightly increased	Decreased
Anoikis	Slightly increased	Decreased
Integrin β1 expression	Unchanged	Increased
Integrin α2 expression	Unchanged	Unchanged
Integrin α5 expression	Decreased	Increased
Integrin α6 expression	Slightly increased	Increased
Drug sensitivity profile	Slight decreased sensitivity	Increased sensitivity

3.4 Proteomic analysis of MiaPaCa-2 and sub-populations Clone #3 and Clone #8 by two-dimensional difference in-gel electrophoresis (2-D DIGE)

Adhesion and degradation of the extracellular matrix (ECM) or basement membrane is one of the first critical steps during the invasive/metastatic cascade *in vivo* (Hood and Cheresh, 2002). Cell-ECM interaction can lead to the activation of essential signalling pathways, therefore to study these stimulated mechanisms, MiaPaCa-2, Clone #3 and Clone #8 were grown on matrigel for 24 hrs (Chapter 2.5.5).

During control conditions, Clone #3 displays a 2.5-fold increase in invasion, while Clone #8 has a 6-fold decrease in invasion compared to the parental cell line, MiaPaCa-2 (Figure 3.4.1). However, pre-incubation of the cells to matrigel for 24 hours prior to the *in vitro* invasion assay induced a further increase in the invasive potential of the cells and a new phenomenon termed superinvasion was also observed (Chapter 3.5). Superinvasion is defined as a process by which cells invade through the matrigel in the Boyden chamber and attach to the bottom of the plate (Glynn *et al.*, 2005).
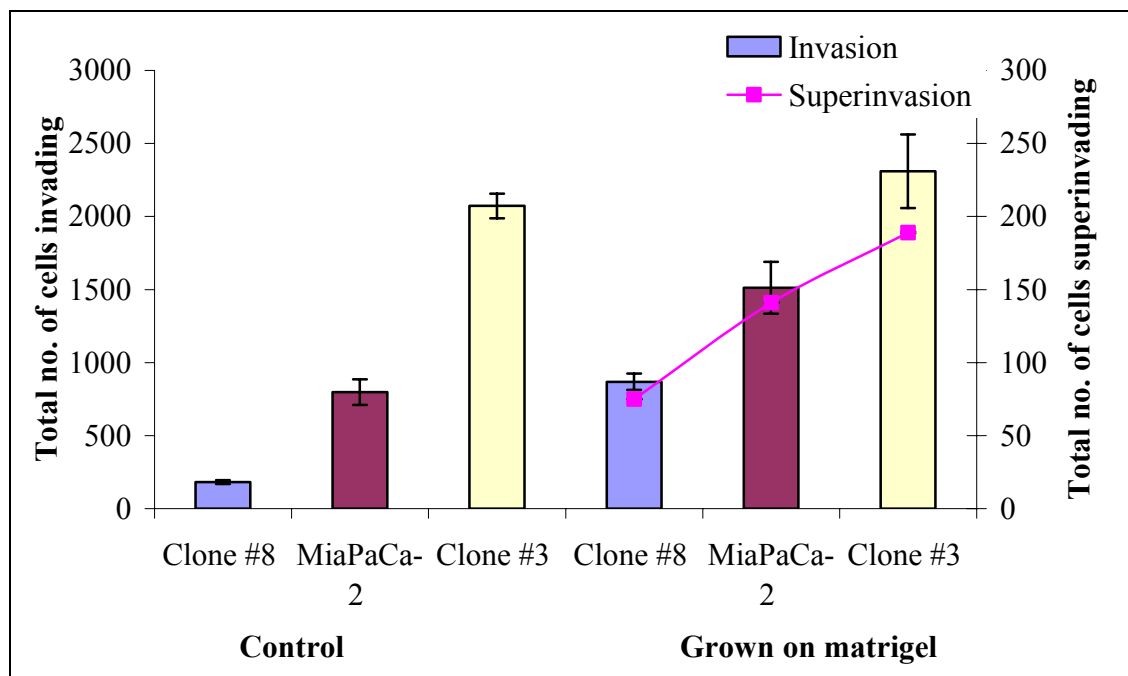
Figure 3.4.1 Total number of cells invading under control conditions and also after 24 hrs incubation on matrigel. Line graph displays the total number of superinvading cells counted after 24 hrs incubation on matrigel of Clone #8, MiaPaCa-2 and Clone #3.

To determine expression differences between the parental cell line and the sub-populations Clone #3 and Clone #8, proteomic analysis was carried out on MiaPaCa-2, Clone #3 and Clone #8 (Chapter 2.10) grown on matrigel for 24 hrs. Investigations into differential protein expression between the cell lines grown on matrigel in relation to their altered invasive phenotype could potentially identify significant functions of proteins and the complexities of cell-ECM interactions and may be critical for developing effective diagnostic techniques and early invasive detection markers for pancreatic cancer.

3.4.1 Experimental outline for 2D-DIGE analysis of the samples

2D-DIGE protein separation is performed by separating proteins first by isoelectric point and then by molecular weight. Protein spots in a gel are visualised using fluorescent markers (Görg *et al.*, 2004). 2-D DIGE enables the incorporation of the same internal standard on every 2-D gel. The internal standard is a pool of all the samples within the experiment, and therefore contains every protein from every sample (e.g. MiaPaCa-2, Clone #3 and Clone #8). Duplicate technical repeats were also carried out as well as reverse labelling. Once proteins are separated and quantified, they are identified by MALDI-TOF MS (Chapter 1.7.1). Identification of proteins enables lists to be generated detailing differentially regulated proteins between samples.

Gel number	Cy2	Cy3	Cy5
Gel 1	Pool	MiaPaCa-2 (1)	Clone #3 (1)
Gel 2	Pool	MiaPaCa-2 (2)	Clone #3 (2)
Gel 3	Pool	MiaPaCa-2 (3)	Clone #3 (3)
Gel 4	Pool	Clone #3 (1)	Clone #8 (1)
Gel 5	Pool	Clone #3 (2)	Clone #8 (2)
Gel 6	Pool	Clone #3 (3)	Clone #8 (3)
Gel 7	Pool	Clone #8 (1)	MiaPaCa-2 (1)
Gel 8	Pool	Clone #8 (2)	MiaPaCa-2 (2)
Gel 9	Pool	Clone #8 (3)	MiaPaCa-2 (3)
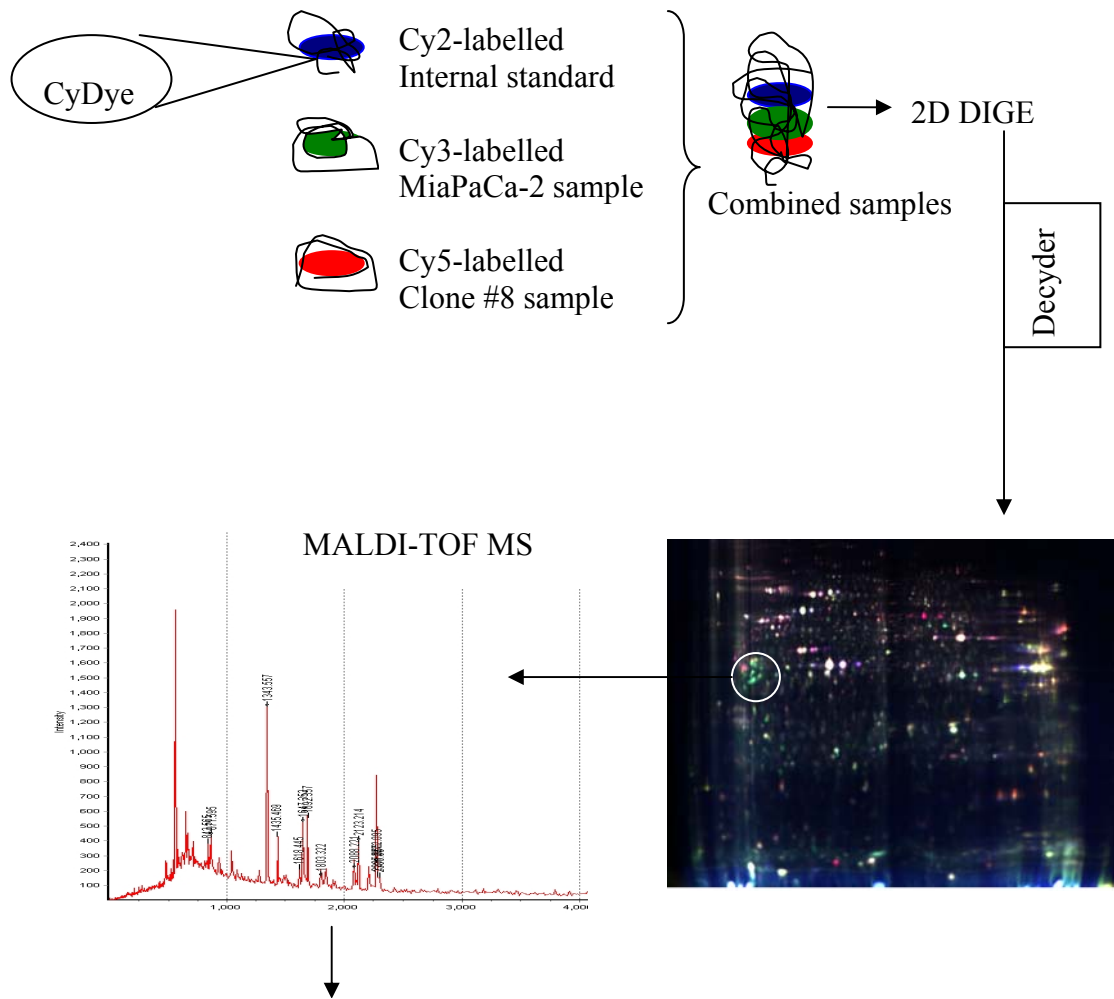
Figure 3.4.2 Normalised pool comprising all the samples from all samples (MiaPaCa-2, Clone #3 and Clone #8) is labelled with Cy2 dye. Each 2D-DIGE gel comprises pool (Cy2), condition 1 (Cy3/Cy5) and condition 2 (Cy3/Cy5) samples. The three scanned images from each 2D-DIGE are further analysed by DeCyder Image analysis software to generate the differentially regulated protein spots. The differentially regulated protein spots, as depicted in the 2D gel, are further processed by MALDI-TOF MS for peptide mass fingerprinting for protein identification.

3.4.1.1 Identification of differentially regulated proteins

Differential protein expression between triplicate biological replicates of MiaPaCa-2, Clone #3 and Clone #8 (exposed to matrigel for 24 hrs) were examined using 2D-DIGE. DeCyder^{TM} 6.5 software was used to identify differentially regulated proteins in each comparison. Biological variation analyses of these spots showing greater that 1.2-fold change in expression with a t-test score of less that 0.05 were identified.

To evaluate the differentially expressed proteins in the cell lines MiaPaCa-2, Clone #3 and Clone #8, three comparative protein lists were generated. A total number of 113 protein spots were identified in each comparison. Of these, 52 proteins were changed in the comparison of MiaPaCa-2 versus Clone #8; Clone #3 versus MiaPaCa-2 resulted in 37 differentially regulated proteins, and in the comparison of Clone #3 versus Clone #8, 60 proteins were identified as differentially regulated (Chapter 7.0, Appendix).

In order to further determine the biological relevance of these differentially expressed proteins, the design analysis was laid out to specifically identify protein changes (either up-regulated or down-regulated) that consistently correlated with the invasion status of the cell lines, that is from high to low invasion (MiaPaCa-2 versus Clone #8 and Clone #3 versus MiaPaCa-2 and Clone #3 versus Clone #8). The three protein lists were overlaid, determining unique and common proteins between lists, as outlined in the next section.

3.4.1.2 Identification of unique proteins differentially regulated with the invasion status of the cell lines

The unique proteins abundantly expressed between each of the comparison lists (MiaPaCa-2 versus Clone #8 and Clone #3 versus MiaPaCa-2 and Clone #3 versus Clone #8) were determined to assess the potential role of uniquely expressed proteins in each comparison.

The fold change in spot intensity in each comparison was determined from the Cy5/Cy3/Cy2 images of replicate repeats. The cell lines are compared from high to low invasion, therefore, proteins that are up-regulated, are increased in the more invasive cells lines and are represented as positive fold changes. The proteins that are down-regulated have negative fold changes, as these proteins are lowly expressed in the invasive cell lines compared to the less invasive cell lines.

Table 3.4.1 outlines the 12 unique expressed proteins in the comparison of MiaPaCa-2 to Clone #8. Among these proteins, 5 were up-regulated while 7 were down-regulated.

In the comparison of Clone #3 to MiaPaCa-2, 9 proteins were identified as uniquely expressed (Table 3.4.2). This list identified 8 up-related protein and 1-down regulated proteins.

Table 3.4.3 displays 13 unique differentially expressed proteins in the comparison of Clone #3 to Clone #8. Of these 13 proteins, 12 proteins were up-regulated, while 1 protein was down-regulated.

Table 3.4.1 **Proteins unique in the comparison of MiaPaCa-2 versus Clone #8**

Protein name	Gene symbol	Protein AC number	pI/Mw	% coverage	Fold change MiaPaCa-2 versus Clone #8
Aldolase	ALDOA	gi|4930291|	8.8/39.7	28.9	-1.4 **
14-3-3 Protein Epsilon	YWHAE	gi|67464424|	4.6/29.1	27.3	-1.3 *
Heat shock protein 60 (b)	HSPD1	gi|77702086|	5.7/61.4	35.5	-1.5 *
Peroxiredoxin 2	PRDX2	gi|33188452|	6.1/16.0	25.9	-1.4 ***
Heat shock protein 60 (c)	HSPD1	gi|77702086|	5.7/61.4	31.3	-1.3 *
Aldehyde dehydrogenase 1 family; member B1	ALDH1B1	gi|2183299|	6.4/57.7	25.9	-1.3 *
Glutathione synthetase	GSS	gi|8248826|	5.7/52.5	27.8	-1.2 *
Beta actin (d)	ACTB	gi|15277503|	5.6/40.5	21.7	1.2 *
Heat shock 70kDa protein 1A	HSPA1A	gi|5123454|	5.5/70.3	33.5	1.3 ***
Nucleoside diphosphate kinase	NDPK	gi|1421614|	5.3/46.4	12.8	1.7 ***
Gamma actin (b)	ACTG1	gi|17511847|	8.8/17.3	43.7	2.0 ***
Beta actin (b)	ACTB	gi|15277503|	5.3/42.1	45.6	2.3 ***

The theoretical isoelectric point (pI) and molecular weight (Mw) were calculated from the sequence of the protein in the database. Isoforms of the same protein are referred to as (a), (b) etc. The percentage coverage is the amount of the protein sequence covered by the matched peptides. Statistical analysis between replicates is referred to as; * $p \leq$ 0.05, *** $p \leq$ 0.01, *** $p \leq$ 0.005. For protein identification, all proteins were digested and identified at least twice from separate gels with MALDI-TOF MS. An expectation value of <0.02 was used for all reported identifications, which indicates a 0.2% chance that the identification is random.

Table 3.4.2   Proteins unique to Clone #3 versus MiaPaCa-2

Protein name	Gene symbol	Protein AC number	pI/Mw	% Coverage	Fold change Clone #3 versus MiaPaCa-2
90kDa heat shock protein	HSP90ab1	gi|306891|	5.0/83.6	12.2	-1.2 *
Aspartate aminotransferase 2 precursor variant	GOT2	gi|62898103|	9.4/47.9	23	1.2 *
Glyceraldehyde-3-phosphate dehydrogenase (d)	GAPDH	gi|31645|	8.7/36.2	22.1	1.2 *
Transketolase	TKT	gi|37267|	6.5/58.8	33.6	1.3 *
Triosephosphate Isomerase (Tim) (b)	TPI1	gi|66360366|	6.5/26.8	19.4	1.3 **
ATP synthase 5 alpha 1 protein (a)	ATP5A1	gi|34782901|	9.2/48.9	27.8	1.3 ***
ATP synthase beta subunit	ATP5B	gi|179279|	5.4/56.9	31.4	1.3 **
Hydroxyacyl dehydrogenase; subunit B	HADHB	gi|44890770|	9.6/51.6	31.6	1.5 **
Beta actin (a)	ACTB	gi|15277503|	5.6/40.5	17.2	1.7 **

The theoretical isoelectric point (pI) and molecular weight (Mw) were calculated from the sequence of the protein in the database. Isoforms of the same protein are referred to as (a), (b) etc. The percentage coverage is the amount of the protein sequence covered by the matched peptides. Statistical analysis between replicates is referred to as; * $p \leq$ 0.05, *** $p \leq 0.01$, *** $p \leq 0.005$. For protein identification, all proteins were digested and identified at least twice from separate gels with MALDI-TOF MS. An expectation value of <0.02 was used for all reported identifications, which indicates a 0.2% chance that the identification is random.

Table 3.4.3   Proteins unique to Clone #3 versus Clone #8

Protein name	Gene symbol	Protein AC number	pI/Mw	% coverage	Fold change Clone #3 versus Clone #8
Heat shock 70kDa protein 8 isoform (b)	HSPA8	gi|62897129|	4.9/26.9	23.5	-1.3 **
Eukaryotic translation elongation factor 2	EEF2	gi|33869643|	9.1/65.4	13.6	1.2 *
Malate dehydrogenase 2	MDH2	gi|49168580|	9.4/36.0	49.7	1.4 **
Tubulin; beta polypeptide (a)	TUBB	gi|18088719|	4.7/50.1	33.1	1.3 **
Tubulin; beta polypeptide (b)	TUBB	gi|18088719|	5.0/50.5	29.4	1.4 **
Tubulin alpha 6 variant	TUBA6	gi|62897609|	5.0/46.5	29	1.4 **
Protein disulfide isomerise protein 5	PDIA5	gi|1710248|	5.3/71.1	30.5	1.4 ***
Heat shock 70kDa protein 8 isoform (b)	HSPA8	gi|62897129|	6.1/47.1	27	1.3 *
Translation initiation factor	EIF4A3	gi|496902|	4.7/50.2	32.9	1.5 ***
Beta-tubulin	TUBB	gi|18088719|	5.9/57.2	26.9	1.5 ***
ER-60 protein (b)	PDIA3	gi|2245365|	8.1/18.1	30.3	1.7 ***
Cyclophilin A complexed with 2-Thr cyclosporine A	PPIA	gi|3659980|	5.0/50.5	18.9	1.7 **
Stress induced phosphoprotein (b)	STIP1	gi|54696884|	6.4/63.3	11.6	1.8 ***

The theoretical Pi and Mw were calculated from the sequence of the protein in the database. Isoforms of the same protein are referred to as (a), (b) etc. The % coverage is the amount of the protein sequence covered by the matched peptides. Statistical analysis between replicates is referred to as; * $p \leq 0.05$, *** $p \leq 0.01$, *** $p \leq 0.005$. An expectation value of <0.02 was used for all reported MS identifications.

3.4.1.3 Identification of common proteins differentially regulated with the invasion status of the cell lines by overlapping two lists

Proteins commonly expressed between the cell lines, MiaPaCa-2, Clone #3 and Clone #8 were examined. The three generated protein comparison lists (MiaPaCa-2 versus Clone #8, Clone #3 versus MiaPaCa-2 and Clone #3 versus Clone #8) were then overlaid to identify common proteins expressed in two lists.

Each generated comparison (from high to low invasion) was overlapped with another comparison to identify key differentially regulated proteins common to both proteins lists. Proteins that are up-regulated are increased in the more invasive cells lines due to high invasion status and have positive fold changes. The proteins that are down-regulated have negative fold changes, as these proteins are lowly expressed in the invasive cell lines compared to the less invasive cell lines. To further define the involvement of the overlapping proteins in each comparison, the proteins with consistent expression (either positively or negatively) in each comparison were considered consistently expressed and deemed more associated with invasion trend of the cell lines.

Two comparison lists, MiaPaCa-2 versus Clone #8 and Clone #3 versus MiaPaCa-2 were overlapped. Table 3.4.4 displays the 4 proteins that were identified as commonly regulated between the lists. The 4 proteins identified were inconsistently expressed in this comparison .i.e. the expression (fold change) did not consistently correlate to the invasive trend of the cell lines.

The comparison of Clone #3 versus MiaPaCa-2 and Clone #3 versus Clone #8 resulted in 11 differentially regulated proteins (Table 3.4.5). Of these 11 proteins, 10 proteins were up-regulated and 1 protein was down-regulated. All proteins were consistently expressed in both comparisons.

Table 3.4.6 outlines the 23 proteins commonly differentially expressed between the comparison of MiaPaCa-2 versus Clone #8 and Clone #3 versus Clone #8. Of these 23 proteins, 17 were up-regulated and 6 were down-regulated. All proteins were consistently expressed in both comparisons.

Table 3.4.4 **Proteins commonly expressed in the comparison of MiaPaCa-2 to Clone #8 and Clone #3 to MiaPaCa-2**

Protein name	Gene symbol	Protein AC number	pI/Mw	% Coverage	Fold change	
					MiaPaCa2 versus Clone #8	Clone #3 versus MiaPaCa2
Peroxiredoxin	PRDX1	gi|55959887|	6.4/19.1	38.6	-1.4 ***	1.2 **
14-3-3 Protein Theta	YWHAQ	gi|71042777|	5.2/29.4	24.2	-1.4 ***	1.5 ***
Annexin I (a)	ANXA1	gi|442631|	7.9/35.3	23.9	1.5 **	-1.5 *
Annexin A2 isoform 2 variant	ANXA2	gi|62896643|	6.9/38.9	25.7	1.6 ***	-1.3 *

The theoretical isoelectric point (pI) and molecular weight (Mw) were calculated from the sequence of the protein in the database. Isoforms of the same protein are referred to as (a), (b) etc. The percentage coverage is the amount of the protein sequence covered by the matched peptides. Statistical analysis between replicates is referred to as; * $p \le$ 0.05, *** $p \le 0.01$, *** $p \le 0.005$. For protein identification, all proteins were digested and identified at least twice from separate gels with MALDI-TOF MS. An expectation value of <0.02 was used for all reported identifications, which indicates a 0.2% chance that the identification is random.

Table 3.4.5   **Proteins commonly expressed in the comparison of Clone #3 to MiaPaCa-2 and Clone #3 to Clone #8**

Protein name	Gene symbol	Protein AC number	pI/Mw	% Cov	Fold change	
					Clone #3 versus MiaPaCa-2	Clone #3 versus Clone #8
Heat shock 70kDa protein 8 isoform 1 variant (c)	HSPA8	gi|62897129|	5.3/71.1	18.3	-1.2 *	-1.3 **
Mortalin (a)	HSPA9	gi|21040386|	6.0/74.1	38.5	1.2 ***	1.2 *
Aldolase (b)	ALDOA	gi|4930291|	8.8/39.7	27.8	1.3 *	1.3 *
Mortalin (b)	HSPA9	gi|292059|	6.0/74.1	17.5	1.4 ***	1.6 ***
Aconitase 2, mitochondrial	ACO2	gi|49168620|	7.2/86.2	11.9	1.4 ***	1.3 *
Annexin I (b)	ANXA1	gi|442631|	7.9/35.3	14.6	1.5 ***	1.3 *
ER-60 protein	PDIA3	gi|2245365|	5.9/57.2	25.5	1.5 *	1.7 ***
Translation initiation factor	EIF4A3	gi|496902|	6.1/47.1	27	1.5 ***	1.5 ***
ATP synthase 5 alpha 1 (b)	ATP5A1	gi|34782901|	8.4/54.6	36.2	1.5 **	1.5 *
Translation elongation factor 1 alpha 1-like 14 (b)	EEF1A1	gi|15277711|	9.1/43.3	12.1	1.6 *	2.2 ***
Elongation factor 1 alpha 1 (a)	EEF1A1	gi|28848610|	5.3/43.2	10.1	2.0 **	2.4 ***

The theoretical pI and Mw were calculated from the sequence of the protein in the database. Isoforms of the same protein are referred to as (a), (b) etc. The % coverage is the amount of the protein sequence covered by the matched peptides. Statistical analysis between replicates is referred to as; * $p \leq 0.05$, *** $p \leq 0.01$, *** $p \leq 0.005$. An expectation value of <0.02 was used for all reported MS identifications.

Table 3.4.6 Proteins commonly expressed in the comparison of MiaPaCa-2 to Clone #8 and Clone #3 to Clone #8

Protein name	Gene symbol	Protein AC number	pI/MW	% coverage	Fold change	
					MiaPaCa-2 versus Clone #8	Clone #3 versus Clone #8
Glyceraldehyde dehydrogenase (a)	GAPDH	gi|31645|	8.4/36.2	16.1	-1.7 ***	-1.9 ***
Profilin	PFN1	gi|30582841|	8.7/15.2	24.3	-1.6 ***	-1.4 **
Heat shock protein 60 (a)	HSPD1	gi|77702086|	5.7/61.4	42.8	-1.6 ***	-1.5 ***
Beta Actin (c)	ACTB	gi|15277503|	5.6/40.5	20.0	-1.5 ***	-1.6 **
Ubiquinol-cytochrome c reductase complex core protein I	UQCRC1	gi|731047|	5.9/53.3	20.0	-1.3 ***	-1.3 ***
Stomatin-like 2	STOML2	gi|6841440|	6.9/38.6	23.6	-1.3 **	-1.2 *
Alpha tubulin	TUBA	gi|340021|	4.9/50.8	32.6	1.3 *	1.4 **
Tubulin alpha 6 variant	TUBA6	gi|62897609|	5.0/50.5	28.7	1.3 **	1.4 ***
Heat shock 70kDa protein 8 isoform 1 variant (d)	HSPA8	gi|62897129|	5.6/53.6	41.4	1.5 ***	1.7 ***
Dissociation inhibitor 2	GDI2	gi|285975|	5.9/51.1	31.7	1.6 ***	1.8 ***
Enolase 1 variant	ENO1	gi|62897945|	7.0/47.5	31.8	1.6 ***	1.9 ***
Heat shock 70kDa protein 8 isoform 1 variant (a)	HSPA8	gi|62897129|	5.3/71.1	28.2	1.6 ***	1.9 ***

Protein	Gene	Accession	pI/Mw	% Coverage	Ratio 1	Ratio 2
Pyruvate kinase 3 isoform 1 variant (a)	PKM2	gi|67464392|	8.8/58.5	44.8	1.6 ***	1.9 ***
Pyruvate kinase 3 isoform 1 variant (b)	PKM2	gi|67464392|	7.8/58.5	41.8	1.6 **	2.4 ***
GARS	GARS	gi|12652637|	8.2/85.4	19.7	1.7 ***	1.8 ***
Chaperonin TCP1, subunit 5 (epsilon)	CCT5	gi|58257644|	5.5/61.5	38.3	1.7 ***	1.8 ***
Vimentin (d)	VIM	gi|57471646|	5.2/49.7	18.1	1.8 ***	2.0 ***
Vinculin	VCL	gi|24657579|	5.8/117.3	15.6	1.8 ***	2.2 ***
Heat shock 70kDa protein 4 isoform a variant	HSPA4	gi|62087882|	5.4/88.8	10.5	2.0 ***	2.4 ***
Eukaryotic translation elongation factor 1 alpha 1 variant (c)	EEF1A1	gi|62897525|	9.3/50.5	16.5	2.0 ***	1.8 *
Eukaryotic translation elongation factor 2	EEF2	gi|33869643|	6.5/58.2	17.6	2.1 ***	2.0 ***
Vimentin (b)	VIM	gi|57471646|	5.2/49.7	33.2	2.2 ***	2.8 ***
Aldehyde dehydrogenase 1 (c)	ALDH1A1	gi|2183299|	6.3/55.4	28.5	3.8 ***	5.3 ***

The theoretical pI and Mw were calculated from the sequence of the protein in the database. Isoforms of the same protein are referred to as (a), (b) etc. The % coverage is the amount of the protein sequence covered by the matched peptides. Statistical analysis between replicates is referred to as; * $p \leq 0.05$, *** $p \leq 0.01$, *** $p \leq 0.005$. An expectation value of <0.02 was used for all reported MS identifications.

3.4.2 Identification of common proteins differentially regulated with the invasion status of the cell lines by overlapping three lists

The three generated protein comparison lists (MiaPaCa-2 versus Clone #8, Clone #3 versus MiaPaCa-2 and Clone #3 versus Clone #8) were then overlaid to determine the common proteins in all the lists.

Table 3.4.7 outlines the list of proteins, in which 13 proteins were commonly regulated between all the lists generated. Of these 13 proteins, 9 proteins were consistently changed across all the lists either increasing/decreasing in expression relative to the invasion status of the cell lines. These 9 proteins are highlighted in bold, KRT19, GAPDH, STIP1, GANAB, UBE1, VIM, TPI1 and ALDH1A1 (a) (b).

Keratin 18 (KRT18) and GAPDH are expressed at lower levels in the high invasive cell line, Clone #3, and expression of these two proteins are increased in the low invasive cell line Clone #8. Their expression in all three lists (going from high to low invasion) is consistently down-regulated as the invasion status of the cell lines increases.

Seven proteins, ALDH1A1 isoforms (a) and (b), TPI1 isoform (a), VIM isoform (a), UBE1, GANAB and STIP1 isoform (a) were all expressed at higher levels in the invasive cell line, Clone #3 compared to the low invasive cell line, Clone #8. Their expression is consistently up-regulated as the invasive status of the cell lines increases.

Figure 3.4.3 represents protein expression map of common differentially regulated proteins between all three list comparisons.

Validation by Western blot was carried out on proteins, ALDH1A1, VIM, TPI1, KRT18, GAPDH, TPI1, ALDH1A1, STIP1 and VIM. Immunofluorescence was also carried out on KRT18 and VIM.

Further functional analysis was carried out on the proteins aldehyde dehydrogenase (ALDH1A1), vimentin (VIM) and stress-induced phosphoprotein 1 (STIP1).

Table 3.4.7   **Overlapping proteins spots between the comparisons MiaPaCa-2 versus Clone #8 and Clone #3 versus MiaPaCa-2 and Clone #3 versus Clone #8**

Protein name	Gene symbol	Protein AC number	pI/MW	% coverage	Fold change			Protein expression as invasion increases
					MiaPaCa-2 versus Clone #8	Clone #3 versus MiaPaCa-2	Clone #3 versus Clone #8	
Antiquitin (b)	ALDH7A1	gi|34783121|	6.2/55.9	17.6	-4.7 ***	2.2 ***	-2.2 ***	n/a
Antiquitin (a)	ALDH7A1	gi|34783121|	6.2/55.9	13.7	2.6 ***	1.7 ***	-1.5 **	n/a
Glyceraldehyde-3-phosphate dehydrogenase (b)	**GAPDH**	**gi|31645|**	**8.4/36.2**	**29.6**	**-1.9 *****	**-1.3 ****	**-2.6 *****	**decreasing**
Keratin 18	**KRT18**	**gi|12653819|**	**5.4/48.0**	**37.7**	**-1.6 ***	**-1.8 ***	**-2.9 *****	**decreasing**
Gamma actin (a)	ACTG1	114865	5.3/42.1	40.3	-1.2 *	-1.3 **	1.5 *	n/a
Stress-induced-phosphoprotein 1 (a)	**STIP1**	**gi|54696884|**	**6.4/63.3**	**17.9**	**1.3 ***	**1.5 ***	**2.0 *****	**increasing**
Glucosidase II	**GANAB**	**gi|2274968|**	**5.7/107**	**11.3**	**1.4 *****	**1.6 *****	**2.2 *****	**increasing**
Ubiquitin-activating enzyme E1	**UBE1**	**gi|57209338|**	**5.5/119**	**4.9**	**1.6 ****	**1.6 ****	**2.6 *****	**increasing**
Human Tryptophanyl-Trna Synthetase	WARS	gi|50513261|	7.1/43.6	35.2	1.8 ***	1.3 **	1.4 ***	n/a

Vimentin (a)	**VIM**	**gi|57471646|**	**5.2/49.7**	**37.9**	**2.2 *****	**2.5 *****	**5.5 *****	**increasing**
Chain B; Human Triosephosphate Isomerase (a)	**TPI1**	**gi|66360366|**	**6.5/26.8**	**19.4**	**2.2 *****	**1.8 ****	**4.0 *****	**increasing**
Aldehyde dehydrogenase 1 (a)	**ALDH1A1**	**gi|2183299|**	6.3/55.4	21.8	**5.3 *****	**1.7 *****	**8.9 *****	**increasing**
Aldehyde dehydrogenase 1 (b)	ALDH1A1	gi|2183299|	5.2/49.7	33.2	6.8 ***	1.2 *	8.4 ***	increasing

The theoretical isoelectric point (pI) and molecular weight (Mw) were calculated from the sequence of the protein in the database. Isoforms of the same protein are referred to as (a), (b) etc. The percentage coverage is the amount of the protein sequence covered by the matched peptides. n/a refers to expression not consistent between protein lists. Statistical analysis between replicates is referred to as; * $p \leq 0.05$, *** $p \leq 0.01$, *** $p \leq 0.005$. For protein identification, all proteins were digested and identified at least twice from separate gels with MALDI-TOF MS. An expectation value of <0.02 was used for all reported identifications, which indicates a 0.2% chance that the identification is random.
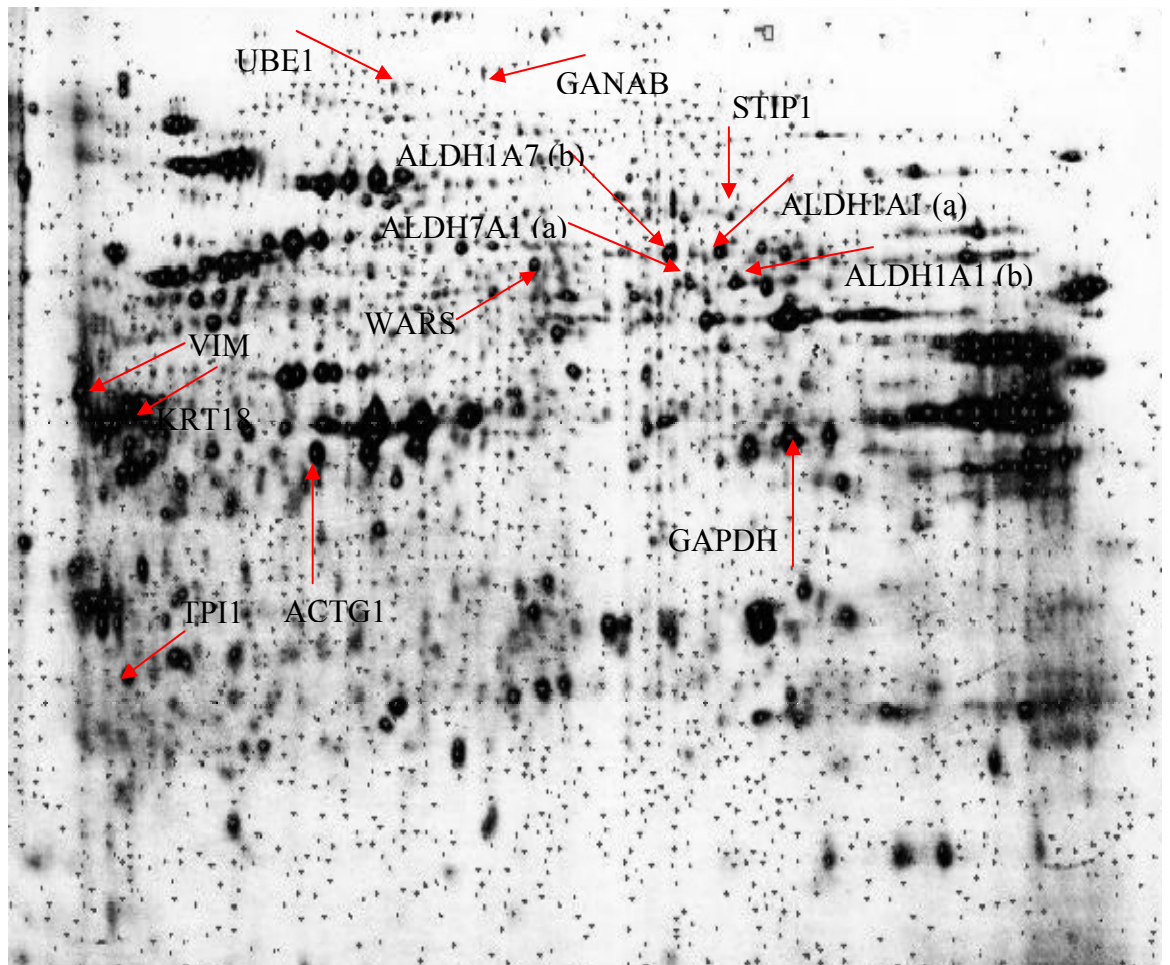
Figure 3.4.3 Protein expression map of MiaPaCa-2, Clone #3 and Clone #8. Arrows highlight 13 proteins commonly differentially regulated in three comparative protein lists.

3.4.3 Bioinformatic analysis of differentially regulated proteins

Bioinformatic analysis was carried out on all differentially regulated proteins identified in our proteomic comparison of MiaPaCa-2, Clone #3 and Clone #8. Figure 3.4.4 represents a Venn diagram outlining the distribution of proteins between the three generated lists, MiaPaCa-2 versus Clone #8, Clone #3 versus MiaPaCa-2 and Clone #3 versus Clone #8.

Using DAVID gene ID tool software (http://david.abcc.ncifcrf.gov), the proteins differentially regulated in our model were converted to their gene IDs. Gene ontology (GO STAT) (http://gostat.wehi.edu.au/cgi-bin/goStat.pl) was then used to classify the proteins and their corresponding genes into gene categories. Enrichment of a particular ontology term, for significantly expressed genes in response to the process under study, means that the ontology term is likely to be involved in the process. In our study, the process refers to invasion in pancreatic cancer. Using the over-expression function of the software and false discovery rate (Benjamini) stats, 52 GO terms were found significantly enriched. The "cytoplasm" term achieved the highest degree of significance in the up-regulated gene class (p = 1.40E-09), with "glycolysis" (p = 4.05E-07) and "nucleotide binding" (p = 1.04E-06) also highly significant terms. In the down-regulated class, "oxioreductase activity" (p = 0.0006), "aldehyde dehydrogenase activity" (p = 0.003) and "mitochondrion" (p = 0.03) were also significantly enhanced. Figure 3.4.5 outlines the top ten ranked functional categories using GO terms in the differentially expressed proteins in the pancreatic cancer model.

Pathway studio is a bioinformatics tool that allows the visualisation and analysis of biological pathways, gene regulation networks and protein interaction maps of groups of genes or proteins (Chapter 2.15). Direct interactions between the differentially regulated proteins in our pancreatic cancer cell line invasion model are shown in figure 3.4.6.

ANXA1
YWHAQ
PRDX1
ANXA2

Table 3.4.4

MiaPaCa-2 vs Clone #8
(52 proteins)

HSPA1A	ACTB (d)
PRDX2	HSPD1 (c)
HSPD1 (b)	NDPK
YWHAE	ACTG1 (b)
ALDH1B1	ALDOA (b)
GSS	ACTB (b)

Table 3.4.1

Clone #3 vs MiaPaCa-2
(37 proteins)

HSP90ab1	ATP5A1 (a)
GOT2	GAPDH (d)
HADHB	ACTB (b)
TPI1 (b)	ATPB
TKT	

Table 3.4.2

12   4   9

13

GAPDH (a)	HSPA8 (d)
PFN1	GDI2
HSPD1 (a)	ENO1
ACTB (c)	HSPA8 (a)
UQCRC1	PKM2 (a)
STOML2	PKM2 (b)
TUBA	GARS
PDIA3 (b)	CCT5

HSPA4
EEF1A1 (c)
EEF2 (a)
VIM (b)
ALDH1A1 (c)
VCL
VIM (d)

23   11

EEF1A1	HSPA9B	HSPA9
EEF1A1	ATP5A1 (a	ANXA1 (b)
HSPA8 (c	ALDOA (a	ACO2
PDIA3 (a	EIF4F	

Table 3.4.5

13

UBE1	ALDH1A1 (a)
WARS	ALDH1A1 (b)
VIM (a)	ALDH7A1 (b)
KRT18	ALDH7A1 (a)
STIP1(a)	GAPDH (b)
GANAB	ACTG1 (a)
TPI1 (a)	

Table 3.4.7

Table 3.4.6

PPIA	
TUBB (a)	EEF2 (b)
PDIA5	HSPA8 (b)
EIF4A3	STIP1 (b)
TUBB (b)	TUBB
MDH2	TUBA6 (a)
HSPA8 (c)	TUBA6 (c)

Clone #3 vs Clone #8
(60 proteins)

Table 3.4.3

Figure 3.4.4 Venn diagram of outlining overlapping proteins between the three lists generated (Clone #8 versus MiaPaCa-2 and MiaPaCa-2 versus Clone #3 and Clone #8 versus Clone #3).

Figure 3.4.5 Representation of the 10 top-ranked functional categories, using GO terms that are enriched in all significantly differentially expressed proteins between all three lists.

171
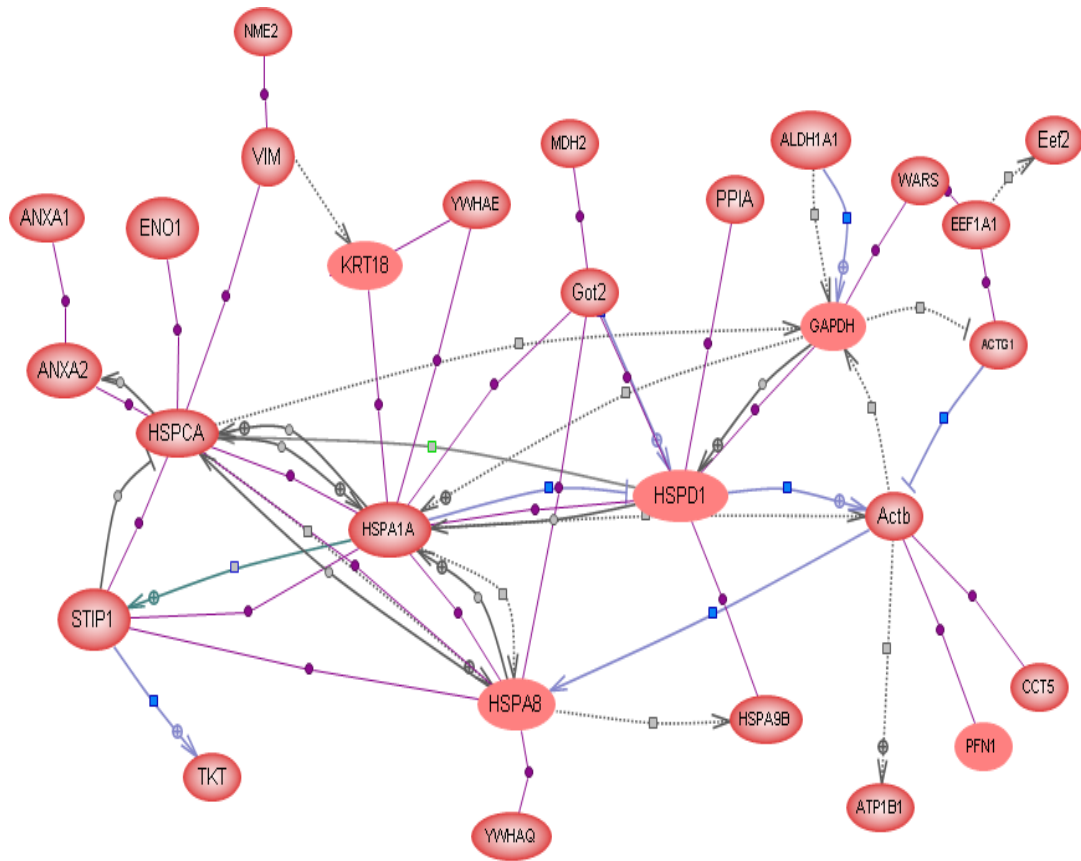
Figure 3.4.6 Pathway studio analysis of direct interaction between all differentially regulated proteins in MiaPaCa-2, Clone #3 and Clone #8. Each arrow represents as a type of control/action between proteins

3.4.4 Protein validation

The identified proteins showing consistent expression in terms of the invasion status of the cell lines (Table 3.4.7) were further analysed by literature searches, Western blot and/or fluorescence validation before final targets for functional analysis were chosen.

3.4.4.1 Western blot and immunofluorescence confirmation of proteomic data analysis

Western blot and immunofluorescence analysis of six proteins was carried out. The proteins highlighted in bold in table 3.4.7 were subjected to validation across the three cell lines exposed to matrigel for 24 hrs, MiaPaCa-2, Clone #3 and Clone #8.

Western blot verification was carried out on ALDH1A1, VIM, STIP1, KRT18, TPI1 and GAPDH. Immunofluorescence was performed on VIM and KRT18 to illustrate the localisation of the protein within the cells (Chapter 2.8.2).

Aldehyde dehydrogenase 1A1, vimentin, stress-induced phosphoprotein 1, cytokeratin 18 and glyceraldehyde-3-phosphate dehydrogenase confirmed the trends indicated in the proteomic analysis. However, Western blot analysis of triosephosphate isomerase 1 did not fully correspond to the trend of expression identified in the 2D proteomic analysis of the cell lines. This discrepancy may be due to the many isoforms caused by post-transcriptional modifications of the protein (Figures 3.4.7-3.4.12).

Three proteins, aldehyde dehydrogenase 1A1, vimentin and stress-induced phosphoprotein 1 were chosen for further functional analysis.

3.4.4.2 Aldehyde dehydrogenase 1A1

Clone #3   Clone #8

MiaPaCa-2   Clone #3   Clone #8

BiP (loading control)
78 kDa

Aldehyde dehydrogenase 1A1

55 kDa
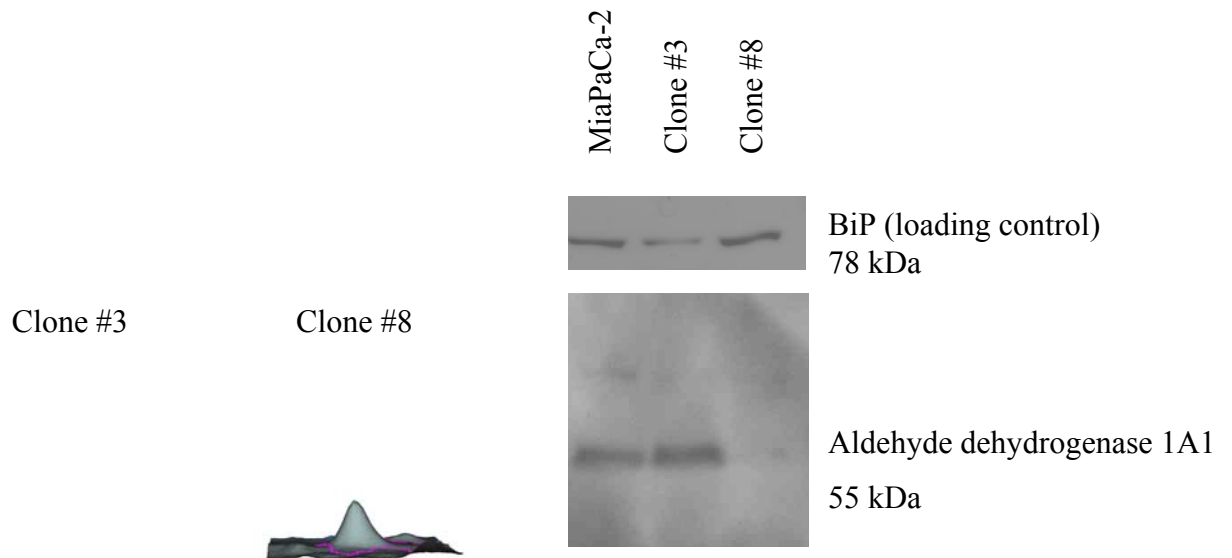
Figure 3.4.7 3D spot images from 2D DIGE gels (Decyder BVA module) and Western blot images of aldehyde dehydrogenase 1A1 protein expression in MiaPaCa-2, Clone #3 and Clone #8. Western blot is representative of three replicates.

3.4.4.3 Vimentin

A. MiaPaCa-2   **B. Clone #3**   **C. Clone #8**

Clone #3   Clone #8

Bip (loading control)
78 kDa
Vimentin 55 kDa
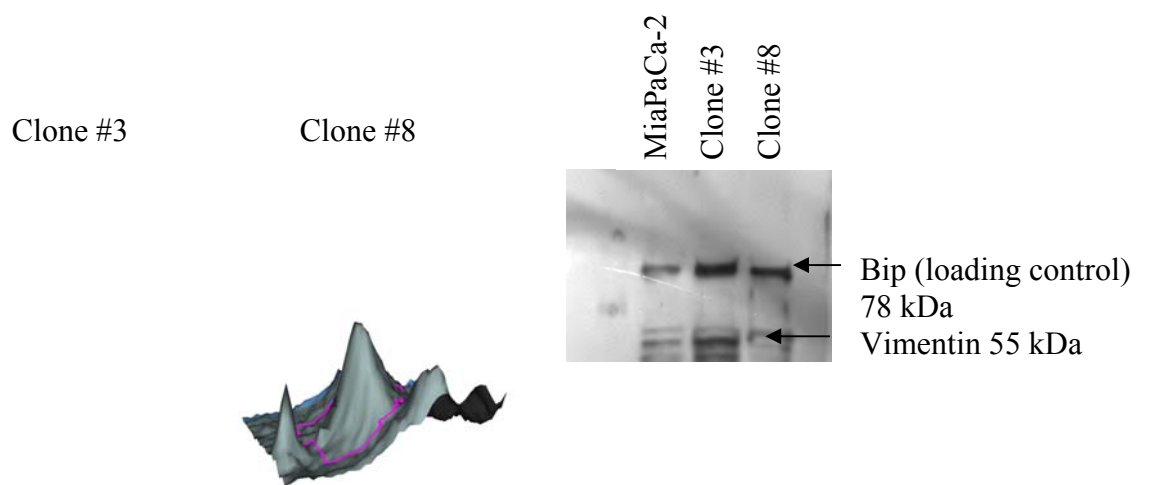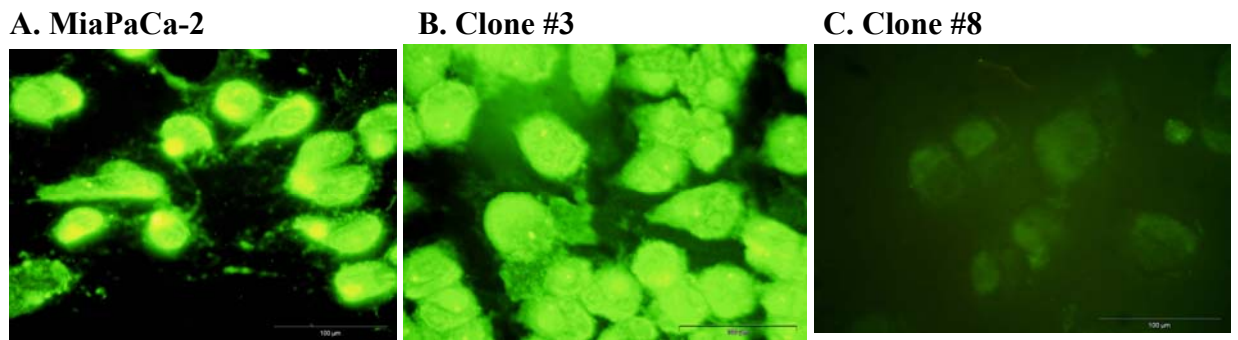
Figure 3.4.8 Immunofluorescence, 3D spot images from 2D DIGE gels (Decyder BVA module) and Western blot images of vimentin protein expression in A. MiaPaCa-2, B. Clone #3 and C. Clone #8. Western blot is representative of three replicates.

3.4.4.4 Stress-induced phosphoprotein 1

Clone #3   Clone #8

MiaPaCa-2   Clone #3   Clone #8

BiP (loading control)
78 kDa

STIP1 60 kDa
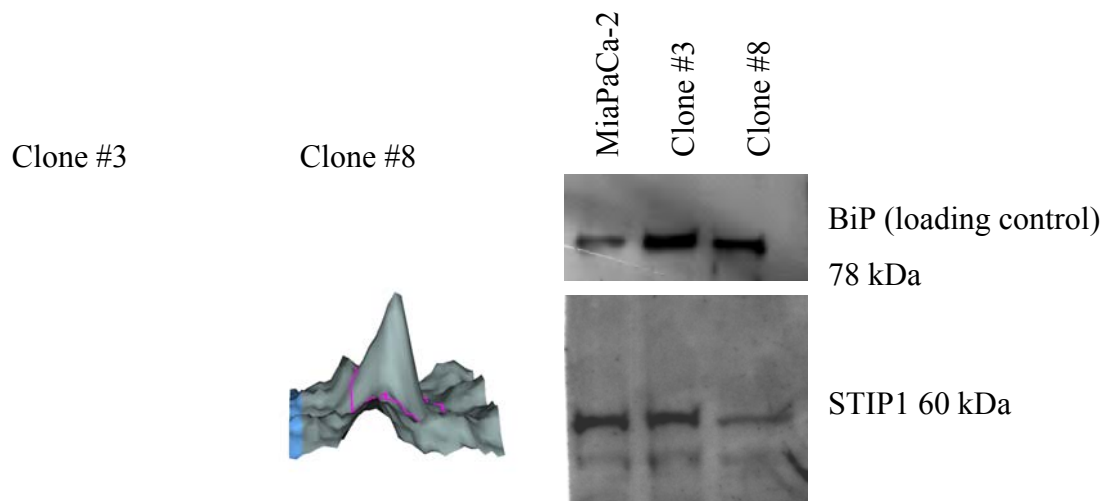
Figure 3.4.9 3D spot images from 2D DIGE gels (Decyder BVA module) and Western blot images of STIP1 protein expression in MiaPaCa-2, Clone #3 and Clone #8. Western blot is representative of two replicates.

3.4.4.5 Triosephosphate isomerase 1

Clone #3   Clone #8

MiaPaCa-2
Clone #3
Clone #8

Bip (loading control)
78 kDa

TPI1
27 kDa
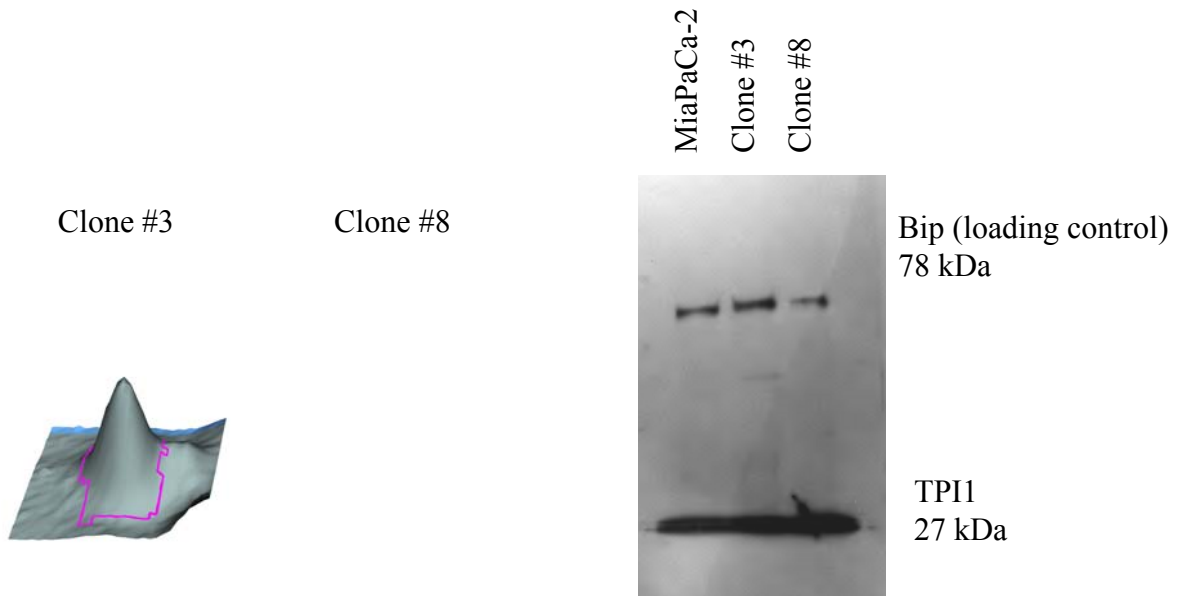
Figure 3.4.10 3D spot images from 2D DIGE gels (Decyder BVA module) and Western blot images of triosephosphate isomerase protein expression in MiaPaCa-2, Clone #3 and Clone #8. Western blot is representative of two replicates.

3.4.4.6 Cytokeratin 18

A. MiaPaCa-2 **B. Clone #3** **C. Clone #8**

Clone #3   Clone #8

MiaPaCa-2 Clone #3 Clone #8

Bip (loading control)
78 kDa
Cytokeratin 18
48 kDa
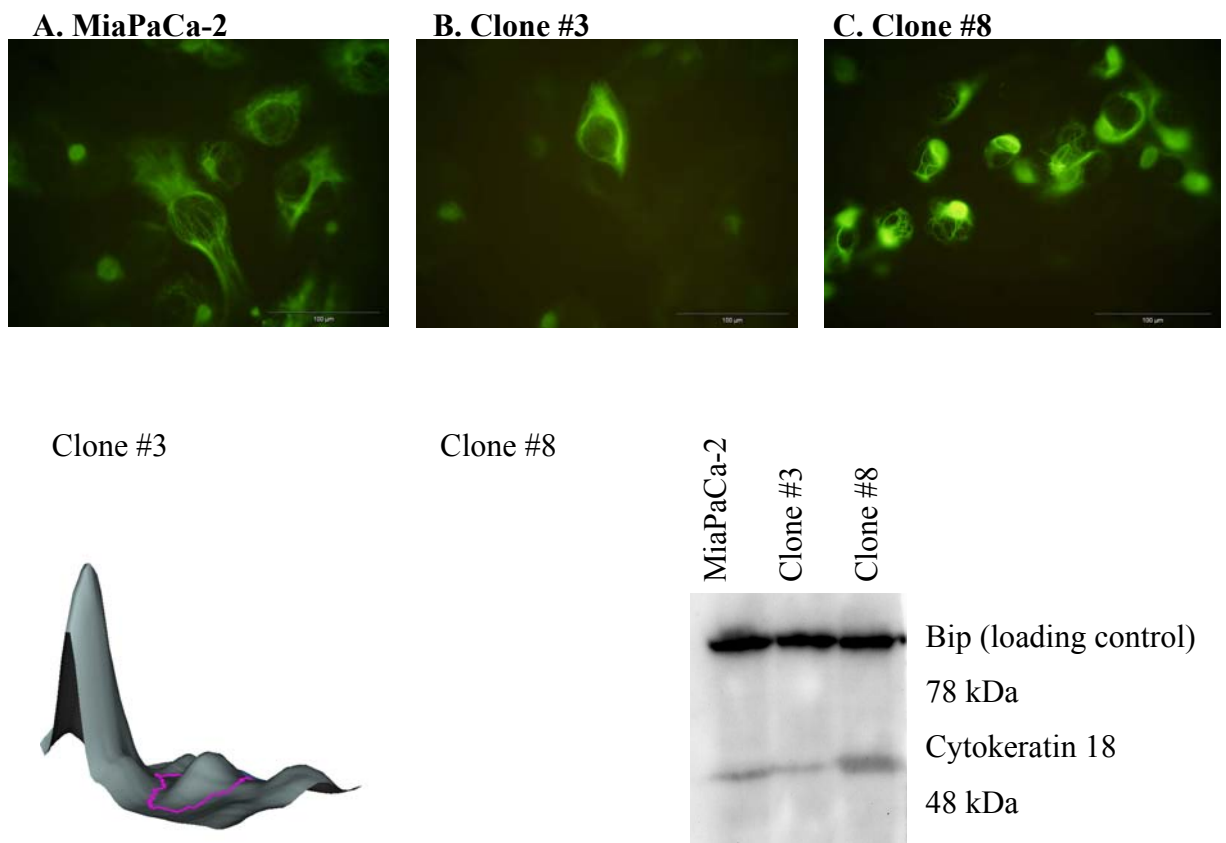
Figure 3.4.11 Immunofluorescence, 3D spot images from 2D DIGE gels (Decyder BVA module) and Western blot images of cytokeratin 18 protein expression in A. MiaPaCa-2, B. Clone #3 and C. Clone #8. Western blot is representative of three replicates.

3.4.4.7 Glyceraldehyde-3-phosphate dehydrogenase

Clone #3   Clone #8

MiaPaCa-2

Clone #3

Clone #8

BiP (loading control)

78 kDa

GAPDH

36 kDa
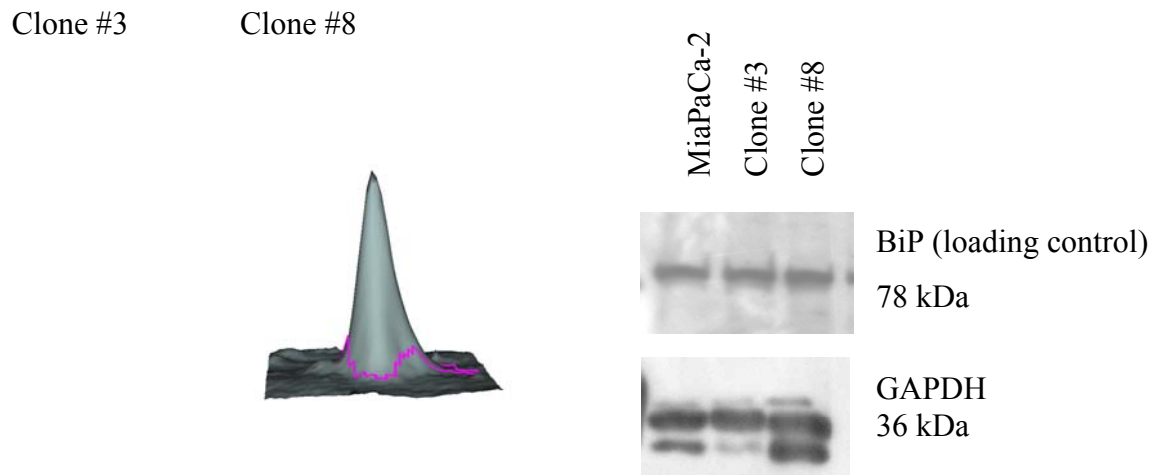
Figure 3.4.12 3D spot images from 2D DIGE gels (Decyder BVA module) and Western blot images of glyceraldehydes-3-phosphate dehydrogenase protein expression in MiaPaCa-2, Clone #3 and Clone #8. Western blot is representative of three replicates.

3.4.4.8 siRNA functional analysis of targets

SiRNA targets specific to invasion were chosen based on proteomic analysis of MiaPaCa-2, Clone #3 and Clone #8 grown on matrigel for 24 hrs. The conditions for siRNA transfection were optimised in 96- and 6-well plates using GAPDH and kinesin as positive controls, and scrambled siRNA as a siRNA transfection control.

Three siRNAs were selected for each of the 3 targets chosen and transfected into cells (Chapter 2.16.2). For each set of siRNA transfections carried out, a non-transfected cell line (control) and a scrambled (SCR) siRNA transfected control were used. Kinesin (Kin) was used as a control for efficient transfection as Kin siRNA reduces proliferation in the cells.

The three chosen targets, aldehyde dehydrogenase 1A1 (ALDH1A1), vimentin (VIM) and stress-induced phosphoprotein 1 (STIP1) were all up-regulated in the high invasive Clone #3, and therefore knockdown of these targets was expected to reduce the level of invasion.

Invasion assays (Chapter 2.16.3) were carried out to confirm whether or not these targets played an important role in invasion, as suggested by proteomic analysis.

Further functional analyses, including adhesion, anoikis, proliferation and chemosensitivity were assessed to investigate the potential role of these targets in characterising the malignant phenotype. In these experiments, all data was normalised to non-treated control cells and statistical analysis to determine significance was obtained by comparing scrambled cells to siRNA treated cells.

3.4.5 Investigation into the role of ALDH1A1 in pancreatic cancer cell invasion

Aldehyde dehydrogenase was identified as a protein potentially involved in invasion in our *in vitro* pancreatic cancer cell line model. The analysis showed that ALDH1A1 was 9-fold up-regulated in the more invasive sub-population, Clone #3 compared to the low invasive cell line, Clone #8 (Table 3.4.7).

3.4.5.1 Effect of ALDH1A1 siRNA transfection on Clone #3

The protein aldehyde dehydrogenase 1A1 was shown to be up-regulated as the invasion status of the cell lines increased, therefore the more invasive cell line, Clone #3 expressed an abundance of the protein. Clone #3 was used for siRNA knockdown and further functional analysis.

Figure 3.4.13 shows by Western blot, the efficient knockdown of ALDH1A1 in three siRNA transfected Clone #3 cells compared to non-treated control and siRNA scrambled transfected cells.
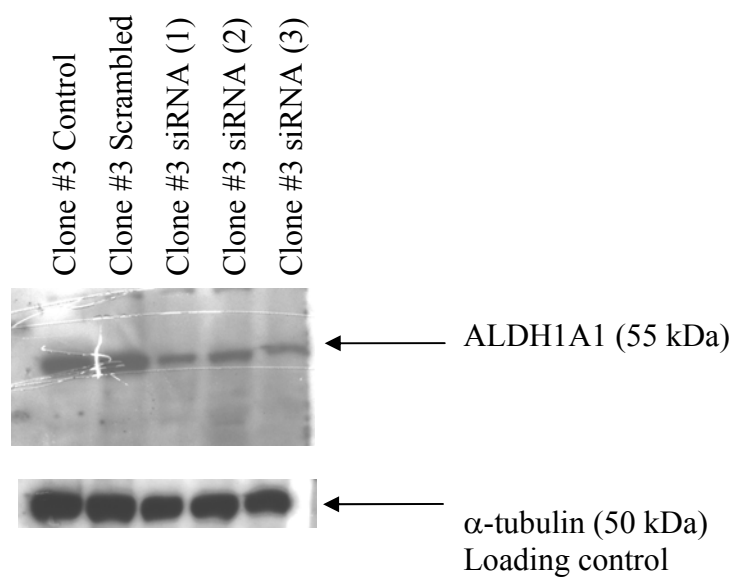
Figure 3.4.13 Western blot of siRNA ALDH1A1 knockdown in Clone #3. Three independent target siRNA of ALDH1A1 were transfected into Clone #3 cells. Protein was harvested 48 hrs post-transfection and used to determine an ALDH1A1-siRNA specific decrease at protein level in response to siRNA transfection by Western blot. α-tubulin antibody was used to demonstrate even loading between the samples.

3.4.5.2 Effect of ALDH1A1 siRNA on invasion

Fourty-eight hours post-transfection with ALDH1A1 siRNA, invasion assays were performed. The total number of cells invading was reduced in Clone #3 cells transfected with ALDH1A1 siRNA. Figure 3.4.14 (A) shows representative pictures of invading cells, and (B) highlights the total number of cells invading. ALDH1A1 siRNA transfection reduced the invasive capabilities of the cells. Invasion was significantly reduced by 2.2-fold (p=0.0013) with siRNA ALDH1A1 (1), 1.8-fold (p=0.00035) with siRNA ALDH1A1 (2) and 2.8-fold (p=0.0018) with ALDH1A1 (3) transfection.

3.4.5.3 Effect of ALDH1A1 siRNA on adhesion

Adhesion assays were also carried out to assess the involvement of ALDH1A1 in adhesion to matrigel. Figure 3.4.15 shows that ALDH1A1 siRNA transfection in Clone #3 cells increased the percentage of adhesion relative to untreated control cells. Adhesion was increased by all three ALDH1A1 siRNA targets. Adhesion was increased 27% with siRNA ALDH1A1 (1) (p=0.04), 23% with siRNA ALDH1A1 (2) (p=0.07) and 32% with siRNA ALDH1A1 (3) (p=0.001) to matrigel, compared to scrambled control cells.

(A)
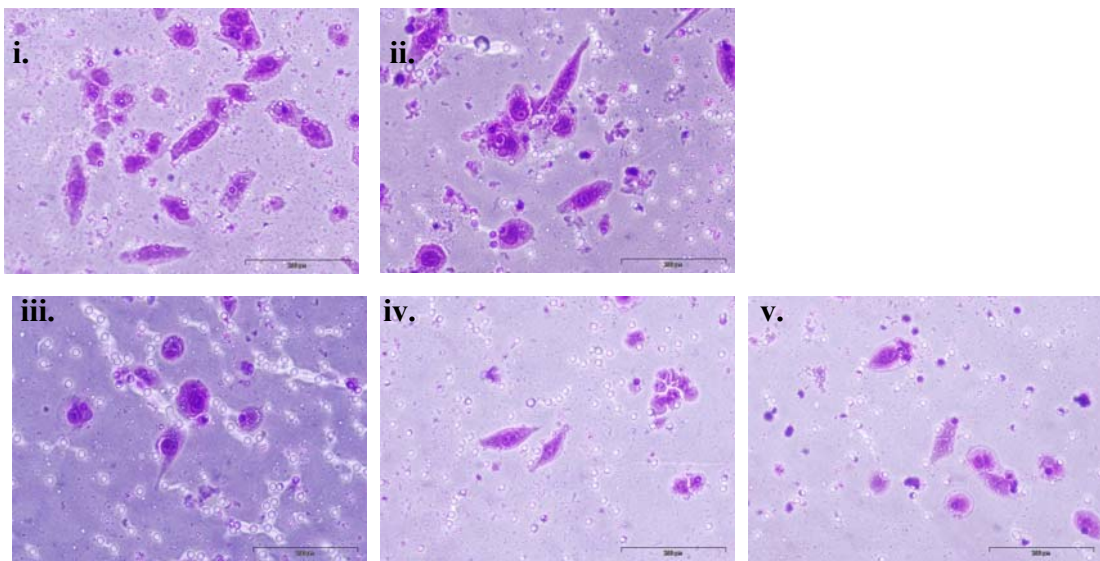
(B)
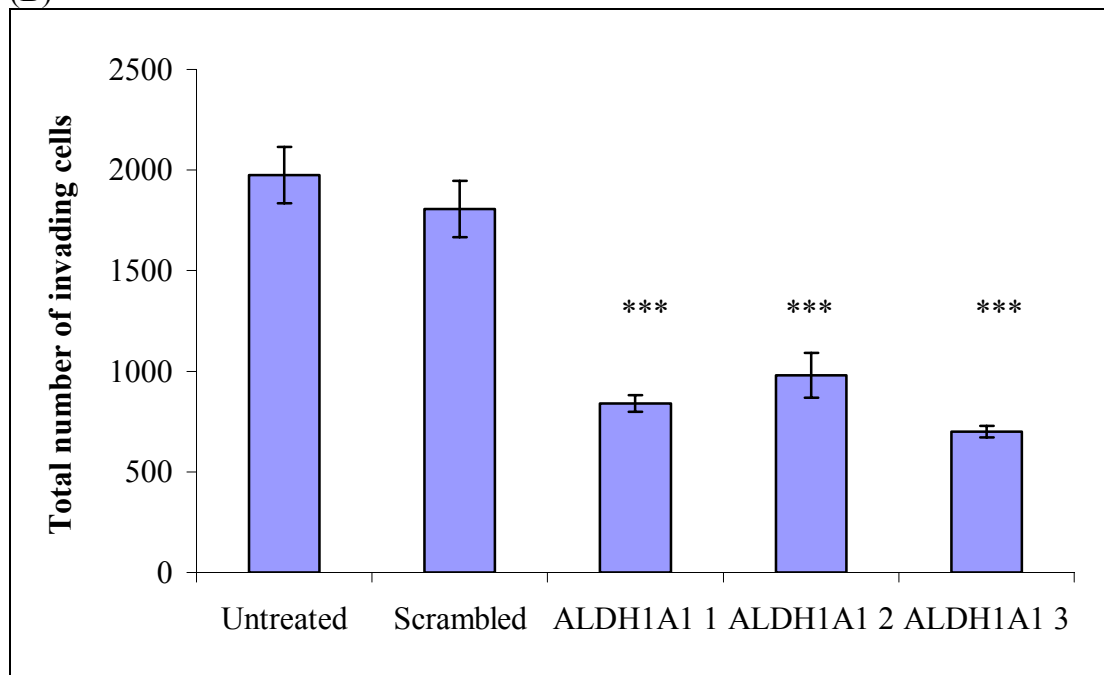
Figure 3.4.14 (A) Invasion assays of Clone #3 (i) under control conditions (ii) transfected with scrambled siRNA (iii) transfected with ALDH1A1 siRNA (1) (iv) transfected with ALDH1A1 siRNA (2) (v) transfected with ALDH1A1 siRNA (3), 48 hrs post transfection. Magnification, 200x. Scale bar, 200μm. (B) Total number of Clone #3 cells invading post ALDH1A1 siRNA transfection.

Statistics: $p \leq 0.05^*, 0.01^{**}, 0.005^{***}$ (unpaired t-test) to scrambled controls
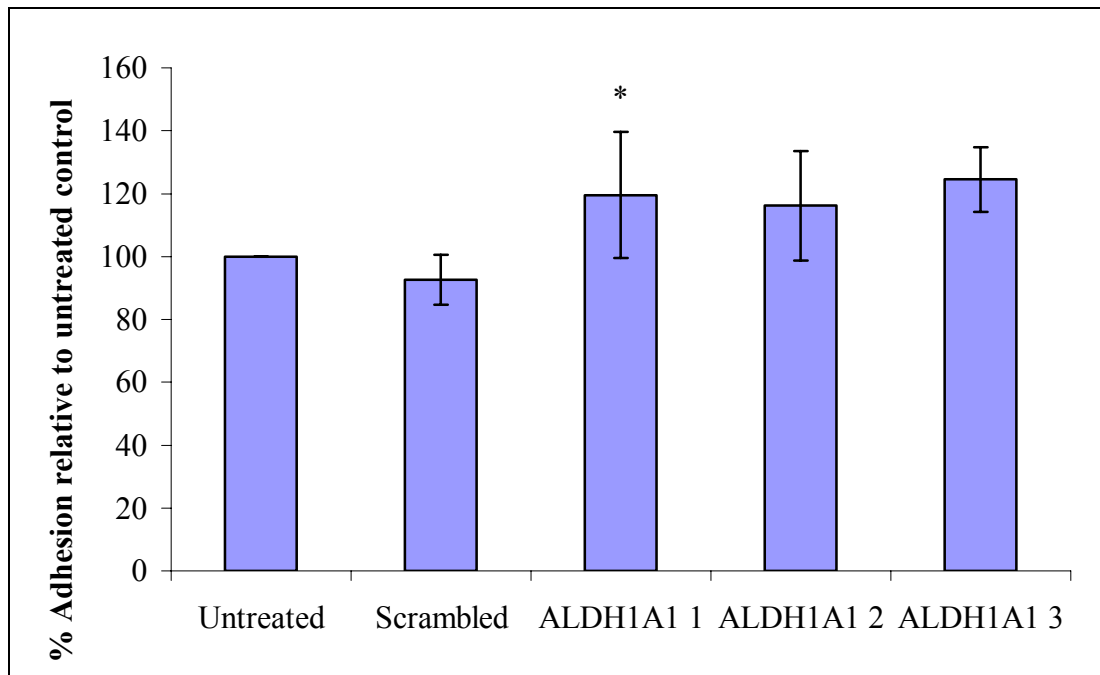
Figure 3.4.15 Percentage adhesion of Clone #3 untreated, scrambled and treated with three target ALDH1A1 siRNAs to matrigel 48 hrs after transfection. Results are expressed as % adhesion relative to untreated control cells. Data shown is mean ± standard deviation ($n = 3$).

Statistics: $p \leq 0.05$*, 0.01**, 0.005*** (unpaired t-test) to scrambled controls

3.4.5.4 Effect of ALDH1A1 siRNA on anoikis

To determine the effect of ALDH1A1 knockdown on suspension survival in Clone #3, anoikis assays were performed with ALDH1A1 siRNAs. Figure 3.4.16 shows that anoikis is modestly induced in siRNA ALDH1A1 (1) and (2) transfected cells compared to scrambled treated cells. Treatment with ALDH1A1 siRNA (3) statistically induces anoikis (p=0.03) compared to the scrambled control. However, no significant difference is observed in anoikis of cells transfected with ALDH1A1 siRNA (1) and (2) compared to the scrambled controls.
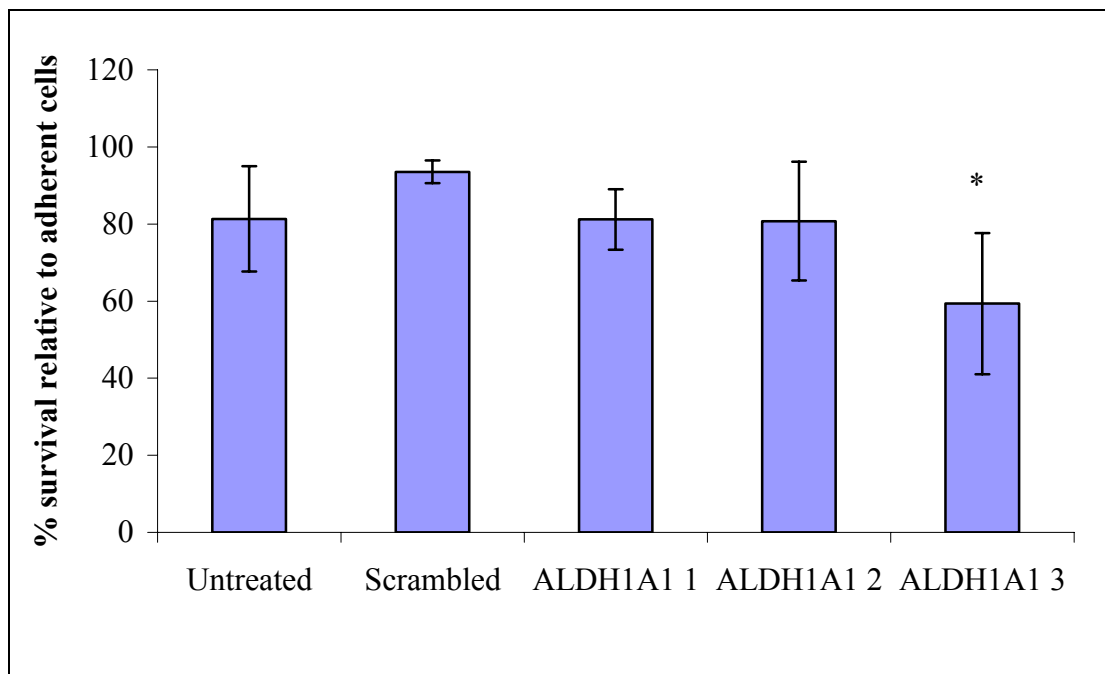
Figure 3.4.16 Percentage survival of Clone #3, untreated, scrambled and transfected with three independent ALDH1A1 siRNA targets in suspension compared to adherent cells. Data shown is mean ± standard deviation (n = 3). Statistics: $p \leq 0.05^{*}$, 0.01^{**}, 0.005^{***} (unpaired t-test).

3.4.5.5 Effect of ALDH1A1 siRNA on proliferation

Proliferation assays were carried out over 5 days after transfection of ALDH1A1 siRNAs into Clone #3 cells. Figure 3.4.17 displays the percentage survival of transfected cells relative to untreated control. Kinesin was used as a control for efficient transfection. There was no significant difference in proliferation of siRNA ALDH1A1 treated cells compared to control cells, therefore loss of ALDH1A1 did not affect proliferation in Clone #3 cells.
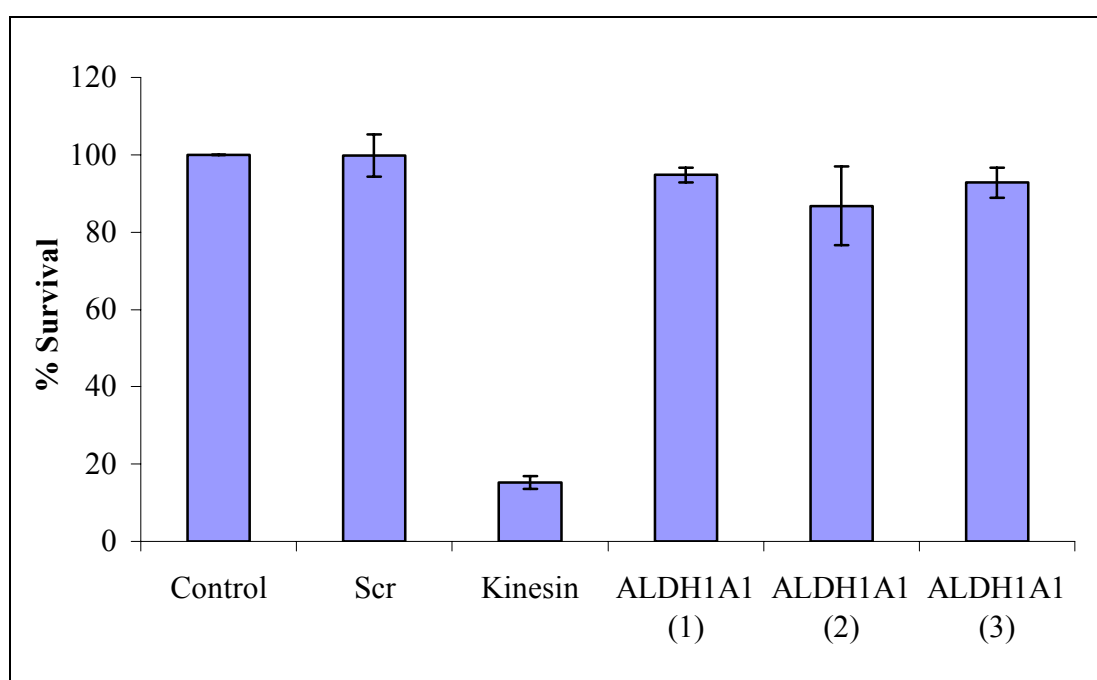
Figure 3.4.17 Percentage survival of Clone #3 transfected with ALDH1A1 target siRNAs relative to untreated control cells (*n*=3).

3.4.5.6 ALDH1A1 cDNA transfection in the low invasive cell line, Clone #8

Proteomic data and Western blot validation confirmed that ALDH1A1 expression was highest in the invasive sub-population, Clone #3 and lowest in the lesser invasive sub-population, Clone #8. To determine whether increasing ALDH1A1 expression in Clone #8 would have an effect on invasion, ALDH1A1 cDNA was transfected into Clone #8. Figure 3.4.18 displays ALDH1A1 expression in Clone #8 control, empty vector and ALDH1A1 cDNA transfected cells. Western blot analysis clearly shows that ALDH1A1 expression was induced in the ALDH1A1 cDNA transfected Clone #8 cells confirming efficient transfection. Two time points, 48 and 72 hrs post transfection were used to assess optimal length of transient transfection.
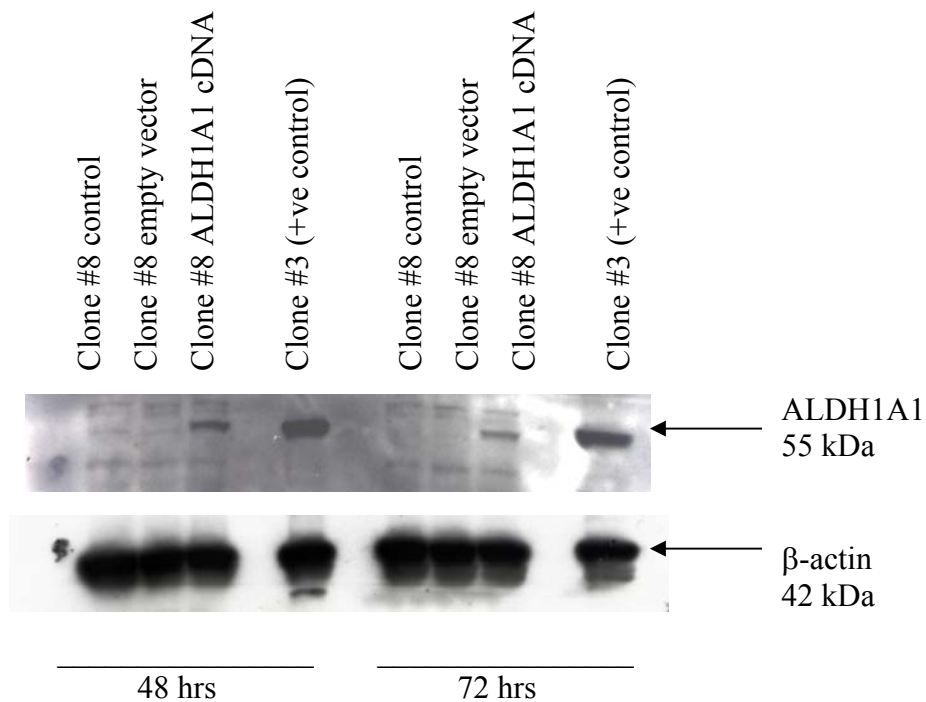
Figure 3.4.18 Western blot analysis of ALDH1A1 cDNA transient transfection in Clone #8. Two time points of 48 hrs and 72 hrs post cDNA transfection were used and β-actin was used as loading control.

3.4.5.6.1 Evaluation of ALDH1A1 cDNA transient transfection of Clone #8 on invasion

The effect of increasing ALDH1A1 expression in the poorly invasive Clone #8 was examined. Invasion assay analysis was performed 48 hrs post transfection. Figure 3.4.19 (A) shows representative pictures of invading cells, and (B) highlights the total number of invading cells of Clone #8 control (untreated), Clone #8 transfected with empty vector and Clone #8 transfected with ALDH1A1 cDNA. ALDH1A1 transfection of Clone #8 cells increased the invasive capacities of the cells, compared to empty vector control.

Invasion was significantly increased 2.1-fold (p=0.01) in Clone #8 ALDH1A1 cDNA transfected cells compared to Clone #8 cells transfected with empty vector.

(A)
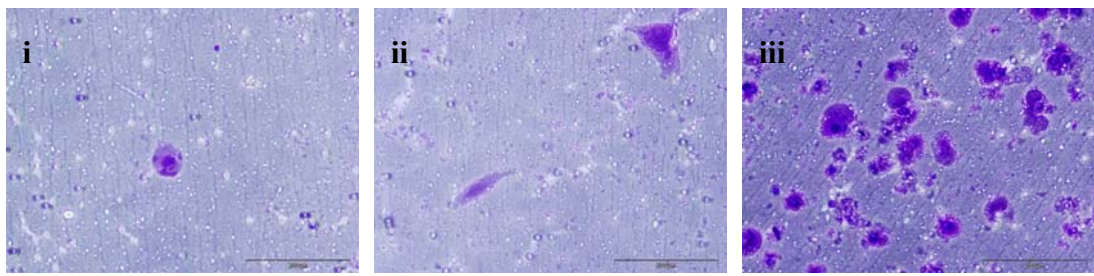
Clone #8 control   Clone #8 EV   Clone #8 ALDH1A1 cDNA

(B)
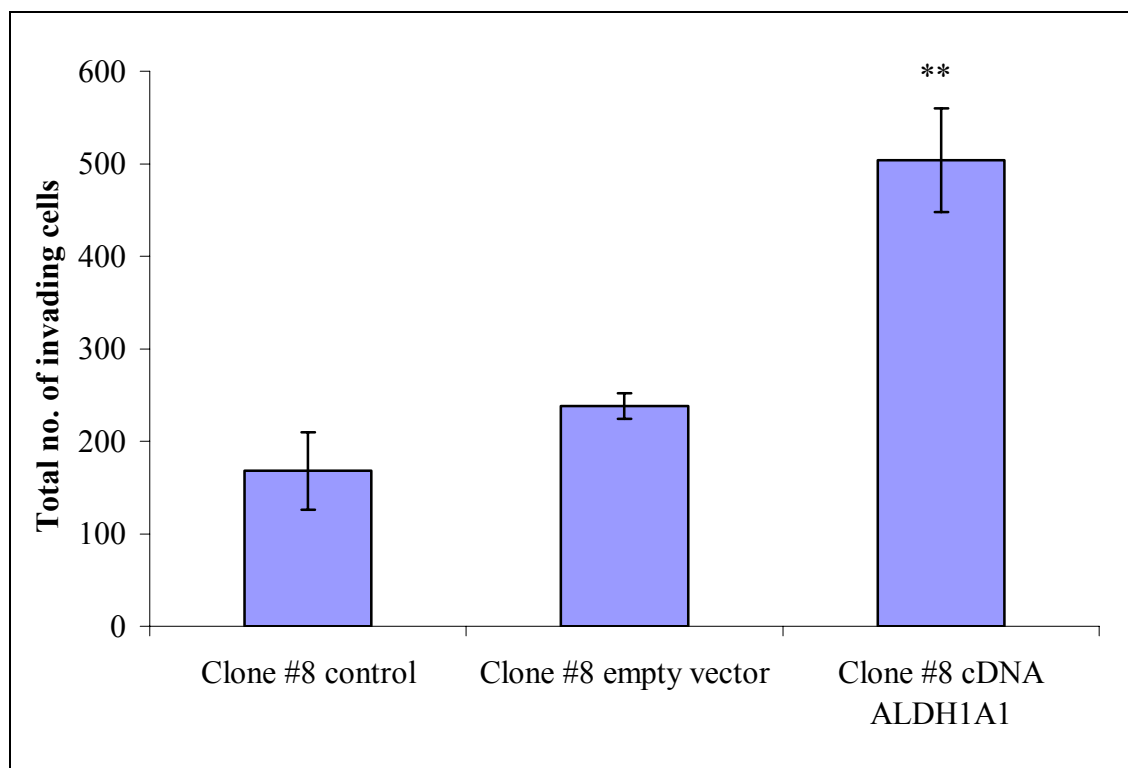
Figure 3.4.19 Invasion assays of (A) (i) Clone #8 under control conditions (ii) Clone #8 transfected with empty vector (EV) (iii) Clone #8 transfected with ALDH1A1 cDNA. Magnification, 200x. Scale bar, 200μm. (B) Invasion assay of Clone #8 of total number of cells invading 48 hrs post ALDH1A1 cDNA transfection.

Statistics: $p \leq 0.05^*$, 0.01^{**}, 0.005^{***} (unpaired t-test) to empty vector control

3.4.5.7 Correlation of ALDH1A1 expression on drug resistance

Chemosensitivity assays were carried out in the three cell lines, MiaPaCa-2, Clone #3 and Clone #8. 4-hydroxycyclophosphamide (4-HC) and mafosfamide are known to be detoxified by ALDH1A1. 4-diethylaminobenzaldehyde (DEAB) is a specific inhibitor of ALDH1A1 and ALDH1A1 converts retinal to retinoic acid. The high invasive cell line, Clone #3 is more resistant to the cytotoxic effects of cyclophosphamide metabolite, 4-HC and analogue, mafosfamide. However, the parental cell line, MiaPaCa-2 and the low invasive cell line, Clone #8 are more sensitive to the drugs (Table 3.4.8).

Table 3.4.8 IC$_{50}$ of MiaPaCa-2, Clone #3 and Clone #8

Drug (µg/ml)	MiaPaCa-2	Clone #3	Clone #8
4-hydroxycyclophosphamide	0.5±0.02	0.8±0.1	0.4±0.02
Mafosfamide	7.2±3.1	10.3±5.2	6.2±2.6
Diethylaminobenzaldehyde	14.4±2.0	16.8±1.0	15.0±1.4
All trans Retinoic Acid (ATRA)	3.4±0.3	6.2±0.6	2.3±0.6

IC$_{50}$s calculated represent half maximal inhibitory concentration of each drug in MiaPaCa-2, Clone #3 and Clone #8.

3.4.5.7.1 Effect of ALDH1A1 siRNA on drug resistance

Chemosensitivity assays were performed on Clone #3 cells transfected with ALDH1A1 siRNA to determine whether ALDH1A1 silencing sensitised the cells to the toxic effects of 4-HC. Figure 3.4.20 shows that ALDH1A1 siRNA slightly increased sensitivity to 4-HC and may be associated with 4-HC resistance in pancreatic cancer cells. Table 3.4.9 outlines the IC_{50}s of Clone #3 untreated control, scrambled and transfected with three independent siRNA ALDH1A1.

Figure 3.4.20 Percentage survival of Clone #3, untreated, scrambled and transfected with three independent ALDH1A1 siRNA targets in 4-HC chemosensitivity assay. Data shown is mean ± standard deviation ($n = 3$).

Table 3.4.9 IC_{50} of Clone #3 control, scrambled and ALDH1A1 siRNA treated cells to 4-HC

µg/ml	Control	Scrambled	SiRNA ALDH1A1 (1)	SiRNA ALDH1A1 (2)	SiRNA ALDH1A1 (3)
4-HC	**1.5 ± 0.5**	**1.6 ± 0.5**	**1.1 ± 0.1**	**1.4 ± 0.2**	**1.1 ± 0.1**

3.4.5.8 Effect of ATRA treatment on Clone #3 and Clone #8

ALDH1A1 acts as a catalyst irreversibly converting retinaldehyde to retinoic acid (RA). Analyses were performed to investigate whether accumulation of intracellular retinoic acid may lead to the suppression of ALDH expression (Moreb *et al.*, 2005). Clone #3 and Clone #8 were incubated with 1.5 µg/ml (5 µM) of ATRA to assess a possible feedback loop of high levels of retinoic acid on ALDH1A1 expression. This effect was measured by Western blot, invasion assays and morphological changes in the cells.

3.4.5.8.1   Western blot analysis of ALDH1A1 expression in Clone #3 cells incubated with ATRA

ALDH1A1 expression was determined by Western blot in Clone #3 cells treated with 5 µM ATRA for 48 hrs and continuous 5 µM ATRA treatment. Figure 3.4.21 shows by Western blot that ALDH1A1 expression is not altered in Clone #3 after ATRA treatment.
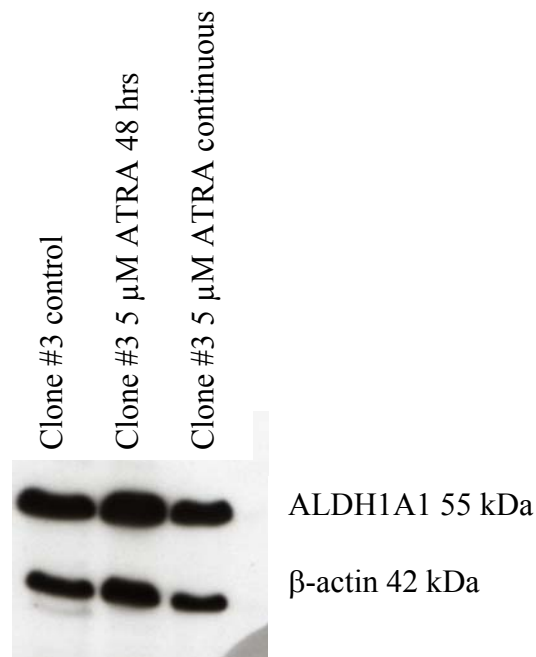
Figure 3.4.21 Western blot of Clone #3 control, treated with 5 µM ATRA for 48 hrs and after continuous ATRA treatment. β-actin was used as loading control.

3.4.5.8.2 **Invasion assays of Clone #3 and Clone #8 cells incubated with ATRA**

Invasion assays were performed in Clone #3 and Clone #8 cells after 48 hrs treatment with 5 μM ATRA. Initial experiments were negative as invasion was not altered in either cell line after ATRA treatment. However, after long-term continuous treatment of 5 μM ATRA for 8 days, Clone #3 displayed unchanged invasion levels, yet invasion of Clone #8 was significantly increased (p=0.03) (Figure 3.4.22 (A) and (B)).

(A)
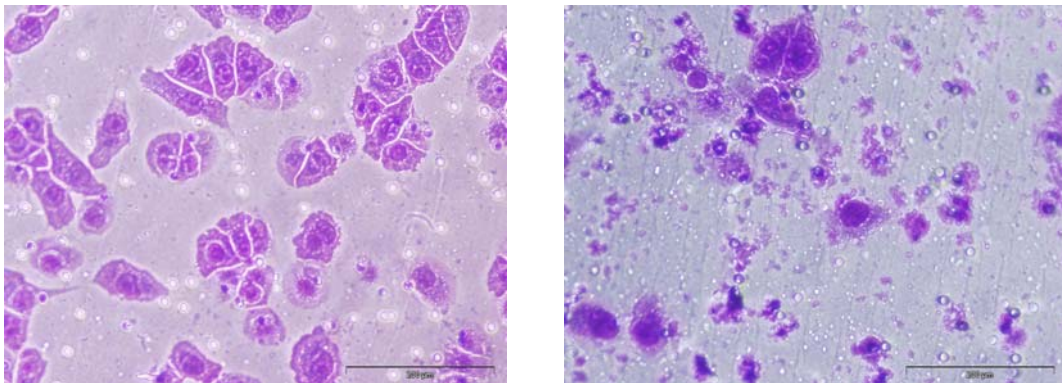
(B)
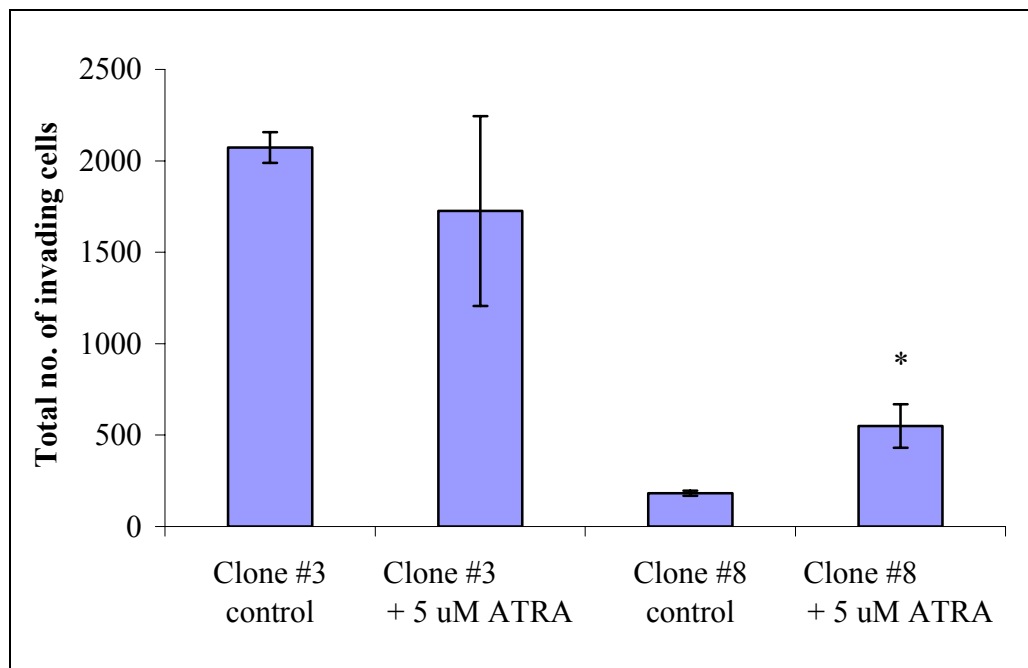
Figure 3.4.22 (A) Invasion of (i) Clone #3 and (ii) Clone #8 after 8 days continuous exposure to 5 μM ATRA. (B) Total number of cells invading.

Statistics: $p \leq 0.05$*, 0.01**, 0.005*** (unpaired t-test) to control

3.4.5.8.3 Morphology of Clone #3 and Clone #8 cells incubated with ATRA

Figure 3.4.23 (i) displays the morphology of control Clone #3 cells, while (ii) highlights the morphology of these cells after continuous exposure to ATRA. These results show that the morphology is unchanged.

Clone #8 under control conditions is depicted in (iii), while (iv) represents the morphology of the cells after long-term treatment with ATRA. The typical phenotype of the cells is obviously different. The cells are spread out, spindle-shaped and elongated compared to colony-type rounded phenotype of the control cells.
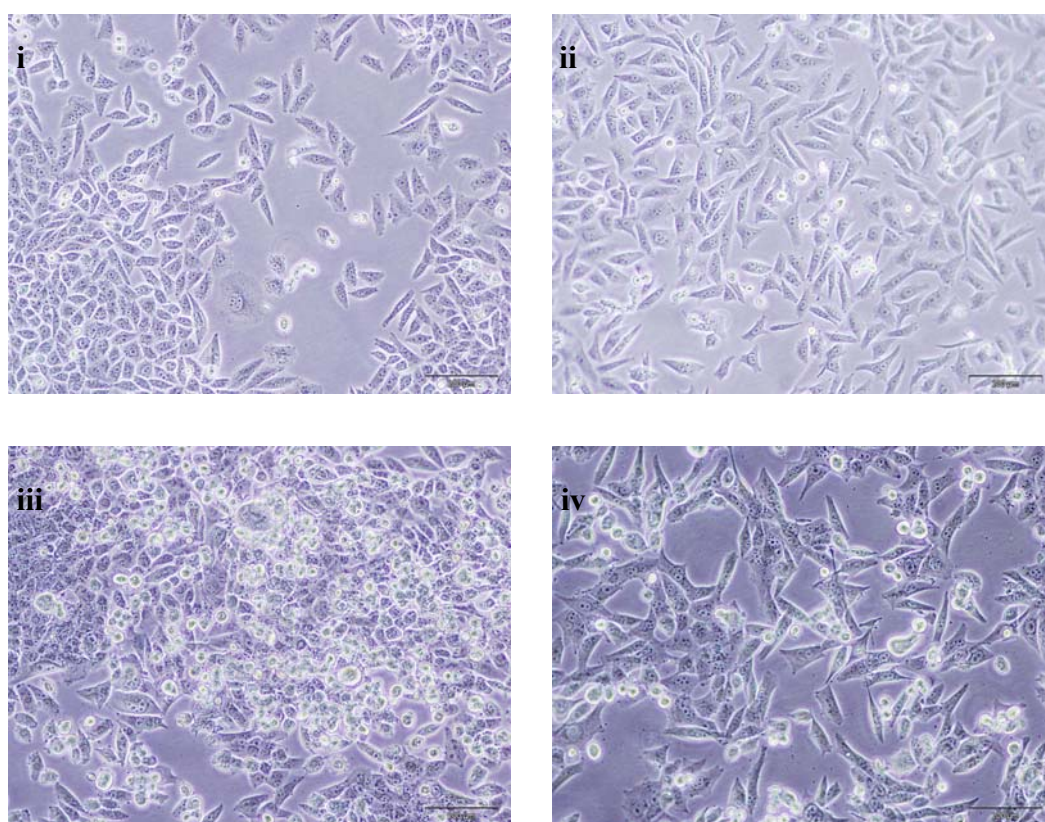
Figure 3.4.23 Morphology of Clone #3 (i) under normal culture conditions (ii) 5 μM ATRA treatment (iii) Clone #8 under normal culture conditioned and (iv) 5 μM ATRA treatment. Magnification, 100x. Scale bar, 200 μm.

3.4.6 Investigation into the role of vimentin in pancreatic cancer cell invasion

Vimentin (VIM) was identified as a protein involved in invasion in our *in vitro* pancreatic cancer cell line model. The analysis showed that VIM was 5.5-fold up-regulated in the more invasive sub-clone, Clone #3 compared to the low invasive cell line, Clone #8 (Table 3.4.7).

3.4.6.1 Effect of VIM siRNA transfection on Clone #3

The protein vimentin was shown to be up-regulated as the invasion status of the cell lines increased, therefore the more invasive cell line, Clone #3 expressed high levels of the protein. Clone #3 was used for siRNA knockdown and further functional analysis. Figure 3.4.24 shows by Western blot the efficient knockdown of VIM in Clone #3 cells transfected with three VIM siRNAs compared to non-treated control and siRNA scrambled transfected cells.
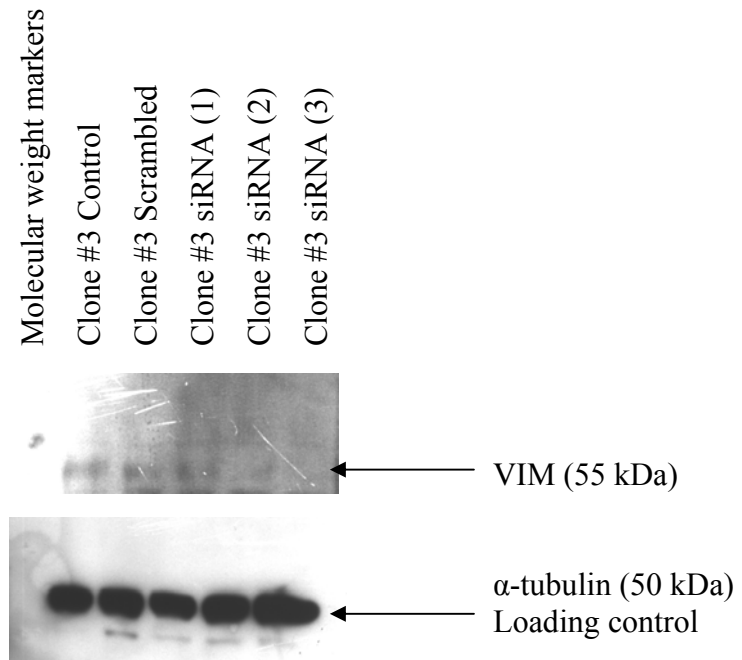
Figure 3.4.24 Western blot of siRNA VIM knockdown in Clone #3. Three independent target siRNA of VIM were transfected into Clone #3 cells.

Protein was harvested 48 hrs post-transfection and used to determine a VIM-siRNA specific decrease at protein level in response to siRNA transfection by Western blot. α-tubulin antibody was used to demonstrate even loading between the samples. This is a representative picture of at least 3 independent analyses.

3.4.6.2 Effect of VIM siRNA on invasion

Fourty-eight hours post-transfection with VIM siRNA, invasion assays were performed. The total number of cells invading was reduced in Clone #3 cells transfected with VIM siRNA. Figure 3.4.25 (A) shows representative pictures of invading cells, and (B) highlights the total number of cells invading. VIM siRNA transfection reduces the invasive capabilities of the cells, by 4-fold (p=0.00036) with VIM siRNA (1), 6-fold (p=0.00031) with VIM siRNA (2) and 6-fold (p=0.0004) with VIM siRNA (3) transfection. The loss of VIM expression through siRNA knockdown in Clone #3 cells reduces invasion and confirms proteomics results.

3.4.6.3 Effect of VIM siRNA on adhesion

Adhesion assays were also carried out to assess the involvement of vimentin in adhesion of Clone #3 to matrigel. Figure 3.4.26 shows the percentage adhesion relative to untreated control cells. siRNA VIM (1) transfection increased the percentage of adhesion (35%) relative to cells treated with scrambled control (p=0.08). Percentage adhesion was significantly increased by 25% with VIM (2) and 32% with VIM (3) siRNAs (p=0.02 and p=0.02) compared to scrambled siRNA transfected control cells. Therefore, these results suggest that siRNA VIM (2) and (3) are more efficient inhibitors of VIM protein translation and that VIM expression is involved in adhesion to matrigel in Clone #3 cells.

(A)
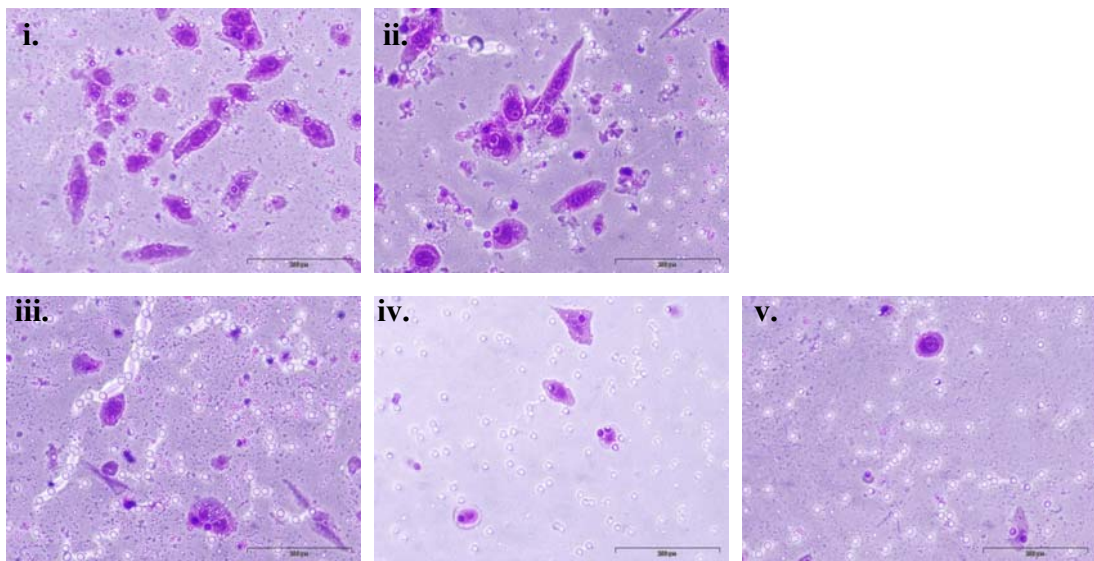
(B)
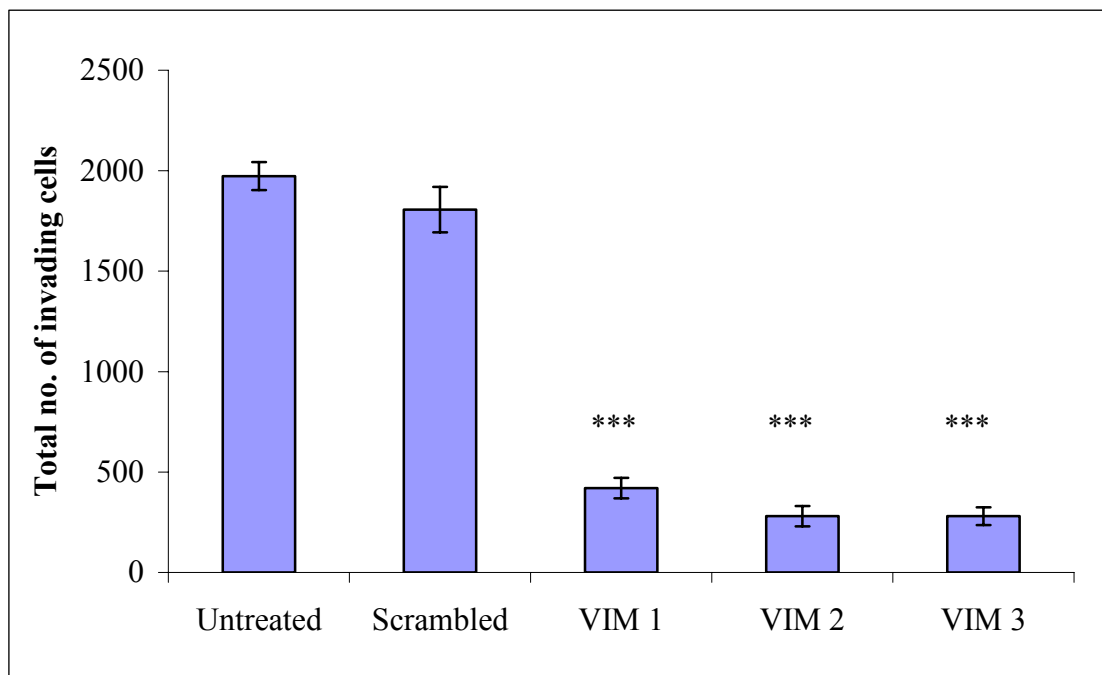
Figure 3.4.25 (A) Invasion assays of Clone #3 (i) under control conditions (ii) transfected with scrambled siRNA (iii) transfected with VIM siRNA (1) (iv) transfected with VIM siRNA (2) (v) transfected with VIM siRNA (3). Magnification, 200x. Scale bar, 200µm.

(B) Invasion assay of Clone #3 of total number of cells invading post siRNA vimentin transfection.

Statistics: $p \leq 0.05*, 0.01**, 0.005***$ (unpaired t-test) to scrambled control
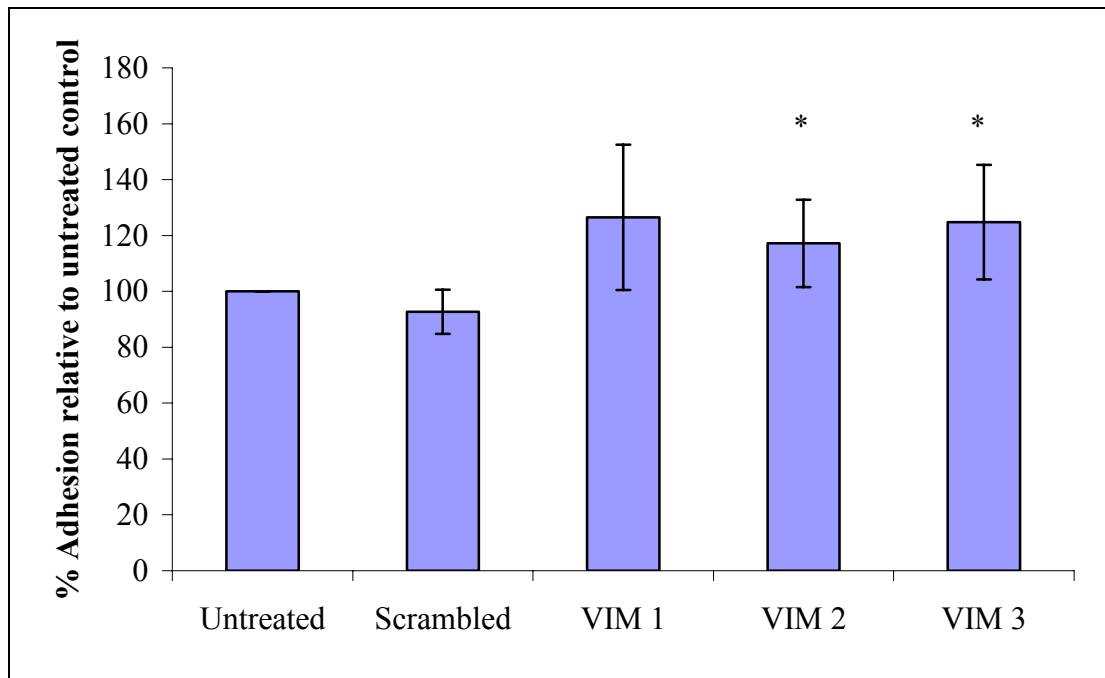
Figure 3.4.26 Percentage adhesion of Clone #3 control, scrambled and treated with three target VIM siRNAs to matrigel. Results are expressed as % adhesion relative to scrambled cells. Data shown is mean ± standard deviation (n = 3). Statistics: $p \leq 0.05^*$, 0.01^{**}, 0.005^{***} (unpaired t-test) compared to scrambled control.

3.4.6.4 Effect of VIM siRNA on anoikis

Anoikis assays showed that VIM siRNA (3) caused a slight but statistically significant decrease in anoikis resistance compared to scrambled control (p=0.02) (Figure 3.4.27). Sensitivity to anoikis was slightly induced in VIM siRNA (1) and (2) transfected cells but only significant in siRNA VIM (3) compared to the scrambled control, indicating that role of VIM in anoikis is unclear.

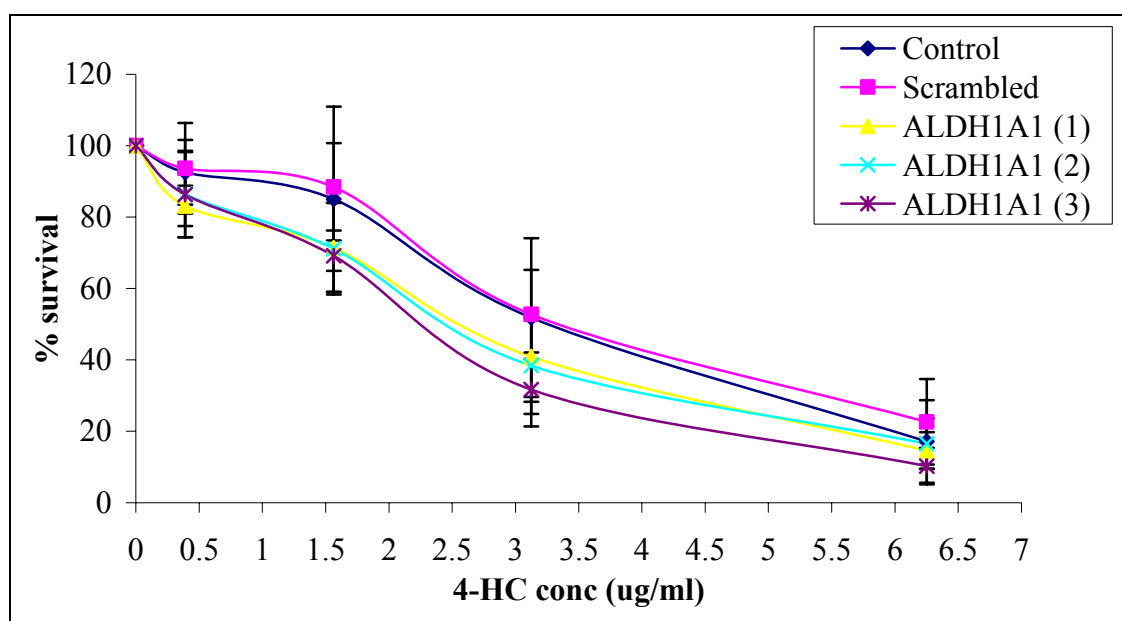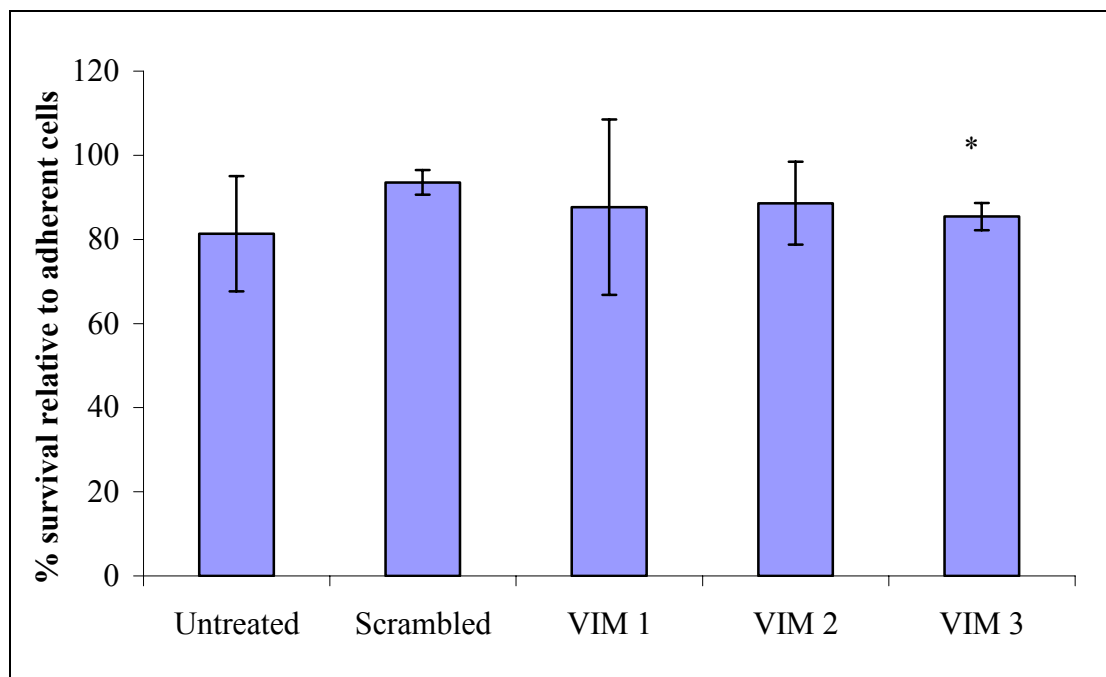**Figure 3.4.27 Percentage survival of Clone #3, untreated, scrambled and transfected with three independent VIM siRNA targets in suspension compared to adherent cells. Data shown is mean ± standard deviation (n = 3).**

Statistics: $p \leq 0.05^*$, 0.01^{**}, 0.005^{***} (unpaired t-test) compared to scrambled control.

3.4.6.5 Effect of VIM siRNA on proliferation

The effect of silencing VIM protein expression on proliferation was studied. Figure 3.4.28 displays the percentage survival of Clone #3 cells transfected with VIM siRNAs. Loss of VIM did not affect proliferation in Clone #3 cells, and VIM is not essential for proliferation of these cells.
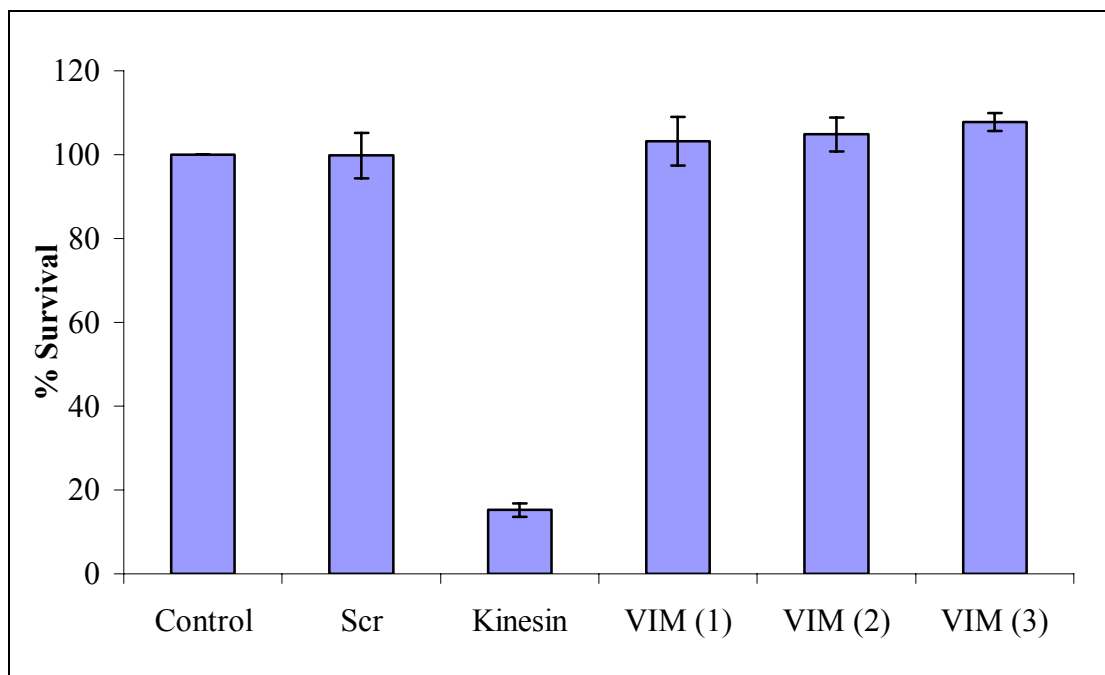
Figure 3.4.28 Proliferation assay of Clone #3 control, scrambled and transfected with siRNA VIM (1), (2) and (3). Results graphed as % survival relative to non-treated control (*n*=3).

3.4.6.6 Effect of VIM siRNA on epithelial to mesenchymal transition (EMT)

EMT is characterised by morphological and behavioural changes in cells (Maeda *et al*., 2005). Investigations into the involvement of VIM, a mesenchymal marker (Leader *et al*., 1987) were determined. Figure 3.4.29 (i-iii) shows the morphological changes of Clone #3 and Clone #8 compared to the parental cell line, MiaPaCa-2 under normal culture conditions. Clone #3 exhibits a more fibroblast phenotype with spindle shaped elongated cells. Clone #8 cells appear rounded and grow in clusters. Clone #3 transfected with siRNA VIM exhibits a rounded phenotype as observed in Clone #8 cells. The morphological changes of Clone #3 after loss of VIM expression may implicate the role of vimentin in the epithelial to mesenchymal transition.
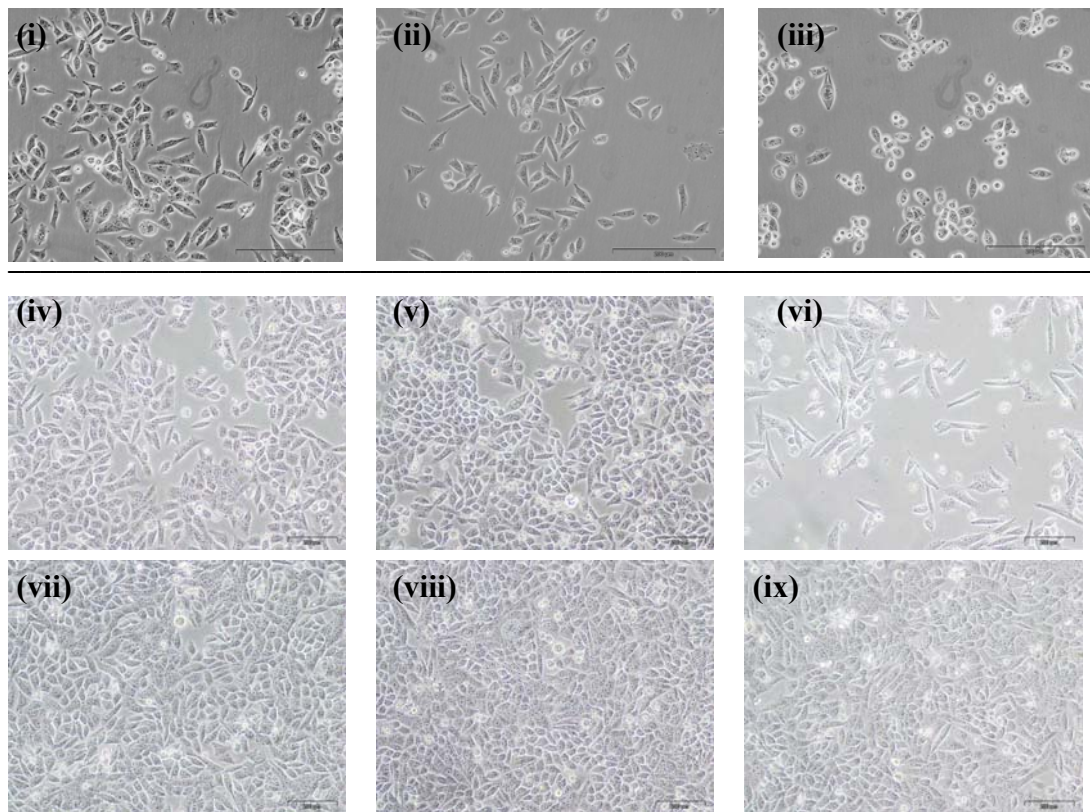
Figure 3.4.29 Morphology of (i) MiaPaCa-2, (ii) Clone #3 and (iii) Clone #8 and after transfection (iv) Clone #3 control (v) Clone #3 scrambled (vi) Clone #3 siRNA kinesin (vii) Clone #3 transfected with VIM (1) (viii) Clone #3 transfected with VIM (2) and (ix) Clone #3 transfected with VIM (3) 48 hours post-transfection. Magnification at 20x, scale bar, 200μm.

3.4.7 Investigation into the role of stress-induced phosphoprotein 1 in pancreatic cancer cell invasion

STIP1 was identified as 2-fold up-regulated in the high invasive sub-population, Clone #3, compared to the low invasive sub-population, Clone #8 (Table 3.4.7). The expression of STIP1 increased as the invasion status of the cells increased suggesting it may correlate to invasion in pancreatic cancer.

3.4.7.1 Effect of STIP1 siRNA transfection on Clone #3

The protein stress-induced phosphoprotein 1 was shown to be up-regulated as the invasion status of the cell lines increased, therefore the more invasive cell line, Clone #3 expressed high levels of the protein. Clone #3 was used for siRNA knockdown and further functional analysis.

Figure 3.4.30 showed by Western blot the efficient knockdown of STIP1 in siRNA treated Clone #3 cells compared to non-treated and scrambled controls.
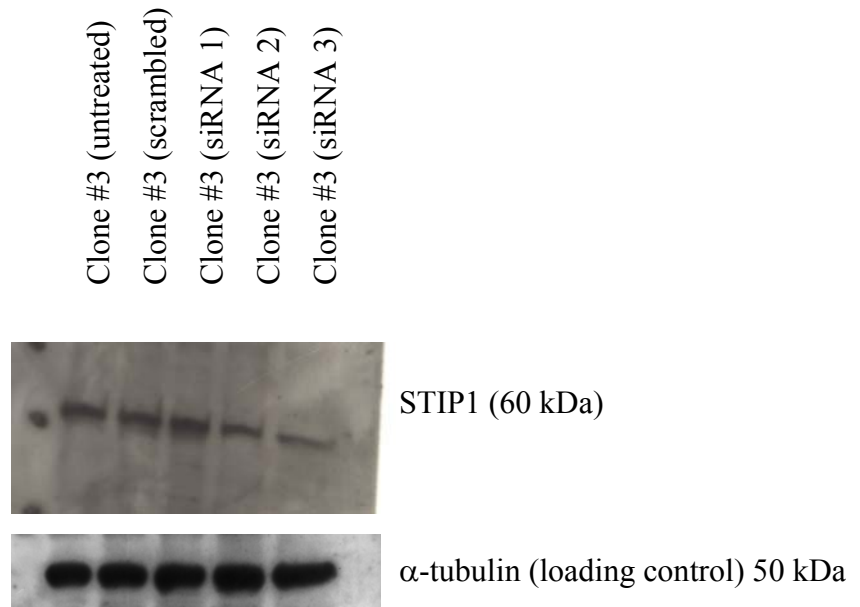
Figure 3.4.30 Western blot of siRNA STIP1 knockdown in Clone #3. Three independent target siRNA of STIP1 were transfected into Clone #3 cells.

Protein was harvested 48 hrs post-transfection and used to determine a STIP1-siRNA specific decrease at protein level. α-tubulin antibody was used to demonstrate even loading between the samples. This is a representative picture of at least 2 independent analyses.

3.4.7.2 Effect of STIP1 siRNA on invasion

Invasion assays were carried out on Clone #3 cells untreated, treated with scrambled siRNA and three independent siRNA targets for STIP1. Figure 3.4.31 displays (A) representative pictures of the level of invasion and (B) the total number of cells invading. STIP1 siRNA transfection reduced the invasive capabilities of Clone #3 cells. Invasion was significantly reduced 3-fold (p=0.0002) with STIP1 siRNA (1), 2-fold (p=0.0002) with STIP1 siRNA (2) and 2-fold (p=0.0003) with STIP1 siRNA (3) transfection. These results confirm proteomic analysis suggesting STIP1 is involved in invasion of Clone #3 cells.

3.4.7.3 Effect of STIP1 siRNA on adhesion

Figure 3.4.32 shows the percentage adhesion to matrigel of STIP1 siRNA transfected cells relative to untreated cells. Adhesion was increased by 31% compared to scrambled controls with all STIP1 targeted siRNAs. Adhesion was significantly increased with siRNA STIP1 (2) and STIP1 (3) (p=0.02 and p=0.03). These results suggest that STIP1 has a role in adhesion of Clone #3 cells to matrigel.

(A)

(B)
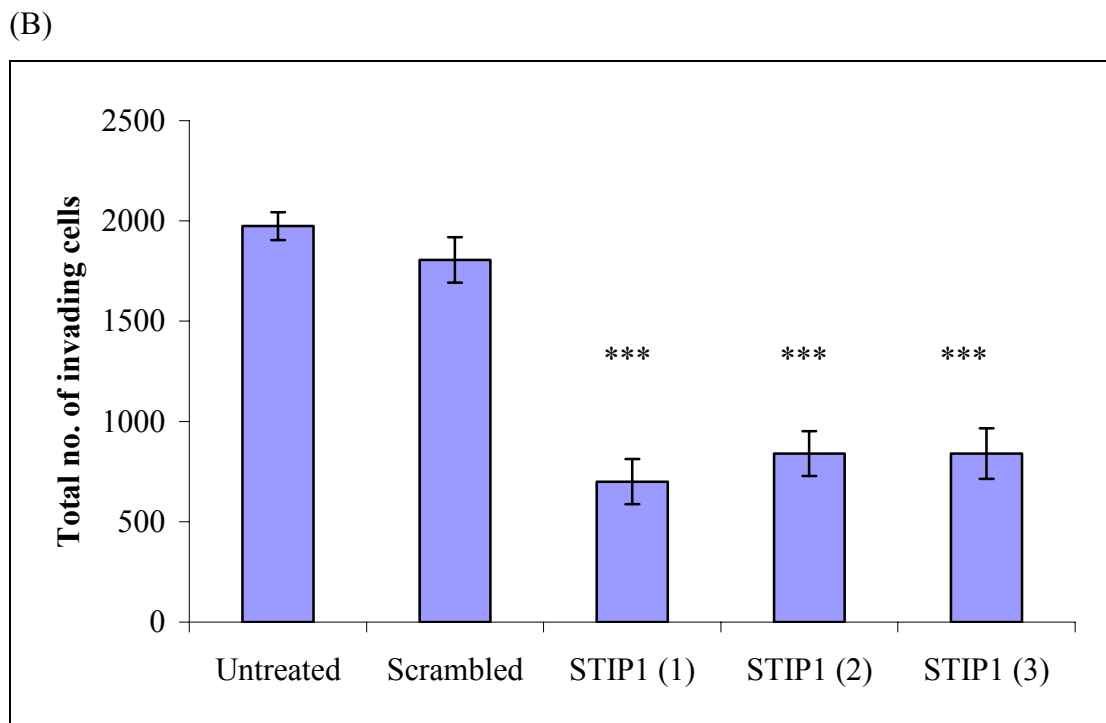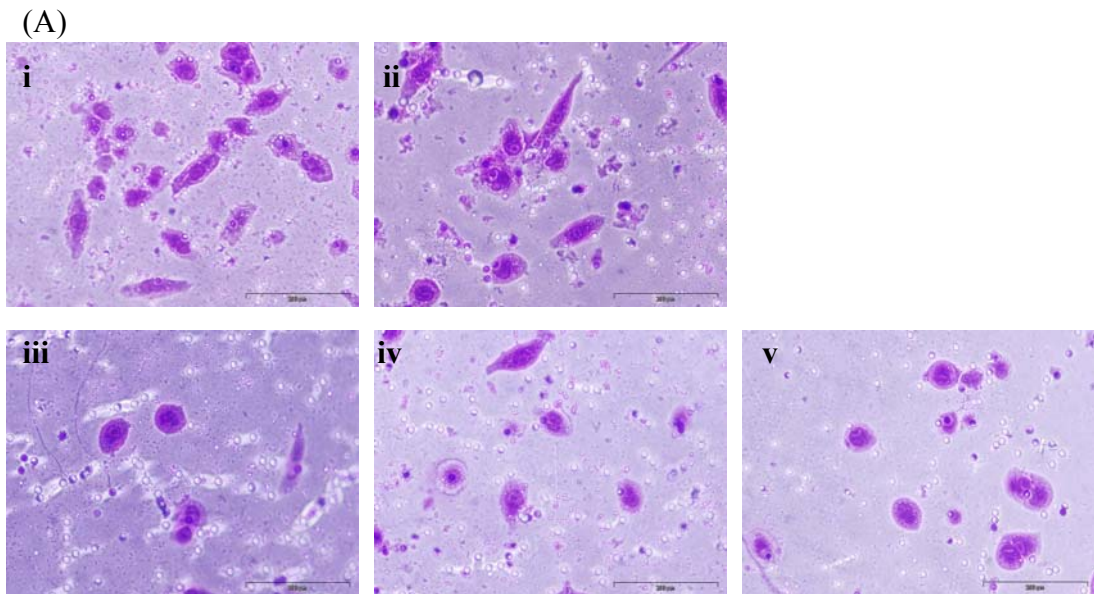
Figure 3.4.31 (A) Invasion assays of Clone #3 (i) under control conditions (ii) transfected with scrambled siRNA (iii) transfected with STIP1 siRNA (1) (iv) transfected with STIP1 siRNA (2) (v) transfected with STIP1 siRNA (3). Magnification, 200x. Scale bar, 200μm. (B) Invasion assay of Clone #3 of total number of cells invading post siRNA STIP1 transfection.

Statistics: $p \leq 0.05^*$, 0.01^{**}, 0.005^{***} (unpaired t-test) to scrambled control.
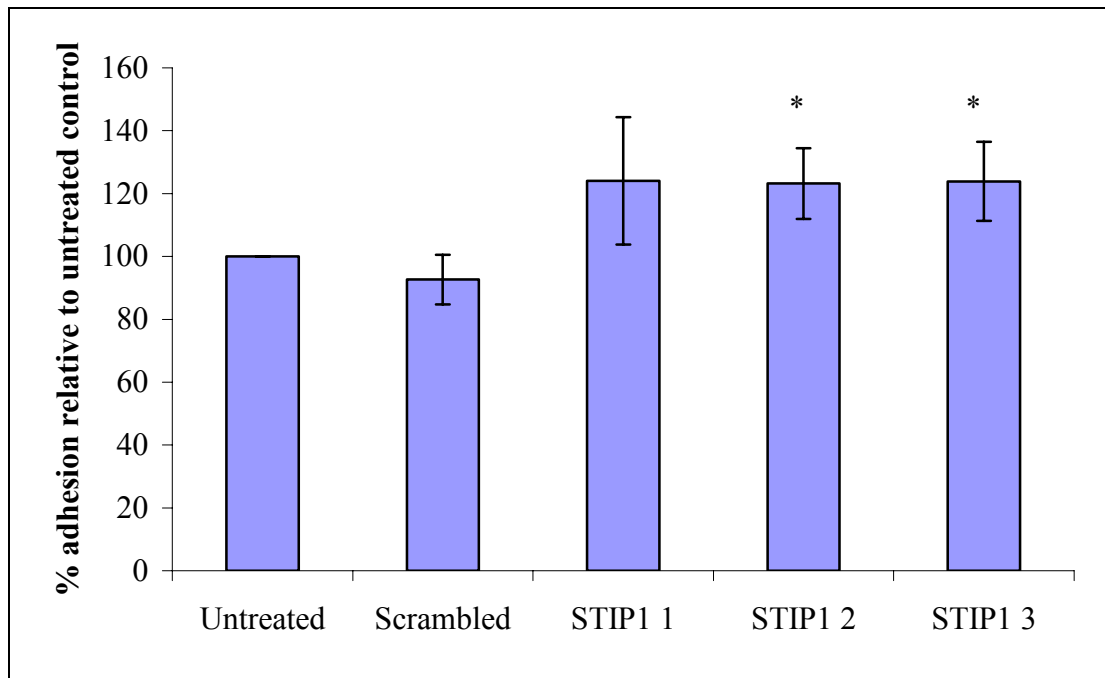
Figure 3.4.32 Percentage adhesion of Clone #3 control, scrambled and treated with three target siRNA STIP1 to matrigel. Results are expressed as % adhesion relative to untreated cells. Data shown is mean ± standard deviation (n = 3). Statistics: $p \leq 0.05*, 0.01**, 0.005***$ (unpaired t-test) compared to scrambled control.

3.4.7.4 Effect of STIP1 siRNA on anoikis

The percentage survival relative to adherent cells of Clone #3 treated with STIP1 siRNAs compared to scrambled controls is displayed in figure 3.4.33. Results show a modest decrease in anoikis resistance with STIP1 siRNA transfection; however, this decrease in survival was not significant, relative to scrambled control cells. Therefore, STIP1 does not appear to play a role in anoikis in these cells.
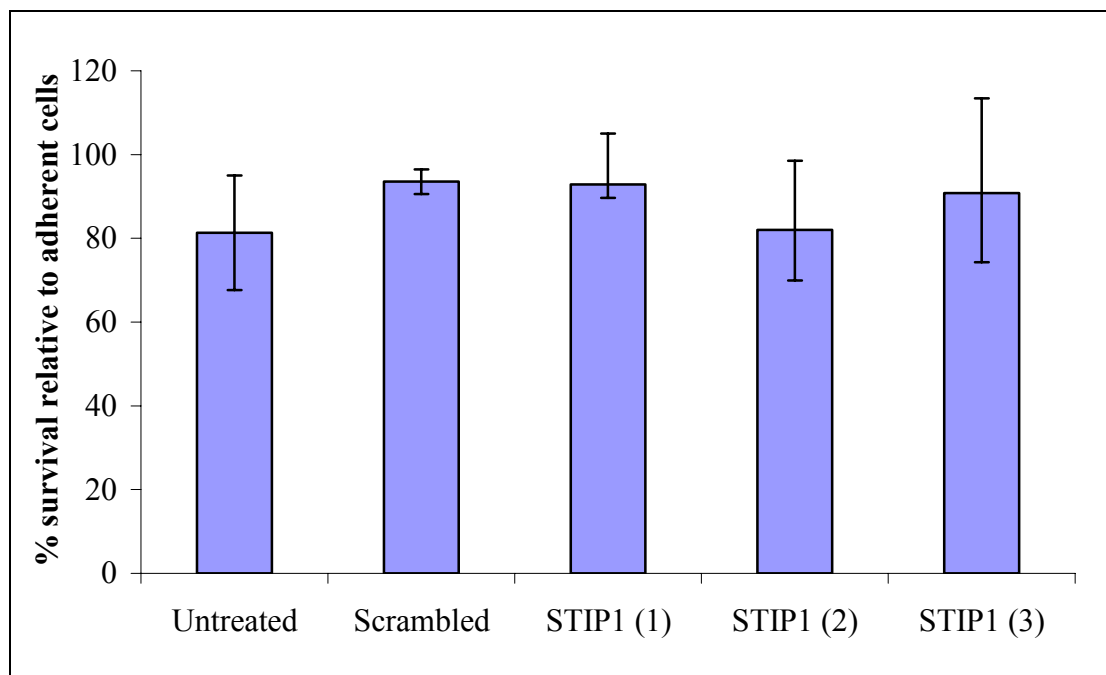
Figure 3.4.33 Percentage survival of Clone #3, untreated, scrambled and transfected with three independent STIP1 siRNA targets in suspension compared to adherent cells. Data shown is mean ± standard deviation ($n = 3$).

Statistics: $p \leq 0.05$*, 0.01**, 0.005*** (unpaired *t*-test) compared to scrambled control.

3.4.7.5 Effect of STIP1 siRNA on proliferation

Proliferation assays were carried out to assess the role of STIP1 on proliferation in Clone #3 cells. Figure 3.4.34 shows the percentage survival of Clone #3 cells, scrambled control and transfected with STIP1 siRNAs (1), (2) and (3). The percentage survival is statistically significantly reduced in STIP1 siRNA (1) and (2) transfected cells. Inhibition of growth is reduced 13% ($p=0.04$) and 27% ($p=0.003$). Proliferation was not reduced with siRNA STIP1 (3). These results suggest that siRNA (1) and (2) are more efficient at STIP1 knockdown and that STIP1 may play a role in proliferation of Clone #3 cells.
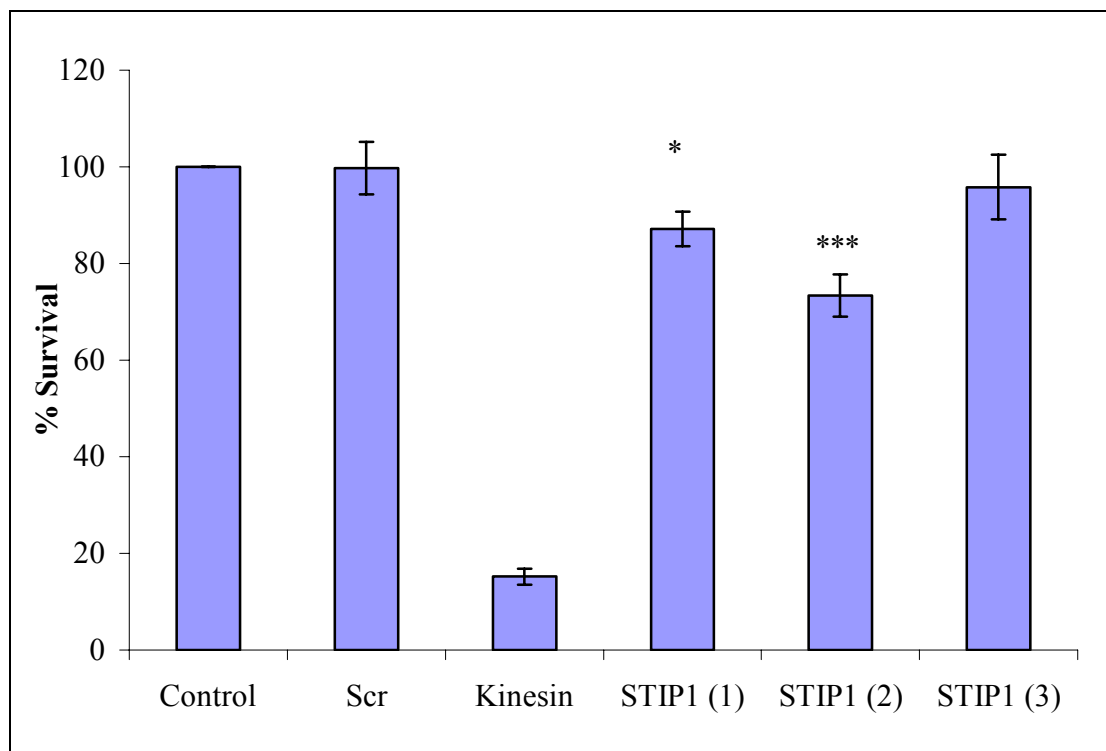
Figure 3.4.34 Proliferation assay of Clone #3 control, scrambled and transfected with siRNA STIP1 (1), (2) and (3). Results graphed as percentage survival relative to non-treated control ($n=3$). Statistics: $p \leq 0.05*$, $0.01**$, $0.005***$ (unpaired t-test) compared to scrambled control.

3.5 Analysis of effects of conditioned media from Clone #3 (CM#3) and Clone #8 (CM#8)

Conditioned media from the clonal populations CM#3 and CM#8 was investigated to assess its role as an autocrine stimulatory and inhibitory factor of pancreatic cancer cell invasion. Conditioned media without serum was obtained from Clone #3 (CM#3) and Clone #8 (CM#8) after 72 hrs incubation. The CM was centrifuged and filtered through a 0.22 μm filter to remove any cell debris (Chapter 2.2.1). Invasion, adhesion and anoikis assays were carried out as described in chapter 2.5 and 2.6, with the addition of either conditioned media CM#3 or CM#8 diluted at a ratio of 1:1 with fresh media, above and below the invasion chamber insert at equal dilution to ensure no gradient for invasion assays.

3.5.6 Effect of CM#3 and CM#8 on invasion of MiaPaCa-2 and sub-populations, Clone #3 and Clone #8

CM#3 enhanced invasion of MiaPaCa-2 by 2.2-fold (p=0.001) compared to an invasion assay control containing fresh medium. MiaPaCa-2 containing CM#8 in the invasion assay shows a 3.33-fold decrease in invasion (p=0.002) (Figure 3.5.1).

Conditioned media from Clone #3 and Clone #8 were also tested on Clone #3 and Clone #8. Figure 3.5.2 shows the enhanced effect of CM#3 on invasion of the cell line, Clone #3. The significant increase in invasion is 1.8-fold (p=0.0008) compared to an invasion assay control containing fresh medium. Clone #3 containing CM#8 in the invasion assay shows a 3.33-fold decrease in invasion (p <0.001).

CM#3 also significantly increased the invasion, 4.2-fold (p=0.005) of Clone #8 compared to an invasion assay control containing fresh medium (Figure 3.5.3). CM#8 caused a very slight (1.1-fold) decrease in invasion of Clone #8 (p=0.7).

(A)
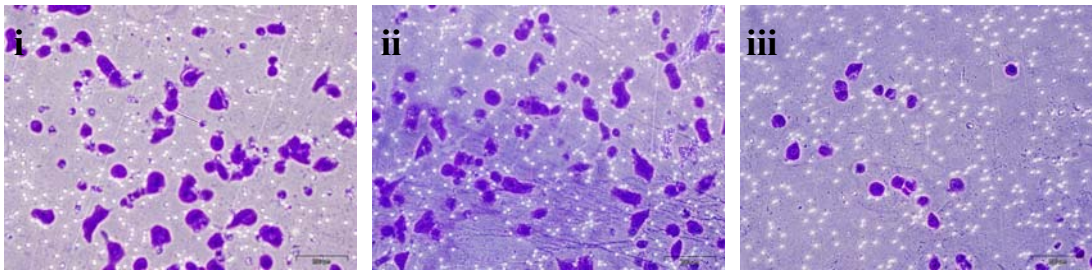
(B)
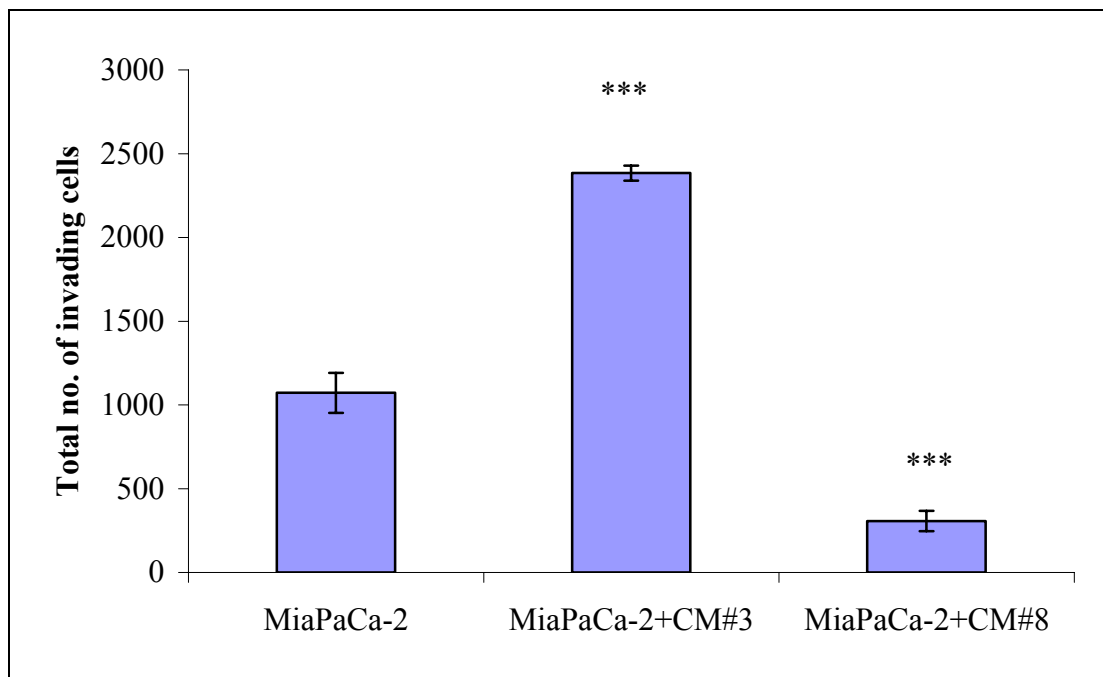
Figure 3.5.1 (A) Invasion assays of MiaPaCa-2 (i) under control conditions (ii) with CM #3 (iii) with CM #8. Magnification, 100x. Scale bar, 200μm. (B) Invasion assay of parental cell line, MiaPaCa-2 containing conditioned media from Clone #3 and Mia clone #8.

Statistics; * $p \leq 0.05$, ** $p \leq 0.01$, *** $p \leq 0.005$ Student's t-test.

(A)
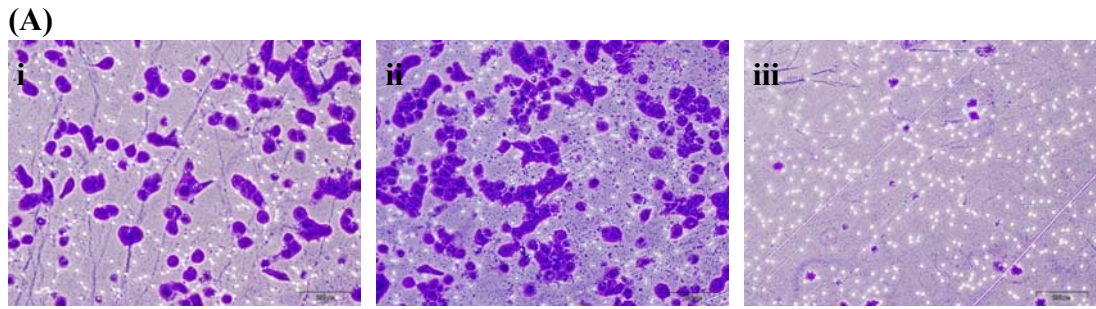
(B)
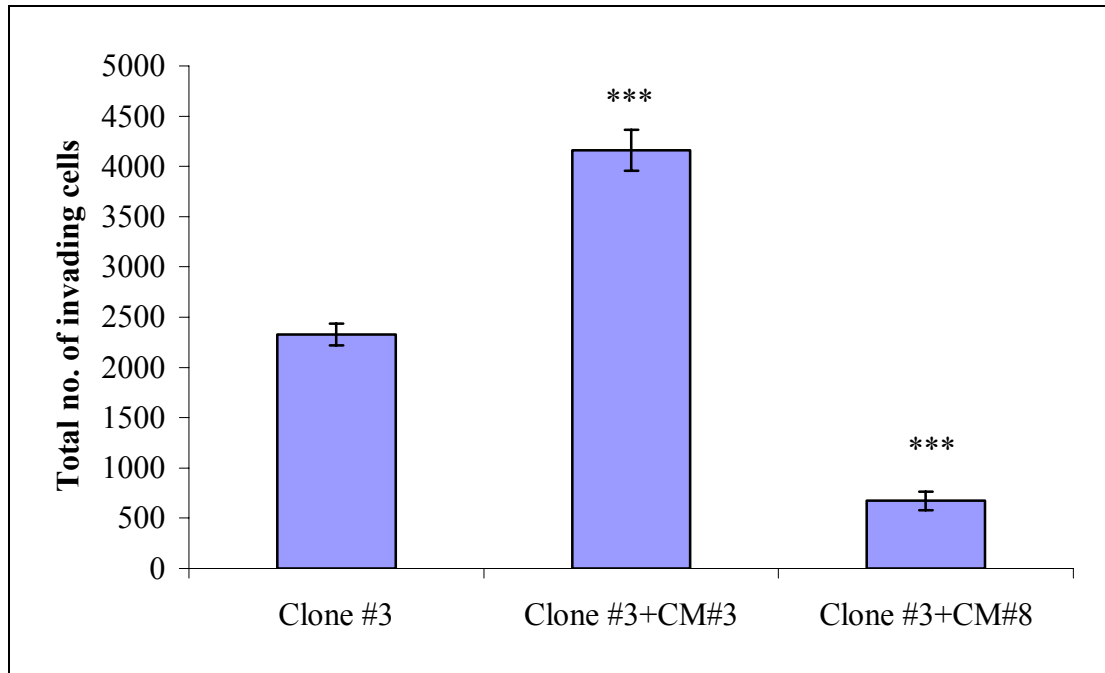
Figure 3.5.2 (A) Invasion assays of Clone #3 (i) under control conditions (ii) with CM #3 (iii) with CM #8. Magnification, 100x. Scale bar, 200μm. (B) Invasion assay of the high invasive cell line, Clone #3 containing conditioned media from Clone #3 and Clone #8.

Statistics; * $p \leq 0.05$, ** $p \leq 0.01$, *** $p \leq 0.005$ Student's t-test.

(A)

(B)
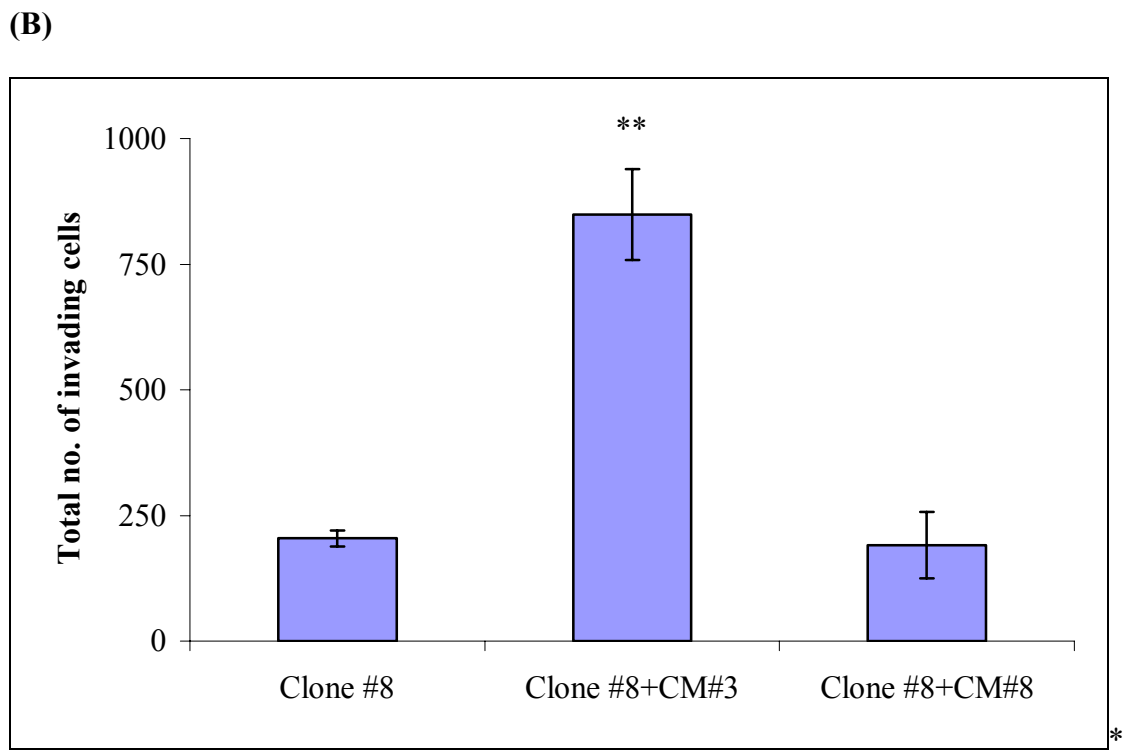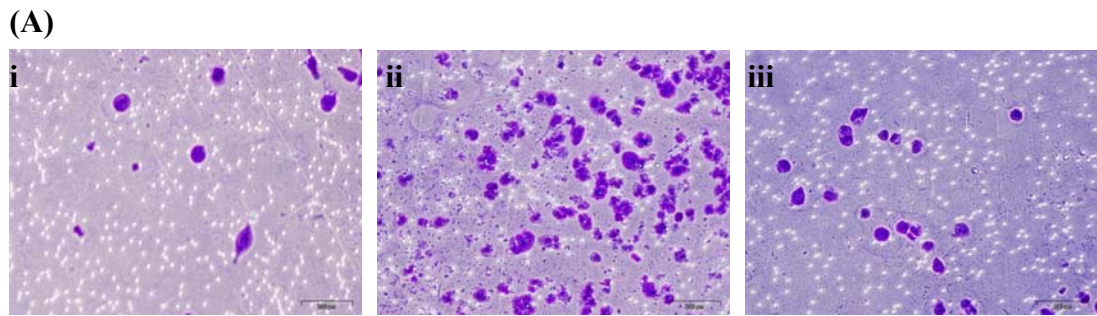
Figure 3.5.3 (A) Invasion assays of Clone #8 (i) under control conditions (ii) with CM #3 (iii) with CM #8. Magnification, 100x. Scale bar, 200μm.

(B) Invasion assay of the low invasive cell line, Clone #8 containing conditioned media from Clone #3 and Clone #8.

Statistics; * $p \leq 0.05$, ** $p \leq 0.01$, *** $p \leq 0.005$ Student's t-test.

3.5.1.2 Effect of CM#3 and CM#8 on adhesion

Adhesion assays of MiaPaCa-2, Clone #3 and Clone #8 were performed in the presence of CM#3 and CM#8 to matrigel. Figure 3.5.4 shows the level of adhesion of the cell lines to matrigel by absorbance readings. The incubation of CM#3 in the assays decreased the percentage adhesion of MiaPaCa-2, Clone #3 and Clone #8, (18%, 19% and 12%) whereas CM#8 enhanced the percentage adhesion by 24%, 22% and 27 % in MiaPaCa-2, Clone #3 and significantly in Clone #8 (p=0.03).

3.5.1.3 Effect of CM#3 and CM#8 on anoikis

CM#3 and CM#8 were also included in anoikis assays to assess whether secreted factors from the CM had an effect on apoptosis due to loss of anchorage (Figure 3.5.5). CM#3 slightly increased resistance to anoikis in MiaPaCa-2, Clone #3 and Clone #8. CM#8 induced sensitivity to anoikis in MiaPaCa-2 and Clone #3, and significantly promoted anoikis in Clone #8 (p=0.05).
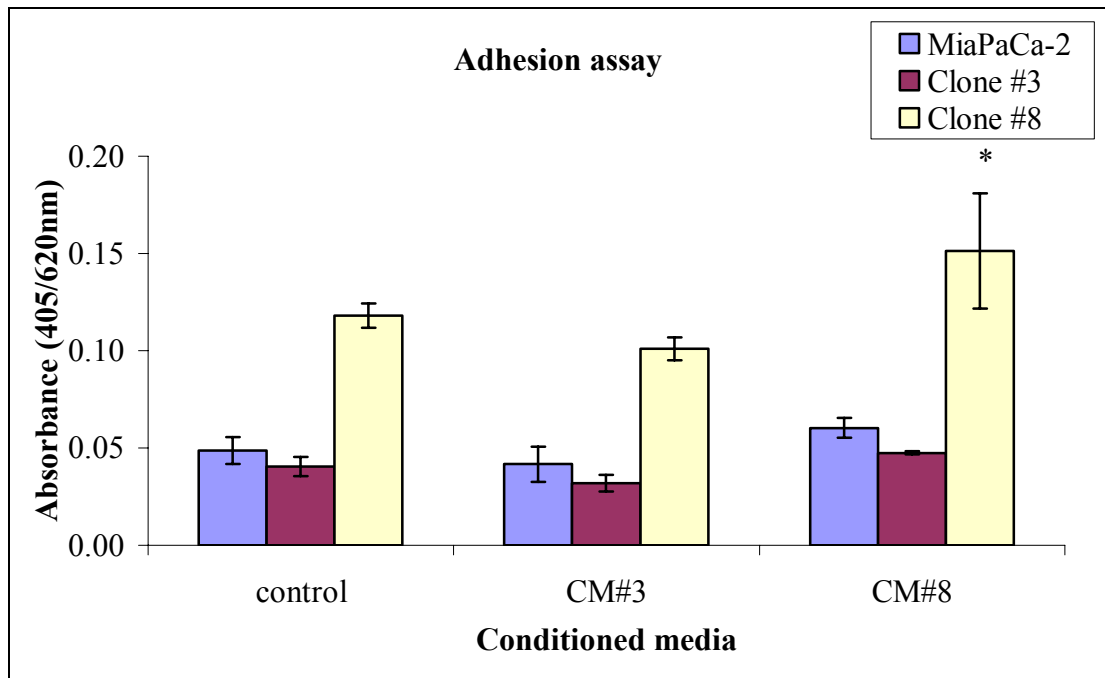
Figure 3.5.4 Effect of conditioned media from Clone #3 (CM#3) and Clone #8 (CM#8) on adhesion of MiaPaCa-2 and its sub-populations, Clone #3 and Clone #8 to matrigel.
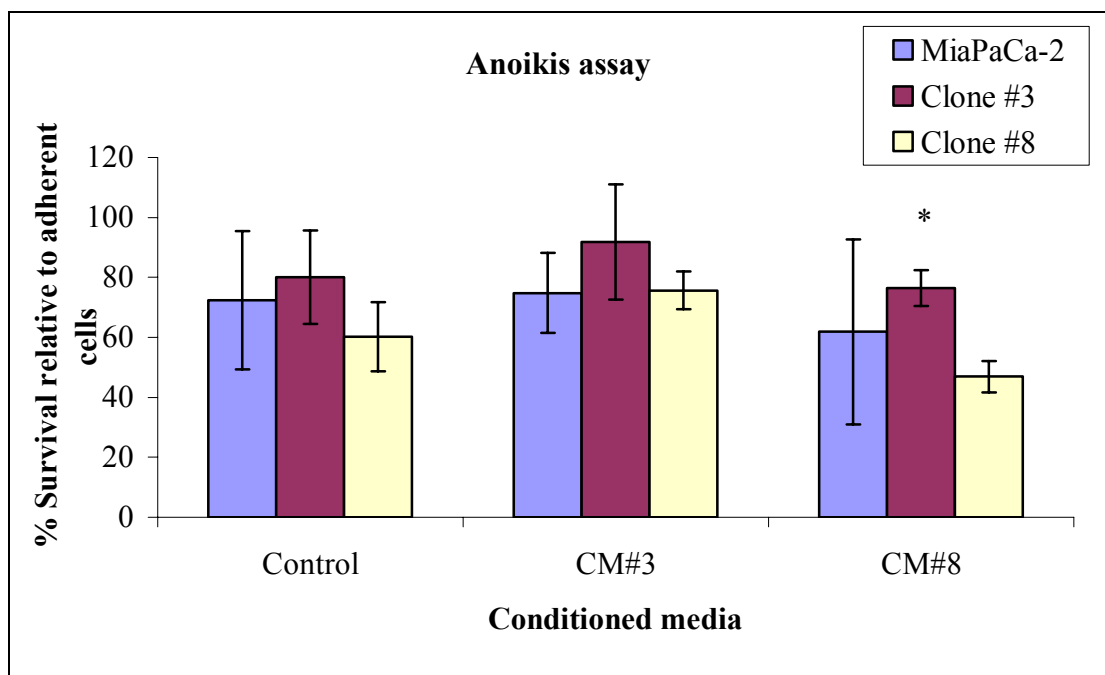
Figure 3.5.5 Effect of conditioned media from Clone #3 (CM#3) and Clone #8 (CM#8) on anoikis of MiaPaCa-2 and its sub-populations, Clone #3 and Clone #8. Statistics; * $p \leq 0.05$, ** $p \leq 0.01$, *** $p \leq 0.005$ Student's t-test.

3.5.1.4 Effect of 24 hour pre-incubation with CM#3 and CM#8 on invasion of MiaPaCa-2

MiaPaCa-2 was incubated with conditioned media for 24 hours and invasiveness assessed. The level of invasion is significantly increased after 24 hours pretreatment of the parental cell line, MiaPaCa-2 with CM#3 (p=0.02), compared to cells not exposed to CM#3. Invasion induced by pre-treatment with CM#3 was similar to that seen when CM#3 was added to the invasion assay (Figure 3.5.6). In contrast, CM#8 pre-treatment of MiaPaCa-2 significantly reduces the level of invasion (p=0.02), again similar to addition of CM#8 to the invasion assay.
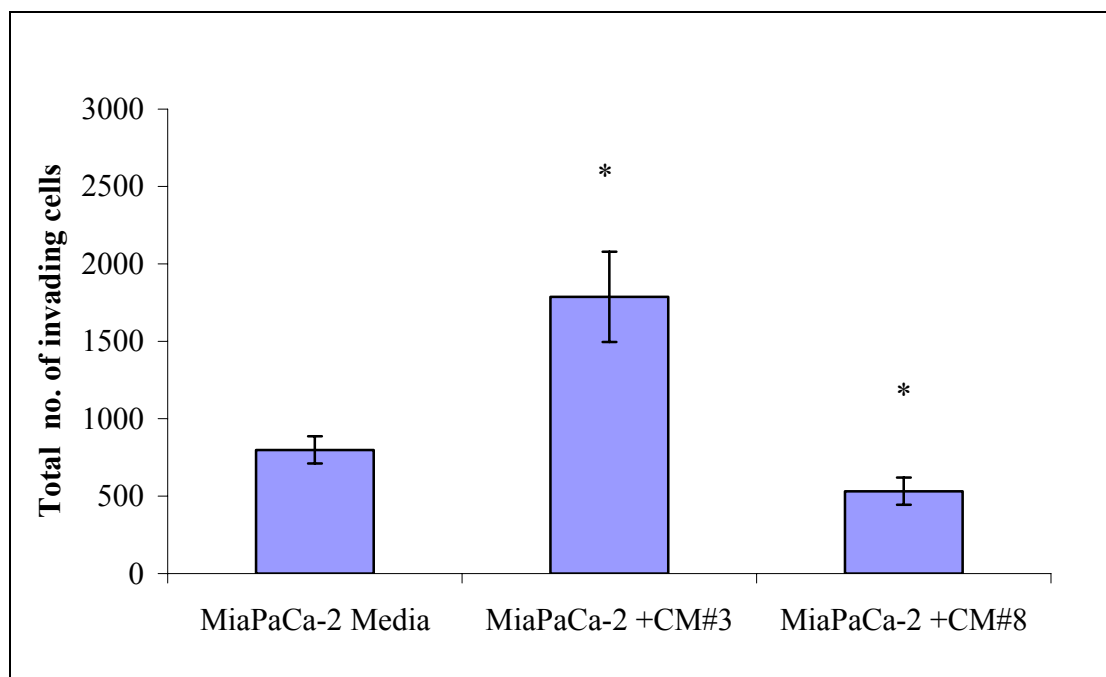
Figure 3.5.6 Invasion assay of MiaPaCa-2 cells incubated with CM#3 and CM#8 for 24 hrs prior to invasion assay.
Statistics; * $p \leq 0.05$, ** $p \leq 0.01$, *** $p \leq 0.005$ Student's t-test.

3.5.2 Effect of pre-incubation on matrigel of MiaPaCa-2 and sub-populations, Clone #3 and Clone #8 on invasion

Adhesion to the extracellular matrix (ECM) is one of the first steps of invasion. The cell utilises different mechanisms to disrupt the basement membrane or ECM. In order to further stimulate these mechanisms that the cells use to degrade the extracellular matrix, the cells were grown on matrigel for 24 hours prior to invasion assays (Chapter 2.5.5).

The invasion and superinvasion of MiaPaCa-2 after pre-incubation for 24 hours on matrigel in the presence of CM#3 and CM#8 were assessed. Figure 3.5.7 (A) shows the number of cells invading is higher for the cells grown on matrigel in the presence of normal fresh media. Superinvasive cells were also observed after pre-incubation of the cells on matrigel. Superinvasion is defined as cells that invade through the matrigel and attach to the bottom of the plate (Glynn *et al*., 2005). However, the invasion of the cell line, MiaPaCa-2 is increased even further when grown on matrigel in the presence of CM#3. The superinvasion of the cell line also increased. In the presence of CM#8, invasion is decreased compared to cells grown in media alone and superinvasion is also significantly decreased (p=0.01). Figuure 3.5.7 (B) represents the number of Clone #3 cells invading through the matrigel insert, after pre-incubation on matrigel for 24 hours. Clone #3 pre-incubated on matrigel displays a slight increase in invasion compared to the control cells not pre-incubated on matrigel. The numbers of cells invading cells are increased, and the superinvading cells are significantly increased (p=0.006) after preincubation on matrigel in the presence of CM#3. Clone #3 shows decreased invasion and superinvasion when preincubated with CM#8, though not significantly.

Figure 3.5.7 (C) shows the low invasive potential of Clone #8 under normal invasion assay conditions. When the cell line is grown on matrigel for 24 hours, invasion increases and superinvasion is also observed. The cell line grown on matrigel in the presence of CM#3 displays further increased invasion and superinvasion, whereas after preincubation with CM#8, the invasion and superinvasion are decreased slightly.
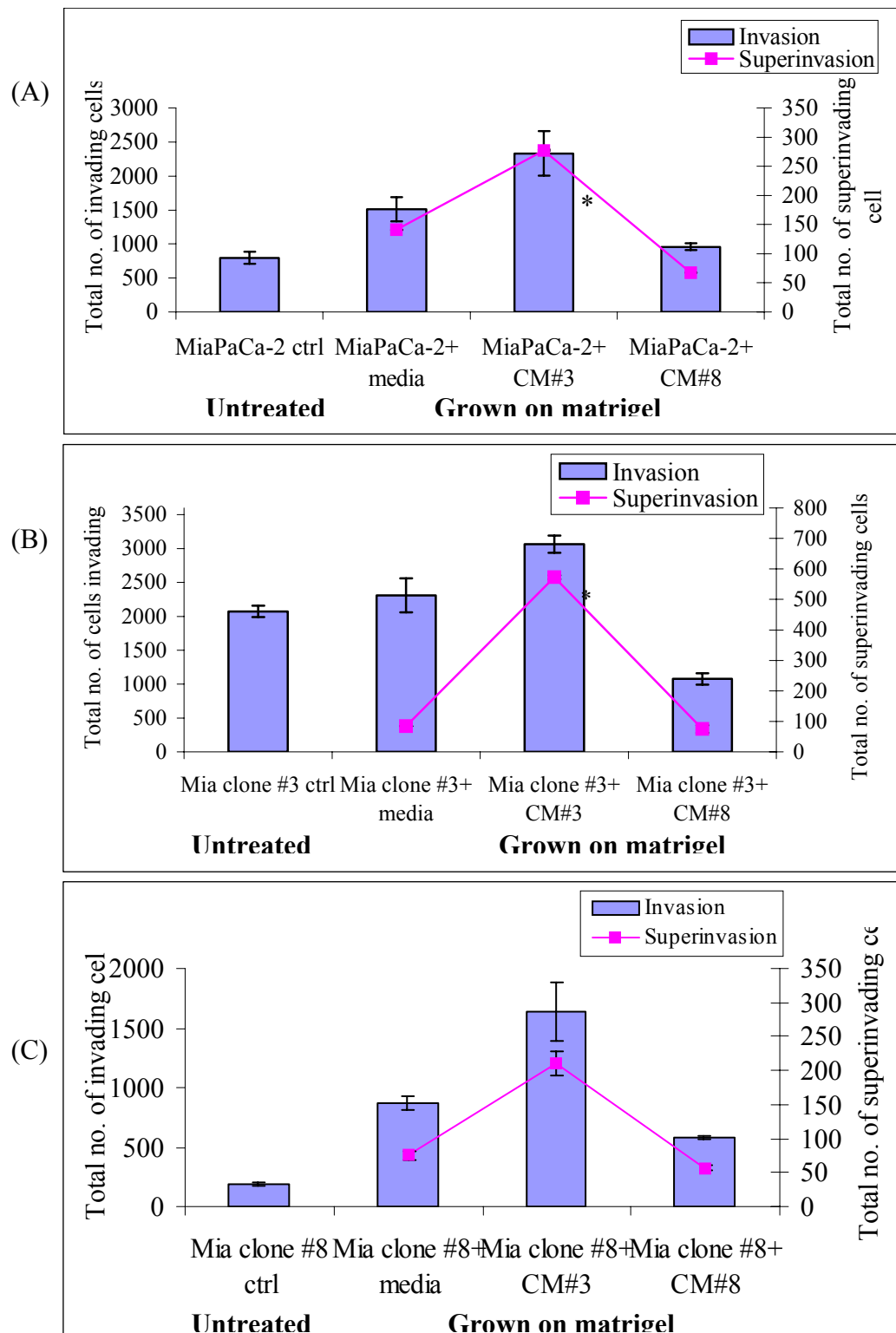
Figure 3.5.7 Invasion and superinvasion levels of (A) MiaPaCa-2 (B) Clone #3 (C) Clone #8 under normal control conditions, grown on matrigel and grown on matrigel in the presence of CM#3 and CM#8. Statistics; * p ≤ 0.05, ** p ≤ 0.01, *** p ≤ 0.005 Student's t-test.

3.5.3 Characterisation of CM#3 and CM#8

Conditioned media from both Clone #3 and #8 were collected over time and pooled to generate a stock of conditioned media. This CM was characterised by temperature, dilution and pH stability in order to determine the stability of the CM.

3.5.3.1 Temperature stability of CM#3 and CM#8

To investigate the temperature stability of the conditioned media, invasion assays were performed on MiaPaCa-2 to evaluate the CM stored at 4° C, -20° C and -80° C over 3 months.

Conditioned media, CM#3 and CM#8 was diluted at a 1:1 ratio with fresh media, above and below the insert. Therefore no gradient was present in the experiments.

The conditioned media CM #3 showed little variability, in terms of inducing increased invasion on the pancreatic cell line MiaPaCa-2 (Figure 3.5.8), when stored at different temperatures. However, storage of CM#3 at -80^0C yielded slightly better results.

Figure 3.5.9 shows that conditioned media CM #8 stored at -80^0C displayed better stability in terms of effectiveness on MiaPaCa-2 in invasion assays. Therefore for all future experiments the conditioned media CM#3 and CM#8 was stored at -80^0C.
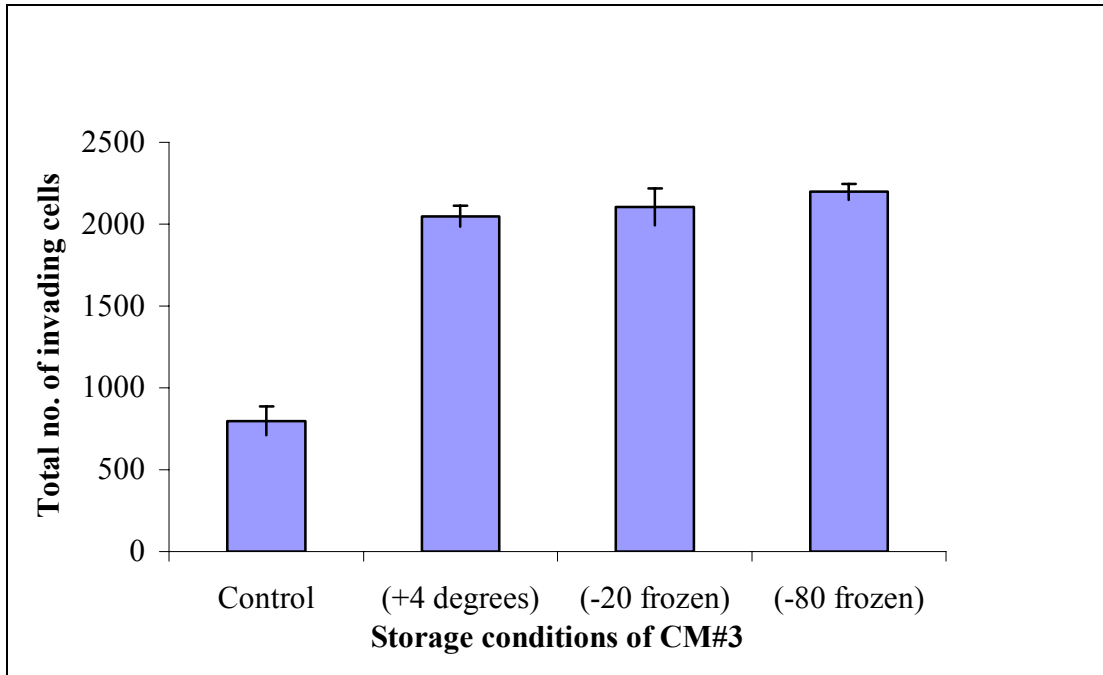
Figure 3.5.8 Invasion assay of MiaPaCa-2 with conditioned media from clone #3 stored at different temperatures.
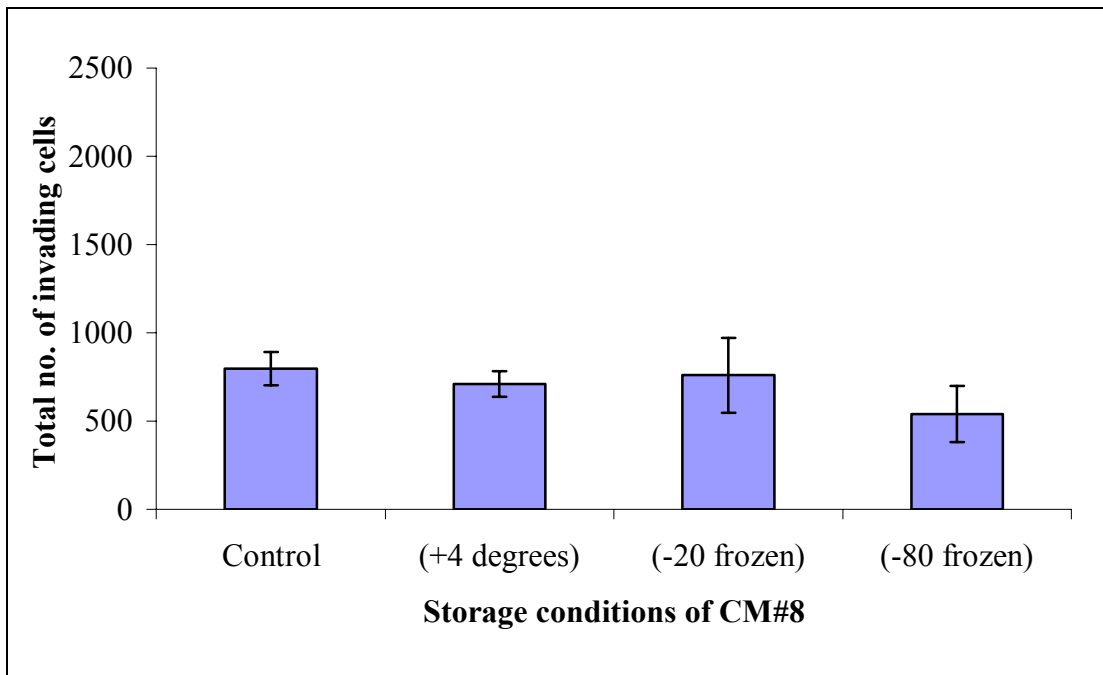
Figure 3.5.9 Invasion assay of MiaPaCa-2 with conditioned media from clone #8 stored at different temperatures.

The control column is based on the average number of invading cells of MiaPaCa-2 under normal fresh media conditions.

3.5.3.2 Effect of dilution of CM#3 and CM#8 on invasion of MiaPaCa-2

Conditioned media from Clone #3 and #8 stored at −80 $^{\circ}$C was used in invasion assays of MiaPaCa-2 diluted at 1:4, 1:8 and 1:16 with fresh media to determine the maximum dilution factor.

Figure 3.5.10 shows that a dilution factor of 1:4 of CM#3 is optimal to achieve increased induction of invasion of MiaPaCa-2 through the matrigel-coated inserts. Dilution of the CM#3 to 1:8 or 1:16 with fresh media dilutes the invasion inducing factors present in the conditioned media thereby reducing the increased invasive effects.

Figure 3.5.11 shows that a dilution factor of 1:4 of CM#8 is also optimal to achieve decreased invasion of MiaPaCa-2 through the matrigel-coated inserts. Dilution of the CM#8 to 1:8 or 1:16 with fresh media dilutes the inhibitory effects of the conditioned media thereby reverts the level of invasion similar to the control containing fresh media.

All future experiments were carried out using the conditioned media diluted with fresh media not more than 1:4.
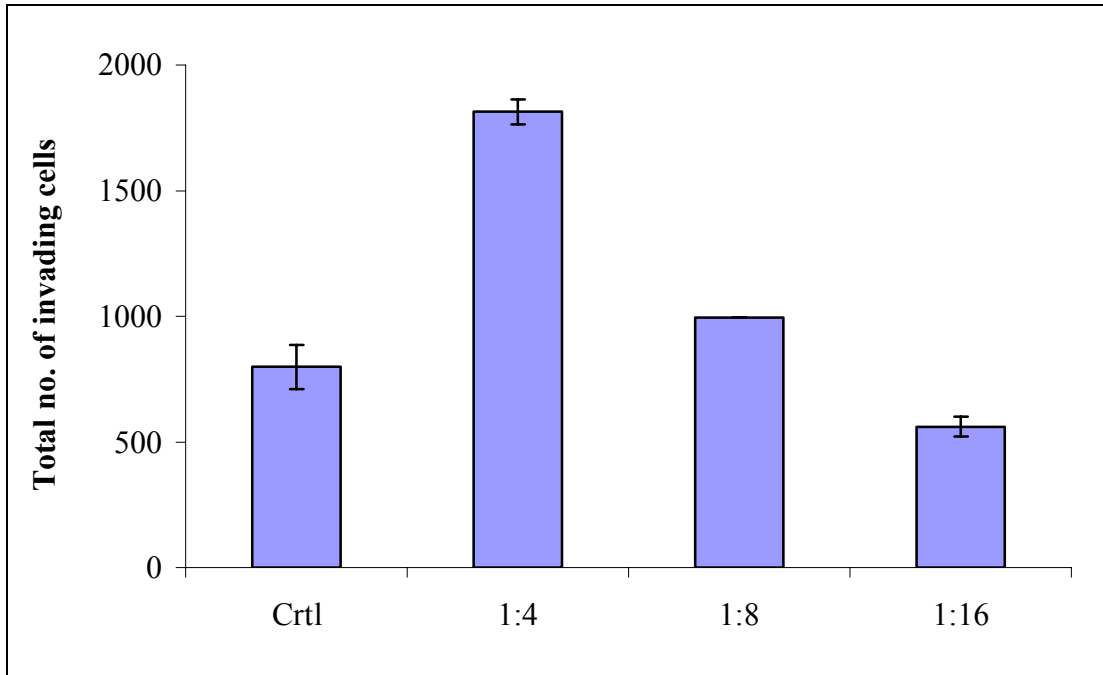
Figure 3.5.10 Invasion assay of parental cell line, MiaPaCa-2 with conditioned media from Clone #3 at variable dilution factors.
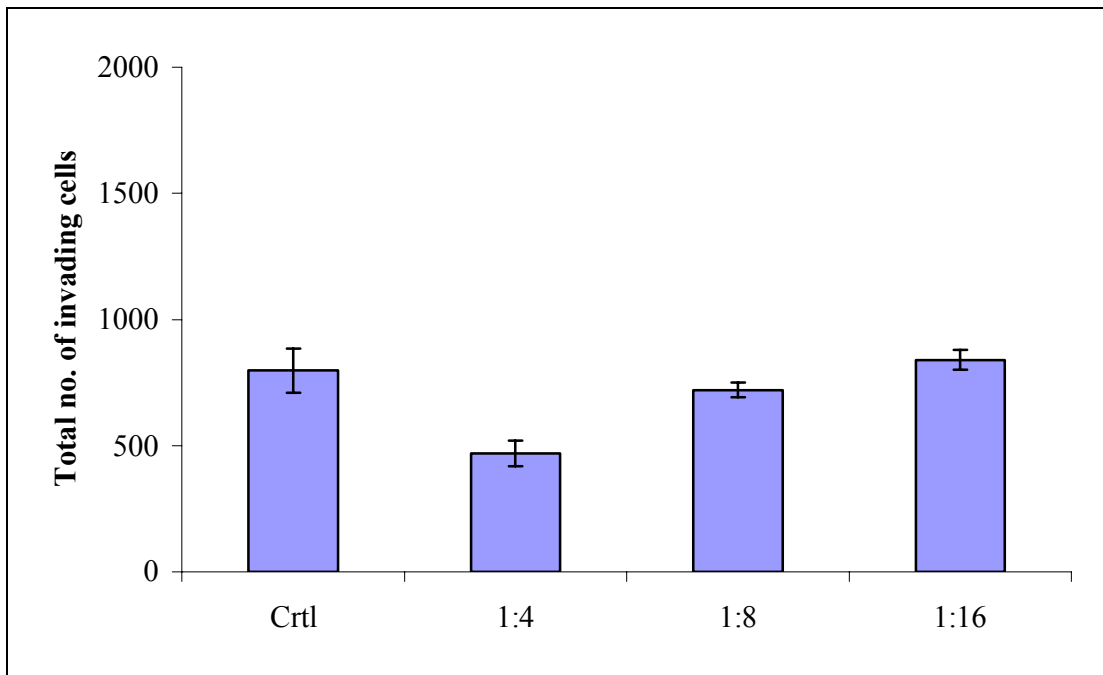
Figure 3.5.11 Invasion assay of parental cell line, MiaPaCa-2 with conditioned media from Clone #8 at variable dilution factors.

The control column represents the average number of invading cells of MiaPaCa-2 under normal fresh media conditions.

3.5.3.3 Characterisation of pH stability of CM#3 and CM#8 on invasion

Serum-free conditioned media from both Clone #3 and Clone #8 were collected over time and pooled (as previously described). To investigate the pH stability of the conditioned media compared to fresh media (treated under the same conditions); invasion assays were performed on MiaPaCa-2 to evaluate stability of the CMs at different pHs.

Figure 3.5.12 shows a summary of the level of invasion in MiaPaCa-2 under control conditions and with the addition of CM#3 and CM#8, as previously observed in figure 3.5.1.

To alter the pH of the media, CM#3 and CM#8, aliquots of media were exposed to acid/base to a range of pHs, kept at new pH for 2 hrs and brought back to pH 7 (original pH) (Chapter 2.2.1).

Fresh media was treated under the same conditions as CM#3 and CM#8 to ensure that the effect of altering the pHs of CMs was not due to the addition of acid/base. Figure 3.5.13 shows invasion of MiaPaCa-2 relative to fresh media treated at the same pH as CM#3 and CM#3. The level of invasion is slightly decreased when media is treated at different pHs. The highest level of invasion observed in control media treatment was in cells treated with media @ pH 3-7. The lowest level of invasion was shown in MiaPaCa-2 treated cells with media at pH 9-7. This results confirms that the addition of acid/base into fresh media does not significantly alter the invasive abilities of the cells.

(A)

(B)
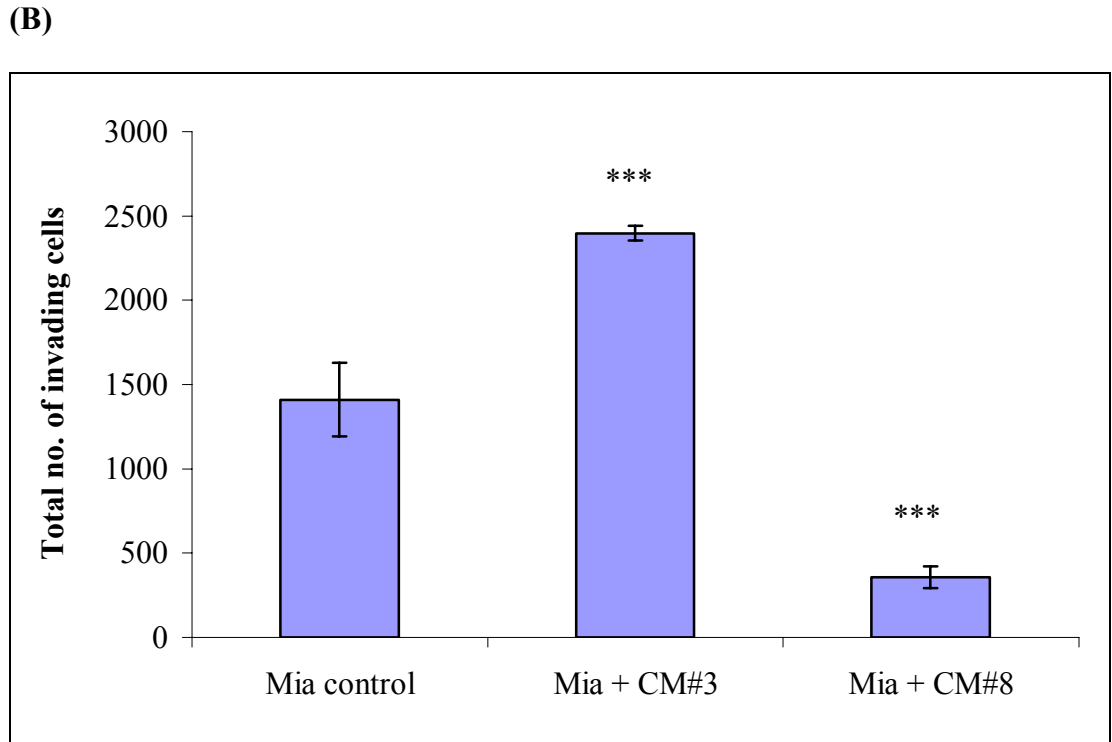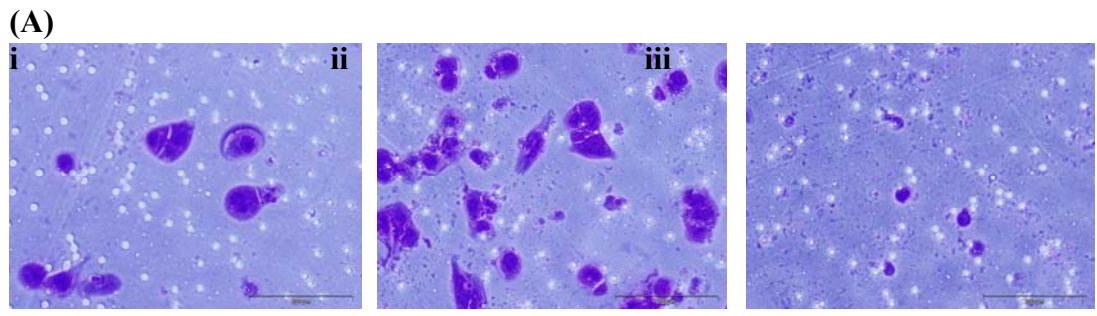
Figure 3.5.12 (A) Invasion assays of (i) MiaPaCa-2 under control conditions, (ii) addition of CM#3 into the invasion insert and (iii) addition of CM#8 into the invasion insert. Scale bar, 200 μm. (B) Total number of cell invading in invasion assay of MiaPaCa-2 under control conditions, with the addition of CM#3 and CM#8

(A)
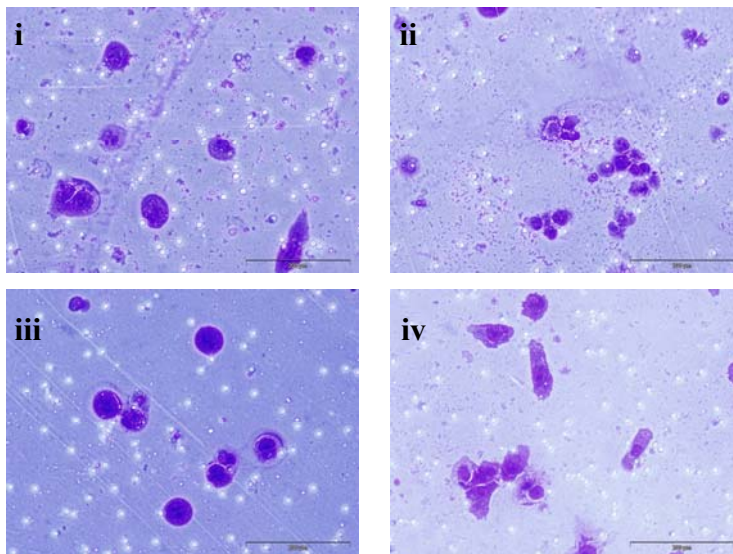
(B)
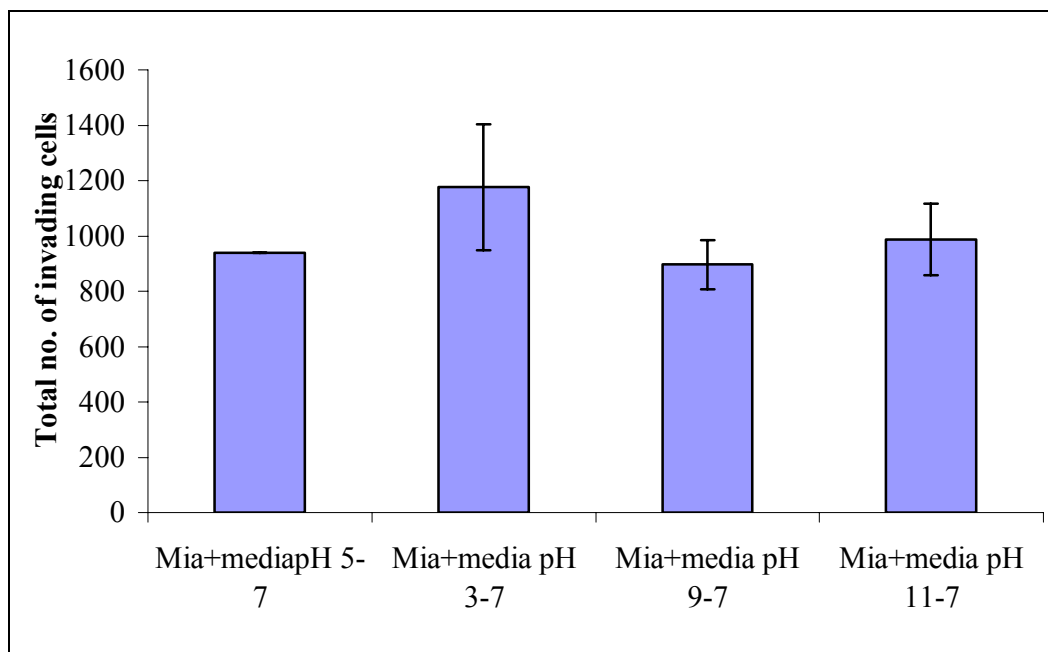
Figure 3.5.13 (A) Invasion assays of MiaPaCa-2 (i) with media @ pH 5-7 (ii) with media @ pH 3-7 (iii) with media @ pH 9-7 (iv) with media @ pH 11-7. Magnification, 200x. Scale bar, 200µm.

(B) Invasion assay MiaPaCa-2 containing media @ different pH.

3.5.3.3.1 Characterisation of pH stability on CM#3 invasion stimulatory activity

Conditioned media from Clone #3 (obtained as previously described) was exposed to differing pH for 2 hours at room temperature and then readjusted back to original pH of the CM#3. Unconditioned media samples were also pH adjusted and treated as controls (Figure 3.5.13). Invasion assays were performed using the parental cell line, MiaPaCa-2. The CM#3 was used at a 1:1 dilution with fresh media.

Table 3.5.1 Stability of CM#3 after pH treatment and readjustment on invasion

Volume added	pH	Volume added	Final pH	CM#3 Invasion	Control Invasion
HCL (20 ul)	5	NaOH (20 μl)	7.2	+++++ Invasion	+ Invasion
HCL (50μl)	3	NaOH (50 μl)	7.2	++++ Invasion	++ Invasion
NaOH (30 μl)	9	HCL (30 μl)	7.2	+++ Invasion	+ Invasion
NaOH (60 μl)	11	HCL (60 μl)	7.2	+++ Invasion	+ Invasion

These experiments indicate that the invasion stimulatory effects of CM#3 are enhanced with acid treatment and readjustment. Slight base sensitivity was observed, although residual activity remained between pH 9 and 11 (Table 3.5.1). pH treatment on control media had greater inhibitory effects on invasion compared to CM#3 (Figure 3.5.14).

The pH stability was also examined by exposing the CM#3 to a range of pH values without readjustment. CM#3 displayed no invasion effect at pH 3 and moderate invasion at pH 9. A higher level of invasion was observed at pH 7.8 (Table 3.5.2). This may be due to the fact that the original pH of CM#3 is slightly more acidic compared to control media.

Table 3.5.2 Stability of CM#3 after pH treatment on invasion

pH	CM#3 Invasion	Control Invasion
3	- Invasion	+ Invasion
7.8	++ Invasion	+ Invasion
9	+ Invasion	+ Invasion

(A)
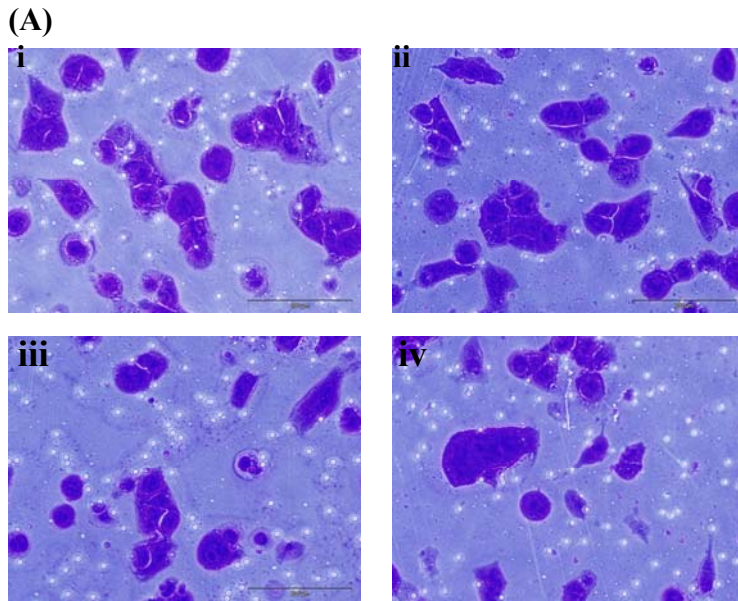
(B)
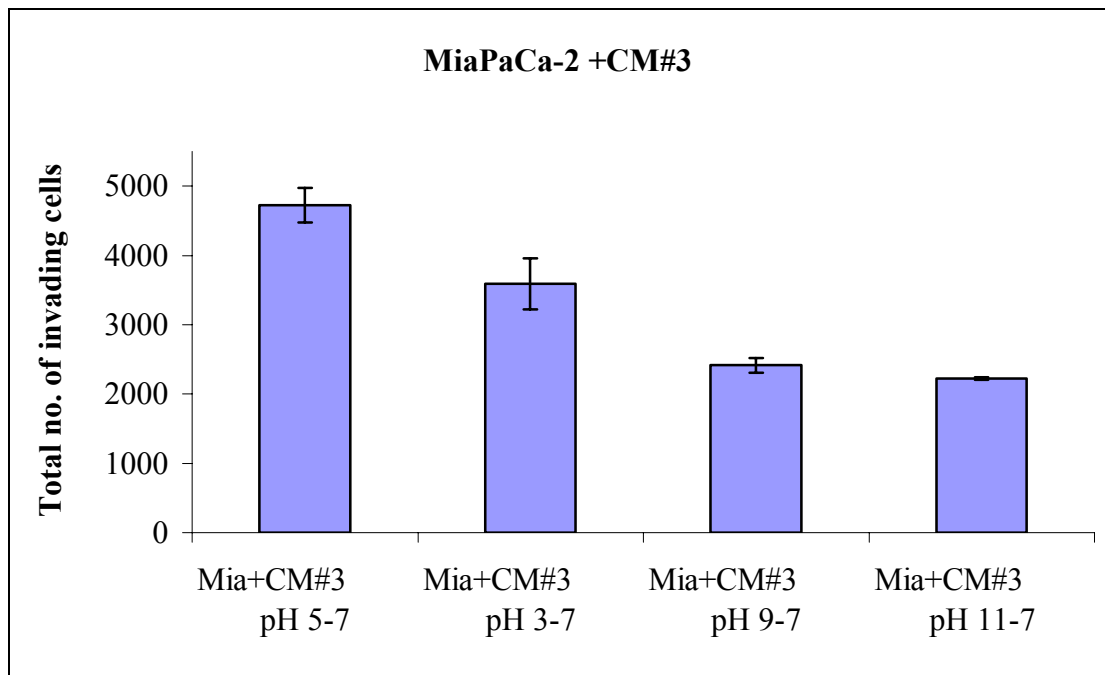
Figure 3.5.14 (A) Invasion assays of MiaPaCa-2 (i) with CM #3 @ pH 5-7 in invasion chamber (ii) with CM #3 @ pH 3-7 in invasion chamber (iii) with CM #3 @ pH 9-7 in invasion chamber (iv) with CM #3 @ pH 11-7 in invasion chamber. Magnification, 200x. Scale bar, 200μm.

(B) Invasion assay MiaPaCa-2 containing conditioned media from CM #3 @ varying pH.

3.5.3.3.2   Characterisation of pH stability CM#8 invasion inhibitory activity

Conditioned media from Clone #8 (obtained as previously described) was exposed to differing pH for 2 hours at room temperature and then readjusted back to original pH of the CM#8. Unconditioned media samples were also pH adjusted and treated as control (Figure 3.5.13). Invasion assays were performed using the parental cell line, MiaPaCa-2. The CM#8 was used at a 1:1 dilution with fresh media.

Table 3.5.3 Stability of CM#8 after pH treatment and readjustment on invasion

Volume added	pH	Volume added	Final pH	CM#8 Invasion	Control Invasion
HCL (20 μl)	5	NaOH (20 μl)	7.4	++ Invasion	+ Invasion
HCL (50 μl)	3	NaOH (50 μl)	7.4	+ Invasion	++ Invasion
NaOH (30 μl)	9	HCL (30 μl)	7.4	+ Invasion	+ Invasion
NaOH (30 μl)	11	HCL (60 μl)	7.4	+ Invasion	+ Invasion

These experiments indicate that the invasion inhibitory effects of CM#8 are enhanced with basic treatment and readjustment. Slight acid sensitivity was observed, whereby the invasion levels increased similar to that of the untreated control media at pH 5-7 (Table 3.5.3). pH treatment on control media had less inhibitory effects on invasion compared to CM#8, optimal CM#8 inhibitory effects were observed at higher pH range between 9-11 (Figure 3.5.15).

The pH stability was also examined more closely by exposing the CM#8 to a range of pH values without readjustment. CM#8 displayed no invasion effect at pH 2 and moderate invasion at pH 8. A higher level of invasion was observed at pH 7.2 (Table 3.5.4) and inhibitory effects optimal at pH8. This may be due to the fact that the original pH of CM#8 is slightly more basic compared to control media.

Table 3.5.4 Stability of CM#8 after pH treatment on invasion

pH	CM#3 Invasion	Control Invasion
2	- Invasion	+ Invasion
7.2	++ Invasion	+ Invasion
8	+ Invasion	+ Invasion

(A)
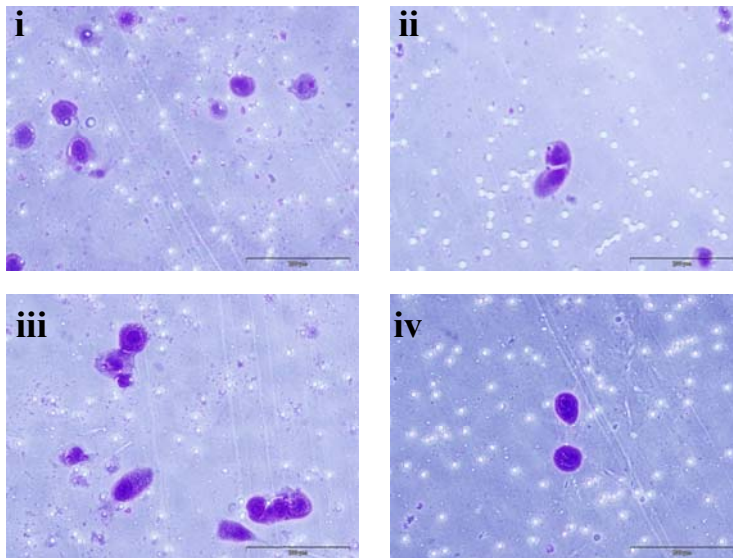
(B)
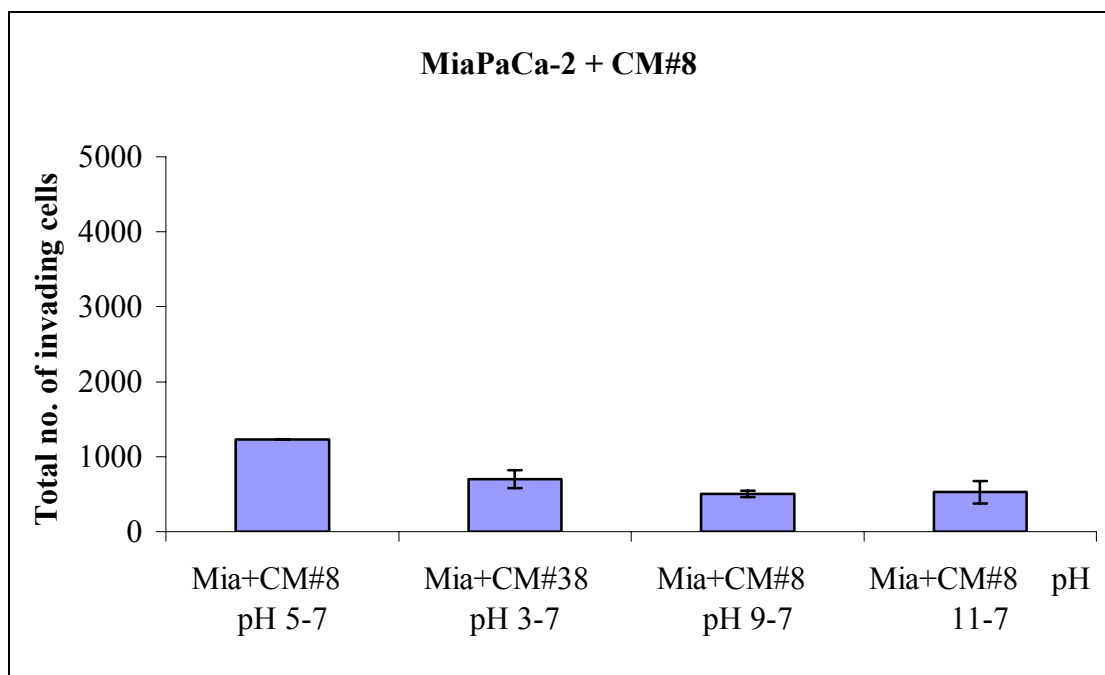
Figure 3.5.15 (A) Invasion assays of MiaPaCa-2 (i) with CM #8 @ pH 5-7 in invasion chamber (ii) with CM #8 @ pH 3-7 in invasion chamber (iii) with CM #8 @ pH 9-7 in invasion chamber (iv) with CM #8 @ pH 11-7 in invasion chamber. Magnification, 200x. Scale bar, 200μm.

(B) Invasion assay MiaPaCa-2 containing conditioned media from CM #8 @ different pH.

3.5.4 Analysis of fractionation samples of CM#3 and CM#8 on invasion of Clone #3

Serum-free conditioned media from Clone #3 and Clone #8 were concentrated to five molecular weight cut off fractions. Approximately 11 ml of CM#3 and CM#8 were concentrated to fractions of below 10 kDa, between 10-30 kDa, 30-50 kDa, 50-100 kDa and above 100 kDa. These concentrated samples were then re-established to their original volume. CM#3 and CM#8 fractions were then used in invasion assays to assess whether a secreted factor in the media causing the promotion or inhibition of invasion was concentrated in a specific CM fraction.

Invasion assays of Clone #3 in the presence of CM#3 fractions were performed. Invasion at the lower concentration cut off showed a decrease in invasion, (p=0.01 and p=0.02), while invasion levels of Clone #3 including fractions, 30-50 kDa, 50-100 kDa and 100 kDa increased significantly (p=0.001, p=0.0002 and p=0.0001) (Figure 3.5.16).

Figure 3.5.17 shows the invasion of Clone #3 in the presence of the different isolated fractions of CM#8. Control invasion was monitored using normal media. The addition of CM#8 at fractions 10 kDa and 10-30 kDa showed the largest reduction in invasion (p=0.002 and p=0.03). As the molecular weight cut off points began to increase, so did the invasion. Invasion increased back to control levels and at 100 kDa invasion was increased 1.1-fold (p=0.05).

These results suggest that important fractions are secreted into Clone #8, acting as an inhibitory factor at lower concentrations, while CM#3 seems to contain high molecular weight fractions that promote invasion.

(A)
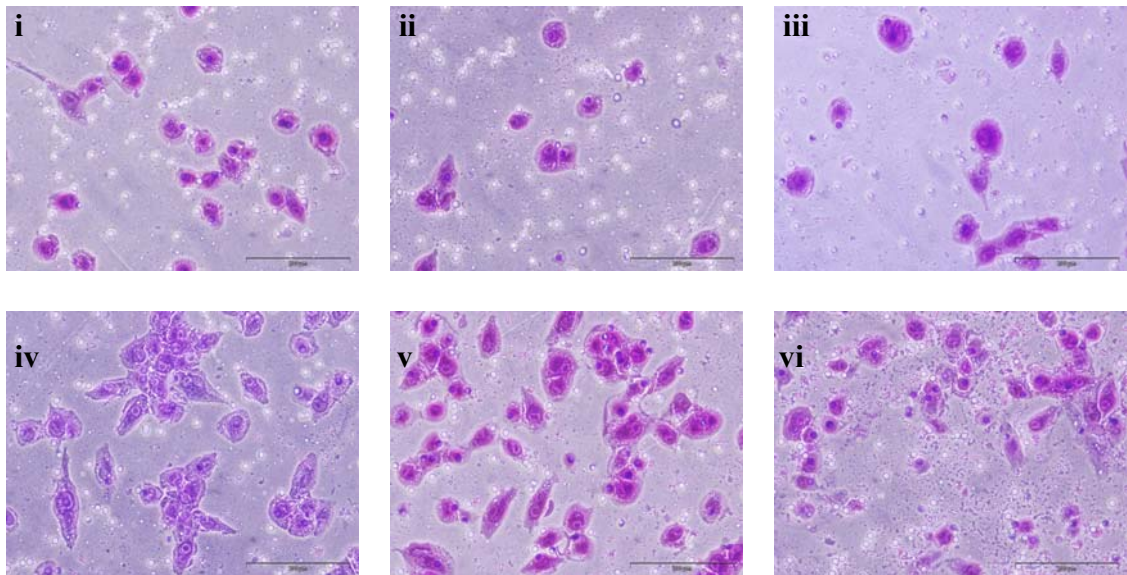
(B)
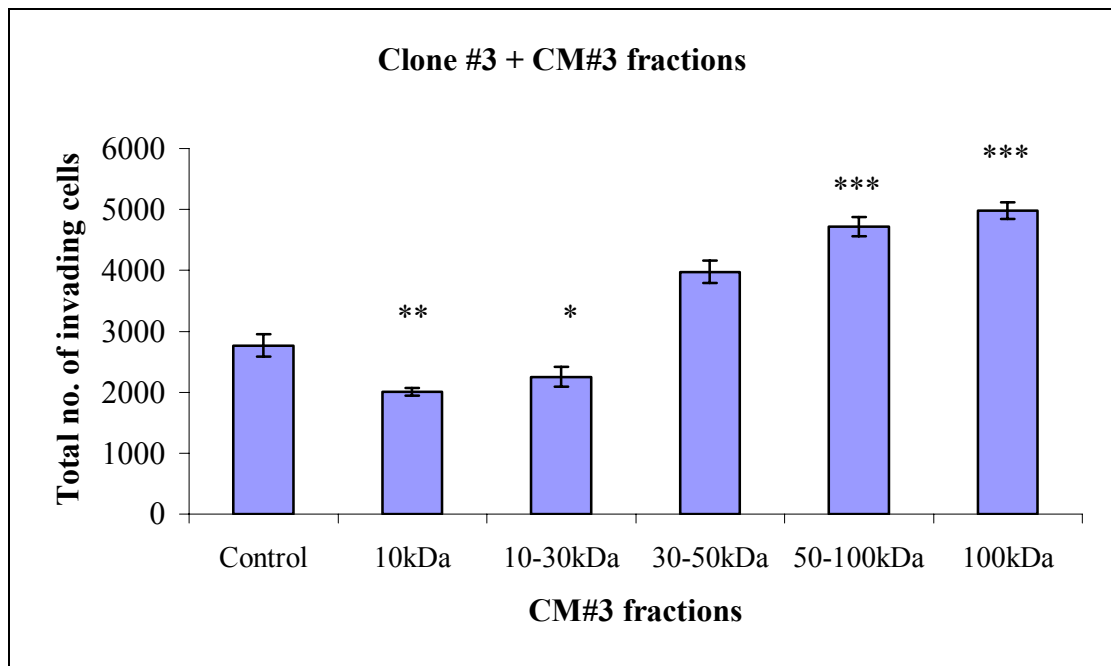
Figure 3.5.16 (A) Invasion of Clone #3 (i) under control conditions (ii) with CM #3 fraction 10 kDa (iii) with CM #3 fraction 10-30 kDa (iv) with CM #3 fraction 30-50 kDa (v) with CM #8 fraction 50-100 kDa (vi) Clone #3 with CM #3 fraction 100 kDa. Magnification, 200x. Scale bar, 200μm.

(B) Invasion of Clone #3 containing CM#3 fractions.

(A)

(B)
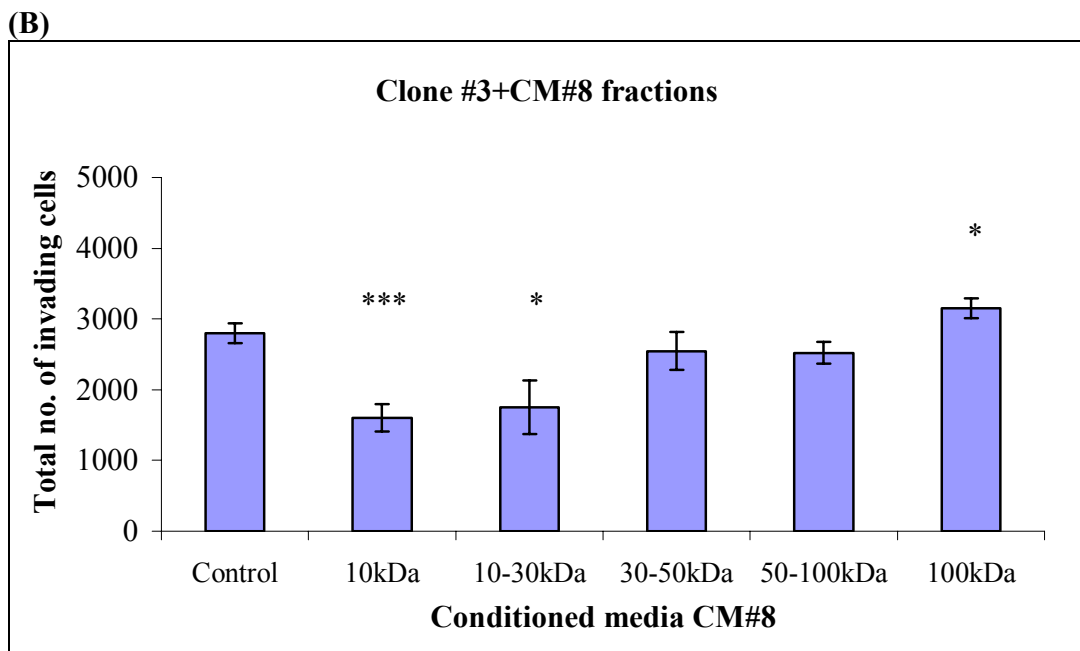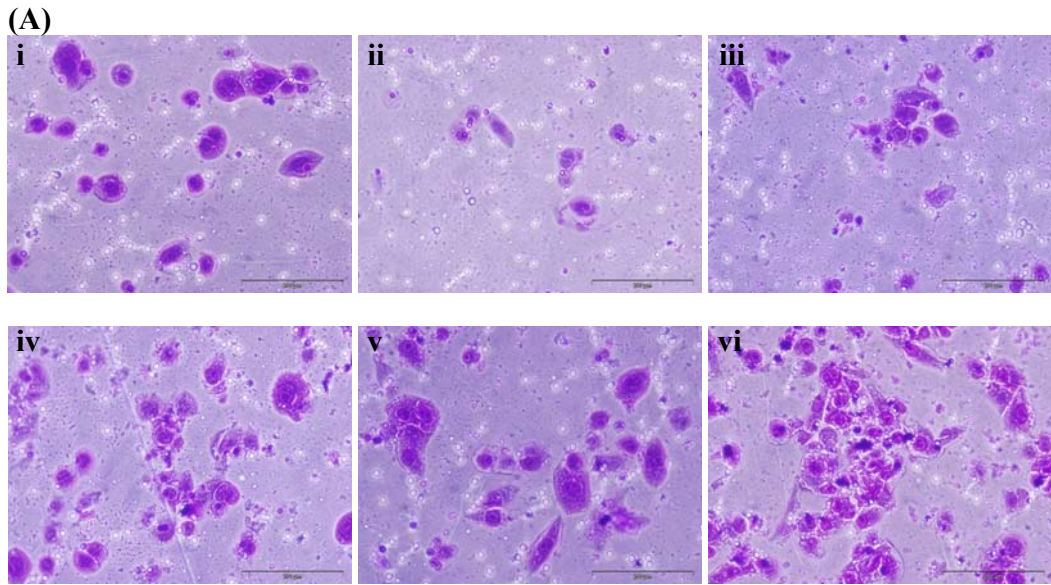
Figure 3.5.17 (A) Invasion assays of Clone #3 (i) under control conditions (ii) with CM #8 fraction 10 kDa (iii) with CM #8 fraction 10-30 kDa (iv) with CM #8 fraction 30-50 kDa (v) with CM #8 fraction 50-100 kDa (vi) with CM #8 fraction 100 kDa. Magnification, 200x. Scale bar, 200μm.

(B) Invasion assay of Clone #3 containing CM#8 fractions.

3.6 Proteomic analysis of conditioned media from MiaPaCa-2 and sub-populations Clone #3 and Clone #8 by two-dimensional difference gel electrophoresis (2-D DIGE)

Proteomic analysis was carried on the conditioned media (CM) of MiaPaCa-2, Clone #3 and Clone #8. Differential protein expression was investigated by 2-D DIGE in the CM samples (Chapter 2.10).

CM #3 and CM #8 were added into the *in vitro* invasion assay model to assess the potential effects of secreted factors on invasion (Chapter 3.5).
CM#3 enhanced invasion of MiaPaCa-2 by 2.2-fold, Clone #3 by 1.8-fold and also significantly increased the invasion, 4.2 fold, of Clone #8 compared to an invasion assay control containing fresh medium.

In contrast, the addition of CM#8 into the invasion chamber caused a reduction in the invasive potential of the cell lines. MiaPaCa-2 containing CM#8 in the invasion assay showed a 3.3-fold decrease in invasion. CM#8 added onto Clone #3 in the invasion assay showed a 3.3-fold decrease in invasion and added onto Clone #8, a 1.1-fold decrease in invasion was observed.

3.6.1 Experimental outline for 2-D DIGE analysis of the samples

Differential secreted proteins between CM Mia, CM#3 and CM#8 were analysed by 2-D DIGE as outlined in Chapter 3.4. Triplicate biological repeats with duplicate technical repeats were reverse labelled with Cy3 and Cy5. All samples used in the experiment were pooled and labelled with the internal dye Cy2. Each sample was compared internally to the same standard, to account for any gel-to-gel variation.

3.6.1.1 DeCyder analysis

Differential protein expression between CM of MiaPaCa-2, Clone #3 and Clone #8 was observed using 2D-DIGE. DeCyder image analysis merged the Cy2, Cy3 and Cy5 images for each gel and detected spot boundaries for the calculation of normalised protein abundance. All paired images were then matched to generate comparative cross-gel statistical analysis. DeCyder^{TM} software revealed a total of 54 secreted protein spots identified in each comparison of CM Mia versus CM #8, CM #3 versus CM Mia and CM #3 versus CM #8.

Biological variation analysis of these spots showing greater that 1.2-fold change in expression with a t-test score of < 0.05 revealed 37 proteins which are significantly changed between CM Mia versus CM #8, while 32 proteins changed between CM #3 versus CM Mia, and 41 proteins were significantly differentially regulated between CM #3 versus CM #8. Protein expression maps (PEM) of all identified proteins between CM#3 and CM#8 are shown in figure 3.6.1 (Position number corresponds to table 3.6.3).

3.6.1.2 Protein identification

For protein identification, all proteins were digested and identified at least twice from separate gels with MALDI-TOF MS. An expectation value of <0.02 was used for all reported identifications, which indicates a 0.2% chance that the identification is random.

3.6.2 Secreted protein list generation

To evaluate the differentially expressed secreted proteins in the conditioned media of MiaPaCa-2, Clone #3 and Clone #8, three comparative protein lists were generated.

Table 3.6.1 outlines the 37 differentially regulated secreted proteins altered between CM of Mia versus CM #8. In this comparison, 5 secreted proteins are up-regulated and 32 secreted proteins are down-regulated with respect to fold change in protein secretion in CM Mia.

Table 3.6.2 outlines the 32 differentially regulated secreted proteins between the comparison of CM #3 versus CM #Mia. Of the 32 secreted proteins, 22 secreted proteins are up-regulated and 10 secreted proteins are down-regulated in relation to CM #3.

The third list compares the secreted proteins between CM #3 and CM #8 (Table 3.6.3). 41 proteins are significantly secreted, 14 secreted proteins are up-regulated and 27 secreted proteins are down-regulated in relation to CM #3.

Figure 3.6.1 displays a representative protein expression map of differentially abundant proteins expressed in CM Mia, CM#3 and CM#8.

Table 3.6.1 Secreted proteins significantly expressed in CM Mia versus CM #8

Protein name	Gene symbol	Protein AC number	PI/Mw	% Coverage	Fold change CM Mia versus CM #8
Gelsolin isoform b (a)	GSN	gi|38044288|	5.6/80.9	17.9	-2.6 ***
Gelsolin isoform b (b)	GSN	gi|38044288|	5.6/80.9	24.4	-2.4 ***
Gelsolin isoform b (c)	GSN	gi|38044288|	5.6/80.9	18.6	-2.3 ***
Gelsolin isoform b (d)	GSN	gi|38044288|	5.6/80.9	18.3	-1.9 ***
Proteasome activator Reg	PSME1	gi|2780883|	7.1/16.3	44.3	-1.9 ***
Beta actin (a)	ACTB	gi|15277503|	5.6/40.5	36.6	-1.9 ***
Phosphoglycerate kinase 1 (a)	PGK1	gi|48145549|	8.6/44.9	25.7	-1.8 ***
Phosphoglycerate kinase 1 (b)	PGK1	gi|48145549|	8.6/44.9	34.8	-1.8 ***
Phosphoglycerate kinase 1 (c)	PGK1	gi|48145549|	8.6/44.9	27.3	-1.7 ***
Beta actin (b)	ACTB	gi|15277503|	5.6/40.5	24.2	-1.7 ***
Nucleoside-diphosphate kinase 2 isoform 1	NDPK	gi|66392203|	9.3/30.3	21.7	-1.7 ***
Heat shock 70kDa protein 8 isoform 2 variant (a)	HSPA8	gi|62896815|	5.6/53.6	28.8	-1.7 ***
Heat shock protein HSP 90-alpha (HSP86)	HSP86	gi|92090606|	4.9/85.0	24.5	-1.6 ***
Gelsolin isoform b (e)	GSN	gi|38044288|	5.6/80.9	12.7	-1.6 *
Heat shock 70kDa protein 8 isoform 2 variant (b)	HSPA8	gi|62896815|	5.6/53.6	16.8	-1.6 ***
S-adenosylhomocysteine hydrolase	AHCY	gi|178277|	6.0/48.2	10.6	-1.6 ***

Malate dehydrogenase cytosolic	MDH1	gi|74311531|	5.9/36.6	20.1	-1.5 ***
Transketolase	TKT	gi|31417921|	8.4/50.3	18.2	-1.5 ***
Thioredoxin peroxidase	PRDX2	gi|9955016|	5.7/21.6	28.4	-1.5 ***
Gelsolin (amyloidosis: finnish type)	GSN	gi|55960299|	5.9/86.0	9.5	-1.5 **
NM23-H1	NM23-H1	gi|29468184|	5.4/19.8	27.1	-1.5 ***
Heat shock 70kDa protein 8 isoform 2 variant (c)	HSPA8	gi|62896815|	5.6/53.6	19.7	-1.5 ***
Peroxidase enzyme	1PRXB	gi|55959887|	6.0/24.9	53.2	-1.4 ***
Beta actin (c)	ACTB	gi|15277503|	5.6/40.5	24.4	-1.4 *
Beta actin (d)	ACTB	gi|15277503|	5.6/40.5	27.3	-1.4 **
Protein disulfide isomerase	PDI	gi|860986|	6.1/57.0	16.0	-1.4 ***
Beta tubulin	TUBB	gi|16198437|	4.8/30.6	14.7	-1.3 ***
Aldolase (a)	ALDOA	gi|4930291|	8.8/39.7	32.0	-1.2 ***
Aldolase (b)	ALDOA	gi|4930291|	8.8/39.7	35.8	-1.2 ***
Pi glutathione transferase	GSTP1	gi|34811304|	5.7/23.4	36.4	-1.2 **
Triosephosphate isomerase	TPI1	gi|999893|	6.5/26.8	29.0	-1.2 *
Glycerate-3-phosphate dehydrogenase (a)	GAPDH	gi|31645|	8.4/36.2	19.4	-1.2 *
Alpha enolase	ENO1	gi|2661039|	7.0/47.4	15.5	1.2 **
Glycerate-3-phosphate dehydrogenase (b)	GAPDH	gi|31645|	8.4/36.2	23.6	1.3 ***
Beta actin (e)	ACTB	gi|15277503|	5.6/40.5	24.4	1.4 *
Mu-protocadherin isoform 1	MUCDHL	gi|62020550|	4.8/88.4	18.2	1.7 ***
Aldehyde dehydrogenase 1A1	ALDH1A1	gi|2183299|	6.3/55.4	18.4	11.4 ***

Table 3.6.2 Secreted proteins significantly expressed in CM #3 versus CM #Mia

Protein name	Gene symbol	Protein AC number	PI/Mw	% coverage	Fold change CM #3 versus CM Mia
Gelsolin isoform b (a)	GSN	gi|38044288|	5.6/80.9	17.9	-8.0 ***
Gelsolin isoform b (b)	GSN	gi|38044288|	5.6/80.9	24.4	-6.3 ***
Gelsolin isoform b (c)	GSN	gi|38044288|	5.6/80.9	18.6	-4.7 ***
Gelsolin isoform b (f)	GSN	gi|38044288|	5.6/80.9	15.2	-3.8 ***
Gelsolin isoform b (e)	GSN	gi|38044288|	5.6/80.9	12.7	-2.1 **
Pro-MMP-2TIMP2 complex	TIMP2	gi|22218678|	6.5/22.4	30.9	-1.9 ***
Gelsolin isoform b (d)	GSN	gi|38044288|	5.6/80.9	18.3	-1.8 *
Gelsolin (amyloidosis: finnish type)	GSN	gi|55960299|	5.6/86.0	9.5	-1.7 **
Mu-protocadherin isoform 1	MUCDHL	gi|62020550|	4.8/88.4	18.2	-1.3 ***
Glycerate-3-phosphate dehydrogenase (b)	GAPDH	gi|31645|	8.4/36.2	23.6	-1.2 **
Glyoxalase I	GLO1	gi|562056|	5.1/20.9	28.3	1.2 ***
Heat shock 70kDa protein 8 isoform 2 variant (c)	HSPA8	gi|62896815|	5.6/53.6	19.7	1.2 ***
Sadenosylhomocysteine hydrolase	AHCY	gi|178277|	6.0/48.2	10.6	1.2 ***
Heat shock 70kDa protein 8 isoform 2 variant (b)	HSPA8	gi|62896815|	5.6/53.6	16.8	1.2 ***
Malate dehydrogenase cytosolic	MDH1	gi|7431153|	5.9/36.6	20.1	1.2 ***
Proteasome activator Reg	PSME1	gi|2780883|	7.1/16.3	44.3	1.2 ***

Phosphoglycerate kinase 1 (c)	PGK1	gi|48145549|	8.6/44.9	27.3	1.3 ***
Alpha enolase (a)	ENO1	gi|2661039|	7.0/47.4	15.5	1.3 ***
Human rab GDI	GDIA	gi|285975|	5.9/51.1	38.7	1.3 ***
Phosphoglycerate kinase 1 (a)	PGK1	gi|48145549|	8.6/44.9	25.7	1.3 ***
Heat shock 70kDa protein 8 isoform 2 variant (a)	HSPA8	gi|62896815|	5.6/53.6	28.8	1.3 ***
Phosphoglycerate kinase 1 (b)	PGK1	gi|62896815|	8.6/44.9	16.8	1.3 ***
Protein disulfide isomerase	PDI	gi|8609861|	6.1/57.0	16.0	1.3 ***
Glycerate-3-phosphate dehydrogenase (a)	GAPDH	gi|31645|	8.4/36.2	19.4	1.4 ***
Peroxiredoxin 1	PRDX1	gi|55959887|	6.4/19.1	53.2	1.4 ***
Alpha enolase (b)	ENO1	gi|2661039|	7.0/47.4	28.6	1.4 ***
Galectin-1	LGALS1	gi|56554350|	5.1/14.8	38.1	1.4 **
Pi glutathione transferase	GSTP1	gi|34811304|	5.7/23.4	36.4	1.6 ***
Human peroxidase enzyme	1PRXB	gi|3318842|	6.0/24.9	40.2	1.6 ***
Mitochondrial malate dehydrogenase	MDH2	gi|12804929|	9.4/35.9	37.0	1.6 ***
Transkelolase	TKT	gi|31417921|	8.4/50.3	18.2	1.7 ***
Aldehyde dehydrogenase	ALDH1A1	gi|2183299|	6.3/55.4	18.4	6.3 ***

Table 3.6.3 Secreted proteins significantly expressed in CM #3 versus CM #8

No.	Protein name	Gene symbol	Protein AC number	PI/MW	% Cov	Fold change CM #3 versus CM #8
1	**Gelsolin isoform b (a)**	**GSN**	**gi|38044288|**	**5.6/80.9**	**17.9**	**-21.0 *****
2	Gelsolin isoform b (b)	GSN	gi|38044288|	5.6/80.9	24.4	-15.2 ***
3	Gelsolin isoform b (c)	GSN	gi|38044288|	5.6/80.9	18.6	-10.7 ***
4	Gelsolin isoform b (f)	GSN	gi|38044288|	5.6/80.9	15.2	-6.4 ***
5	Gelsolin isoform b (d)	GSN	gi|38044288|	5.6/80.9	18.3	-3.8 ***
6	Gelsolin isoform b (g)	GSN	gi|38044288|	5.6/80.9	18.5	-3.4 ***
7	Gelsolin (amyloidosis: Finnish type)	GSN	gi|55960299|	5.9/86.0	9.5	-2.5 ***
8	Pro-MMP-2TIMP2 complex	TIMP2	gi|22218678|	6.5/22.4	30.9	-1.8 ***
9	Beta actin (a)	ACTB	gi|15277503|	5.6/40.5	36.6	-1.7 ***
10	**Nucleoside-diphosphate kinase 2 isoform**	**NDPK2**	gi|66392203|	**9.3/30.5**	**21.7**	**-1.7 ****
11	Beta actin (c)	ACTB	gi|15277503|	5.6/40.5	24.4	-1.6 ***
12	Proteasome activator Reg(Alpha)	PSME1	gi|2780883|	7.1/16.3	44.3	-1.5 ***
13	Beta actin (b)	ACTB	gi|15277503|	5.6/40.5	24.2	-1.5 ***
14	Heat shock protein HSP 90-alpha (HSP86)	HSP86	gi|92090606|	4.9/85.0	24.5	-1.5 ***
15	Phosphoglycerate kinase 1 (a)	PGK1	gi|48145549|	8.6/44.9	25.7	-1.4 ***
16	Thioredoxin peroxidase	PRDX2	gi|9955016|	5.7/21.6	28.4	-1.4 ***
17	Phosphoglycerate	PGK1	gi|48145549|	8.6/44.9	25.7	-1.4 ***

	kinase 1 (b)					
18	Phosphoglycerate kinase 1 (c)	PGK1	gi|48145549|	8.6/44.9	27.3	-1.4 ***
19	Heat shock 70kDa protein 8 isoform 2 variant (b)	HSPA8	gi|62896815|	5.6/53.6	16.8	-1.3 ***
20	Beta actin (d)	ACTB	gi|15277503|	5.6/40.5	27.3	-1.3 ***
21	NM23-H1	NME1	gi|29468184|	5.4/19.8	27.1	-1.3 ***
22	Triosephosphate isomerase	TPI1	gi|999893|	6.5/26.8	29.0	-1.3 ***
23	Heat shock 70kDa protein 8 isoform 2 variant (a)	HSPA8	gi|62896815|	5.6/53.6	28.8	-1.3 ***
24	S-adenosylhomocysteine hydrolase	AHCY	gi|178277|	6.0/48.2	10.6	-1.3 ***
25	Malate dehydrogenase cytosolic	MDH1	gi|7431153|	5.9/36.6	20.1	-1.2 ***
26	Heat shock 70kDa protein 8 isoform 2 variant (c)	HSPA8	gi|62896815|	5.6/53.6	19.7	-1.2 ***
27	Nucleoside phosphorylase	PNP	gi|58176568|	6.5/32.2	36.1	-1.2 ***
28	CAPZA1	CAPZA1	gi|12652789|	5.4/33.0	39.9	1.2 ***
29	Beta actin (g)	ACTB	gi|15277503|	5.6/40.5	30.6	1.2 *
30	Beta actin (f)	ACTB	gi|15277503|	5.6/40.5	24.4	1.2 *
31	Glycerate-3-phosphate dehydrogenase (a)	GAPDH	gi|31645|	8.4/36.2	19.4	1.2 **
32	Beta actin (e)	ACTB	gi|15277503|	5.6/40.5	24.5	1.2 *
33	**Galectin-1**	**LGALS1**	gi|56554350|	**5.1/14.8**	**38.1**	**1.3 ***

34	Mu-protocadherin isoform	MUCDHL	gi|62020550|	4.8/88.4	18.2	1.3 ***
35	Pi glutathione transferase	GSTP1	gi|34811304|	5.7/23.4	36.4	1.3 ***
36	Elongation factor	EEF1A1	gi|15277711|	9.3/46.5	12.1	1.4 ***
37	Alpha enolase (b)	ENO1	gi|2661039|	7.0/47.4	28.6	1.5 ***
38	Peroxiredoxin 1	PRDX1	gi|55959887|	6.4/19.1	53.2	1.5 ***
39	Alpha enolase (a)	ENO1	gi|2661039|	7.0/47.4	15.5	1.5 ***
40	Mitochondrial malate dehydrogenase	MDH2	gi|12804929|	9.4/35.9	37.0	1.6 ***
41	**Aldehyde dehydrogenase 1A1**	**ALDH1A1**	gi|2183299|	**6.3/55.4**	**18.4**	**21.0 *****

The nominal isoelectric point (pI) and molecular weight (Mw) were calculated from the sequence of the protein in the database. Isoforms of the same protein are referred to as (a), (b) etc. The percentage coverage is the amount of the protein sequence covered by the matched peptides. Statistical analysis between replicates is referred to as; * $p \leq 0.05$, *** $p \leq 0.01$, *** $p \leq 0.005$. For protein identification, all proteins were digested and identified at least twice from separate gels with MALDI-TOF MS. An expectation value of <0.02 was used for all reported identifications, which indicates a 0.2% chance that the identification is random.
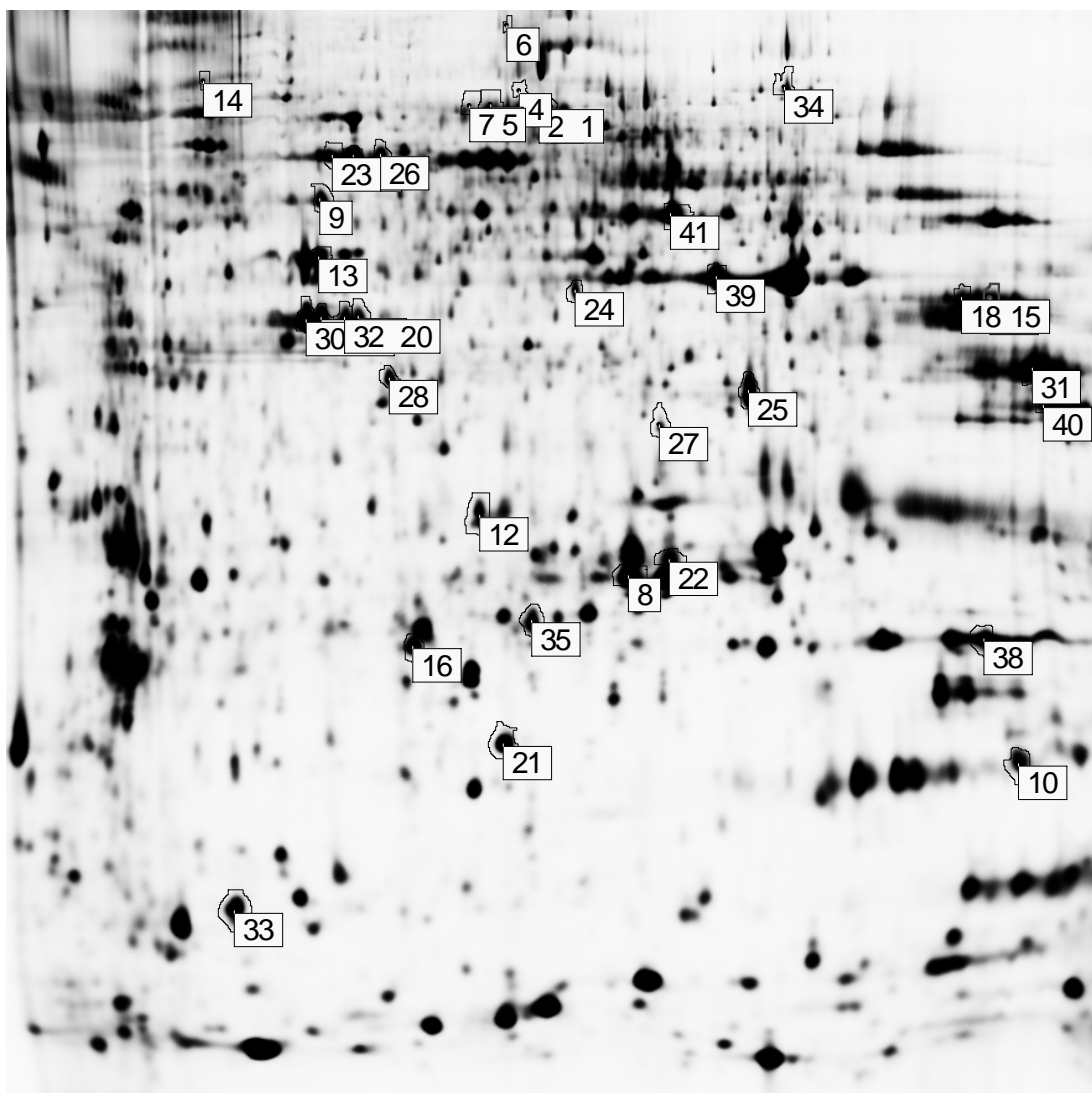
Figure 3.6.1 Protein expression map of CM Mia, CM#3 and CM#8. Numbers correspond to proteins of interest between CM#3 and CM#8.

3.6.3 Bioinformatic analysis of differentially regulated secreted proteins

Bioinformatic analysis was carried out on all differentially identified secreted proteins in our proteomic comparison of the conditioned media of MiaPaCa-2, Clone #3 and Clone #8.

As outlined in section 2.8, DAVID gene ID tool software (http://david.abcc.ncifcrf.gov) was used to generate gene ID matching the significant secreted proteins in our model. Gene ontology (GO STAT) (http://gostat.wehi.edu.au/cgi-bin/goStat.pl) was then used to classify the proteins and their corresponding genes into gene categories. Using the over-expression function of the software and false discovery rate (Benjamini) stats, 91 GO terms were found significantly enriched. The "cytoplasm" term achieved the highest degree of significance in the up-regulated gene class ($p = 0.0013$), with "glycolysis" ($p = 5.4E-07$) and "glucose/alcohol catabolic process" ($p = 9.05E-07/9.5E-07$) also highly significant terms. In the down-regulated class, "cytoplasm" ($p = 0.0076$) and "glycolysis" ($p = 1.8E-09$) were also significantly enhanced. Figure 3.6.2 outlines the top eight ranked functional categories using GO terms in the differentially expressed proteins in the pancreatic cancer model.

Pathway studio is a bioinformatics tool that allows the visualisation and analysis of biological pathways, gene regulation networks and protein interaction maps of groups of genes or proteins (Chapter 2.15). Direct interactions between the differentially regulated proteins in our pancreatic cancer cell line invasion model are shown in figure 3.6.3.
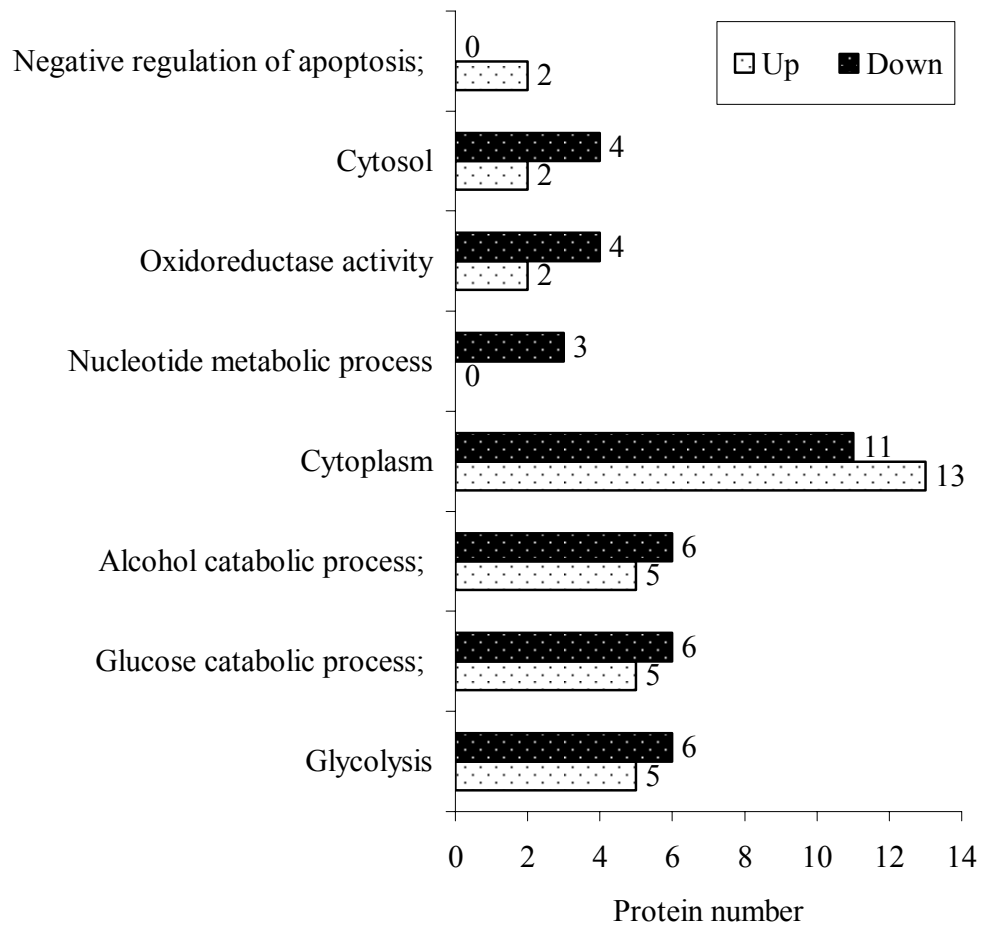
Figure 3.6.2 Term-ranking GO categories. Representation of the 8 top-ranked functional categories, using GO terms that are enriched in all significantly differentially secreted proteins identified between MiaPaCa-2, Clone #3 and Clone #8..
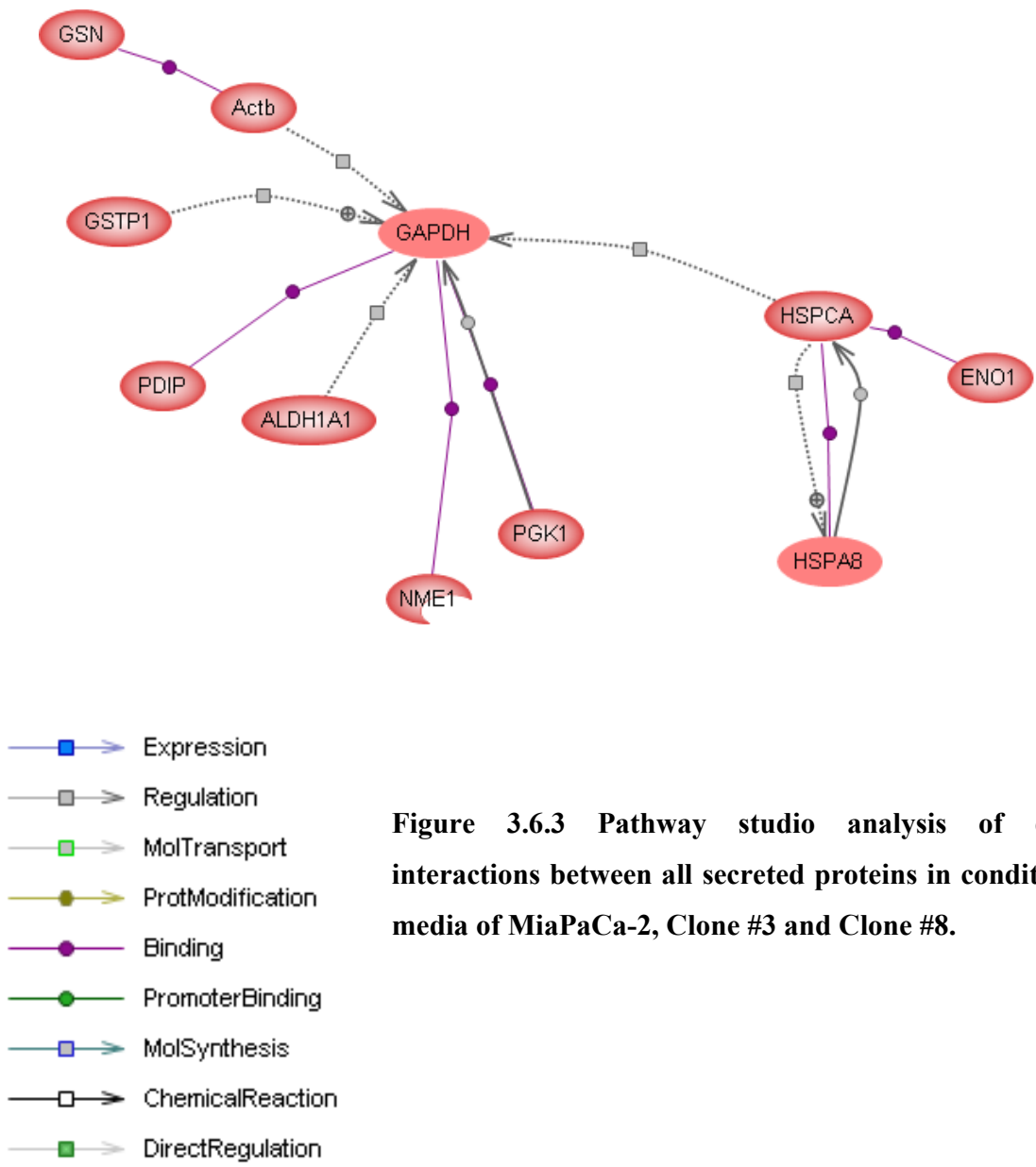
Figure 3.6.3 Pathway studio analysis of direct interactions between all secreted proteins in conditioned media of MiaPaCa-2, Clone #3 and Clone #8.

3.6.4 Identification and validation of target secreted proteins

Table 3.6.3 outlines the comparison of the conditioned media from Clone #3 to the conditioned media of Clone #8. This comparison represents the greatest difference in invasion status as the addition of CM #3 and CM #8 into the invasion chamber had the greatest effect on invasion (either increasing or decreasing).

Four secreted proteins have been chosen for further analysis. Of these 4 secreted proteins, 2 are up-regulated and 2 are down-regulated in the comparison.

Gelsolin (GSN) is -21-fold down-regulated in the CM of Clone #3 compared to CM #8. Nucleotide-diphosphate kinase 2 (NDPK) is -1.7-fold less expressed in CM#3 compared to CM#8.
Of the up-regulated secreted proteins, galectin (LGALS1) is 1.3-fold, while aldhehyde dehydrogenase 1A1 (ALDH1A1) expression is 21-fold more highly secreted in CM #3 versus CM #8.

Western blotting was carried out to confirm the expression of the proteins, as indicated from the proteomic data. Figure 3.6.4 (A, B, D) validates the secretion of GSN, NDPK and ALDH1A1. However, secretion of LGALS1 was difficult to confirm, as the proteins seemed to be over-secreted and the antibody and Western blot technique were not sensitive enough to differentiate between expression levels in CM#3 compared to CM#8 (Figure 3.6.4, C).

Two proteins, GSN and ALDH1A1 were chosen for further functional analysis.
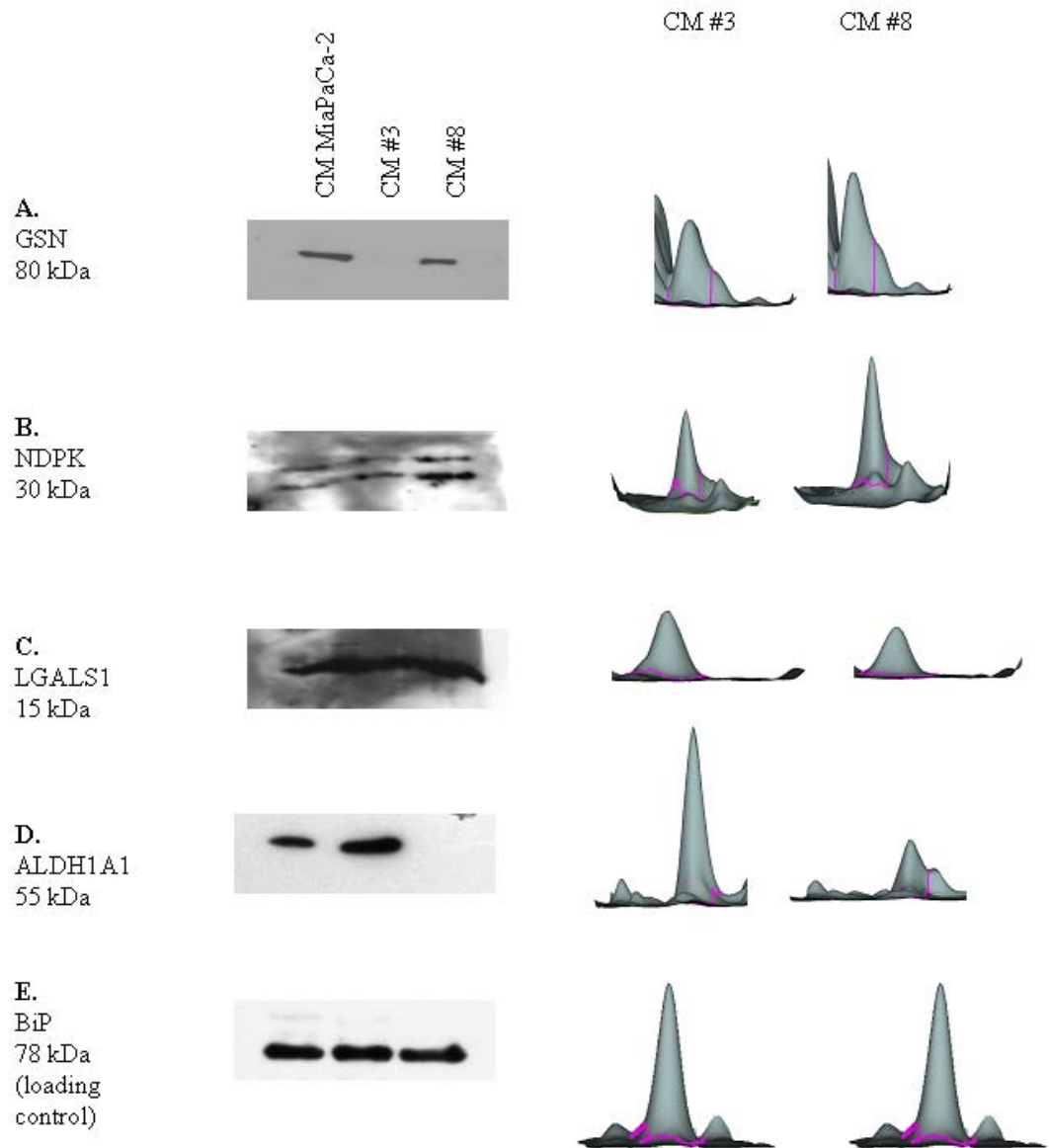
Figure 3.6.4 Western blot validation and 3D spot images of A. GSN, B. NDPK, C. LGALS1, D. ALDH1A1, E. BiP (loading control) in conditioned media of MiaPaCa-2, Clone #3 and Clone #8.

249

3.6.5 Investigation into the role of secreted gelsolin in pancreatic cancer invasion

Gelsolin was identified as a secreted protein potentially involved in invasion in our *in vitro* pancreatic cancer cell line model. The analysis showed that GSN was up-regulated (21-fold) in the less invasive sub-clone, Clone #8 compared to the high invasive cell line, Clone #3.

3.6.5.1 Effect of GSN siRNA transfection on invasion

The secretion of gelsolin was shown to be up-regulated in the conditioned media of the less invasive cell line, Clone #8. Using two siRNA targets for GSN, the secreted expression of GSN was knocked down in the conditioned media of Clone #8. CM#8 was used for siRNA knockdown and further functional analysis. Figure 3.6.4 shows by Western blot the efficient knockdown of GSN in the CM#8 using two GSN target siRNAs in Clone #8 cells.
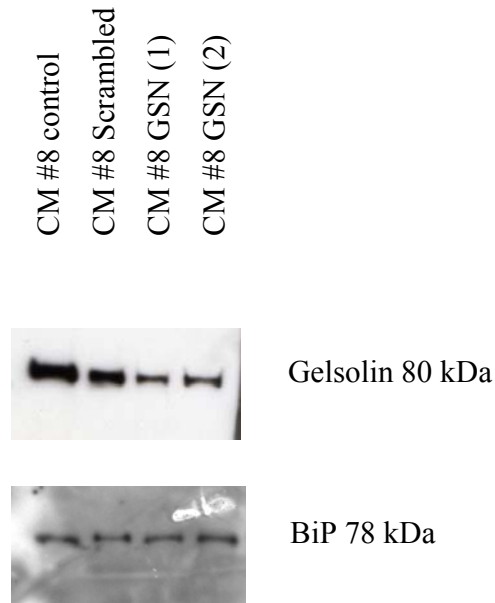
Figure 3.6.5 Western blot of siRNA GSN knockdown in CM#8. Two independent target siRNAs for GSN were transfected into Clone #8 cells. SFCM was harvested 72 hrs post-transfection and used to determine GSN-siRNA specific decrease of secreted protein compared with non-treated and scrambled controls. Bip antibody was used to demonstrate even loading between the samples.

3.6.4.2 Effect of siRNA GSN CM#8 on invasion

Conditioned media derived from Clone #8 cells treated with GSN siRNA was added into invasion assays of Clone #8 to assess the potential involvement of GSN in invasion. GSN siRNA CM#8 was added above and below the insert at equal dilution to ensure no gradient was present in the assay. Clone #8 was chosen; as this cell line is low invasive and any increase in invasion could be easily observed. Figure 3.6.6 represents (A) pictures of the invasion level after addition of CM#8 untreated control, scrambled and GSN (1) and (2) transfected siRNA. Figure 3.6.6 (B) displays the total number of invading cells. GSN knockdown in CM#8 resulted in increased invasion through matrigel. Invasion was increased 1.3-fold (p=0.01) with siRNA GSN (1) in CM#8 and 1.5-fold (p=0.2) with siRNA GSN (2) in CM#8.

(A)
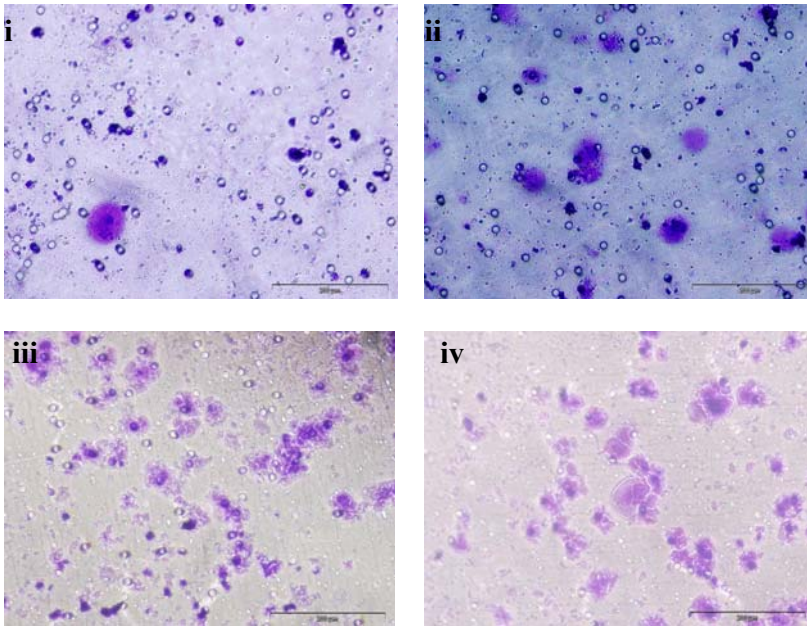
(B)
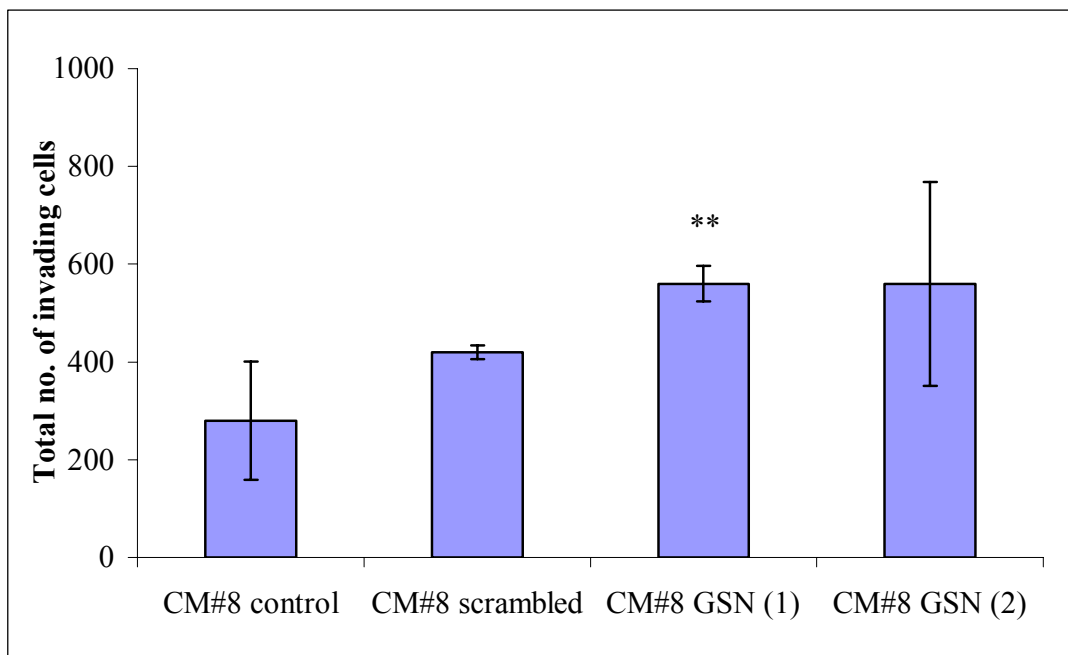
Figure 3.6.6 (A) Invasion assay pictures of Clone #8 cells with the addition of (i) untreated control CM#8, (ii) scrambled transfected CM#8, (iii) GSN siRNA (1) CM#8 and (iv) GSN siRNA (2) CM#8. Magnification, 200x. Scale bar, 200 μm. (B) Total number of invading cells (*n*=3). Statistics; * ≤ 0.05, ** ≤ 0.01, * ≤ 0.005.**

3.6.4.3 Cytoplasmic GSN expression

Figure 3.6.7 shows by Western blot the expression of GSN in the whole cell lysates of MiaPaCa-2, Clone #3 and Clone #8. GSN is expressed at low levels in Clone #8; however, the expression of GSN is increased in Clone #8 when the cells are grown on matrigel for 24 hrs. This suggests that GSN expression is induced when the cells are exposed to matrigel. GSN expression is not detected in MiaPaCa-2 or Clone #3.
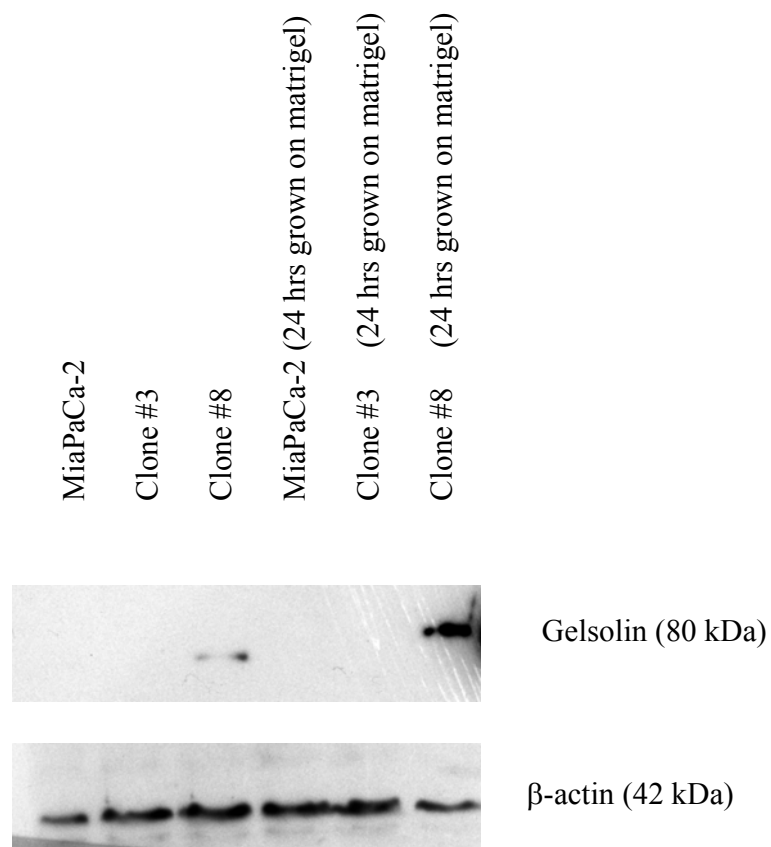
Figure 3.6.7 Western blot of GSN expression in MiaPaCa-2, Clone #3 and Clone #8 cells and after 24 hrs grown on matrigel. β-actin, used as loading control.

3.6.5.4 Effect of GSN siRNA on invasion

Invasion assays were performed on Clone #8 cells transfected with GSN siRNA. Figure 3.6.8 (A) shows representative pictures of the level of invasion observed in Clone #8 non-treated and scrambled control cells and cells transfected with GSN siRNA, (B) displays the total number of cells invading. Loss of GSN expression through siRNA induces increased invasion in Clone #8 cells. Invasion was significantly increased 2.6–fold with GSN siRNA (1) (p=0.02) and 2.4-fold with GSN siRNA (2) (p=0.05).

These results suggest that silencing of GSN cytoplasmic expression within the cells has more of a functional effect that reducing the GSN secreted fraction.

(A)
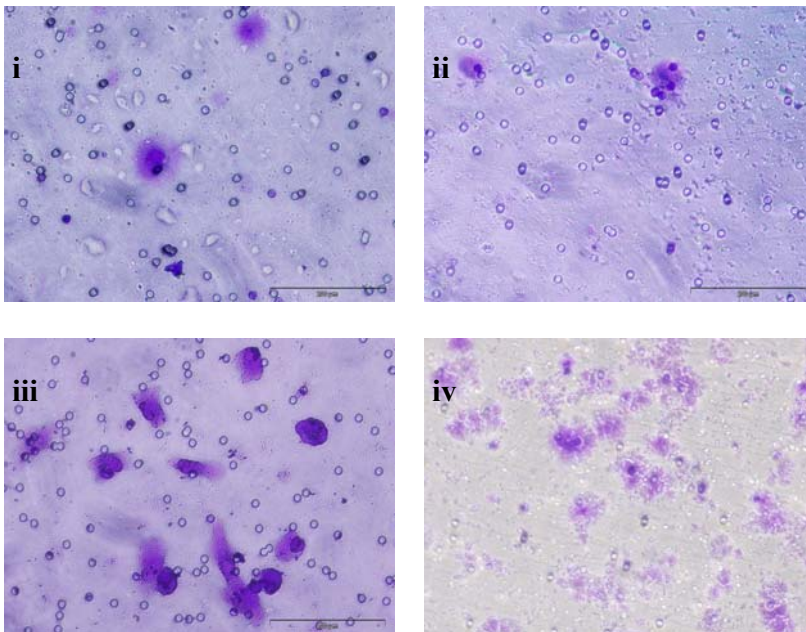
(B)
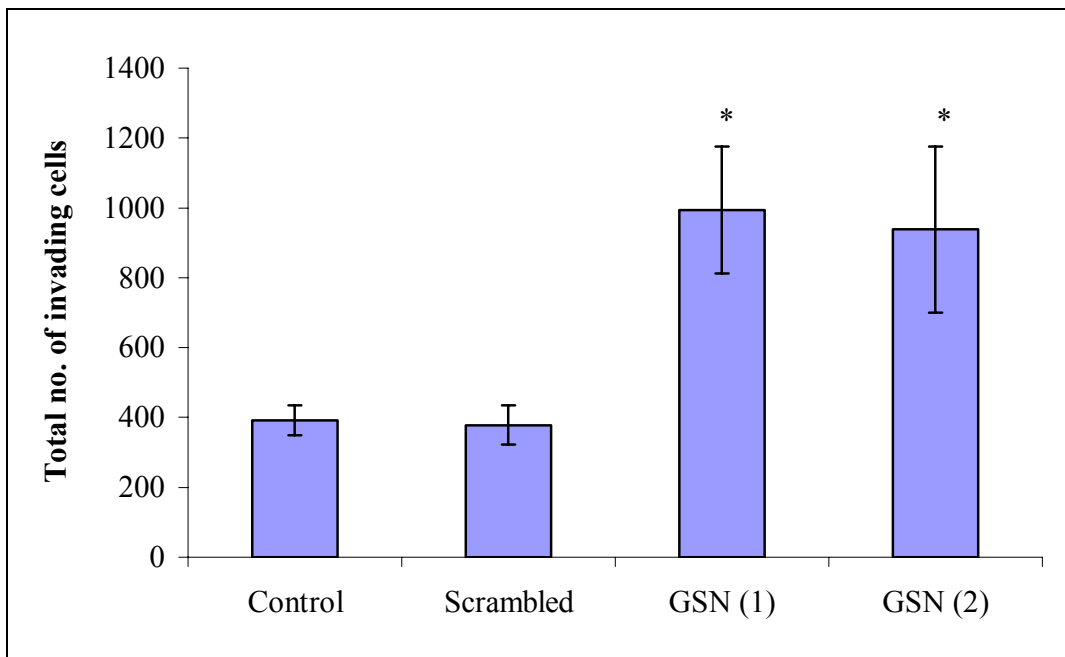
Figure 3.6.8 (A) Invasion assay pictures of Clone #8 (i) untreated control, (ii) scrambled transfected, (iii) GSN siRNA (1) and (iv) GSN siRNA (2) transfected cells. Magnification, 200x. Scale bar, 200 μm. (B) Total number of invading cells (*n*=3). Statistics; * ≤ 0.05, ** ≤ 0.01, *** ≤ 0.005.

3.6.6 Investigation into the role of secreted aldehyde dehydrogenase 1A1 in pancreatic cancer invasion

ALDH1A1 was identified as a secreted protein potentially involved in invasion in our *in vitro* pancreatic cancer cell line model. The analysis showed that ALDH1A1 was up-regulated (21-fold) in the more invasive sub-population, Clone #3 compared to the low invasive cell line, Clone #8.

3.6.6.1 Effect of ALDH1A1 siRNA CM#3 on invasion

Figure 3.6.9 shows efficient knockdown of secreted ALDH1A1 in conditioned media of Clone #3 after ALDH1A1 siRNA transfection. Invasion assays were then carried out with the addition of CM#3 untreated control, scrambled, and three independent ALDH1A1 siRNAs into the invasion chamber above and below to ensure no gradient.

Figure 3.6.10 (A) highlights the representative pictures of invasion, and (B) displays the total number of invading cells. Invasion is significantly decreased after siRNA knockdown of ALDH1A1 secretion.

ALDH1A1 siRNA (1) in CM#3 reduced invasion 4.2-fold ($p=0.01$), ALDH1A1 siRNA (2) in CM#3 decreased invasion 2.7-fold ($p=0.003$) and ALDH1A1 siRNA (3) in CM#3 also significantly reduced the invasive abilities of Clone #3 2.5-fold ($p=0.02$), compared to the scrambled control.
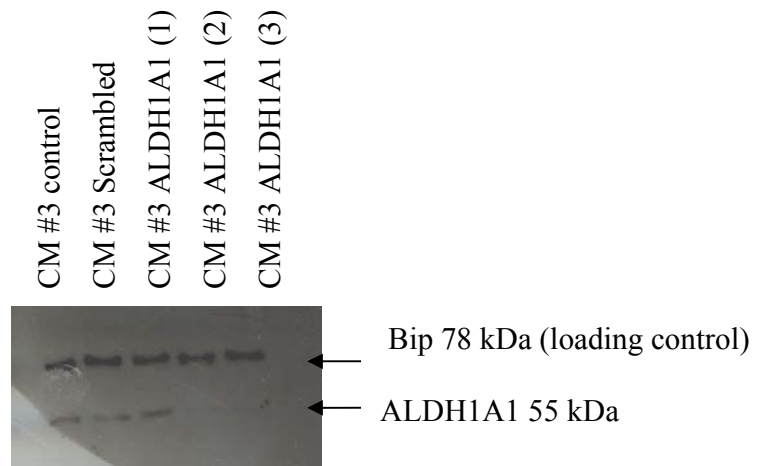
Figure 3.6.9 Western blot of ALDH1A1 knockdown in CM#3 untreated control, scrambled, siRNA ALDH1A1 (1), siRNA ALDH1A1 (2) and siRNA ALDH1A1 (3).

(A)
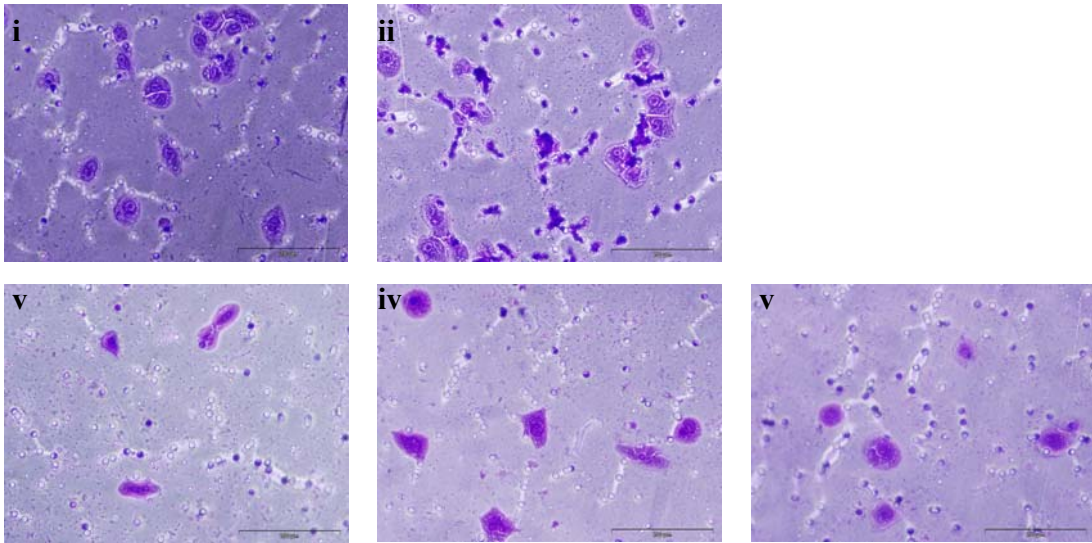
(B)
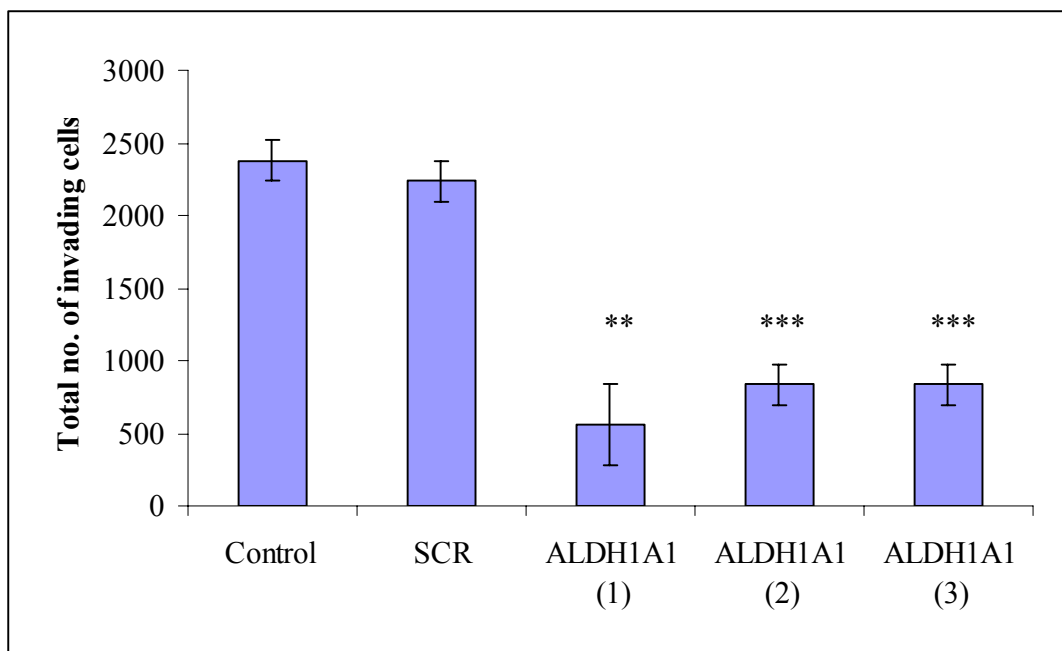
Figure 3.6.10 (A) Invasion assays of Clone #3 with addition of (i) CM#3 media (control) (ii) CM#3 media with scrambled (iii) CM#3 treated with ALDH1A1 siRNA (1) (iv) CM#3 treated with ALDH1A1 siRNA (2) (v) CM#3 treated with ALDH1A1 siRNA (3). SFCM was collected 72-96 hrs post transfection. Magnification, 200x. Scale bar, 200µm. (B) Invasion assay of Clone #3 showing total number of cells invading post ALDH1A1 siRNA transfection. Statistics; * ≤ 0.05, ** ≤ 0.01, *** ≤ 0.005.

3.7 Investigation of EGFR and HER2 expression in pancreatic cancer

3.7.1 EGFR expression

EGFR levels were investigated by Western blot and ELISA in a panel of five pancreatic cancer cell lines (Chapter 2.9). Figure 3.7.1 (A) shows the protein expression of EGFR. (B) Quantitatively measures the level of EGFR (pg/µl total protein). EGFR is highly expressed in Panc-1, BxPc-3, AsPc-1 and expressed in lower levels in KCI-MOH1 and MiaPaCa-2.

(A)

(B)
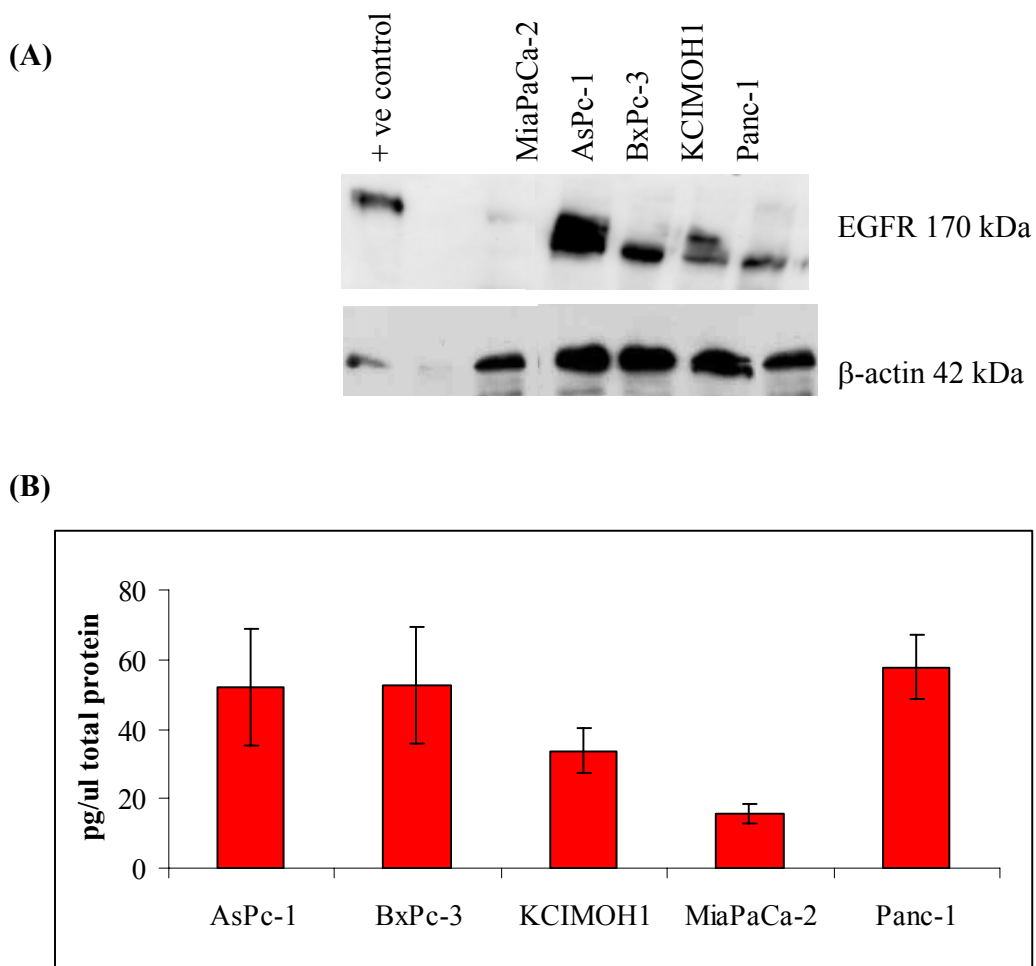
Figure 3.7.1 EGFR expression in panel of pancreatic cancer cell lines (A) Western blot of EGFR and (B) ELISA quantification of EGFR pg/µl total protein.

3.7.2 HER2 expression

HER2 expression levels were investigated by Western blot in a panel of five pancreatic cancer cell lines. Figure 3.7.2 shows the protein expression of HER2. HER2 is expressed in BxPc-3, AsPc-1 and expressed in lower levels in KCI-MOH1 and Panc-1. No detectable level of HER2 in MiaPaCa-2 was observed.
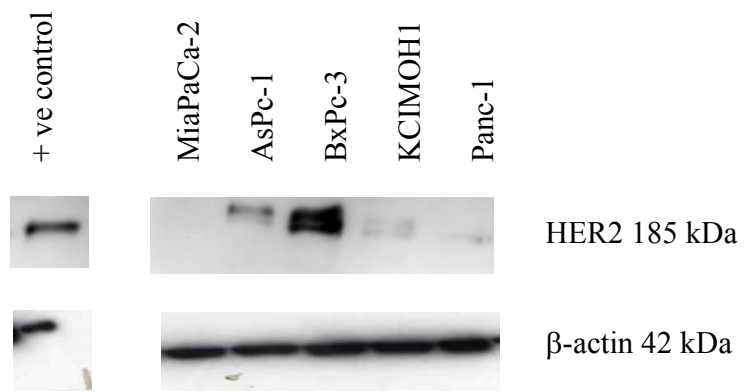
Figure 3.7.2 HER2 expression in panel of pancreatic cancer cell lines by Western blot. β-actin used as loading control.

3.7.3 Chemosensitivity profile of BxPc-3 and KCIMOH1

The dual EGFR and HER2 inhibitor, lapatinib, was tested in two of the EGFR/HER2 positive cell lines, BxPc-3 and KCIMOH1. Table 3.7.1 shows the IC_{50}s for lapatinib in the pancreatic cancer cell lines compared to two lapatinib sensitive breast cancer cell lines, which express low levels of EGFR (+) and over-express HER2 (+++++).

The chemosensitivity profile of BxPc-3 and KCIMOH1 was also analysed using an *in vitro* proliferation assay (Chapter 2.3) to determine the IC_{50} (concentration of drug that inhibits proliferation of 50% of the cell population) of cisplatin, gemcitabine, taxotere and 5'dFUrd (Table 3.7.2).

Table 3.7.1   Lapatinib IC_{50} values for pancreatic and breast cancer cell lines (results are expressed as $IC_{50} \pm$ SD, n=3).

	EGFR	HER2	Lapatinib IC_{50}
BxPc-3	+++	++	1.4 ± 0.1 µg/ml
KCIMOH1	+	+	1.4 ± 0.2 µg/ml
BT474	+	+++++	142 ± 28 ng/ml
SKBR3	+	+++++	113 ± 38 ng/ml

Table 3.7.2 IC_{50} values of pancreatic cell lines to chemotherapeutic agents (results are expressed as $IC_{50} \pm$ SD, n=3).

(ng/ml)	BxPc-3	KCI-MOH1
Cisplatin	225.6 ± 56.3	226.4 ± 10.7
Gemcitabine	1.4 ± 0.6	0.5 ± 0.01
Taxotere	0.4 ± 0.05	0.4 ± 0.1
5'dFUrd (µg/ml)	$2.9 + 0.2$	8.3 ± 1.1

3.7.4 Scheduling combination assays

Combination assays assessing the drug effect/combination index analysis of lapatinib, a dual EGFR/HER2 tyrosine kinase inhibitor, in combination with chemotherapeutic agents, cisplatin, gemcitabine, taxotere and 5'dFUrd against BxPc-3 and KCIMOH1, two EGFR/HER2 expressing pancreatic cancer cell lines *in vitro* were performed.

The combination assays were carried out using a fixed ratio of lapatinib:chemotherapeutic drug. Initial experiments combined lapatinib and chemotherapeutic drug together during assays, however antagonism was observed. Figure 3.7.3 displays a representative graph of combining treatments together in KCIMOH1.
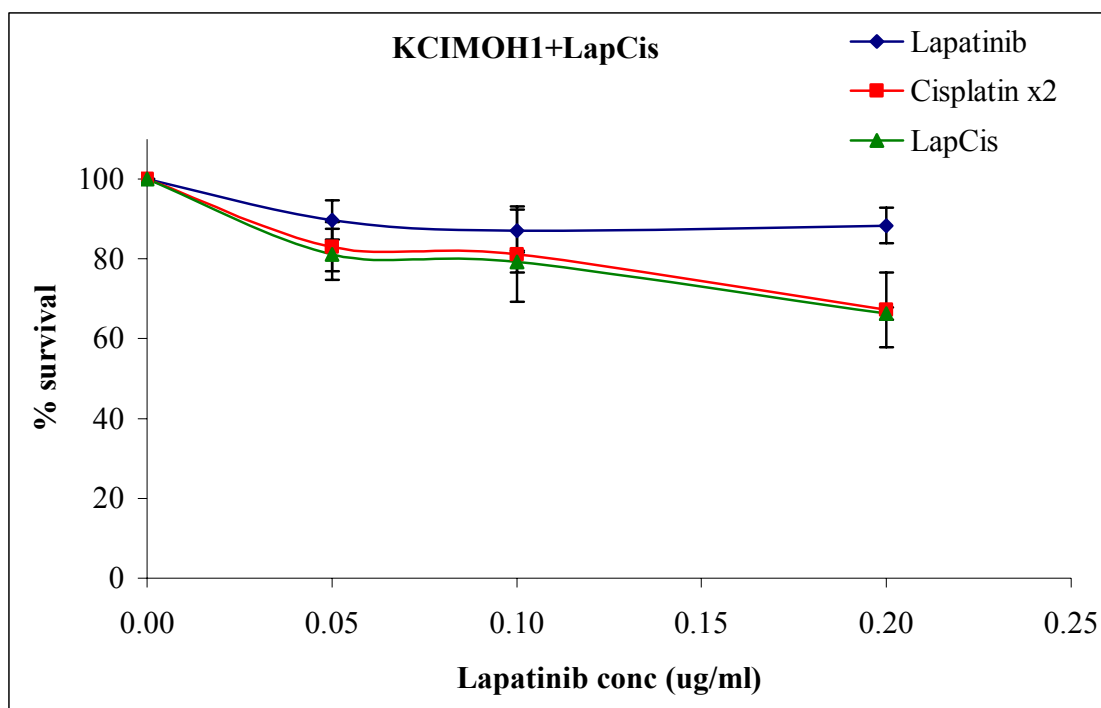
Figure 3.7.3 Percentage survival of KCIMOHI in combination with lapatinib and cisplatin

However, when cells were pre-treated with lapatinib for 24 hours before addition of chemotherapeutic drugs, more efficacy of the combination was observed. Therefore, all combinations were performed using this method of scheduling (Chapter 2.3.1).

Combination indices (CI) were calculated using the model of Chou and Talalay for drug combinations and the CalcuSyn software package. CI < 0.8 denotes synergy, CI > 0.8 but < 1.2 denotes additivity and CI > 1.2 denotes antagonism.

3.7.4.1 Drug effect/combination index analysis of lapatinib in combination with cisplatin against BxPc-3 and KCI-MOH1, EGFR/HER2 expressing pancreatic cancer cell lines *in vitro*

Lapatinib was added to the cells 24 hours prior to the addition of cisplatin, this was to ensure the EGFR/HER2 inhibitory effects of lapatinib were maximised. The combinations of lapatinib and cisplatin were carried out at a constant ratio of 1:0.1, lapatinib:cisplatin to obtain a complete dosage range in both cell lines.

Figure 3.7.4 (A) and (B) outlines the percentage survival of BxPc-3 and KCIMOH1 with lapatinib and cisplatin alone and in combination.

Synergism was observed between cisplatin and lapatinib in BxPc-3 cells at lower concentrations of lapatinib and cisplatin with a CI value at ED25 of 0.60 ± 0.09. At the ED50 concentrations, the interaction was additive and at ED75, the interaction became antagonistic (Table 3.7.3).
Synergism was also observed in KCIMOH1 at ED50 (CI value, 0.65 ± 0.05), and at ED25 and ED75, the interaction in additive (Table 3.7.3).
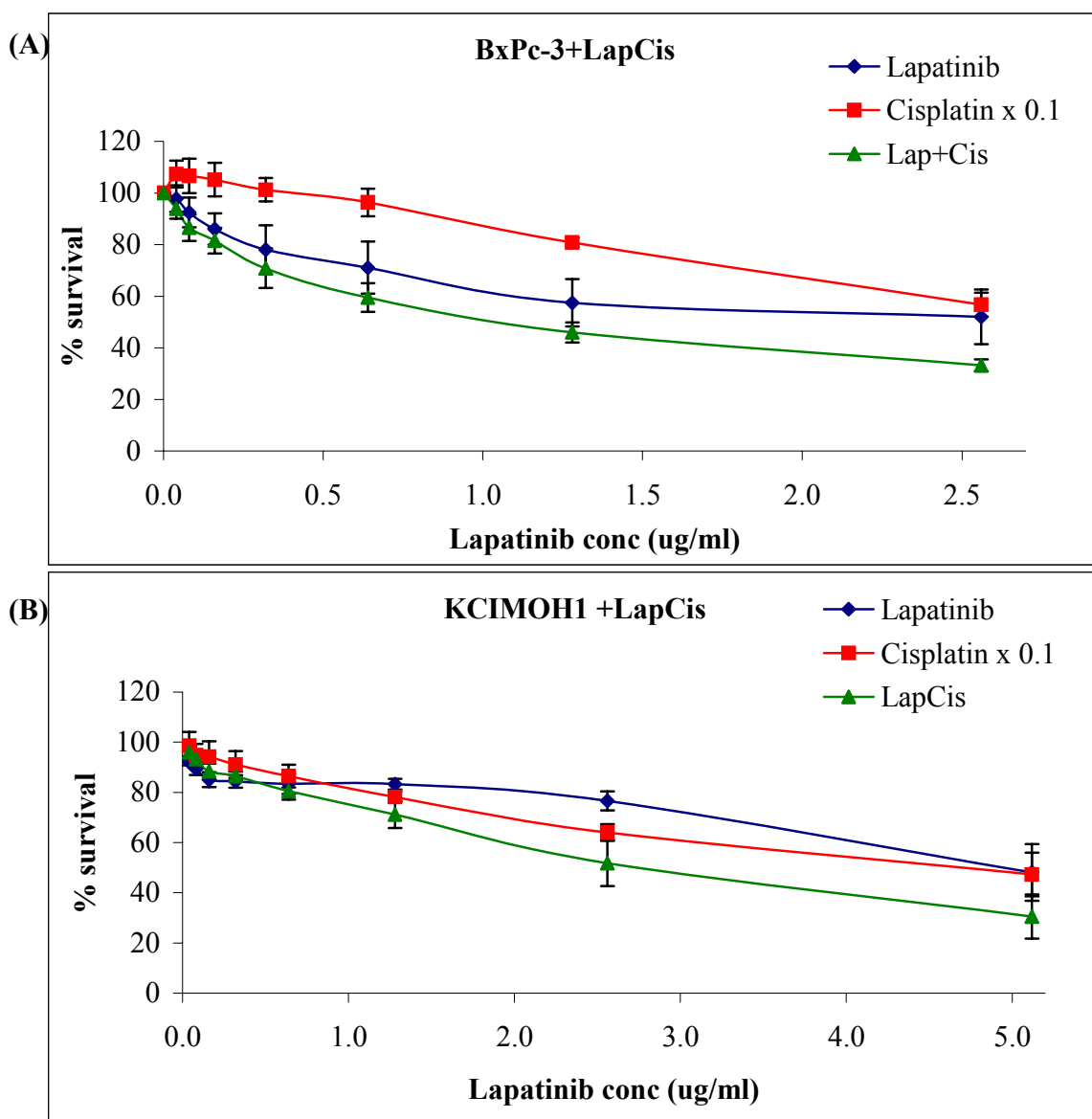
Figure 3.7.4 Percentage survival of lapatinib and cisplatin combinations in (A) BxPc-3 and (B) KCIMOH1 (*n*=3).

Table 3.7.3 Mutually non-exclusive CI values at ED25, ED50 and ED75 (results are expressed as ED ± SD, *n*=3)

Drug	Combination Index Values		
Lapatinib:Cisplatin , 1:0.1	ED25	ED50	ED75
BxPc-3	0.60 ± 0.09	0.97 ± 0.18	1.17 ± 0.16
KCI-MOH1	0.81 ± 0.23	0.65 ± 0.05	0.88 ± 0.20

3.7.4.2 Drug effect/combination index analysis of lapatinib in combination with gemcitabine against BxPc-3 and KCIMOH1, EGFR/HER2 expressing pancreatic cancer cell lines *in vitro*

BxPc-3 and KCIMOH1 cells were pre-incubated with lapatinib 24 hours prior to the addition of gemcitabine, this was to ensure the EGFR/HER2 inhibitory effects of lapatinib were maximised. The combinations of lapatinib and gemcitabine were carried out at a constant ratio of 1:0.02, lapatinib:gemcitabine to obtain a complete dosage range in both cell lines.

Figure 3.7.5 (A) and (B) outlines the average percentage survival of BxPc-3 and KCIMOH1 with lapatinib and gemcitabine alone and in combination.

The combination of lapatinib and gemcitabine in BxPc-3 was additive at ED25-75, with CI values in the range of 0.9-1.0 (Table 3.7.4).

The relationship between lapatinib and gemcitabine in the KCIMOH1 cell line displayed additivity at ED25 (CI value, 0.93 ± 0.10). The combination was additive at ED50 and at ED75 (Table 3.7.4).
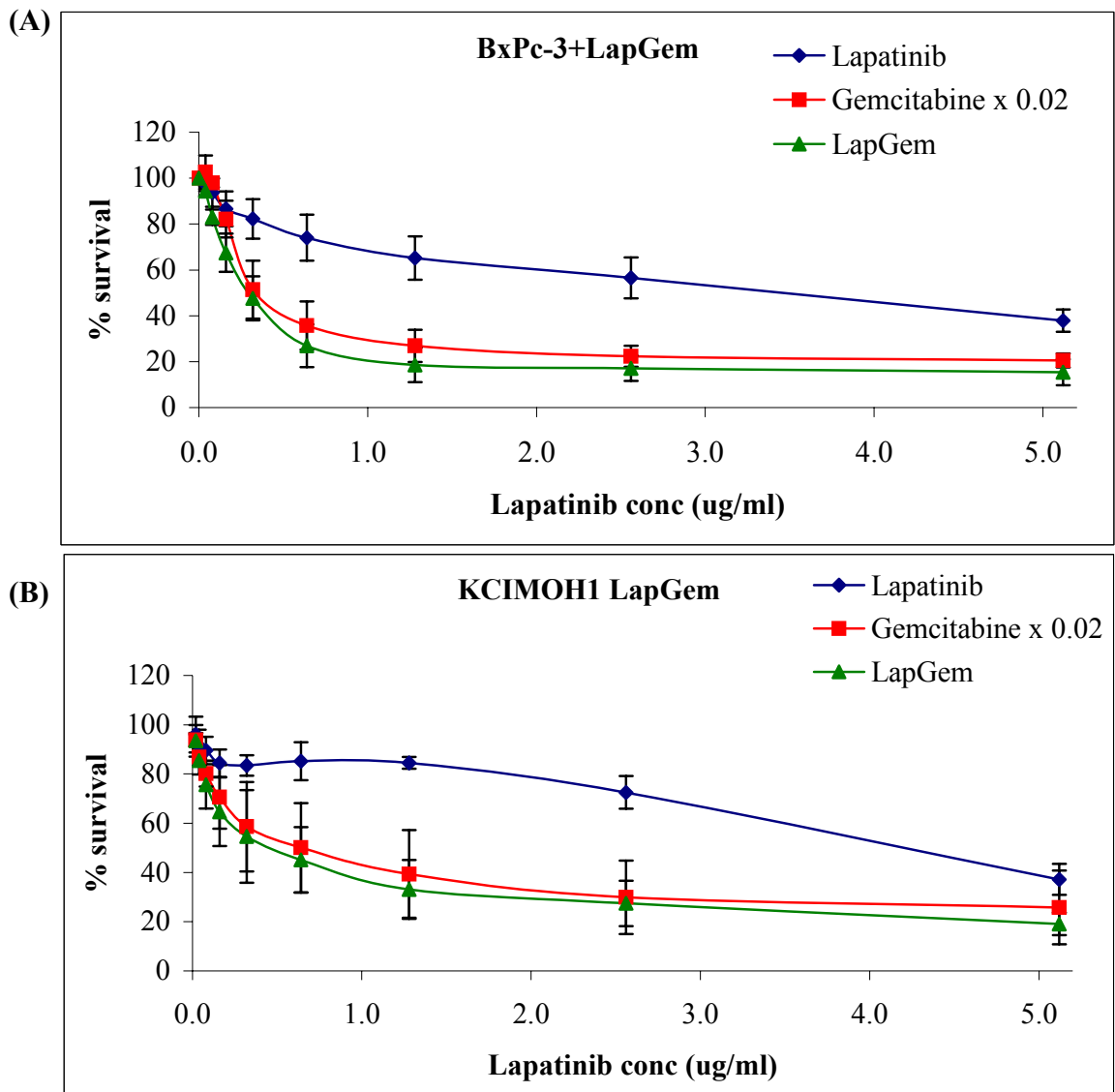
Figure 3.7.5 **Percentage survival of lapatinib and gemcitabine combinations in (A) BxPc-3 and (B) KCIMOH1 (*n*=3).**

Table 3.7.4 **Mutually non-exclusive CI values at ED25, ED50 and ED75 (results are expressed as ED ± SD, *n*=3)**

Drug	Combination Index Values		
Lapatinib:Gemcitabine , 1:0.02	ED25	ED50	ED75
BxPc-3	0.79 ± 0.23	0.89 ± 0.28	1.07 ± 0.41
KCI-MOH1	0.93 ± 0.10	1.00 ± 0.17	1.12 ± 0.35

3.7.4.3 Drug effect/combination index analysis of lapatinib in combination with taxotere against BxPc-3 and KCI-MOH1, EGFR/HER2 expressing pancreatic cancer cell lines *in vitro*

Lapatinib was added to the cells 24 hours prior to the addition of taxotere, this was to ensure the EGFR/HER2 inhibitory effects of lapatinib were maximised. The combination of lapatinib and taxotere were carried out at a constant ratio of 1:0.01, lapatinib:taxotere to obtain a complete dosage range.

Figure 3.7.6 (A) and (B) displays the average percentage survival of BxPc-3 and KCIMOH1 with lapatinib and taxotere alone and in combination. These results show that taxotere is a very potent drug and that pancreatic cancer cell lines, BxPc-3 and KCIMOH1 are sensitive at very low concentrations. The high toxicity of taxotere masked any anti-proliferative effects of lapatinib. Therefore, as an accurate dose response curve was not generated, the combination could not be analysed by Calcusyn.
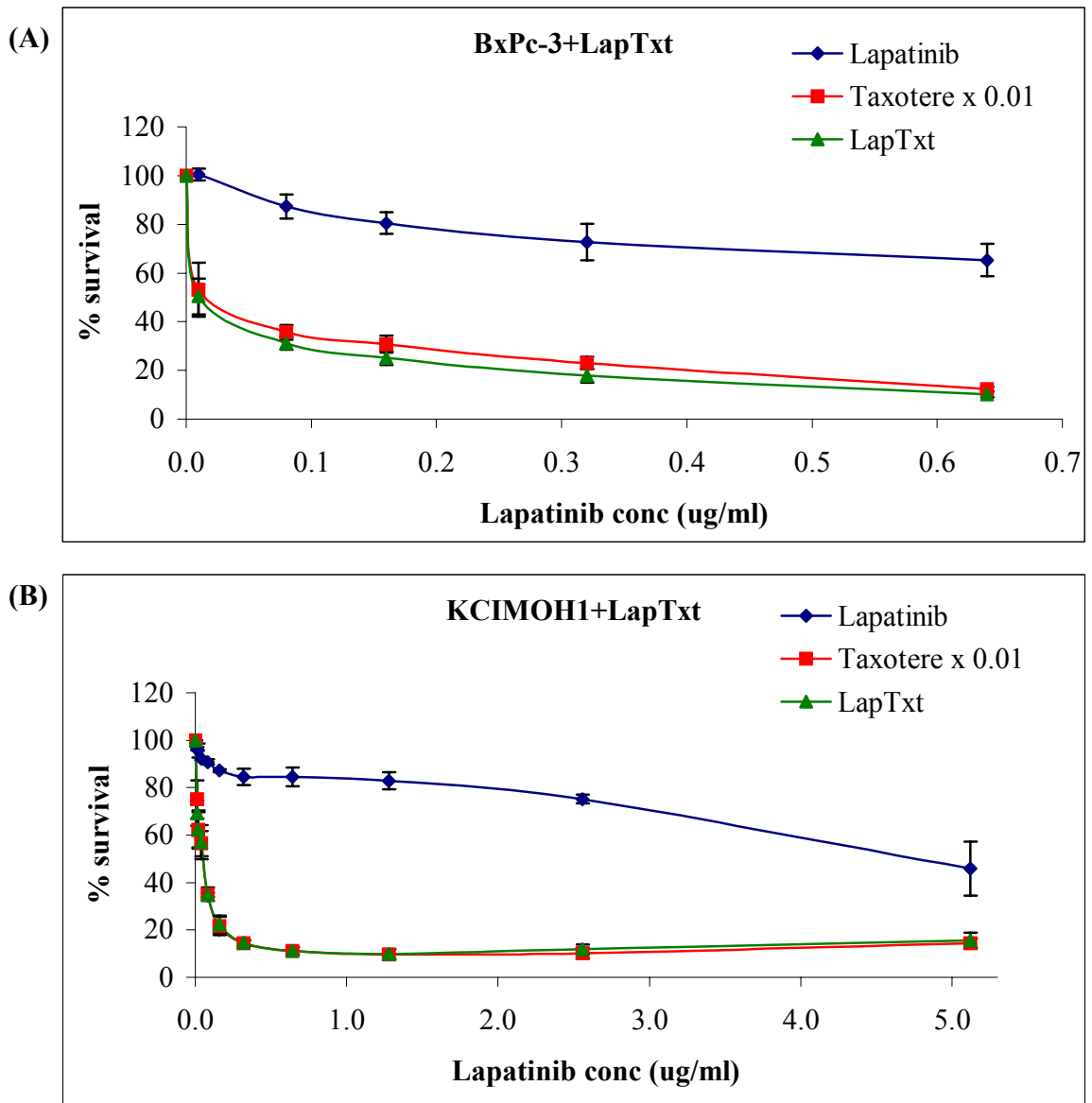
Figure 3.7.6 Percentage survival of lapatinib and taxotere combinations in (A) BxPc-3 and (B) KCIMOH1 (*n*=3).

3.7.4.4 Drug effect/combination index analysis of lapatinib in combination with 5'dFUrd against BxPc-3 and KCIMOH1, EGFR/HER2 expressing pancreatic cancer cell lines *in vitro*

Lapatinib was added to the cells 24 hours prior to the addition of 5'dFUrd, this was to ensure the EGFR/HER2 inhibitory effects of lapatinib were maximised. The combination of lapatinib and 5'dFUrd were carried out at a constant ratio of 1:2, lapatinib:5'dFUrd to obtain a complete dosage range.

Figure 3.7.7 (A) and (B) displays the average percentage survival of BxPc-3 and KCIMOH1 with lapatinib and 5'dFUrd alone and in combination.

The interaction of lapatinib and 5'dFUrd in BxPc-2 at lower concentrations, ED25-50 is synergistic to additive. However, at ED75, the CI value is 1.12 ± 0.24 and displays an antagonistic effect (Table 3.7.5).

In KCIMOH1 cells, the relationship between lapatinib and 5'dFUrd is antagonistic at ED25, and displays an additive to synergistic interaction at ED50-75. Table 3.7.5 displays that the CI values at ED25-75, these are in the range of 1.17-0.95.
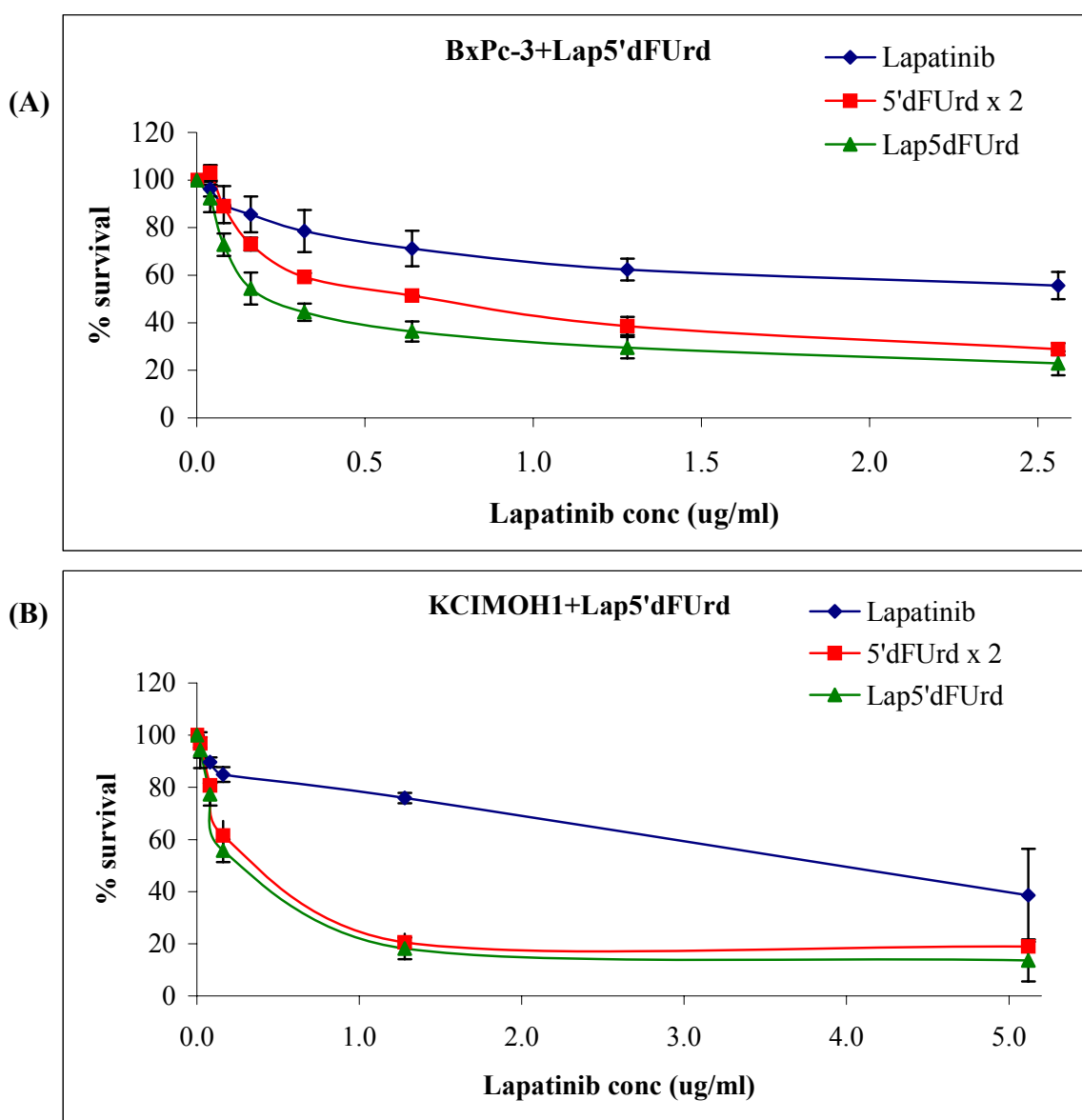
Figure 3.7.7 Percentage survival of lapatinib and 5'dFUrd combinations in (A) BxPc-3 (*n*=3) and (B) KCIMOH1 (*n*=3).

Table 3.7.5   Mutually non-exclusive CI values at ED25, ED50 and ED75

(results are expressed as ED ± SD, *n*=3)

Drug	Combination Index Values		
Lapatinib:5'dFUrd , 1:2	**ED25**	**ED50**	**ED75**
BxPc-3	0.73 ± 0.22	0.88 ± 0.03	1.12 ± 0.24
KCI-MOH1	1.17 ± 0.20	1.00 ± 0.21	0.95 ± 0.40

4.0 Discussion

4.1 Establishment of drug-selected variants

Multi-drug resistance (MDR) in invasive and metastatic cancer are major causes of death for patients with cancer. The relationship between drug resistance and invasion/metastasis in cancer is not fully elucidated. In this thesis, three pancreatic cell lines, BxPc-3, KCI-MOH1 and MiaPaCa-2, each with differing degrees of sensitivity to chemotherapeutic drugs were chosen for pulse selection with epirubicin, taxotere and gemcitabine in order to investigate any relationship between invasion and drug response.

The level of resistance observed to the selecting drugs is low compared to the high levels of resistance that have been previously shown when selecting continuously with a chemotherapeutic drug. The tumour resistance observed in patients is approximately 3- to 6-fold to the agent of therapy (Wolf *et al.*, 1987). However, the pulse selection method outlined in chapter 2.4.6 is more closely related to the *in vivo* situation, whereby patients receiving chemotherapy are treated every 1-3 weeks and also uses clinically relevant doses of the drugs.

4.1.1 Epirubicin selections

Epirubicin is a member of the anthracycline family of chemotherapeutic drugs. The use of this drug for the treatment of advanced pancreatic cancer is currently undergoing clinical trials. Reni *et al.* (2006) demonstrated that dose intense cisplatin, epirubicin, 5-fluorouracil and gemcitabine in a randomised controlled phase III clinical trial regime appeared more suitable than gemcitabine alone for the treatment of advanced pancreatic cancer.

Multi-drug resistance is a common problem in the treatment of cancer, in particular pancreatic cancer. MDR may occur intrinsically or may be acquired after drug treatment. P-gp is intrinsically expressed in paraffin embedded sections of untreated pancreatic cancer tumours (Suwa *et al.*, 1996) and in cell lines (Zhao *et al.*, 2004).

Epirubicin is a P-gp substrate and other mechanisms of resistance to anthracyclines include: increased glutathione peroxidase and/or glutathione S-tranferase, MRP-1 and

decreased topoismoerase II α expression (Uchiyama-Kokubu *et al*., 2001; Bader *et al*., 1998; Kuriyama *et al*., 1997).

In an attempt to identify the mechanisms of MDR in epirubicin-selected pancreatic cell lines, and to investigate the effect of acquired epirubicin resistance on invasion, cross-resistance proliferation assays were carried out. Invasion status was also assessed.

Bx/Epi was generated after 10 pulses with 50 ng/ml epirubicin. The epirubicin-variant exhibited a modest 1.4-fold increase in resistance to epirubicin and a significant cross-resistance to adriamycin and vincristine. The cell line exhibited cross-sensitivity to 5-fluorouracil and taxotere. KCI/Epi was established after 10 pulses with 100 ng/ml epirubicin. The selected-variant displayed 8-fold resistance to epirubicin compared to the parental cell line. Cross-resistance profiling showed that a significant increase in resistance was also observed for gemcitabine, carboplatin and VP-16. A significant decrease in cross-resistance to adriamycin and vincristine was demonstrated suggesting an alternative mode of multi-drug resistance other than MDR-1 and MRP-1. Mia/Epi was established after 10 pulses with 64 ng/ml epirubicin. The selected-variant displayed a significant 1.7-fold increase in resistance to epirubicin compared to the parental cell line. Cross-resistance profiling showed an increase in resistance to gemcitabine, taxotere, adriamycin, carboplatin, cisplatin, VP-16 and vincristine.

Both Bx/Epi and Mia/Epi displayed significant cross-resistance to adriamycin and vincristine. Epirubicin, adriamycin and vincristine are classified as MDR-related drugs and this resistance may be consistent with a P-gp or MRP-1 drug resistant phenotype. However, the cross-resistance profile for the epirubicin-selected pancreatic cell lines is varied. Takeshita *et al*. (2000) highlighted the involvement of sub-populations within an ADR-resistant osteosarcoma cell line. The ADR-resistant cell line and its sub-population displayed cross-resistance to P-gp substrates, doxorubicin, vincristine and etoposide, while the sub-populations also exhibited resistance to cisplatin and methotrexate, indicating that intrinsic resistance to multiple drugs exists within resistant cell lines.

273

Anthracycline-induced resistance in cells can often show cross-resistance to other members of the family. Pesic *et al.* (2006) established a resistant doxorubicin NSCL cancer cell line that displayed cross-resistance to VP-16, taxol, vinblastine and epirubicin, which was mediated by P-gp expression and not MRP-1 and LRP. Marks *et al.* (1996) developed an 8-fold epirubicin resistant haemopoietic cell line, which displayed cross-resistance to vinblastine, paclitaxel, etoposide and cisplatin demonstrating an extended MDR phenotype. The cells showed P-gp expression, although the P-gp was not functional as decreased drug accumulation was not restored in the presence of verapamil. Therefore, the induction of an extended MDR phenotype may explain why the pancreatic cell lines pulsed with epirubicin displayed cross-resistance to drugs of different families.

In our study, all epirubicin selected variants showed very low, non-significant cross-resistance to 5-fluorouracil. This sensitivity may have clinical relevance, whereby tumours that develop low to moderate resistance to epirubicin may be treated with 5-fluorouracil in order to hinder the development of an MDR tumour.

To investigate the relationship between invasion and epirubicin acquired resistance in pancreatic carcinoma, the invasive status of the epirubicin-selected cell lines was assessed (Chapter 3.1.4). Pancreatic cancer cell lines pulse-selected with epirubicin, displayed a significant increase in invasion relative to untreated parental cells.

Table 4.1.1 summarises the association between epirubicin drug resistance and invasion in the selected pancreatic cell lines. There is no literature available on acquired epirubicin resistance and its effect on invasion. From our results it is clear that exposure to epirubicin increases invasion through matrigel, to varying degrees. This may be caused by selecting the more invasive cell populations or by inducing genetic/translational alterations that lead to a more invasive phenotype.

Table 4.1.1 **Summary of fold drug resistance and invasion status of epirubicin selected pancreatic cancer variants**

Cell line	Drug	Fold resistance	Fold invasion
BxPc-3	Epirubicin	1.4	1.3
MiaPaCa-2	Epirubicin	1.7	3
KCI-MOH1	Epirubicin	8.0	1.7

4.1.2 Taxotere-selections and effects on cell invasion

Taxotere is a semi-synthetic microtubule inhibitor belonging to the family of taxanes. The mechanisms of taxotere resistance *in vivo* and *in vitro* are still poorly understood. Taxotere is a substrate for the multi-drug resistance P-glycoprotein (P-gp) which confers cross-resistance to a wide variety of chemotherapeutic substances. Many reports have found that cells selected with taxotere display an increased cross-resistance to other chemo-drugs and elevated levels of P-gp (Liu *et al*., 2001). Liang *et al*. (2004) investigated the mechanism of taxotere resistance in the human lung carcinoma cell line, DLKP. The taxotere-selected cell line established was 36-fold more resistant than the parental cell line. This new resistant "Txt" variant displayed high levels of MDR-1/P-gp and MRP-1 shown by Western blot and RT-PCR suggesting taxotere resistance is mediated in part through MDR-1/P-gp and MRP-1.

Brown *et al*. (2004) investigated a novel mechanism of taxotere resistance in breast cancer cells. Two taxotere resistant breast cancer cell lines (MCF-7 and MDA-MB-231) were created and analysed by microarray to identify genes associated with taxotere resistance. A reduction in the expression of p27, the cyclin-dependent kinase inhibitor was observed in the taxotere resistant cell lines. Other studies implicate that alterations in the β-tubulin isotypes are associated with acquired taxotere resistance in breast cancer cells (Shalli *et al*., 2005).

Three pancreatic cancer cell lines, BxPc-3, KCI-MOH1 and MiaPaCa-2, were chosen for pulse selection with varying concentrations of taxotere (Chapter 3.1).

The taxotere-selected variant, KCI/Txt was established after 10 pulses with 2 ng/ml of taxotere. No resistance was observed to the selecting drug; in fact a marked sensitivity to taxotere was displayed. Adriamycin, cisplatin, and vincristine also showed a decrease in resistance. An increase in cross-resistance was observed for epirubicin, gemcitabine, 5-fluorouracil, taxol, carboplatin and VP-16. In this cell line, pulse selection exposure to taxotere did not lead to the development of taxotere resistance. Perhaps, clinically this tumour would have responded to taxotere treatment. It would be interesting to study the inherent differences in cell lines that develop resistance and those that do not, as it may result in the identification of predictive markers.

The taxotere-selected variant, Mia/Txt was established after 10 pulses with 1.2 ng/ml taxotere. Resistance to taxotere was increased 1.2-fold, while taxol resistance was also increased. Cross-resistance profiling showed a modest increase in resistance to gemcitabine, cisplatin and carboplatin. A decrease in resistance was observed for epirubicin, 5-fluorouracil, adriamycin, VP-16 and vincristine.

Taxotere promotes the polymerisation of tubulin. Microtubules are involved in many aspects of cell functions such as cell division, cell movement and intracellular protein translocation, and therefore acquired resistance of cells to taxotere may induce an altered *in vitro* invasive phenotype. Taxotere has been shown to up- or down-regulate the expression of metastasis-associated proteins and genes such as metalloproteinases, urokinase-type plasminogen activator and E-cadherin. Guo *et al*. (2003) demonstrated that treatment of colon cancer cell lines with non-toxic concentrations of taxotere resulted in a decrease in expression of MMP-2 and -9 and induced a reduction in their activities. MMP-2 and MMP-9 play a vital role in the degradation of collagen type IV in the basement membrane, which is a crucial event in the metastatic cascade.

To investigate the relationship between taxotere resistance and invasion, the invasion status of the taxotere selected cell lines was assessed. Table 4.1.2 summarises the connection between taxotere acquired resistance and invasion.

Table 4.1.2   Summary of fold drug resistance and invasion status of taxotere selected pancreatic cancer variants

Cell line	Drug	Fold resistance	Fold invasion
MiaPaCa-2	Taxotere	1.2	1.0
KCI-MOH1	Taxotere	0.8	0.9

Invasion assays of the taxotere-selected pancreatic cell lines, MiaPaCa-2 and KCI-MOH1, indicated no change in invasion status. These findings may be due to the low level of taxotere resistance observed in the selected cell lines. Many other reports show taxotere treatment has inhibitory effects on tumour cell invasion. Liu *et al*. (2001) investigated the role of acquired and intrinsic resistance of the pancreatic cell line, SUIT-2 to taxotere. The study showed resistance to taxotere was mediated mainly by P-gp and concluded that taxotere inhibits the invasive ability of drug-sensitive cells but not drug resistant cells. Glynn *et al*. (2004) also observed decreased invasion in a taxol-resistant variant.

4.2.3   Gemcitabine-selection and effects on cell invasion

Gemcitabine [2′-deoxy-′, 2′-difluorocytidine monohydrochloride], a pyrimidine nucleoside analogue, is the most common principal agent used to treat advanced pancreatic cancer. However, acquired resistance to gemcitabine, a clinical trait, may result in treatment failure. To investigate the mechanisms involved in gemcitabine resistance, three pancreatic cell lines were pulse-selected with varying concentrations of gemcitabine for 4 hours once a week for 10 weeks as described in Chapter 2.4.2.

Molecular markers relating to gemcitabine chemo-resistance that have been described include genes involved in cell cycle regulation, proliferation and apoptosis. However, the genes most frequently associated with gemcitabine resistance are related to nucleoside transport and metabolism, which may be involved in the intracellular activation of gemcitabine *in vivo*.

Apoptotic factors have been implicated in the development of resistance to gemcitabine in carcinoma cell lines. Nakai *et al.* (2005) investigated genes relating to gemcitabine

sensitivity by using gene expressions profiles from gemcitabine resistant human pancreatic cell lines under continuous gemcitabine exposure. Fas ligand (TNFSF6), a gene related to Fas mediated apoptosis signalling was down-regulated at the mRNA and protein level in a gemcitabine-resistant cell line. The TNFSF6 protein has also been implicated in cisplatin resistance, whereby cells unable to up-regulate the protein displayed reduced levels of apoptosis in response to cisplatin.

BNIP3 (Bcl2/adenovirus E1B 19 kDa protein interacting protein), which is a member of the BH3-only subfamily of Bcl-2 proteins and is known to promote apoptosis, was expressed at lower levels in gemcitabine-resistant cell lines. Silencing of BNIP3 with siRNA resulted in a marked reduction of gemcitabine-induced toxicity *in vitro* (Akada *et al*., 2005).

In NSCLC (non small cell lung cancer), increased hENT1 (human equilibrative nucleoside transporter 1) expression is a determinant of gemcitabine sensitivity and decreased dCK (deoxycytidine kinase) expression has been shown to be associated with resistance in a gemcitabine-resistant cell line (Achiwa *et al*., 2004). However, Bergman *et al*. (2005) determined that decreased dCK activity *in vivo* was not as important to gemcitabine resistance as RRM1 (ribonucleotide reductase subunit M1) expression (Jordheim *et al*., 2005).

We induced acquired gemcitabine resistance in the cell lines KCI-MOH1 and MiaPaCa-2. Pulse selection with gemcitabine in the BxPc-3 cell line did not induce acquired resistance after ten consecutive pulses.

The KCI-MOH1 gemcitabine-selected variant was generated after 10 pulses with 50 ng/ml gemcitabine. A significant increase in resistance of 2608-fold was observed to gemcitabine. KCI/Gem also displayed significant cross-resistance to epirubicin, taxol and VP-16. Slight increases in resistance to taxotere and cisplatin were observed. Resistance to 5-fluorouracil, adriamycin, carboplatin and vincristine were decreased.

The cross-resistance profile of the KCI-MOH1 gemcitabine variant correlates with other studies investigating gemcitabine cross-resistance. Bergman *et al*. (2000) developed a

30,000-fold gemcitabine resistant ovarian cell line with no dCK activity and investigated the cross-resistance profile. Large increase in resistance was observed to taxol, taxotere and epirubicin. Slight cross-resistance was displayed for 5-fluorouracil, cisplatin, VP-16 and adriamycin.

KCI/Gem showed some cross-resistance to taxotere and taxol, which may be related to toxicity associated with the taxanes; however, no P-gp protein expression was observed in this gemcitabine-selected cell line.

KCI/Gem displayed a high level of resistance to gemcitabine but was not resistant to 5-fluorouracil. Shi *et al*. (2002) showed that pancreatic cell lines are intrinsically resistant to 5-fluorouracil and more sensitive towards gemcitabine. The precise mechanisms of gemcitabine and 5-fluorouracil chemo-resistance in cancer patients are still unknown. Gemcitabine and 5-fluorouracil have similar molecular structures, mechanisms and metabolic characteristics. Both drugs interfere with DNA and RNA synthesis. However the drugs target multiple mechanisms, and therefore resistance to either drug is multifactorial. Over-expression of thymidylate synthase (TS) (5-FU initiates apoptosis by inhibiting TS) and down-regulation of key enzymes (thymidine kinase and pyrimidine nucleoside phosphorylase) are involved in 5-FU resistance (Wang *et al*., 2004). 5-FU sensitivity is also dependent on expression of dihydropyrimidine dehydrogenase, p53 status and DNA mismatch-repair genes (Longley *et al*., 2003). Shi *et al*. (2002) investigated the role of apoptosis genes in 5-FU/gemcitabine resistance in pancreatic cancer cell lines. Following long term exposure to 5-FU and gemcitabine, some pancreatic cell lines displayed acquired resistance to the drugs, partially mediated by the up-regulation of apoptosis inhibitors bcl-$_{xL}$ and mcl-1. This study also showed that the ratio of bax/bcl-2 is predictive of sensitivity toward 5-FU and gemcitabine. These results suggest that common anti-apoptotic genes between 5-FU and gemcitabine may play an important role in predicting cross-resistance.

Unfortunately, our KCI/Gem cell line could not be cultured further as frozen stocks were not viable.

Mia/Gem was established after 10 pulses with 20 ng/ml gemcitabine and showed a 1.3-fold increase in resistance. Cross-resistance was observed to adriamycin, VP-16 and vincristine. Increasing knowledge of cross-resistance profiles of gemcitabine resistance

tumour cells may help to increase our knowledge on future chemotherapeutic combinations.

To study the relationship between gemcitabine resistance and invasion, the invasion status of the gemcitabine-selected variants was investigated. Acquired drug resistance after gemcitabine treatment of pancreatic cancer is often encountered and may lead to further more aggressive metastasis. Verma *et al*. (2006) showed that elevated levels of tissue transglutaminase (TG2) in pancreatic ductal adenocarcinoma (PDAC) cells can add to the development of gemcitabine drug resistance and invasive phenotypes by activation of the FAK/phosphatidylinositol 3-kinase (PI3K)/AKT pathway.

Table 4.1.3 summarises the relationship between gemcitabine drug resistance and invasion. BxPc-3 did not acquire resistance to gemcitabine after pulse selection and therefore, did not show any increase in invasion. However, interestingly MiaPaCa-2 and KCI-MOH1 displaying different levels of gemcitabine resistance showed the same rate of increased invasion. This suggests that even low levels of gemcitabine resistance may contribute to enhanced invasion.

Table 4.1.3 **Summary of fold drug resistance and invasion status of gemcitabine selected pancreatic cancer variants**

Cell line	Drug	Fold resistance	Fold invasion
BxPc-3	Gemcitabine	1.0	1.0
MiaPaCa-2	Gemcitabine	1.3	2.5
KCI-MOH1	Gemcitabine	2608	2.5

In summary, pulse-selection treatment of pancreatic cancer cell lines with epirubicin, taxotere and gemcitabine did not result in major multi-drug resistance phenotypes. Our method of selection reflected clinical conditions and exposure was efficient enough to observe a significant effect on invasion. Further selection with continuous chemotherapeutic exposure has previously resulted in stable resistant cell lines (Frei *et al*., 1985); however this is not representative of clinical settings.

This may be an important finding, in terms of pancreatic cancer patient treatment as adjuvant treatment with anti-invasive molecules and chemotherapy may have a more efficient outcome than drug treatment alone.

4.2 Investigation of MDR associated protein expression in pancreatic carcinoma patients

Intrinsic and acquired drug resistance to a wide variety of molecularly diverse and structurally different chemotherapeutic drugs is a clinical phenomenon that is mainly responsible for the high mortality rates among patients with pancreatic cancer.
The two main drug efflux pump transport families involved in multi-drug resistance (MDR) are multi-drug resistant gene P-glycoprotein (MDR-1/P-gp) and multi-drug resistance protein (MRP-1).
The expression of P-gp has been found in neoplastic and normal tissues such as the kidney, liver (Silverman *et al*., 1995), pancreas, large intestine, and heart (Abu-Qare *et al*., 2003) as well as in several cancer cell lines before or after treatment with cytotoxic agents.

The expression of multi-drug resistant gene 1 (MDR-1/P-gp) and MRP-1 are the major factors for failure of chemotherapy in cancer patients. Studies of the prevalence of these drug efflux pumps in pancreatic tumours are limited and contradictory. This study is the first of its kind to measure the expression of both MDR-1/P-gp and MRP-1 in pancreatic tumours.

Conflicting results have been reported in studies regarding P-gp in pancreatic cancer. Miller *et al*. (1996) examined the expression of P-gp and its function as a drug efflux system in pancreatic cancer. They found no functional P-gp present in pancreatic cancer cell lines, Panc-1, BxPc-3 and AsPc-1, suggesting that intrinsic MDR in pancreatic cancer may be in part mediated by MRP-1 and not MDR-1/P-gp. This observation was also supported by Izquierdo *et al*. (1996) whereby MRP-1 was detected in 97% and 87% of pancreatic tumour cell lines.

However, as P-gp is central in multi-drug resistance, it may have a role in the development of acquired resistance after exposure to drug treatment. Liu *et al*. (2001) verified the acquired resistance caused by P-gp in a study examining the effect of taxotere on the pancreatic carcinoma cell line SUIT-2 and its taxotere-selected variant S2/Txt, established by exposure to increasing taxotere concentrations. The Txt variant was 9.5-fold more resistant that the parental cell line. The parental cell line showed no MDR-1 expression while the S2/Txt line expressed MDR-1 mRNA. This shows that P-gp may mediate acquired resistance in pancreatic cancer.

Suwa *et al*. (1996) also investigated the role of P-gp in 103 paraffin embedded sections of previously untreated pancreatic cancer patients. MDR-1 was detected in all tumours at a significantly higher levels compared to normal pancreas tissue. Higher MDR-1/P-gp expression levels correlated significantly with better prognosis of patients with ductal carcinoma. Among patients with ductal carcinoma, the group with high P-gp staining revealed a 3.5-fold better prognosis compared with the low staining group. They concluded that MDR-1 gene/P-gp expression in pancreatic cancer without chemotherapy inversely correlates with biological aggressiveness and is an independent indicator of favourable prognosis.

MRP-1 (multi-drug resistance-associated protein) is a drug efflux pump that actively transports selected chemotherapeutic agents out of the cell. The potential importance of MRP-1 in pancreatic carcinoma is as yet unknown. A recent study analysed the mRNA expression of MRP 1-9 in normal pancreatic tissue and pancreatic carcinoma. MRP-1 mRNA levels were found not to change significantly between normal pancreatic tissue and pancreatic carcinoma samples with different grading. Furthermore, MRP-1 protein was localised only in the fibroblasts and not in the acinar cells or pancreatic carcinoma cells and expression did not correlate with tumour stage or grading (König *et al*., 2005).

The potential involvement of MDR-1/P-gp and MRP-1 in pancreatic cancer and the implications of their expression in the clinical setting have not been fully defined.

In this study, we detailed the expression of both MDR-1/P-gp and MRP-1 expression in pancreatic tumours. MDR-1/P-gp expression was detected in 93% of tumours stained, while MRP-1 was expressed in 36% of pancreatic carcinomas. Co-expression of multi-drug proteins was observed in 36% of specimens, no cases were observed where MRP-1 was expressed independently of MDR-1/P-gp. However, 61% stained MDR-1/P-gp positive and MRP-1 negative. Only 6.7% of cases expressed neither drug efflux pumps.

The results from this study show that MDR-1/Pgp and MRP-1 are frequently co-expressed in pancreatic tumours. We suggest that these efflux pumps contribute in part to the chemo-resistance phenotype observed in pancreatic cancer. However as the pre-operative chemotherapy history of these patients is unknown, we can not identify whether this resistance is inherent or acquired.

The frequent over-expression of MDR-1/P-gp in particular highlights the need to investigate the functional roles of drug efflux pumps in pancreatic cancer, and inhibition of multiple drug efflux pumps may be essential for the complete control of multi-drug resistance in pancreatic cancer. Future work may involve examining the functional role of P-gp and MRP-1 in pancreatic cancer. Targeting these drug efflux pumps with siRNA or antibodies in combination with chemotherapy may allow for improved treatment efficiency.

4.3 Analysis of the malignant characteristics of MiaPaCa-2 and sub-populations, Clone #3 and Clone #8

Current therapies are unsuccessful in the treatment of metastatic cancer, mainly due to the advanced stage of the cancer at diagnosis. Other rationale behind the high mortality rate of metastatic cancers may be the location and specific organ environment, which may alter the efficiency of chemotheraptic drugs. The heterogeneous composition of tumours is another underlying cause for ineffective treatment as the process of metastasis is highly selective. Heterogenic neoplasms contain a variety of sub-populations, which have differing metastatic potential (Fidler and Kripke, 1977).

4.3.1 Analysis of invasion, adhesion, anoikis and anchorage independent growth in the malignant phenotype

In this thesis, sub-populations of the human pancreatic cancer cell line, MiaPaCa-2 were successfully isolated by single cell cloning to effectively obtain homogeneous clonal populations with differing degrees of invasion. Two of these clones, Clone #3 and Clone #8, showed the most divergent invasive abilities compared to the parent cell line. *In vitro* invasion assays were carried out using the extracellular matrix proteins, matrigel, laminin, fibronectin and collagen type IV and I. A high level of invasion through matrigel, laminin, fibronectin was observed for Clone #3. Invasion through collagens type IV and I showed a modest increase compared to the parent cell line, MiaPaCa-2. Motility for this cell line was also highly increased. In contrast, Clone #8 showed a significant reduction in invasion through matrigel, laminin, fibronectin and collagens type IV and I. Motility of this cell line was similar to the parental cell line.

Tumour cell invasion through the basement membrane is central to the metastatic process. One of the first events during cancer cell invasion is the loss of junctional contact between adjacent cells in the epithelial tissue by disruption of the cell-cell and/or cell-ECM association. Loss of tissue cohesiveness involves alterations in adhesion molecules. Cell adhesion to the ECM is mediated in part by the integrin family of transmembrane receptor proteins. It is understood that adhesion molecules prevent cell migration and invasion via the cell-ECM association. However, disruption of these connections may lead to increased

motility of the tumour cells that have the ability to detach from the original tumour. Therefore, cell surface adhesion molecules play a significant function in cell invasion, migration and metastasis. Changes in the integrin expression during malignant transformation are dependent on the type of cancer. Vodelmann *et al.* (1999) demonstrated altered adhesion properties and integrin expression in a human pancreatic metastatic cell line and a non-metastatic cell line derived from the same original tumour. The metastatic cell line exhibited decreased adhesion to fibronectin, collagens type IV and I. However, an increase in adhesion was observed to laminin. The non-metastatic cell line displayed an increase in adhesion to the ECM proteins, fibronectin, collagens type IV and I. A decrease in adhesion was also observed to laminin. Altered integrin expression on these cell lines was determined by flow cytometry. The metastatic cell line displayed a higher expression of $\alpha6$ (binding to laminin). The non-metastatic cell line highly expressed integrins $\alpha3$ (collagen), $\alpha5$ (fibronectin) and integrins $\beta1$ and $\beta3$.

Adhesion of the pancreatic clonal populations of MiaPaCa-2 to the ECM proteins, matrigel, laminin, fibronectin and collagens type IV and I, was investigated. The results in this thesis agree in part with the above findings, whereby the highly invasive cell line Clone #3 displayed significantly reduced adhesion to matrigel, fibronectin, laminin and collagen type IV. The low invasive cell line, Clone #8, exhibited a significant increase in adhesion to matrigel and laminin. Adhesion to fibronectin and collagen type I was also increased, though not significantly. Adhesion to the ECM proteins, especially fibronectin and laminin represents an important step in metastasis (Shaw *et al*., 1996).

The effect of anoikis in our pancreatic cell line model was also investigated to determine whether detachment from cell-cell or cell-ECM/adherent matrix had an effect on cell survival. Clone #3 displayed increased resistance to anoikis, while Clone #8 displayed significant sensitivity to anoikis compared to the parental cell line. Transformed cells often display anchorage independent growth that results in increased motility and invasion. Changes in cell morphology are common characteristics of malignant transformation in many tumour cells. A feature of transformation is the ability of the cells to grow in the absence of cell anchorage, as revealed by their ability to grow in soft agar. To determine whether anoikis patterns correlated with the ability of the cell lines,

MiaPaCa-2, sub-populations, Clone #3 and Clone #8 to grow in an anchorage-independent environment, the *in vitro* soft agar assay was used. Clone #3 showed an increased ability to form colonies compared to the parental cell line. Clone #8 displayed a significant reduction in colony formation.

Previous studies in other cancer types have also shown a correlation between increased invasion, decreased adhesion, resistance to anoikis and anchorage independent growth. Minard *et al*. (2006) demonstrated a relationship between reduced cellular adhesion and resistance to anoikis mediated by Tiam1 (T-lymphoma invasion and metastasis gene 1) in colon tumour cells. Abraham *et al*. (2003) showed that prostate cancer cells transfected with maspin (a member of the serine protease inhibitor family) displayed decreased metastasic potential *in vivo* and this correlated with increased adhesion to laminin and fibronectin, decreased invasion as well as anchorage independent growth *in vitro*. Zhu *et al*. (2001) selected an anoikis resistant melanoma cell line, which displayed increased proliferation and higher invasive and metastatic abilities than the anoikis sensitive parent.

In pancreatic cancer, links have been established between increased invasion and decreased adhesion to ECM proteins *in vitro* and to high metastatic potential *in vivo*. Satoh *et al*. (2000) reported that MUC-1 expression in S2-013, a human pancreatic cell line population of SUIT-2, resulted in increased invasion and motility and decreased adhesion to ECM proteins. Duxbury *et al*. (2004) described that resistance to anoikis facilitates tumourigenesis and metastasis in pancreatic cancer studies. Over-expression of certain genes, such as CEACAM6 and FAK, are common in pancreatic cancer, and knockdown of such genes by siRNA have successfully resulted in increased anoikis.

4.3.2 Role of integrin expression

Tumour progression and metastasis is associated with changes in a multitude of integrin signalling cascades. Transformed cells are often characterised by the loss/reduction of integrin expression. ECM-ligand binding to an integrin initiates signals which are transmitted via different yet interconnecting pathways and elicit various cell functions such as morphological changes, adhesion, migration and gene activation. All of these functions take part in the metastatic cascade of tumour progression. Investigations into the

role of integrin expression in our pancreatic cancer cell line model were based on the variable invasive and adhesive differences to ECM components in the cells. Integrins β1, α5 and α6 were investigated (Chapter 3.3) and are associated with binding to fibronectin and laminin (Lefcort *et al.*, 1992; Shaw *et al.*, 1996).

We therefore examined the expression of α2, α5, α6 and β1 integrin receptors in our pancreatic cancer cell lines by Western blot and determined whether their expression could account for differences in adhesion and invasion. In our model, the integrins β1, α5 and α6 subunits were over-expressed in the low invasive/high adhesive pancreatic cell line Clone #8, suggesting a role for this integrin in increasing adhesion and inhibiting invasion in pancreatic cancer. Integrin β1 is the unique partner for α5 and also forms heterodimers with integrins α2 and α6.

4.3.2.1 Role of integrin β1 siRNA transfection in Clone #8 cells

Efficient functional siRNA knockdown of integrin β1 in Clone #8 was determined by Western blot. Significantly increased invasion through matrigel and fibronectin was observed, but there was no significant change in invasion through laminin. The adhesion of this cell line to matrigel and fibronectin were also reduced with treatment of integrin β1 siRNAs; however no decrease in adhesion to laminin was observed. These results suggest that integrin β1 plays a role in the adherence of Clone #8 to matrigel and fibronectin, and the knockdown of integrin β1 resulted in reduction of the adhesiveness of the cell line and subsequently increased the cells ability to become motile, invade and transverse the matrigel coated membrane. We therefore investigated changes in migration in the integrin β1 siRNA transfected Clone #8 cells. Motility of the cells was significantly increased due to the loss of integrin β1 expression.

Our results suggest that integrin β1 plays a role in promoting adhesion and inhibiting invasion/motility in the Clone #8 population, while the decreased expression of integrin β1 in Clone #3 may also contribute to the more invasive phenotype of these cells. Ellerbroek *et al*. (1999) determined that inhibition of integrin β1 through aggregation induced pro-activation of MMP-2 in ovarian cancer cells. In fact other studies have

reported that anti-integrin β1 antibodies stimulate collagenase activity in keratinocytes (Larjava *et al.*, 1993) and melanoma (Seftor *et al.*, 1993).

The involvement of integrin β1 in anoikis was also investigated by RNAi. Decreasing the expression of integrin β1 in Clone #8 revealed a more anoikis resistant phenotype. Interaction of the ECM proteins and integrin receptors are known to activate proliferation and survival signals. Once ECM-cell or cell-cell detachment occurs, survival mechanisms are down-regulated, proliferation ceases and cells undergo anoikis (Frisch and Screaton, 2001). Our findings suggest that loss of integrin β1 signalling resulted in enhanced invasion through matrigel, decreased adhesion to matrigel and increased anoikis resistance. These findings correlate with a recent study, which determined that drug selected resistant variants of a breast cancer cell line showed increased invasion status and anoikis resistance through the loss of integrin β1 expression (Morozevich *et al.*, 2006).

Integrin β1 expression in melanoma metastases has been shown to forecast a longer disease-free period (Vihinen *et al.*, 2000). In prostate cancer the integrin β1 splice variant of β1A, β1C, has been shown to inhibit proliferation by regulating the cell cycle inhibitor, p27(Kip1). β1C integrin has been shown by immunohistochemistry to be down-regulated in prostate cancer cells compared to benign prostate tissue (Fornaro *et al.*, 1996). Ramachandra *et al.* (2002) showed that increased p21 and integrin β1 expression reduced colony formation efficiency in soft agar, and that anoikis sensitivity was due to SMAD4 expression in a SMAD4-transfected cell line, which in turn restores transforming growth factor beta (TGF-β) signalling.

Howlett *et al.* (1995) established a rapid 3-D assay for discrimination of normal and malignant human breast epithelial cells where normal epithelial cells differentiate into well-organised acinar structures, whereas tumour cells produce large, disordered colonies. Immunocytochemical analysis showed that normal cells expressed integrins α1, α2, α3, α6, β1 and β4 integrin subunits, whereas breast carcinoma cells show variable losses, disordered expression, or down-regulation of these subunits. Function-blocking analysis using anti-β1 or anti-α3 antibodies showed a > 5-fold inhibition of the formation of acinar structures by normal cells, whereas anti-α2 or -α6 antibodies had little or no effect. In

experiments where collagen type I gels were used instead of basement membrane, acinar morphogenesis was blocked by anti-β1 and -α2 antibodies but not by anti-α3. These data suggest a specificity of integrin utilisation dependent on the ECM ligands encountered by the cell and that loss of proper integrin-mediated cell-ECM interaction may be critical to breast tumour formation.

Plath *et al*. (2000) demonstrated that p16^{INK4a} induces anoikis via up-regulation of α5β1, fibronectin receptor in the pancreatic cell line, Capan-1. Addition of soluble fibronectin completely inhibits the p16^{INK4a} mediated anoikis. Further investigations showed that with the added addition of a monoclonal integrin α5 antibody, the fibronectin-mediated inhibition of anoikis was abolished. Integrin α5 and β1 were up-regulated in our low invasive, anoikis sensitive clonal population, Clone #8. This may suggest that by inhibiting integrin β1 (unique partner for α5 to form the α5β1 receptor) by siRNA, α5 and β1 integrins are unable to partner, and therefore the anoikis induction is lost in our cell line model resulting in resistance to anoikis.

4.3.2.2 Role of integrins α5 and α6 siRNA transfection in Clone #8 cells

Expression of the α5 subunit, which binds to fibronectin, was elevated in Clone #8, the less invasive/more adhesive cell line. Functional knockdown of integrin α5 expression by siRNA in Clone #8 resulted in a significant increase in invasion through matrigel, laminin and fibronectin. The level of motility was also increased after integrin α5 siRNA transfection. Adhesion to fibronectin was statistically significantly reduced, while adhesion to matrigel and laminin was slightly reduced. Resistance to anoikis was slightly increased in integrin α5 siRNA transfected cells compared to Clone #8 cells transfected with scrambled siRNA, although not significantly. Our findings confirm other reports suggesting that the expression of integrin α5 may be related to loss of tumourigenicity. By reducing integrin α5 protein expression, a more invasive, less adhesive, anoikis resistant phenotype was observed, similar to the more invasive clone, Clone #3. Recent research indicates that altered α5β1 expression may inhibit tumour development and metastasis (Felding-Habermann, 2003). Chintala *et al*. (1996) determined that loss of integrins α3β1 and α5β1 increased the invasiveness of glioma cells through up-regulation of MMP-2.

Hall *et al.* (1991) examined the incidence of integrin α5β1 in pancreatic cancer sections. Pancreatic adenocarcinomas and ampullary tumours showed expression of integrins α2, α3, α6 and β1, β4 and the vitronectin receptor (integrin αv associated with integrin β1 or β5). However, no staining of integrin α5 was observed. Loss of integrin complex α5β1 (fibronectin receptor) facilitates the tumourigenicity of transformed colon cells. The capacity to form tumours in nude mice was significantly lower for α5 positive than α5 negative clones of the cell line, HT 29 (Stallmach *et al.*, 1994). Giancotti and Ruoslahti (1990) showed that in transformed CHO cells, co-expression of integrin α5 and β1 made the cells non-tumourigenic.

We also characterised the involvement of integrin α6, which functions as an adhesive receptor for laminin (Mercurio *et al.*, 1995). We functionally knocked down integrin α6 expression. Invasion assays showed a moderate increase in invasion through matrigel and laminin; however, invasion through fibronectin was significantly increased. Adhesive properties to laminin were reduced (20-34%), while adhesion to matrigel and fibronectin were unchanged. Resistance to anoikis was unaltered suggesting that loss of integrin α6 results in increased invasion, with decreased adhesion to laminin and no change in anoikis. The role of integrin α6 in our pancreatic cancer cell line model may be more associated with interactions with specific components of the ECM. The expression and distribution patterns of integrins and ECM molecules in chronic pancreatitis (CP) and pancreatic adenocarcinoma (PC) compared with normal pancreas (NP) were investigated by Shimoyama *et al.* (1995). Integrins α2, α3, and α6 were strongly expressed and diffuse, while no α5 expression was seen in PC. Continuous staining in CP was observed in the basement membrane (BM), whereas it showed discontinuous/absent staining in PC with anti-collagen type IV, laminin, and vitronectin antibodies. Some carcinoma cells showed reverse correlation between expression of integrins α2, α3, and α6 and type IV collagen and laminin expression. Weinel *et al.* (1992) studied the expression of integrins α2, α3, α5 and α6 by IHC in tissue samples from ductal PC, CP, NP and in 8 cell lines of ductal human pancreatic cancer. Pancreatic carcinoma showed intense staining for integrins α2 and α6 with redistribution, which may reflect a loss of spatial arrangement of tumour cells and their ability to interact randomly with extracellular matrix structures during invasion

and metastasis. Furthermore, adhesion assays on purified extracellular matrix (ECM)-compounds were used to define the function of α2, α3, α5 and α6 in pancreatic cancer cell lines (PC 3 and PC 44). Monoclonal antibodies (MAbs) against α6 (GoH3) inhibited tumour-cell adhesion to laminin (52%-86%) in both cell lines. These results suggest that α6 is a laminin-binding site in pancreatic cancer cells. Weinel *et al.* (1995) performed *in vitro* adhesion, migration, and invasion experiments to investigate the role of α6 in pancreatic cancer. Integrin α6 was differentially expressed in NP and PC. Immunoprecipitation of different pancreatic carcinoma cell lines revealed that integrin α6 was expressed together with the β4 subunit as α6β4 complex. However, adhesion of pancreatic cancer cells to laminin was inhibited by anti-α6 and anti-β1 integrin antibodies but not by anti-β4 integrin antibodies. Migration of the cells through laminin was almost completely inhibited by anti-β1 antibody but not by other anti-integrin antibodies. Tumour cell invasion through a matrigel was only slightly inhibited by anti-α6 antibodies. In contrast, a marked inhibition was observed using anti-β1 antibody, anti-α2, anti-α5 antibodies, and RGDS. We have also shown that the integrin α6 is a laminin adhesion receptor in pancreatic carcinoma cells, and could possibly be involved in tumour invasion and adhesion through the basement membrane.

4.3.3 Drug resistance

To characterise the relationship between invasion and drug resistance, toxicity assays were carried out using a panel of ten chemotherapeutic drugs. The IC_{50} values of each of the chemotherapeutic agents were determined for the parental line and its sub clones, Clone #3 and Clone #8 (Chapter 3.3.7, table 3.3.1). Clone #3 exhibited a significantly higher level of resistance to taxotere and VP-16, while resistance levels to epirubicin, adriamycin and vincristine were also increased compared to MiaPaCa-2. No increase in resistance was observed for 5-FU, taxol, cisplatin and carboplatin. Interestingly, a significant sensitivity to gemcitabine was observed.

The general drug resistance of Clone #3 was in fact quite small, less than 2-fold however this level of inherent resistance may have important implications *in vivo*. Clinically, many patients develop drug resistance, where the tumour resistance is approximately 3- to 6-fold (Wolf *et al.*, 1987). Therefore, the study of low level resistance in invasive tumours may

be more relevant than the study of acquired resistance after long term exposure to chemotherapeutic agents (Belvedere *et al*., 1996). Clone #8 displayed an increase in sensitivity to all ten chemotherapeutic drugs compared to the parental cell line.

An important aspect of the toxicity profile of Clone #3 and Clone #8 compared to the parental cell line may be the cross-resistance to chemotherapeutic agents of the same family. Clone #3 showed no resistance to the platinum family, cisplatin and carboplatin. The main mechanisms of resistance to platinum compounds are decreased cellular transport of the drug, enhanced repair of platinum-related DNA damage, absence of mismatch repair and increased expression of glutathione and glutathione-S-transferase. However, Clone #8 displayed a significant sensitivity to the platinum family; this may suggest that there may be a more defined link between low invasion and inherent platinum sensitivity compared to the high invasion and lack of platinum resistance status of Clone #3. Interestingly, Clone #3 and Clone #8 are sensitive to gemcitabine and 5-fluorouracil. These drugs are members of the anti-metabolite family; both drugs have similar molecular structures, mechanisms and metabolic characteristics. Recent pharmacogenetic studies focuses on genes encoding proteins directly involved in anti-metabolite activity, showing the role of thymidylate synthase and human equilibrate nucleoside transporter-1 as prognostic factor in 5-FU and gemcitabine treated patients, respectively (Giovannetti *et al*., 2006). Gemcitabine and 5-FU interfere with DNA and RNA synthesis; however, the drugs target multiple mechanisms, therefore resistance to either drug is multifactorial. Clone #3 showed significant increased sensitivity to gemcitabine compared to Clone #8. This may suggest that the toxicity potential of gemcitabine is exerted more efficiently to invasive pancreatic cancer cells.

Clone #3 displayed a typical multidrug resistance (MDR) phenotype, whereby increased resistance was observed for taxotere, VP-16, epirubicin, adriamycin and vincristine compared to MiaPaCa-2 parental cells. These drugs are substrates for P-gp and MRP-1, which are drug efflux pumps that mediate drug transport from the cell. However, no inherent resistance was observed for taxol. Taxotere and taxol are microtubule inhibitors belonging to the family of taxanes. The two taxanes share major part of their structure and mechanisms of action, but differ in other aspects. There are differences in their tubulin polymer generation and taxotere is twice as active in the inhibition of depolymerisation.

Ishitobi *et al*. (2001) demonstrated the treatment of resistant metastatic breast cancer, whereby, resistance to anthracycline and taxotere could be successfully treated with taxol. *In vitro* studies have also confirmed the lack of cross-resistance between the taxanes, and that some human tumour cell lines resistant to taxol are not resistant to taxotere; thus, resistance to taxol does not automatically indicate resistance to taxotere (Untch *et al*., 1994). The clinical implications for the results in this thesis suggest that treatment with chemotherapeutic drugs could potentially select for the invasive cells. However, the invasive cells are sensitive to gemcitabine which is the standard drug for pancreatic cancer.

4.3.4 Summary

In summary, this chapter discusses the occurrence of sub-populations within a pancreatic cancer cell line, displaying variable invasion abilities and correlates the invasive phenotype with malignant transformation. Clone #3 displayed an inherent increased invasive potential, high motility, distinct reduction in adhesion to ECM proteins, anoikis resistance, and the ability to form colonies in soft agar. Integrins β1, α5 and α6 were undetectable in this cell line by Western blot, suggesting a role for the loss of their expression in invasion and adhesion in pancreatic cancer. Functional knockdown of integrins β1, α5 and α6 protein expressions in Clone #8 revealed a more aggressive phenotype with increased invasive and motility abilities corresponding to a decrease in cell attachment to ECM. The role of integrins in anoikis was less clear, as integrin β1 knockdown significantly increased anoikis resistance. However, loss of either integrins α5 or α6 revealed no significant change in the induction of anoikis. Clone #3 corresponding to the more invasive/less adhesive phenotype, displayed increased drug resistance compared to the parental cell lines, whereas Clone #8, corresponding to the low invasive/high adhesive phenotype was significantly sensitive to a panel of chemotherapeutic drugs.

4.4 Proteomic analysis of MiaPaCa-2 and sub-populations, Clone #3 and Clone #8 grown on matrigel

Characterisation of MiaPaCa-2, Clone #3 and Clone #8, previously determined a relationship between invasion and the malignant transformation. Differing invasive abilities within the cells corresponding to an aggressive phenotype is a complex process, requiring an organised interaction between proteins, signalling pathways and genetic mutations. The tumour microenvironment plays an essential role in cancer progression, invasion and metastasis. The microenvironment consists of many features including stromal fibroblasts, inflammatory cells, vasculature components, normal epithelial cells and the extracellular matrix (ECM). Tumour-tumour cell interaction, tumour-stromal cell interaction, as well as tumour-ECM interaction, all contribute to "cross-talk" among tumour cells through the release of growth factors, cytokines, proteases, and other bioactive molecules (Ariztia *et al*., 2006). Therefore, to stimulate the interaction of MiaPaCa-2, Clone #3 and Clone #8 to the ECM, the cells were grown on matrigel (reconstituted ECM) for 24 hrs prior to analysis. Proteomic analysis was applied to investigate crucial events underlying *in vitro* pancreatic cancer invasion tumourigenesis and to exploit this knowledge for early detection and better intervention.

4.4.1 Generation of protein lists

Three lists of differentially expressed proteins between MiaPaCa-2 versus Clone #8 (list 1), Clone #3 versus MiaPaCa-2 (list 2) and Clone #3 versus Clone #8 (list 3) were established. The generated protein lists and analysis was from high to low invasion status of the cell lines. Therefore, in order to further determine the significance of these differentially changed proteins, the design analysis was laid out to specifically identify proteins that were consistently altered (either up-regulated or down-regulated) corresponding with the invasion status of the cell lines.

The three generated differentially expressed protein lists were overlaid, determining unique and common expressing proteins between lists. Common proteins consistently expressed (positively or negatively) between all three lists, associated with the invasive position of the cells were determined (Chapter 3.4, table 3.4.7).

4.4.2 Invasion specific proteins chosen for siRNA functional analysis

Three proteins were chosen for siRNA silencing based on specificity to invasion in our proteomic profiling results (Chapter 3.4), relevance to cancer/invasion in the literature, fold difference and *p*-value. Table 4.4.1 summarises fold difference between each comparison to the chosen target proteins.

Table 4.4.1   Proteins commonly and consistently expressed between the comparisons, MiaPaCa-2 vs Clone #8, Clone #3 versus MiaPaCa-2 and Clone #3 versus Clone #8 chosen for further analysis

Protein	Description	MiaPaCa-2 vs Clone #8	Clone #3 vs MiaPaCa-2	Clone #3 vs Clone #8
ALDH1A1	Aldehyde dehydrogenase 1A1	5.3	1.7	8.9
VIM	Vimentin	2.2	2.6	5.5
STIP1	Stress-induced phosphoprotein 1	1.3	1.5	2.0

There is increasing evidence that siRNAs can affect the expression of multiple genes (Jackson *et al*., 2003). These non-specific results are termed "off-target" effects; therefore it is vital that appropriate controls are used during siRNA experiments. In our analysis, each set of siRNA experiments included accurate controls of siRNA target sequencing, in each experiment the siRNA targeted the same mRNA using three different siRNA sequences. Consequently, any changes induced by one siRNA and not the other two could be attributed to off-target effects and multiple non-homologous siRNAs are most likely to be responsible for specific target suppression/knockdown. Three non-homologous ALDH1A1, VIM and STIP1 siRNAs were used in this set of experiments, each targeting different regions of the transcript.

Western blots were used to analyse the efficiency of target siRNA knockdown of protein expression in our model; however, it is worth noting the role of monitoring mRNA knockdown validation. With an effective siRNA, target reduction should be observed at both protein and mRNA level, however, this may not always be true. Reduction in mRNA levels without corresponding reduction in protein levels could indicate slow protein turnover. Pai *et al*. (2006) demonstrated that the targeting of proteins with a long half-life

may not produce the desired phenotypic effect because silencing at the level of transcription will not affect pre-existing proteins, suggesting further optimisation of time points may be required. In contrast, protein reduction without a decrease in mRNA could signify a siRNA mediating its effects at the translational level as microRNA (miRNA). siRNAs trigger mRNA degradation through the RNAi pathway, however, miRNA can inhibit translation without affecting mRNA levels.

Appropriate controls were used during each siRNA experiment; comparing non-treated control to scrambled siRNA (nonsense target) treated cells revealed changes specifically caused by siRNA delivery ensuring that siRNA results are due to efficient targeted RNAi molecules and not an artefact of the delivery. siRNA delivery through transfection can result in temporary changes in the cell, and in some cases cells may become resistant to conditions of delivery, to further ensure optimal target knockdown siPORT™ *NeoFX*™, a lipid-based agent was used to minimise serum RNase digestion of siRNA and to maximize delivery of siRNA to the cells.

All experiments also included efficient transfection control/positive control, kinesin 11 (Kif11). Kinesin facilitates cellular mitosis, therefore silencing kinesin causes cellular arrest. Weil *et al*. (2002) showed that a siRNA targeting the mRNA of the Kif11 induces a rapid mitotic arrest and provides a convenient assay for the optimisation of siRNA transfection in mammalian cells. Examination of cell morphology and reduced cell proliferation after transfection indicated a successful transfection.

The duration of gene silencing varies greatly between cells with slow growing cells still showing the effects of siRNA after several weeks, but more rapidly dividing cells not seeing an effect for longer than 1 week (Ryther *et al*., 2005). This was important to consider when choosing time points for protein, invasion, adhesion, and anoikis assays. All assays were carried out within a maximum of 72 hrs post transfection. Proliferation and chemosensitivity assays were carried out within 5 days of the initial transfection to ensure the siRNA was still having an effect.

4.4.3 Aldehyde dehydrogenase 1A1 (ALDH1A1)

Aldehyde dehydrogenase 1A1 (ALDH1A1) is an enzyme, belonging to the aldehyde dehydrogenase family of proteins which are involved in the conversion of aldehydes to their corresponding acids by $NAD(P)^+$ dependent reactions (Yoshida *et al.*, 1998). Three major liver isoforms of this enzyme exists, cytosolic (1), mitochondrial (2), cytosolic and mitrochondrial (3) and can be distinguished by their electrophoretic mobilities, kinetic properties, and subcellular localisations. ALDH1A1 is a cytosolic enzyme ubiquitously distributed in many tissues, including brain (Bhave *et al.*, 2006) and red blood cells (Collard *et al.*, 2007).

ALDH1A1 was chosen as a target for siRNA based on the comparative proteomic data analysis which compared protein expression in MiaPaCa-2, Clone #3 and Clone #8. ALDH1A1 was expressed at higher levels in the parent MiaPaCa-2 than Clone #8 (5.3-fold) and at higher levels in Clone #3 compared to either the parent or Clone #8 (1.7- and 8.9-fold, repectively). As the comparisons generated were from high to low invasion, the overall status of ALDH1A1 expression is increasing as the invasive status of the cell lines increase. Validation analysis was carried out by Western blot and results confirmed that Clone #3 showed the highest expressed of ALDH1A1.

4.4.3.1 Effect of ALDH1A1 siRNA in Clone #3

RNAi technology was used to study ALDH1A1 protein expression; therefore, using three independent ALDH1A1 siRNA target sequences, ALDH1A1 protein expression was specifically down-regulated in Clone #3 cells and its role in invasion, adhesion, anoikis, proliferation and drug resistance was investigated.

We suggest that as our model has significant altered ALDH1A1 expression consistently correlating with differences in invasion, ALDH1A1 may potentially play a role in pancreatic cancer invasion and the transformed phenotype. Invasion assays performed 48 hrs post-transfection showed significant inhibition of invasion in Clone #3 cells. The invasive abilities of the ALDH1A1 siRNA (3) transfected Clone #3 cells were reduced up to 2.8-fold compared to scrambled control cells.

Adhesion to matrigel was significantly increased (23-32%) after knockdown of ALDH1A1 protein expression in Clone #3 cells. Anoikis sensitivity was only induced by ALDH1A1 siRNA (3); the two other ALDH1A1 siRNA targets did not have an effect on anoikis. This result may suggest that the role of ALDH1A1 in anoikis is unclear and further analysis may need to be carried out to determine its involvement.

Proliferation assays of ALDH1A1 siRNA transfected Clone #3 cells carried out over 5 days, determined that loss of ALDH1A1 does not affect cell growth in Clone #3 cells. Recent studies have reported that ALDH1A1$^{-/-}$ mice do not exhibit defects in growth and survival (Molotkov e*t al*., 2002) or obvious developmental defects in the retina or other tissues (Fan *et al*., 2003).

Difference in drug resistance was also previously observed in our characterisation of the *in vitro* invasive pancreatic cancer cell line model (Chapter 3.3.7). Clone #8 was significantly sensitive to a panel of 10 chemotherapeutic drugs tested (Table 3.3.1). Recent research has determined a relationship between ALDH1A1 expression and resistance to certain chemotherapeutic drugs. To investigate this phenomenon further, we established the relative IC$_{50}$s of MiaPaCa-2, Clone #3 and Clone #8 to 4-hydroxycyclophosphamide (4-HC), masfosfamide, 4-diethylaminobenzaldehyde (DEAB) and all-trans retinoic acid. ALDH1A1 activity in cancer has been found to be responsible for resistance to oxazaphosphorines such as cyclophosphamide. Cyclophosphamide (CPA), an alkylating agent, is one of the most widely used drugs in the treatment of breast cancer. CPA is metabolised by enzymes in the liver, so its preactivated form, 4-HC and mafosfamide, a preactivated cyclophosphamide analogue were used in *in vitro* chemosensitivity assays. Our results show that ALDH1A1 expression correlated with resistance of these drugs. Clone #3 was more resistant to 4-HC and mafosfamide than MiaPaCa-2 or Clone #8. Although many other molecular enzymes are involved in CPA resistance we showed that RNAi-mediated knockdown of ALDH1A1 sensitised Clone #3 cells to the toxic effects of 4-HC. This result supports numerous studies indicating ALDH1A1s involvement in CPA resistance. Sladek *et al*. (2002) showed by a retrospective study that the ALDH1A1 expression level was higher in metastatic tumours that did not respond to CPA-based treatment than those that did respond to the regime.

ALDH1A1 expression has also been reported in lung cancer cell line, A549, where its expression along with ALDH1A3 was knocked down by RNAi and determined to mediate CPA resistance (Moreb *et al.*, 2007). However, our findings are the first report to show ALDH1A1 mediates 4-HC resistance in pancreatic cancer.

Although no direct evidence exists linking ALDH1A1 mediated drug resistance, invasion and the malignant phenotype, studies have shown that increased drug resistance may also increase invasion in certain cancers. Liang *et al.* (2004) used pulse-selections to induce drug resistant variants of the lung cancer cell line, DLKP. The cell line was exposed to VP-16, vincristine, taxotere, mitoxantrone, 5-fluorouracil, methotrexate, CCNU, BCNU, cisplatin and chlorambucil, resulting in resistance to the selecting agents and, in some cases, cross-resistance to methotrexate, vincristine, adriamycin and taxotere. A marked increase in *in vitro* invasion and motility was observed with variants pulsed with mitoxantrone, 5-fluorouracil, methotrexate, BCNU, cisplatin and chlorambucil suggesting that drug exposure may induce not only resistance but also invasiveness in cancer cells. Drug selection of RPMI 2650, a non-invasive human nasal epithelium cell line, with the chemotherapeutic agents, paclitaxel and melphalan, resulted in multiple drug resistant phenotypes and in the case of melphalan but not paclitaxel, a highly invasive phenotype (Liang *et al.*, 2001). Glynn *et al.* (2004) established drug resistant variants using doxorubicin and paclitaxel pulse-selection method of an *in vitro* invasive clonal population of the human breast cancer cell line, MDA-MB-435S. A novel 'superinvasive' phenotype was observed; this phenotype was characterised by an ability to relocate to another surface following invasion through matrigel and membrane pores, by decreased adhesion to extracellular matrix proteins and by increased motility.

To further develop our hypothesis linking ALDH1A1 expression and increased invasion in pancreatic cancer, we studied the effects of all-trans retinoic acid (ATRA) on Clone #8 and Clone #3. ALDH1A1 was shown to be 9-fold up-regulated in Clone #3 compared to Clone #8 by proteomic profiling. Cells were exposed to ATRA every 72 hrs, as studies have shown that ATRA is degraded *in vitro* every 48-72 hrs.

ALDH1A1 is involved in the irreversible oxidisation of retinal to retinoic acid (Duester, 1996). Retinoic acid (RA) is an acidic derivative of Vitamin A and regulates cell differentiation, growth inhibition and apoptosis in many cell types (De luca, 1991). The differentiation and anti-proliferative effects of RA has been established in cervical cancer (Borutinskaite *et al*., 2006), hepatoma (Li and Wan, 1998) and breast cancer (Lopez-Boado *et al*., 1994). RA inhibits cell proliferation but induces scattering and invasion of the pancreatic cancer cell line, Capan-1, through c-met up-regulation (Leelawat *et al*., 2004) and also been shown to inhibit adhesion to laminin in pancreatic cancer cells through the $\alpha6\beta1$ integrin receptor (Rosewicz *et al*., 1997).

Clone #3 is 2.7-fold more resistant to ATRA than Clone #8, however, ALDH1A1 may not involved in the anti-proliferative effects of ATRA. The biological actions of ATRA and derivates are mediated by the retinoic acid receptor (RAR) and retinoid X receptor (RXR) each with α, β γ isoforms, which are ligand dependent transcription factors expressed in the nucleus of cells (Chambon, 1996). These homodimers and heterodimers receptors, then bind to specific RA response elements (RARE), and regulate positive/negative transcription activities of target genes. ATRA inhibits proliferation of gastric cancer cells by up-regulating RARα expression (Liu *et al*., 2001) and induced G1 cell cycle arrest in breast cancer cells (Wilcken *et al*., 1996) and apoptosis (Mangiarotti *et al*., 1998). These events require ubiquitylation and degradation of Skp2, an F-box protein that targets p27^{Kip1} for degradation and cyclin D (Dow *et al*., 2001).

RA metabolites are currently used in treatment of colon cancer (Park *et al*., 2007) and leukemia (Huang *et al*., 1988). Studies have also confirmed the ability of RA to inhibit invasion by decreasing expression of proteolytic enzymes and motility factors in melanoma cells (Hendrix *et al*., 1990; Wood *et al*., 1990) and colonic cancer cells (Park *et al*., 2007). Therefore, conflicting results exist and there is a need for further study into the presence of high ALDH1A1 activity, retinoic acid and cancer cell invasion.

We hypothesised that accumulation of ATRA intracellularly in Clone #3 may reduce ALDH1A1 expression and therefore lead to decreased invasion of the cells by a possible negative feedback loop. However, we did not observe any decrease in ALDH1A1 protein

expression after 5 μM ATRA exposure for 48 hrs or long-term continuous exposure. Previous studies have shown that ATRA treatment can decrease ALDH1A1 protein expression and enzyme activity, but not corresponding mRNA. This observed decrease resulted in a significant increase in toxicity in treated lung cancer cells to 4-HC and acetaldehyde, indicating a post-translational mechanism, involving the ubiquitin-proteasome pathway, through which ATRA decreases ALDH1A1 expression (Moreb *et al*., 2004).

The lack of ATRA effect on Clone #3 cells may be due to the inherent resistance of these cells to ATRA. Although the use of RA is valid in the clinical setting, many cancer cells exhibit resistance (Lotan and Nicolson, 1979). ATRA-resistant breast cancer cell lines are generally negative for the expression of estrogen receptor-α (ERα) (Fontana, 1987) and have low levels of RARs, particularly RARα (Schneider *et al*., 2000). Tari *et al*., (2002) showed that HER2 over-expression in breast cancer cell lines exhibited resistance to ATRA. In pancreatic cancer, Pettersson *et al*. (2002) reported the involvement of the Bcl-2 family of proteins in ATRA resistance. Over-expression of Bcl-2 resulted in inhibition of apoptosis induced by retinoic acid. Kaiser *et al*. (1998) reported loss of RARγ expression in two pancreatic cancer retinoid-resistant cell lines, suggesting RARγ as a predictive marker for retinoid treatment of pancreatic cancer.

However, Clone #8 (low invasion) cells displayed increased invasion and displayed morphological changes of elongated spindle shaped cells after continuous treatment with ATRA. Leelawat *et al*. (2005) determined that the pancreatic cancer cell line, Capan-1 displayed increased invasion through matrigel after ATRA treatment. The increase in invasion of these cells correlated with an up-regulation of c-Met (mesenchymal epithelial transition factor), a proto-oncogene that encodes for a tyrosine kinase membrane receptor for hepatocyte growth factor/scatter factor (HGF/SF).

These results suggest that increased ALDH1A1 expression in Clone #3 could potentially contribute to the invasive phenotype by the production of RA.

The role of ALDH1A1 activity as a marker for hematopoietic progenitor stem cells is well established (Kastan *et al*., 1990). ALDH1A1 activity appears to be responsible for the resistance of hematopoietic progenitor stem cells (HSCs) to cyclophosphamide and 4-

hydroxyperoxycyclophosphamide (Sahovic *et al.*, 1988). Therefore, these drugs are used in purging regimens for autologous bone marrow transplants, as HSCs are capable of repopulation (Yeager *et al.*, 1986). Storms *et al.* (1999) described a fluorescent substrate of ALDH (termed Aldefluor) that can be used to isolate cells with increased ALDH activity by fluorescence-activated cell sorting (FACS). The substrate is an amino acetaldehyde molecule conjugated to a BODIPY (4, 4-difluoro-5, 7-dimethyl-4-bora-3a, 4adiaza-5-proprionic acid) fluorochrome that is metabolised by ALDH to an aminoacetate anion, retained within the cell because of its negative charge. Thus, the amount of fluorescent product that accumulates in viable cells correlates to ALDH activity, and cells with high ALDH activity can be selected from human umbilical cord blood (UCB). Therefore, isolation of stem and progenitor cells based on ALDH activity also represents a novel tool to explore the heterogeneity of selected stem cells.

Cancer stem cells (CSCs) are a distinct sub-population within a tumour that has self-renewing properties. The existence of CSCs was verified in myelogenous leukaemia (Bonnet *et al.*, 1997), breast (Al-Hajj *et al.*, 2003) and brain tumours (Hemmati *et al.*, 2003). More recently, Li *et al.* (2007) identified a highly tumourigenic sub-population of pancreatic cancer stem cells expressing the cell surface markers CD44, CD24, and epithelial-specific antigen (ESA) using a xenograft model in which primary human pancreatic adenocarcinomas were grown in immunocompromised mice. Pancreatic cancer stem cells with the CD44(+)CD24(+)ESA(+) phenotype (0.2-0.8% of pancreatic cancer cells) had a 100-fold increased tumourigenic potential compared with nontumourigenic cancer cells. The CD44(+)CD24(+)ESA(+) pancreatic cancer cells, in an orthotopic pancreatic mouse model, showed the stem cell properties of self-renewal, the ability to produce differentiated progeny, and increased expression of the developmental signalling molecule sonic hedgehog (sHh). Feldmann *et al.* (2007) showed that blockade of Hh by cyclopamine treatment in pancreatic cancer significantly reduced invasion *in vitro*. However, *in vivo*, cyclopamine had no significant effect on primary tumour mass but had profound effect on the tumour metastasis of orthotopic xenograft pancreatic cancer mouse model. Furthermore, cyclopamine reduced the expression of ALDH (3-fold) *in vitro*, suggesting existence of a sub-population dependent on Hh and therefore, more sensitive to cyclopamine specific Hh inhibition. The authors also implied that cyclopamine may

inhibit the functional abilities of invading cells through down-regulation of EMT or by preferentially targeting the minor proportion of cells capable of tumour initiation within the tumour mass, without reducing overall invasive capacity.

These recent reports along with our own findings linking the expression of ALDH1A1 with pancreatic cancer cell invasion and drug resistance may warrant further studies as identification of pancreatic cancer stem cells markers and further elucidation of the signalling pathways that regulate their growth and survival may provide novel therapeutic approaches to treat pancreatic cancer, which is highly invasive and metastatic with inherent chemotherapy resistance.

4.4.4 Vimentin

Vimentin (VIM) is the main member of the intermediate filaments (IF) of mesenchymal cells and is frequently used as a developmental marker for cells and tissues. IFs are important structural features within the cell and along with microtubules, and actin microfilaments, make up the cytoskeleton. IF networks form a physical link between the plasma membrane and nuclear envelope of the cell (Georgatos *et al*., 1987) and have been suggested to play a role in intracellular transport and signal transduction to the nucleus. Vimentin shows a high degree of sequence homology between species (Schaffeld *et al*., 2006), indicating an important and evolutionary conserved physiological function. Essentially, vimentin is responsible for maintaining cell shape, integrity of the cytoplasm, and stabilising cytoskeletal interactions (Goldman *et al*., 1996).

VIM was chosen as a target for siRNA based on the comparative proteomic data analysis which compared protein expression in MiaPaCa-2, Clone #3 and Clone #8. VIM was expressed at higher levels in MiaPaCa-2 compared to Clone #8 (2.2-fold), VIM was 2.5-fold up-regulated in Clone #3 versus MiaPaCa-2 and in the comparison of Clone #3 versus Clone #8, VIM was 5.5-fold up-regulated. As the comparisons generated were from high to low invasion, the overall status of vimentin expression is increasing as the invasive status of the cell lines increase.

4.4.4.1 Effect of VIM siRNA in Clone #3

VIM has a long half-life of 15-17 hrs (Podolin and Prystowsky, 1991) and studies have demonstrated that siRNA targeting of proteins with a long half-life may not produce the desired phenotypic effect because silencing at the level of transcription will not affect pre-existing proteins (Pai *et al.*, 2006). However, Western blot analysis of Clone #3 cells transfected with VIM siRNA showed efficient protein knockdown.

Chiu and Goldman (1984) studied the kinetics of synthesis and protein turnover in VIM, and observed a fast-decaying pool with a half-life of 12–18 h contributed about 40% of the total activity. A major portion, about 60%, however, decayed much more slowly, exhibiting a half-life of about 8 days. This may suggest that post-translational modifications (phosphorylation) of selective vimentin pools may result in different rates of turnover. Several isoforms of VIM were identified in our proteomic analysis. Phosphorylation and reorganisation of the vimentin network have been implicated in mediating smooth muscle contraction, cell migration and cell mitosis (Li *et al.*, 2006).

Invasion assays carried out 48 hrs after VIM siRNA transfection in our high invasive cell line, Clone #3, showed a significant decrease in the total number of invading cells (Chapter 3.4.6). Studies of many carcinomas have shown that VIM expression is related to high invasion.

Gilles *et al.* (1996) showed that VIM expression *in vivo* is associated with high invasive and migratory potential in cervical carcinomas. Furthermore, VIM expression correlates with poor prognosis (Kim *et al.*, 2004) and poor survival in breast cancer (Domagala *et al.*, 1990). However, another study reported contradictory evidence, Seshadri *et al.* (1996) determined that VIM expression was associated with several features of tumour aggressiveness; yet, expression was not associated with increased in risk of relapse or death from breast cancer. Nevertheless, the consensus from literature suggests that VIM expression is related to high invasive abilities (Sommers *et al.*, 1992; Polette *et al.*, 1998). Hendrix *et al.* (1997) showed the *in vitro* invasive potential was decreased after transfection VIM antisense into MDA-MD-231, a highly invasive, VIM positive cell line. These results, along with our own, suggest VIM plays a functional role in cancer cell invasion.

The functional relationship of VIM expression in our invasive Clone #3 cells, and the epithelial to mesenchymal transition (EMT) of the malignant phenotype, was further characterised by adhesion, anoikis and proliferations assays.

Adhesion of VIM siRNA transfected Clone #3 cells to matrigel was significantly increased in two out of three independent VIM siRNA targets. These results suggest that silencing of VIM expression increases the cells ability to interact with ECM proteins. Loss of the epithelial phenotype and disruption of adhesion molecules is a hallmark in the epithelial-mesenchymal transition (EMT) reported in several types of cancer. VIM, a mesenchymal marker has been implicated in epithelial to mesenchymal transition (EMT) in pancreatic cancer (Jungert *et al*., 2007; Yang *et al*., 2006). EMT is a process initially seen in the development of the embryo, whereby cells lose epithelial characteristics and gain a mesenchymal phenotype such as increased invasion and motility. Recent research has shown that EMT may be an important factor in cancer progression; epithelial-derived tumour cells switch properties to a more mesenchymal phenotype facilitating tumour invasion and metastasis. The epithelial state is characterised by E-cadherin expression (Ozawa *et al*., 1990) and cytokeratin expression, such as cytokeratin 18 (Brabletz *et al*., 2001). Nakajima *et al*. (2004) immunohistochemically examined the expression of VIM, N- and E- cadherin in pancreatic cancer tissue specimens. In epithelial cells, the loss of E-cadherin and the increase in N-cadherin expression results in a metastatic phenotype. VIM expression was observed in a few cancer cells of pancreatic primary tumours but was substantially expressed in liver metastasis of pancreatic tumours.

McInroy and Määttä (2007) determined that cell adhesion to fibrilliar collagen was reduced in VIM siRNA transfected MDA-MD-231 cells; however, VIM knockdown did not have an effect on adhesion of SW480 cells. This suggests that the effect of VIM on adhesion may be cell specific and that cells that have retained expression of keratins could circumvent the requirement of VIM for adhesion. Bühler *et al*. (2005) transfected the human KRT18 gene into MDA-MB-231 cells, which displayed an up-regulation of adhesive proteins, dramatic reduction of *in vitro* invasion and *in vivo* tumourigenicity. Schaller *et al*. (1996) determined that elevated KRT18 protein expression indicates a favourable prognosis in patients with breast cancer. It is interesting to note, that in our proteomic analysis, Clone #8 (low invasive cell line) expressed 2.9-fold higher levels of

KRT18 compared to Clone #3 (high invasive cell line). The relationship between VIM and KRT18 was further described by Thomas *et al*. (1999), and this study concluded that dual expression of KRT18 and VIM in relative amounts characterised breast tumours with the poorest prognosis. Melanoma cells transfected with cDNAs for KRT18 and KRT8 co-expressed VIM, showed increased invasion and migration *in vitro* and displayed increased cytoskeletal interactions at focal contacts within extracellular matrices involving integrin cell signaling events (Chu *et al*., 1996).

Proliferation assays were carried out on Clone #3 transfected with three independent siRNA VIM targets. VIM transfection did not effect growth rate (Chapter 3.4.6), indicating that VIM does not play an important role in proliferation of Clone #3.

Mice homozygous for a null mutation in the VIM gene developed and reproduced without an obvious deviant phenotype. No compensatory expression of another intermediate filament could be demonstrated, suggesting VIM could play a significant role only in pathologic or unusual conditions (Colucci-Guyon *et al*., 1994). However, Eckes *et al*. (1998) determined that primary fibroblasts derived from vimentin-deficient mouse embryos displayed 40% decrease in fibroblast stiffness, reduced mechanical stability, motility and directional migration towards different chemo-attractive stimuli compared to VIM (+/+) wild-type cells suggesting that absence of VIM does not impair basic cellular functions needed for growth but have mechanical instable function.

In our study, a morphological change in Clone #3 cells after VIM siRNA transfection was observed. Cells changed from scattered fibroblast/mesenchymal type to a more epithelial tightly connected phenotype. This change in morphology is a common feature observed in mesenchymal to epithelial transition (MET) (Kokkinos *et al*., 2007). During EMT, cell-cell contact is decreased as cellular motility, invasion and skeletal rearrangement are promoted. The reorganisation of the cytoskeleton proteins within cancer cells may have significant implications in the invasion and metastasis of pancreatic cancer. Transcription factors, TWIST (Cheng *et al*., 2007) and Sp1 (Jungert *et al*., 2007) have also been associated with EMT phenotype of high VIM and low KRT18 expression. Previous studied have also linked the EMT with MMP up-regulation (Taki *et al*., 2006), down-regulation of E- cadherin and disruption of adhesion molecules (Blanco *et al*., 2004). All

these characteristics may help to further establish future potential protein markers by which aggressive invasive pancreatic cancer can be detected in early stages of malignancy. Javle *et al*. (2007) investigated whether EMT markers (low E-cadherin, high fibronectin and VIM) correlated with the activation on P13K and Ras/Erk pathways in pancreatic cancer. Fibronectin over-expression correlated with the presence of VIM and activated Erk. There was a borderline association of fibronectin with worsening grade, and a negative association between vimentin and E-cadherin was observed. Increased fibronectin or VIM and decreased E-cadherin correlated with poor survival.

In this thesis, we have investigated the effect of VIM silencing in the invasive cell line, Clone #3. We have shown that siRNA knockdown of VIM results in significant reduction of invasion through matrigel in an *in vitro* boyden chamber. Adhesion to matrigel and anoikis sensitivity is increased, and we have determined that VIM knockdown does not affect the proliferation rate of the cells. These results support the hypothesis that VIM expression is associated with a more aggressive invasive phenotype and may be also required for loss of adhesion and anoikis resistance. We conclude that targeting VIM through RNAi may potentially be effective in modulating pancreatic cancer invasion and the malignant EMT phenotype.

4.4.5 Stress-induced phosphoprotein 1

Stress-induced-phosphoprotein 1 (STIP1, Hop or Hsp70/Hsp90-organising protein) mediates the association, and forms a physical complex with the molecular chaperones Hsp90 and Hsp70 (Carrigan *et al*., 2006), which is dependent on the hydrolysis of ATP and ADP/ATP exchange. STIP1 optimises the functional co-operation for Hsp70 and Hsp90 which require highly co-ordinated interactions for the folding and conformational regulation of a variety of proteins, such as steroid hormone receptors and many other signal transduction regulators (Hernández *et al*., 2002).

STIP1 was chosen as a target for siRNA based on the comparative proteomic data analysis which compared protein expression in MiaPaCa-2, Clone #3 and Clone #8. STIP1 expression was higher in MiaPaCa-2 versus Clone #8 (1.3-fold) and 1.5-fold up-regulated

in the comparison of Clone #3 to MiaPaCa-2. STIP1 was 2.0-fold higher expressed in Clone #3 compared to Clone #8. As the comparisons generated were from high to low invasion, the overall status of STIP1 expression is increasing as the invasive status of the cell lines increase.

4.4.5.1 Effect of STIP1 siRNA in Clone #3

STIP1 protein expression was knocked down in Clone #3 cells by siRNA transfection. Forty-eight hours post-transfection of three independent STIP1 siRNA targets, invasion, adhesion, anoikis and proliferation assays were carried out to investigate the potential role of STIP1 in pancreatic cancer invasion and the malignant phenotype. Invasion was significantly reduced by all three STIP1 siRNAs in Clone #3 cells. The optimal reduction in invasion was observed with STIP1 siRNA (1), which displayed a 2.7-fold decrease in invasion of Clone #3 cells. Adhesion to matrigel was statistically significantly increased after knockdown of STIP1 protein expression in Clone #3 cells. Increased adhesion was observed in 2/3 independent STIP1 siRNAs. Anoikis sensitivity was not altered by STIP1 siRNA transfection, indicating that STIP1 did not have an effect on anoikis in Clone #3 cells. Interestingly, proliferation assays of STIP1 siRNA transfected Clone #3 cells carried out over 5 days determined that loss STIP1 effected cell growth in Clone #3 cells. Proliferation of STIP1 siRNA transfected cells reduced the growth rate between 13-27% signifying a role for STIP1 in pancreatic cancer cell proliferation.

The molecular chaperone complex of Hsp70, Hsp90 and STIP1 is involved in the folding and maturation of key regulatory proteins, like steroid hormone receptors, transcription factors, and kinases, some of which are involved in cancer progression. The connection and interplay between these complexes is of crucial importance for cell viability (Wegele *et al.*, 2004). There is increasing evidence that heat shock proteins play an important role in the development, maintenance and progression of cancer (Pick *et al.*, 2007).

Heat shock proteins (Hsp) are highly conserved molecules, which protect cells from various environmental damages, including stress and carcinogenesis (Lindquist, 1986). Heat shock proteins are activated by the ubiquitin-proteasome pathway. The covalent attachment of ubiquitin to protein regulates a number of cellular processes including responses to stress. This process is responsible for selective targeting of proteins for

degradation. The ubiquitin-proteosome pathway (UPP) can regulate expression of MMPs and their tissue inhibitors (TIMPs) in some tissues (Ikebe *et al.*, 1998). The induced HSPs play roles as cellular chaperones, and many modulate apoptotic pathways, particularly those involving mitochondria, conferring protection from stressful stimuli including chemotherapeutic agents.

The role of STIP1 in cancer invasion is currently unknown; however increasing evidence is emerging for the role of heat shock proteins in cancer progression. Ogata *et al.* (2000) examined the expression of Hsp90 and its relationship to pancreatic cancer by IHC, *in situ* hybridisation and RT-PCR. mRNA of Hsp90 was over-expressed in pancreatic tumour samples compared to control tissues, and Hsp90 expression correlated with pancreatic cancer proliferation. Eustace *et al.* (2004) showed that Hsp90α interacts with MMP-2 in the extracellular compartment of the cell. Inhibition of the extracellular Hsp90α decreases MMP-2 activity and invasiveness. Hsp90s association is required for the stability and function of multiple mutated, chimeric and over-expressed signalling proteins that promote cancer cell growth and/or survival. Hsp90 client proteins include mutated p53, Bcr-Abl, Raf-1, Akt, HER2 (ErbB2) and hypoxia inducible factor-1alpha (HIF-1alpha) (Powers and Workman, 2006).

Hsp70 is an anti-apoptotic protein (Jaattela *et al.*, 1998) and is over-expressed in breast, (Larazis *et al.*, 1997) lung (Bonay *et al.*, 1994), colorectal (Larazis *et al.*, 1995) and pancreatic cancer (Gress *et al.*, 1994), and the level of Hsp70 expression correlates with poor clinical outcome in certain cancers (Ciocca and Calderwood, 2005). Hsp70 increases tumourigenicity and inhibits apoptosis in pancreatic cancer (Aghdassi *et al.*, 2007). Havik *et al.* (2007) investigated the impact of Hsp70 protein expression and its close family member, Hsc70, on breast cancer cell viability and on the activity of the STIP1 (Hsp90/Hsp70) chaperone complex. Simultaneous blocking of Hsp70, Hsc70 and Hsp90 reduced breast cancer cell viability. Alone Hsp90 inhibition also displayed low cell viability and reduced Hsp70/Hsp90 chaperone complex activity; however, the single or mixed reduction in Hsp70 and Hsc70 expression displayed no ability to reduce the activity of the Hsp90/Hsp70 chaperone complex. Therefore, targeting the Hsp70/Hsp90 family shows greater effect on cancer cell survival, even though their pathways of action are separate. Recently, modulators of chaperone activities introduced an emerging field of

drug development. Inhibitors of Hsp70's sister chaperone Hsp90, such as 17-AAG, exhibit a broad spectrum of anti-tumour activity and appear promising in clinical trails (Neckers and Neckers, 2005).

Our findings determine that STIP1 has a functional effect in invasion and adhesion of Clone #3 to matrigel. Functional knockdown of STIP1 failed to induced anoikis sensitivity; however, there is little evidence in literature connecting Hsp activation and anoikis. Interestingly, loss of STIP1 affected proliferation, indicating that STIP1 chaperone activity is required for pancreatic cancer cell growth.

4.5 Analysis of effects of CM#3 and CM#8 on MiaPaCa-2 and sub-populations Clone #3 and Clone #8

Serum-free conditioned media (CM) collected from Clone #3 and Clone #8 was added into the Boyden chamber invasion assay to assess whether secreted factors produced from the cells contained in the media would have an effect on invasion. CM#3 significantly enhanced the relative level of invasion of MiaPaCa-2, Clone #3 and Clone #8, whereas in contrast CM#8 decreased the invasion of MiaPaCa-2 and Clone #3. No obvious decrease in invasion was observed in Clone #8, as the cells invade at very low levels, therefore, it was difficult to detect a significant reduction in invasion. Adhesion assays showed that incubation of CM#3 with MiaPaCa-2, Clone #3 and Clone #8 had no effect on adhesion to matrigel; this affect was not altered by addition of CM#8, however, a significant increase in adhesion was observed in Clone #8 cells incubated with CM#8. Anoikis was also not stimulated in the cells by CM#3 exposure, and CM#8 incubation only statistically reduced anoikis resistance in Clone #3 cells. It is evident from these results that factors secreted in CM#3 and CM#8 can affect invasion and to a lesser extent adhesion and anoikis.

We suggest that factors secreted into the CM#3 and CM#8 augment the cell-ECM contact and the invasive potential of the cells studied. To address this comment, the parental cell line, MiaPaCa-2 was incubated with CM#3 and CM#8 for 24 hrs prior to invasion assay. Invasion of MiaPaCa-2 was stimulated with preincubation of CM#3 and inhibited with

preincubation of CM#8. These results show that the factors secreted in the CM of both Clone #3 and Clone #8 are potentially capable of interacting with the proteins on the cell surface, and once secreted into the extracellular media, may induce a series of molecular events leading to modulation of the invasive abilities of the cells. We further demonstrated that preincubation of MiaPaCa-2, Clone #3 and Clone #8 with matrigel (reconstituted ECM) in the presence of CM#3 showed higher invasive abilities compared to exposure to CM#3 alone and induced a phenomenon termed 'superinvasion'. In contrast, exposure of the cells to matrigel in the presence of CM#8 effectively reduced the invasion, however, superinvasion was still observed. During normal *in vitro* invasion, cells invade to the underside of the invasion chamber and are stained at this point, however during 'superinvasion', a large proportion of the cells, invade through the underside of the chamber and attach to the bottom of the 24-well plate. This phenomenon of superinvasion, first described by Glynn *et al*. (2004), whereby doxorubicin- and paclitaxel-selected variants of an *in vitro* invasive clonal population of the human breast cancer cell line, MDA-MB-435S, were established by pulse selection, and exhibited a novel 'superinvasive' phenotype. This phenotype was characterised by an ability to relocate to another surface following invasion through matrigel and membrane pores, by decreased adhesion to extracellular matrix proteins and by increased motility.

The occurrence of further increased invasion and superinvasion after exposure of the cell lines to matrigel for 24 hrs prior to invasion assays shows that the cell-ECM contact stimulates the invasive potential of MiaPaCa-2, Clone #3 and even the low invasive cell line, Clone #8. The stimulatory invasive effects of CM#3 were further enhanced when combined with cells incubated with matrigel, suggesting that the factor(s) secreted in CM#3 interact with cell-matrigel contact. The invasive inhibitory effects of CM#8 in combination with cells exposed to matrigel, was not sufficient to eradicate invasion or superinvasion completely, and only a modest reduction was observed. These results suggest that cell-ECM contact may induce important modulations within the cells, creating a highly invasive, superinvasive phenotype. Addition of CM#3 further transformed the invasive and superinvasive abilities of the cells, whereas CM#8 modestly decreased invasion and superinvasion of the cells similar to that observed in cells exposed to matrigel in the presence of control media. Interaction of the cells with matrigel may

represent an *in vitro* model for a step in the metastasis process subsequent to invasion, and hence may lead to a better understanding of the metastatic process.

Recent studies have identified that many cancer types can secrete cytokines and growth factors to stimulate proliferation and tumourigenesis. The protein, melanoma inhibitory activity (MIA) is correlated with tumour progression and development of metastatic disease. MIA, secreted by melanoma cells, is known to inhibit tumour cell attachment to the extracellular matrix enhancing their invasive potential (Callejo *et al*., 2004). Barak *et al*. (2007) determined that elevated serum osteopontin (OPN), S-100beta and MIA levels correlate with metastatic uveal melanoma (UM) to the liver. OPN is over-expressed in metastatic UM, while S-100beta and MIA serum levels are elevated in metastatic cutaneous melanoma. In combination, these markers provide a highly sensitive and specific method to detect hepatic metastases and therefore provide for earlier therapeutic intervention that can prolong survival.

Tumour cells secreting invasion or tumourigenic inhibitory factors are of critical importance. Butt *et al*. (2003) determined the effect of the insulin-like growth factor-binding protein (IGFBP)-5 in human breast cancer *in vivo* and *in vitro*. Expression of IGFBP-5, both by stable transfection and adenoviral-mediated infection, was inhibitory to the growth of human breast cancer cell lines over a 13-day period. Secreted IGFBP-5 when added exogenously to breast cancer cells was not internalised and had no effect on cell growth or apoptosis, suggesting that IGFBP-5 may elicit its inhibitory effects via a novel, intracrine mechanism.

WISP3 (WNT-1 inducible signalling pathway protein 3) is secreted into the CM of human inflammatory breast cancer (IBC). Once secreted, WISP3 decreases directly or through induction of other molecules the IGF-1-induced activation of the IGF-IR, and two of its main downstream signalling molecules IRS1 and ERK-1/2, in SUM149 IBC cells. WISP3 is lost in 80% of human IBC tumours and it has growth- and angiogenesis-inhibitory functions in breast cancer *in vitro* and *in vivo*. Furthermore, WISP3-containing conditioned media decreased the growth rate of SUM149 cells. WISP3 can modulate IGF-IR signalling pathways and cellular growth in IBC cells (Kleer *et al*., 2004).

The results presented here clearly show that exposure of pancreatic cancer cells to exogenous factors secreted in the CM could potentially inhibit or enhance *in vitro* invasion. In general, CM can undergo compositional changes throughout cell cultivation, therefore several characteristic experiments were carried out to determine the stability of the unknown factor(s) in the CM. Varying the storage conditions determined that both CM#3 and CM#8 retained their enhancement/inhibitory affects on MiaPaCa-2 more effectively at -80 ^{0}C. The ability to dilute the effects of CM#3 and CM#8 in the invasion assays were determined by serially diluting CM#3 and CM#8 with normal media and observing the effects on invasion of the parental cell line, MiaPaCa-2. The optimal dilution factor for both CMs was determined as 1:4, after this dilution point the effects of the CM were no longer observed.

To detect the optimal pH of the factor(s) exhibiting altered affects on invasion in CM#3 and CM#8, the CMs were exposed to differing pHs for 2 hrs at room temperature and then brought back to pH ~7 (the original pH). Invasion assays using these CM #3 pH fractions showed that invasion was optimal at pH 5 for the enhancement factor in CM#3 compared to normal media under the same conditions. These results suggest that a lower pH is more favourable to induce invasion. In contrast, CM#8 exhibited optimal inhibitory effects on invasion of MiaPaCa-2 at pH 9-11 compared to control media under the same conditions, suggesting alkaline conditions have a favourable effect. These findings are in agreement with Kato *et al.* (1992); this study examined the effect of culture medium pH on the secretion of gelatinases from both murine melanoma and human tumour cell lines. Gelatinases were not secreted at neutral pHs but at lower pH range of 5.4-6.1, secretion of a 103 kDa gelatinase was observed. *In vitro* invasion assays showed that cells incubated in an acidic medium exerted more active migration through collagen type IV than those in a neutral medium. These results in conjunction with our own, suggest that an acidic environment around tumour cells may be an important factor in invasion and metastasis of some cell lines. It is well established that tumours consistently rely on anaerobic pathways to convert glucose to ATP even in the presence of abundant oxygen, resulting in increased tumour cell acid production. Tumour cells evolve resistance to acid-induced toxicity during carcinogenesis, allowing them to survive and proliferate in low pH microenvironments. This permits them to invade the damaged adjacent normal tissue

313

despite the acid gradients (Gatenby *et al.*, 2006). Extracellular pH (pH(e)) is lower in many tumours than in the corresponding normal tissue. Melanoma cells cultured at acidic pH(e) showed increased secretion of proteinases and proangiogenic factors, enhanced invasive and angiogenic potential, and enhanced potential to develop experimental metastases (Rofstad *et al.*, 2006).

The approximate molecular weight range of the factor(s) involved in CM#3 and CM#8 were determined by concentration of the CMs into fractions of below 10 kDa, between 10-30 kDa, 30-50 kDa, 50-100 kDa and above 100 kDa. Invasion assays of Clone #3 cells with the addition of the molecular weight fractions from CM#3 showed that the highest level of enhanced invasion was observed at high molecular weight of between 50-100 kDa and above 100 kDa; interestingly, the lower molecular weight fractions (below 10 kDa and 10-30 kDa) of CM#3 had an inhibitory effect on invasion of Clone #3 cells. Invasion was optimally reduced in Clone #3 cells with the lower molecular weight fractions of CM#8 (below 10 kDa and 10-30 kDa); in contrast, invasion was also increased at the high molecular weight fractions of CM#8. These results suggest that the enhancement factor of invasion secreted by Clone #3 in CM#3 is isolated in the higher molecular weight fractions, whereas the inhibitory factor of invasion secreted by Clone #8 in CM#8 is contained in the lower molecular weight fractions. The fact that both CMs have opposite enhancement and inhibitory effects at different molecular weight fractions could be possibly explained by the fact that the cells originate from the same parental cell line, and therefore may secrete similar factors into the CM. The effects of these secreted factors on invasion may be due to their relative secreted abundance within the conditioned media and isolation of fractions from CM#3 and CM#8 may in fact concentrate factors that may otherwise be very low in abundance in the CMs.

In summary, we present evidence that "hypothetical factor(s)" secreted into the media from Clone #3 and Clone #8 modulates the invasive abilities of the cells when co-cultured with the CM. The pre-incubation of cells with matrigel in the presence of CM#3 further enhanced the *in vitro* invasion and increased superinvasion, in the presence of CM#8 invasion and superinvasion were modestly reduced similar to control experiments.

Furthermore, characterisation of this 'factor' revealed an optimal storage condition of -80 °C with a maximum diluent ratio of 1:4 with fresh media. The factor(s) secreted into CM#3 were found to behave more aggressively at lower pH ranges with a higher molecular weight, in the range of between 50-100 kDa and above 100 kDa, while analyses of the secreted 'factors' in CM#8 revealed the inhibitory effects are more favourable with alkaline pHs with a lower molecular weight (mass range below 10 kDa and between 10-30 kDa).

At present, we can only speculate to the potential clinical and therapeutic benefit of the role of secreted factors in CM#3 and CM#8 in pancreatic cancer invasion and metastasis progression. Recently, Ramachandran *et al*. (2007) identified adrenomedullin as a potential secreted autocrine regulator of pancreatic cancer cell line function. Exogenous adrenomedullin treatment of Panc-1, BxPC3, and MPanc96 cells *in vitro* stimulated cell proliferation, invasion, and nuclear factor kappaB activity, indicating the ability of the cells to respond to adrenomedullin. Treatment of the cell cultures with an adrenomedullin antagonist inhibited basal levels of proliferation and nuclear factor kappaB activity, supporting the autocrine function of this molecule. Furthermore, increasing adrenomedullin levels by gene transfer to Panc-1 cells increased, whereas adrenomedullin small hairpin RNA silencing in MPanc96 cells inhibited, tumour growth and metastasis *in vivo*. Adrenomedullin acts through at least two different receptors, including adrenomedullin receptor (ADMR) and calcitonin receptor-like receptor (CRLR). Pancreatic cancer cell lines only express ADMR, as determined by Reverse transcription-PCR and Western blotting. However, cells found in the tumour microenvironment, such as primary human pancreatic stellate and endothelial cells, expressed both ADMR and CRLR. Silencing of ADMR in pancreatic cancer cells by shRNA blocked adrenomedullin-induced growth and invasion, demonstrating that this receptor is involved in the autocrine actions of adrenomedullin. This data indicates that adrenomedullin acts via ADMR increasing the aggressiveness of pancreatic cancer cells and suggests that these molecules may be useful therapeutic targets.

Further analysis and identification of the secreted functions in CM#3 and CM#8 may lead to the development of novel biomarkers or therapeutic targets for pancreatic cancer.

4.6 Proteomic profiling of conditioned media from CM Mia, CM#3 and CM#8

The malignant progression of invasive and metastatic pancreatic cancer is a complex and poorly understood process. In this study, we established the proteomic profile of proteins secreted into the media from pancreatic cancer cell lines with varying invasive and malignant transformation characteristics. Identification of secreted proteins from cell lines could be an important step toward discovering molecular markers of invasion in pancreatic cancer and could potentially form the basis for diagnosis and treatment prognosis. Theoretically, proteins secreted by tumour cells are more likely to be detected easily in bodily fluids such as urine, blood serum and pancreatic ductal juice. Therefore, secreted proteins and their metabolites found *in vivo* could represent a panel of potential bio-markers.

4.6.1 Generation of protein lists

In this study, secreted proteins were obtained from culture of MiaPaCa-2, Clone #3 and Clone #8 in serum-free conditions (SF). Cells were first allowed to attach under normal conditions, and once appropriately confluent, cells were adapted to SF conditions for 48 hrs. SF conditions have the advantage of reducing the abundance of bovine proteins in the samples. Three comparative lists of differentially secreted proteins between CM Mia versus CM #8, CM #3 versus CM Mia and CM #3 versus CM #8 were established. Bio-informatic analysis (GO STAT and pathway studio) was applied to all differentially secreted proteins between our pancreatic cancer CM model. Gene ontology (GO STAT) classified the differentially secreted proteins and their corresponding genes into gene categories. Although membrane-bound and extracellular proteins are more likely to be cleaved and found in the circulation (Kulasingam and Diamandis, 2007), our GO STAT analysis determined that most up-regulated and down-regulated proteins were involved in the cytoplasm. However, secreted heat shock proteins and actins, generally viewed as cytoplasmic markers, increasingly have been implicated in extracellular functions. Altmeyer *et al*. (1996) showed that gp96 (protypical Hsp) normally resides in the lumen of the endoplasmic reticulum (ER), however a significant proportion of intact gp96 molecule

is expressed on the cell surface and that this surface expression is not a result of gp96 from dead cells. Cell surface expression of gp96 is enhanced by heat shock and exposure to reducing agents suggesting that gp96 and perhaps other HSPs are anchored to the cell surface as part of larger molecular complexes, which also transport them to the cell surface. Wang *et al*. (2004) showed that beta-actin is present on the extracellular membranes of some cancer cells and can mediate plasmin binding to the cell surface and autoproteolysis to angiostatin 4.5 (a naturally occurring human angiostatin isoform).

Eukaryotic protein secretion normally routes through the endoplasmatic reticulum (ER) and Golgi, ending up in a secretory vesicle fusing to the cell membrane. Studies have shown that the non-classical secretory pathway works independently of the ER–Golgi network; the secreted proteins do not enter the ER and have not been glycosylated (Bendtsen *et al*., 2004). Non-classical secretion of proteins was verified by Tanudji *et al*. (2002), whereby the cytosolic green fluorescent protein (GFP) was secreted by cell lines experimentally, as export was not hampered by inhibitors of the classical secretory pathway, such as monensin and brefeldin A.

Therefore, it is feasible to include these cytoplasmic proteins as potential secreted bio-markers in our study.

4.6.2 Invasion specific proteins chosen for siRNA functional analysis

The greatest fold difference between secreted proteins was observed in the comparison of CM#3 versus CM#8, and as CM from these cell lines produced an effective inhibitory/enhancement of invasion (Chapter 3.5), we decided to concentrate primarily on this comparison for functional analysis.

Four proteins were chosen for secretion validation in CM Mia, CM#3 and CM#8 by Western blot analysis. Gelsolin (GSN), nucleoside diphosphate kinase (NDPK) and aldehyde dehydrogenase 1A1 (ALDH1A1) correlated with proteomic data. Galectin-1 (GAL-1) secretion did not correlate with fold difference determined by proteomic profiling; this may have been due to many reasons such as unspecificity of antibody or the low fold difference between CM#3 and CM#8 (1.3-fold).

Two secreted proteins, GSN and ALDH1A1, were chosen for siRNA silencing based on specificity to invasion, relevance to cancer/invasion in the literature, fold difference and *p*-

value. Table 4.6.1 summarises fold difference between each comparison to the chosen target proteins.

Table 4.6.1 Proteins differentially secreted between CM#8 and CM#3 chosen for further analysis

Protein	Description	CM#8 vs CM Mia	CM Mia vs CM#3	CM#8 vs CM#3
GSN	Gelsolin isoform b (a)	2.6	8.0	21.0
ALDH1A1	Aldehyde dehydrogenase 1A1	-11.4	-6.3	-21.0

4.6.3 Gelsolin (GSN)

GSN is a calcium-binding protein which binds to and regulates actin filaments. GSN binds to the barbed ends of actin filaments and prevents capping (Kumar *et al*., 2004). Severing and capping of actin filament enhances the rate of cell motility and migration (Cunningham *et al*., 1991). Gelsolin is located intracellularly in the cytoplasm and mitochondria (Koya *et al*., 2000) as well as extracellularly in the blood plasma (Chaponnier *et al*., 1979). The intracellular form termed cytoplasmic, and the secreted form termed plasma GSN are derived from a single gene by alternative transcription initiation sites and differential sequencing (Kwiatkowski *et al*., 1988). Plasma GSN differs to cytoplasmic GSN, in that it is larger (93 kDa and 90 kDa, respectively), contains 25 extra amino acids at its NH_2 terminus, and is more positively charged (Kwiatkowski *et al*., 1986). Yin *et al*. (1984) determined plasma GSN is more highly labelled relative to cytoplasmic GSN, suggesting that it is synthesised more rapidly or catabolised more slowly. Plasma GSN is removed from the cells more rapidly, consistent with a secreted protein, and only the plasma form of GSN is secreted in HepG2, a human hepatoma-derived cell line.

GSN was chosen as a target for siRNA based on the comparative proteomic data analysis, which compared secretion of proteins in the conditioned media of MiaPaCa-2, Clone #3 and Clone #8. GSN was secreted at lower levels in all three lists (CM Mia vs CM #8 (-2.6-fold), CM #3 vs CM Mia (-8.0-fold) and CM #3 vs CM #8 (-21-fold)). Therefore,

secretion of GSN is highest in the low invasive cell line, Clone #8, and lowest in Clone #3.

4.6.3.1 Effect of GSN siRNA in CM#8

RNAi technology was used to study GSN protein secretion in CM#8. Using two independent GSN siRNA target sequences, GSN protein expression was specifically down-regulated in Clone #8 cells, resulting in decreased secretion of GSN. The role of secreted GSN in invasion was investigated in Clone #8 cells by addition of GSN siRNA transfected CM#8 into the invasion chamber. Invasion of Clone #8 was increased after addition of GSN siRNA CM#8; however, only one siRNA GSN showed a statistically significant increase in invasion. The high standard deviations between triplicate repeats may be due to the inherent unevenness of Clone #8 cell invasion, it is possible that GSN was not knocked down efficiently enough to observe complete invasion. This may be as a result of the high proportion of secreted GSN in CM#8, as in order to observe optimal reduction of GSN secretion by Western blot in CM#8, the total amount of protein loaded had to be reduced to 5 μg of total protein. This suggests that GSN is highly secreted in CM#8.

To address this issue, the level of cytoplasmic GSN was determined by Western blot. MiaPaCa-2 and Clone #3 showed no detectable levels of GSN expression, while Clone #8 expressed low levels of GSN. However, after incubation on matrigel for 24 hrs the expression of GSN was increased further in Clone #8 cells. This finding suggests that GSN expression is up-regulated due to Clone #8 cell-matrigel contact. Invasion assays of siRNA GSN transfected Clone #8 cells showed that loss of cytoplasmic GSN significantly increased invasion in both siRNA targets.

Our results suggest that both plasma and cytoplasmic GSN have functional effects on invasion in Clone #8 cells. We showed that cytoplasmic GSN was up-regulated after cell-matrigel contact. We confirmed that silencing secreted GSN in CM#8 was not sufficient to completely increase invasion as the cells in the invasion assays highly express cytoplasmic GSN when in contact with an extracellular matrix. Targeting cytoplasmic GSN by siRNA was sufficient to statistically increase invasion.

Decreased expression of cytoplasmic GSN has been shown in several types of human cancers, including urinary bladder carcinogenesis (Tanaka *et al*., 1995), NSCLC (Dosaka-Akita *et al*., 1998), prostatic adenocarcinoma (Lee *et al*., 1999) and breast (Winston et al., 2001) suggesting a possible role as a tumour suppressor. Noske *et al*. (2005) determined that reduced expression of GSN in 75 ovarian carcinoma specimens was significantly associated with a high tumour grade; this study also showed that up-regulation of GSN in ovarian cancer cell lines, OAW42 and ES-2 reduced tumour colony formation. Our studies suggest that the inhibitory invasive effects of CM#8 may be in part due to GSN secretion and are in agreement with the above findings. Sagawa *et al*. (2003) suggested that GSN expression suppresses the activation of phospholipases C (PLC)/protein kinase C (PKCs) involved in phospholipid signalling pathways, thus inhibiting cell proliferation and tumourigenicity. Furthermore, Tanaka *et al*. (2006) functionally knocked down GSN expression by siRNA in the human mammary epithelial cell line, MCF10A, and suggested that GSN functions as a switch that controls E- and N-cadherin conversion via Snail, and demonstrated that its knockdown led to EMT, characterised by fibroblastic morphology, loss of contact inhibition, focus formation in monolayer growth and enhanced motility and invasiveness *in vitro*. Therefore, silencing GSN expression could possibly lead to the development of human mammary tumours.

However, Thor *et al*. (2001) determined the GSN over-expression in 56% of breast cancers was associated with the over-expression of EGFR and HER2, as well as a more aggressive phenotype. High GSN levels have also been identified as a negative prognostic factor in pulmonary carcinomas, stage I non-small cell lung carcinomas (Shieh *et al*., 1999), where they have been linked to enhanced cellular motility.

Several studies have implicated GSN in regulating cell motility. Thompson *et al*. (2006) showed the over-expression of GSN in pancreatic cancer cells and demonstrated that reducing the level of GSN decreases the motility of pancreatic cancer cell lines, suggesting the marked up-regulation of motility-modulating actin-capping proteins in pancreatic cancer cells may have important consequences for the motility and consequently the dissemination of these cells.

GSN secreted in the plasma has an actin-scavenging function, and its level has been shown to be reduced in response to increase tissue injury and hepatocellular carcinoma, possibly due to an increase in binding and clearance of shed actin (Ito *et al.*, 1992). Orchekowski *et al.* (2005) revealed through antibody microarray profiling of combined serum proteins associated with pancreatic cancer a significant reduction of plasma GSN in pancreatic cancer serum. Okano *et al.* (2006) also confirmed the decrease of plasma GSN expression in lung cancer serum by proteomic profiling.

In conclusion, the results presented here clearly determine that both cytoplasmic and plasma GSN have a role in the invasive potential of pancreatic cancer. GSN may have a role as a functional bio-marker for the early detection of invasive/metastatic pancreatic cancer.

4.6.4 Aldehyde dehydrogenase 1A1 (ALDH1A1)

ALDH1A1 as previously discussed in Chapter 4.4 was chosen as a target for siRNA as proteomic profiling revealed its secretion highly up-regulated in the CM of the more invasive cell line, Clone #3. ALDH1A1 is highly secreted in CM Mia compared to CM#8 (11.4-fold) and in the comparison of CM#3 compared to CM Mia (6.3-fold change). The comparison of CM#3 versus CM#8 showed a 21.0-fold up-regulation of ALDH1A1 secretion in CM#3. The secretion of ALDH1A1 is higher in the invasive cell line Clone #3.

Secreted ALDH1A1 expression was reduced in CM#3 through siRNA sequence targeting of three independent sequences of the ALDH1A1 gene. Addition of ALDH1A1 siRNA transfected CM#3 into the invasion chamber significantly reduced invasion of Clone #3 cells. These findings along with our previous analysis of cytosolic ALDH1A1 suggest that both secreted and cytosolic ALDH1A1 have an important role to play in pancreatic cancer invasion.

No literature is available on the occurrence or incidence of secreted ALDH1A1 in serum of cancer patients or conditioned media of cancer cells. Therefore, we can only speculate

on its involvement in the pancreatic cancer invasion cascade. The cytosolic form of ALDH1A1, expressed in high levels intracellularly, could possibly be secreted into the media by active diffusion or transport.

In summary, identification of secreted proteomes from cancer cell lines may serve as an ideal and efficient method in the establishment of a panel of potential bio-markers correlating to invasion/metastatic cascade of pancreatic cancer. The non-invasive detection of bio-markers may be useful for clinical application in early diagnosis and prognosis of pancreatic cancer.

4.7   Role of EGFR and HER2 in pancreatic carcinoma

Tyrosine kinase growth factor receptors and their ligands act to influence tumour cell growth, differentiation, invasion, metastasis and angiogenesis. EGFR over-expression occurs in 30% to 50% of pancreatic ductal adenocarcinomas and over-expression is thought to often confer a poor prognosis in several malignancies (Garcea *et al.*, 2005). It often correlates with poorly differentiated histology and a more advanced stage.

Increased expression of HER2 has also been observed in pancreatic adenocarcinoma. Over-expression is more common in well and moderately differentiated tumours compared to poorly differentiated and anaplastic tumours. The oncogene HER2 is over-expressed in 50-70% of pancreatic cancer cases (Bũchler *et al.*, 2002). Therefore, an agent against the combination of EGRF/HER2 is a tempting target for therapeutic strategy in pancreatic cancer.

Lapatinib is a reversible, dual EGFR/HER2 tyrosine kinase inhibitor. *In vivo* and *in vitro*, lapatinib has inhibited EGFR and HER2 phosphorylation, resulting in decreased activation and phosphorylation of Erk-1/2 and Akt (Xia *et al.*, 2002). Lapatinib has shown clinical activity in cancers resistant to agents targeted at ErbB receptors. Patients resistant to gefinitib or herceptin, experienced minor-partial response to lapatinib treatment (Burris *et al.*, 2003; Blackwell *et al.*, 2004).

The analysis method of Chou and Talalay was used in this study to calculate the median effect and the combination index (CI) equation. The CI method is based on the median-effect equation, which correlates the drug dose and the cytotoxicity or cytostatic effect (Chou and Talalay, 1984). The drugs used in this study have "mutually nonexclusive" mechanisms of action (i.e., drugs that are non-competitive inhibitors of each other). The CalcuSyn program automatically analyses the data and the CI equation determines the additive effect of the drug combinations. Synergism is defined as a greater than expected additive effect.

CI < 0.8 indicates synergism, CI > 0.8 but < 1.2 indicates an additive effect and CI > 1.2 indicates antagonism. The CI values are presented for each effective dose (ED) tested, (e.g., ED25, ED50 and ED75) because the CI values may change with the fraction affected in a non-linear manner (Reynolds and Maurer, 2005). ED is the minimal dose that produces the desired effect of a drug. The effective dose is determined based on analysing the dose-response relationship specific to the drug. The dosage that produces a desired effect in half the test population is referred to as the ED-50, for "Effective Dose, 50%".

This study details quantitative interactions between lapatinib and four different chemotherapeutic drugs: cisplatin, gemcitabine, taxotere and 5'dFUrd. BxPc-3 and KCI-MOH1, two pancreatic cancer cell lines that expressed both EGFR and HER2, were tested in combination with lapatinib and the cytotoxic drugs. Analysis of the scheduling regime identified that pre-incubation of lapatinib 24 hrs prior to chemotherapy was more efficient than using the combination together. Wakeling *et al*. (2002) determined that pre-incubation with gefitinib prior to EGF treatment inhibited autophosphorylation of EGFR TK in a dose-dependent manner in human tumour cell lines from lung, prostate, colon, and head and neck cancers and these results correlated with inhibition of tumour xenograft growth *in vivo*.

Lapatinib was added to the cells 24 hours prior to the addition of cytotoxic drugs, this was to ensure the EGFR/HER2 inhibitory effects of lapatinib were maximised. Fixed ratio analyses of drug interactions were calculated. Accurate dose-response curves for lapatinib and the chemotherapeutic drugs both alone and in combination was generated. Synergy,

additivity and antagonism were quantified at different concentrations and effect levels, whereby, the maximum anti-tumour efficacy of the combination was determined.

4.7.1 Combination of lapatinib and cisplatin

In our study, a synergistic to additive interaction was observed between cisplatin and lapatinib in both EGFR/HER2 expressing cell lines, BxPc-3 and KCI-MOH1 at ED25-50. These results suggest that toxic effects of the lapatinib and cisplatin combination are further enhanced compared to either drug alone. Recent studies have supported this observation; McHugh *et al*. (2007) demonstrated a synergistic effect with the combination of lapatinib, gemcitabine and cisplatin regime in two bladder cancer cell lines, expressing high levels of EGFR/HER2 (RT112) and low levels of EGFR/HER2 (J82). Results showed that lapatinib reduced cell viability in both cells lines in a dose-dependent manner, and the IC_{50} results for both cell lines to lapatinib were similar irrespective of their EGFR/HER2 expression level. In both cases, addition of lapatinib before or during gemcitabine and cisplatin treatment was optimal and resulted in a synergistic effect. Coley *et al*. (2006) showed that the RTK inhibitor GW282974A (an analogue of GW2016; lapatinib) is synergistically effective in combination with cisplatin in platinum resistant, EGFR over-expressing ovarian cancer cell lines. A reduction in the downstream signalling effector phosphorylated ERK was observed when the combination was applied to the cells.

This data, in conjunction with our own work suggests that dual EGFR/HER2 inhibition in combination with cisplatin is effective in the chemosensitisation of cancer cell lines.

Baselga *et al*. (2000) reported responses in patients with head-and-neck cancer treated with erbitux (an anti-EGFR antibody) and cisplatin. The interactions between anti-EGFR antibodies and cisplatin may be due to inhibition of DNA repair mechanisms, alteration in paracrine growth factor production and promotion of apoptotic cell death (Fan and Mendelson, 1998). Tanaoka *et al*. (2007) investigated the effects of combining an anti-EGFR monoclonal antibody (C225) or an EGFR-selective tyrosine kinase inhibitor (AG1478) with cisplatin on the oral SCC (OSCC) cell lines, NA and Ca9-22. OSCC cell proliferation was inhibited by C225, AG1478 and cisplatin in a dose-dependent manner.

The combination of C225 or AG1478 with cisplatin at concentrations <IC_{50} synergistically inhibited cell proliferation and induced apoptosis in these cells. Furthermore, treatment with C225 or AG1478 OSCC reduced phosphorylation of EGFR and Akt, as well as Bad. EGFR inhibitors down-regulated expression levels of the anti-apoptotic proteins cellular IAP-1 (cIAP-1), X-linked IAP (XIAP), Bcl-2 and Bcl-xL, whereas those of the pro-apoptotic proteins Bax and Bak were up-regulated. EGFR inhibitors provide partial regulation of cisplatin-mediated apoptosis in OSCC cells by modulating expression of cIAP-1, XIAP, Bcl-2, Bcl-xL, Bax and Bak.

4.7.2 Combination of lapatinib and gemcitabine

Our finding show that on average, there was an additive interaction between gemcitabine and lapatinib in both cell lines, BxPc-3 and KCI-MOH1 at ED25-75. However, at low combination effective doses (ED25) in BxPc-3 cells, there is a synergistic interaction (CI value, 0.79 ± 0.23). This may suggest that dosage and treatment regime may be critical in the treatment of pancreatic cancer with lapatinib and gemcitabine combinations.

Baerman *et al*., (2005) studied the biochemical and biological impact of lapatinib in pancreatic cancer cell lines. All cell lines were shown to variably express EGFR, HER2, and HER3, while HER4 mRNA levels were lower than other EGFR family members. Lapatinib inhibited anchorage-dependent growth in all cell lines and markedly inhibited EGF or heregulin initiated phosphorylation of Akt and 44/42 MAPK. This study concluded that lapatinib inhibits EGFR dependent proliferation and anchorage-independent colony formation in pancreatic cancer cell lines through inhibition of MAPK and Akt pathways. A recent two-stage, phase I evaluation of lapatinib, gemcitabine and lapatinib, gemcitabine and oxaliplatin (GEMOX) resulted in dramatic responses in patients with diffuse liver and peritoneal metastases; this study suggests that EGFR/HER2 signaling is important in pancreaticobiliary cancers (Safran *et al*., 2006). Currently, Safran and colleagues are recruiting for a phase II study of lapatinib and gemcitabine for patients with metastatic pancreatic cancer.

EGFR inhibition has become an important target in pancreatic carcinoma. Buchsbaum *et al*. (2002) treated pancreatic cancer xenografts with erbitux, an anti-EGFR antibody,

gemcitabine and radiation. This study showed the combination had significantly greater efficacy over single or double therapies. Erbitux and gemcitabine has previously shown to inhibit human pancreatic xenografts in subcutaneous or orthotopically in nude mice and reduce metastases (Overholser *et al*., 2000; Bruns *et al*., 2000).

Feng *et al*. (2006) reported that treatment with gemcitabine stimulates phosphorylation of EGFR. As phosphorylation of EGFR is known to precede receptor degradation, gemcitabine treatment resulted in EGFR degradation. In two human head and neck cancer cell lines, UMSCC-1 and UMSCC-6, an approximately 80% decrease in total EGFR levels at 72 h after a 2-h treatment with gemcitabine was demonstrated. Neither cisplatin nor 5-fluorouracil, which are used to treat head and neck cancer, caused EGFR degradation. EGFR down-regulation did not occur at the level of transcription, as assessed by RT-PCR, but instead occurred via phosphorylation and ubiquitination of the receptor along a proteosome/lysosome-mediated pathway. Inhibition of EGFR degradation, by either pretreatment with the EGFR tyrosine kinase inhibitor, gefitinib or by exposure to the proteosome/lysosome inhibitor MG132, significantly reduced gemcitabine-induced cell death. These results suggest that EGFR degradation may be a novel mechanism for gemcitabine-mediated cell death. These findings also indicate that caution should be exercised when combining gemcitabine with agents that may prevent EGFR degradation, such as EGFR tyrosine kinase inhibitors administered in a suboptimal sequence or proteosome inhibitors.

A phase III study determined the effects of combining the EGFR-targeted agent, erlotinib with gemcitabine in patients with unresectable, locally advanced, or metastatic pancreatic cancer. Overall survival (OS) was significantly prolonged on the erlotinib/gemcitabine arm compared with gemcitabine alone, median survival was 6.25 versus 5.91 months, with a one-year survival of 23% versus 17% (Moore *et al*., 2007). These results led to the FDA approval of erlotinib in combination with gemcitabine in advanced, unresectable or metastatic pancreatic cancer.

Our results in conjunction with recent literature reports, suggest that the combination of lapatinib and gemcitabine may be therapeutically more efficient than gemcitabine alone in the treatment of pancreatic cancer.

4.7.3 Combination of lapatinib and taxotere

Lapatinib and taxotere combination in both BxPc-3 and KCIMOH1 cells showed a modest interaction, as shown in Chapter 3.7 (Figure 3.7.5). The combination response was not evaluated by Calcusyn and CI analysis was not carried out on this data. A perquisite of fixed ratio calculations is the generation of an accurate dose response curve of all the drugs tested. It is obvious from the graphs that taxotere is a very potent drug and the pancreatic cancer cell lines, BxPc-3 and KCI-MOH1, are sensitive to the drug at very low concentrations. Therefore, the dynamic range of the assay was not accurate as the combination of taxotere and lapatinib were not combined at an equipotent ratio (the ratio of the IC_{50} concentrations). The combination ratio concentration of lapatinib:taxotere used was 1:0.01 ng/ml; however, due to the scheduling of the combination including 24 hr pre-incubation with lapatinib, the overall kill of taxotere alone was higher than expected and the anti-proliferative effects of lapatinib were masked. These results highlight the importance of lapatinib: taxotere scheduling. It is unclear from this data whether this combination would be an effective treatment for pancreatic cancer.

Taxotere has been used in combination with gemcitabine in the treatment of pancreatic cancer. The combination in unresectable pancreatic carcinoma has been well tolerated. Survival time and 1-year survival rate has proved promising and the regimen appears suitable for further evaluation in a prospective phase-III study setting (Ridwelski *et al.*, 2006; Meyer *et al.*, 2004).

Ignatiadis *et al*. (2006) evaluated the efficacy and tolerance of the taxotere/gefitinib combination as a second-line treatment in patients with advanced pancreatic cancer after failure of gemcitabine-based chemotherapy. This study concluded that this combination, although safe, did not offer an active salvage treatment.

A phase I-II study of lapatinib and taxotere as neoadjuvant treatment for locally advanced breast cancer is currently undergoing clinical assessment.

4.7.4 Combination of lapatinib and 5'dFUrd

Lapatinib in combination with 5'dFUrd (active capecitabine intermediate) shows synergism in BxPc-3 cells at ED25, as the concentrations increases the combination indices also increases displaying an additive to antagonistic interaction at ED50-75. This shows that the combined effect of the two drugs are maximised at lower concentration levels. However, the opposite is true for KCIMOH1 cells. Antagonism is observed at ED25, and additivity to synergism is observed as the concentration increases (ED50-75). These results suggest that synergy is observed in both cell lines with the combination of lapatinib and 5'dFUrd, although at different concentration ranges. This may be an important consideration in pre-clinical studies.

Herrmann *et al*. (2007) in a phase III randomised trial compared the efficacy and safety of gemcitabine plus capecitabine versus single-agent gemcitabine alone in advanced/metastatic pancreatic cancer. Although the median overall survival (OS) time was slightly improved (8.4 compared to 7.2 months), GemCap failed to improve OS significantly compared to gemcitabine alone. This study concluded that GemCap may be considered as an alternative to single-agent gemcitabine for the treatment of advanced/metastatic pancreatic cancer patients with a good performance status.

Capecitabine in combination with trastuzumab (Herceptin) caused complete remission of a patient with recurrent breast cancer and liver metastasis (Morohashi *et al*., 2007). The combination of capecitabine and trastuzumab has been further validated in a phase II study of HER2 over-expressing advanced/metastatic breast cancer. Schaller *et al*. (2007) showed that the combination of capecitabine and trastuzumab is highly active in patients with HER-2 over-expressing anthracycline- and/or taxane-pretreated breast cancer, with only slight restrictions regarding quality of life. These recent studies suggest that the combination of capecitabine and EGFR/HER2 targeting therapies could possibly be used to treat other cancer at advanced/metastatic stage. Geyer *et al*. (2006) recently completed a clinical trial comparing lapatinib plus capecitabine with capecitabine alone in women with

HER2-positive metastatic breast cancer that has progressed after trastuzumab-based therapy. The median time to progression was 8.4 months in the combination-therapy group as compared with 4.4 months in the monotherapy group. This improvement was achieved without an increase in serious toxic effects or symptomatic cardiac events. This study concluded that lapatinib plus capecitabine is superior to capecitabine alone in women with HER2-positive advanced breast cancer refractive after treatment with regimens that included an anthracycline, a taxane, and trastuzumab.

Clinical trials are now underway investigating the combination of capecitabine with gemcitabine and erlotinib for advanced pancreatic cancer.

Our data presents evidence that lapatinib cooperates with cytotoxic drugs and may have a therapeutic role in the treatment and management of EGFR/HER2 expressing pancreatic cancers. We have demonstrated that the anti-proliferative effect of lapatinib is optimal with 24 hrs exposure before addition of chemotherapeutic drug to the cells. Further consideration to the optimal scheduling regimes in pre-clinical trials may show a more beneficial outcome.

4.8 Conclusions

In this thesis, we have successfully established an *in vitro* pancreatic cancer invasion model, which represents the malignant transformation in pancreatic cancer cell lines; this model could potentially signify a model of invasion and metastasis *in vivo*. Novel proteins and secreted biomarkers differentially regulated in our model, through identification by 2-D DIGE proteomics, siRNA and cDNA analysis, showed functional involvement in invasion and the malignant phenotype of pancreatic cancer cells. This could possible help to further determine key targets/biomarkers in pancreatic cancer patients in an aim to therapeutically assist the early detection of the disease. The expression of MDR pumps, P-gp and MRP-1 in pancreatic cancer specimens showed that these pumps are an important mechanism of drug resistance in pancreatic cancer patients. Furthermore, treatment with lapatinib in combination with chemotherapeutic lapatinib has shown to exert additive effects, and could be used to target EGFR/HER2 expressing pancreatic cancers.

5.0 Summary & Future work

5.1 Summary

Pancreatic cancer is characterised by an inherent drug resistance phenotype with a propensity for early invasion and local metastasis. The main focus of this thesis was to develop relevant human *in vitro* models that would allow us search for molecular signatures involved in these processes and to identify novel markers that may therapeutically assist the detection and treatment of this disease.

5.1.1 Drug resistance profile of pancreatic cancer cell lines and clinical specimens

Pulse-selection of three pancreatic cancer cell lines with epirubicin, gemcitabine and taxotere led to the establishment of eight novel cell lines with relatively low resistance.

- The low level of resistance observed to the selecting drug may be more clinically relevant and better represent acquired resistance observed *in vivo*.

- No obvious cross-resistance pattern of variants was observed to a panel of ten chemotherapeutic drugs, even with drugs within the same chemical family (e.g. taxanes, platinum compounds etc). Inherent or induced expression of the multidrug resistant pumps, P-gp or MRP-1 was not obviously detectable in our panel of pulsed pancreatic cancer cell lines.

- Epirubicin and gemcitabine pulse-selected cell lines showed increased invasive capacities. The resistance levels, however, did not correlate with invasive abilities of the cells, suggesting that even modest resistance can induce a more invasive phenotype. In contrast, taxotere-selected variants did not display any increase in invasion abilities.

- Pancreatic cancer specimens were stained for the multi-drug resistance pumps, P-gp and MRP-1. 93% (42/45) of pancreatic cancer specimens stained positive for P-gp. Approximately 12% (5/42) scored 1+, 10% (4/42) scored 2+, 24% (10/42) scored 3+, while 55% (23/42) scored 4+. Weak staining was observed 10% (4/42),

intermediate staining in 52% (22/42) and strong staining in 38% (16/42) of cases. Three cases showed no P-gp expression.

- MRP-1 protein was expressed in 31% of pancreatic tumour specimens. Approximately 14% (2/14) scored 1+, 14% (2/14) scored 2+, 57% (8/14) scored 3+ and 14% (2/14) scored 4+. Weak staining was observed in 36% (5/14) of cases, intermediate staining in 29% (4/14) and strong staining in 36% (5/14). Sixty-nine percent (31/45) of tumours did not show MRP-1 protein expression.

- Co-expression of multi-drug proteins was observed in 36% of specimens, no cases were observed where MRP-1 was expressed independently of MDR-1/P-gp. However, 61% stained MDR-1/P-gp positive and MRP-1 negative. 6.7% of cases expressed neither drug efflux pumps.

- These results suggest that P-gp may be functionally more important in the role of mediating pancreatic cancer chemotherapy resistance than MRP-1. However, no direct link can be made from this data as the chemotherapy resistance history of the patients is unknown, therefore, we cannot identify whether this MDR phenotype is inherent or acquired.

- These results show that drug efflux pumps, in particular that of P-gp, are frequently expressed in pancreatic cancer. The absence of these pumps in the cell lines we used may represent a limitation of the degree in which they model pancreatic carcinoma *in vivo*. This fact should be considered when selecting chemotherapy/drug efflux pump inhibitors for future therapies.

5.1.2 Characterisation of sub-populations within the pancreatic cancer cell line, MiaPaCa-2

Heterogeneity within tumours may signify existence of sub-populations with inherent invasive/metastatic and drug resistance potentials (Fidler, 1978).

- Clonal sub-populations of the pancreatic cancer cell line, MiaPaCa-2 which displayed variable levels of invasion were established. Clone #3 is 2.5-fold more invasive, while Clone #8 is 6-fold less invasive than the parental cell line.

- Characterisation of these clones revealed that Clone #3 is consistent with the malignant transformation phenotype, exhibiting increased invasion through ECM

proteins, decreased adhesion to ECM proteins, increased anoikis resistance, ability to form colonies in anchorage independent conditions. The reverse of this pattern is observed for Clone #8 cells.

- Integrins β1, α5 and α6 are up-regulated in the less invasive, high adhesive Clone #8. Functional knockdown by siRNA of integrin β1 revealed its involvement in the invasion and adhesion to matrigel and fibronectin. The loss of integrin β1 expression also increases motility and anoikis resistance of Clone #8 cells. Our results show that integrin β1 may play a role as the main β-chain for the αβ chain heterodimer to form a fibronectin receptor. Expression of integrin β1 may act as an invasion and motility suppressor and encourage increased adhesiveness and anoikis sensitivity. However, invasion and adhesion to laminin was unaltered, suggesting that integrin β1 is not the main β-chain involved in laminin binding.

- Loss of integrin α5 in Clone #8 cells induces increased motility and invasion through matrigel, laminin and fibronectin. Silencing of integrin α5 expression reduced adhesion to fibronectin. However, no reduction in adhesion was observed to matrigel and laminin. Anoikis was not altered when integrin α5 was down-regulated. Therefore, our results suggest that integrin α5 plays a vital role in suppressing motility, invasion through matrigel, laminin and fibronectin, but is only involved in increased adhesion to the ECM protein, fibronectin.

- Loss of integrin α6 in Clone #8 cells increases motility and invasion through matrigel and fibronectin, but decreases adhesion to laminin. Anoikis is also unaffected by loss of integrin α6.

- Drug resistance profiling of MiaPaCa-2, Clone #3 and Clone #8 to a panel of ten chemotherapeutic drugs suggest a relationship between drug resistance and increased invasion in this cell line model. Clone #3 displays significant resistance to taxotere and VP-16. Clone #8 shows a significant sensitivity to nine out of ten drugs tested compared to the parent, MiaPaCa-2.

The occurrence of sub-populations within cancer cell lines and the correlation with *in vitro* malignant transformation may offer an important tool for identifying markers of more aggressive metastatic cells *in vivo*.

5.1.3 Proteomic profiling of MiaPaCa-2 and sub-populations, Clone #3 and Clone #3

- Proteomic comparative analysis of MiaPaCa-2, Clone #3 and Clone #8 in order of high to low invasion of the cell lines (MiaPaCa-2 versus Clone #8, Clone #3 versus MiaPaCa-2 and Clone #3 versus Clone #8) generated lists of differentially expressed proteins.

- The distinctive design analysis of overlapping the three generated proteins lists to specifically identify proteins that were consistently altered (either up-regulated or down-regulated) with the invasion status of the cell lines led to the identification of three proteins which were verified as having significant roles in invasion and the malignant process of pancreatic cancer.

Aldehyde dehydrogenase 1A1 (ALDH1A1)

ALDH1A1 is a cytosolic enzyme involved in the conversion of aldehydes to their corresponding acids by $NAD(P)^+$ dependent reactions. The role of ALDH1A1 in mediating resistance to the family of oxazaphosphorines has been clearly demonstrated in breast and lung cancer (Sladek *et al.*, 2002; Moreb *et al.*, 2007); however, its role in invasion is undefined. ALDH1A1 was found to be up-regulated in the invasive Clone #3 cell line and subsequent siRNA gene silencing revealed a novel role for this enzyme in pancreatic cancer invasion, adhesion and drug resistance. Exogeneous increase of ALDH1A1 expression by cDNA transfection in Clone #8 cells further confirmed the ability of ALDH1A1 to modulate invasion. ALDH1A1 acts as a catalyst in the oxidation of retinal to retinoic acid. We determined no evidence of a negative feedback loop on ALDH1A1 expression through ATRA exposure in Clone #3 cells. However, morphological changes and increased invasion of Clone #8 were observed after long-term continuous ATRA exposure, suggesting a further link to the invasive phenotype characterised by pancreatic cancer.

ALDH1A1 may have dual potential as a therapeutic target as a treatment to inhibit invasion as well as sensitising cancer cells to certain chemotherapy regimes. This may be especially beneficial since drug resistant cells are refractory to chemotherapy and exhibit an aggressive invasive phenotype and highly metastatic cells are inherently more resistant

to chemotherapeutic treatment. Thus, targeting ALDH1A1 as an anti-invasive therapy in combination with selected chemotherapy may provide a more effective cancer treatment.

Vimentin (VIM)

VIM is a structural intermediate filament of the cytoskeleton. Its expression confers an epithelial to mesenchymal transition (EMT) phenotype characterised by increased invasion/metastasis and poorer survival times in many cancers (Gilles *et al*., 1996; Domagala *et al*., 1990). Our study confirms these previous reports and determined a functional role of VIM in pancreatic cancer cell invasion and adhesion; furthermore, the silencing of VIM expression in Clone #3 cells by siRNA induced morphological changes in the cells consistent with the reversal of the EMT phenotype termed mesenchymal to epithelial transition (MET). In agreement with *in vivo* studies (Colucci-Guyon *et al*., 1994; Eckes *et al*., 1998) loss of VIM expression did affect cell growth, therefore, VIM could be identified as a suitable adjuvant therapy specifically reversing the EMT phenotype while targeting cancer invasion and metastasis in conjunction with conventional chemotherapy treatment for the solid tumour mass.

Stress-induced phosphoprotein 1 (STIP1)

STIP1 mediates the association, and forms a physical complex with the molecular chaperones Hsp90 and Hsp70 (Carrigan *et al*., 2006). Little evidence exists determining a role for STIP1 in cancer cell invasion and the malignant phenotype. However, STIP1 acts as a co-chaperone for Hsp90 and Hsp70, whose involvement in cancer progression, development and maintenance has previously been identified (Pick *et al*., 2007; Aghdassi *et al*., 2007). Through RNAi knockdown of STIP1 expression in the invasive sub-population, Clone #3, a functional role of STIP1 in invasion, adhesion and proliferation was observed in our study. Therefore, further studies on the novel anti-invasive and anti-proliferative effects of STIP1 as a therapeutic target for pancreatic cancer needs to be assessed. Whether or not loss of STIP has functional consequences for Hsp90 and Hsp70, it could represent an effective strategy for combating invasive pancreatic cancer.

5.1.4 Characterisation and proteomic analysis of conditioned media, CM#3 and CM#8

The ability of tumour cells to respond to microenvironmental factors present in the target organ may be necessary for successful metastasis. The potential role of secreted factors in conditioned media from Clone #3 and Clone #8 on invasion was investigated.

- Conditioned media (CM) collected from Clone #3 and Clone #8 and added into the *in vitro* invasion chamber at equal dilution ensuring no gradient (no chemotaxis) revealed that CM#3 significantly enhances invasion and CM#8 significantly inhibits invasion of MiaPaCa-2, Clone #3 and Clone #8 compared to an invasion assay control containing fresh medium. Pre-incubation of the cells with either CM#3 or CM#8 24 hrs prior to invasion assays displays the same trends indicating that the CMs secrete factor(s) that can modulate invasion.

- MiaPaCa-2, Clone #3 and Clone #8 grown on matrigel for 24 hrs (in the presence of CM#3 and CM#8) prior to invasion assays display further increased invasion and superinvasion, suggesting that the cell-ECM contact highly activates molecules involved in invasion, and that this pathway may be essential in determining potential invasive markers.

- Temperature storage stability analysis of CM#3 and CM#8 determined that both CM#3 and CM#8 showed better stability in terms of inducing and inhibiting invasion when stored at -80° C compared to storage at 4 $^{\circ}$C and -20 $^{\circ}$C.

- The maximum diluent factors for CM#3 and CM#8 to exert their respective promotion and inhibitory effects on invasion was determined to be 1:4 with fresh media.

- pH stability experiments with CM#3 and CM#8 demonstrate that, compared to controls (fresh media treated with same pH changes), invasion was promoted to the greatest degree when CM#3 was exposed to acidic pH for 2 hrs at RT and brought back to pH 7, whereas CM#8 displayed the greatest inhibitory effect on invasion when exposed to alkaline pHs for 2 hrs RT and brought back to pH 7, then added into the invasion assay chamber.

- Fractionation of CM#3 and CM#8 showed that invasion was significantly increased when higher molecular weight fractions of CM#3 (30-50 kDa, 50-100

kDa and 100 kDa) were added to the invasion insert. Invasion was significantly decreased when CM#8 fractions 10 kDa and 10-30 kDa were added into the invasion insert. Important fractions are secreted into CM#8, acting as an inhibitory factor at lower molecular weights, while CM#3 seems to promote invasion at higher molecular weight cut off points.

5.1.5 Proteomic profiling of CM Mia, CM#3 and CM#8

Secreted markers for pancreatic cancer invasion were profiled by proteomic analysis, revealing comparative differentially secreted protein between CMs. Emphasis was placed on the comparison of CM#3 versus CM#8, as the greatest difference in invasion modulation was observed. Two secreted targets chosen for functional analysis showed distinct roles in the invasive process of pancreatic cancer.

Gelsolin (GSN)

GSN is a calcium-binding protein which binds to and regulates actin filaments. The majority of work to date shows that GSN may act as a tumour suppressor in many cancer tissues. In our study, we confirmed that both cytoplasmic and secreted plasma GSN are expressed by Clone #8 and are functionally involved in suppressing pancreatic cancer invasion. Gene silencing of GSN reduced plasma and cytoplasmic GSN expression, revealing a more invasive phenotype. However, we also determined that cytoplasmic GSN expression may have an additional role in invasion suppression. Additional analysis of GSN expression and ECM contact, in this cell system may present a clearer picture for both cytoplasmic and plasma GSN, as an invasion inhibitory factor.

Aldehyde dehydrogenase 1A1 (ALDH1A1)

The nature of ALDH1A1 secretion has not been determined in literature. In our model, ALDH1A1 was found to be highly secreted in the invasive inducing CM#3. Silencing of ALDH1A1 secretion by siRNA in CM#3 significantly reduced the invasive promoting activities of CM#3. This study, to our knowledge, is the first report to implicate secreted ALDH1A1 as an invasive enhancer and further characterisation and study needs to be carried out to verify its effects in other caner types.

5.1.6 Role of EGFR and HER2 in pancreatic cancer

Over-expression of EGFR and HER2 has been associated with reduced overall survival and disease free survival in some cancers. The potential use of lapatinib, a dual EGFR/HER2 tyrosine kinase inhibitor in combination with chemotherapeutic drugs in pancreatic cancer cell lines was assessed.

- EGFR was expressed in all five of our pancreatic cancer cell lines, as determined by western blot and ELISA. HER2 was expressed at low levels in four out of five of our pancreatic cell line panel. High expression was observed only in one cell line, BxPc-3.

- Combination assays of lapatinib with four chemotherapeutic drugs, cisplatin, gemcitabine, taxotere and 5'dFUrd in BxPc-3 and KCIMOH1 revealed that the combination of lapatinib and cisplatin, gemcitabine and 5'dFUrd has an overall additive effect compared to either drug alone. The combination of lapatinib and taxotere did not show any additivity, possibly because the potent toxicity of taxotere masked any additional anti-proliferation effects of lapatinib.

- The scheduling regime is an important factor, as optimal effects of lapatinib and chemotherapeutic drugs was observed after 24 hrs pre-treatment with lapatinib followed by addition of chemo-drugs. This may be an important factor in pre-clinical trials, as optimisation of scheduling regimes may determine a more beneficial outcome.

5.2 Future work

1. The proteomic profiling carried out in this thesis generated vast amounts of data. Only a fraction of the data was functionally analysed, and consequently, many potential targets remain to be examined. The analysis mainly focused on pancreatic cancer cell invasion; however, similar analysis could be carried out to determine functional involvement of differentially regulated proteins in other parameters relevant to cancer such as, adhesion, anoikis, proliferation and drug resistance.

2. The metastatic potential of Clone #3 and Clone #8 will be verified in *in vivo* orthotopic mouse models. Stable transfected cell lines will be established with a fluorescent tag, the growth and metastatic spread of the cells will be followed by an *in vivo* fluorescent imager, to correlate metastasis with our *in vitro* work.

3. ALDH1A1, VIM and STIP1 will be further analysed by transfection of their cDNA into the low invasive cell line, Clone #8. It would be interesting to see if modulation of the target proteins by cDNA transfection could be capable of inducing invasion and if their expression correlates with the invasive phenotype without non-specific effects. It is possible that individual silencing of any one of protein will not be enough to completely reduce invasion, and therefore, the next step would be combined silencing of two or more simultaneously.

4. The role of the selected targets *in vivo* could be determined by measuring their expression in patient tissues sections.

5. Tumour cells expressing CD44, CD24 and ESA have previously been found to characterise breast and pancreatic cancer stem cells, therefore ALDH1A1 expression in pancreatic cancer could also be investigated as a potential marker for pancreatic cancer stem cells.

6. Identification of secreted targets may be clinically relevant as serum markers. Purification of secreted factors involved in the promotion/inhibition of invasion in CM of Clone #3 and Clone #8 could determine novel biomarkers and/or therapeutic targets. Techniques such as ultrafiltration, size-exclusion, gel-filtration and reverse-phase column chromatography could help to purify the secreted pancreatic tumour markers in conditioned media and may be applicable to serum biomarkers.

7. Proteomic profiling of secreted proteins in CM#3 and CM#8 resulted in the identification of two secreted proteins functionally involved in the invasive modulation of CM to pancreatic cancer cells. Further validation of these and other targets identified in our analysis will be confirmed in pancreatic cancer patient serum. Comparison of our secreted factors in CM relating to invasion with patient serum may highlight the clinical importance of these 'secreteomes' in pancreatic cancer invasion.

8. Co-expression of EGFR and HER2 needs to be assessed in pancreatic tumours to determine if a sub-population of pancreatic cancer patients exists to which lapatinib treatment in combination with chemotherapeutic drugs would be clinically applicable. This study will be carried out on paraffin-embedded pancreatic cancer tissue sections by immunohistochemistry.

6.0 Bibliography

Aalinkeel, R., Nair, M.P., Sufrin, G., Mahajan, S.D., Chadha, K.C., Chawda, R.P. and Schwartz, S.A. (2004) Gene expression of angiogenic factors correlates with metastatic potential of prostate cancer cells. *Cancer Res.,* **64,** 5311-5321.

Abraham, S., Zhang, W., Greenberg, N. and Zhang, M. (2003) Maspin functions as tumor suppressor by increasing cell adhesion to extracellular matrix in prostate tumor cells. *J. Urol.,* **169,** 1157-1161.

Abu-Qare, A.W., Elmasry, E. and Abou-Donia, M.B. (2003) A role for P-glycoprotein in environmental toxicology. *J. Toxicol. Environ. Health B Crit. Rev.,* **6,** 279-288.

Achiwa, H., Oguri, T., Sato, S., Maeda, H., Niimi, T. and Ueda, R. (2004) Determinants of sensitivity and resistance to gemcitabine: the roles of human equilibrative nucleoside transporter 1 and deoxycytidine kinase in non-small cell lung cancer. *Cancer. Sci.,* **95,** 753-757.

Aghdassi, A., Phillips, P., Dudeja, V., Dhaulakhandi, D., Sharif, R., Dawra, R., Lerch, M.M. and Saluja, A. (2007) Heat shock protein 70 increases tumorigenicity and inhibits apoptosis in pancreatic adenocarcinoma. *Cancer Res.,* **67,** 616-625.

Ahmad, A. and Hart, I.R. (1997) Mechanisms of metastasis. *Crit. Rev. Oncol. Hematol.,* **26,** 163-173.

Aigner, A. (2006) Gene silencing through RNA interference (RNAi) in vivo: strategies based on the direct application of siRNAs. *J. Biotechnol.,* **124,** 12-25.

Akada, M., Crnogorac-Jurcevic, T., Lattimore, S., Mahon, P., Lopes, R., Sunamura, M., Matsuno, S. and Lemoine, N.R. (2005) Intrinsic chemoresistance to gemcitabine is associated with decreased expression of BNIP3 in pancreatic cancer. *Clin. Cancer Res.,* **11,** 3094-3101.

Alban, A., David, S.O., Bjorkesten, L., Andersson, C., Sloge, E., Lewis, S., Currie, I. (2003) A novel experimental design for comparative two-dimensional gel analysis; two-dimensional gel difference gel electrophoresis incorporating a pooled internal standard. *Proteomics*, **3**, 36-44.

Albini, A., Iwamoto, Y., Kleinman, H.K., Martin, G.R., Aaronson, S.A., Kozlowski, J.M. and McEwan, R.N. (1987) A rapid in vitro assay for quantitating the invasive potential of tumor cells. *Cancer Res.,* **47,** 3239-3245.

Al-Hajj, M., Wicha, M.S., Benito-Hernandez, A., Morrison, S.J. and Clarke, M.F. (2003) Prospective identification of tumorigenic breast cancer cells. *Proc. Natl. Acad. Sci. U. S. A.,* **100,** 3983-3988.

Altenberg, B. and Greulich, K.O. (2004) Genes of glycolysis are ubiquitously overexpressed in 24 cancer classes. *Genomics,* **84,** 1014-1020.

Altmeyer, A., Maki, R.G., Feldweg, A.M., Heike, M., Protopopov, V.P., Masur, S.K. and Srivastava, P.K. (1996) Tumor-specific cell surface expression of the-KDEL containing, endoplasmic reticular heat shock protein gp96. *Int. J. Cancer,* **69,** 340-349.

Altomare, D.A., Wang, H.Q., Skele, K.L., De Rienzo, A., Klein-Szanto, A.J., Godwin, A.K. and Testa, J.R. (2004) AKT and mTOR phosphorylation is frequently detected in ovarian cancer and can be targeted to disrupt ovarian tumor cell growth. *Oncogene,* **23,** 5853-5857.

Anderson, L. and Seilhamer, J. (1997) A comparison of selected mRNA and protein abundances in human liver. *Electrophoresis,* **18,** 533-537.

Andre, T., Balosso, J., Louvet, C., Gligorov, J., Callard, P., de Gramont, A. and Izrael, V. (1998) Adenocarcinoma of the pancreas. General characteristics. *Presse Med.,* **27,** 533-536.

Androulakis, N., Kourousis, C., Dimopoulos, M.A., Samelis, G., Kakolyris, S., Tsavaris, N., Genatas, K., Aravantinos, G., Papadimitriou, C., Karabekios, S., et al (1999) Treatment of pancreatic cancer with docetaxel and granulocyte colony-stimulating factor: a multicenter phase II study. *J. Clin. Oncol.,* **17,** 1779-1785.

Ariztia, E.V., Lee, C.J., Gogoi, R. and Fishman, D.A. (2006) The tumor microenvironment: key to early detection. *Crit. Rev. Clin. Lab. Sci.,* **43,** 393-425.

Arora, A. and Scholar, E.M. (2005) Role of tyrosine kinase inhibitors in cancer therapy. *J. Pharmacol. Exp. Ther.,* **315,** 971-979.

Asanuma, K., Moriai, R., Yajima, T., Yagihashi, A., Yamada, M., Kobayashi, D. and Watanabe, N. (2000) Survivin as a radioresistance factor in pancreatic cancer. *Jpn. J. Cancer Res.,* **91,** 1204-1209.

Bader, P., Fuchs, J., Wenderoth, M., von Schweinitz, D., Niethammer, D. and Beck, J.F. (1998) Altered expression of resistance associated genes in hepatoblastoma xenografts incorporated into mice following treatment with adriamycin or cisplatin. *Anticancer Res.,* **18,** 3127-3132.

Baeckström, D.
www.dan1.medkem.gu.se (2006)

Baerman, K.M., Caskey, L.S., Dasi, F., Earp, H.S., Calvo, B.F. (2005) EGFR/HER2 targeted therapy inhibits growth of pancreatic cancer cells. *ASCO Annual Meeting*, **84,** Abstract.

Bakin, A.V., Tomlinson, A.K., Bhowmick, N.A., Moses, H.L. and Arteaga, C.L. (2000) Phosphatidylinositol 3-kinase function is required for transforming growth factor beta-mediated epithelial to mesenchymal transition and cell migration. *J. Biol. Chem.,* **275,** 36803-36810.

Barak, V., Frenkel, S., Kalickman, I., Maniotis, A.J., Folberg, R. and Pe'er, J. (2007) Serum markers to detect metastatic uveal melanoma. *Anticancer Res.,* **27,** 1897-1900.

Barker, A.J., Gibson, K.H., Grundy, W., Godfrey, A.A., Barlow, J.J., Healy, M.P., Woodburn, J.R., Ashton, S.E., Curry, B.J., Scarlett, L., et al (2001) Studies leading to the identification of ZD1839 (IRESSA): an orally active, selective epidermal growth factor receptor tyrosine kinase inhibitor targeted to the treatment of cancer. *Bioorg. Med. Chem. Lett.,* **11,** 1911-1914.

Barrallo-Gimeno, A. and Nieto, M.A. (2005) The Snail genes as inducers of cell movement and survival: implications in development and cancer. *Development,* **132,** 3151-3161.

Baselga, J., Pfister, D., Cooper, M.R., Cohen, R., Burtness, B., Bos, M., D'Andrea, G., Seidman, A., Norton, L., Gunnett, K., et al (2000) Phase I studies of anti-epidermal growth factor receptor chimeric antibody C225 alone and in combination with cisplatin. *J. Clin. Oncol.,* **18,** 904-914.

Bates, R.C., Bellovin, D.I., Brown, C., Maynard, E., Wu, B., Kawakatsu, H., Sheppard, D., Oettgen, P. and Mercurio, A.M. (2005) Transcriptional activation of integrin beta6 during the epithelial-mesenchymal transition defines a novel prognostic indicator of aggressive colon carcinoma. *J. Clin. Invest.,* **115,** 339-347.

Batlle, E., Sancho, E., Franci, C., Dominguez, D., Monfar, M., Baulida, J. and Garcia De Herreros, A. (2000) The transcription factor snail is a repressor of E-cadherin gene expression in epithelial tumour cells. *Nat. Cell Biol.,* **2,** 84-89.

Baulcombe, D.C. (2006) Short silencing RNA: the dark matter of genetics? *Cold Spring Harb. Symp. Quant. Biol.,* **71,** 13-20.

Bendtsen, J.D., Jensen, L.J., Blom, N., Von Heijne, G. and Brunak, S. (2004) Feature-based prediction of non-classical and leaderless protein secretion. *Protein Eng. Des. Sel.,* **17,** 349-356.

Bergman, A.M., Eijk, P.P., Ruiz van Haperen, V.W., Smid, K., Veerman, G., Hubeek, I., van den Ijssel, P., Ylstra, B. and Peters, G.J. (2005) In vivo induction of resistance to gemcitabine results in increased expression of ribonucleotide reductase subunit M1 as the major determinant. *Cancer Res.,* **65,** 9510-9516.

Bergman, A.M., Giaccone, G., van Moorsel, C.J., Mauritz, R., Noordhuis, P., Pinedo, H.M. and Peters, G.J. (2000) Cross-resistance in the 2',2'-difluorodeoxycytidine (gemcitabine)-resistant human ovarian cancer cell line AG6000 to standard and investigational drugs. *Eur. J. Cancer,* **36,** 1974-1983.

Bernards, R. and Weinberg, R.A. (2002) A progression puzzle. *Nature,* **418,** 823.

Bhave, S.V., Hoffman, P.L., Lassen, N., Vasiliou, V., Saba, L., Deitrich, R.A. and Tabakoff, B. (2006) Gene array profiles of alcohol and aldehyde metabolizing enzymes in brains of C57BL/6 and DBA/2 mice. *Alcohol. Clin. Exp. Res.,* **30,** 1659-1669.

Bi, X., Lin, Q., Foo, T.W., Joshi, S., You, T., Shen, H.M., Ong, C.N., Cheah, P.Y., Eu, K.W. and Hew, C.L. (2006) Proteomic analysis of colorectal cancer reveals alterations in metabolic pathways: mechanism of tumorigenesis. *Mol. Cell. Proteomics,* **5,** 1119-1130.

Birchmeier, C., Birchmeier, W. and Brand-Saberi, B. (1996) Epithelial-mesenchymal transitions in cancer progression. *Acta Anat. (Basel),* **156,** 217-226.

Blackstock, W.P. and Weir, M.P. (1999) Proteomics: quantitative and physical mapping of cellular proteins. *Trends Biotechnol.,* **17,** 121-127.

Blackwell, K.L., Kaplan, E.H., Franco, S.X., et al (2004) A phase II, open-label, multicenter study of GW572016 in patients with trastuzumab-refractory metastatic breast cancer. *Proc Annu Meet Am Soc Clin Oncol.,* **22**, Abstract.

Blanco, D., Vicent, S., Elizegi, E., Pino, I., Fraga, M.F., Esteller, M., Saffiotti, U., Lecanda, F. and Montuenga, L.M. (2004) Altered expression of adhesion molecules and epithelial-mesenchymal transition in silica-induced rat lung carcinogenesis. *Lab. Invest.,* **84,** 999-1012.

Bloomston, M., Zervos, E.E. and Rosemurgy, A.S.,2nd (2002) Matrix metalloproteinases and their role in pancreatic cancer: a review of preclinical studies and clinical trials. *Ann. Surg. Oncol.,* **9,** 668-674.

Blum, J.L., Jones, S.E., Buzdar, A.U., LoRusso, P.M., Kuter, I., Vogel, C., Osterwalder, B., Burger, H.U., Brown, C.S. and Griffin, T. (1999) Multicenter phase II study of capecitabine in paclitaxel-refractory metastatic breast cancer. *J. Clin. Oncol.,* **17,** 485-493.

Bolós, V., Peinado, H., Pérez-Moreno, M.A., Fraga, M.F., Esteller, M. and Cano, A. (2003) The transcription factor Slug represses E-cadherin expression and induces epithelial to mesenchymal transitions: a comparison with Snail and E47 repressors. *J Cell Sci.,* **116**, 499-511.

Bonay, M., Soler, P., Riquet, M., Battesti, J.P., Hance, A.J. and Tazi, A. (1994) Expression of heat shock proteins in human lung and lung cancers. *Am. J. Respir. Cell Mol. Biol.,* **10,** 453-461.

Bonnet, D. and Dick, J.E. (1997) Human acute myeloid leukemia is organized as a hierarchy that originates from a primitive hematopoietic cell. *Nat. Med.,* **3,** 730-737.

Borutinskaite, V.V., Navakauskiene, R. and Magnusson, K.E. (2006) Retinoic acid and histone deacetylase inhibitor BML-210 inhibit proliferation of human cervical cancer HeLa cells. *Ann. N. Y. Acad. Sci.,* **1091,** 346-355.

Boulton, S.J. (2006) Cellular functions of the BRCA tumour-suppressor proteins. *Biochem. Soc. Trans.,* **34,** 633-645.

Brabec, V. and Kasparkova, J. (2002) Molecular aspects of resistance to antitumor platinum drugs. *Drug Resist Updat,* **5,** 147-161.

Brabletz, T., Jung, A., Reu, S., Porzner, M., Hlubek, F., Kunz-Schughart, L.A., Knuechel, R. and Kirchner, T. (2001) Variable beta-catenin expression in colorectal cancers indicates tumor progression driven by the tumor environment. *Proc. Natl. Acad. Sci. U. S. A.,* **98,** 10356-10361.

Bradley, G. and Ling, V. (1994) P-glycoprotein, multidrug resistance and tumor progression. *Cancer Metastasis Rev.,* **13,** 223-233.

Brakebusch, C., Wennerberg, K., Krell, H.W., Weidle, U.H., Sallmyr, A., Johansson, S. and Fassler, R. (1999) Beta1 integrin promotes but is not essential for metastasis of ras-myc transformed fibroblasts. *Oncogene,* **18,** 3852-3861.

Breuninger, L.M., Paul, S., Gaughan, K., Miki, T., Chan, A., Aaronson, S.A. and Kruh, G.D. (1995) Expression of multidrug resistance-associated protein in NIH/3T3 cells confers multidrug resistance associated with increased drug efflux and altered intracellular drug distribution. *Cancer Res.,* **55,** 5342-5347.

Brew, K., Dinakarpandian, D. and Nagase, H. (2000) Tissue inhibitors of metalloproteinases: evolution, structure and function. *Biochim. Biophys. Acta,* **1477,** 267-283.

Brown, B., Lindberg, K., Reing, J., Stolz, D.B. and Badylak, S.F. (2006) The basement membrane component of biologic scaffolds derived from extracellular matrix. *Tissue Eng*., **12**, 519-526.

Brown, I., Shalli, K., McDonald, S.L., Moir, S.E., Hutcheon, A.W., Heys, S.D. and Schofield, A.C. (2004) Reduced expression of p27 is a novel mechanism of docetaxel resistance in breast cancer cells. *Breast Cancer Res.,* **6,** R601-7.

Brummelkamp, T.R., Bernards, R. and Agami, R. (2002) Stable suppression of tumorigenicity by virus-mediated RNA interference. *Cancer. Cell.,* **2,** 243-247.

Bruns, C.J., Harbison, M.T., Davis, D.W., Portera, C.A., Tsan, R., McConkey, D.J., Evans, D.B., Abbruzzese, J.L., Hicklin, D.J. and Radinsky, R. (2000) Epidermal growth factor receptor blockade with C225 plus gemcitabine results in regression of human pancreatic carcinoma growing orthotopically in nude mice by antiangiogenic mechanisms. *Clin. Cancer Res.,* **6,** 1936-1948.

Buchler, P., Reber, H.A., Buchler, M.C., Roth, M.A., Buchler, M.W., Friess, H., Isacoff, W.H. and Hines, O.J. (2001) Therapy for pancreatic cancer with a recombinant humanized anti-HER2 antibody (herceptin). *J. Gastrointest. Surg.,* **5,** 139-146.

Buchsbaum, D.J., Bonner, J.A., Grizzle, W.E., Stackhouse, M.A., Carpenter, M., Hicklin, D.J., Bohlen, P. and Raisch, K.P. (2002) Treatment of pancreatic cancer xenografts with Erbitux (IMC-C225) anti-EGFR antibody, gemcitabine, and radiation. *Int. J. Radiat. Oncol. Biol. Phys.,* **54,** 1180-1193.

Buhler, H. and Schaller, G. (2005) Transfection of keratin 18 gene in human breast cancer cells causes induction of adhesion proteins and dramatic regression of malignancy in vitro and in vivo. *Mol. Cancer. Res.,* **3,** 365-371.

Burris, H.A.,3rd (2004) Dual kinase inhibition in the treatment of breast cancer: initial experience with the EGFR/ErbB-2 inhibitor lapatinib. *Oncologist,* **9 Suppl 3,** 10-15.

Burris, H., Hurwitz, H., Dees, C., et al (2003) EGF10004: a randomized, multicenter, phase Ib study of the safety, biologic activity and clinical efficacy of the dual kinase inhibitor GW572016. *Breast Can Res Treat*., **82**, Abstract 39.

Butt, A.J., Dickson, K.A., McDougall, F. and Baxter, R.C. (2003) Insulin-like growth factor-binding protein-5 inhibits the growth of human breast cancer cells in vitro and in vivo. *J. Biol. Chem.,* **278,** 29676-29685.

Cabral, F. and Barlow, S.B. (1989) Mechanisms by which mammalian cells acquire resistance to drugs that affect microtubule assembly. *FASEB J.,* **3,** 1593-1599.

Caldas, C., Hahn, S.A., da Costa, L.T., Redston, M.S., Schutte, M., Seymour, A.B., Weinstein, C.L., Hruban, R.H., Yeo, C.J. and Kern, S.E. (1994) Frequent somatic mutations and

homozygous deletions of the p16 (MTS1) gene in pancreatic adenocarcinoma. *Nat. Genet.,* **8,** 27-32.

Callejo, S.A., Marshall, J.C., Cools-Lartigue, J., Saraiva, V.S. and Burnier, M.N.,Jr (2004) Macrophage-derived soluble factor enhances melanoma inhibitory activity expression by uveal melanoma cells in vitro. *Melanoma Res.,* **14,** 91-95.

Cameron, M.D., Schmidt, E.E., Kerkvliet, N., Nadkarni, K.V., Morris, V.L., Groom, A.C., Chambers, A.F. and MacDonald, I.C. (2000) Temporal progression of metastasis in lung: cell survival, dormancy, and location dependence of metastatic inefficiency. *Cancer Res.,* **60,** 2541-2546.

Carrigan, P.E., Sikkink, L.A., Smith, D.F. and Ramirez-Alvarado, M. (2006) Domain:domain interactions within Hop, the Hsp70/Hsp90 organizing protein, are required for protein stability and structure. *Protein Sci.,* **15,** 522-532.

Carter, W.G., Wayner, E.A., Bouchard, T.S. and Kaur, P. (1990) The role of integrins alpha 2 beta 1 and alpha 3 beta 1 in cell-cell and cell-substrate adhesion of human epidermal cells. *J. Cell Biol.,* **110,** 1387-1404.

Cascallo, M., Calbo, J., Capella, G., Fillat, C., Pastor-Anglada, M. and Mazo, A. (2005) Enhancement of gemcitabine-induced apoptosis by restoration of p53 function in human pancreatic tumors. *Oncology,* **68,** 179-189.

Cayrol, C., Clerc, P., Bertrand, C., Gigoux, V., Portolan, G., Fourmy, D., Dufresne, M. and Seva, C. (2006) Cholecystokinin-2 receptor modulates cell adhesion through beta 1-integrin in human pancreatic cancer cells. *Oncogene,* **25,** 4421-4428.

Center for drug evaluation and research. U.S Food and drug administration
www.fda.gov (2005)

Centre Hospitalier Universitaire Vaudois
www.chuv.ch (2006)

Chambon, P. (1996) A decade of molecular biology of retinoic acid receptors. *FASEB J.,* **10,** 940-954.

Chang, H. (2007) RNAi-mediated knockdown of target genes: a promising strategy for pancreatic cancer research. *Cancer Gene Ther.,* **14,** 677-685.

Chaponnier, C., Borgia, R., Rungger-Brandle, E., Weil, R. and Gabbiani, G. (1979) An actin-destabilizing factor is present in human plasma. *Experientia,* **35,** 1039-1041.

Chemblink
www.chemblink.com (2007)

Chen, R., Yi, E.C., Donohoe, S., Pan, S., Eng, J., Cooke, K., Crispin, D.A., Lane, Z., Goodlett, D.R., Bronner, M.P., et al (2005) Pancreatic cancer proteome: the proteins that underlie invasion, metastasis, and immunologic escape. *Gastroenterology,* **129,** 1187-1197.

Chen, S., Prapapanich, V., Rimerman, R.A., Honore, B. and Smith, D.F. (1996) Interactions of p60, a mediator of progesterone receptor assembly, with heat shock proteins hsp90 and hsp70. *Mol. Endocrinol.,* **10,** 682-693.

Chen, Y., Lin, M.C., Yao, H., Wang, H., Zhang, A.Q., Yu, J., Hui, C.K., Lau, G.K., He, M.L., Sung, J., et al (2007) Lentivirus-mediated RNA interference targeting enhancer of zeste homolog 2 inhibits hepatocellular carcinoma growth through down-regulation of stathmin. *Hepatology,* **46,** 200-208.

Cheng, G.Z., Chan, J., Wang, Q., Zhang, W., Sun, C.D. and Wang, L.H. (2007) Twist transcriptionally up-regulates AKT2 in breast cancer cells leading to increased migration, invasion, and resistance to paclitaxel. *Cancer Res.,* **67,** 1979-1987.

Chintala, S.K., Sawaya, R., Gokaslan, Z.L. and Rao, J.S. (1996) Modulation of matrix metalloprotease-2 and invasion in human glioma cells by alpha 3 beta 1 integrin. *Cancer Lett.,* **103,** 201-208.

Chiu, F.C. and Goldman, J.E. (1984) Synthesis and turnover of cytoskeletal proteins in cultured astrocytes. *J. Neurochem.,* **42,** 166-174.

Chu, Y.W., Seftor, E.A., Romer, L.H. and Hendrix, M.J. (1996) Experimental coexpression of vimentin and keratin intermediate filaments in human melanoma cells augments motility. *Am. J. Pathol.,* **148,** 63-69.

Cintorino, M., Tripod, S.A., Santopietro, R., Antonio, P., Lutfi, A., Chang, F., Syrjanen, S., Shen, Q., Tosi, P. and Syrjanen, K. (2001) Cytokeratin expression patterns as an indicator of tumour progression in oesophageal squamous cell carcinoma. *Anticancer Res.,* **21,** 4195-4201.

Ciocca, D.R. and Calderwood, S.K. (2005) Heat shock proteins in cancer: diagnostic, prognostic, predictive, and treatment implications. *Cell Stress Chaperones,* **10,** 86-103.

Coley, H.M., Shotton, C.F., Ajose-Adeogun, A., Modjtahedi, H. and Thomas, H. (2006) Receptor tyrosine kinase (RTK) inhibition is effective in chemosensitising EGFR-expressing drug resistant human ovarian cancer cell lines when used in combination with cytotoxic agents. *Biochem. Pharmacol.,* **72,** 941-948.

Collard, F., Vertommen, D., Fortpied, J., Duester, G. and Van Schaftingen, E. (2007) Identification of 3-deoxyglucosone dehydrogenase as aldehyde dehydrogenase 1A1 (retinaldehyde dehydrogenase 1). *Biochimie,* **89,** 369-373.

Colucci-Guyon, E., Portier, M.M., Dunia, I., Paulin, D., Pournin, S. and Babinet, C. (1994) Mice lacking vimentin develop and reproduce without an obvious phenotype. *Cell,* **79,** 679-694.

Cornett, D.S., Reyzer, M.L., Chaurand, P. and Caprioli, R.M. (2007) MALDI imaging mass spectrometry: molecular snapshots of biochemical systems. *Nat. Methods,* **4,** 828-833.

Couch, F.J., Johnson, M.R., Rabe, K.G., Brune, K., de Andrade, M., Goggins, M., Rothenmund, H., Gallinger, S., Klein, A., Petersen, G.M., et al (2007) The prevalence of BRCA2 mutations in familial pancreatic cancer. *Cancer Epidemiol. Biomarkers Prev.,* **16,** 342-346.

Coussens, L.M. and Werb, Z. (1996) Matrix metalloproteinases and the development of cancer. *Chem. Biol.,* **3,** 895-904.

Cunningham, C.C., Stossel, T.P. and Kwiatkowski, D.J. (1991) Enhanced motility in NIH 3T3 fibroblasts that overexpress gelsolin. *Science,* **251,** 1233-1236.

Czito, B.G., Willett, C.G., Bendell, J.C., Morse, M.A., Tyler, D.S., Fernando, N.H., Mantyh, C.R., Blobe, G.C., Honeycutt, W., Yu, D., et al (2006) Increased toxicity with gefitinib, capecitabine, and radiation therapy in pancreatic and rectal cancer: phase I trial results. *J. Clin. Oncol.,* **24,** 656-662.

Dancer, J., Takei, H., Ro, J.Y. and Lowery-Nordberg, M. (2007) Coexpression of EGFR and HER-2 in pancreatic ductal adenocarcinoma: a comparative study using immunohistochemistry correlated with gene amplification by fluorescent in situ hybridization. *Oncol. Rep.,* **18,** 151-155.

De Luca, L.M. (1991) Retinoids and their receptors in differentiation, embryogenesis, and neoplasia. *FASEB J.,* **5,** 2924-2933.

Declerck, Y. (2004) Focus on the cell membrane: the need for dissociation and detachment in tumoral invasion. *Cancer. Biol. Ther.,* **3,** 632-633.

Dedhar, S., Saulnier, R., Nagle, R. and Overall, C.M. (1993) Specific alterations in the expression of alpha 3 beta 1 and alpha 6 beta 4 integrins in highly invasive and metastatic variants of human prostate carcinoma cells selected by in vitro invasion through reconstituted basement membrane. *Clin. Exp. Metastasis,* **11,** 391-400.

Deng, M., Tu, Z., Sun, F. and Chen, T. (2004) Mapping Gene Ontology to proteins based on protein-protein interaction data. *Bioinformatics,* **20,** 895-902.

Deryugina, E.I. and Quigley, J.P. (2006) Matrix metalloproteinases and tumor metastasis. *Cancer Metastasis Rev.,* **25,** 9-34.

Di Gennaro, E., Barbarino, M., Bruzzese, F., De Lorenzo, S., Caraglia, M., Abbruzzese, A., Avallone, A., Comella, P., Caponigro, F., Pepe, S., et al (2003) Critical role of both p27KIP1 and p21CIP1/WAF1 in the antiproliferative effect of ZD1839 ('Iressa'), an epidermal growth factor receptor tyrosine kinase inhibitor, in head and neck squamous carcinoma cells. *J. Cell. Physiol.,* **195,** 139-150.

Domagala, W., Lasota, J., Dukowicz, A., Markiewski, M., Striker, G., Weber, K. and Osborn, M. (1990) Vimentin expression appears to be associated with poor prognosis in node-negative ductal NOS breast carcinomas. *Am. J. Pathol.,* **137,** 1299-1304.

Dosaka-Akita, H., Hommura, F., Fujita, H., Kinoshita, I., Nishi, M., Morikawa, T., Katoh, H., Kawakami, Y. and Kuzumaki, N. (1998) Frequent loss of gelsolin expression in non-small cell lung cancers of heavy smokers. *Cancer Res.,* **58,** 322-327.

Dow, R., Hendley, J., Pirkmaier, A., Musgrove, E.A. and Germain, D. (2001) Retinoic acid-mediated growth arrest requires ubiquitylation and degradation of the F-box protein Skp2. *J. Biol. Chem.,* **276,** 45945-45951.

Duester, G. (1996) Involvement of alcohol dehydrogenase, short-chain dehydrogenase/reductase, aldehyde dehydrogenase, and cytochrome P450 in the control of retinoid signaling by activation of retinoic acid synthesis. *Biochemistry,* **35,** 12221-12227.

Durkin, A.J., Bloomston, P.M., Rosemurgy, A.S., Giarelli, N., Cojita, D., Yeatman, T.J. and Zervos, E.E. (2003) Defining the role of the epidermal growth factor receptor in pancreatic cancer grown in vitro. *Am. J. Surg.,* **186,** 431-436.

Duxbury, M.S., Ito, H., Benoit, E., Ashley, S.W. and Whang, E.E. (2004) CEACAM6 is a determinant of pancreatic adenocarcinoma cellular invasiveness. *Br. J. Cancer,* **91,** 1384-1390.

Duxbury, M.S., Ito, H., Benoit, E., Waseem, T., Ashley, S.W. and Whang, E.E. (2005) RNA interference demonstrates a novel role for integrin-linked kinase as a determinant of pancreatic adenocarcinoma cell gemcitabine chemoresistance. *Clin. Cancer Res.,* **11,** 3433-3438.

Duxbury, M.S., Ito, H., Zinner, M.J., Ashley, S.W. and Whang, E.E. (2004) CEACAM6 gene silencing impairs anoikis resistance and in vivo metastatic ability of pancreatic adenocarcinoma cells. *Oncogene,* **23,** 465-473.

Duxbury, M.S., Ito, H., Zinner, M.J., Ashley, S.W. and Whang, E.E. (2004) EphA2: a determinant of malignant cellular behavior and a potential therapeutic target in pancreatic adenocarcinoma. *Oncogene,* **23,** 1448-1456.

Duxbury, M.S., Ito, H., Zinner, M.J., Ashley, S.W. and Whang, E.E. (2004) Focal adhesion kinase gene silencing promotes anoikis and suppresses metastasis of human pancreatic adenocarcinoma cells. *Surgery,* **135,** 555-562.

Duxbury, M.S., Ito, H., Zinner, M.J., Ashley, S.W. and Whang, E.E. (2004) RNA interference targeting the M2 subunit of ribonucleotide reductase enhances pancreatic adenocarcinoma chemosensitivity to gemcitabine. *Oncogene,* **23,** 1539-1548.

Ebert, M., Yokoyama, M., Friess, H., Buchler, M.W. and Korc, M. (1994) Coexpression of the c-met proto-oncogene and hepatocyte growth factor in human pancreatic cancer. *Cancer Res.,* **54,** 5775-5778.

Eckes, B., Dogic, D., Colucci-Guyon, E., Wang, N., Maniotis, A., Ingber, D., Merckling, A., Langa, F., Aumailley, M., Delouvee, A., et al (1998) Impaired mechanical stability, migration and contractile capacity in vimentin-deficient fibroblasts. *J. Cell. Sci.,* **111 (Pt 13),** 1897-1907.

Eisenhauer, E.A. and Vermorken, J.B. (1998) The taxoids. Comparative clinical pharmacology and therapeutic potential. *Drugs,* **55,** 5-30.

Eisold, S., Linnebacher, M., Ryschich, E., Antolovic, D., Hinz, U., Klar, E. and Schmidt, J. (2004) The effect of adenovirus expressing wild-type p53 on 5-fluorouracil chemosensitivity is related to p53 status in pancreatic cancer cell lines. *World J. Gastroenterol.,* **10,** 3583-3589.

Elbashir, S.M., Harborth, J., Lendeckel, W., Yalcin, A., Weber, K. and Tuschl, T. (2001) Duplexes of 21-nucleotide RNAs mediate RNA interference in cultured mammalian cells. *Nature,* **411,** 494-498.

Elbashir, S.M., Lendeckel, W. and Tuschl, T. (2001) RNA interference is mediated by 21- and 22-nucleotide RNAs. *Genes Dev.,* **15,** 188-200.

Ellerbroek, S.M., Fishman, D.A., Kearns, A.S., Bafetti, L.M. and Stack, M.S. (1999) Ovarian carcinoma regulation of matrix metalloproteinase-2 and membrane type 1 matrix metalloproteinase through beta1 integrin. *Cancer Res.,* **59,** 1635-1641.

Emmert-Buck, M.R., Gillespie, J.W., Paweletz, C.P., Ornstein, D.K., Basrur, V., Appella, E., Wang, Q.H., Huang, J., Hu, N., Taylor, P., et al (2000) An approach to proteomic analysis of human tumors. *Mol. Carcinog.,* **27,** 158-165.

Eustace, B.K. and Jay, D.G. (2004) Extracellular roles for the molecular chaperone, hsp90. *Cell. Cycle,* **3,** 1098-1100.

Fan, X., Molotkov, A., Manabe, S., Donmoyer, C.M., Deltour, L., Foglio, M.H., Cuenca, A.E., Blaner, W.S., Lipton, S.A. and Duester, G. (2003) Targeted disruption of Aldh1a1 (Raldh1) provides evidence for a complex mechanism of retinoic acid synthesis in the developing retina. *Mol. Cell. Biol.,* **23,** 4637-4648.

Fan, Z. and Mendelsohn, J. (1998) Therapeutic application of anti-growth factor receptor antibodies. *Curr. Opin. Oncol.,* **10,** 67-73.

Fang, S.M., Jin, X., Li, Y., Wang, R., Guo, W., Wang, N. and Zhang, J.H. (2005) Correlation of matrix metalloproteinase-3 polymorphism to genetic susceptibility and lymph node metastasis of non-small cell lung cancer. *Ai Zheng,* **24,** 305-310.

Fearon, E.R. and Vogelstein, B. (1990) A genetic model for colorectal tumorigenesis. *Cell,* **61,** 759-767.

Felding-Habermann, B. (2003) Integrin adhesion receptors in tumor metastasis. *Clin. Exp. Metastasis,* **20,** 203-213.

Feldmann, G., Dhara, S., Fendrich, V., Bedja, D., Beaty, R., Mullendore, M., Karikari, C., Alvarez, H., Iacobuzio-Donahue, C., Jimeno, A., et al (2007) Blockade of hedgehog signaling inhibits pancreatic cancer invasion and metastases: a new paradigm for combination therapy in solid cancers. *Cancer Res.,* **67,** 2187-2196.

Feng, F.Y., Varambally, S., Tomlins, S.A., Chun, P.Y., Lopez, C.A., Li, X., Davis, M.A., Chinnaiyan, A.M., Lawrence, T.S. and Nyati, M.K. (2007) Role of epidermal growth factor receptor degradation in gemcitabine-mediated cytotoxicity. *Oncogene,* **26,** 3431-3439.

Ferlay, J., Autier, P., Boniol, M., Heanue, M., Colombet, M., and Boyle, P. (2006) Estimates of the cancer incidence and mortality in Europe in 2006. *Ann Oncol.,* **18**, 581.592.

Festuccia, C., Angelucci, A., Gravina, G.L., Biordi, L., Millimaggi, D., Muzi, P., Vicentini, C. and Bologna, M. (2005) Epidermal growth factor modulates prostate cancer cell invasiveness regulating urokinase-type plasminogen activator activity. EGF-receptor inhibition may prevent tumor cell dissemination. *Thromb. Haemost.,* **93,** 964-975.

Fidler, I.J. and Kripke, M.L. (1977) Metastasis results from preexisting variant cells within a malignant tumor. *Science,* **197,** 893-895.

Filipits, M., Stranzl, T., Pohl, G., Heinzl, H., Jager, U., Geissler, K., Fonatsch, C., Haas, O.A., Lechner, K. and Pirker, R. (2000) Drug resistance factors in acute myeloid leukemia: a comparative analysis. *Leukemia,* **14,** 68-76.

Fire, A., Xu, S., Montgomery, M.K., Kostas, S.A., Driver, S.E. and Mello, C.C (1998) Potent and specific genetic interference by double-stranded RNA in Caenorhabditis elegans. *Nature*, **1**, 806-811.

Fisher, W.E. and Berger, D.H. (2003) Angiogenesis and antiangiogenic strategies in pancreatic cancer. *Int. J. Gastrointest. Cancer.,* **33,** 79-88.

Fjallskog, M.L., Lejonklou, M.H., Oberg, K.E., Eriksson, B.K. and Janson, E.T. (2003) Expression of molecular targets for tyrosine kinase receptor antagonists in malignant endocrine pancreatic tumors. *Clin. Cancer Res.,* **9,** 1469-1473.

Fleming, J.B., Shen, G.L., Holloway, S.E., Davis, M. and Brekken, R.A. (2005) Molecular consequences of silencing mutant K-ras in pancreatic cancer cells: justification for K-ras-directed therapy. *Mol. Cancer. Res.,* **3,** 413-423.

Fontana, J.A. (1987) Interaction of retinoids and tamoxifen on the inhibition of human mammary carcinoma cell proliferation. *Exp. Cell Biol.,* **55,** 136-144.

Fornaro, M., Tallini, G., Bofetiado, C.J., Bosari, S. and Languino, L.R. (1996) Down-regulation of beta 1C integrin, an inhibitor of cell proliferation, in prostate carcinoma. *Am. J. Pathol.,* **149,** 765-773.

Frei, E.,3rd, Cucchi, C.A., Rosowsky, A., Tantravahi, R., Bernal, S., Ervin, T.J., Ruprecht, R.M. and Haseltine, W.A. (1985) Alkylating agent resistance: in vitro studies with human cell lines. *Proc. Natl. Acad. Sci. U. S. A.,* **82,** 2158-2162.

Friess, H., Yamanaka, Y., Kobrin, M.S., Do, D.A., Buchler, M.W. and Korc, M. (1995) Enhanced erbB-3 expression in human pancreatic cancer correlates with tumor progression. *Clin. Cancer Res.,* **1,** 1413-1420.

Frisch, S.M. and Screaton, R.A. (2001) Anoikis mechanisms. *Curr. Opin. Cell Biol.,* **13,** 555-562.

Gallacher, L., Murdoch, B., Wu, D.M., Karanu, F.N., Keeney, M. and Bhatia, M. (2000) Isolation and characterization of human CD34(-)Lin(-) and CD34(+)Lin(-) hematopoietic stem cells using cell surface markers AC133 and CD7. *Blood,* **95,** 2813-2820.

Garcea, G., Neal, C.P., Pattenden, C.J., Steward, W.P. and Berry, D.P. (2005) Molecular prognostic markers in pancreatic cancer: a systematic review. *Eur. J. Cancer,* **41,** 2213-2236.

Gatenby, R.A., Gawlinski, E.T., Gmitro, A.F., Kaylor, B. and Gillies, R.J. (2006) Acid-mediated tumor invasion: a multidisciplinary study. *Cancer Res.,* **66,** 5216-5223.

Georgatos, S.D. and Blobel, G. (1987) Two distinct attachment sites for vimentin along the plasma membrane and the nuclear envelope in avian erythrocytes: a basis for a vectorial assembly of intermediate filaments. *J. Cell Biol.,* **105,** 105-115.

Georgoulias, V. (2002) Docetaxel (Taxotere) in the treatment of non-small cell lung cancer. *Curr Med Chem.*, **9**, 869-877

Gerdes, B., Ramaswamy, A., Ziegler, A., Lang, S.A., Kersting, M., Baumann, R., Wild, A., Moll, R., Rothmund, M. and Bartsch, D.K. (2002) p16INK4a is a prognostic marker in resected ductal pancreatic cancer: an analysis of p16INK4a, p53, MDM2, an Rb. *Ann. Surg.,* **235,** 51-59.

Germann, U.A., Pastan, I. and Gottesman, M.M. (1993) P-glycoproteins: mediators of multidrug resistance. *Semin. Cell Biol.,* **4,** 63-76.

Geyer, C.E., Forster, J., Lindquist, D., Chan, S., Romieu, C.G., Pienkowski, T., Jagiello-Gruszfeld, A., Crown, J., Chan, A., Kaufman, B., et al (2006) Lapatinib plus capecitabine for HER2-positive advanced breast cancer. *N. Engl. J. Med.,* **355,** 2733-2743.

Ghadirian, P., Lynch, H.T. and Krewski, D. (2003) Epidemiology of pancreatic cancer: an overview. *Cancer Detect. Prev.,* **27,** 87-93.

Gharbi, S., Gaffney, P., Yang, A., Zvelebil, M.J., Cramer, R., Waterfield, M.D. and Timms, J.F. (2002) Evaluation of two-dimensional differential gel electrophoresis for proteomic expression analysis of a model breast cancer cell system. *Mol. Cell. Proteomics,* **1,** 91-98.

Giancotti, F.G. and Ruoslahti, E. (1990) Elevated levels of the alpha 5 beta 1 fibronectin receptor suppress the transformed phenotype of Chinese hamster ovary cells. *Cell,* **60,** 849-859.

Gilles, C., Polette, M., Piette, J., Delvigne, A.C., Thompson, E.W., Foidart, J.M. and Birembaut, P. (1996) Vimentin expression in cervical carcinomas: association with invasive and migratory potential. *J. Pathol.,* **180,** 175-180.

Gilles, C., Polette, M., Zahm, J.M., Tournier, J.M., Volders, L., Foidart, J.M. and Birembaut, P. (1999) Vimentin contributes to human mammary epithelial cell migration. *J. Cell. Sci.,* **112 (Pt 24),** 4615-4625.

Giovannetti, E., Del Tacca, M., Mey, V., Funel, N., Nannizzi, S., Ricci, S., Orlandini, C., Boggi, U., Campani, D., Del Chiaro, M., et al (2006) Transcription analysis of human equilibrative nucleoside transporter-1 predicts survival in pancreas cancer patients treated with gemcitabine. *Cancer Res.,* **66,** 3928-3935.

GlaxoSmithKline
www.gsk.com (2006)

Glynn, S.A., Gammell, P., Heenan, M., O'Connor, R., Liang, Y., Keenan, J. and Clynes, M. (2004) A new superinvasive in vitro phenotype induced by selection of human breast carcinoma cells with the chemotherapeutic drugs paclitaxel and doxorubicin. *Br. J. Cancer,* **91,** 1800-1807.

Goan, Y.G., Zhou, B., Hu, E., Mi, S. and Yen, Y. (1999) Overexpression of ribonucleotide reductase as a mechanism of resistance to 2,2-difluorodeoxycytidine in the human KB cancer cell line. *Cancer Res.,* **59,** 4204-4207.

Gobin, A.S. and West, J.L. (2002) Cell migration through defined, synthetic ECM analogs. *FASEB J.,* **16,** 751-753.

Godwin, A.K., Meister, A., O'Dwyer, P.J., Huang, C.S., Hamilton, T.C. and Anderson, M.E. (1992) High resistance to cisplatin in human ovarian cancer cell lines is associated with marked increase of glutathione synthesis. *Proc. Natl. Acad. Sci. U. S. A.,* **89,** 3070-3074.

Goggins, M. (2005) Molecular markers of early pancreatic cancer. *J. Clin. Oncol.,* **23,** 4524-4531.

Goldman, R.D., Khuon, S., Chou, Y.H., Opal, P. and Steinert, P.M. (1996) The function of intermediate filaments in cell shape and cytoskeletal integrity. *J. Cell Biol.,* **134,** 971-983.

Goplen, D., Wang, J., Enger, P.O., Tysnes, B.B., Terzis, A.J., Laerum, O.D. and Bjerkvig, R. (2006) Protein disulfide isomerase expression is related to the invasive properties of malignant glioma. *Cancer Res.,* **66,** 9895-9902.

Gorg, A., Weiss, W. and Dunn, M.J. (2004) Current two-dimensional electrophoresis technology for proteomics. *Proteomics,* **4,** 3665-3685.

Goswami, S., Wang, W., Wyckoff, J.B. and Condeelis, J.S. (2004) Breast cancer cells isolated by chemotaxis from primary tumors show increased survival and resistance to chemotherapy. *Cancer Res.,* **64,** 7664-7667.

Gottesman, M.M. and Pastan, I. (1993) Biochemistry of multidrug resistance mediated by the multidrug transporter. *Annu. Rev. Biochem.,* **62,** 385-427.

Graber, H.U., Friess, H., Kaufmann, B., Willi, D., Zimmermann, A., Korc, M. and Buchler, M.W. (1999) ErbB-4 mRNA expression is decreased in non-metastatic pancreatic cancer. *Int. J. Cancer,* **84,** 24-27.

Gress, T.M., Muller-Pillasch, F., Weber, C., Lerch, M.M., Friess, H., Buchler, M., Beger, H.G. and Adler, G. (1994) Differential expression of heat shock proteins in pancreatic carcinoma. *Cancer Res.,* **54,** 547-551.

Grille, S.J., Bellacosa, A., Upson, J., Klein-Szanto, A.J., van Roy, F., Lee-Kwon, W., Donowitz, M., Tsichlis, P.N. and Larue, L. (2003) The protein kinase Akt induces epithelial mesenchymal transition and promotes enhanced motility and invasiveness of squamous cell carcinoma lines. *Cancer Res.,* **63,** 2172-2178.

Gronborg, M., Bunkenborg, J., Kristiansen, T.Z., Jensen, O.N., Yeo, C.J., Hruban, R.H., Maitra, A., Goggins, M.G. and Pandey, A. (2004) Comprehensive proteomic analysis of human pancreatic juice. *J. Proteome Res.,* **3,** 1042-1055.

Grossmann, J. (2002) Molecular mechanisms of "detachment-induced apoptosis--Anoikis". *Apoptosis,* **7,** 247-260.

Grzesiak, J.J. and Bouvet, M. (2007) Determination of the ligand-binding specificities of the alpha2beta1 and alpha1beta1 integrins in a novel 3-dimensional in vitro model of pancreatic cancer. *Pancreas,* **34,** 220-228.

Grzesiak, J.J. and Bouvet, M. (2006) The alpha2beta1 integrin mediates the malignant phenotype on type I collagen in pancreatic cancer cell lines. *Br. J. Cancer,* **94,** 1311-1319.

Guan, H.T., Xue, X.H., Dai, Z.J., Wang, X.J., Li, A. and Qin, Z.Y. (2006) Down-regulation of survivin expression by small interfering RNA induces pancreatic cancer cell apoptosis and enhances its radiosensitivity. *World J. Gastroenterol.,* **12,** 2901-2907.

Guan, H.T., Xue, X.H., Wang, X.J., Li, A. and Qin, Z.Y. (2006) Effects of siRNA targeted to survivin in suppressing proliferation and inducing apoptosis in breast cancer MCF-7 cells. *Zhonghua Zhong Liu Za Zhi,* **28,** 326-330.

Guo, X.L., Lin, G.J., Zhao, H., Gao, Y., Qian, L.P., Xu, S.R., Fu, L.N., Xu, Q. and Wang, J.J. (2003) Inhibitory effects of docetaxel on expression of VEGF, bFGF and MMPs of LS174T cell. *World J. Gastroenterol.,* **9,** 1995-1998.

Gygi, S.P., Rochon, Y., Franza, B.R. and Aebersold, R. (1999) Correlation between protein and mRNA abundance in yeast. *Mol. Cell. Biol.,* **19,** 1720-1730.

Haber, M., Burkhart, C.A., Regl, D.L., Madafiglio, J., Norris, M.D. and Horwitz, S.B. (1995) Altered expression of M beta 2, the class II beta-tubulin isotype, in a murine J774.2 cell line with a high level of taxol resistance. *J. Biol. Chem.,* **270,** 31269-31275.

Hahn, S.A., Schutte, M., Hoque, A.T., Moskaluk, C.A., da Costa, L.T., Rozenblum, E., Weinstein, C.L., Fischer, A., Yeo, C.J., Hruban, R.H., et al (1996) DPC4, a candidate tumor suppressor gene at human chromosome 18q21.1. *Science,* **271,** 350-353.

Hall, P.A., Coates, P., Lemoine, N.R. and Horton, M.A. (1991) Characterization of integrin chains in normal and neoplastic human pancreas. *J. Pathol.,* **165,** 33-41.

Hansel, D.E., Rahman, A., House, M., Ashfaq, R., Berg, K., Yeo, C.J. and Maitra, A. (2004) Met proto-oncogene and insulin-like growth factor binding protein 3 overexpression correlates with metastatic ability in well-differentiated pancreatic endocrine neoplasms. *Clin. Cancer Res.,* **10,** 6152-6158.

Havik, B. and Bramham, C.R. (2007) Additive viability-loss following hsp70/hsc70 double interference and Hsp90 inhibition in two breast cancer cell lines. *Oncol. Rep.,* **17,** 1501-1510.

Hay, E.D. (1995) An overview of epithelio-mesenchymal transformation. *Acta Anat. (Basel),* **154,** 8-20.

Hemmati, H.D., Nakano, I., Lazareff, J.A., Masterman-Smith, M., Geschwind, D.H., Bronner-Fraser, M. and Kornblum, H.I. (2003) Cancerous stem cells can arise from pediatric brain tumors. *Proc. Natl. Acad. Sci. U. S. A.,* **100,** 15178-15183.

Hendrix, M.J., Seftor, E.A., Seftor, R.E. and Trevor, K.T. (1997) Experimental co-expression of vimentin and keratin intermediate filaments in human breast cancer cells results in phenotypic interconversion and increased invasive behavior. *Am. J. Pathol.,* **150,** 483-495.

Hendrix, M.J., Wood, W.R., Seftor, E.A., Lotan, D., Nakajima, M., Misiorowski, R.L., Seftor, R.E., Stetler-Stevenson, W.G., Bevacqua, S.J. and Liotta, L.A. (1990) Retinoic acid inhibition of human melanoma cell invasion through a reconstituted basement membrane and its relation to decreases in the expression of proteolytic enzymes and motility factor receptor. *Cancer Res.,* **50,** 4121-4130.

Hernandez, M.P., Sullivan, W.P. and Toft, D.O. (2002) The assembly and intermolecular properties of the hsp70-Hop-hsp90 molecular chaperone complex. *J. Biol. Chem.,* **277,** 38294-38304.

Herrera, C.A., Xu, L., Bucana, C.D., Silva el, V.G., Hess, K.R., Gershenson, D.M. and Fidler, I.J. (2002) Expression of metastasis-related genes in human epithelial ovarian tumors. *Int. J. Oncol.,* **20,** 5-13.

Herrmann, R., Bodoky, G., Ruhstaller, T., Glimelius, B., Bajetta, E., Schuller, J., Saletti, P., Bauer, J., Figer, A., Pestalozzi, B., et al (2007) Gemcitabine plus capecitabine compared with gemcitabine alone in advanced pancreatic cancer: a randomized, multicenter, phase III trial of the Swiss Group for Clinical Cancer Research and the Central European Cooperative Oncology Group. *J. Clin. Oncol.,* **25,** 2212-2217.

Hillenkamp, F. and Karas, M. (1990) Mass spectrometry of peptides and proteins by matrix-assisted ultraviolet laser desorption/ionization. *Methods Enzymol.,* **193,** 280-295.

Hofmann, U.B., Westphal, J.R., Waas, E.T., Becker, J.C., Ruiter, D.J. and van Muijen, G.N. (2000) Coexpression of integrin alpha(v)beta3 and matrix metalloproteinase-2 (MMP-2) coincides with MMP-2 activation: correlation with melanoma progression. *J. Invest. Dermatol.,* **115,** 625-632.

Holland, J.F. and Frei, E. 3rd, editors. Cancer medicine 6. Hamilton (ON): BC Decker Inc; 2003.

Holly, S.P., Larson, M.K. and Parise, L.V. (2000) Multiple roles of integrins in cell motility. *Exp. Cell Res.,* **261,** 69-74.

Honda, K., Hayashida, Y., Umaki, T., Okusaka, T., Kosuge, T., Kikuchi, S., Endo, M., Tsuchida, A., Aoki, T., Itoi, T., et al (2005) Possible detection of pancreatic cancer by plasma protein profiling. *Cancer Res.,* **65,** 10613-10622.

Hong, S.H., Misek, D.E., Wang, H., Puravs, E., Giordano, T.J., Greenson, J.K., Brenner, D.E., Simeone, D.M., Logsdon, C.D. and Hanash, S.M. (2004) An autoantibody-mediated immune response to calreticulin isoforms in pancreatic cancer. *Cancer Res., 64,* 5504-5510.

Horizons in cancer therapeutics. From bench to bedside www.meniscus.com (2001)

Hotz, B., Arndt, M., Dullat, S., Bhargava, S., Buhr, H.J. and Hotz, H.G. (2007) Epithelial to mesenchymal transition: expression of the regulators snail, slug, and twist in pancreatic cancer. *Clin. Cancer Res., 13,* 4769-4776.

Howlett, A.R., Bailey, N., Damsky, C., Petersen, O.W. and Bissell, M.J. (1995) Cellular growth and survival are mediated by beta 1 integrins in normal human breast epithelium but not in breast carcinoma. *J. Cell. Sci., 108 (Pt 5),* 1945-1957.

Hruban, R.H., Offerhaus, G.J., Kern, S.E., Goggins, M., Wilentz, R.E. and Yeo, C.J. (1998) Tumor-suppressor genes in pancreatic cancer. *J. Hepatobiliary. Pancreat. Surg., 5,* 383-391.

Hsu, M.Y., Shih, D.T., Meier, F.E., Van Belle, P., Hsu, J.Y., Elder, D.E., Buck, C.A. and Herlyn, M. (1998) Adenoviral gene transfer of beta3 integrin subunit induces conversion from radial to vertical growth phase in primary human melanoma. *Am. J. Pathol., 153,* 1435-1442.

Hu, L., Lau, S.H., Tzang, C.H., Wen, J.M., Wang, W., Xie, D., Huang, M., Wang, Y., Wu, M.C., Huang, J.F., et al (2004) Association of Vimentin overexpression and hepatocellular carcinoma metastasis. *Oncogene, 23,* 298-302.

Huang, M.E., Ye, Y.C., Chen, S.R., Chai, J.R., Lu, J.X., Zhoa, L., Gu, L.J. and Wang, Z.Y. (1988) Use of all-trans retinoic acid in the treatment of acute promyelocytic leukemia. *Blood, 72,* 567-572.

Huang, P., Chubb, S., Hertel, L.W., Grindey, G.B. and Plunkett, W. (1991) Action of 2',2'-difluorodeoxycytidine on DNA synthesis. *Cancer Res., 51,* 6110-6117.

Hugh, T.J., Dillon, S.A., O'Dowd, G., Getty, B., Pignatelli, M., Poston, G.J. and Kinsella, A.R. (1999) Beta-Catenin Expression in Primary and Metastatic Colorectal Carcinoma. *Int. J. Cancer, 82,* 504-511.

Hynes, R.O. (1992) Integrins: versatility, modulation, and signaling in cell adhesion. *Cell, 69,* 11-25.

Iacobuzio-Donahue, C.A., Ashfaq, R., Maitra, A., Adsay, N.V., Shen-Ong, G.L., Berg, K., Hollingsworth, M.A., Cameron, J.L., Yeo, C.J., Kern, S.E., et al (2003) Highly expressed genes in pancreatic ductal adenocarcinomas: a comprehensive characterization and comparison of the transcription profiles obtained from three major technologies. *Cancer Res., 63,* 8614-8622.

Ianniello, G.P., Orditura, M., Rossi, A., De Vita, F., Maiorino, L., Carrozza, F., Manzione, L. and Catalano, G. (2001) Gemcitabine plus epirubicin in advanced pancreatic cancer: a phase II multicenter trial. *Oncol. Rep., 8,* 1111-1115.

Ignatiadis, M., Polyzos, A., Stathopoulos, G.P., Tselepatiotis, E., Christophylakis, C., Kalbakis, K., Vamvakas, L., Kotsakis, A., Potamianou, A. and Georgoulias, V. (2006) A multicenter phase II study of docetaxel in combination with gefitinib in gemcitabine-pretreated patients with advanced/metastatic pancreatic cancer. *Oncology,* **71,** 159-163.

Ikebe, T., Takeuchi, H., Jimi, E., Beppu, M., Shinohara, M. and Shirasuna, K. (1998) Involvement of proteasomes in migration and matrix metalloproteinase-9 production of oral squamous cell carcinoma. *Int. J. Cancer,* **77,** 578-585.

Ishikawa, T., Fukase, Y., Yamamoto, T., Sekiguchi, F. and Ishitsuka, H. (1998) Antitumor activities of a novel fluoropyrimidine, N4-pentyloxycarbonyl-5'-deoxy-5-fluorocytidine (capecitabine). *Biol. Pharm. Bull.,* **21,** 713-717.

Ishitobi, M., Shin, E. and Kikkawa, N. (2001) Metastatic breast cancer with resistance to both anthracycline and docetaxel successfully treated with weekly paclitaxel. *Int. J. Clin. Oncol.,* **6,** 55-58.

Ito, H., Duxbury, M., Zinner, M.J., Ashley, S.W. and Whang, E.E. (2004) Glucose transporter-1 gene expression is associated with pancreatic cancer invasiveness and MMP-2 activity. *Surgery,* **136,** 548-556.

Ito, H., Kambe, H., Kimura, Y., Nakamura, H., Hayashi, E., Kishimoto, T., Kishimoto, S. and Yamamoto, H. (1992) Depression of plasma gelsolin level during acute liver injury. *Gastroenterology,* **102,** 1686-1692.

Izquierdo, M.A., Neefjes, J.J., Mathari, A.E., Flens, M.J., Scheffer, G.L. and Scheper, R.J. (1996) Overexpression of the ABC transporter TAP in multidrug-resistant human cancer cell lines. *Br. J. Cancer,* **74,** 1961-1967.

Jaattela, M., Wissing, D., Kokholm, K., Kallunki, T. and Egeblad, M. (1998) Hsp70 exerts its anti-apoptotic function downstream of caspase-3-like proteases. *EMBO J.,* **17,** 6124-6134.

Jackson, A.L., Bartz, S.R., Schelter, J., Kobayashi, S.V., Burchard, J., Mao, M., Li, B., Cavet, G. and Linsley, P.S. (2003) Expression profiling reveals off-target gene regulation by RNAi. *Nat. Biotechnol.,* **21,** 635-637.

Jallal, H., Valentino, M.L., Chen, G., Boschelli, F., Ali, S. and Rabbani, S.A. (2007) A Src/Abl kinase inhibitor, SKI-606, blocks breast cancer invasion, growth, and metastasis in vitro and in vivo. *Cancer Res.,* **67,** 1580-1588.

Javle, M.M., Gibbs, J.F., Iwata, K.K., Pak, Y., Rutledge, P., Yu, J., Black, J.D., Tan, D. and Khoury, T. (2007) Epithelial-Mesenchymal Transition (EMT) and Activated Extracellular Signal-regulated Kinase (p-Erk) in Surgically Resected Pancreatic Cancer. *Ann. Surg. Oncol.,*

Jawhari, A., Jordan, S., Poole, S., Browne, P., Pignatelli, M. and Farthing, M.J. (1997) Abnormal immunoreactivity of the E-cadherin-catenin complex in gastric carcinoma: relationship with patient survival. *Gastroenterology,* **112,** 46-54.

Jemal, A., Thomas, A., Murray, T. and Thun, M. (2002) Cancer statistics, 2002. *CA Cancer. J. Clin.,* **52,** 23-47.

Jeong, J., Park, Y.N., Park, J.S., Yoon, D.S., Chi, H.S. and Kim, B.R. (2005) Clinical significance of p16 protein expression loss and aberrant p53 protein expression in pancreatic cancer. *Yonsei Med. J.,* **46,** 519-525.

Ji, Z., Mei, F.C., Xie, J. and Cheng, X. (2007) Oncogenic KRAS activates hedgehog signaling pathway in pancreatic cancer cells. *J. Biol. Chem.,* **282,** 14048-14055.

Jiang, D., Ying, W., Lu, Y., Wan, J., Zhai, Y., Liu, W., Zhu, Y., Qiu, Z., Qian, X. and He, F. (2003) Identification of metastasis-associated proteins by proteomic analysis and functional exploration of interleukin-18 in metastasis. *Proteomics,* **3,** 724-737.

Jones, L.E., Humphreys, M.J., Campbell, F., Neoptolemos, J.P. and Boyd, M.T. (2004) Comprehensive analysis of matrix metalloproteinase and tissue inhibitor expression in pancreatic cancer: increased expression of matrix metalloproteinase-7 predicts poor survival. *Clin. Cancer Res.,* **10,** 2832-2845.

Jones, M.B., Krutzsch, H., Shu, H., Zhao, Y., Liotta, L.A., Kohn, E.C. and Petricoin, E.F.,3rd (2002) Proteomic analysis and identification of new biomarkers and therapeutic targets for invasive ovarian cancer. *Proteomics,* **2,** 76-84.

Joo, Y.E., Rew, J.S., Park, C.S. and Kim, S.J. (2002) Expression of E-cadherin, alpha- and beta-catenins in patients with pancreatic adenocarcinoma. *Pancreatology,* **2,** 129-137.

Jordheim, L.P., Guittet, O., Lepoivre, M., Galmarini, C.M. and Dumontet, C. (2005) Increased expression of the large subunit of ribonucleotide reductase is involved in resistance to gemcitabine in human mammary adenocarcinoma cells. *Mol. Cancer. Ther.,* **4,** 1268-1276.

Joshi, S., Guleria, R., Pan, J., DiPette, D. and Singh, U.S. (2006) Retinoic acid receptors and tissue-transglutaminase mediate short-term effect of retinoic acid on migration and invasion of neuroblastoma SH-SY5Y cells. *Oncogene,* **25,** 240-247.

Jung, C.P., Motwani, M.V. and Schwartz, G.K. (2001) Flavopiridol increases sensitization to gemcitabine in human gastrointestinal cancer cell lines and correlates with down-regulation of ribonucleotide reductase M2 subunit. *Clin. Cancer Res.,* **7,** 2527-2536.

Jungert, K., Buck, A., von Wichert, G., Adler, G., Konig, A., Buchholz, M., Gress, T.M. and Ellenrieder, V. (2007) Sp1 is required for transforming growth factor-beta-induced mesenchymal transition and migration in pancreatic cancer cells. *Cancer Res.,* **67,** 1563-1570.

Kaiser, A., Wolf-Breitinger, M., Albers, A., Dorbic, T., Wittig, B., Riecken, E.O. and Rosewicz, S. (1998) Retinoic acid receptor gamma1 expression determines retinoid sensitivity in pancreatic carcinoma cells. *Gastroenterology,* **115,** 967-977.

Kami, K., Doi, R., Koizumi, M., Toyoda, E., Mori, T., Ito, D., Kawaguchi, Y., Fujimoto, K., Wada, M., Miyatake, S., et al (2005) Downregulation of survivin by siRNA diminishes radioresistance of pancreatic cancer cells. *Surgery,* **138,** 299-305.

Kapitein, L.C., Peterman, E.J., Kwok, B.H., Kim, J.H., Kapoor, T.M. and Schmidt, C.F. (2005) The bipolar mitotic kinesin Eg5 moves on both microtubules that it crosslinks. *Nature,* **435,** 114-118.

Karas, M. and Hillenkamp, F. (1988) Laser desorption ionization of proteins with molecular masses exceeding 10,000 daltons. *Anal. Chem.,* **60,** 2299-2301.

Karatzas, G., Karayiannakis, A.J., Syrigos, K.N., Chatzigianni, E., Papanikolaou, S., Riza, F. and Papanikolaou, D. (1999) E-cadherin expression correlates with tumor differentiation in colorectal cancer. *Hepatogastroenterology,* **46,** 232-235.

Kasai, H., Allen, J.T., Mason, R.M., Kamimura, T. and Zhang, Z. (2005) TGF-beta1 induces human alveolar epithelial to mesenchymal cell transition (EMT). *Respir. Res.,* **6,** 56.

Kastan, M.B., Schlaffer, E., Russo, J.E., Colvin, O.M., Civin, C.I. and Hilton, J. (1990) Direct demonstration of elevated aldehyde dehydrogenase in human hematopoietic progenitor cells. *Blood,* **75,** 1947-1950.

Kato, Y., Nakayama, Y., Umeda, M. and Miyazaki, K. (1992) Induction of 103-kDa gelatinase/type IV collagenase by acidic culture conditions in mouse metastatic melanoma cell lines. *J. Biol. Chem.,* **267,** 11424-11430.

Kayahara, M., Nakagawara, H., Kitagawa, H. and Ohta, T. (2007) The nature of neural invasion by pancreatic cancer. *Pancreas,* **35,** 218-223.

Kazmirski, S.L., Isaacson, R.L., An, C., Buckle, A., Johnson, C.M., Daggett, V. and Fersht, A.R. (2002) Loss of a metal-binding site in gelsolin leads to familial amyloidosis-Finnish type. *Nat. Struct. Biol.,* **9,** 112-116.

Kim, D. and Chung, J. (2002) Akt: versatile mediator of cell survival and beyond. *J. Biochem. Mol. Biol.,* **35,** 106-115.

Kim, H.J., Park, C.I., Park, B.W., Lee, H.D. and Jung, W.H. (2006) Expression of MT-1 MMP, MMP2, MMP9 and TIMP2 mRNAs in ductal carcinoma in situ and invasive ductal carcinoma of the breast. *Yonsei Med. J.,* **47,** 333-342.

Kim, J.C., Ali, M.A., Nandi, A., Mukhopadhyay, P., Choy, H., Cao, C. and Saha, D. (2005) Correlation of HER1/EGFR expression and degree of radiosensitizing effect of the HER1/EGFR-tyrosine kinase inhibitor erlotinib. *Indian J. Biochem. Biophys.,* **42,** 358-365.

Kiyomiya, K., Matsuo, S. and Kurebe, M. (2001) Mechanism of specific nuclear transport of adriamycin: the mode of nuclear translocation of adriamycin-proteasome complex. *Cancer Res.,* **61,** 2467-2471.

Kleer, C.G., Zhang, Y., Pan, Q. and Merajver, S.D. (2004) WISP3 (CCN6) is a secreted tumor-suppressor protein that modulates IGF signaling in inflammatory breast cancer. *Neoplasia,* **6,** 179-185.

Klemke, R.L., Yebra, M., Bayna, E.M. and Cheresh, D.A. (1994) Receptor tyrosine kinase signaling required for integrin alpha v beta 5-directed cell motility but not adhesion on vitronectin. *J. Cell Biol.,* **127,** 859-866.

Kohn, E.C., Alessandro, R., Spoonster, J., Wersto, R.P. and Liotta, L.A. (1995) Angiogenesis: role of calcium-mediated signal transduction. *Proc. Natl. Acad. Sci. U. S. A.,* **92,** 1307-1311.

Kokkinos, M.I., Wafai, R., Wong, M.K., Newgreen, D.F., Thompson, E.W. and Waltham, M. (2007) Vimentin and epithelial-mesenchymal transition in human breast cancer--observations in vitro and in vivo. *Cells Tissues Organs,* **185,** 191-203.

Konig, J., Hartel, M., Nies, A.T., Martignoni, M.E., Guo, J., Buchler, M.W., Friess, H. and Keppler, D. (2005) Expression and localization of human multidrug resistance protein (ABCC) family members in pancreatic carcinoma. *Int. J. Cancer,* **115,** 359-367.

Konig, J., Rost, D., Cui, Y. and Keppler, D. (1999) Characterization of the human multidrug resistance protein isoform MRP3 localized to the basolateral hepatocyte membrane. *Hepatology,* **29,** 1156-1163.

Kool, M., de Haas, M., Scheffer, G.L., Scheper, R.J., van Eijk, M.J., Juijn, J.A., Baas, F. and Borst, P. (1997) Analysis of expression of cMOAT (MRP2), MRP3, MRP4, and MRP5, homologues of the multidrug resistance-associated protein gene (MRP1), in human cancer cell lines. *Cancer Res.,* **57,** 3537-3547.

Kornmann, M., Beger, H.G. and Link, K.H. (2003) Chemosensitivity testing and test-directed chemotherapy in human pancreatic cancer. *Recent Results Cancer Res.,* **161,** 180-195.

Koya, R.C., Fujita, H., Shimizu, S., Ohtsu, M., Takimoto, M., Tsujimoto, Y. and Kuzumaki, N. (2000) Gelsolin inhibits apoptosis by blocking mitochondrial membrane potential loss and cytochrome c release. *J. Biol. Chem.,* **275,** 15343-15349.

Krengel, S., Stark, I., Geuchen, C., Knoppe, B., Scheel, G., Schlenke, P., Gebert, A., Wunsch, L., Brinckmann, J. and Tronnier, M. (2005) Selective down-regulation of the alpha6-integrin subunit in melanocytes by UVB light. *Exp. Dermatol.,* **14,** 411-419.

Kubota, S., Ito, H., Ishibashi, Y. and Seyama, Y. (1997) Anti-alpha3 integrin antibody induces the activated form of matrix metalloprotease-2 (MMP-2) with concomitant stimulation of invasion through matrigel by human rhabdomyosarcoma cells. *Int. J. Cancer,* **70,** 106-111.

Kulasingam, V. and Diamandis, E.P. (2007) Proteomic analysis of conditioned media from three breast cancer cell lines: A mine for biomarkers and therapeutic targets. *Mol. Cell. Proteomics,*

Kumar, N., Tomar, A., Parrill, A.L. and Khurana, S. (2004) Functional dissection and molecular characterization of calcium-sensitive actin-capping and actin-depolymerizing sites in villin. *J. Biol. Chem.,* **279,** 45036-45046.

Kuramitsu, Y. and Nakamura, K. (2006) Proteomic analysis of cancer tissues: shedding light on carcinogenesis and possible biomarkers. *Proteomics,* **6,** 5650-5661.

Kuriyama, M., Tsutsui, K., Tsutsui, K., Ono, Y., Tamiya, T., Matsumoto, K., Furuta, T. and Ohmoto, T. (1997) Induction of resistance to etoposide and adriamycin in a human glioma cell line treated with antisense oligodeoxynucleotide complementary to the messenger ribonucleic acid of deoxyribonucleic acid topoisomerase II alpha. *Neurol. Med. Chir. (Tokyo),* **37,** 655-61; discussion 661-2.

Kwiatkowski, D.J., Mehl, R. and Yin, H.L. (1988) Genomic organization and biosynthesis of secreted and cytoplasmic forms of gelsolin. *J. Cell Biol.,* **106,** 375-384.

Kwiatkowski, D.J., Stossel, T.P., Orkin, S.H., Mole, J.E., Colten, H.R. and Yin, H.L. (1986) Plasma and cytoplasmic gelsolins are encoded by a single gene and contain a duplicated actin-binding domain. *Nature,* **323,** 455-458.

Lage, H. and Dietel, M. (2002) Multiple mechanisms confer different drug-resistant phenotypes in pancreatic carcinoma cells. *J. Cancer Res. Clin. Oncol.,* **128,** 349-357.

Languino, L.R., Gehlsen, K.R., Wayner, E., Carter, W.G., Engvall, E. and Ruoslahti, E. (1989) Endothelial cells use alpha 2 beta 1 integrin as a laminin receptor. *J. Cell Biol.,* **109,** 2455-2462.

Larjava, H., Lyons, J.G., Salo, T., Makela, M., Koivisto, L., Birkedal-Hansen, H., Akiyama, S.K., Yamada, K.M. and Heino, J. (1993) Anti-integrin antibodies induce type IV collagenase expression in keratinocytes. *J. Cell. Physiol.,* **157,** 190-200.

Larue, L. and Bellacosa, A. (2005) Epithelial-mesenchymal transition in development and cancer: role of phosphatidylinositol 3' kinase/AKT pathways. *Oncogene,* **24,** 7443-7454.

Lazaris, A.C., Theodoropoulos, G.E., Davaris, P.S., Panoussopoulos, D., Nakopoulou, L., Kittas, C. and Golematis, B.C. (1995) Heat shock protein 70 and HLA-DR molecules tissue expression. Prognostic implications in colorectal cancer. *Dis. Colon Rectum,* **38,** 739-745.

Lazaris, A.C., Chatzigianni, E.B., Panoussopoulos, D., Tzimas, G.N., Davaris, P.S. and Golematis, B.C. (1997) Proliferating cell nuclear antigen and heat shock protein 70 immunolocalization in invasive ductal breast cancer not otherwise specified. *Breast Cancer Res. Treat.,* **43,** 43-51.

Leader, M., Collins, M., Patel, J. and Henry, K. (1987) Vimentin: an evaluation of its role as a tumour marker. *Histopathology,* **11,** 63-72.

Lee, H.K., Driscoll, D., Asch, H., Asch, B. and Zhang, P.J. (1999) Downregulated gelsolin expression in hyperplastic and neoplastic lesions of the prostate. *Prostate,* **40,** 14-19.

Leelawat, K., Ohuchida, K., Mizumoto, K., Mahidol, C. and Tanaka, M. (2005) All-trans retinoic acid inhibits the cell proliferation but enhances the cell invasion through up-regulation of c-met in pancreatic cancer cells. *Cancer Lett.,* **224,** 303-310.

Lefcort, F., Venstrom, K., McDonald, J.A. and Reichardt, L.F. (1992) Regulation of expression of fibronectin and its receptor, alpha 5 beta 1, during development and regeneration of peripheral nerve. *Development,* **116,** 767-782.

Lei, S., Appert, H.E., Nakata, B., Domenico, D.R., Kim, K. and Howard, J.M. (1995) Overexpression of HER2/neu oncogene in pancreatic cancer correlates with shortened survival. *Int. J. Pancreatol.,* **17,** 15-21.

Lemoine, N.R., Jain, S., Hughes, C.M., Staddon, S.L., Maillet, B., Hall, P.A. and Kloppel, G. (1992) Ki-ras oncogene activation in preinvasive pancreatic cancer. *Gastroenterology,* **102,** 230-236.

Levy, L. and Hill, C.S. (2005) Smad4 dependency defines two classes of transforming growth factor {beta} (TGF-{beta}) target genes and distinguishes TGF-{beta}-induced epithelial-mesenchymal transition from its antiproliferative and migratory responses. *Mol. Cell. Biol.,* **25,** 8108-8125.

Lewis, D.L., Hagstrom, J.E., Loomis, A.G., Wolff, J.A. and Herweijer, H. (2002) Efficient delivery of siRNA for inhibition of gene expression in postnatal mice. *Nat. Genet.,* **32,** 107-108.

Li, C., Heidt, D.G., Dalerba, P., Burant, C.F., Zhang, L., Adsay, V., Wicha, M., Clarke, M.F. and Simeone, D.M. (2007) Identification of pancreatic cancer stem cells. *Cancer Res.,* **67,** 1030-1037.

Li, C. and Wan, Y.J. (1998) Differentiation and antiproliferation effects of retinoic acid receptor beta in hepatoma cells. *Cancer Lett.,* **124,** 205-211.

Li, J., Kleeff, J., Giese, N., Buchler, M.W., Korc, M. and Friess, H. (2004) Gefitinib ('Iressa', ZD1839), a selective epidermal growth factor receptor tyrosine kinase inhibitor, inhibits pancreatic cancer cell growth, invasion, and colony formation. *Int. J. Oncol.,* **25,** 203-210.

Li, Q.F., Spinelli, A.M., Wang, R., Anfinogenova, Y., Singer, H.A. and Tang, D.D. (2006) Critical role of vimentin phosphorylation at Ser-56 by p21-activated kinase in vimentin cytoskeleton signaling. *J. Biol. Chem.,* **281,** 34716-34724.

Liang, Y., McDonnell, S. and Clynes, M. (2002) Examining the relationship between cancer invasion/metastasis and drug resistance. *Curr. Cancer. Drug Targets,* **2,** 257-277.

Liang, Y., O'Driscoll, L., McDonnell, S., Doolan, P., Oglesby, I., Duffy, K., O'Connor, R. and Clynes, M. (2004) Enhanced in vitro invasiveness and drug resistance with altered gene expression patterns in a human lung carcinoma cell line after pulse selection with anticancer drugs. *Int. J. Cancer,* **111,** 484-493.

Lindquist, S. (1986) The heat-shock response. *Annu. Rev. Biochem.,* **55,** 1151-1191.

Liotta, L.A. and Stetler-Stevenson, W.G. (1991) Tumor invasion and metastasis: an imbalance of positive and negative regulation. *Cancer Res.,* **51,** 5054s-5059s.

Liu, B., Staren, E., Iwamura, T., Appert, H. and Howard, J. (2001) Taxotere resistance in SUIT Taxotere resistance in pancreatic carcinoma cell line SUIT 2 and its sublines. *World J. Gastroenterol.,* **7,** 855-859.

Liu, B., Staren, E.D., Iwamura, T., Appert, H.E. and Howard, J.M. (2001) Mechanisms of taxotere-related drug resistance in pancreatic carcinoma. *J. Surg. Res.,* **99,** 179-186.

Liu, S., Wu, Q., Chen, Z.M. and Su, W.J. (2001) The effect pathway of retinoic acid through regulation of retinoic acid receptor alpha in gastric cancer cells. *World J. Gastroenterol.,* **7,** 662-666.

Longley, D.B., Harkin, D.P. and Johnston, P.G. (2003) 5-Fluorouracil: Mechanisms of Action and Clinical Strategies. *Nat. Rev. Cancer.,* **3,** 330-338.

Lopez-Boado, Y.S., Tolivia, J. and Lopez-Otin, C. (1994) Apolipoprotein D gene induction by retinoic acid is concomitant with growth arrest and cell differentiation in human breast cancer cells. *J. Biol. Chem.,* **269,** 26871-26878.

Lotan, R. and Nicolson, G.L. (1979) Heterogeneity in growth inhibition by beta-trans-retinoic acid of metastatic B16 melanoma clones and in vivo-selected cell variant lines. *Cancer Res.,* **39,** 4767-4771.

Lowenfels, A.B. and Maisonneuve, P. (2004) Epidemiology and prevention of pancreatic cancer. *Jpn. J. Clin. Oncol.,* **34,** 238-244.

Maeda, M., Johnson, K.R. and Wheelock, M.J. (2005) Cadherin switching: essential for behavioral but not morphological changes during an epithelium-to-mesenchyme transition. *J. Cell. Sci.,* **118,** 873-887.

Mangiarotti, R., Danova, M., Alberici, R. and Pellicciari, C. (1998) All-trans retinoic acid (ATRA)-induced apoptosis is preceded by G1 arrest in human MCF-7 breast cancer cells. *Br. J. Cancer,* **77,** 186-191.

Marco, R.A., Diaz-Montero, C.M., Wygant, J.N., Kleinerman, E.S. and McIntyre, B.W. (2003) Alpha 4 integrin increases anoikis of human osteosarcoma cells. *J. Cell. Biochem.,* **88,** 1038-1047.

Markogiannakis, E., Georgoulias, V., Margioris, A.N., Zoumakis, E., Stournaras, C. and Gravanis, A. (1997) Estrogens and glucocorticoids induce the expression of c-erbB2/NEU receptor in Ishikawa human endometrial cells. *Life Sci.,* **61,** 1083-1095.

Marks, D.C., Su, G.M., Davey, R.A. and Davey, M.W. (1996) Extended multidrug resistance in haemopoietic cells. *Br. J. Haematol.,* **95,** 587-595.

McHugh, L.A., Kriajevska, M., Mellon, J.K. and Griffiths, T.R. (2007) Combined treatment of bladder cancer cell lines with lapatinib and varying chemotherapy regimens--evidence of schedule-dependent synergy. *Urology,* **69,** 390-394.

McInroy, L. and Maatta, A. (2007) Down-regulation of vimentin expression inhibits carcinoma cell migration and adhesion. *Biochem. Biophys. Res. Commun.,* **360,** 109-114.

McKenzie, S.J., DeSombre, K.A., Bast, B.S., Hollis, D.R., Whitaker, R.S., Berchuck, A., Boyer, C.M. and Bast, R.C.,Jr (1993) Serum levels of HER-2 neu (C-erbB-2) correlate with overexpression of p185neu in human ovarian cancer. *Cancer,* **71,** 3942-3946.

Mendelsohn, J. (2003) Antibody-mediated EGF receptor blockade as an anticancer therapy: from the laboratory to the clinic. *Cancer Immunol. Immunother., 52,* 342-346.

Mercurio, A.M. (1995) Laminin receptors: achieving specificity through cooperation. *Trends Cell Biol., 5,* 419-423.

Meyer, F., Lueck, A., Hribaschek, A., Lippert, H. and Ridwelski, K. (2004) Phase I trial using weekly administration of gemcitabine and docetaxel in patients with advanced pancreatic carcinoma. *Chemotherapy, 50,* 289-296.

Mikuriya, K., Kuramitsu, Y., Ryozawa, S., Fujimoto, M., Mori, S., Oka, M., Hamano, K., Okita, K., Sakaida, I. and Nakamura, K. (2007) Expression of glycolytic enzymes is increased in pancreatic cancerous tissues as evidenced by proteomic profiling by two-dimensional electrophoresis and liquid chromatography-mass spectrometry/mass spectrometry. *Int. J. Oncol., 30,* 849-855.

Miller, D.W., Fontain, M., Kolar, C. and Lawson, T. (1996) The expression of multidrug resistance-associated protein (MRP) in pancreatic adenocarcinoma cell lines. *Cancer Lett., 107,* 301-306.

Minakuchi, Y., Takeshita, F., Kosaka, N., Sasaki, H., Yamamoto, Y., Kouno, M., Honma, K., Nagahara, S., Hanai, K., Sano, A., et al (2004) Atelocollagen-mediated synthetic small interfering RNA delivery for effective gene silencing in vitro and in vivo. *Nucleic Acids Res., 32,* e109.

Minard, M.E., Ellis, L.M. and Gallick, G.E. (2006) Tiam1 regulates cell adhesion, migration and apoptosis in colon tumor cells. *Clin. Exp. Metastasis, 23,* 301-313.

Minotti, G., Menna, P., Salvatorelli, E., Cairo, G. and Gianni, L. (2004) Anthracyclines: molecular advances and pharmacologic developments in antitumor activity and cardiotoxicity. *Pharmacol. Rev., 56,* 185-229.

Mizejewski, G.J. (1999) Role of integrins in cancer: survey of expression patterns. *Proc. Soc. Exp. Biol. Med., 222,* 124-138.

Molotkov, A., Deltour, L., Foglio, M.H., Cuenca, A.E. and Duester, G. (2002) Distinct retinoid metabolic functions for alcohol dehydrogenase genes Adh1 and Adh4 in protection against vitamin A toxicity or deficiency revealed in double null mutant mice. *J. Biol. Chem., 277,* 13804-13811.

Moore, M.J., Goldstein, D., Hamm, J., Figer, A., Hecht, J.R., Gallinger, S., Au, H.J., Murawa, P., Walde, D., Wolff, R.A., et al (2007) Erlotinib plus gemcitabine compared with gemcitabine alone in patients with advanced pancreatic cancer: a phase III trial of the National Cancer Institute of Canada Clinical Trials Group. *J. Clin. Oncol., 25,* 1960-1966.

Moreb, J.S., Gabr, A., Vartikar, G.R., Gowda, S., Zucali, J.R. and Mohuczy, D. (2005) Retinoic acid down-regulates aldehyde dehydrogenase and increases cytotoxicity of 4-hydroperoxycyclophosphamide and acetaldehyde. *J. Pharmacol. Exp. Ther., 312,* 339-345.

Moreb, J.S., Mohuczy, D., Ostmark, B. and Zucali, J.R. (2007) RNAi-mediated knockdown of aldehyde dehydrogenase class-1A1 and class-3A1 is specific and reveals that each contributes equally to the resistance against 4-hydroperoxycyclophosphamide. *Cancer Chemother. Pharmacol., ***59,** 127-136.

Morohashi, S., Odagiri, H., Morohashi, H., Kimura, Y. and Sasaki, M. (2007) Complete remission of recurrent breast cancer with multiple liver metastases after oral capecitabine and injected trastuzumab. *Breast Cancer, ***14,** 297-301.

Morozevich, G.E., Kozlova, N.I., Preobrazhenskaya, M.E., Ushakova, N.A., Eltsov, I.A., Shtil, A.A. and Berman, A.E. (2006) The role of beta1 integrin subfamily in anchorage-dependent apoptosis of breast carcinoma cells differing in multidrug resistance. *Biochemistry (Mosc), ***71,** 489-495.

Moyer, J.D., Barbacci, E.G., Iwata, K.K., Arnold, L., Boman, B., Cunningham, A., DiOrio, C., Doty, J., Morin, M.J., Moyer, M.P., et al (1997) Induction of apoptosis and cell cycle arrest by CP-358,774, an inhibitor of epidermal growth factor receptor tyrosine kinase. *Cancer Res., ***57,** 4838-4848.

Murray, D., Morrin, M. and McDonnell, S. (2004) Increased invasion and expression of MMP-9 in human colorectal cell lines by a CD44-dependent mechanism. *Anticancer Res., ***24,** 489-494.

Nakahashi, C., Oda, T., Kinoshita, T., Ueda, T., Konishi, M., Nakagohri, T., Inoue, K., Furuse, J., Ochiai, A. and Ohkohchi, N. (2003) The impact of liver metastasis on mortality in patients initially diagnosed with locally advanced or resectable pancreatic cancer. *Int. J. Gastrointest. Cancer., ***33,** 155-164.

Nakai, Y., Otsuka, M., Hoshida, Y., Tada, M., Komatsu, Y., Kawabe, T. and Omata, M. (2005) Identifying genes with differential expression in gemcitabine-resistant pancreatic cancer cells using comprehensive transcriptome analysis. *Oncol. Rep., ***14,** 1263-1267.

Nakajima, S., Doi, R., Toyoda, E., Tsuji, S., Wada, M., Koizumi, M., Tulachan, S.S., Ito, D., Kami, K., Mori, T., et al (2004) N-cadherin expression and epithelial-mesenchymal transition in pancreatic carcinoma. *Clin. Cancer Res., ***10,** 4125-4133.

Nakazawa, K., Dobashi, Y., Suzuki, S., Fujii, H., Takeda, Y. and Ooi, A. (2005) Amplification and overexpression of c-erbB-2, epidermal growth factor receptor, and c-met in biliary tract cancers. *J. Pathol., ***206,** 356-365.

Napoli, C., Lemieux, C. and Jorgensen, R. (1990) Introduction of a Chimeric Chalcone Synthase Gene into Petunia Results in Reversible Co-Suppression of Homologous Genes in trans. *Plant Cell, ***2,** 279-289.

National Cancer Registry, Ireland
www.ncri.ie (2000)

Naumann, M., Savitskaia, N., Eilert, C., Schramm, A., Kalthoff, H. and Schmiegel, W. (1996) Frequent codeletion of p16/MTS1 and p15/MTS2 and genetic alterations in p16/MTS1 in pancreatic tumors. *Gastroenterology, ***110,** 1215-1224.

Neckers, L. and Neckers, K. (2002) Heat-shock protein 90 inhibitors as novel cancer chemotherapeutic agents. *Expert Opin. Emerg. Drugs,* **7,** 277-288.

Neet, K.E. and Lee, J.C. (2002) Biophysical characterization of proteins in the post-genomic era of proteomics. *Mol. Cell. Proteomics,* **1,** 415-420.

Negm, R.S., Verma, M. and Srivastava, S. (2002) The promise of biomarkers in cancer screening and detection. *Trends Mol. Med.,* **8,** 288-293.

Nelson, G.M., Huffman, H. and Smith, D.F. (2003) Comparison of the carboxy-terminal DP-repeat region in the co-chaperones Hop and Hip. *Cell Stress Chaperones,* **8,** 125-133.

Neoptolemos, J.P., Cunningham, D., Friess, H., Bassi, C., Stocken, D.D., Tait, D.M., Dunn, J.A., Dervenis, C., Lacaine, F., Hickey, H., et al (2003) Adjuvant therapy in pancreatic cancer: historical and current perspectives. *Ann. Oncol.,* **14,** 675-692.

Neri, B., Doni, L., Fulignati, C., Gemelli, M.T., Turrini, M., Di Cello, V., Dominici, A., Mottola, A., Raugei, A., Ponchietti, R., et al (2002) Gemcitabine plus Epi-doxorubicin as first-line chemotherapy for bladder cancer in advanced or metastatic stage: a phase II. *Anticancer Res.,* **22,** 2981-2984.

Nieth, C., Priebsch, A., Stege, A. and Lage, H. (2003) Modulation of the classical multidrug resistance (MDR) phenotype by RNA interference (RNAi). *FEBS Lett.,* **545,** 144-150.

Nitori, N., Ino, Y., Nakanishi, Y., Yamada, T., Honda, K., Yanagihara, K., Kosuge, T., Kanai, Y., Kitajima, M. and Hirohashi, S. (2005) Prognostic significance of tissue factor in pancreatic ductal adenocarcinoma. *Clin. Cancer Res.,* **11,** 2531-2539.

Noske, A., Denkert, C., Schober, H., Sers, C., Zhumabayeva, B., Weichert, W., Dietel, M. and Wiechen, K. (2005) Loss of Gelsolin expression in human ovarian carcinomas. *Eur. J. Cancer,* **41,** 461-469.

Novak, A., Hsu, S.C., Leung-Hagesteijn, C., Radeva, G., Papkoff, J., Montesano, R., Roskelley, C., Grosschedl, R. and Dedhar, S. (1998) Cell adhesion and the integrin-linked kinase regulate the LEF-1 and beta-catenin signaling pathways. *Proc. Natl. Acad. Sci. U. S. A.,* **95,** 4374-4379.

Ochiya, T., Nagahara, S., Sano, A., Itoh, H. and Terada, M. (2001) Biomaterials for gene delivery: atelocollagen-mediated controlled release of molecular medicines. *Curr. Gene Ther.,* **1,** 31-52.

Oda, H., Tsukita, S. and Takeichi, M. (1998) Dynamic behavior of the cadherin-based cell-cell adhesion system during Drosophila gastrulation. *Dev. Biol.,* **203,** 435-450.

Odunuga, O.O., Hornby, J.A., Bies, C., Zimmermann, R., Pugh, D.J. and Blatch, G.L. (2003) Tetratricopeptide repeat motif-mediated Hsc70-mSTI1 interaction. Molecular characterization of the critical contacts for successful binding and specificity. *J. Biol. Chem.,* **278,** 6896-6904.

O'Farrell, P.H. (1975) High resolution two-dimensional electrophoresis of proteins. *J. Biol. Chem.,* **250,** 4007-4021.

Ogata, M., Naito, Z., Tanaka, S., Moriyama, Y. and Asano, G. (2000) Overexpression and localization of heat shock proteins mRNA in pancreatic carcinoma. *J. Nippon Med. Sch.,* **67,** 177-185.

Ohta, T., Terada, T., Nagakawa, T., Tajima, H., Itoh, H., Fonseca, L. and Miyazaki, I. (1994) Pancreatic trypsinogen and cathepsin B in human pancreatic carcinomas and associated metastatic lesions. *Br. J. Cancer,* **69,** 152-156.

Okada, S., Sakata, Y., Matsuno, S., Kurihara, M., Sasaki, Y., Ohashi, Y. and Taguchi, T. (1999) Phase II study of docetaxel in patients with metastatic pancreatic cancer: a Japanese cooperative study. Cooperative Group of Docetaxel for Pancreatic Cancer in Japan. *Br. J. Cancer,* **80,** 438-443.

Okano, T., Kondo, T., Kakisaka, T., Fujii, K., Yamada, M., Kato, H., Nishimura, T., Gemma, A., Kudoh, S. and Hirohashi, S. (2006) Plasma proteomics of lung cancer by a linkage of multi-dimensional liquid chromatography and two-dimensional difference gel electrophoresis. *Proteomics,* **6,** 3938-3948.

Orchekowski, R., Hamelinck, D., Li, L., Gliwa, E., vanBrocklin, M., Marrero, J.A., Vande Woude, G.F., Feng, Z., Brand, R. and Haab, B.B. (2005) Antibody microarray profiling reveals individual and combined serum proteins associated with pancreatic cancer. *Cancer Res.,* **65,** 11193-11202.

Overholser, J.P., Prewett, M.C., Hooper, A.T., Waksal, H.W. and Hicklin, D.J. (2000) Epidermal growth factor receptor blockade by antibody IMC-C225 inhibits growth of a human pancreatic carcinoma xenograft in nude mice. *Cancer,* **89,** 74-82.

Ozawa, M., Ringwald, M. and Kemler, R. (1990) Uvomorulin-catenin complex formation is regulated by a specific domain in the cytoplasmic region of the cell adhesion molecule. *Proc. Natl. Acad. Sci. U. S. A.,* **87,** 4246-4250.

Page, M.J., Amess, B., Townsend, R.R., Parekh, R., Herath, A., Brusten, L., Zvelebil, M.J., Stein, R.C., Waterfield, M.D., Davies, S.C., et al (1999) Proteomic definition of normal human luminal and myoepithelial breast cells purified from reduction mammoplasties. *Proc. Natl. Acad. Sci. U. S. A.,* **96,** 12589-12594.

Pai, S.I., Lin, Y.Y., Macaes, B., Meneshian, A., Hung, C.F. and Wu, T.C. (2006) Prospects of RNA interference therapy for cancer. *Gene Ther.,* **13,** 464-477.

Palmer, D.H., Stocken, D.D., Hewitt, H., Markham, C.E., Hassan, A.B., Johnson, P.J., Buckels, J.A. and Bramhall, S.R. (2007) A randomized phase 2 trial of neoadjuvant chemotherapy in resectable pancreatic cancer: gemcitabine alone versus gemcitabine combined with cisplatin. *Ann. Surg. Oncol.,* **14,** 2088-2096.

Pantel, K. and Brakenhoff, R.H. (2004) Dissecting the metastatic cascade. *Nat. Rev. Cancer.,* **4,** 448-456.

Papouli, E., Cejka, P. and Jiricny, J. (2004) Dependence of the cytotoxicity of DNA-damaging agents on the mismatch repair status of human cells. *Cancer Res.,* **64,** 3391-3394.

Park, E.Y., Wilder, E.T., Chipuk, J.E. and Lane, M.A. (2007) Retinol decreases phosphatidylinositol 3-kinase activity in colon cancer cells. *Mol. Carcinog.,*

Park, E.Y., Wilder, E.T. and Lane, M.A. (2007) Retinol inhibits the invasion of retinoic acid-resistant colon cancer cells in vitro and decreases matrix metalloproteinase mRNA, protein, and activity levels. *Nutr. Cancer,* **57,** 66-77.

Parkin, D.M., Pisani, P. and Ferlay, J. (1999) Global cancer statistics. *CA Cancer. J. Clin.,* **49,** 33-64, 1.

Pellegata, N.S., Sessa, F., Renault, B., Bonato, M., Leone, B.E., Solcia, E. and Ranzani, G.N. (1994) K-ras and p53 gene mutations in pancreatic cancer: ductal and nonductal tumors progress through different genetic lesions. *Cancer Res.,* **54,** 1556-1560.

Peng, B., Fleming, J.B., Breslin, T., Grau, A.M., Fojioka, S., Abbruzzese, J.L., Evans, D.B., Ayers, D., Wathen, K., Wu, T., et al (2002) Suppression of tumorigenesis and induction of p15(ink4b) by Smad4/DPC4 in human pancreatic cancer cells. *Clin. Cancer Res.,* **8,** 3628-3638.

Persad, S. and Dedhar, S. (2003) The role of integrin-linked kinase (ILK) in cancer progression. *Cancer Metastasis Rev.,* **22,** 375-384.

Pesic, M., Markovic, J.Z., Jankovic, D., Kanazir, S., Markovic, I.D., Rakic, L. and Ruzdijic, S. (2006) Induced resistance in the human non small cell lung carcinoma (NCI-H460) cell line in vitro by anticancer drugs. *J. Chemother.,* **18,** 66-73.

Pettersson, F., Dalgleish, A.G., Bissonnette, R.P. and Colston, K.W. (2002) Retinoids cause apoptosis in pancreatic cancer cells via activation of RAR-gamma and altered expression of Bcl-2/Bax. *Br. J. Cancer,* **87,** 555-561.

Pick, E., Kluger, Y., Giltnane, J.M., Moeder, C., Camp, R.L., Rimm, D.L. and Kluger, H.M. (2007) High HSP90 expression is associated with decreased survival in breast cancer. *Cancer Res.,* **67,** 2932-2937.

Plath, T., Detjen, K., Welzel, M., von Marschall, Z., Murphy, D., Schirner, M., Wiedenmann, B. and Rosewicz, S. (2000) A novel function for the tumor suppressor p16(INK4a): induction of anoikis via upregulation of the alpha(5)beta(1) fibronectin receptor. *J. Cell Biol.,* **150,** 1467-1478.

Plebani, M., Herszenyi, L., Cardin, R., Roveroni, G., Carraro, P., Paoli, M.D., Rugge, M., Grigioni, W.F., Nitti, D. and Naccarato, R. (1995) Cysteine and serine proteases in gastric cancer. *Cancer,* **76,** 367-375.

Podolin, P.L. and Prystowsky, M.B. (1991) The kinetics of vimentin RNA and protein expression in interleukin 2-stimulated T lymphocytes. *J. Biol. Chem.,* **266,** 5870-5875.

Polette, M., Gilles, C., de Bentzmann, S., Gruenert, D., Tournier, J.M. and Birembaut, P. (1998) Association of fibroblastoid features with the invasive phenotype in human bronchial cancer cell lines. *Clin. Exp. Metastasis,* **16,** 105-112.

Powell, W.C., Knox, J.D., Navre, M., Grogan, T.M., Kittelson, J., Nagle, R.B. and Bowden, G.T. (1993) Expression of the metalloproteinase matrilysin in DU-145 cells increases their invasive potential in severe combined immunodeficient mice. *Cancer Res.,* **53,** 417-422.

Powers, M.V. and Workman, P. (2006) Targeting of multiple signalling pathways by heat shock protein 90 molecular chaperone inhibitors. *Endocr. Relat. Cancer,* **13 Suppl 1,** S125-35.

Przybylo, J.A. and Radisky, D.C. (2007) Matrix metalloproteinase-induced epithelial-mesenchymal transition: tumor progression at Snail's pace. *Int. J. Biochem. Cell Biol.,* **39,** 1082-1088.

Qian, F., Bajkowski, A.S., Steiner, D.F., Chan, S.J. and Frankfater, A. (1989) Expression of five cathepsins in murine melanomas of varying metastatic potential and normal tissues. *Cancer Res.,* **49,** 4870-4875.

Radisky, D.C. (2005) Epithelial-mesenchymal transition. *J. Cell. Sci.,* **118,** 4325-4326.

Ramachandra, M., Atencio, I., Rahman, A., Vaillancourt, M., Zou, A., Avanzini, J., Wills, K., Bookstein, R. and Shabram, P. (2002) Restoration of transforming growth factor Beta signaling by functional expression of smad4 induces anoikis. *Cancer Res.,* **62,** 6045-6051.

Ramachandran, V., Arumugam, T., Hwang, R.F., Greenson, J.K., Simeone, D.M. and Logsdon, C.D. (2007) Adrenomedullin is expressed in pancreatic cancer and stimulates cell proliferation and invasion in an autocrine manner via the adrenomedullin receptor, ADMR. *Cancer Res.,* **67,** 2666-2675.

Ramos, D.M., Cheng, Y.F. and Kramer, R.H. (1991) Role of laminin-binding integrin in the invasion of basement membrane matrices by fibrosarcoma cells. *Invasion Metastasis,* **11,** 125-138.

Ray, J.M. and Stetler-Stevenson, W.G. (1994) The role of matrix metalloproteases and their inhibitors in tumour invasion, metastasis and angiogenesis. *Eur. Respir. J.,* **7,** 2062-2072.

Rees, J.R., Onwuegbusi, B.A., Save, V.E., Alderson, D. and Fitzgerald, R.C. (2006) In vivo and In vitro Evidence for Transforming Growth Factor-{beta}1-Mediated Epithelial to Mesenchymal Transition in Esophageal Adenocarcinoma. *Cancer Res.,* **66,** 9583-9590.

Rejiba, S., Wack, S., Aprahamian, M. and Hajri, A. (2007) K-ras oncogene silencing strategy reduces tumor growth and enhances gemcitabine chemotherapy efficacy for pancreatic cancer treatment. *Cancer. Sci.,* **98,** 1128-1136.

Reni, M., Cereda, S., Bonetto, E., Vigano, M.G., Passoni, P., Zerbi, A., Balzano, G., Nicoletti, R., Staudacher, C. and Di Carlo, V. (2007) Dose-intense PEFG (cisplatin, epirubicin, 5-fluorouracil, gemcitabine) in advanced pancreatic adenocarcinoma. *Cancer Chemother. Pharmacol.,* **59,** 361-367.

Reynolds, C.P. and Maurer, B.J. (2005) Evaluating response to antineoplastic drug combinations in tissue culture models. *Methods Mol. Med.,* **110,** 173-183.

Richmond, P.J., Karayiannakis, A.J., Nagafuchi, A., Kaisary, A.V. and Pignatelli, M. (1997) Aberrant E-cadherin and alpha-catenin expression in prostate cancer: correlation with patient survival. *Cancer Res.,* **57,** 3189-3193.

Ridwelski, K., Fahlke, J., Kuhn, R., Hribaschek, A., Kettner, E., Greiner, C., Florschuetz, A., Manger, T., Wilhelm, G., Klein, H., et al (2006) Multicenter phase-I/II study using a combination of gemcitabine and docetaxel in metastasized and unresectable, locally advanced pancreatic carcinoma. *Eur. J. Surg. Oncol.,* **32,** 297-302.

Riikonen, T., Westermarck, J., Koivisto, L., Broberg, A., Kahari, V.M. and Heino, J. (1995) Integrin alpha 2 beta 1 is a positive regulator of collagenase (MMP-1) and collagen alpha 1(I) gene expression. *J. Biol. Chem.,* **270,** 13548-13552.

Rodel, F., Hoffmann, J., Distel, L., Herrmann, M., Noisternig, T., Papadopoulos, T., Sauer, R. and Rodel, C. (2005) Survivin as a radioresistance factor, and prognostic and therapeutic target for radiotherapy in rectal cancer. *Cancer Res.,* **65,** 4881-4887.

Rofstad, E.K., Mathiesen, B., Kindem, K. and Galappathi, K. (2006) Acidic extracellular pH promotes experimental metastasis of human melanoma cells in athymic nude mice. *Cancer Res.,* **66,** 6699-6707.

Rosewicz, S., Wollbergs, K., Von Lampe, B., Matthes, H., Kaiser, A. and Riecken, E.O. (1997) Retinoids inhibit adhesion to laminin in human pancreatic carcinoma cells via the alpha 6 beta 1-integrin receptor. *Gastroenterology,* **112,** 532-542.

Rosivatz, E., Becker, I., Specht, K., Fricke, E., Luber, B., Busch, R., Hofler, H. and Becker, K.F. (2002) Differential expression of the epithelial-mesenchymal transition regulators snail, SIP1, and twist in gastric cancer. *Am. J. Pathol.,* **161,** 1881-1891.

Rougier, P., Adenis, A., Ducreux, M., de Forni, M., Bonneterre, J., Dembak, M., Clouet, P., Lebecq, A., Baille, P., Lefresne-Soulas, F., et al (2000) A phase II study: docetaxel as first-line chemotherapy for advanced pancreatic adenocarcinoma. *Eur. J. Cancer,* **36,** 1016-1025.

Rozenblum, E., Schutte, M., Goggins, M., Hahn, S.A., Panzer, S., Zahurak, M., Goodman, S.N., Sohn, T.A., Hruban, R.H., Yeo, C.J., et al (1997) Tumor-suppressive pathways in pancreatic carcinoma. *Cancer Res.,* **57,** 1731-1734.

Rubinson, D.A., Dillon, C.P., Kwiatkowski, A.V., Sievers, C., Yang, L., Kopinja, J., Rooney, D.L., Zhang, M., Ihrig, M.M., McManus, M.T., et al (2003) A lentivirus-based system to functionally silence genes in primary mammalian cells, stem cells and transgenic mice by RNA interference. *Nat. Genet.,* **33,** 401-406.

Ruoslahti, E. (1999) Fibronectin and its integrin receptors in cancer. *Adv. Cancer Res.,* **76,** 1-20.

Ruppert, C., Ehrenforth, S., Scharrer, I. and Halberstadt, E. (1997) Protease levels in breast, ovary, and other gynecological tumor tissues: prognostic importance in breast cancer. *Cancer Detect. Prev.,* **21,** 452-459.

Rusnak, D.W., Lackey, K., Affleck, K., Wood, E.R., Alligood, K.J., Rhodes, N., Keith, B.R., Murray, D.M., Knight, W.B., Mullin, R.J., et al (2001) The effects of the novel, reversible epidermal growth factor receptor/ErbB-2 tyrosine kinase inhibitor, GW2016, on the growth of human normal and tumor-derived cell lines in vitro and in vivo. *Mol. Cancer. Ther.,* **1,** 85-94.

Rustum, Y.M. (2004) Thymidylate synthase: a critical target in cancer therapy? *Front. Biosci.,* **9,** 2467-2473.

Ryther, R.C., Flynt, A.S., Phillips, J.A.,3rd and Patton, J.G. (2005) siRNA therapeutics: big potential from small RNAs. *Gene Ther.,* **12,** 5-11.

Safran, H., Iannitti, D., Miner, T. et al (2006) GW572016, gemcitabine and GW572016, gemcitabine, oxaliplatin, a two-stage, phase I study for advanced pancreaticobiliary cancer. *J Clin Oncol.,* **24,** (18 suppl).

Safran, H., Steinhoff, M., Mangray, S., Rathore, R., King, T.C., Chai, L., Berzein, K., Moore, T., Iannitti, D., Reiss, P., et al (2001) Overexpression of the HER-2/neu oncogene in pancreatic adenocarcinoma. *Am. J. Clin. Oncol.,* **24,** 496-499.

Sagawa, N., Fujita, H., Banno, Y., Nozawa, Y., Katoh, H. and Kuzumaki, N. (2003) Gelsolin suppresses tumorigenicity through inhibiting PKC activation in a human lung cancer cell line, PC10. *Br. J. Cancer,* **88,** 606-612.

Sahovic, E.A., Colvin, M., Hilton, J. and Ogawa, M. (1988) Role for aldehyde dehydrogenase in survival of progenitors for murine blast cell colonies after treatment with 4-hydroperoxycyclophosphamide in vitro. *Cancer Res.,* **48,** 1223-1226.

Sano, A., Maeda, M., Nagahara, S., Ochiya, T., Honma, K., Itoh, H., Miyata, T. and Fujioka, K. (2003) Atelocollagen for protein and gene delivery. *Adv. Drug Deliv. Rev.,* **55,** 1651-1677.

Sato, H., Takino, T. and Miyamori, H. (2005) Roles of membrane-type matrix metalloproteinase-1 in tumor invasion and metastasis. *Cancer. Sci.,* **96,** 212-217.

Satoh, S., Hinoda, Y., Hayashi, T., Burdick, M.D., Imai, K. and Hollingsworth, M.A. (2000) Enhancement of metastatic properties of pancreatic cancer cells by MUC1 gene encoding an anti-adhesion molecule. *Int. J. Cancer,* **88,** 507-518.

Savagner, P. (2001) Leaving the neighborhood: molecular mechanisms involved during epithelial-mesenchymal transition. *Bioessays,* **23,** 912-923.

Sawai, H., Funahashi, H., Yamamoto, M., Okada, Y., Hayakawa, T., Tanaka, M., Takeyama, H. and Manabe, T. (2003) Interleukin-1alpha enhances integrin alpha(6)beta(1) expression and metastatic capability of human pancreatic cancer. *Oncology,* **65,** 167-173.

Sawai, H., Okada, Y., Funahashi, H., Matsuo, Y., Takahashi, H., Takeyama, H. and Manabe, T. (2006) Integrin-linked kinase activity is associated with interleukin-1 alpha-induced progressive behavior of pancreatic cancer and poor patient survival. *Oncogene,* **25,** 3237-3246.

Schaffeld, M., Herrmann, H., Schultess, J. and Markl, J. (2001) Vimentin and desmin of a cartilaginous fish, the shark Scyliorhinus stellaris: sequence, expression patterns and in vitro assembly. *Eur. J. Cell Biol., 80,* 692-702.

Schaller, G., Fuchs, I., Gonsch, T., Weber, J., Kleine-Tebbe, A., Klare, P., Hindenburg, H.J., Lakner, V., Hinke, A. and Bangemann, N. (2007) Phase II study of capecitabine plus trastuzumab in human epidermal growth factor receptor 2 overexpressing metastatic breast cancer pretreated with anthracyclines or taxanes. *J. Clin. Oncol., 25,* 3246-3250.

Schaller, G., Fuchs, I., Pritze, W., Ebert, A., Herbst, H., Pantel, K., Weitzel, H. and Lengyel, E. (1996) Elevated keratin 18 protein expression indicates a favorable prognosis in patients with breast cancer. *Clin. Cancer Res., 2,* 1879-1885.

Schellens, J.H. (2007) Capecitabine. *Oncologist, 12,* 152-155.

Scheufler, C., Brinker, A., Bourenkov, G., Pegoraro, S., Moroder, L., Bartunik, H., Hartl, F.U. and Moarefi, I. (2000) Structure of TPR domain-peptide complexes: critical elements in the assembly of the Hsp70-Hsp90 multichaperone machine. *Cell, 101,* 199-210.

Schlessinger, J. (2000) Cell signaling by receptor tyrosine kinases. *Cell, 103,* 211-225.

Schneider, S.M., Offterdinger, M., Huber, H. and Grunt, T.W. (2000) Activation of retinoic acid receptor alpha is sufficient for full induction of retinoid responses in SK-BR-3 and T47D human breast cancer cells. *Cancer Res., 60,* 5479-5487.

Science Creative Quarterly
www.scq.ubc.ca (2007)

Seftor, R.E., Seftor, E.A., Stetler-Stevenson, W.G. and Hendrix, M.J. (1993) The 72 kDa type IV collagenase is modulated via differential expression of alpha v beta 3 and alpha 5 beta 1 integrins during human melanoma cell invasion. *Cancer Res., 53,* 3411-3415.

Sellers, T.A. and Yates, J.R. (2003) Review of proteomics with applications to genetic epidemiology. *Genet. Epidemiol., 24,* 83-98.

Seshadri, R., Raymond, W.A., Leong, A.S., Horsfall, D.J. and McCaul, K. (1996) Vimentin expression is not associated with poor prognosis in breast cancer. *Int. J. Cancer, 67,* 353-356.

Shalli, K., Brown, I., Heys, S.D. and Schofield, A.C. (2005) Alterations of beta-tubulin isotypes in breast cancer cells resistant to docetaxel. *FASEB J., 19,* 1299-1301.

Shaw, L.M., Chao, C., Wewer, U.M. and Mercurio, A.M. (1996) Function of the integrin alpha 6 beta 1 in metastatic breast carcinoma cells assessed by expression of a dominant-negative receptor. *Cancer Res., 56,* 959-963.

Shen, J., Person, M.D., Zhu, J., Abbruzzese, J.L. and Li, D. (2004) Protein expression profiles in pancreatic adenocarcinoma compared with normal pancreatic tissue and tissue affected by pancreatitis as detected by two-dimensional gel electrophoresis and mass spectrometry. *Cancer Res., 64,* 9018-9026.

Shi, X., Liu, S., Kleeff, J., Friess, H. and Buchler, M.W. (2002) Acquired resistance of pancreatic cancer cells towards 5-Fluorouracil and gemcitabine is associated with altered expression of apoptosis-regulating genes. *Oncology, 62,* 354-362.

Shieh, D.B., Godleski, J., Herndon, J.E.,2nd, Azuma, T., Mercer, H., Sugarbaker, D.J. and Kwiatkowski, D.J. (1999) Cell motility as a prognostic factor in Stage I nonsmall cell lung carcinoma: the role of gelsolin expression. *Cancer, 85,* 47-57.

Shimoyama, S., Gansauge, F., Gansauge, S., Oohara, T. and Beger, H.G. (1995) Altered expression of extracellular matrix molecules and their receptors in chronic pancreatitis and pancreatic adenocarcinoma in comparison with normal pancreas. *Int. J. Pancreatol., 18,* 227-234.

Shore, S., Raraty, M.G., Ghaneh, P. and Neoptolemos, J.P. (2003) Review article: chemotherapy for pancreatic cancer. *Aliment. Pharmacol. Ther., 18,* 1049-1069.

Sigma-Aldrich
www.sigmaaldrich.com (2007)

Silverman, J.A. and Thorgeirsson, S.S. (1995) Regulation and function of the multidrug resistance genes in liver. *Prog. Liver Dis., 13,* 101-123.

Sirivatanauksorn, V., Sirivatanauksorn, Y. and Lemoine, N.R. (1998) Molecular pattern of ductal pancreatic cancer. *Langenbecks Arch. Surg., 383,* 105-115.

Sladek, N.E., Kollander, R., Sreerama, L. and Kiang, D.T. (2002) Cellular levels of aldehyde dehydrogenases (ALDH1A1 and ALDH3A1) as predictors of therapeutic responses to cyclophosphamide-based chemotherapy of breast cancer: a retrospective study. Rational individualization of oxazaphosphorine-based cancer chemotherapeutic regimens. *Cancer Chemother. Pharmacol., 49,* 309-321.

Slebos, R.J., Hoppin, J.A., Tolbert, P.E., Holly, E.A., Brock, J.W., Zhang, R.H., Bracci, P.M., Foley, J., Stockton, P., McGregor, L.M., et al (2000) K-ras and p53 in pancreatic cancer: association with medical history, histopathology, and environmental exposures in a population-based study. *Cancer Epidemiol. Biomarkers Prev., 9,* 1223-1232.

Sommers, C.L., Heckford, S.E., Skerker, J.M., Worland, P., Torri, J.A., Thompson, E.W., Byers, S.W. and Gelmann, E.P. (1992) Loss of epithelial markers and acquisition of vimentin expression in adriamycin- and vinblastine-resistant human breast cancer cell lines. *Cancer Res., 52,* 5190-5197.

Song, H.Y., Liu, Y.K., Feng, J.T., Cui, J.F., Dai, Z., Zhang, L.J., Feng, J.X., Shen, H.L. and Tang, Z.Y. (2006) Proteomic analysis on metastasis-associated proteins of human hepatocellular carcinoma tissues. *J. Cancer Res. Clin. Oncol., 132,* 92-98.

Sorenson, C.M. and Eastman, A. (1988) Mechanism of cis-diamminedichloroplatinum(II)-induced cytotoxicity: role of G2 arrest and DNA double-strand breaks. *Cancer Res., 48,* 4484-4488.

Spinelli, G.P., Zullo, A., Romiti, A., Di Seri, M., Tomao, F., Miele, E., Spalletta, B., Eramo, A., Hassan, C. and Tomao, S. (2006) Long-term survival in metastatic pancreatic cancer. A case report and review of the literature. *JOP,* **7,** 486-491.

Stallmach, A., von Lampe, B., Orzechowski, H.D., Matthes, H. and Riecken, E.O. (1994) Increased fibronectin-receptor expression in colon carcinoma-derived HT 29 cells decreases tumorigenicity in nude mice. *Gastroenterology,* **106,** 19-27.

Standop, J., Standop, S., Itami, A., Nozawa, F., Brand, R.E., Buchler, M.W. and Pour, P.M. (2002) ErbB2 oncogene expression supports the acute pancreatitis-chronic pancreatitis sequence. *Virchows Arch.,* **441,** 385-391.

Stierum, R., Gaspari, M., Dommels, Y., Ouatas, T., Pluk, H., Jespersen, S., Vogels, J., Verhoeckx, K., Groten, J. and van Ommen, B. (2003) Proteome analysis reveals novel proteins associated with proliferation and differentiation of the colorectal cancer cell line Caco-2. *Biochim. Biophys. Acta,* **1650,** 73-91.

Storms, R.W., Trujillo, A.P., Springer, J.B., Shah, L., Colvin, O.M., Ludeman, S.M. and Smith, C. (1999) Isolation of primitive human hematopoietic progenitors on the basis of aldehyde dehydrogenase activity. *Proc. Natl. Acad. Sci. U. S. A.,* **96,** 9118-9123.

Sugiura, T. and Berditchevski, F. (1999) Function of alpha3beta1-tetraspanin protein complexes in tumor cell invasion. Evidence for the role of the complexes in production of matrix metalloproteinase 2 (MMP-2). *J. Cell Biol.,* **146,** 1375-1389.

Sun, Z.L., Zhu, Y., Wang, F.Q., Chen, R., Peng, T., Fan, Z.N., Xu, Z.K. and Miao, Y. (2007) Serum proteomic-based analysis of pancreatic carcinoma for the identification of potential cancer biomarkers. *Biochim. Biophys. Acta,* **1774,** 764-771.

Suwa, H., Ohshio, G., Arao, S., Imamura, T., Yamaki, K., Manabe, T., Imamura, M., Hiai, H. and Fukumoto, M. (1996) Immunohistochemical localization of P-glycoprotein and expression of the multidrug resistance-1 gene in human pancreatic cancer: relevance to indicator of better prognosis. *Jpn. J. Cancer Res.,* **87,** 641-649.

Taghavi, M.H. and Davoodi, J. (2007) Restoration of p53 functions suppresses tumor growth of pancreatic cells with different p53 status. *Cancer Biother. Radiopharm.,* **22,** 322-332.

Takano, S., Kanai, F., Jazag, A., Ijichi, H., Yao, J., Ogawa, H., Enomoto, N., Omata, M. and Nakao, A. (2007) Smad4 is essential for down-regulation of E-cadherin induced by TGF-beta in pancreatic cancer cell line PANC-1. *J. Biochem. (Tokyo),* **141,** 345-351.

Takaoka, S., Iwase, M., Uchida, M., Yoshiba, S., Kondo, G., Watanabe, H., Ohashi, M., Nagumo, M. and Shintani, S. (2007) Effect of combining epidermal growth factor receptor inhibitors and cisplatin on proliferation and apoptosis of oral squamous cell carcinoma cells. *Int. J. Oncol.,* **30,** 1469-1476.

Takeshita, H., Kusuzaki, K., Murata, H., Suginoshita, T., Hirata, M., Hashiguchi, S., Ashihara, T., Gebhardt, M.C., Mankin, H.J. and Hirasawa, Y. (2000) Osteoblastic differentiation and P-glycoprotein multidrug resistance in a murine osteosarcoma model. *Br. J. Cancer,* **82,** 1327-1331.

Taki, M., Verschueren, K., Yokoyama, K., Nagayama, M. and Kamata, N. (2006) Involvement of Ets-1 transcription factor in inducing matrix metalloproteinase-2 expression by epithelial-mesenchymal transition in human squamous carcinoma cells. *Int. J. Oncol.,* **28,** 487-496.

Tanaka, H., Shirkoohi, R., Nakagawa, K., Qiao, H., Fujita, H., Okada, F., Hamada, J., Kuzumaki, S., Takimoto, M. and Kuzumaki, N. (2006) siRNA gelsolin knockdown induces epithelial-mesenchymal transition with a cadherin switch in human mammary epithelial cells. *Int. J. Cancer,* **118,** 1680-1691.

Tanaka, M., Mullauer, L., Ogiso, Y., Fujita, H., Moriya, S., Furuuchi, K., Harabayashi, T., Shinohara, N., Koyanagi, T. and Kuzumaki, N. (1995) Gelsolin: a candidate for suppressor of human bladder cancer. *Cancer Res.,* **55,** 3228-3232.

Tang, Z.H., Zou, S.Q., Hao, Y.H., Wang, B.J., Yang, X.P., Chen, Q.Q. and Qiu, F.Z. (2002) The relationship between loss expression of DPC4/Smad4 gene and carcinogenesis of pancreatobiliary carcinoma. *Hepatobiliary. Pancreat. Dis. Int.,* **1,** 624-629.

Tanno, S., Tanno, S., Mitsuuchi, Y., Altomare, D.A., Xiao, G.H. and Testa, J.R. (2001) AKT activation up-regulates insulin-like growth factor I receptor expression and promotes invasiveness of human pancreatic cancer cells. *Cancer Res.,* **61,** 589-593.

Tannu, N.S. and Hemby, S.E. (2006) Two-dimensional fluorescence difference gel electrophoresis for comparative proteomics profiling. *Nat. Protoc.,* **1,** 1732-1742.

Tanudji, M., Hevi, S. and Chuck, S.L. (2002) Improperly folded green fluorescent protein is secreted via a non-classical pathway. *J. Cell. Sci.,* **115,** 3849-3857.

Tari, A.M., Lim, S.J., Hung, M.C., Esteva, F.J. and Lopez-Berestein, G. (2002) Her2/neu induces all-trans retinoic acid (ATRA) resistance in breast cancer cells. *Oncogene,* **21,** 5224-5232.

Taxotere
www.taxotere.com (2007)

Thomas, P.A., Kirschmann, D.A., Cerhan, J.R., Folberg, R., Seftor, E.A., Sellers, T.A. and Hendrix, M.J. (1999) Association between keratin and vimentin expression, malignant phenotype, and survival in postmenopausal breast cancer patients. *Clin. Cancer Res.,* **5,** 2698-2703.

Thompson, C.C., Ashcroft, F.J., Patel, S., Saraga, G., Vimalachandran, D., Prime, W., Campbell, F., Dodson, A., Jenkins, R.E., Lemoine, N.R., et al (2007) Pancreatic cancer cells overexpress gelsolin family-capping proteins, which contribute to their cell motility. *Gut,* **56,** 95-106.

Thor, A.D., Edgerton, S.M., Liu, S., Moore, D.H.,2nd and Kwiatkowski, D.J. (2001) Gelsolin as a negative prognostic factor and effector of motility in erbB-2-positive epidermal growth factor receptor-positive breast cancers. *Clin. Cancer Res.,* **7,** 2415-2424.

Tobita, K., Kijima, H., Dowaki, S., Kashiwagi, H., Ohtani, Y., Oida, Y., Yamazaki, H., Nakamura, M., Ueyama, Y., Tanaka, M., et al (2003) Epidermal growth factor receptor expression in human pancreatic cancer: Significance for liver metastasis. *Int. J. Mol. Med.,* **11,** 305-309.

Torimura, T., Ueno, T., Kin, M., Ogata, R., Inuzuka, S., Sugawara, H., Kurotatsu, R., Shimada, M., Yano, H., Kojiro, M., et al (1999) Integrin alpha6beta1 plays a significant role in the attachment of hepatoma cells to laminin. *J. Hepatol.,* **31,** 734-740.

Tsao, M.S., Sakurada, A., Cutz, J.C., Zhu, C.Q., Kamel-Reid, S., Squire, J., Lorimer, I., Zhang, T., Liu, N., Daneshmand, M., et al (2005) Erlotinib in lung cancer - molecular and clinical predictors of outcome. *N. Engl. J. Med.,* **353,** 133-144.

Tsuji, N., Asanuma, K., Kobayashi, D., Yagihashi, A. and Watanabe, N. (2005) Introduction of a survivin gene-specific small inhibitory RNA inhibits growth of pancreatic cancer cells. *Anticancer Res.,* **25,** 3967-3972.

Tsutsumida, H., Swanson, B.J., Singh, P.K., Caffrey, T.C., Kitajima, S., Goto, M., Yonezawa, S. and Hollingsworth, M.A. (2006) RNA interference suppression of MUC1 reduces the growth rate and metastatic phenotype of human pancreatic cancer cells. *Clin. Cancer Res.,* **12,** 2976-2987.

Turashvili, G., Bouchal, J., Burkadze, G. and Kolar, Z. (2005) Differentiation of tumours of ductal and lobular origin: II. Genomics of invasive ductal and lobular breast carcinomas. *Biomed. Pap. Med. Fac. Univ. Palacky Olomouc Czech. Repub.,* **149,** 63-68.

Uchiyama-Kokubu, N. and Watanabe, T. (2001) Establishment and characterization of adriamycin-resistant human colorectal adenocarcinoma HCT-15 cell lines with multidrug resistance. *Anticancer Drugs,* **12,** 769-779.

Uhm, J.H., Gladson, C.L. and Rao, J.S. (1999) The role of integrins in the malignant phenotype of gliomas. *Front. Biosci.,* **4,** D188-99.

University of Chicago
www.home_uchicago.edu (1999)

University of Trieste, Department of Chemical Sciences
www.dsch.univ.trieste.it (2004)

Unlu, M., Morgan, M.E. and Minden, J.S. (1997) Difference gel electrophoresis: a single gel method for detecting changes in protein extracts. *Electrophoresis,* **18,** 2071-2077.

Untch, M., Untch, A., Sevin, B.U., Angioli, R., Perras, J.P., Koechli, O. and Averette, H.E. (1994) Comparison of paclitaxel and docetaxel (Taxotere) in gynecologic and breast cancer cell lines with the ATP-cell viability assay. *Anticancer Drugs,* **5,** 24-30.

Varner, J.A., Emerson, D.A. and Juliano, R.L. (1995) Integrin alpha 5 beta 1 expression negatively regulates cell growth: reversal by attachment to fibronectin. *Mol. Biol. Cell,* **6,** 725-740.

Verma, A., Wang, H., Manavathi, B., Fok, J.Y., Mann, A.P., Kumar, R. and Mehta, K. (2006) Increased expression of tissue transglutaminase in pancreatic ductal adenocarcinoma and its implications in drug resistance and metastasis. *Cancer Res.,* **66,** 10525-10533.

Verovski, V.N., Van den Berge, D.L., Delvaeye, M.M., Scheper, R.J., De Neve, W.J. and Storme, G.A. (1996) Low-level doxorubicin resistance in P-glycoprotein-negative human pancreatic tumour PSN1/ADR cells implicates a brefeldin A-sensitive mechanism of drug extrusion. *Br. J. Cancer,* **73,** 596-602.

Vihinen, P., Nikkola, J., Vlaykova, T., Hahka-Kemppinen, M., Talve, L., Heino, J. and Pyrhonen, S. (2000) Prognostic value of beta1 integrin expression in metastatic melanoma. *Melanoma Res.,* **10,** 243-251.

Vogelmann, R., Kreuser, E.D., Adler, G. and Lutz, M.P. (1999) Integrin alpha6beta1 role in metastatic behavior of human pancreatic carcinoma cells. *Int. J. Cancer,* **80,** 791-795.

Voss, T., Ahorn, H., Haberl, P., Dohner, H. and Wilgenbus, K. (2001) Correlation of clinical data with proteomics profiles in 24 patients with B-cell chronic lymphocytic leukemia. *Int. J. Cancer,* **91,** 180-186.

Wakeling, A.E., Guy, S.P., Woodburn, J.R., Ashton, S.E., Curry, B.J., Barker, A.J. and Gibson, K.H. (2002) ZD1839 (Iressa): an orally active inhibitor of epidermal growth factor signaling with potential for cancer therapy. *Cancer Res.,* **62,** 5749-5754.

Wang, H., Schultz, R., Hong, J., Cundiff, D.L., Jiang, K. and Soff, G.A. (2004) Cell surface-dependent generation of angiostatin4.5. *Cancer Res.,* **64,** 162-168.

Wang, K.L., Wu, T.T., Choi, I.S., Wang, H., Reseetkova, E., Correa, A.M., Hofstetter, W.L., Swisher, S.G., Ajani, J.A., Rashid, A., et al (2007) Expression of epidermal growth factor receptor in esophageal and esophagogastric junction adenocarcinomas: association with poor outcome. *Cancer,* **109,** 658-667.

Wang, W., Cassidy, J., O'Brien, V., Ryan, K.M. and Collie-Duguid, E. (2004) Mechanistic and predictive profiling of 5-Fluorouracil resistance in human cancer cells. *Cancer Res.,* **64,** 8167-8176.

Wang, Z., Banerjee, S., Li, Y., Rahman, K.M., Zhang, Y. and Sarkar, F.H. (2006) Down-regulation of notch-1 inhibits invasion by inactivation of nuclear factor-kappaB, vascular endothelial growth factor, and matrix metalloproteinase-9 in pancreatic cancer cells. *Cancer Res.,* **66,** 2778-2784.

Wegele, H., Muller, L. and Buchner, J. (2004) Hsp70 and Hsp90--a relay team for protein folding. *Rev. Physiol. Biochem. Pharmacol.,* **151,** 1-44.

Weil, D., Garcon, L., Harper, M., Dumenil, D., Dautry, F. and Kress, M. (2002) Targeting the kinesin Eg5 to monitor siRNA transfection in mammalian cells. *BioTechniques,* **33,** 1244-1248.

Weinel, R.J., Rosendahl, A., Neumann, K., Chaloupka, B., Erb, D., Rothmund, M. and Santoso, S. (1992) Expression and function of VLA-alpha 2, -alpha 3, -alpha 5 and -alpha 6-integrin receptors in pancreatic carcinoma. *Int. J. Cancer,* **52,** 827-833.

Weinel, R.J., Rosendahl, A., Pinschmidt, E., Kisker, O., Simon, B. and Santoso, S. (1995) The alpha 6-integrin receptor in pancreatic carcinoma. *Gastroenterology,* **108,** 523-532.

Wewer, U.M., Shaw, L.M., Albrechtsen, R. and Mercurio, A.M. (1997) The integrin alpha 6 beta 1 promotes the survival of metastatic human breast carcinoma cells in mice. *Am. J. Pathol.,* **151,** 1191-1198.

Wijnholds, J., Mol, C.A., van Deemter, L., de Haas, M., Scheffer, G.L., Baas, F., Beijnen, J.H., Scheper, R.J., Hatse, S., De Clercq, E., et al (2000) Multidrug-resistance protein 5 is a multispecific organic anion transporter able to transport nucleotide analogs. *Proc. Natl. Acad. Sci. U. S. A.,* **97,** 7476-7481.

Wilcken, N.R., Sarcevic, B., Musgrove, E.A. and Sutherland, R.L. (1996) Differential effects of retinoids and antiestrogens on cell cycle progression and cell cycle regulatory genes in human breast cancer cells. *Cell Growth Differ.,* **7,** 65-74.

Winston, J.S., Asch, H.L., Zhang, P.J., Edge, S.B., Hyland, A. and Asch, B.B. (2001) Downregulation of gelsolin correlates with the progression to breast carcinoma. *Breast Cancer Res. Treat.,* **65,** 11-21.

Woelfle, U., Sauter, G., Santjer, S., Brakenhoff, R. and Pantel, K. (2004) Down-regulated expression of cytokeratin 18 promotes progression of human breast cancer. *Clin. Cancer Res.,* **10,** 2670-2674.

Wolff, J.A. and Budker, V. (2005) The mechanism of naked DNA uptake and expression. *Adv. Genet.,* **54,** 3-20.

Wood, W.R., Seftor, E.A., Lotan, D., Nakajima, M., Misiorowski, R.L., Seftor, R.E., Lotan, R. and Hendrix, M.J. (1990) Retinoic acid inhibits human melanoma tumor cell invasion. *Anticancer Res.,* **10,** 423-432.

Wooster, R. and Weber, B.L. (2003) Breast and ovarian cancer. *N. Engl. J. Med.,* **348,** 2339-2347.

Xi, S. and Grandis, J.R. (2003) Gene therapy for the treatment of oral squamous cell carcinoma. *J. Dent. Res.,* **82,** 11-16.

Xia, W., Mullin, R.J., Keith, B.R., Liu, L.H., Ma, H., Rusnak, D.W., Owens, G., Alligood, K.J. and Spector, N.L. (2002) Anti-tumor activity of GW572016: a dual tyrosine kinase inhibitor blocks EGF activation of EGFR/erbB2 and downstream Erk1/2 and AKT pathways. *Oncogene,* **21,** 6255-6263.

Xiong, H.Q. and Abbruzzese, J.L. (2002) Epidermal growth factor receptor-targeted therapy for pancreatic cancer. *Semin. Oncol.,* **29,** 31-37.

Xiong, H.Q., Rosenberg, A., LoBuglio, A., Schmidt, W., Wolff, R.A., Deutsch, J., Needle, M. and Abbruzzese, J.L. (2004) Cetuximab, a monoclonal antibody targeting the epidermal growth factor receptor, in combination with gemcitabine for advanced pancreatic cancer: a multicenter phase II Trial. *J. Clin. Oncol.,* **22,** 2610-2616.

Xu, L., Li, Y.M., Yu, C.H., Li, L., Liu, Y.S., Zhang, B.F., Fang, J., Zhou, Q., Hu, Y. and Gao, H.J. (2006) Expression of p53, p16 and COX-2 in pancreatic cancer with tissue microarray. *Hepatobiliary. Pancreat. Dis. Int., 5,* 138-142.

Yamamoto, H., Itoh, F., Iku, S., Adachi, Y., Fukushima, H., Sasaki, S., Mukaiya, M., Hirata, K. and Imai, K. (2001) Expression of matrix metalloproteinases and tissue inhibitors of metalloproteinases in human pancreatic adenocarcinomas: clinicopathologic and prognostic significance of matrilysin expression. *J. Clin. Oncol., 19,* 1118-1127.

Yamanaka, Y., Friess, H., Kobrin, M.S., Buchler, M., Kunz, J., Beger, H.G. and Korc, M. (1993) Overexpression of HER2/neu oncogene in human pancreatic carcinoma. *Hum. Pathol., 24,* 1127-1134.

Yang, A.D., Camp, E.R., Fan, F., Shen, L., Gray, M.J., Liu, W., Somcio, R., Bauer, T.W., Wu, Y., Hicklin, D.J., et al (2006) Vascular endothelial growth factor receptor-1 activation mediates epithelial to mesenchymal transition in human pancreatic carcinoma cells. *Cancer Res., 66,* 46-51.

Yang, J., Mani, S.A. and Weinberg, R.A. (2006) Exploring a new twist on tumor metastasis. *Cancer Res., 66,* 4549-4552.

Yang, X., Staren, E.D., Howard, J.M., Iwamura, T., Bartsch, J.E. and Appert, H.E. (2001) Invasiveness and MMP expression in pancreatic carcinoma. *J. Surg. Res., 98,* 33-39.

Yano, J., Hirabayashi, K., Nakagawa, S., Yamaguchi, T., Nogawa, M., Kashimori, I., Naito, H., Kitagawa, H., Ishiyama, K., Ohgi, T., et al (2004) Antitumor activity of small interfering RNA/cationic liposome complex in mouse models of cancer. *Clin. Cancer Res., 10,* 7721-7726.

Yao, V.J., Ozawa, M.G., Varner, A.S., Kasman, I.M., Chanthery, Y.H., Pasqualini, R., Arap, W. and McDonald, D.M. (2006) Antiangiogenic therapy decreases integrin expression in normalized tumor blood vessels. *Cancer Res., 66,* 2639-2649.

Yarden, Y. (2001) The EGFR family and its ligands in human cancer. signalling mechanisms and therapeutic opportunities. *Eur. J. Cancer, 37 **Suppl 4,*** S3-8.

Yarden, Y. and Peles, E. (1991) Biochemical analysis of the ligand for the neu oncogenic receptor. *Biochemistry, 30,* 3543-3550.

Yates, J.R.,3rd (2000) Mass spectrometry. From genomics to proteomics. *Trends Genet., 16,* 5-8.

Yau, C.Y., Wheeler, J.J., Sutton, K.L. and Hedley, D.W. (2005) Inhibition of integrin-linked kinase by a selective small molecule inhibitor, QLT0254, inhibits the PI3K/PKB/mTOR, Stat3, and FKHR pathways and tumor growth, and enhances gemcitabine-induced apoptosis in human orthotopic primary pancreatic cancer xenografts. *Cancer Res., 65,* 1497-1504.

Yeager, A.M., Kaizer, H., Santos, G.W., Saral, R., Colvin, O.M., Stuart, R.K., Braine, H.G., Burke, P.J., Ambinder, R.F. and Burns, W.H. (1986) Autologous bone marrow transplantation in patients with acute nonlymphocytic leukemia, using ex vivo marrow treatment with 4-hydroperoxycyclophosphamide. *N. Engl. J. Med., 315,* 141-147.

Yin, H.L., Kwiatkowski, D.J., Mole, J.E. and Cole, F.S. (1984) Structure and biosynthesis of cytoplasmic and secreted variants of gelsolin. *J. Biol. Chem.,* **259,** 5271-5276.

Yin, T., Wang, C., Liu, T., Zhao, G. and Zhou, F. (2006) Implication of EMT induced by TGF-beta1 in pancreatic cancer. *J. Huazhong Univ. Sci. Technolog Med. Sci.,* **26,** 700-702.

Yokoyama, K., Kamata, N., Fujimoto, R., Tsutsumi, S., Tomonari, M., Taki, M., Hosokawa, H. and Nagayama, M. (2003) Increased invasion and matrix metalloproteinase-2 expression by Snail-induced mesenchymal transition in squamous cell carcinomas. *Int. J. Oncol.,* **22,** 891-898.

Yoshida, A., Rzhetsky, A., Hsu, L.C. and Chang, C. (1998) Human aldehyde dehydrogenase gene family. *Eur. J. Biochem.,* **251,** 549-557.

Yoshida, H. (2007) ER stress and diseases. *FEBS J.,* **274,** 630-658.

Yosuico, V.D., Khoury, T., Yu, J., Pande, A. and Javle, M. (2006) Epithelial-mesenchymal transition (EMT) in resected pancreatic cancer. *J Clin Oncol.*, **24**, abstract 4094.

Zalatnai, A. (2006) Familial pancreatic cancer. *Magy Onkol.,* **50,** 163-168.

Zaman, G.J., Flens, M.J., van Leusden, M.R., de Haas, M., Mulder, H.S., Lankelma, J., Pinedo, H.M., Scheper, R.J., Baas, F. and Broxterman, H.J. (1994) The human multidrug resistance-associated protein MRP is a plasma membrane drug-efflux pump. *Proc. Natl. Acad. Sci. U. S. A.,* **91,** 8822-8826.

Zelcer, N., Saeki, T., Reid, G., Beijnen, J.H. and Borst, P. (2001) Characterization of drug transport by the human multidrug resistance protein 3 (ABCC3). *J. Biol. Chem.,* **276,** 46400-46407.

Zeng, Z., Weiser, M.R., D'Alessio, M., Grace, A., Shia, J. and Paty, P.B. (2004) Immunoblot analysis of c-Met expression in human colorectal cancer: overexpression is associated with advanced stage cancer. *Clin. Exp. Metastasis,* **21,** 409-417.

Zhang, L., Chenwei, L., Mahmood, R., van Golen, K., Greenson, J., Li, G., D'Silva, N.J., Li, X., Burant, C.F., Logsdon, C.D., et al (2006) Identification of a putative tumor suppressor gene Rap1GAP in pancreatic cancer. *Cancer Res.,* **66,** 898-906.

Zhang, X., Kon, T., Wang, H., Li, F., Huang, Q., Rabbani, Z.N., Kirkpatrick, J.P., Vujaskovic, Z., Dewhirst, M.W. and Li, C.Y. (2004) Enhancement of hypoxia-induced tumor cell death in vitro and radiation therapy in vivo by use of small interfering RNA targeted to hypoxia-inducible factor-1alpha. *Cancer Res.,* **64,** 8139-8142.

Zhang, X., Shan, P., Jiang, D., Noble, P.W., Abraham, N.G., Kappas, A. and Lee, P.J. (2004) Small interfering RNA targeting heme oxygenase-1 enhances ischemia-reperfusion-induced lung apoptosis. *J. Biol. Chem.,* **279,** 10677-10684.

Zhao, Y.P., Zhang, L.Y., Liao, Q., Guo, J.C., Chen, G. and Li, J.Y. (2004) Detection of multidrug resistant gene 1 in pancreatic cancer. *Hepatobiliary. Pancreat. Dis. Int.,* **3,** 307-310.

Zhou, W., Sokoll, L.J., Bruzek, D.J., Zhang, L., Velculescu, V.E., Goldin, S.B., Hruban, R.H., Kern, S.E., Hamilton, S.R., Chan, D.W., et al (1998) Identifying markers for pancreatic cancer by gene expression analysis. *Cancer Epidemiol. Biomarkers Prev.,* **7,** 109-112.

Zhu, Z., Sanchez-Sweatman, O., Huang, X., Wiltrout, R., Khokha, R., Zhao, Q. and Gorelik, E. (2001) Anoikis and metastatic potential of cloudman S91 melanoma cells. *Cancer Res.,* **61,** 1707-1716.

7.0 Appendix

Table 7.1 All proteins differentially regulated between MiaPaCa-2 versus Clone #8

Protein name	Gene ID	Protein AC	Fold change MiaPaCa2 versus Clone #8
Antiquitin (b)	ALDH7A1	gi|34783121|	-4.7 ***
Antiquitin (a)	ALDH7A1	gi|34783121|	-2.6 ***
Glyceraldehyde-3-phosphate dehydrogenase (b)	GAPDH	gi|31645|	-1.9 ***
Glyceraldehyde-3-phosphate dehydrogenase (a)	GAPDH	gi|31645|	-1.7 ***
Profilin 1	PFN1	gi|30582841|	-1.6 ***
Keratin 18	KRT18	gi|12653819|	-1.6 *
Heat shock protein 60 (a)	HSPD1	gi|77702086|	-1.6 ***
Heat shock protein 60 (b)	HSPD1	gi|77702086|	-1.5 *
Beta actin (c)	ACTB	gi|15277503|	-1.5 ***
Peroxiredoxin 1	PRDX1	gi|55959887|	-1.4 ***
Peroxiredoxin 2 isoform b	PRDX2	gi|33188452|	-1.4 ***
Muscle Fructose 1; 6-Bisphosphate Aldolase	ALDOA	gi|4930291|	-1.4 **
14-3-3 Protein Theta (Human) Complexed To Peptide	YWHAQ	gi|71042777|	-1.4 ***
Ubiquinol-cytochrome c reductase complex core protein1	UQCRC1	gi|731047|	-1.3 ***
Heat shock protein 60 (c)	HSPD1	gi|77702086|	-1.3 *
Epsilon (Human) Complexed To Peptide	YWHAE	gi|67464424|	-1.3 *
Stomatin-like 2	STOML2	gi|6841440|	-1.3 **
Aldehyde dehydrogenase 1 family;	ALDH1B1	gi|30583675|	-1.3 *

member B1			
Glutathione synthetase	GSS	gi|8248826|	-1.2 *
Gamma actin (a)	ACTG1	gi|17511847|	1.2 *
Beta actin (d)	ACTB1	gi|15277503|	1.2 *
Alpha-tubulin	TUBA	gi|340021|	1.3 *
Stress-induced-phosphoprotein 1 (a)	STIP1	gi|54696884|	1.3 *
ER-60 protein	PDIA3	gi|2245365|	1.3 *
Tubulin alpha 6 variant	TUBA6	gi|62897609|	1.3 **
Heat shock 70kDa protein 1A	HSPA1A	gi|5123454|	1.3 ***
Glucosidase II	GANAB	gi|2274968|	1.4 ***
Eukaryotic translation initiation factor 4A; isoform 1	EIF4A1	gi|40786436|	1.4 *
Annexin I (a)	ANXA1	gi|442631|	1.5 **
heat shock 70kDa protein 8 isoform 1 variant (d)	HSPA8	gi|62897129|	1.5 ***
Human rab GDI	GDI2	gi|285975|	1.6 ***
Enolase 1	ENO1	gi|62897945|	1.6 ***
Heat shock 70kDa protein 8 isoform 1 variant (a)	HSPA8	gi|62897129|	1.6 ***
Ubiquitin-activating enzyme E1	UBE1	gi|57209338|	1.6 **
Pyruvate kinase 3 isoform 1 variant (a)	PKM2	gi|62897413|	1.6 ***
Muscle Pyruvate Kinase (b)	PKM2	gi|67464392|	1.6 **
Annexin A2 isoform 2 variant	ANXA2	gi|62896643|	1.6 ***
GARS protein	GARS	gi|12652637|	1.7 ***
Nucleoside Triphosphate; Nucleoside Diphosphate	NDPK	gi|1421614|	1.7 ***
Chaperonin TCPI, subunit 5 (epsilon)	CCT5	gi|58257644|	1.7 ***
Vimentin (d)	VIM	gi|57471646|	1.8 **

382

Vinculin	VCL	gi|24657579|	1.8 ***
Tryptophanyl-Trna Synthetase	WARS	gi|50513261|	1.8 ***
Heat shock 70kDa protein 4 isoform a variant	HSPA4	gi|62087882|	2.0 ***
Eukaryotic translation elongation factor 1 alpha 1 variant (c)	EEF1A1	gi|62897525|	2.0 ***
Gamma actin (b)	ACTG1	gi|17511847|	2.0 ***
Eukaryotic translation elongation factor 2	EEF2	gi|33869643|	2.1 ***
Vimentin (a)	VIM	gi|57471646|	2.2 ***
Triosephosphate Isomerase (a)	TPI1	gi|66360366|	2.2 ***
Vimentin (b)	VIM	gi|57471646|	2.2 ***
Beta actin (b)	ACTB	gi|15277503|	2.3 ***
Aldehyde dehydrogenase 1 (c)	ALDH1A1	gi|2183299|	3.8 ***
Aldehyde dehydrogenase 1 (a)	ALDH1A1	gi|2183299|	5.3 ***
Aldehyde dehydrogenase 1 (b)	ALDH1A1	gi|2183299|	6.8 ***

Table 7.2 All proteins differentially regulated between Clone #3 versus MiaPaCa-2

Protein name	Gene ID	Protein AC	Fold change Clone #3 versus MiaPaCa-2
Keratin 18	KRT18	gi|12653819|	-1.8
Annexin I (a)	ANXA1	gi|442631|	-1.5
glyceraldehyde-3-phosphate dehydrogenase (b)	GAPDH	gi|31645|	-1.3
annexin A2 isoform 2 variant	ANXA2	gi|62896643|	-1.3
Fragment Of Human Tryptophanyl-Trna Synthetase	WARS	gi|50513261|	-1.3
90kDa heat shock protein	HSP90ab1	gi|306891|	-1.2
heat shock 70kDa protein 8 isoform 1 variant (c)	HSPA8	gi|62897129|	-1.2
aspartate aminotransferase 2 precursor variant	GOT2	gi|62898103|	1.2
heat shock 70kD protein 9B (mortalin-2)	HSPA9	gi|21040386|	1.2
peroxiredoxin 1	PRDX1	gi|55959887|	1.2
glyceraldehyde-3-phosphate dehydrogenase (d)	GAPDH	gi|32891805|	1.2
aldehyde dehydrogenase 1 (b)	ALDH1A1	gi|2183299|	1.2
transketolase	TKT	gi|37267|	1.3
Human Muscle Fructose 1; 6-Bisphosphate Aldolase	ALDOA	gi|4930291|	1.3
Triosephosphate Isomerase (b)	TPI1 (b)	gi|999893|	1.3
ACTG1 protein (a)	ACTG1	gi|17511847|	1.3
ATP5A1 protein (a)	ATP5A1	gi|34782901|	1.3
ATP synthase beta subunit	ATPB	gi|179279|	1.3
MTHSP75	HSPA9B	gi|292059|	1.4

ACO2	ACO2	gi|49168620|	1.4
Annexin I (b)	ANXA1	gi|442631|	1.5
Chain B; 14-3-3 Protein Theta (Human) Complexed To Peptide	YWHAQ	gi|71042777|	1.5
ER-60 protein	PDIA3	gi|2245365|	1.5
translation initiation factor	EIF4F	gi|496902|	1.5
ATP5A1	ATP5A1	gi|34782901|	1.5
Hydroxyacyl dehydrogenase; subunit B	HADHB	gi|44890770|	1.5
stress-induced-phosphoprotein 1 (a)	STIP1	gi|54696884|	1.5
Glucosidase II	GANAB	gi|2274968|	1.6
translation elongation factor 1 alpha 1-like 14 (b)	EEF1A1	gi|15277711|	1.6
ubiquitin-activating enzyme E1	UBE1	gi|57209338|	1.6
aldehyde dehydrogenase 1 (a)	ALDH1A1	gi|2183299|	1.7
ACTB protein (a)	ACTB	gi|15277503|	1.7
Antiquitin (a)	ALDH7A1	gi|34783121|	1.7
Chain B; Human Triosephosphate Isomerase (a)	TPI1	gi|66360366|	1.8
elongation factor 1-alpha 1 (a)	EEF1A1	gi|28848610|	2.0
Antiquitin (b)	ALDH7A1	gi|34783121|	2.2
vimentin (a)	VIM	gi|57471646|	2.5

Table 7.3 All proteins differentially regulated between Clone #3 versus Clone #8

Protein name	Gene ID	Protein AC	Fold change Clone #3 versus Clone #8
aldehyde dehydrogenase 1 (a)	ALDH1A1	gi|2183299|	8.9
aldehyde dehydrogenase 1 (b)	ALDH1A1	gi|2183299|	8.4
vimentin (a)	VIM	gi|57471646|	5.5
aldehyde dehydrogenase 1 (c)	ALDH1A1	gi|2183299|	5.3
Triosephosphate Isomerase (a)	TPI1	gi|66360366|	4.0
vimentin (b)	VIM	gi|57471646|	2.8
vimentin (c)	VIM	gi|37852|	2.7
ubiquitin-activating enzyme E1	UBE1	gi|57209338|	2.6
heat shock 70kDa protein 4 isoform a variant	HSPA4	gi|62087882|	2.4
Chain A; Structure Of Human Muscle Pyruvate Kinase (Pkm2)	PKM2	gi|67464392|	2.4
elongation factor 1-alpha 1 (a)	EEF1A1	gi|28848610|	2.4
translation elongation factor 1 alpha 1-like 14 (b)	EEF1A1	gi|15277711|	2.2
VCL protein	VCL	gi|24657579|	2.2
Glucosidase II	GANAB	gi|2274968|	2.2
ER-60 protein (a)	PDIA3	gi|2245365|	2.0
stress-induced-phosphoprotein 1 (a)	STIP1	gi|54696884|	2.0
vimentin (d)	VIM	gi|57471646|	2.0
EEF2 protein (a)	EEF2	gi|33869643|	2.0
pyruvate kinase 3 isoform 1 variant	PKM2	gi|62897413|	1.9
heat shock 70kDa protein 8 isoform 1	HSPA8	gi|62897129|	1.9
enolase 1 variant	ENO1	gi|62897945|	1.9

eukaryotic translation elongation factor 1 alpha 1 variant (c)	EEF1A1	gi|62897525|	1.8
GARS protein	GARS	gi|12652637|	1.8
human rab GDI	GDI2	gi|285975|	1.8
KIAA0098 protein	CCT5	gi|58257644|	1.8
stress-induced-phosphoprotein 1 (b)	STIP1	gi|54696884|	1.8
Chain A; Human Cyclophilin A Complexed With 2-Thr Cyclosporin	PPIA	gi|3659980|	1.7
tubulin alpha 6 variant (a)	TUBA6	gi|62897609|	1.7
heat shock 70kDa protein 8 isoform 1	HSPA8	gi|62897129|	1.7
ER-60 protein (b)	PDIA3	gi|2245365|	1.7
MTHSP75	HSPA9	gi|292059|	1.6
beta-tubulin (a)	TUBB	gi|338695|	1.5
translation initiation factor	EIF4A3	gi|496902|	1.5
heat shock 70kDa protein 8 isoform 1 variant (b)	HSPA8	gi|62897129|	1.5
ATP5A1 protein	ATP5A1	gi|34782901|	1.5
ACTG1 protein (a)	ACTG1	gi|17511847|	1.5
tubulin alpha 6 variant (b)	TUBA6	gi|62897609|	1.4
Tubulin; beta polypeptide (b)	TUBB	gi|18088719|	1.4
protein disulfide isomerase-related protein 5	PDIA5	gi|1710248|	1.4
tubulin alpha 6 variant (c)	TUBA6	gi|62897609|	1.4
alpha-tubulin	TUBA	gi|340021|	1.4
Tubulin; beta polypeptide (c)	TUBB	gi|18088719|	1.4
Fragment Of Human Tryptophanyl-Trna Synthetase	WARS	gi|50513261|	1.4
MDH2	MDH2	gi|49168580|	1.4
ACO2	ACO2	gi|49168620|	1.3
Bisphosphate Aldolase	ALDOA	gi|4930291|	1.3

Annexin I (b)	ANXA1	gi|442631|	1.3
EEF2 protein	EEF2	gi|33869643|	1.2
Mortalin-2	HSPA9	gi|21040386|	1.2
HSPC108	STOML2	gi|6841440|	-1.2
Ubiquinol-cytochrome-c reductase complex core protein I	UQCRC1	gi|731047|	-1.3
heat shock 70kDa protein 8 isoform 1 variant (c)	HSPA8	gi|62897129|	-1.3
profilin 1	PFN1	gi|30582841|	-1.4
heat shock protein 60 (a)	HSPD1	gi|77702086|	-1.5
Antiquitin (a)	ALDH7A1	gi|34783121|	-1.5
ACTB protein (c)	ACTB	gi|15277503|	-1.6
glyceraldehyde-3-phosphate dehydrogenase (a)	GAPDH	gi|31645|	-1.9
Antiquitin (b)	ALDH7A1	gi|34783121|	-2.2
glyceraldehyde-3-phosphate dehydrogenase (b)	GAPDH	gi|31645|	-2.6
Keratin 18	KRT18	gi|12653819|	-2.9